School of Earth and Planetary Sciences

Mesozoic Tectono-stratigraphic evolution of the Exmouth Plateau, North West Shelf Australia

Hayley Rebecca Rohead-O'Brien

0000-0002-4626-455X

This thesis is presented for the Degree of

Doctor of Philosophy

of

Curtin University

November 2023

Declaration

To the best of my knowledge and belief, this thesis contains no material previously

published by any other person except where due acknowledgement has been made.

This thesis contains no material which has been accepted for the award of any other

degree or diploma in any university.

Signature: …….

Date: 14-11-2023

ABSTRACT

The Exmouth Plateau sits at the outer limits of the northwest margin of the Australian continent and remains poorly understood. Previously, our understanding of the Exmouth Plateau, part of the Northern Carnarvon Basin, has been largely based on observations from the surrounding sub-basins or the northwestern margin as a whole. The current breadth of studies that focus on the Exmouth Plateau are generally based on single datasets and seek to apply the learnings to the broader plateau. Consequently, this dissertation takes a more regional approach and looks at the southern part of the Exmouth Plateau, utilising several high-quality 3D seismic surveys, deeply-imaged 2D seismic data, and information from several hydrocarbon wells. Using information from deeply buried Mesozoic sequences, a series of tectono-stratigraphic mega-sequences have been defined to describe and to examine the relationship between Mesozoic rift activity and the formation of the Exmouth Plateau.

Detailed interpretation shows that the onset of fault activity across the plateau was variable. With the earliest onset of fault activity occurring in the Uppermost Triassic, prominently on NNE-SSW and NE-SW trending faults. These faults are the expression of a period of rifting that culminated in sea-floor spreading in the Argo Abyssal Plain, although fault orientation and uplift patterns indicate that other processes may also have been operating. Fault orientation is strongly controlled by underlying Palaeozoic and basement structures. Faults with a NW-SE orientation were most prominent during the Lower Cretaceous and are related to the separation of the Australian and Greater Indian plates, although the persistence of this fault orientation throughout the Mesozoic is an indication that stress from the Greater India separation event began to build earlier than commonly accepted. This highlights two prominent phases of rift-activity which have influenced the development of the Exmouth Plateau.

The pattern of faulting is also reflected in the rift morphology, with the more faulted regions in the north west of the Plateau being persistently higher in elevation. The prolonged pattern of outer margin elevation is maintained

throughout the Jurassic and Cretaceous resulting in reduced sedimentation in the area, and the development of the Exmouth Plateau Depocentre. The elevation of the south east margin of the Exmouth Plateau during the Lower Jurassic was short-lived and controlled by uplift of the failed Barrow-Dampier rift flank. This uplift created the mechanical subsidence adjacent to the Rankin Platform, resulting the formation of the Kangaroo Syncline. The uplift of individual fault blocks limited Jurassic sedimentation on the plateau. These fault blocks provided a barrier to sediment supply, preventing deposition in areas of greater fault activity. However, uplift also affected sediment supply to the Kangaroo Syncline and Exmouth Plateau Depocentre. The Lower Jurassic uplift of the rift-flank altered the supply pathway from the east, and some of that material was deflected into the adjacent depocentre. Secondly, the uplift resulted in the erosion and recycling of the flank into the syncline, further driving the subsidence of the Kangaroo Syncline.

A shelf prograded onto the plateau from the south-west in the latest Jurassic and sediment slowly infilled the previously starved half-graben. The fresh influx of sediment utilised pathways created by the fault activity to allow accumulation over an area of greater bathymetric relief. This concentration developed in the position of the younger Exmouth Plateau Arch, above part of the area of greater Jurassic elevation. At this time fault activity was most prominent on NW-SE orientated faults, which are related to the Valanginian separation of Greater India and Australia. Sedimentation then continued in a more widespread manner but was limited to the northeast by an elevated feature, the Wanthaya High (newly identified feature of the plateau). Fault activity had decreased considerably by the Valanginian and all but ceased by the mid-Aptian, but subsidence continued in a depocentre above the Jurassic Kangaroo Syncline until the end of the Cretaceous.

This research has also identified that the formation of uplifted rift flanks is crucial to the resulting architecture of rift basins. In the case of the Exmouth Plateau, there are two uplifted flanks in response to rift processes and both have been key to the formation of prominent depocentres. While uplift on the flanks of the marginal rift basin is similar to that in other rift systems, the

fundamental processes pertaining to the uplift of the outer margin remain enigmatic.

Acknowledgement to Country

I want to begin by acknowledging the Traditional Owners of the land on which I undertook this research, the Noongar Wadjuk peoples, and any peoples of the Land and Sea over the Exmouth Plateau. I extend my humble respect to the Elders of this Country, past, present, and future. I offer my thanks for sharing this country and my sorrow for the pain and suffering that sharing has and is still causing. I hope our many peoples are beginning to build a strong relationship after many years of injustice. My greatest hope is that my Wardandi nephews grow up in a world where their culture and traditions are celebrated and accepted.

Acknowledgments

This dissertation has literally resulted from so many people supporting me through difficult, unfair, and unavoidable periods of my life. When I embarked on this adventure in 2016, I never would have predicted the downward mental health spiral that plagued me nearly constantly until sometime in 2019. I also would not have expected my diagnosis of aggressive bilateral breast cancer in 2020. On the long road that has been this research, I also discovered I have CPTSD, ADHS and likely Autism. So, thank you to everyone who helped me along the way in getting to this point; notable mentions below.

To my primary supervisor, the esteemed Professor Chris Elders. Thank you for giving me encouragement and understanding. For providing me space to feel, following a bad case of sexism that nearly resulted in me stepping away from this field, and for then being upset and angry that I went through that for six months without speaking to you about why I was barely functioning. Thank you for supporting me through chemotherapy even when it felt like I had no remaining brain cells. However, I still disagree, I could have obtained my Doctorate posthumously, but I am somewhat glad I did it this way. Otherwise, how would I have kept myself entertained whilst trying to decipher your handwriting….and my own. Thank you also to my co-supervisors, Jane Cunneen and Greg Smith, for offering chats and advice when needed.

Thank you to my Aunt Marianne for taking me in during my late teens and pushing me to look into studying, even if I spent a lot of my tertiary education regretting tertiary education. Thank you also for the many phone calls from me just venting about my mother and how her actions continue to impact me even though she is long gone. Thank you to my cousin Jorja for being there for me at my lowest and enduring my IBS text cries for help regularly. Thank you to my adoptive family, the Nicolson-Begg Clan (and descendants) for putting up with me, feeding me and caring for me.

Thank you to my dog Alfonso Geoffrey Charles Nicolson Begg for never wavering in your love for food above all else; it’s nice to know your priorities never faltered.

Thank you to the Cheese Sluts for eating all of the cheese with me and abstaining from this pleasure when I had to. Particular thanks to Laura and Richard for sticking by me, even if it cost you friendships too.

Thank you to my primary Breast Care Nurse, Joan Burgess, for being on call for my uneducated and needy questions even after treatment was over.

Thank you to Dr Elizabeth Sinclair for not dismissing my concerns and giving me the devastating news straight, then letting me cry for way longer than my allotted appointment.

Thank you to Professor Saunders and her staff for guiding me through the process of an early breast cancer diagnosis and then for removing the offensive material from my body.

Thank you to Professor Daphne Tsoi, her medical receptionist Jacquie, and all the Bendat Family Cancer Centre staff in Subiaco. The intense treatment saved my life, but I would not recommend the hairdressing services; I just wanted a trim.

Thank you to Dr Brigid Corrigan for performing my reconstruction surgeries with last-minute panicked changes.

Thank you to Dr Stuart Salfinger for performing preventive surgery for my BRCA-1 gene mutation and not making me fight to have it.

Thank you to Dr Lesley Ramage for assisting me with my urgent medical needs following a round of surgery not long before the first submission of this thesis.

Thank you to my therapist while I studied Ali Marland for guiding me through trauma and anxiety and, jeez, probably a million other things, including most of my medical treatment.

Thank you to Katie at Breast Care WA for providing me therapy in the aftermath of surgery and chemo when I needed someone who had more of a hold on what I was going through.

Thank you to all those I work with for making me feel included even when I couldn’t be. Especially thank you to Barry, Channel, Nicole, Wayne, and Zory

for carrying my extra weight on your shoulders while I was sick from chemo. I hope you never need the same from me.

Thank you to those who have made me laugh, made me cry-laugh and made me smile.

Additional Acknowledgments for Final Submission

Thank you to Dr Hacking for providing me with a C-PTSD and ADHD diagnosis and a way forward.

Thank you to April at the PAX Centre for getting me out of crisis and guiding me through reframing my trauma.

Thank you to Helena Green for teaching me how to move past my body image issues after cancer.

Attribution Statement

This thesis is the product of work which I undertook in a Petrel project which contained seismic and well data. The project was provided to me by my primary supervisor Professor Chris Elders. I added some additional well data and undertook the seismic interpretation. I then wrote and prepared the first draft of the dissertation with figures. Extensive discussion of the first draft occurred between myself and my supervisory panel, Professor Elders, Dr Cunneen, and Dr Smith.

During preparation and development of ideas I had regular discussions with my supervisory panel. This includes the preparation of documents for several conferences as paper or poster presentations, some involving oral presentations.

Student Name, Hayley (Halla) Rebecca Rohead-O'Brien

Signature……..

Date, 14-11-2023

Funding Statement

I received a stipend in the form of an Australian Postgraduate Award (APA) from the Australian Government to aid in undertaking this research

TABLE OF CONTENTS

Table of Figures

List of Tables

1. Introduction

1.1. Rifting at Continental Margins

The formation of global continental margins, as observed at the present day, is the result of continental rifting, extension, and deformation (Alves et al., 2021; Elders et al., Manuscript; Grasemann & Stuwe, 2011; Mondy, 2019) resulting in the separation of one or more continental fragments (Brownfield & Charpentier, 2006; Cameron et al., 1999; Heine et al., 2013). Rifting is the result of a wide-range of geodynamic processes (Alves et al., 2021; Grasemann & Stuwe, 2011; Khain, 1992; Mondy, 2019; Turcotte & Emermann, 1983) that are the result of deviatoric stress acting on the lithosphere and/or thermal upwelling of the mantle (Figure 1.1; Bastia & Radhakrishna, 2012; Bott, 1993; Burke & Dewey, 1973; Franke, 2013; Kearey et al., 2009; McKenzie, 1978; Ribeiro et al., 2002; Turcotte & Emermann, 1983; Turcotte & Oxburgh, 1973).

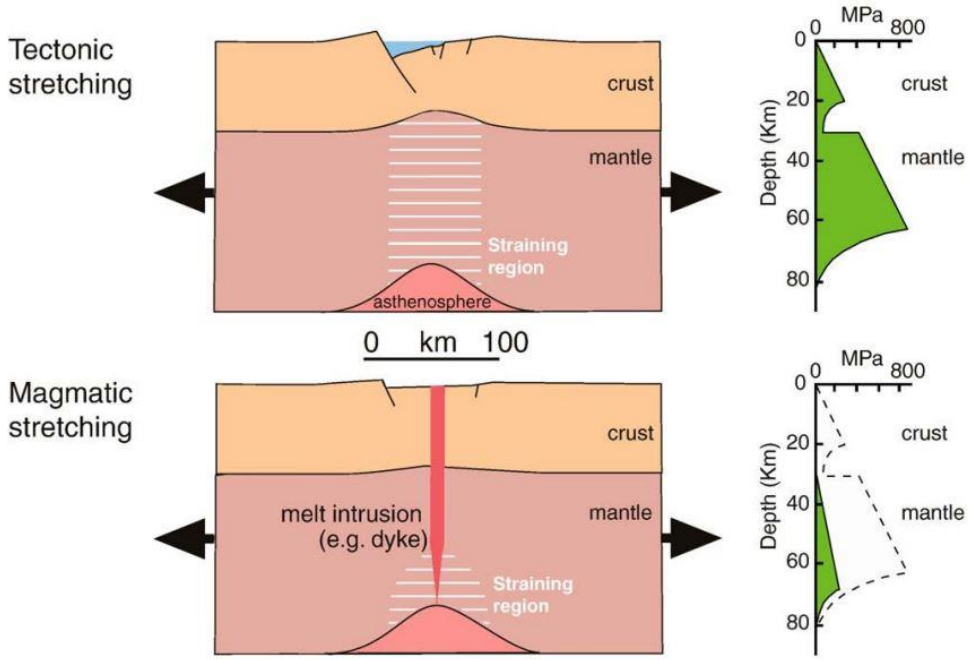

Figure 1.1 Extension of crustal material resulting in rift formation, tectonic stretching and magmatic stretching. Note the larger volume of stress required to generate crustal separation without magma, as per Corti (2009).

Additional aspects which impact upon the development of a rifted margin are the composition and density of the lithosphere, structural heritage, thermal gradient, and rate of plate motion (Bott, 1993; Cloetingh et al., 2013; Davis & Lavier, 2017; Falvey & Mutter, 1981; Forsyth & Uyeda, 1975; Frison de Lamotte et al., 2015; Gueydan & Précigout, 2014; Ju et al., 2015, 2022; Korchinski et al., 2021; Moore et al., 1986; Sleep, 1971; Wessel & Müller, 2007; Wheeler & Cheadle, 2014; Ziegler, 1993).

Magmatic underplating (Figure 1.2; Fyfe & Leonardos, 1973) is a process that impacts the evolution of a rifted margin by altering the thermal conditions of a region, the lithospheric composition and the relative buoyancy of the resulting crust (Ju et al., 2022). The location of basins -forming on continental margins, as a result of rift processes- impact upon the magmatic, thermal and topographic history of the basin. Close proximity to the rift centre causes thermal and magmatic processes to drive both uplift and subsidence, whereas distance from the rift axis reduces or removes any magmatic driver (Manatschal et al., 2021). The extent of magmatic influence on a rifted margin impacts upon the regional stress, and the thermal and compositional nature of the margin (Chenin et al., 2022; Grasemann & Stuwe, 2011). Magma alters the rheology of the lithosphere, altering the thermal gradient of the region (Chenin et al., 2022), where there is a greater -and prolonged- thermal impact based on the volume of magmatic influence (Grasemann & Stuwe, 2011). Magmatic influence can temporarily weaken the rifted crust making it prone to deformation (Grasemann & Stuwe, 2011; Neugebauer, 1978). In the long-term magmatic influence may strengthen the newly formed basin by creation of a mechanically stronger rheology (Grasemann & Stuwe, 2011). Rifted margins are commonly classed as either magma-rich or -poor, resulting from different proportions of primary rift triggers (Alves et al., 2021; Chenin et al., 2022; Franke, 2013; Sawyer et al., 2007). Magma-rich margins add complexity to the tectonic-magmatic relation of the rift processes (Alves et al., 2021). The increase in thermal alteration from magmatic influence can alter the time-scale of the rift activity (Alves et al., 2021; Bai et al., 2020).

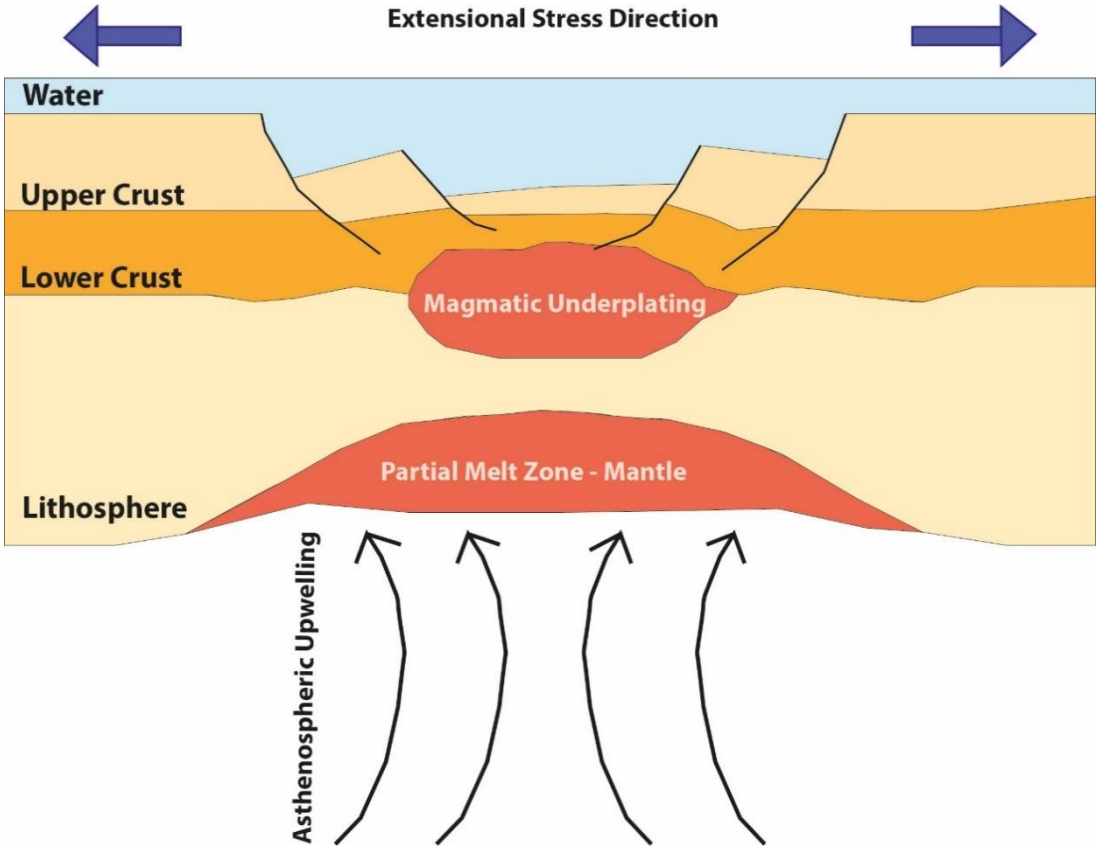

Figure 1.2 Diagrammatic representation of upwelling asthenosphere and resulting partial melt or underplating of the lithosphere, based on the work of Watts (2001) and Zhu et al. (2019).

Thermal energy transfer is a key geodynamic process, both driving rifting and deforming the resulting basin (Grasemann & Stuwe, 2011; Hu et al., 2001). Continental crust heats up before any rift event, remaining high until rifting has ceased (Boillot, 1979; Dewey & Bird, 1970; Falvey, 1974). The speed at which cooling occurs is related to the size of the rifted area (Pitman & Andrews, 1985). Additional factors which can impact the thermal nature of a rifted margin are deformation and erosion (Grasemann & Stuwe, 2011; Rouby et al., 2013) and the input of material through surface processes (Ju et al., 2015, 2020).

The density and composition of the lithosphere plays a key role in the response to stress and the resulting deformation and loading (Rouby et al., 2013; Wheeler & Cheadle, 2014) where gravity plays a part in the geodynamics of rifted margins (Ju et al., 2022; Morgan et al., 2016). Loading causes plates to deform during rift activity via flexure (Figure 1.3a; Rouby et al., 2013; White &

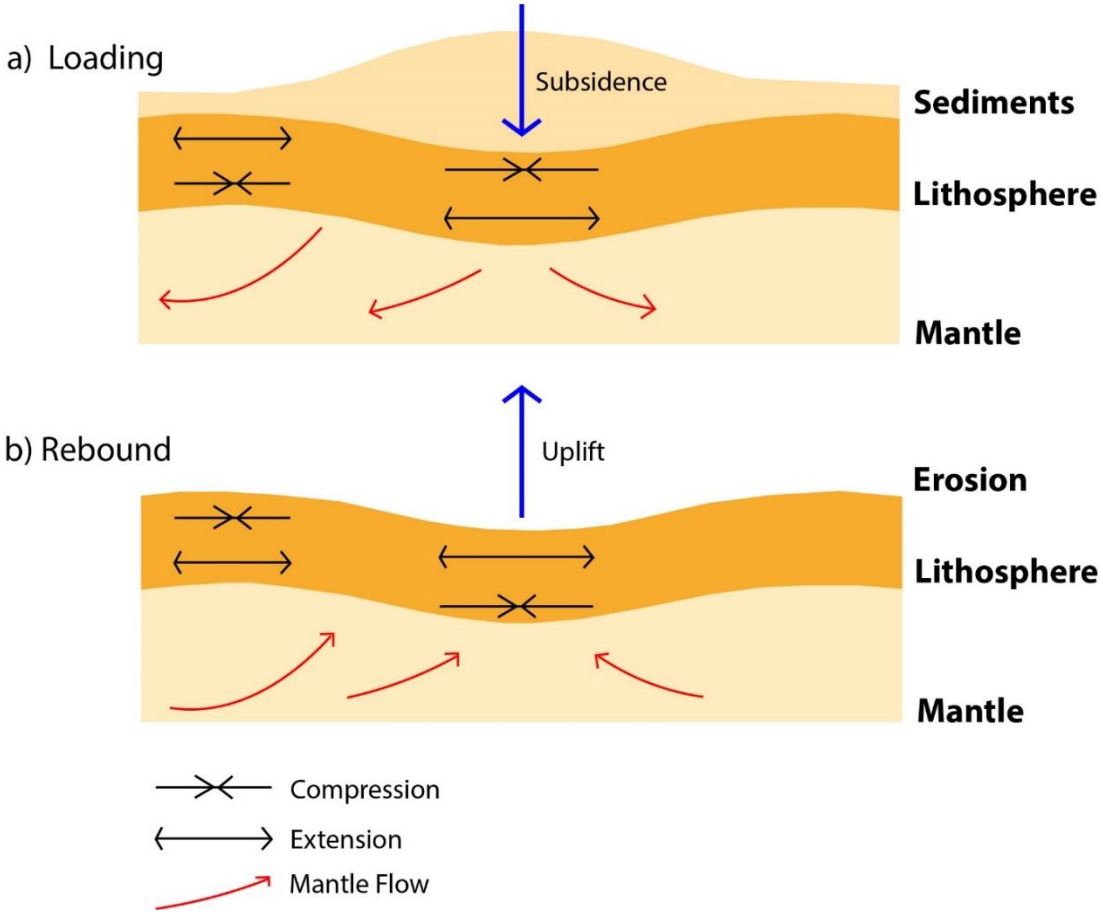

Figure 1.3 Impacts of loading and unloading on the lithosphere, based on the work of Shaw et al. (2013), Watts (2001), and White and McKenzie (1988).

McKenzie, 1988). The density of the lithosphere and crust can be altered by the introduction or removal of heat (Chenin et al., 2022), in addition loading of the crust will be impacted by changes surrounding the addition or removal of water and sediments (Figure 1.4; Allen, 2008; Ju et al., 2022; Mondy, 2019; Ribeiro et al., 2002). Indeed, the reduction of the rift induced thermal anomaly following the cessation of rift activity reduces the mechanical flexure of the crust in response to loading (Watts, 1978; Watts et al., 1982; Beaumont et al., 1982).

1.1.1. EVOLUTION OF RIFTING AT CONTINENTAL MARGINS

The deformation of the lithosphere represents the initial stage of continental break-up (Kearey et al., 2009). Falvey (1974) described this stage as early basement subsidence prior to the rift opening. Following the rift opening along

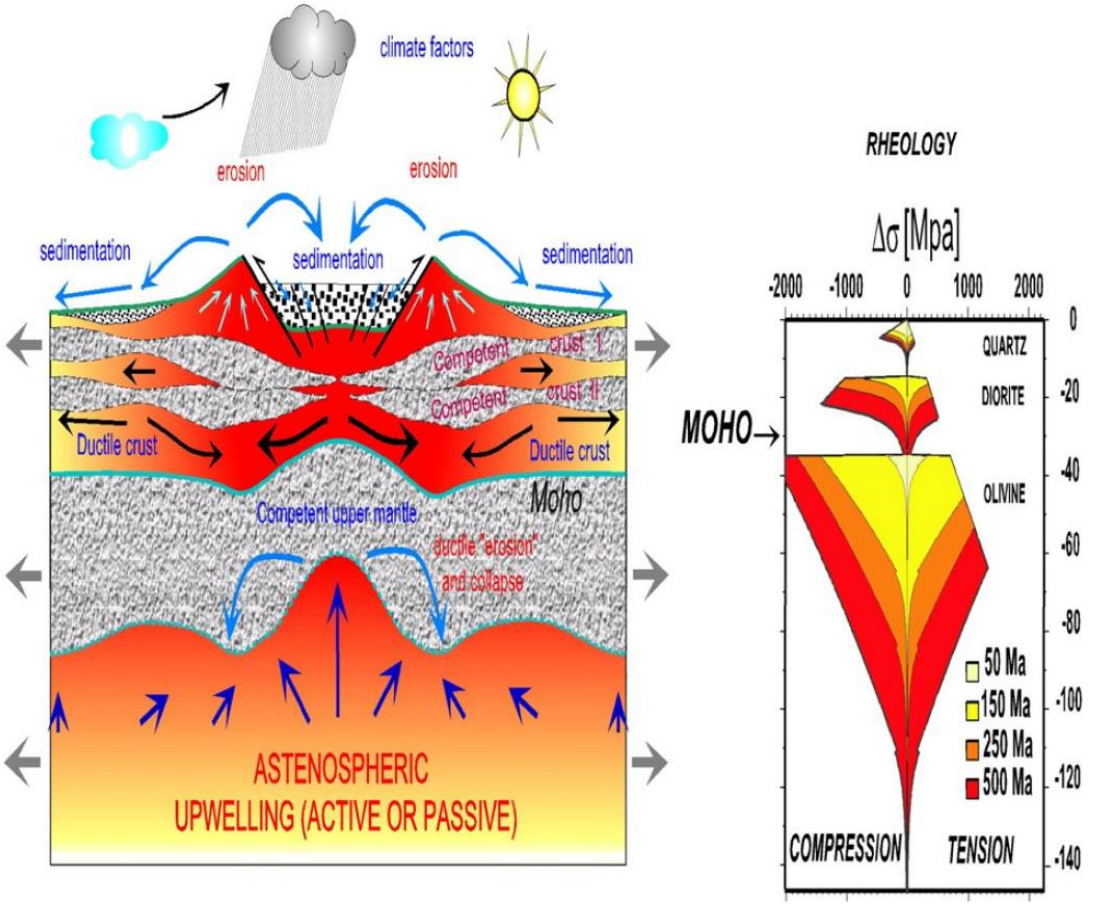

Figure 1.4 The impacts of surface processes, such as deposition of sediment, weather and climate, on the loading of a rifting margin, as per Cloetingh et al. (2013).

a continental margin, the subsequent development of accommodation space (Chenin et al., 2022; McKenzie, 1978) and the sedimentary basin will occur (Frison de Lamotte et al., 2015; Kearey et al., 2009; Khain, 1992; Grasemann & Stuwe, 2011). However, there may be one or several stages of extension which result in the development of a continental margin (Chenin et al., 2022; Péron-Pinvidic & Manatschal, 2010). The impacts of the rifting occur at various spatial locations and extents as the margin develops (Chenin et al., 2022; Nabliboff et al., 2017; Péron-Pinvidic & Manatschal, 2010). These are termed the Proximal, Necking, and Coupled (distal) domains (Figure 1.5; Péron-Pinvidic et al., 2013) or more simply in the older nomenclature the Proximal and Distal domains (Boillot et al., 1979).

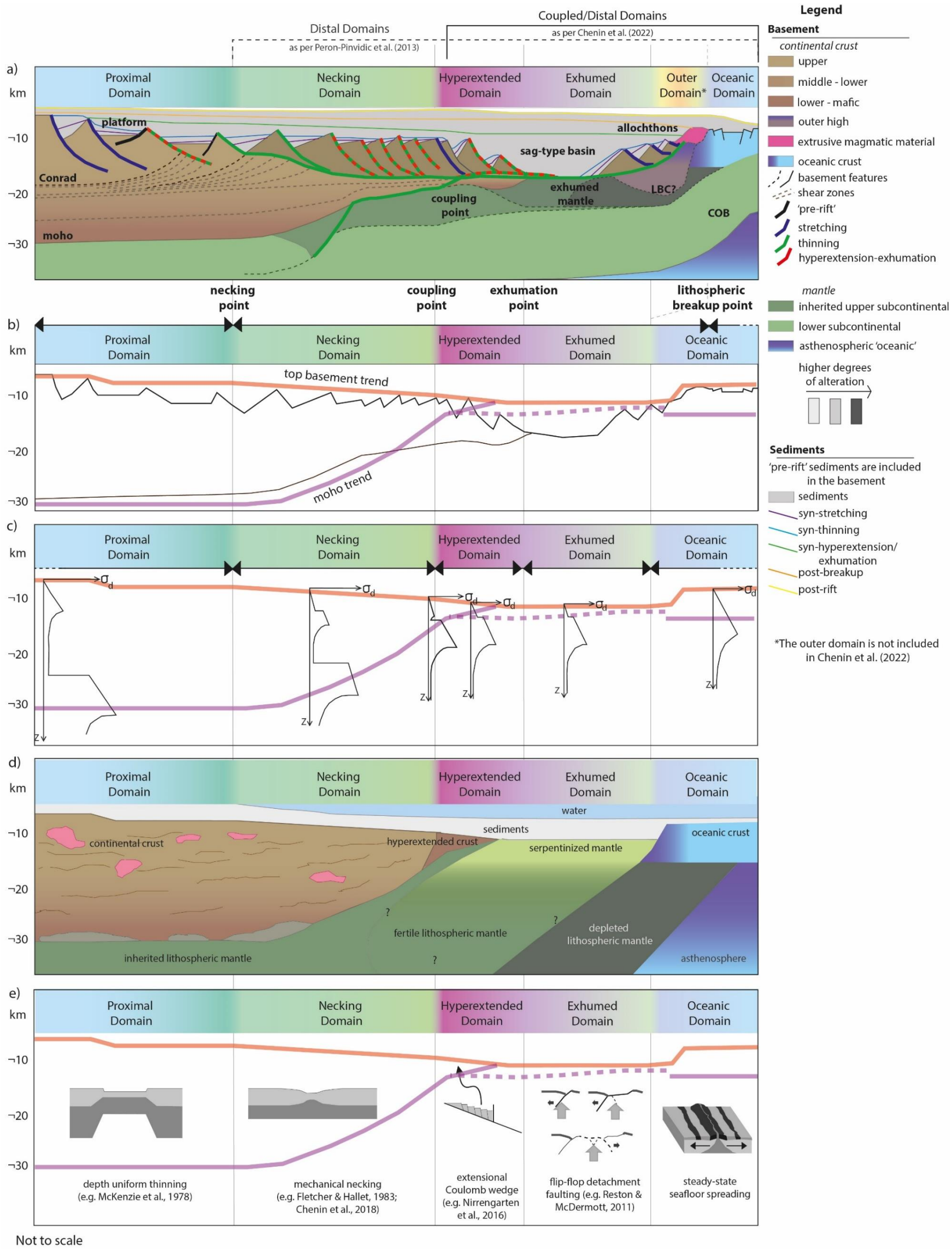

Figure 1.5 Schematics of a typical magma-poor rifted margin, showing a) Schematic section of a typical rifted margin illustrating the various terms used by Chenin et al. (2022) and Péron-Pinvidic et al. (2013), modified from Péron-Pinvidic et al. (2013); b) Schematic cross-section highlighting the primary morphology of magma-poor rifted margins, modified from Chenin et al. (2022); c) Schematic depth-dependent stress profiles (σd: deviatoric stress; z: depth) for the rheological evolution of a typical magma-poor rifted margin, modified from Chenin et al. (2022); d) Schematic cross-section displaying the first-order lithology across a typical magma-poor rifted margin, modified from Chenin et al. (2022); e) Schematic cross-section displaying the dominant deformation mechanism associated with the different rift domains of magma-poor rifted margins, modified from Chenin et al. (2022).

1.1.1.1. DOMAINS AND THEIR PHASES

PROXIMAL DOMAIN AND THE STRETCHING PHASE

The proximal domain sits furthest from the rift axis and is characterised by large high-angle fault blocks forming graben and half-graben architecture (Figure 1.5; Manatschal et al., 2021, 2022; Nabliboff et al., 2017; Péron-Pinvidic et al., 2013). The proximal domain develops during an initial period of lithospheric stretching (the stretching phase, Figure 1.6; Chenin et al., 2022; Manatschal et al., 2021, 2022). This is the onset of mechanically driven lithospheric thinning (Buck, 1986; Cloetingh et al., 2013; Elders et al., Manuscript; Grasemann & Stuwe, 2011; Huismans et al., 2001; Ribeiro, 2002; Richter & McKenzie, 1978; White & McKenzie, 1989a, 1989b; Wilson, 1993) as the initial stage of rift activity (Kearey et al., 2009; Lavier & Manatschal, 2006; Manatschal et al., 2022; Nabliboff et al., 2017). However, crustal thinning is the most limited in this phase and domain (Chenin et al., 2022). The Moho and top basement are sub- horizontal to parallel (Figure 1.6; Chenin et al., 2022; Nabliboff et al., 2017).

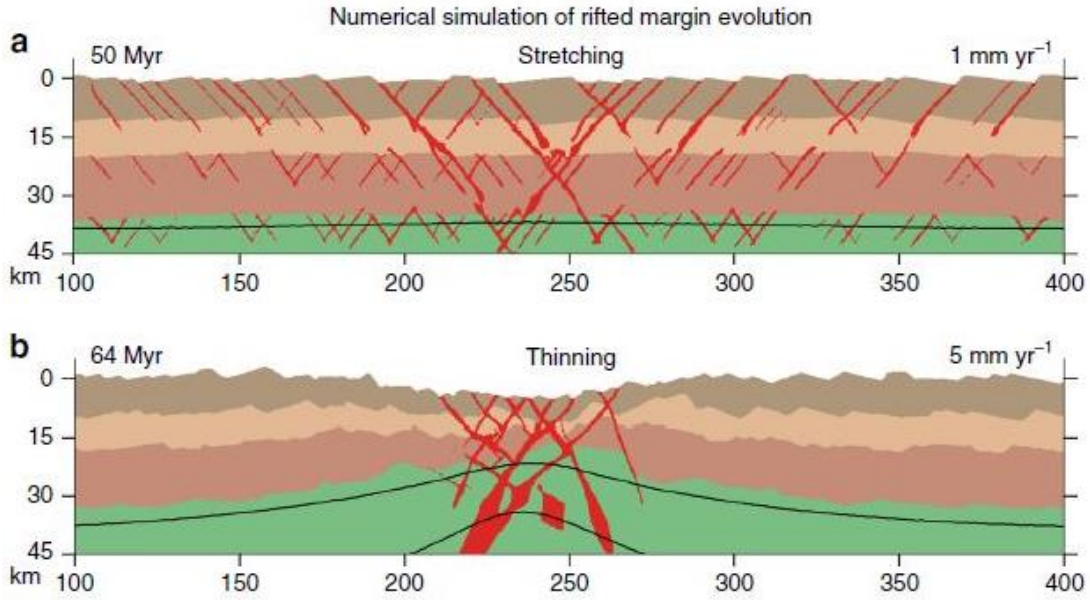

Figure 1.6 Modelled simulation of the a) stretching caused by a 50 Myr slow continental extension at 1mmyr−1 causes; and b) an increase in velocity to 5mmyr−1 progressively localizes deformation towards the model centre in the thinning phase of rifting, modified from Naliboff et al. (2017). Images show a 400 by 45 km subset of the total model domain of 500 by 110 km. Black lines mark temperature contours of 600, 900, and 1200 °C.

The proximal areas have usually experienced the lowest increase in accommodation space in the basin, as a result of rift activity, with faults here most often of low throw and strain (Chenin et al., 2022; Manatschal et al., 2021, 2022), resulting in minimal deformation (Lavier & Manatschal, 2006; Péron-Pinvidic et al., 2013). These faults are seeded in the mid-crustal level, although deeper faults can occur (Péron-Pinvidic et al., 2013). Extension is minimal but broadly distributed during this stage of rifting (Figure 1.6; Elders et al., Manuscript; Lavier & Manatschal, 2006; Manatschal et al., 2021; Nabliboff et al., 2017; Manatschal et al., 2022). Proximal domains of rifted continents display the most similarity to one another across geographic regions (Péron-Pinvidic et al., 2013). Fault activity is limited in the proximal domain following the onset of the successive necking phase, but uplift, subsidence and intrusive activity are ongoing (Péron-Pinvidic et al., 2013).

Necking Domain and Thinning Phase

The area sitting between the proximal and the distal domains (Figure 1.5) as the transition zone from decoupled to coupled lithospheric deformation is known as the necking domain (Péron-Pinvidic et al., 2013). The necking domain forms from the thinning or necking phase (Chenin et al., 2017, 2022; Fletcher & Hallet, 1983; Manatschal et al., 2021; Nabliboff et al., 2017). Thinning occurs at a ratio of approximately 3:1 (i.e., a 30-35 km thick crust will have thinned to about 10 km in a necked domain; Chenin et al., 2022; Mohn et al., 2010; Péron-Pinvidic & Manatschal, 2009; Ribeiro, 2002).

The impact of extension from the prior stretching phase is reduced spatially (Figure 1.6; Chenin et al., 2017, 2022; Fletcher & Hallet, 1983; Manatschal et al., 2021, 2022) but the lithosphere is thinned more dramatically than in the earlier stretching phase (Manatschal et al., 2022; Nabliboff et al., 2017). The necking is primarily controlled by large scale detachment faulting (Figure 1.5; Elders et al., Manuscript; Mohn et al., 2012; Nabliboff et al., 2017; Péron-Pinvidic et al., 2013) and depth (Karner et al., 2004). Faulting continues from the earlier stretching phase, and new faults nucleate at this time (Nabliboff et al., 2017) with the domain considered highly faulted (Péron-Pinvidic et al., 2013). As well as uplift of the more outboard regions, rapid subsidence occurs

due in part to loading and thermal differentiation (Chenin et al., 2018; Manatschal et al., 2021, 2022; McKenzie, 1978) and in part due to the plasticity of the lithosphere in this stage (Chenin et al., 2018, 2022; Péron-Pinvidic et al., 2013).

The syn-rift deposits are often preserved and are more complex than those in the proximal setting, including significant unconformities which document changes to sediment supply (Manatschal et al., 2021). These fill oceanward increasing accommodation space (Péron-Pinvidic et al., 2013). Fundamental similarities across geographical regions are the oceanward decrease in crustal thickness, increase in accommodation space and the convergence of the Moho and basement (Figure 1.5; Péron-Pinvidic et al., 2013).

Coupled Domains and Their Phases

During the earlier phases of rift formation, the crust is considered to be decoupled (Lavier & Manatschal, 2006) and ductile crustal layers are still present (Péron-Pinvidic et al., 2013). There are several expressions of a coupled domain, the hyperextended and exhumed domains of the distal domain region (Figure 1.5), as well as the outer and oceanic domains (Figure1.5), these are described below. The crust in these coupled domains lack ductile properties, which allows for faults to completely penetrate the crust to the mantle (Péron-Pinvidic et al., 2013). Coupling is highly dependent on the composition of the crust and mantle at the location of mantle breakthrough (Franke, 2013; Lavier & Manatschal, 2006).

Distal Domains

In the distal zones, the lower crust is considered to be thin due to rift activity (Franke, 2013). No ductile crustal layers remain in these regions, which permits the propagation and/or initiation of faults from surface to mantle (Péron-Pinvidic et al., 2013; Pinto et al., 2015). This full crustal penetration results in pathways for mantle exhumation (Figure 1.5; Franke, 2013; Lavier & Manatschal, 2006; Manatschal et al., 2022) which occurs in the exhumation domain (Péron-Pinvidic et al., 2013). The hyperextension domain also sits within the distal realm (Péron-Pinvidic et al., 2013). These domains are often

highly variable but fundamentally similar regardless of geography (Péron-Pinvidic et al., 2013).

Basement in these areas is often less than 5km in thickness and is likely highly modified from its original state (Péron-Pinvidic et al., 2013). Magmatic intrusions and extrusions are likely to be most common in these domains, regardless of whether the margin is considered magma-rich or -poor (Péron-Pinvidic et al., 2013). Detachment surfaces and high frequency faulting are commonplace (Péron-Pinvidic et al., 2013). Sag-induced stratal patterns are seen in these areas, along with syn-rift fill (Péron-Pinvidic et al., 2013). More accommodation space tends to be created in the distal domains than in the proximal domains (Péron-Pinvidic et al., 2013).

Hyperextension Domain and Phase

The hyperextended domain (Figure 1.5; formed during the hyperextension phase) is adjacent to the oceanic crust of the older sea-floor spreading zone (exhumation domain; Manatschal et al., 2021). This region contains detachment faults and ample syn-rift deposition (though, not always preserved; Manatschal et al., 2021; Nabliboff et al., 2017). Detachment faulting results in a wedge of sub-crustal material forming adjacent to the oceanic centre (Chenin et al., 2022; Manatschal et al., 2021) as the rift centre migrates oceanward (Elders et al., Manuscript). These detachment faults can penetrate the entire thickness of the crust, driving the mantle upwards (Lavier & Manatschal, 2006; Manatschal et al., 2022; Naliboff et al., 2017). In the hyperextension stage subsidence is controlled by cooling and crustal thinning (limited to the oceanward region; Grasemann & Stuwe, 2011; Manatschal et al., 2021) where the crust may be completely thinned or removed (i.e., exhumation; Chenin et al., 2022). The basement in this region is thin, less than 10 km in thickness (Chenin et al., 2022; Péron-Pinvidic et al., 2013).

Exhumation Domain and Phase

In the exhumation domain (Figure 1.5) the mantle zone is at the surface and the uppermost layers have been serpentinised (Chenin et al., 2022; Lavier & Manatschal, 2006; Manatschal et al., 2021; Péron-Pinvidic et al., 2013). This

occurs only where the rift results in oceanic basin development (Ribeiro, 2002). Exhumation is reliant on the presence of listric faults, though these have little impact on topography due to the upwelling mantle (Lavier & Manatschal, 2006). The rheology of the exhumed mantle varies based on spatial distance from the spreading centre, as does the mass of accumulated magma (Ribeiro, 2002). Sedimentary deposition occurs over these domains but remains limited by comparison to the adjacent rift-basin area (Manatschal et al., 2021). Fault activity continues or reactivates from earlier phases though orientational changes in the stress associated with a developing rift likely results in the rotation, lengthening and flattening of existing faults (Nabliboff et al., 2017). This domain does not always occur at rifted margins (Péron-Pinvidic et al., 2013).

Outer Domains

A key area for identification of a magma-poor or -rich margin, the outer domain is the most variable domain across geographic regions (Péron-Pinvidic et al., 2013). Due to this variability the spatial extent of the outer domain is difficult to define (Péron-Pinvidic et al., 2013). Any remaining basement material has been highly intruded during the final rift episodes during the magmatic phase (Péron-Pinvidic & Manatschal, 2010; Péron-Pinvidic et al., 2013).

Oceanic Domain and Spreading Phase

Where rift processes result in the formation of an ocean basin, an oceanic domain forms (Figure 1.5; Ribeiro, 2002). The exact boundaries of this domain are likely to be obscured (Péron-Pinvidic et al., 2013). It represents the true spreading centre of a sea-floor spreading zone where the mantle is closest to the surface (Manatschal et al., 2021) and formed during the spreading phase (Péron-Pinvidic & Manatschal, 2010; Péron-Pinvidic et al., 2013). This domain is highly reliant on the amount of magma involved in the rift process (Péron-Pinvidic et al., 2013). Fault activity and fluid flow are both highly active and have significant impact on the topography of this zone (Manatschal et al., 2021).

1.1.2. THE FORMATION OF MARGINAL RIFT BASINS

1.1.2.1. THERMAL SUBSIDENCE

Significant subsidence occurs at continental margins during and following rift activity, including in the location of failed rifts (Boillot, 1979) resulting in the development of sedimentary basins (Şengör & Burke, 1978; Khain, 1992; Ziegler, 1992). Kearey et al (2009) furthered this definition by stipulating that a passive margin subsides below sea-level due to isostatic compensation of the thinned continental crust and as heat (originally transferred to the lithosphere from the asthenosphere during rifting) dissipates. Subsidence is understood to be the prominent geodynamic effect leading to the development of accommodation space to form a sedimentary basin on continental margins (Figure 1.7; Boillot, 1979; Kearey et al., 2009; Li et al., 2004; Martins-Neto & Catuneanu, 2010; Ruppel, 1995).

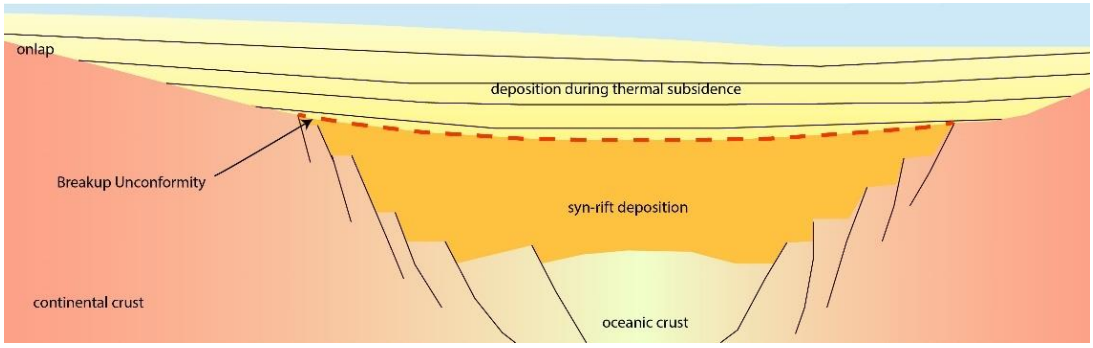

Figure 1.7 Schematic of thermal sag (subsidence) and basin fill following rift activity. Where the subsidence is the product of isostatic readjustment following cooling of the rift forming new accommodation space, based on the works of McKenzie (1978).

Thermal subsidence following rift activity results in the creation of accommodation space (White & McKenzie, 1988). Initially this subsidence is related to the significant amount of thermal energy lost during lithosphere thinning at the start of the rifting process (See Section 1.1.1; Pitman & Andrews, 1985; Sandiford et al., 1998; Sleep 1971; Steckler & Watts 1980; Manatschal et al., 2022). When the crust first rifts, heat floods the region causing thermal uplift (Keen, 1979; Turcotte & Emerman, 1983). The temperature anomalies generated during rifting then cool, resulting in

subsidence (Karner et al., 2004; Keen, 1979; Keen & Boutilier, 1990; McKenzie, 1978; Moore et al., 1986; Pitman & Andrews, 1985; Manatschal et al., 2022) during a protracted period of thermal readjustment (Keen, 1979; McKenzie, 1978; Pitman & Andrews, 1985). Thermally controlled changes in base-level are also interrelated to both magmatic and load induced uplift and subsidence (Cloetingh et al., 2013).

Magmatic underplating results in the isostatic uplift of the area due to thermal thinning (melting) of the crust (Franke, 2013; Ju et al., 2022; Mohr, 1992; Turcotte & Emermann, 1983; Watts & Fairhead, 1997). Once the magmatically uplifted area begins to cool subsidence is induced (Chenin et al., 2022; Ju et al., 2022; Mohr, 1992; Skogseid et al., 2000; Watts & Fairhead, 1997; Zastrozhnov et al., 2020).

The weight of deposited strata can contribute towards subsidence (isostatic), as deposition occurs, the density of the crust is altered (as the density of sediments is higher than that of water) resulting in isostatic sea-level rise (Boillot, 1979; Hu et al., 2001; Li et al., 2004; Martins-Neto & Catuneanu, 2010; Mondy, 2019; Ribeiro, 2002; Rouby et al., 2013). Loading of the depocenter occurs over extended periods of time, reaching “considerable thickness” (Allen & Allen, 2013). When large-scale removal of sediment occurs, isostatic uplift can begin to occur in response to the reduction in load induced flexure (Boillot, 1979; Grasemann & Stuwe, 2011; Martins-Neto & Catuneanu, 2010; Mondy, 2019; Watts, 2001; White & McKenzie, 1988). Changes to the load of the rifted or rifting crust can significantly alter the thermal character of the crust, resulting in thermally driven subsidence and or uplift (Burov & Cloetingh, 1997; Gilchrist & Summerfield, 1994; Kooi & Beaumont, 1994; Sandiford et al., 1998; Van der Beek et al., 1994, 1995; Watts, 1989; Watts et al., 1982; Rouby et al., 2013) and the upwelling of the mantle (Mondy, 2019). Loading of the crust becomes the sole driver of subsidence after post-rift thermal equilibrium is reached (Cloetingh et al., 2013).

Mechanical subsidence (fault activity) can also alter local sea-level and increase or reduce accommodation space (Boillot, 1979; Franke, 2013; Martins-Neto & Catuneanu, 2010; Weissel & Karner, 1989). As tectonic

processes shaped the evolution of the rifted margins, they also impacted on the subtler developments of the local basins through fluctuations in base-level, the expression of which is seen in sediment transport and delivery (Korchinski, 2019; Mondy, 2019; Martins-Neto & Catuneanu, 2010; Mosher & Yanez-Carrizo, 2021; Rouby et al., 2013; Weissel & Karner, 1989; Wopfner, 1994) to accommodate the extension of rift activity.

1.1.2.2. STRENGTH AND INHERITANCE

The thinning of the lithosphere increases the thermal flow and gradient of the thinned area (Hu et al., 2001) feeding back these changes to the other key aspects of rift and basin formation. The thickness of the crust and its thermal state act as a control on the evolution of the initial, and therefor latter, rift phase (Cloetingh et al., 2013; Gillard et al., 2019; Issautier et al., 2020). Of chief importance is the distribution of the stretching phase, which is in turn controlled by the physical and mechanical properties of the lithosphere (Cloetingh et al., 2013; Issautier et al., 2020; Reston & Pérez-Gussinyé, 2007; White & McKenzie, 1988).

The mechanical strength of the lithosphere prior to rift initiation impacts upon the formation of the rift through inherited rock property strength (Figure 1.8; Elders et al., Manuscript; Gillard et al., 2019; Issautier et al., 2020). The initial strength will control the stretching of the lithosphere and resulting key early fault formations (Cloetingh et al., 2013; Elders et al., Manuscript; Gillard et al., 2019; White & McKenzie, 1988) and evolving phases of rift development (Alves et al., 2021; Beaumont & Ings, 2012; Issautier et al., 2020; Naliboff et al., 2017; Sapin et al., 2021; White & McKenzie, 1988). This controls the distribution and intensity of fault activity to stretch the crust (Cloetingh et al., 2013). Rheology of the crustal layers is equally as important to the volume of deformation through crustal structuring and particularly where changes in rheology occur (Figure 1.8; Alves et al., 2021; Reston & Pérez-Gussinyé, 2007; Lavier & Manatschal, 2006).

With limited magmatic input into a rift zone, the thermal gradient is significantly impacted including the initial geotherm (Lavier & Manatschal, 2006), with the

thermal state of the evolving basin controlling subsidence (Pitman & Andrews, 1985). The ability of faults to intersect significant depth allowing for mantle exhumation is thought to be reliant on the original composition of the crust (Gillard et al., 2015, 2019). The presence and amount of magma involved in the rifting of a margin has little influence on the development of the distinct inboard rift domains (Alves et al., 2021; Menzies et al., 2002; Péron-Pinvidic et al., 2013; Sapin et al., 2021; Tugend et al., 2020). However, it will impact on the development and expression of the oceanic and outer domains (Alves et al., 2021; Péron-Pinvidic et al., 2013).

1.1.2.3. RESULTING ARCHITECTURE

The structural expression of rifted margins is controlled by mechanical activity (the processes of rifting, and the resulting fault activity; Beaumont & Ings, 2012; Corti, 2012; Elders et al., Manuscript; Issautier et al., 2020; Manatschal et al., 2022; Naliboff et al., 2017, Sapin et al., 2021), orientation (Brune et al., 2012; Sapin et al., 2021; Zwaan & Schreurs, 2017) and rate of extension (Brune et al., 2014; Naliboff et al., 2017; Tetreault & Buiter, 2018), or by structures of previous rift events (Elders et al., Manuscript; Issautier et al., 2020; Morley et al., 2004).

It is the earliest formed faults in a rifted margin, formed during the initial stretching phase (Figure 1.5 & 1.6) that control the later evolution of the margin, including any mantle exhumation and eventual sea-floor spreading (Nabliboff et al., 2017; White & McKenzie, 1988). These early faults form a series of half-graben, with the key boundary faults of these features then linking, increasing the size of the new basin (Sakai et al., 2013). Fault activity in the later phases of rift development are important for local architecture of the basin segments, forming through linkage, inversion, reactivation and abandonment (Nabliboff et al., 2017; Péron-Pinvidic et al., 2013). It is common for rifted regions to display clusters of multiple fault populations (Bonali et al., 2018, 2019). The geometry of these fault clusters can be related to the crustal structure and composition (Aanyu & Koehn, 2011; Ring, 1994), magnitude of

stress axes (Angelier, 1984; Krantz, 1988; Reches, 1978; Tibaldi, 1989) or volcanic deposits (Tibaldi & Bonali, 2018).

The location of the various domains created by the unique phases of rifting impact on the structural architecture of the resulting basin (Alves et al., 2021; Chenin et al., 2022; Nabliboff et al., 2017; O'Brien et al., 1996). The expression of tectonic activity through fault activity is most concentrated to the necking domain (Figure 1.5; Manatschal et al., 2022; Nabliboff et al., 2017). Indeed, the architecture of a rifted margin can be largely predicted from identification of the rift domains (Chenin et al., 2022; Nabliboff et al., 2017; Péron-Pinvidic et al., 2013) as a type of structural segmentation (Bosworth, 1985; Cartwright, 1987; Chapin et al., 1978; Crossley, 1979; Jackson & McKenzie, 1983; Rosendahl, 1987; Milani & Davison, 1988; Trudgill & Cartwright, 1994).

1.1.3. BASIN DEPOSITS

The accumulation of sedimentary deposits is directly tied to the tectonic evolution of a passive margin. Key evolutionary influences (magmatic, thermal, loading, and others) directly impact on the location, thickness and geometry of depositional packages, and are recorded as sediment accumulation, subsidence and base-level variation (Blaich et al., 2011; Gernigon et al., 2014; Martins-Neto & Catuneanu, 2010; Mondy, 2019; Rouby et al., 2013). Fault activity and subsidence are the primary drivers for the development of accommodation space in rifted margins (Martins-Neto & Catuneanu, 2010). Other prominent factors influencing the sedimentary history of a basin, such as climate, hydrodynamics, and biological actions (Ju et al., 2022) further complicate the record.

The methods of supply to sedimentary basins are considered to be a key control on basin development (Allen, 2008; Helland-Hansen & Martinsen, 1996; Manatschal et al., 2022; Martins-Neto & Catuneanu, 2010; Mondy, 2019; Mosher & Yanez-Carrizo, 2021; Zhao et al., 2021). The accumulation of sedimentary material occurs most prominently within ocean terrains, specifically in continental margins (Cook & Carleton, 2000; Grotzinger & Jordan, 2007). The manner of sediment dispersal at continental margins

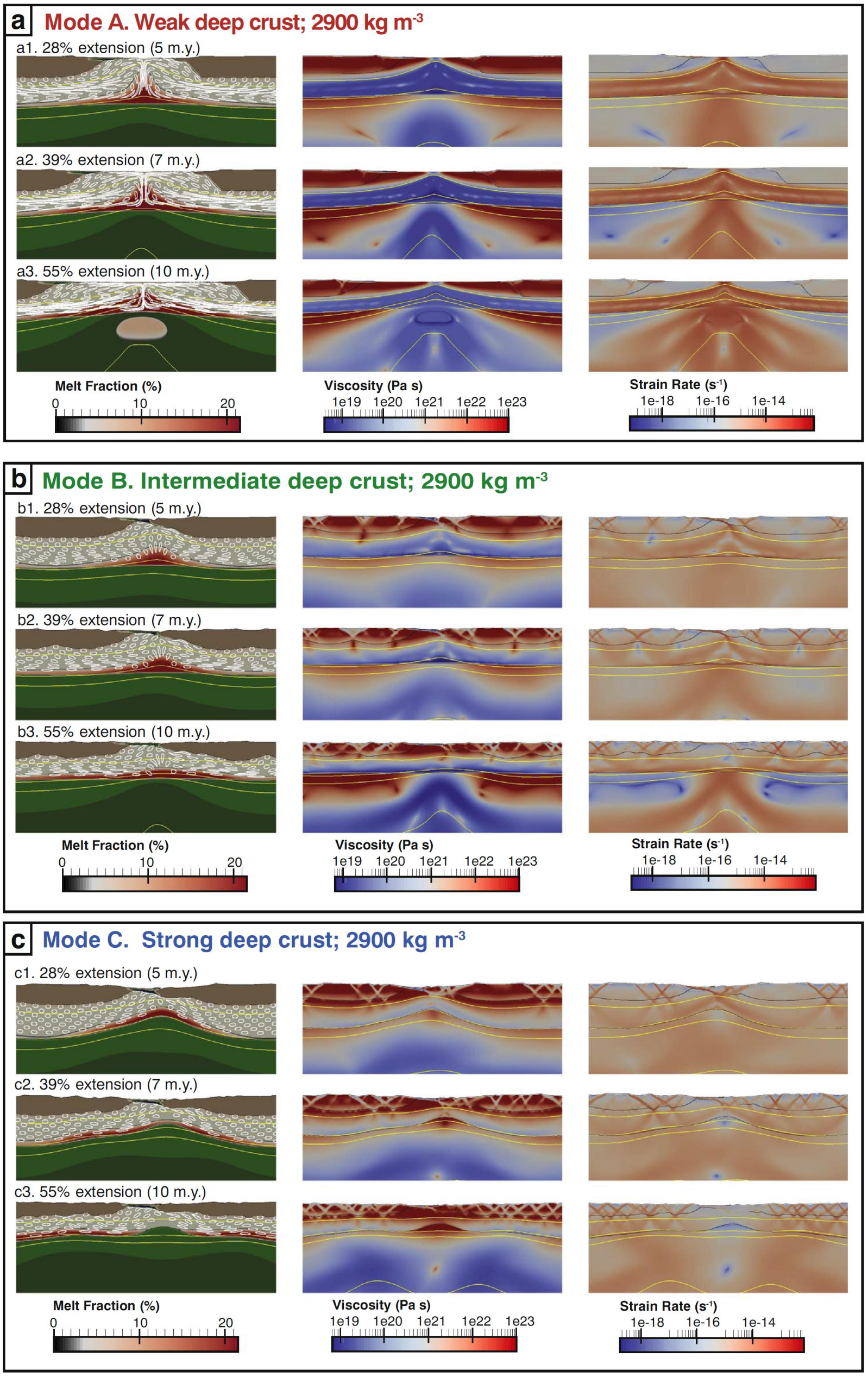

Figure 1.8 Experiment snapshots from numerical modelling showing the results of different crustal strengths on, effective viscosity, and strain rate of Mode A (panel a), Mode B (panel b), and Mode C (panel c) exhumation mechanisms for the fast experiment suite, as per Korchinski et al. (2018).

remains a widely debated and researched topic (Bhattacharya et al., 2016; Boyd et al., 2008; Carvajal & Steel, 2009; Gauchery et al., 2021; Goodwin et al., 2016; Harris, 1988; Pellegrini et al., 2020; Romans et al., 2016; Sømme et al., 2009; 2013a; Weaver et al., 2000; Zhao et al., 2021) of high importance to ongoing exploration activities (Martins-Neto & Catuneanu, 2010; Zhao et al., 2021). Sediment dispersal should be considered when observing the evolution of continental margins as they are complex and often the relation to slope and active tectonics is not clear-cut (Mosher & Yanez-Carrizo, 2021).

As tectonic processes shape the evolution of the rifted margins, they also impact on the subtler developments of local basins through fluctuations in base-level, the expression of which is seen in sediment transport and delivery (Burov & Cloetingh, 1997; Gilchrist & Summerfield, 1994; Korchinski, 2019; Martins-Neto & Catuneanu, 2010; Mondy, 2019; Mosher & Yanez-Carrizo, 2021; Rouby et al., 2013; Van der Beek et al., 1995; Watts, 1989; Watts et al., 1982; Weissel & Karner, 1989; Wopfner, 1994). These dynamics are crucial in the development of lithospheric deformation and basin fill (Ju et al., 2022). The resulting stratigraphic successions are divided into observable breakup packages (Soares et al., 2012; Lei et al., 2019) related to rift phases (pre-, syn- and post-rift; Bastia & Radhakrishna, 2012; Williams 1993). These packages assist in identifying the evolutionary history of a rifted margin (Alves et al., 2021; Morag et al., 2019) which is key to uncovering the origins of present-day deep-water rifted continental margins (Manatschal et al., 2022).

1.1.4. THE ROLE OF OBSERVATIONAL GEOSCIENCE

Observations of historic earth processes are vital to our quest to further understand the manner of continental evolution and breakup. Not all of the geological record has survived to the present, yet many reconstructions of plate tectonics rely on the observations of the geological past (Karner et al., 2004; Manatschal et al., 2022; Wopfner, 1994; Zahirovic et al., 2016) from terrains across the globe. In seeking to understand the way basins formed along rifted margins we also expose key parts of the controlling forces on resource accumulation and development (Alves et a., 2021; Chalmers et al.,

1993; Goldfarb et al., 2014; Grantz & May, 1982; Ju et al., 2022; Plafker, 1987; Zaw et al., 2014; Manatschal et al., 2022), ocean circulation (Gaina & Müller, 2007; Gourlan et al., 2008; Heine et al., 2004; Schiffer et al., 2020), climate, and sea-level (Allen, 2008; Allen & Allen, 2013; Carvajal & Steel, 2009; Herold et al., 2014; Ju et al., 2022; Lee et al., 2013; Müller et al., 2008; Schiffer et al., 2020; Scotese et al., 1999; Spasojevic & Gurnis, 2012; Wang, 2004).

By examining the impact of fault activity and depositional processes we can observe the manner in which the evolution of a basin is impacted by changes in both systems (Naliboff et al., 2017; Zhao et al., 2021; Manatschal et al., 2022). The history of rifted margins is gleaned from the strata deposited during the rift activity (Keen, 1979; Manatschal et al., 2022). However, until recently observations have been largely focussing on the proximal areas of rifted margins which studies show to be highly variable in comparison to the proximal domains, and to other distal domains (Péron-Pinvidic et al., 2013).

Previous work using mega-sequences (Blunes & McClay, 1998; Fontes et al., 2022; Hubbard, 1988; Totterdell et al., 2000), tectono-sedimentary (Chenin et al., 2022; Manatschal et al., 2022) or breakup sequences (Figure 1.9; Soares et al., 2012; Lei et al., 2019; Franke, 2013) to further the understanding of tectonic and deposition history of a geological region have proven useful. Analysis of the geometry of stratal packages in basins to reveal history is a primary analytical tool used in geological reconstruction (Chenin et al., 2022; Roberts & Bally, 2012; Rouby et al., 2013; Alves et al., 2020) where observations can be tied to discrete periods of geological history (Chenin et al., 2022; Manatschal et al., 2022; Roberts & Bally, 2012).

Insights into the state of lithosphere prior to and during rift activity can be gained from observations of the present day. We know that the behaviour of the lithosphere changes across specific domains, due to the phases of rifting (Beaumont & Ings, 2012; Elders et al., Manuscript; Falvey, 1974; Grasemann & Stuwe, 2011; Heezen, 1960; McKenzie, 1978; Naliboff et al., 2017; Sapin et al., 2021) and we can identify these structural changes through investigations. Drilling profiles (Duncan et al., 1996; Eldholm et al., 1989; Larsen et al., 1994; Larsen & Saunders, 1998; Roberts & Schnitker, 1984), seismic imaging (Davis

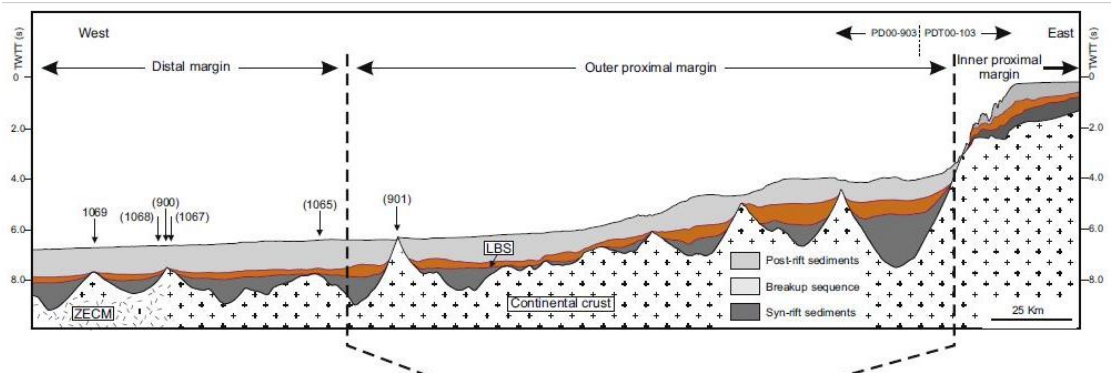

		DISTAL	OUTER PROXIMAL	INNER PROXIMAL	
Seismic Character	Earliest syn-rift	Transparent reflectors onlaping structural highs and LBS	Transparent reflectors onlaping structural highs and LBS	donwlaping (with toplap) reflectors on the LBS	
	Latest post-rift	Chaotic, divergent, strong reflectors	Chaotic, parallel and divergent reflectors	Parallel reflectors	
Depositional environment	Earliest syn-rift	Pelagic deposition below CCD	Pelagic deposition below CCD	Deltaic to fluvial deposition	
	Latest post-rift	Pelagic deposition below CCD	Pelagic deposition below (distally) and above CCD (proximally)	Neritic	
Lithology	Earliest syn-rift	Black shales (in starved depocentres)	Black shales (in balanced depocentres)	Fine to coarse siliciclastics (overfilled depocentres)	
	Latest post-rift	Mass flow deposits (hemipelagic background.)	Mass flow deposits (hemipelagic background)	Marls to fine siliciclastics	
Stratigraphic contact		Diastem?	Diastem/conformable (probable short hiatus or condensed level)	Unconformity (hiatus less expressive basinwards)	Composite subaerial unconformity
Sequence stratigraphic surface		Correlative conformity	Correlative conformity	Erosive basal surface of forced regression	Subaerial unconformity
				OFFSHORE	ONSHORE

Figure 1.9 Example of breakup sequences identified on a continental margin (Iberian margin). Work is an amalgamation of the studies undertaken by Soares et al. (2012) and references therein, as per Soares et al. (2012).

& Kusznir, 2004; Gomez-Romeu et al., 2020; Lymer et al., 2019; McDermott & Reston, 2015; Ranero & Pérez-Gussinyé, 2010; Reston, 2005), gravity, magnetic imaging and other tools help shed light on the development of rifted margins by illuminating the condition of the lithosphere, location of mantle and relevant structuring (Clerc et al., 2018; Gillard et al., 2016; Grasemann & Stuwe, 2011). In cases where rift overprinting occurs the structuring from the earlier rift(s) have some impact on the structural development of the younger rifting (Zastrozhnov et al., 2020).

1.1.4.1. OBSERVATIONS GEOSCIENCE AND MODELLING

Formation of the continents as they are at present remains an active field of study (O'Neill & Zhang, 2019) with much still remaining unresolved

(Manatschal et al., 2022). Models are used to further our understanding of the geological evolution of rifts in the formation of continents and global plate tectonics (Manatschal et al., 2022; Zahirovic et al., 2016). However, models often lack the complexity of real-world histories (Mondy, 2019; O'Neill & Zhang, 2019) and so we must rely our observations to deliver a full history of rifts, and these models rely on detailed observational data to accurately constrain them (Wopfner, 1994; Zahirovic et al., 2016).

Observational data is also vital to the geological discipline of numerical modelling. Many numerical models focused on the key dynamics that result in the final architecture, stratigraphy and structure of the developing rift margin (Manatschal et al., 2015; Moresi & Solomatov, 1998; Naliboff et al., 2017; O'Neill et al., 2007a, b; O'Neill & Lenardic, 2007; Tackley, 2000; Wheeler & Cheadle, 2014; Ziegler, 1996; Ziegler & Cloetingh, 2004). That is, they focus on the magmatic, thermal and rheological composition of the lithosphere (Allen & Allen, 2013; Elders et al., Manuscript; Ju et al., 2015; Korchinski et al., 2021; Miall, 2013; Wheeler & Cheadle, 2014). However, observational data allows us to feed accurate constraints into the modelling process (Chenin et al., 2022; Manatschal et al., 2022).

Observational data of the geometries, spatial location, structures, unconformities, and surface processes of rocks in basins provides us with the key baseline on which we build and constrain our most detailed geological models and reconstructions (Franke, 2013; Grasemann & Stuwe, 2011; O'Neill & Zhang, 2019). The data gathered from observations of rifted margins can aid in reconstruction studies globally, and are not limited to their exact geographic province (Grasemann & Stuwe, 2011). As discussed by O'Neill and Zhang (2019) due to the ever-increasing technology and tomes of dynamic observations, models are, and should be, in a constant cycle of repetition to provide ever greater reconstructions with accurate constraints. These observations should also be validated against global and regional models by (O'Neill & Zhang, 2019).

Continental margins are complex geological features, with many containing important economic resources (Cloetingh et al., 2013; Grasemann & Stuwe,

2011). Sand-rich reservoirs are primarily developed on continental margins (Cook & Carleton, 2000; Grotzinger & Jordan, 2007; Karner et al., 2004). As the world continues to be reliant on fossil fuels, even during the transition to greener energy sources, more hydrocarbon resources are needed to meet demand. Understanding the formation of these hydrocarbon rich areas is vital to the future of the hydrocarbon industry (Karner et al., 2004) and to carbon sequestration efforts.

1.2. This Dissertation

The margin of North Western Australia (also the North West Shelf; Figure 1.10) is still the focus of a number of modelling activities where it has been attempted to address the development of the rifting margin, crustal strength, rift overprinting and tectonic plate reconstruction (Audley-Charles, 1988; l'Anson, 2020; l'Anson et al., 2019; Metcalfe, 1994; 2006; Pigram & Panggabean, 1984; Zahirovic et al., 2016). The North West Shelf (NWS) of Australia (Figure 1.10) sits within the realm of the Gondwanan breakup, the reconstruction of which is still considered unsolved (Müller et al., 1998). The Northern Carnarvon Basin is an important oil and gas province in offshore Western Australia, with many national and international companies continuing to explore for future resources, and search for suitable storage sites for CO_2 for reducing greenhouse gas emissions. Both these factors have resulted in a significant trove of open-source seismic and well data over a largely marine rift system.

The NWS (Figure 1.10) has undergone several episodes of rift activity to result in its current configuration through diverse geodynamic processes. The various rifts impacting this region have resulted from major plate movements (Elders et al., Manuscript). Significant rift events are also observed prior to the early Permian, but are believed to have limited impact on the following events or present structure of the basins (Etheridge & O'Brien, 1994, Longley et al., 2002). The early Permian (or Permo-Carboniferous) extensional rift activities imposed structural controls on the later Mesozoic rift activities through structural inheritance (Elders et al., Manuscript; Etheridge & O'Brien, 1994, Longley et al., 2002). This early rift failed and a period of subsidence gave way

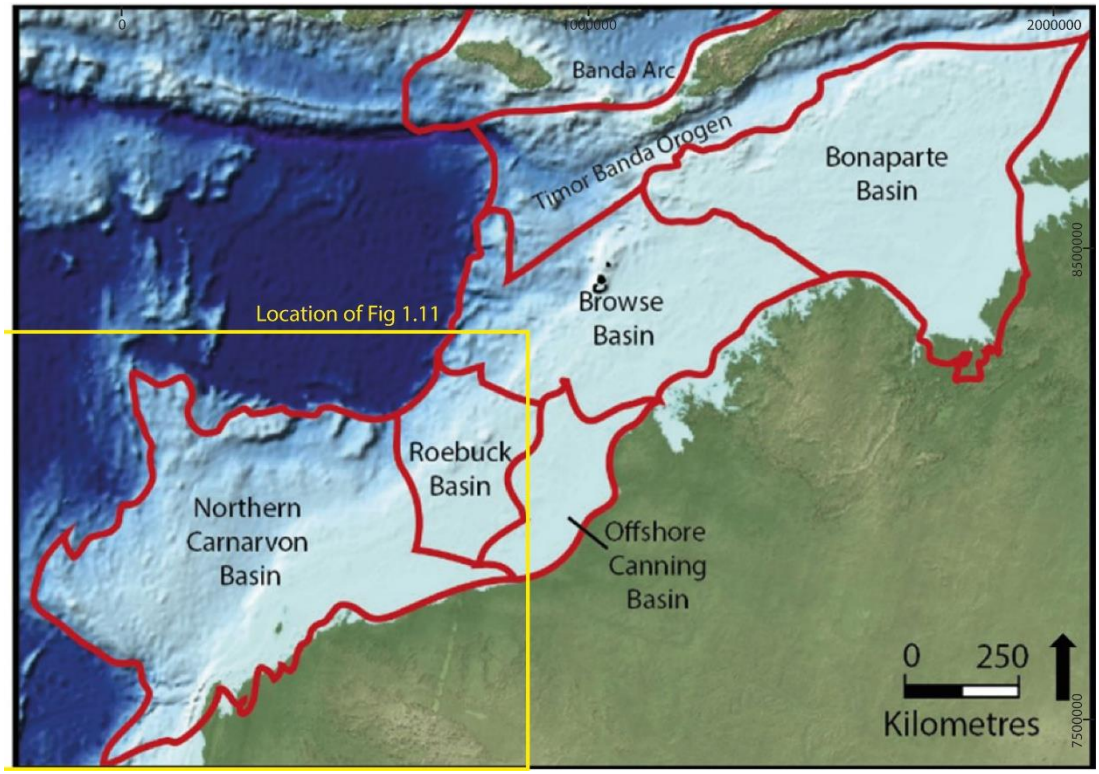

Figure 1.10 The North West Shelf of Australia and the Timor Banda Orogen, modified from Rohead-O'Brien and Elders (2018). The location of the Exmouth Plateau is identified in a sequential Figure (1.11) the location of this figure is indicated here by the square (yellow).

to renewed rifting in the Triassic which stretched into the Jurassic (Bilal & McClay, 2022; Elders et al., Manuscript; Jitmahantakul & McClay, 2013; Marshall & Lang, 2013) as a series of continental ribbons, or blocks, separated from the continent (AGSO North West Shelf Study Group, 1994; Bradshaw et al., 1988; Etheridge & O'Brien, 1994; Longely et al., 2002; Marshall & Lang, 2013; Metcalfe, 1999, 2013; O'Brien et al., 1993; Pryer et al., 2002; Purcell & Purcell, 1988; Stagg et al., 1999; Veevers, 2006). The loci of extension shifted resulting in a secondary Mesozoic rift event, leading to the Lower Cretaceous separation of Australia and Greater India (Elders et al., Manuscript; Gibbons et al., 2013).

The NWS region (Figure 1.10) exhibits different characteristics from other rifted continental margins, with limited necking and outer domains having formed (Elders et al., Manuscript). Complex multi-phase rifted margins are poorly understood (Manatschal et al., 2022). The resulting region has several

similar, yet distinct regions (basins) that can be further segmented by structural formations and/or stratigraphic characteristics (Elders et al., Manuscript).

This study focuses on the Exmouth Plateau (Figure 1.11), which sits at the southern end of the extensive North West Shelf of Australia (Figure 1.10) within the Northern Carnarvon Basin (Figure 1.11). The plateau has been chosen for its ample data availability, importance to the resource industry, and because it is a distal domain, which Manatschal et al. (2022) highlights as being typically understudied. In addition, this margin has undergone multiple rift episodes and is therefore complicated by the inclusion, or reactivation, of older rift structures and tectono-stratigraphic architecture (Chenin et al., 2022), producing unusual stratal geometry. The impacts of multiple stages of rift history, its location between a failed rift (the Barrow-Dampier rift: Hocking, 1987, 1990b; Stagg & Colwell, 1994; Veevers, 1988; Wulff & Barber, 1995) and the successful rift of successive continental fragments (AGSO North West Shelf Study Group,

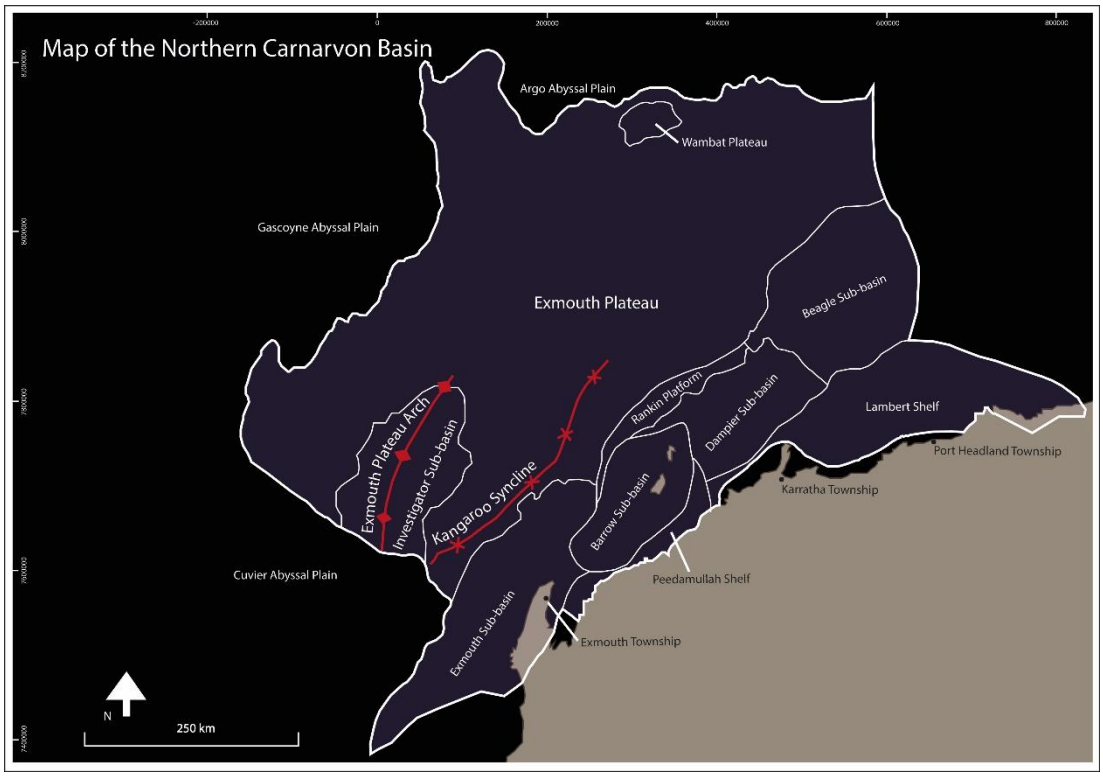

Figure 1.11 The Northern Carnarvon Basin on the northwestern margin of the Australian mainland. The Northern Carnarvon Basin is shown here sub-divided into its main structural sub-basins, and displaying the prominent structural features of the southern Exmouth Plateau Arch and the Kangaroo Syncline. The surrounding abyssal plains, Argo, Cuvier, and Gascoyne are also annotated.

1994; Bradshaw et al., 1988; Etheridge & O'Brien, 1994; Jablonski & Saitta, 2004; Marshall & Lang, 2013; Metcalfe, 1996, 1999, 2013; O'Brien et al., 1993; Pryer et al., 2002, 2014; Stagg et al., 1999; Veevers, 2006) and Greater India (i.e., Gibbons et al., 2012, 2013; Veevers, 2006) pose interesting questions about the formation of marginal rifts and marine rifts. Observation of the rift overprinting, and latter sedimentary responses, is important geological evidence of rift history. The rich depositional history of the plateau (Cathro & Karner, 2006; Felton et al., 1992; Hocking, 1990b; Jablonski, 1997; Jablonski & Saitta, 2004; Marshall & Lang, 2013; Stagg & Colwell, 1994), as well as magmatic interactions (AGSO North West Shelf Study Group, 1994; Chen, 2018; Exon & Buffler, 1992; Gartrell, 2000; Rohrman, 2013, 2015) have resulted in a history of isostatic alteration not well documented at present. In addition, the fault mechanics of the plateau in response to rift stresses have created several key fault orientations over several stages of rift history.

The Exmouth Plateau (Figure 1.11) is a large outboard portion of this rich hydrocarbon province. This study covers approximately 400 km^2 in the southern half of the plateau, where fault blocks form half-graben and graben architecture. The Triassic sequence is several kilometres thick, and relatively uniform in thickness, while the Jurassic and Lower Cretaceous sequences vary from a few metres (where present) to 560 m and 1.2 km's, respectively. The Exmouth Plateau remains somewhat understudied despite its proximity to actively producing hydrocarbon fields and premier exploration acreage. Investigation into the history of the plateau have been minimal to date, with many authors combining the Exmouth Plateau into studies undertaken as part of a broader area of interest, despite its increased size and complexity. Despite this, the outboard area - the Exmouth Plateau, Figure 1.11 - is largely understudied with many investigations mainly focused on the Mesozoic development of the inboard sub-basins.

1.3. Aims and Objectives

The aim of this research is to uncover the timing and distribution of uplift of a rifted continental margin and to relate this to the overall evolution of the rift in

order to better understand the geodynamic processes that have controlled its evolution. A further aim is to investigate the consequent response of sedimentary systems within a marine rift system.

To undertake this task, this study will define a series of mega-sequences which highlight the evolution of this part of the margin. These mega-sequences will then be used to analyse the timing and variability of fault activity during the stages of rift activities. Further analysis of these mega-sequences will uncover the regional uplift and subsidence history, including spatial changes over the evolution of the rift. As the strata records a history of the geodynamic break-up processes, an investigation of the sediment supply pathways in a marine rift system will also be of valuable insight to the history of rifted marine basins.

This research focuses on the outboard Exmouth Plateau (Figure 1.11), a more distal domain of the expansive North West Shelf (Figure 1.10). Investigations utilise seismic and well data to observe and analyse the evolution of the rift system in the area of interest between the Triassic and Cretaceous. The Mesozoic event is readily imaged on seismic data and is the most important event for the generation, migration and storage of accessible and economic hydrocarbons, and thus is the focus of this investigation. Earlier Paleozoic events sit much too deeply for a detailed investigation, with available data.

1.4. Structure of Thesis

This thesis consists of seven chapters, including this introductory chapter which also presents the data and methodology used in the research. Relevant background information is presented as a literature review in chapter 2; including the geological history of the NWS and Northern Carnarvon Basin and the geology of rifted margins.

Chapters 3 to 5 present the observations made during this research and provide some discussion by way of analysis. The third chapter (Tectono-stratigraphic Framework) describes the observed stratigraphic packages (mega-sequences) that aid in the analysis of the Mesozoic rift history. The mega-sequences form an integral portion of this research and are referenced

in the subsequent chapters. The fourth chapter (Structural Architecture of the Exmouth Plateau) details the timing and orientation of Mesozoic faults within the studied area. The fifth chapter (Rift-Related Morphology of the Exmouth Plateau) describes and analyses timing of uplift and subsidence on the Exmouth Plateau.

A detailed discussion of the observations and analysis forms the sixth chapter (Tectono-stratigraphic Evolution of the Exmouth Plateau) and the conclusions are presented in the final chapter, chapter 7. Suggestions for further work are also listed as a part of the conclusions chapter. Following this a full bibliography is provided.

1.4.1. GEOLOGICAL TIME SCALE

For the purposes of consistency all references to geological time used within this dissertation have been calibrated to the International Chronostratigraphic Chart (Version 7.0, 2018; Figure 1.12) from the international Commission on Stratigraphy. This includes all geological ages used from reference material in the introduction, discussion and conclusion sections of this dissertation.

Each geological Period of the Mesozoic is divided into Epochs (Figure 1.12). The Triassic and Jurassic are both divided into three epochs (Figure 1.12), formally termed Upper, Middle and Lower. The Cretaceous is divided into the Upper and Lower (Figure 1.12). Often in literature these terms are switched for informal nomenclature such as early and late. In many cases this follows the work of Haile (1987), but not in all cases. In reviewing Haile (1987) it is observed that no accommodation was made for the use of proper nouns when using the descriptive prefix. Proper nouns should be used as labelled/named for each Epoch in the International Chronostratigraphic Chart (Version 7.0, 2018) provided here as Figure 1.12, and may not always correlate to Haile (1987). Halie (1987) is instead referring to the usage of upper/late, early/lower in terms of the best descriptive manner for referring to geological time in reference to the timing of events (termed by Halie (1987) as geochronological) and describing the age of a formation or seismic reflector (chronostratigraphic), and not related to the use of capitalisation (Table 1.1).

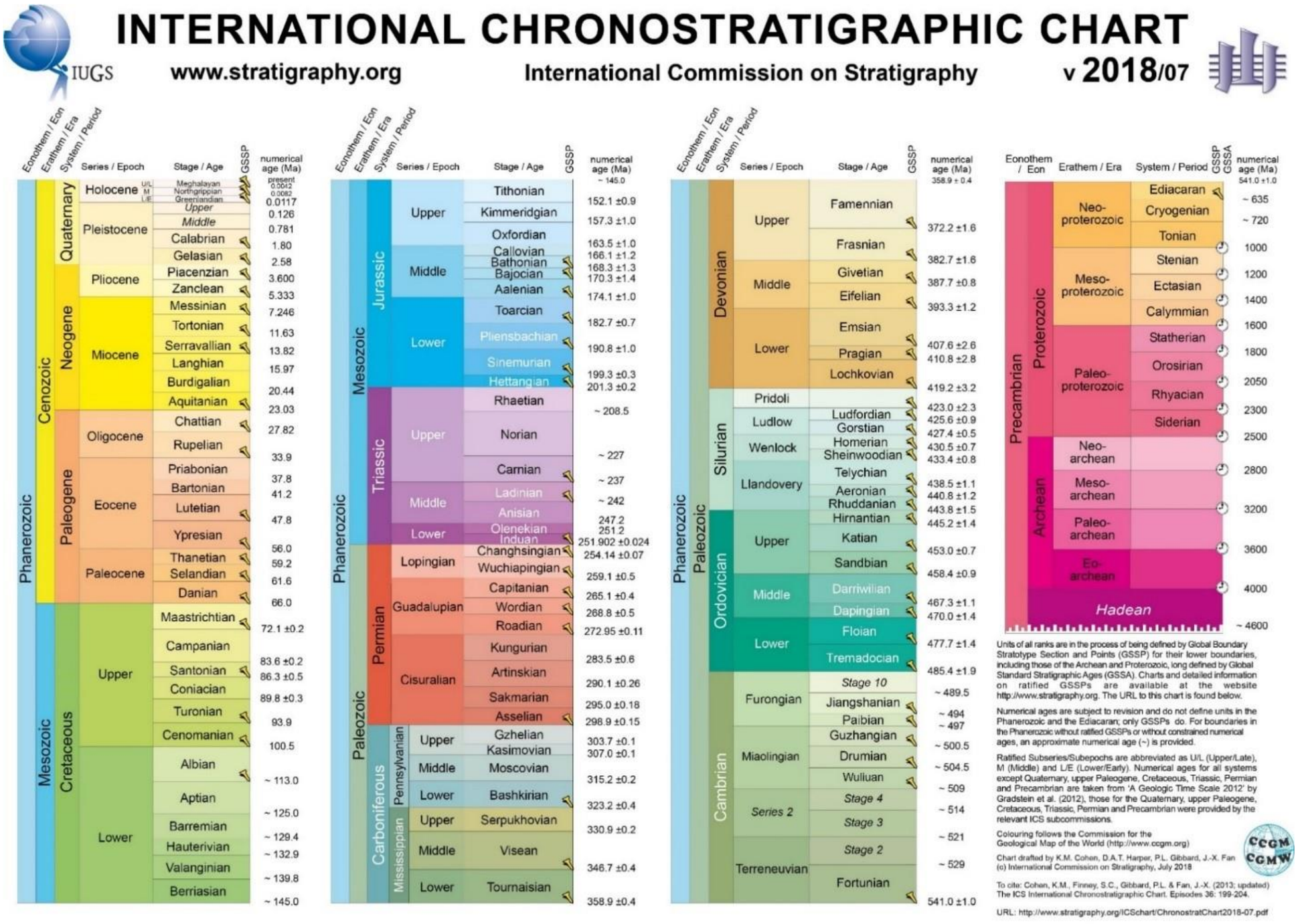

Figure 1.12 The International Chronostratigraphic Chart, Version 7.0 2018 as per Cohen et al. (2013).

Table 1.1 Review of Haile (1987) and the use of proper nouns and capitalisation.

	Correct geochronological an per Halie (1978)*	Correct chronostratigraphic as per Halie (1978)*
Correct use of capitalisation for a proper noun	The rift events continued into the **Upper** Jurassic.	The seismic reflector sits at a depth of approximately -2500 ms (TWT) and has been calculated to be of **late** Jurassic age.
Incorrect use of capitalisation for a proper noun	The rift events continued into the **upper** Jurassic.	The seismic reflector sits at a depth of approximately -2500 ms (TWT) and has been calculated to be of **Late** Jurassic age.
	Incorrect geochronological an per Halie (1978)*	Incorrect chronostratigraphic as per Halie (1978)*
Correct use of capitalisation for a proper noun	The rift events continued into the **late** Jurassic.	The seismic reflector sits at a depth of approximately -2500 ms (TWT) and has been calculated to be of **Upper** Jurassic age.
Incorrect use of capitalisation for a proper noun	The rift events continued into the **Late** Jurassic.	The seismic reflector sits at a depth of approximately -2500 ms (TWT) and has been calculated to be of **upper** Jurassic age.

*Halie (1978) does not cover capitalisation of a proper noun

This dissertation includes both the formal (as named in the International Chronostratigraphic Chart, i.e., Upper Cretaceous) and informal nomenclature (i.e., late Jurassic), where appropriate as per Haile (1987). Only the formal nomenclature has been capitalised, in keeping with the English standards of capitalisation for proper nouns.

1.5. Data

The primary data source for this research is a series of overlapping and adjacent high-quality 3D seismic surveys. These surveys are the Bonaventure, Duyfken, Glencoe, Honeycomb, Io-Jansz, Mary-Rose Northern Extension, Scarborough, Thebe, and Willem-Pluto seismic surveys (Figure 1.13). The location of these surveys is just south of the centre of the Exmouth Plateau, covering a portion of the Investigator Sub-basin and stretching east towards the inboard margin of the plateau and the Rankin Platform.

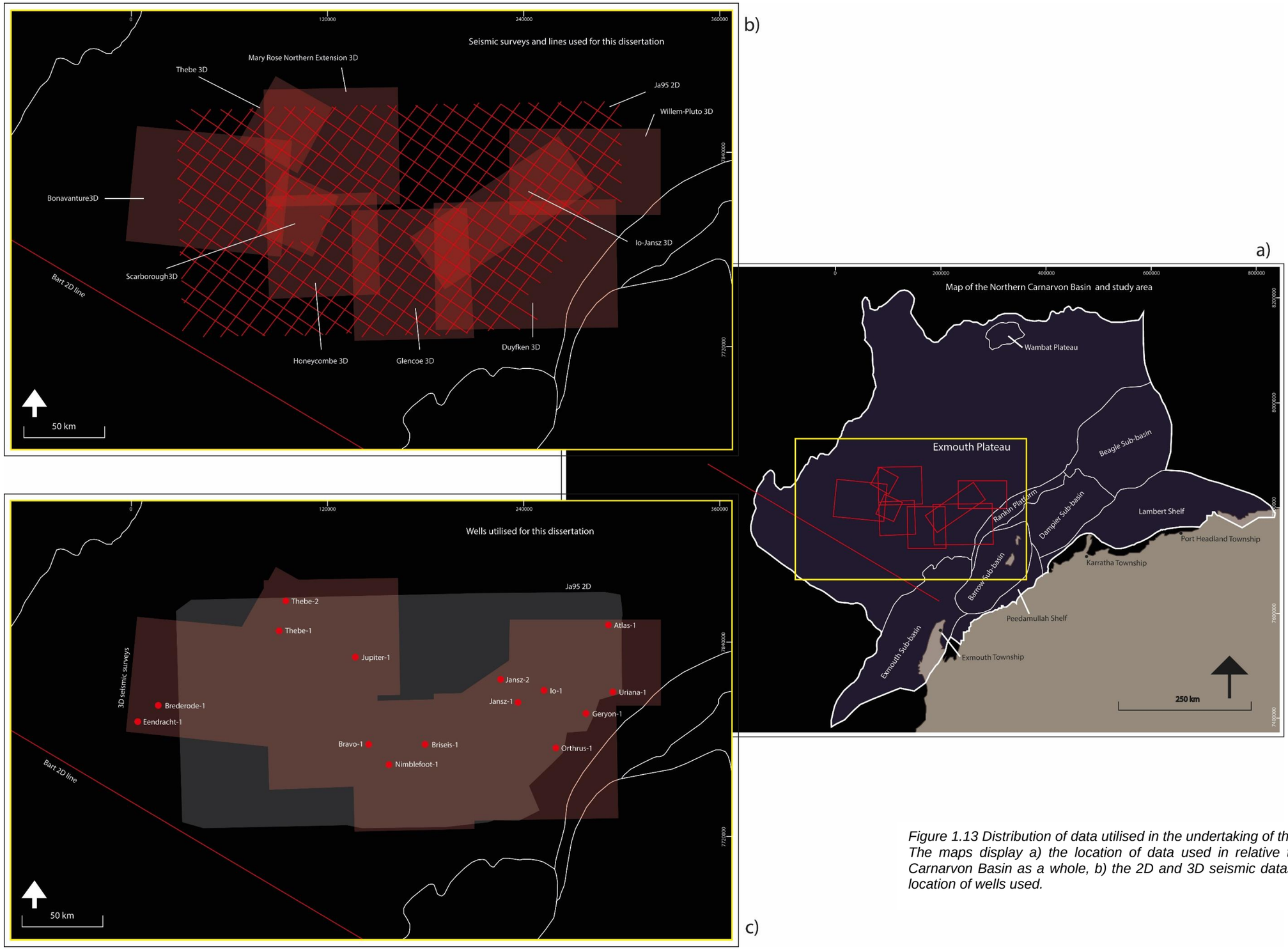

Figure 1.13 Distribution of data utilised in the undertaking of this body of work. The maps display a) the location of data used in relative to the Northern Carnarvon Basin as a whole, b) the 2D and 3D seismic datasets, and c) the location of wells used.

Additionally, two 2D surveys (Figure 1.13) were also utilised to fill gaps between the 3D seismic surveys and to provide more regional context. The details of the seismic surveys used for this study are listed in Tables 1.2 and 1.3. The majority of these surveys are available in the public domain; however, industry service company TGS provided the Honeycomb and Mary-Rose Northern Extension surveys. All the seismic surveys are provided and interpreted in the time domain.

Table 1.2 Details of the 3D seismic surveys used for interpretation of the Exmouth Plateaus' rift history.

Survey	Area (km^2)	Record Length (ms)	Inline Spacing (m)	Crossline Spacing (m)
Bonaventure	4131.50	7200	18.75	12.50
Duyfken	1941.00	6000	18.75	12.50
Glencoe	3968.70	8100	25.00	25.00
Honeycomb	3448.14	6088	18.75	25.00
Io-Jansz	2777.46	6144	18.75	12.50
Mary-Rose Northern Extension	2687.50	6200	18.75	25.00
Scarborough	900.00	6000	18.75	12.50
Thebe	1197.98	4600	20.00	12.50
Willem-Pluto	2734.56	6000	25.00	12.50

A series of wells were used to tie the seismic data to the stratigraphy. There are many wells over the area, but only 16 wells (Table 1.4 & Figure 1.13) had the required velocity information which allowed for the seismic tie, and stratigraphic information. The stratigraphic information was provided in well completion reports as either the top of a specified geological Stage or the top of a geological formation intersected by a well. In many cases this information was not available for wells within the area of interest or the well was not yet available in the public domain. The depths of the 16 wells used is highly

variable, as some wells do not penetrate deeper than the early Cretaceous or the Middle Jurassic (Table 1.4).

Table 1.3 Details of 2D seismic surveys on the Exmouth Plateau, used for the completion of this research.

Survey	Area (km^2)	Record Length (ms)	Inline Spacing (m)	Crossline Spacing (m)	Number of lines
Ja95	36170.47	7000	75-85	75-85	66
*Bart	*	18432	-	-	*1

**Of the Nemo_Bart 2D survey, only a single line, the Bart 2D OBS depth, was used to provide geological observations at depths greater than those imaged in other seismic data, and to provide a regional context to work undertaken in this study. The length of the single line is 280 km.*

Table 1.4 Wells within the study area which were utilised for this research.

Well Name	Latitude	Longitude	TVDSS (m)	Formation at TD
Atlas-1	-19.427836	115.022912	4181.76	Mungaroo Formation
Bravo-1	-20.064375	113.599837	2706.00	Mungaroo Formation
Bredoerode-1	-19.818856	112.370821	2749.82	Barrow Group
Briseis-1	-20.073959	113.93314	3525.30	Mungaroo Formation
Eendracht-1	-19.906758	112.244464	3399.51	Mungaroo Formation
Geryon-1	-19.920351	114.883838	3514.88	Mungaroo Formation
Io-1	-19.785538	114.637504	2972.28	Athol Formation
Jansz-1	-19.847561	114.483313	2955.80	Athol Formation
Jansz-2	-19.718616	114.382053	3226.46	Mungaroo Formation
Jupiter-1	-19.580202	113.534215	4936.50	Mungaroo Formation
Nimblefoot-1	-20.181142	113.716938	4161.67	Mungaroo Formation
Orthus-1	-20.108688	114.700493	3388.55	Mungaroo Formation
Scarbourogh-1	-19.883859	113.147036	2360.00	Barrow Group
Thebe-1	-19.423469	113.088733	2487.70	Mungaroo Formation
Thebe-2	-19.260049	113.131273	2527.70	Mungaroo Formation
Urania-1	-19.800145	115.044164	3979.32	Mungaroo Formation

1.6. Methodology

1.6.1. SEISMIC INTERPRETATION

The interpretation of critical Mesozoic horizons is based on the recognition of seismically visible tectono-stratigraphic relationships tied to well data. Where changes in the tectonic environment or depositional processes form geological basins, this is reflected in the subsurface structure. The interpretation of mega-sequences highlights a group of seismically similar packages, spanning a period of time between two regional unconformity events (Roberts & Bally, 2012). In this case, broad mega-sequence horizons were interpreted over the entire area of interest. In some cases, these mega-sequences displayed significant internal variations and additional sub-divisions were interpreted where variations in tectonic or depositional behaviour were observed. These sub-divisions can be large, spanning several seismic surveys or small, spanning part of a single survey.

Interpretation was carried out using Petrel software. When interpreting the 3D seismic surveys the 3D seismic interpretation tool was used. Occasional use of the manual interpretation tool was necessary where reflectors became chaotic and the 3D interpretation tool could not adequately interpret the selected reflector. Surfaces were then generated using the same spacing as the surveys to preserve detail. The separate 3D grids were then merged together. Further 2D interpretation utilised the 2D seeded auto-tracking and manual interpretation tools. The largest faults sitting outside of any 3D surveys where then interpreted. A fault map was created from the original horizon interpretation and the faults, forming grids. Data from these 2D was then eliminated within the overlapping 3D survey areas, and where necessary polygons were used to remove areas of excessive interpolation, substantial fault throw and/or heave, non-deposition and erosion. These 2D grids were then merged with the 3D grids. These grids are then used to create detailed thickness maps. Thickness maps were created using surface operation tools within Petrel.

1.6.2. GEOLOGICAL INTERPRETATION

The patterns observed within the created surface, thickness maps and seismic cross-sections were used to describe the formation of faults, the timing of fault activity and the response of depositional processes. Direct observations from seismic data aided in the description of specific features and formations during specified time periods to create the Exmouth Plateau mega-sequences.

These mega-sequences were then used to describe the different phases in the evolution of the rift system in the Exmouth Plateau. Fault activity was analysed through thickness changes, onlap patterns and stratigraphic relationships surrounding faults; sedimentary fill was investigated using observed differences between thickness maps and on seismic cross-sections. The analysis and formation of mega-sequences enables a breakdown of the individual phases of basin development, specific to the Exmouth Plateau. The use of mega-sequences allows for the appropriate resolution of interpretation required for the broadness of the plateau, catering for changes over the region, and for more localised changes. The mega-sequences can be further divided in successive investigations and extended further over the plateau.

A description of these mega-sequences is provided in Chapter 3.

1.6.3. DEPTH CONVERSIONS

With most of the seismic data provided in the time domain, it is necessary to convert the seismic travel times to depth to aid in the description of subsurface features and remove distortions such as variations in water depth. This relies on the checkshot and velocity information provided with the wells. Using the information from the suitable wells, velocity information is used to convert the time-based depth domain into a meters-based depth domain. This is done in one of two ways;

1. When describing a feature in close proximity to a single well, an average velocity was derived from the velocity information obtained from the well completion reports (WCR's), for the appropriate time/depth. The equation

is provided below (Equation 1.1) in its original form, and the modified form used in this study.

2. When describing a broader scale feature, or a series of features which occur across a large area, the average interval velocity was used to calculate the depth of the feature(s). This was calculated from the seabed to the top of the Mungaroo Formation. There are ten wells within the study area that intersect the Mungaroo Formation. The average interval velocity between the seabed and the top of the Mungaroo Formation was calculated for all ten wells (Equation 1.2) by first calculating the interval velocity of each well and calculating the average of those values.

Equation 1.1 The calculation of depth in meters from depth in time using the velocity data provided in well completion reports.

$V = \frac{d}{t}$	$d = t \times V$
The original equation used to determine the velocity of a subsurface feature.	The converted equation used in this calculation the determine the depth in meters of a feature in the subsurface.

V *is the velocity, or interval velocity*
d *is the depth in meters*
t *is he depth in time*

1.6.4. FAULT ORIENTATIONS AND ROSE DIAGRAMS

Fault orientation was measured by averaging the orientation of the fault over the length of the faults through measurement of the orientation of a line joining fault tips. Faults were counted and catalogued manually by the candidate and then graphed in Adobe Illustrator, the most efficient method given the software available for use. The fault data was catalogued by main orientation/strike of the fault, per mega-sequence and timing of activity relevant to the pattern of deposition associated with the fault and mega-sequence. The strike of faults

was catalogued in 10-degree increments – i.e., all faults striking between 1º and 10º fall into the 10º cluster – based on number of faults identified as striking in that orientation. Faults was then classified as either active during deposition or post-depositional or remnant. This data was then plotted graphically onto a rose diagram in the common manner used for geological data in literature. That is, the strike of the faults (in 10º cluster) was plotted radially along the degrees of the rose circle, and the count of faults was plotted on the 'ladders' originating from the rose circle centre (count of 0) to the outer ring (count of 100 or another amount as supplied in each rose diagram).

Equation 1.2 The equation used when converting depth in time to depth in meters over large expanses of the study area, relying on all available well information.

Step 1 $(t_1 - t_2) \div (d_1 - d_2)$ The equation used to calculate the interval velocity.	t_1 *is the depth in time at the seabed* t_2 *is the depth in time at the top of the Mungaroo Fm* d_1 *is the depth in meters at the seabed* d_2 *is the depth in meters at the top of the Mungaroo Fm*

2. Regional And Background Geology

2.1. The North West Shelf

The northwestern margin of Australia has a geologically complex polyphase rift-drift history relating to the separation of several continental blocks from the Australian continent (Figures 2.1, 2.2, & 2.3; AGSO North West Shelf Study Group, 1994; Anfiloff, 1988; Bradshaw et al., 1988; Etheridge & O'Brien, 1994; Longely et al., 2002; Marshall & Lang, 2013; Metcalfe, 1999, 2013; O'Brien et al., 1993; Pryer et al., 2002; Purcell & Purcell, 1988; Stagg et al., 1999; Veevers, 2006). Like other divergent passive margins of Australia, the region evolved from breakup of the supercontinent Gondwana (Figure 2.4; Falvey & Mutter, 1981; Gartrell, 2000; Longley et al., 2002; Marshall & Lang, 2013; Purcell & Purcell, 1988; Veevers, 1988). The breakup occurred over several phases of extension (Gartrell, 2000; Stagg et al., 1999; Veevers, 1988). Rifting of the area began in the Permo-Carboniferous and continued to the Lower Cretaceous (Figures 2.1, 2.2, & 2.3; Stagg et al., 1999). Before the development of the modern margin, the earlier geological province experienced growth-fault-controlled subsidence and volcanic extrusions (Playford et al., 1976; Yeates et al., 1987). The geological province was periodically connected to the Tethys oceans and straddled the separating plates of Gondwana (Yeates et al., 1987).

Australia's northwestern continental margin is a rich hydrocarbon province (Geoscience Australia, 2014a, 2019), currently referred to as the North West Shelf (hereafter abbreviated to NWS; Geoscience Australia, 2014a, 2019). The NWS is a marginal rift system infilled with Permo-Triassic intracratonic sediments and overlain by the younger Mesozoic to Cenozoic syn-rift and post-rift successions (Longley et al., 2002). There are four sedimentary basins (Figure 1.10), the Northern Carnarvon, Roebuck (Offshore Canning), Browse and Bonaparte basins and an orogenic belt, the Timor-Banda Orogen (Geoscience Australia, 2014a; Longley et al., 2002; Marshall & Lang, 2013; Purcell & Purcell, 1988; Stagg et al., 1999).

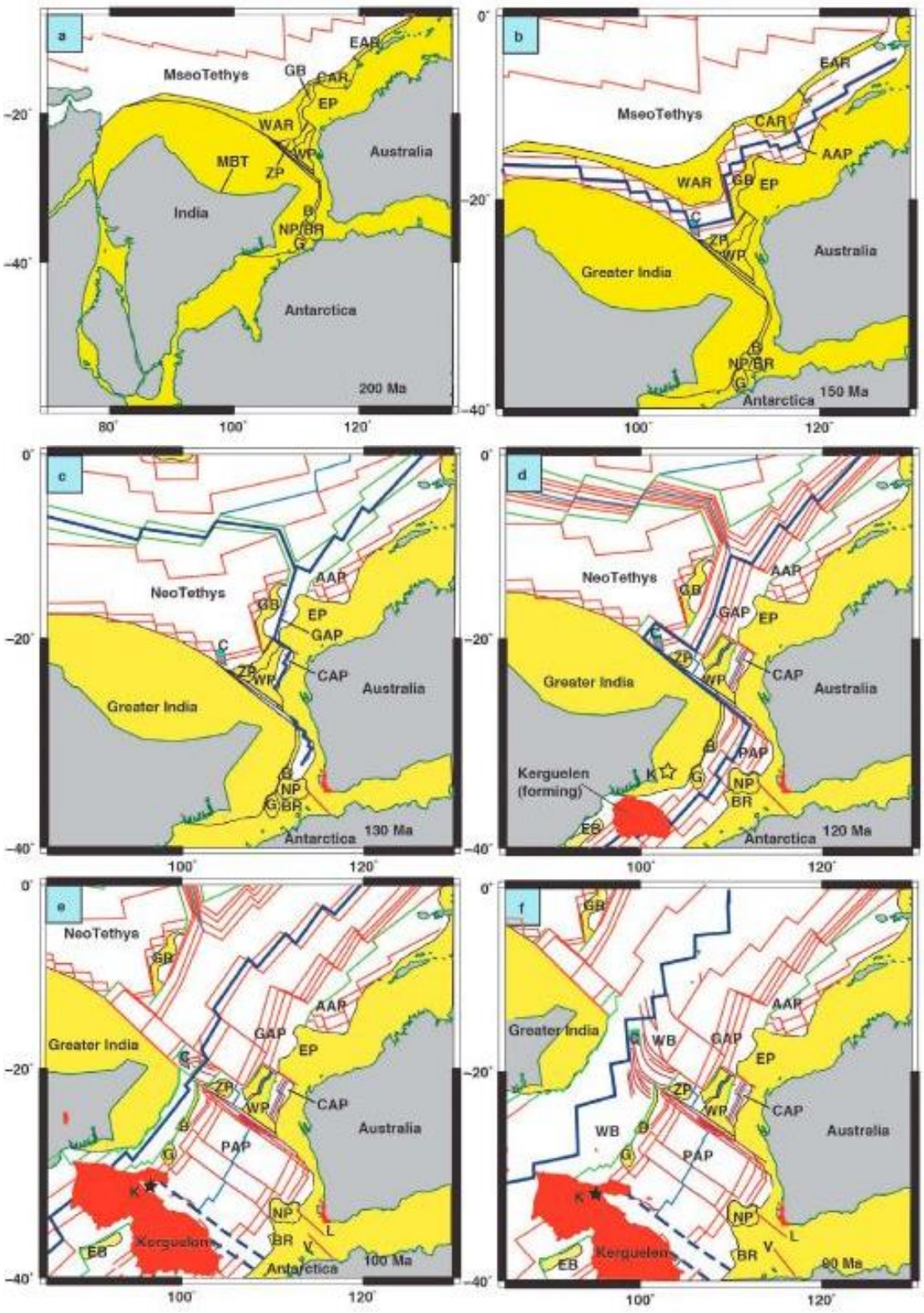

Figure 2.1 Continental breakup history of the Western Australian margin, as per Gibbons et al. (2012).

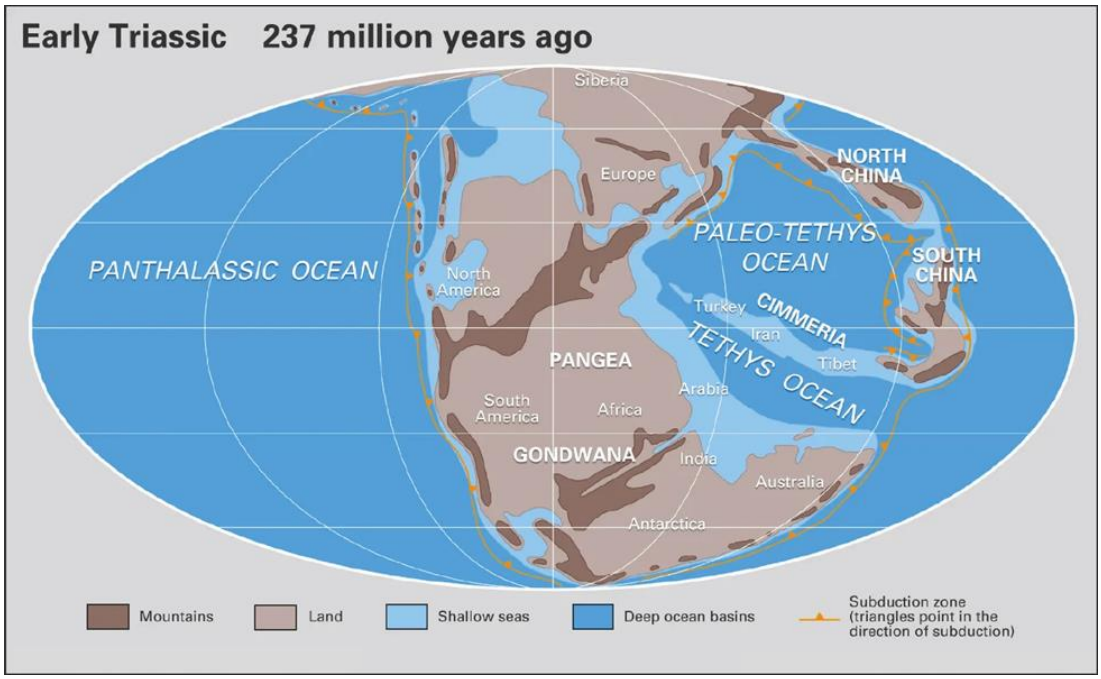

Figure 2.2 The Pangean Supercontinent, as per Scotese (2001).

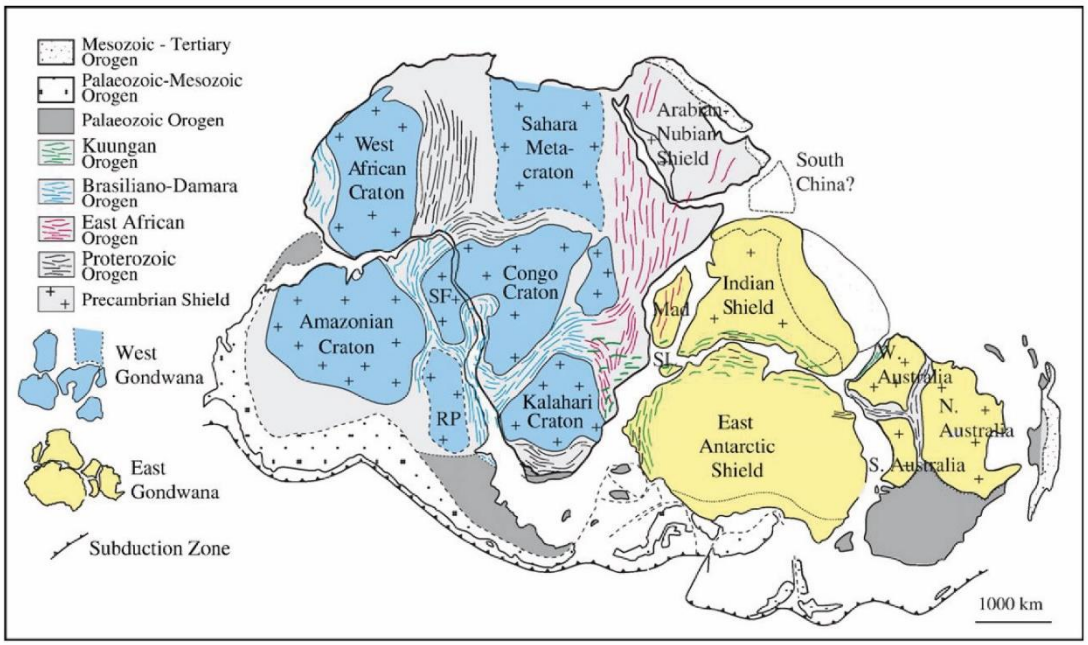

Figure 2.3 Gondwana supercontinent displaying the east (yellow) and west (blue) as the later division of cratons, blocks and shields and orogens. MB: Mozambique Belt, RP: Rio de la Plata Craton, TC: Tanzanian Craton, as per Meert and Lieberman (2008).

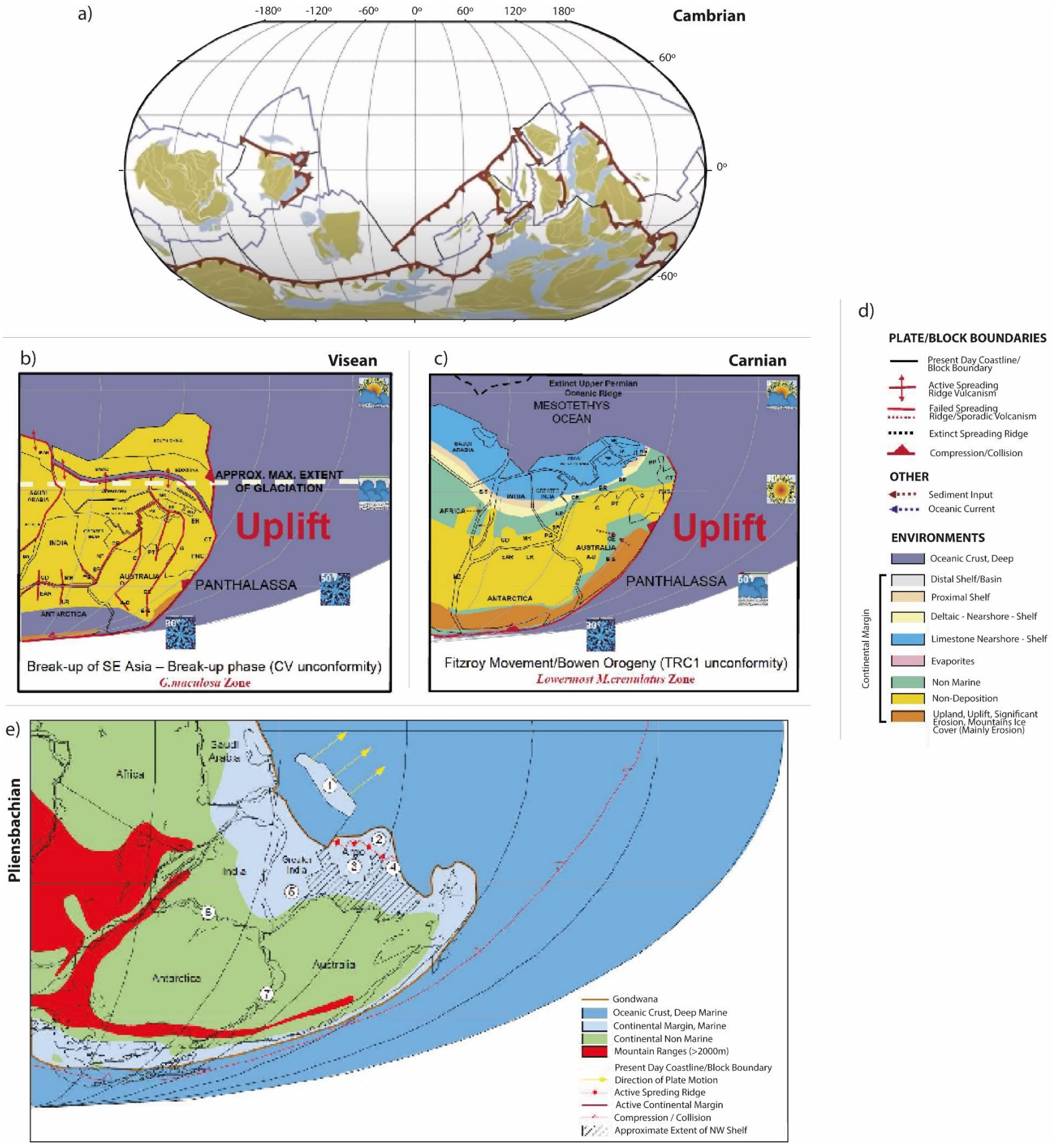

Figure 2.4 The formation of the northwestern margin of Western Australia over time in relation to global tectonics. The early state of the region in a) the Cambrian Earth, modified from Merdith et al. (2020); b) the Early Carboniferous (Visean), modified from Jablonski and Saitta, (2004); c) the early Upper Triassic (Carnian), modified from Jablonski and Saitta, (2004); d) the legend for images b) and c); and e) the mid-Lower Jurassic (Pilensbachian), modified from Longely et al. (2002).

1 – Lhasa Block, 2 – West Burma I Block, 3 – West Burma II Block, 4 – West Burma III Block, 5 – India Separation, 6 – India-Antarctica Separation, 7 – Antarctica Separation, A – Arkaringa Basin, AP – Ashmore Platform, B – Bowen Basin, BP – Bonaparte Basin, BR – Browse Basin, B-D – Barrow-Dampier Failed Rift, BH – Birdís Head (Irian Jaya), C – Canning Basin, CE – Cooper-Eromanga Basin, CR – Carnarvon Basin, CT – Central Ranges (Irian Jaya), D - Denman Basin, EAR – East Antarctic Rift, G – Goulburn Graben, GD – GodavarI Basin (India), H-V – Heywood-Vulcan Failed Rift, L – Lamu Basin (Kenya), LR – Lambert Rift (Antarctica), M – Malita Failed Rift, MG – Madagascar, RMR – Mahanadi Rift, MZ – Mozambique, NP – Northern Perth Basin, P – Perth Basin, PM – Paternoster-Meratus, PG – Panagarh Area (India), PNG – Papua New Guinea, PT – Petrel sub-basin, R – Roebuck Basin, S – Sydney Basin, SH – Sahul Platform, SK – Sikuleh (Western Sumatra), SP – Southern Perth Basin, T – Timor, WB – West Burma, WS – West Sulawesi.

The dominant structural grain in northern Australia is a northwest-southeast trend (Etheridge & O'Brien, 1994). Etheridge and Wall (1994) interpreted this as the extensional grain of the underlying rift basin system formed in the Paleoproterozoic. O'Brien et al. (1993) and Etheridge and O'Brien (1994) describe the early north to south trending Precambrian and early Paleozoic structures as important in controlling the distribution of later basins. This control would occur through the mechanical inheritance of the rifted zones (Section 1.1.2. The Formation of Marginal Rift Basins; Elders et al., Manuscript; Issautier et al., 2020; Morley et al., 2004), where the earliest developed faults continue to impact the evolution of a rift throughout its maturation (Nabliboff et al., 2017; Péron-Pinvidic et al., 2013; White & McKenzie, 1988). The Northern Carnarvon and Bonaparte basins display this Precambrian trend (Etheridge & O'Brien, 1994; O'Brien et al., 1993). The older structures remain unimaged due to constraints on current investigative techniques and are invoked to explain what is observed in the younger sections of the basins.

2.2. The Northern Carnarvon Basin

The Northern Carnarvon Basin sits mostly offshore, on Australia's northwestern continental shelf (Geoscience Australia, 2019). The basin extends for 500 km across the northwest Australian coast (Geoscience Australia, 2019), sitting at the southern end of the NWS (Gartrell, 2000; Geoscience Australia, 2014a; Longley et al., 2002; Marshall & Lang, 2013). In the north, the Jurassic Argo Abyssal Plain bounds the basin along the Exmouth Plateau, while to the northwest and southwest, the Cretaceous Gascoyne and Cuvier abyssal plains bound the southern portion of the Exmouth Plateau and the Exmouth Sub-basin (Figures 1.11, & 2.5; Stagg & Colwell, 1994; Stagg et al., 1999; Yeates et al., 1987). The Pilbara Craton is the prominent basin bounding feature in the east, while the northeast transitions into the Roebuck Basin (Figures 1.11, & 2.5). The Northern Carnarvon Basin is separated from its southern counterpart by a hinge zone. This structural hinge zone formed in either the Jurassic (Condon, 1967b) or Cretaceous (Yeates et al., 1987),

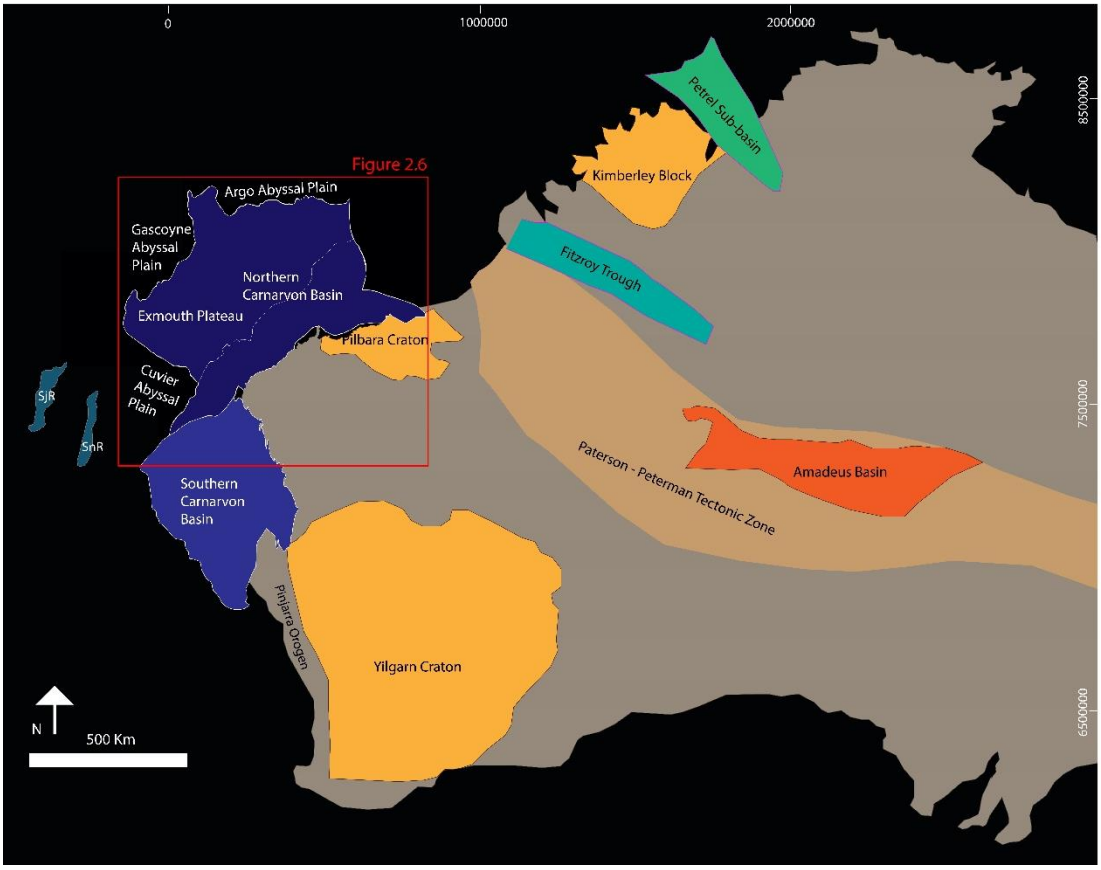

Figure 2.5 The Northern Carnarvon Basin in relation to the prominent blocks, tectonic zones of its formation, based on the work of various authors, such as Anfiloff (1988), Bagas (2004), Bradshaw et al. (1988), Condon (1967), de Gromard et al. (2019), Exon and Wilcox (1978), Felton et al. (1992), and Gunn (1988).

SjR – Sonja Ridge, SnR – Sonne Ridge

separating the Southern and Northern Carnarvon Basins. The hinge zone remains elusive in literature and is never specifically named and rarely discussed in more than passing detail. Condon (1967b) described hinges as not being well understood.

After much review, there are *two* possibilities, this hinge zone, designated as the separation point of the Grater Carnarvon Basin is either a hinge line formed over the Long Island Fault System or a structural feature on the ‘Cape Range High/Anticline’ (Figure 2.6). The Long Island Fault System is sometimes referenced as the hinge zone responsible for Lower Cretaceous aged depositional and subsidence divides (Felton et al., 1992; Romine & Durrant,

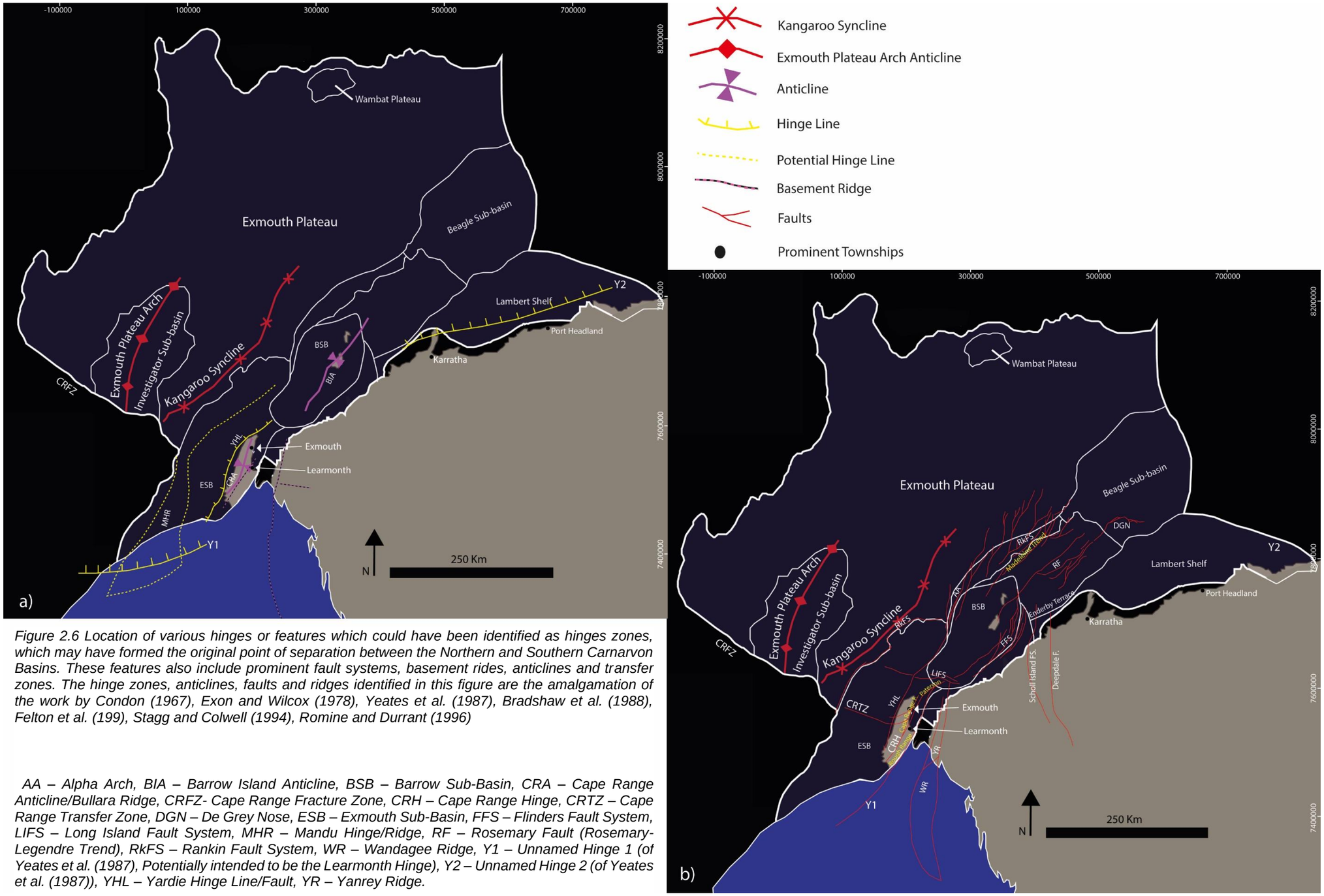

Figure 2.6 Location of various hinges or features which could have been identified as hinges zones, which may have formed the original point of separation between the Northern and Southern Carnarvon Basins. These features also include prominent fault systems, basement rides, anticlines and transfer zones. The hinge zones, anticlines, faults and ridges identified in this figure are the amalgamation of the work by Condon (1967), Exon and Wilcox (1978), Yeates et al. (1987), Bradshaw et al. (1988), Felton et al. (199), Stagg and Colwell (1994), Romine and Durrant (1996)

AA – Alpha Arch, BIA – Barrow Island Anticline, BSB – Barrow Sub-Basin, CRA – Cape Range Anticline/Bullara Ridge, CRFZ- Cape Range Fracture Zone, CRH – Cape Range Hinge, CRTZ – Cape Range Transfer Zone, DGN – De Grey Nose, ESB – Exmouth Sub-Basin, FFS – Flinders Fault System, LIFS – Long Island Fault System, MHR – Mandu Hinge/Ridge, RF – Rosemary Fault (Rosemary-Legendre Trend), RkFS – Rankin Fault System, WR – Wandagee Ridge, Y1 – Unnamed Hinge 1 (of Yeates et al. (1987), Potentially intended to be the Learmonth Hinge), Y2 – Unnamed Hinge 2 (of Yeates et al. (1987)), YHL – Yardie Hinge Line/Fault, YR – Yanrey Ridge.

1996). In other literature, the hinge zone is indicated to be a structural feature in the vicinity of the ‘Cape Range High’ (Figure 2.6), referred to as the Learmonth Hinge or Ridge (from investigations into references in Condon, 1967a; Yeates et al., 1987). It seems most likely that this Hinge Zone referenced in literature is the Learmonth Hinge, despite its apparent obscurity, as the Long Island Fault System sits too far to the North to act as a separation feature between the two segments of the Greater Carnarvon Basin. It remains unclear if the Learmonth Hinge is the hinge feature identified by Yeates et al. (1987; Figure 2.6, as ‘Y1’) on their structural map of the Westralian Superbasin relics (Figure 2.7), or if this feature is a third option for the elusive hinge point between basins.

2.2.1. BASEMENT STRUCTURE

The basement remains poorly understood (Felton et al., 1992). Pryer et al. (2014) described the basement as highly variable and a key contributor to the overlying structure of the sedimentary basins. This aligns with the findings of Alves et al. (2021), Cloetingh et al. (2013), Gillard et al. (2019), Issautier et al. (2020), Lavier and Manatschal (2006), Morley et al. (2004), Reston and Pérez-Gussinyé (2007) and White and McKenzie (1988) who identified that early variations in the crustal structure during rifting influence the later formation of basins (Section 1.1.2. The Formation of Marginal Rift Basins). The Archaean and Proterozoic basement structures of the Northern Carnarvon Basin trend northwest, northeast and north (Pryer et al., 2002). These structures are primarily responsible for forming depocenters and basement topography and influence the later structural development across the margin (Section 1.1.2.3. Resulting Architecture; Elders et al., Manuscript; Etheridge et al., 1991; Issautier et al., 2020; Morley et al., 2004; Pryer et al., 2002). There is a north-northeast trend that bends into a clear northeast trend at the southern end of the Exmouth Sub-basin and a northern trend extending from the onshore cratons (Figure 2.8; Gartrell, 2000; Jitmanhantakul & McClay, 2013; Pryer et al., 2002, Czarnota, 2009). Gravity data across the NWS has shown the presence of a dense network of gravity anomalies (Figure 2.9) in comparison to Australia's other continental margins (Anfiloff, 1988). In the vicinity of the

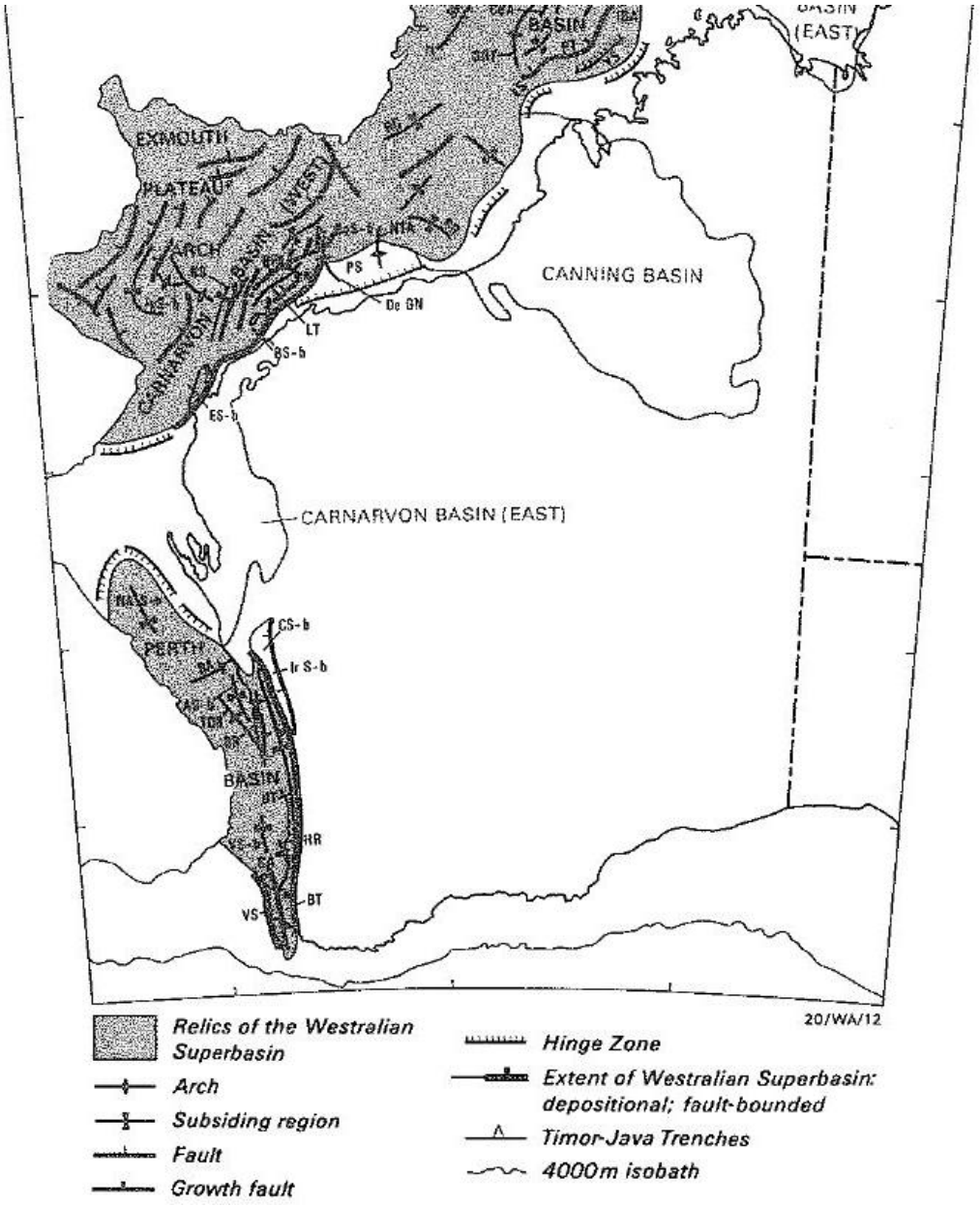

Figure 2.7 Original image by Yeates et al. (1987) of the relics of the Westralian Superbasin showing a Hinge separating the Northern and Southern Carnarvon basins, labelled here as the east and west Carnarvon Basins.

PERTH BASIN - CS-b Coolcalalaya Sub-basin; NAS-b North Abrolhos Sub-basin; BA Batavia Arch; AS-b Abrolhos Sub-basin; TDR Turtle Dove Ridge; BR Beagle Ridge; DT Dandaragan Trough; IrS-b Irwin Sub-basin; VS-b Vlaming Sub-basin; HR Harvey Ridge; SA Sugarloaf Arch; VS Vasse Shelf; BT Bunbury Trough: CARNARVON BASIN (WEST) - NTA North Turtle Arch; BeS-b Beagle Subbasin; DeGN De Grey Nose; KS Kangaroo Syncline; DS-b Dampier Subbasin; RP Rankin Platform; LT Lewis Trough; BS-b Barrow Sub-basin; ES-b Exmouth Sub-basin; EXMOUTH PLATEAU ARCH - IvS-b Investigator Sub-basin; BD Bedout Depression; RD Rowley Depression; LS Leveque Shelf; BROWSE BASIN - BT Buffon Trend; SRT Scott Reef Trend; CBA Central Basin Arch; IBA Inner Basin Arch; PT Prudhoe Terrace; YS Yampi Shelf: SR Seringapatam Rise; AP Ashmore Platform; LA Londonderry Arch; VS-b Vulcan Sub-basin; DR Dillon Ridge; CT Cartier Trough; BONAPARTE BASIN (WEST) - SP Sahul Platform; MG Malita Graben; CG Calder Graben; SD Sahul Depression.

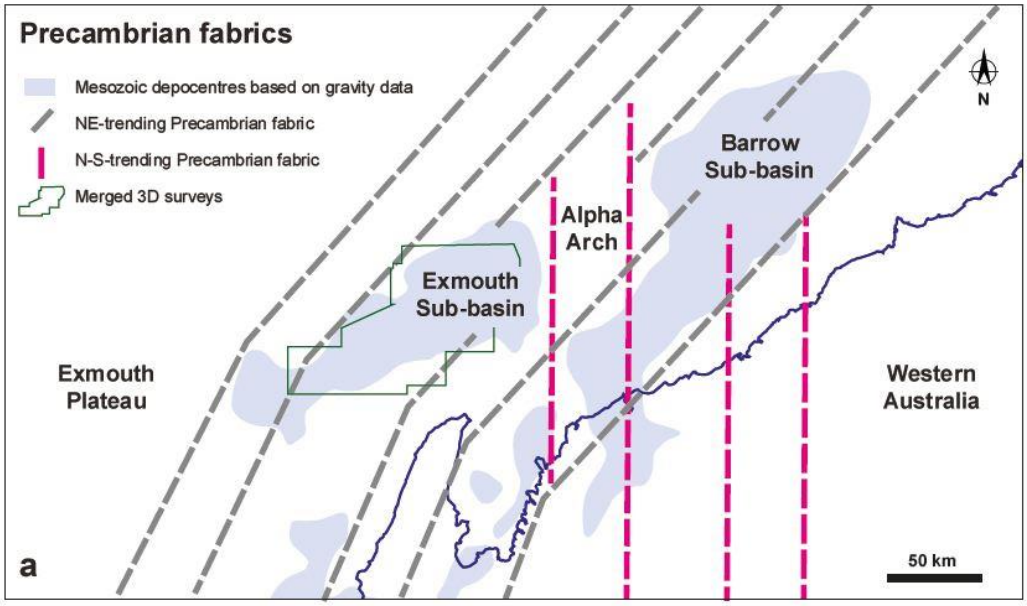
Precambrian fabrics
Mesozoic depocentres based on gravity data
NE-trending Precambrian fabric
N-S-trending Precambrian fabric
Merged 3D surveys
N
Barrow
Sub-basin
Alpha
Arch
Exmouth
Sub-basin
Exmouth
Plateau
Western
Australia
a
50 km

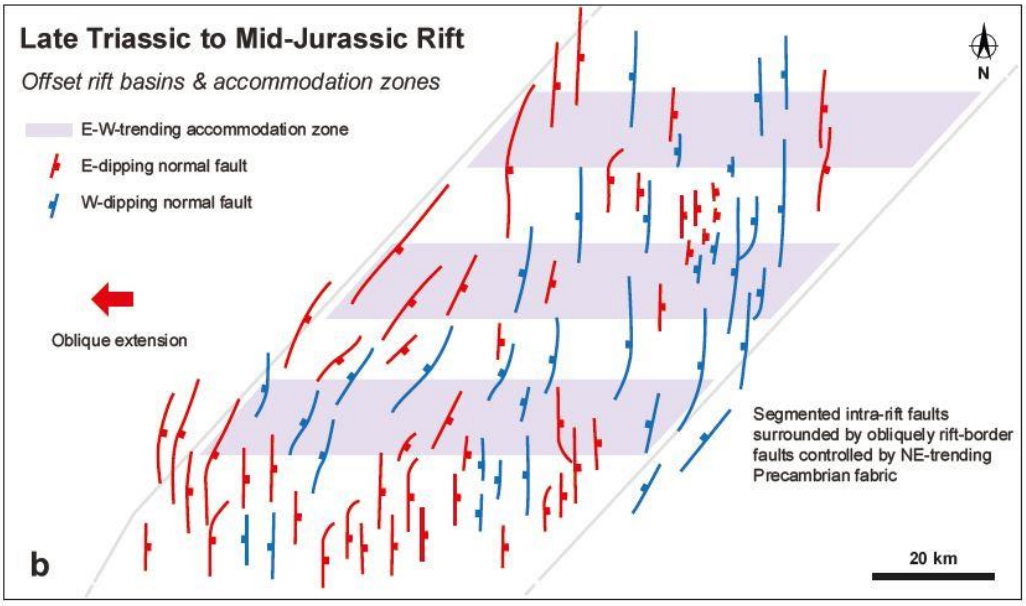
Late Triassic to Mid-Jurassic Rift
Offset rift basins & accommodation zones
N
E-W-trending accommodation zone
E-dipping normal fault
W-dipping normal fault
Oblique extension
Segmented intra-rift faults
surrounded by obliquely rift-border
faults controlled by NE-trending
Precambrian fabric
b
20 km

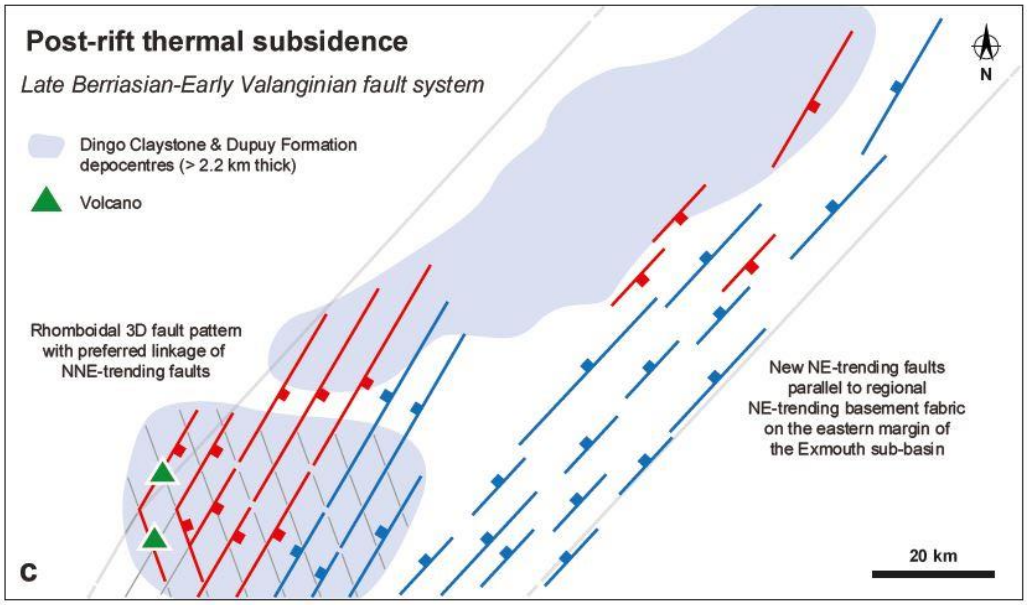
Post-rift thermal subsidence
Late Berriasian-Early Valanginian fault system
N
Dingo Claystone & Dupuy Formation
depocentres (> 2.2 km thick)
Volcano
Rhomboidal 3D fault pattern
with preferred linkage of
NNE-trending faults
New NE-trending faults
parallel to regional
NE-trending basement fabric
on the eastern margin of
the Exmouth sub-basin
c
20 km

Figure 2.8 Orientation of deformation associated with Precambrian plate organisation events which now underlie the Exmouth Sub-basin, as per Jitmahantakul and McClay (2013).

On previous page

Northern Carnarvon Basin, these alternating gravity highs and lows occur in a northeast trend (Figure 2.9a & b; Anfiloff, 1988) with a major northeast trend identified as the North West Shelf Megashear (Figures 2.9 & 2.10; ASGO North West Shelf Study Group, 1994; Pryer et al., 2002; Gartrell et al., 2022). The megashear has been previously described as the remnant of a northeast trending strike-slip zone between the Pilbara and Kimberley Cratons of Australia and the Kaapvaal Craton in Africa; and an extension of the Limpopo Mobile Belt of South Africa (Pryer et al., 2002), now a relic of what was once a zone of orogeny (Gartrell et al., 2022). More recent analysis (i.e., Belgarde et al., 2015; MacNeill et al., 2018; Rollet et al., 2019) of these gravity anomalies using potential field, magnetic, gravity (Figure 2.11) and seismic (Figure 2.12) data link shallower expressions to a thick (c.10km) large igneous province of Triassic age. This magmatic extrusion is the result of early failed rifting on the margin in the Lower to Middle Triassic (MacNeill et al., 2018; Rollet et al., 2019).

2.2.2. STRUCTURAL ELEMENTS

The divisions of the Northern Carnarvon Basin have changed over time, likely due to the limit of clear divisional features within the basin– structural or stratigraphic. This lack of clear division is then further confused by the similarity of the sub-basins to one another. Currently, the Exmouth Plateau, Wombat Plateau, Investigator Sub-basin, Rankin Platform, Exmouth Sub-basin, Barrow Sub-basin, Dampier Sub-basin, Beagle Sub-basin, Peedamullah Shelf and Lambert Shelf form the dominant sub-divisions of the Northern Carnarvon Basin (Figures 1.11, & 2.6; Geoscience Australia, 2019).

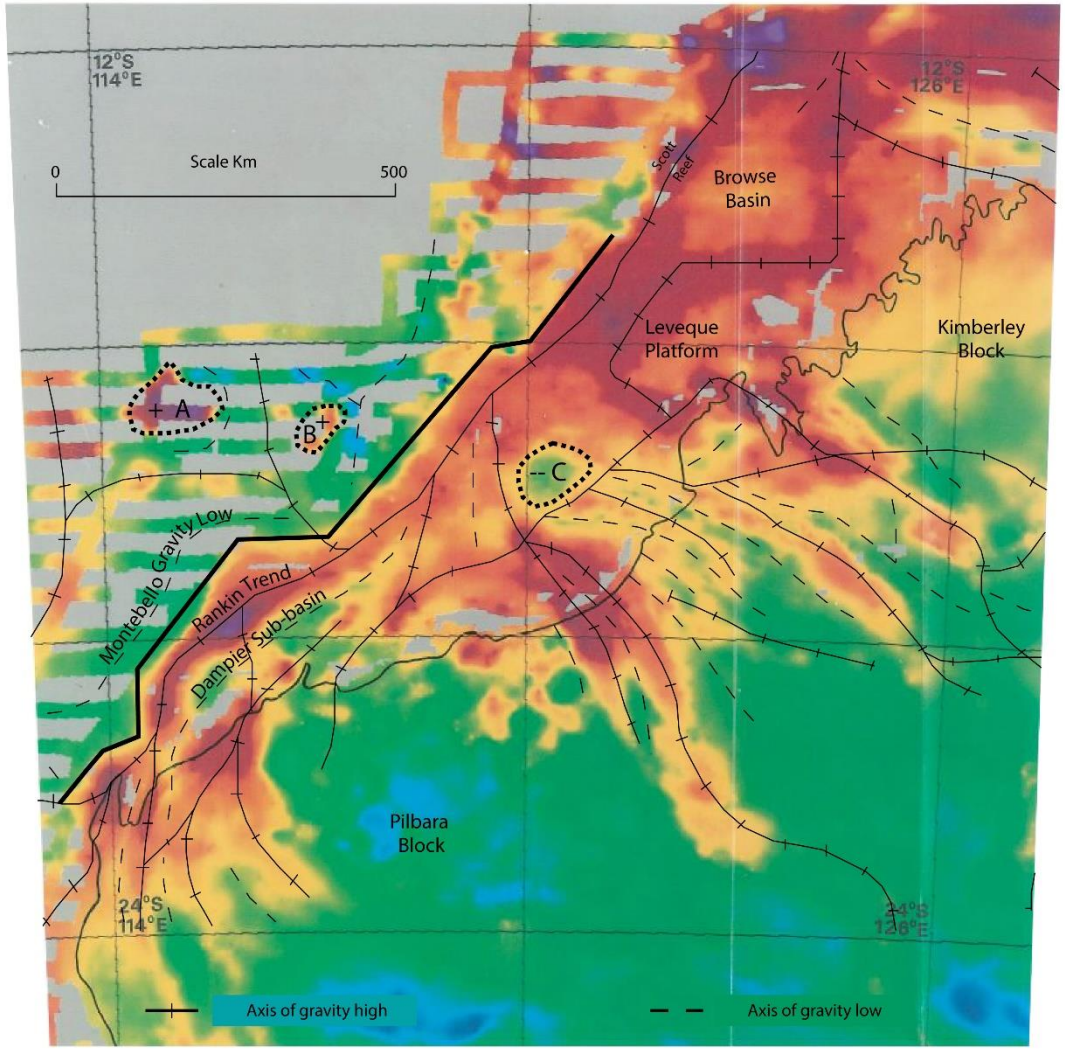
12°S
114°E
0
Scale Km
500
Scott Reef
Browse Basin
12°S
126°E
Leveque Platform
Kimberley Block
A
B
C
Montebello Gravity Low
Rankin Trend
Dampier Sub-basin
Pilbara Block
24°S
114°E
24°S
126°E
Axis of gravity high
Axis of gravity low
Local anomaly
Shelf edge faults

a)

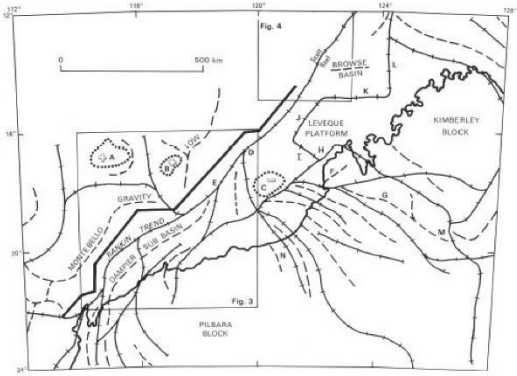
Fig. 4
BROWSE BASIN
LEVEQUE PLATFORM
KIMBERLEY BLOCK
GRAVITY TREND
Fig. 3
PILBARA BLOCK
Axis of gravity high
Axis of gravity low
Local anomaly
Shelf edge faults

b)

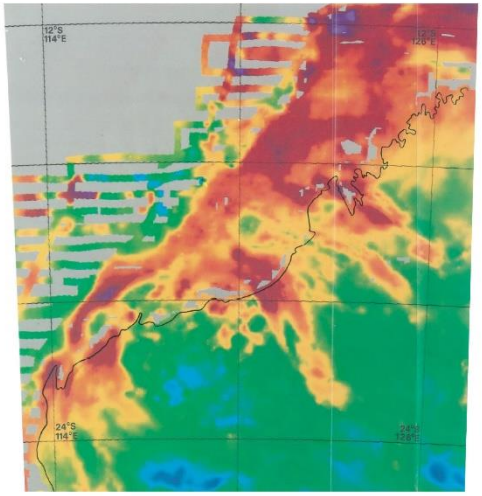
12°S
114°E
24°S
114°E

c)

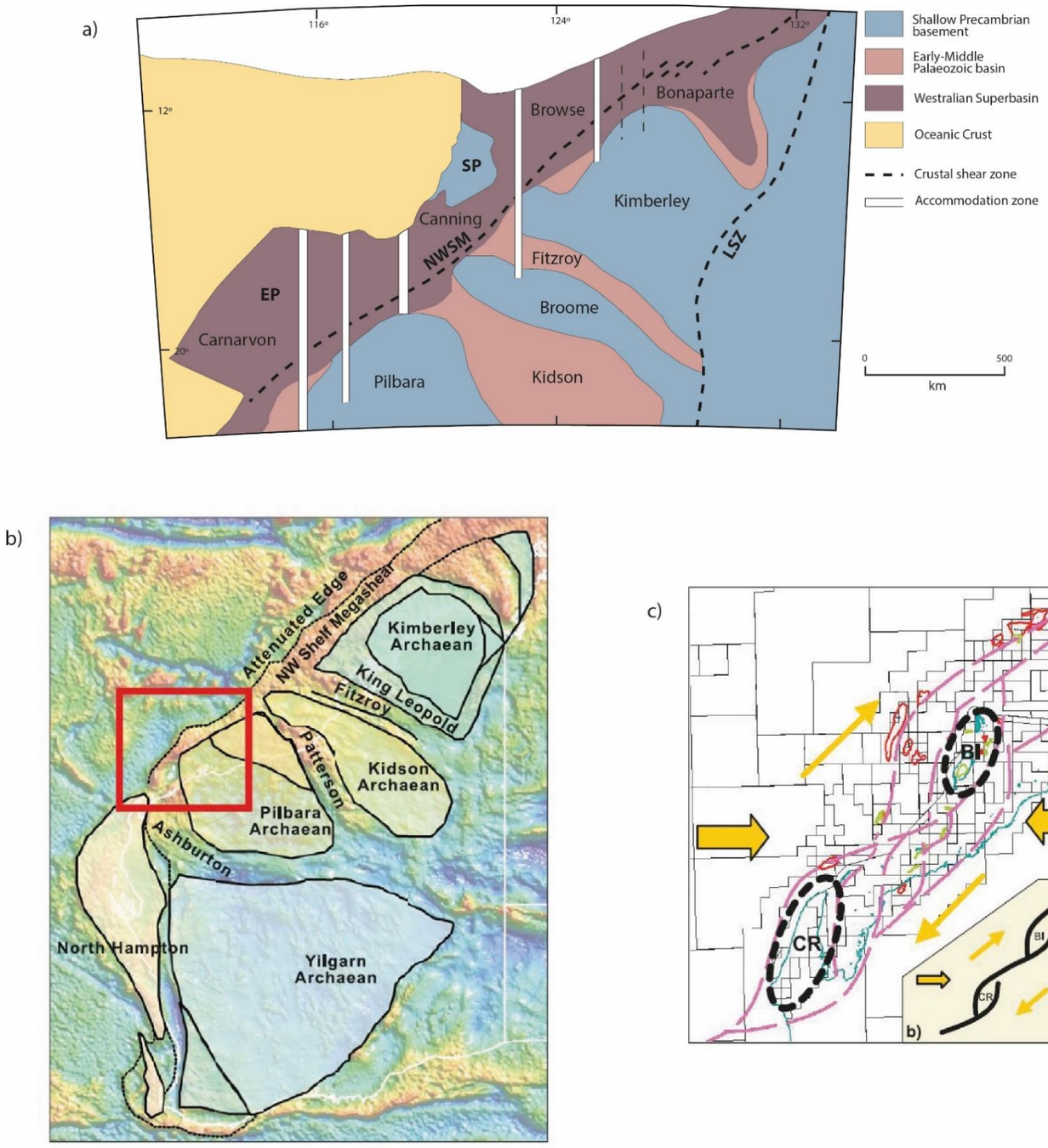

Figure 2.9 Gravity anomalies and interpretation of the North West Shelf, modified from Anfiloff (1988). NOTE: The shelf edge faults as identified here correspond to the location of the NWS Megashear as identified by Pryer et al. (2002), see Figure 2.10.

On previous page

Figure 2.10 NWS Megashear a) principle components of the Westralian Superbasin: LSZ- Lasseter Shear Zone, NWSM- North West Shelf Megashear, EP- Exmouth Plateau, SP- Scott Plateau, modified from AGSO North West Shelf Study Group (1994); b) Reginal gravity profile of Reginal gravity profile of Western Australia with the study area of Pryer et al. (2002) indicated, as per Pryer et al. (2002): c) map view of Cape Range (CR) and Barrow Island (BI) anticline formation as a result of the Miocene reactivation of the NWS Megashear, as per Pryer et al. (2002): d) formation of Barrow Sub-basin pull-apart structures as a result of reactivation along the NWS Megashear, as per Pryer et al. (2002).

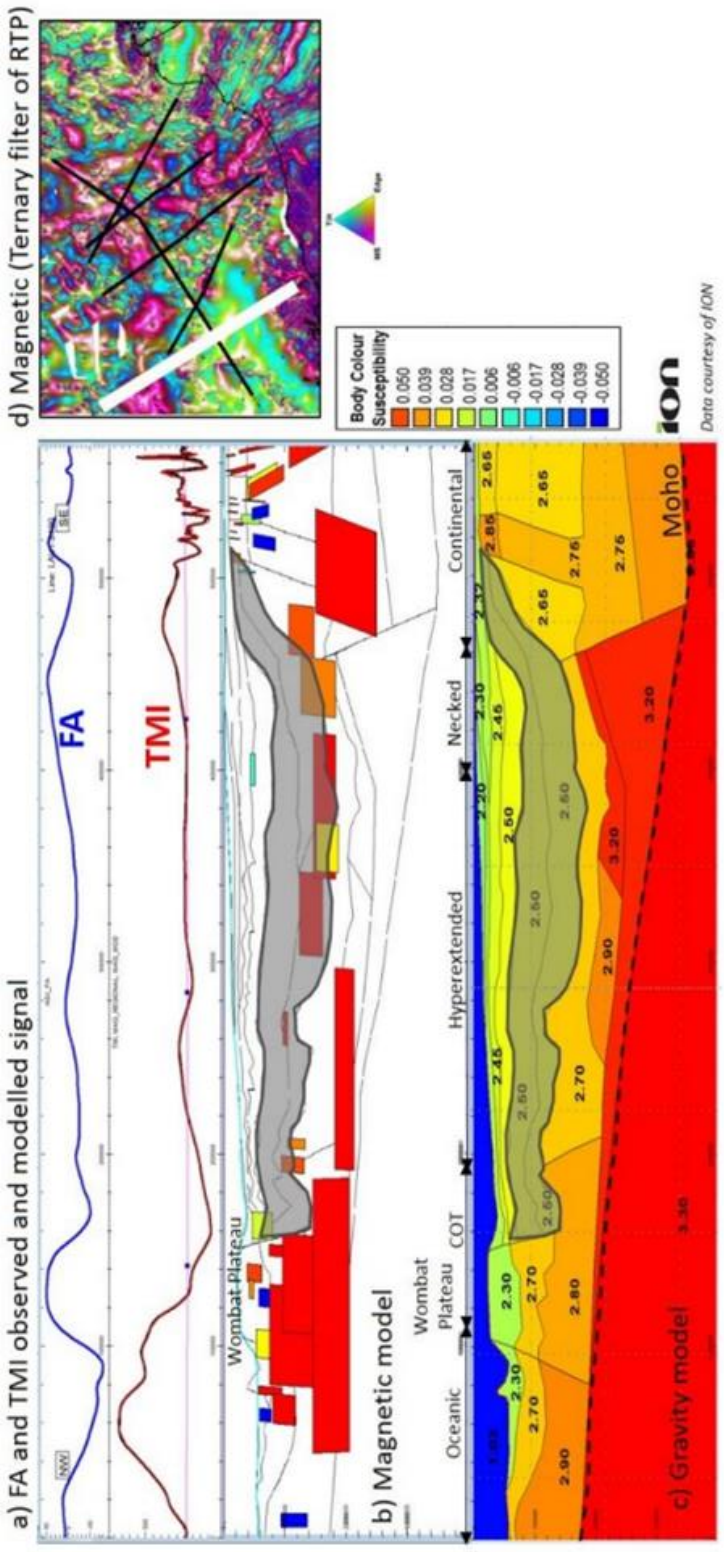

Figure 2.11 Gravity and magnetic modelling of the Lower and Middle Triassic in the northern portion of the Northern Carnarvon Basin, displaying correlation with a large, extruded igneous body. Th low density and high magnetic intensity bodies (grey outline on panels b and c). (d) Line location (white line) shown on RTP processed magnetic image. Note the high magnetic response of the Wombat Plateau within the Continental-Ocean Transition (COT) zone. Figure as per Rollet et al. (2019).

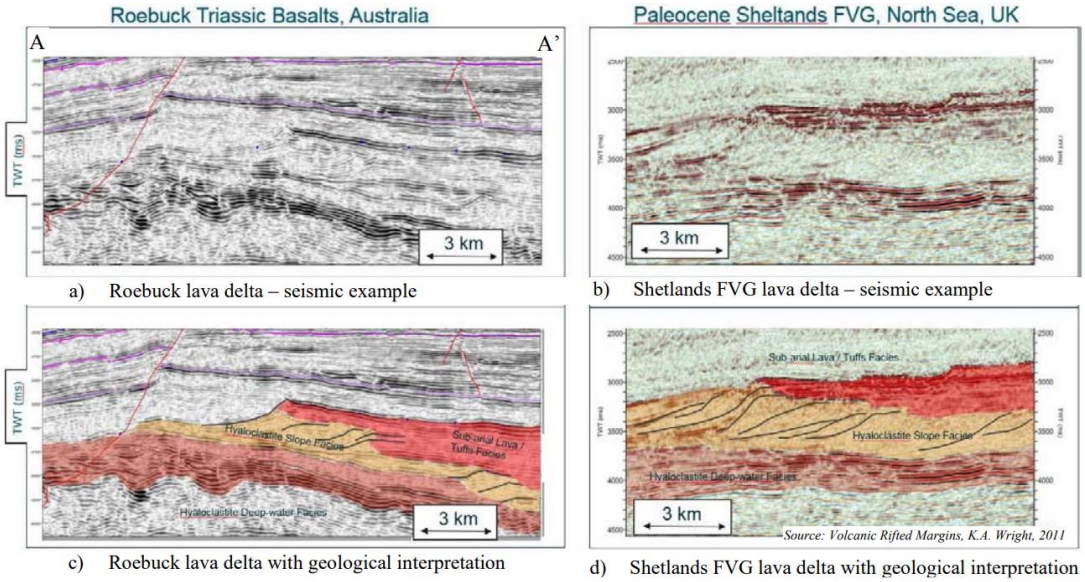

Figure 2.12 Comparison of seismic data from the North Sea and the Roebuck Basin, highlighting the similarities which indicate a large magmatic flow during in the Lower to Middle Triassic, as per MacNeill et al. (2018).

2.2.2.1. THE EXMOUTH PLATEAU

The Exmouth Plateau is an 800 to 3,000 m deep bathymetric plateau (Exon & Buffler, 1992; Exon & Willcox, 1978; Geoscience Australia, 2014a, 2014b; Falvey & Mutter, 1981; Felton et al., 1992; Purcell & Purcell, 1988; Stagg et al., 2004; Wulff & Barber, 1995) which has undergone crustal thinning (Driscoll & Karner, 1998; Exon & Buffler, 1992). The plateau is a significant basin feature (Figures 1.11, 2.5 & 2.6), approximately 600 km in length and 350 km in width (Bilal et al., 2018; Scarselli, 2014). The most distinct stratigraphic difference of the plateau from the inboard sub-basins is a thick Triassic sequence and a thin Jurassic sequence; by comparison of one to the other (Figure 2.13; Zabanbark, 2010). Early works describe the plateau as a sunken continental feature (e.g., Exon et al., 1982). This is at odds with the mechanical and physical properties of the crust which are reflected in the overlaying basin features (see Section 1.1.2 The Formation of Marginal Rift Basins; Beaumont & Ings, 2012; Cloetingh et al., 2013; Issautier et al., 2020; Reston & Pérez-Gussinyé, 2007; White & McKenzie, 1988). Later modelling work has

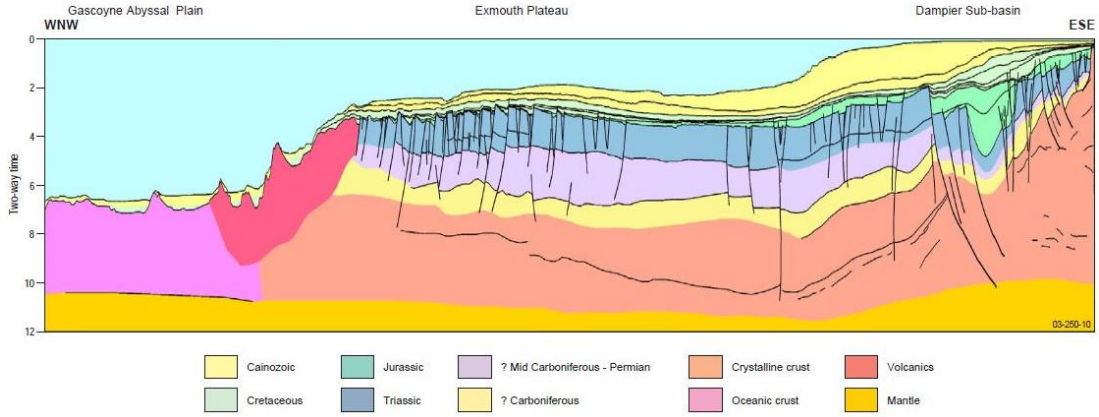

Figure 2.13 Broad Triassic and Jurassic stratal thickness changes between thin inboard and outboard Northern Carnarvon Sub-basin and the thicker Permo-Triassic deposition oceanwards, as per Stagg et al. (2004).

highlighted the crustal strength discrepancies and indicated the plateau might have formed over remnant oceanic crust (Belgarde et al., 2015; I'Anson, 2020).

The plateau can be divided into key structural domains; the Rankin Platform, the Kangaroo Syncline, the Investigator Sub-basin (often interchanged with the Exmouth Plateau Arch) and the Wombat Plateau (Figures 1.11, & 2.6; Geoscience Australia, 2014a; Stagg et al., 2004; Tindale et al., 1998).

Structural Architecture

Normal fault activity (Figure 2.14), occurring on northeast trending faults, is the plateau's primary characteristic (Figure 2.8; Exon & Willcox, 1978; Hocking, 1990b). Landward tilting fault blocks (Figure 2.14) are prominent and may be listric at depth (Exon et al., 1982) indicating the plateau formed as a distal domain (as per Péron-Pinvidic et al., 2013; See Section 1.1.1.1. Domains and Their Phases) which is in-line with the identification of exhumed and hyperextended domains by Belgarde et al. (2015). The central and southern plateau have fault trends that occur obliquely to the direction of extension and breakup (Stagg et al., 2004). Exon and Willcox (1978) describe the southern plateau as less faulted due to the later seafloor spreading in the Gascoyne Abyssal Plain in the Cretaceous, identifying Triassic and Jurassic fault activity

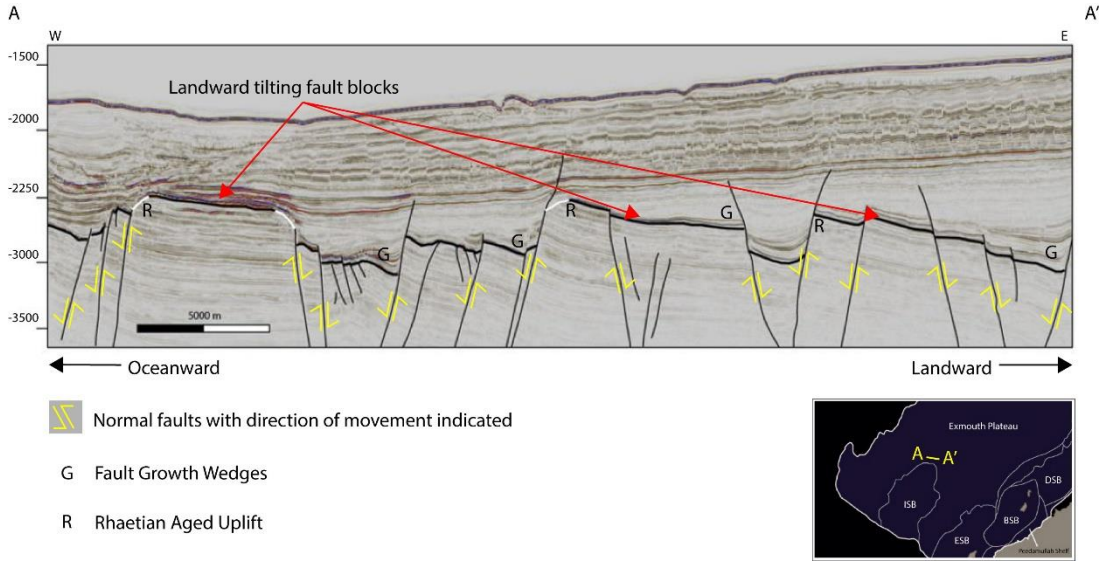

Figure 2.14 Seismic cross-section displaying the prominent structural characteristics of the Exmouth Plateau, landward dipping fault blocks and normal faults, growth wedges and fault block uplift of Rhaetian age, modified from Rohead-O'Brien and Elders (2018).

as largely confined to the northern plateau. The northern margin is considered the most structurally complex area (Stagg et al., 2004) with significant structural relief emanating from both the Argo rifting and the underlying Palaeozoic structure of the onshore Canning Basin (Exon & Willcox, 1978; Stagg et al., 2004). The northwest margin is a low gradient slope, dominated by volcanic extrusions and intrusions (Stagg et al., 2004). The southwest margin is a transform margin, which underwent significant uplift and erosion (±2 km) due to the Cuvier spreading centre (Stagg et al., 2004).

There are two dominant structural trends on the Exmouth Plateau, north and northeast (Figure 2.8; Geoscience Australia, 2014a; Stagg et al., 2004). These trends vary across the plateau, a reflection of both the underlying structural grain (north trend) and episodes of oblique extension (northeast trend; Refer to Section 1.1.2.3. Resulting Architecture for a more detailed review of the origin of structural trends on rifted margins; Geoscience Australia, 2014a; Stagg et al., 2004). The northeast trend is the primary structural control on the plateau (Exon & Willcox, 1978).

In the southern plateau faults are north or northeast-trending and occur in the Upper Triassic strata. They are more frequent in the western regions and less

common in the east of the plateau (Stagg & Colwell, 1994). North-trending faults are also seen in the Investigator Sub-basin area and its surroundings and the northwestern extent of the plateau (Geoscience Australia, 2014a, 2015; McHarg, 2018). Early descriptions of the northern plateau by Exon and Willcox (1978) found fault populations with west to northwest trends. These faults interacted with the northeast to north-trending faults on the northwestern plateau forming troughs and highs (Exon & Willcox, 1978). Hocking et al. (1987) described the northeast trend as "bending around to a more easterly direction in the eastern part of the plateau".

DEEP STRUCTURE OF THE EXMOUTH PLATEAU

AGSO North West Shelf Study Group (1994) identified two (C1 and C2) flat-lying reflectors at 15 - 18 km depth in the Exmouth Plateau (Figure 2.15), shallowing slightly into the Rankin Platform (12 - 18 km), and interpreted them as likely detachment surfaces. Etheridge and O'Brien (1994) described the crustal detachment as west-dipping, while Driscoll and Karner (1998) favour an east-dipping detachment. Velocity information indicated that these reflectors likely represent crystalline crust that forms the basement to the Northern Carnarvon Basin (AGSO North West Shelf Study Group, 1994). Gartrell (2000) favoured changes in the composition of the crust to explain the shallower reflector (C1; Figure 2.15), while maintaining that the deeper of the two reflectors (C2; Figure 2.15) was indeed a detachment surface (Gartrell, 2000; Mutter & Larson, 1989). The identification of an expansive extrusion (large igneous province, or LIP) over much of the area to in the north of the Northern Carnarvon Basin (Belgarde et al., 2015; MacNeill et al., 2018; Rollet et al., 2019) would support that invoking geometrical detachments to explain current architecture of the basin is redundant and overly complex where more simplistic explanations are probable (LIP).

2.2.2.2. MARGINAL SUB-BASINS

Four sub-basins, the Dampier, Barrow, Beagle and Exmouth sub-basins (Figures 1.11 & 2.16; Stagg & Colwell, 1994) form a string of depocentres that sit between the continental shelf and upper continental slope (Stagg & Colwell,

a) **Northern Carnarvon Basin – Line 110/12.**

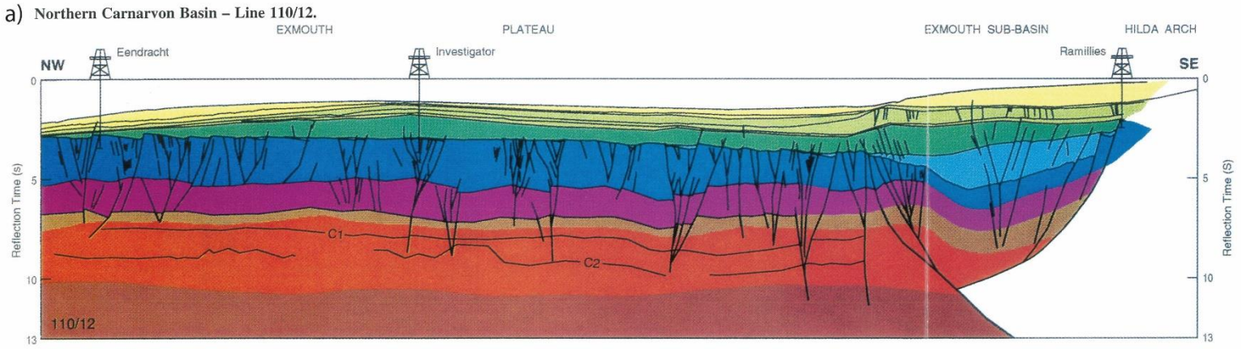

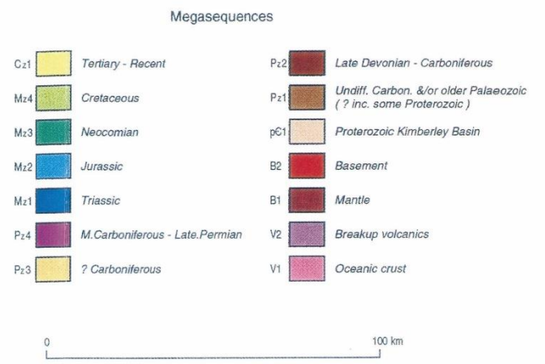

b) **Northern Carnarvon Basin – Lines 101/07 & 110/15.**

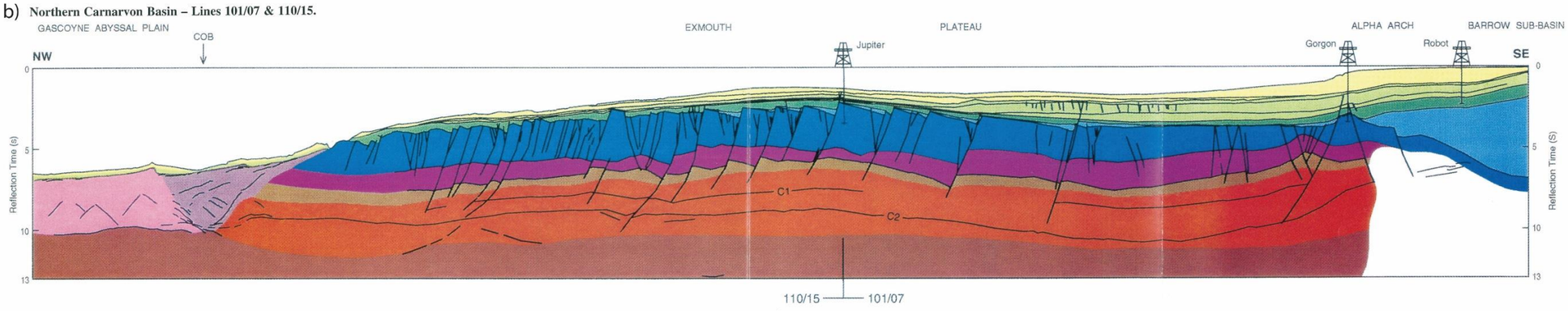

c)

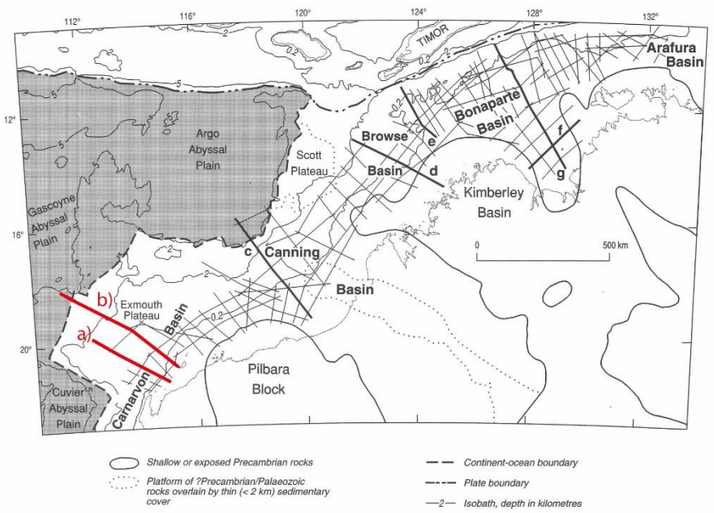

Figure 2.15 Interpretation of deep seismic profiles within the Northern Carnarvon Basin displaying the thickness of the sedimentary successions, depth of basement and deep reflectors (C1 & C2), modified from AGSO North West Shelf Study Group (1994). Location of lines a) and b) are shown on map in figure c).

1994). The Dampier, Barrow, Beagle and Exmouth sub-basins form a collection of large trough style depocentres (Hocking, 1990b) resulting from Mesozoic extension (Geoscience Australia, 2014a, 2015; Gartrell, 2000). Originally these sub-basins formed a linked system of Jurassic depocentres, often referred to as a major component of the rift system (Hocking, 1992; Stagg & Colwell, 1994; Wulff & Barber, 1995). This rift system is over 400 km in length (Wulff & Barber, 1995). Originally classed as a series of graben and half-graben, Stagg and Colwell (1994) found that these basins were better described as synclinal depocentres, whose boundaries were originally constrained by the localised fault activity on the Rankin, Rosemary and Flinders fault systems (Figure 2.6). The structural outline of the rift formed between the Upper Triassic and earliest Jurassic, over a zone of rapid change in crustal thickness (Stagg & Colwell, 1994).

Oblique extension has resulted in a northeast fault trend for the Dampier, Barrow and Exmouth sub-basins (Figure 2.16), with a series of *en-echelon* highs and troughs (Geoscience Australia, 2014a, 2015; Stagg & Colwell, 1994; Woodside Offshore Petroleum, 1988). The Beagle Sub-basin is different and contains a series of north-trending fault blocks, anticlines and troughs (Blevin et al., 1994; Geoscience Australia, 2014a, 2015). Consequently, the fault orientations in the Beagle Sub-basin also differ, occurring in a north to northeast orientation (Figures 2.16 & 2.17; I'Anson et al., 2019; McCormack & McClay, 2018).

2.2.2.3. LAMBERT AND PEEDAMULLAH SHELVES

The most landward areas of the Northern Carnarvon Basin form the Peedamullah and Lambert shelves (Figure 1.11; Stagg & Colwell, 1994). They are described as Precambrian basement material overlain by up to 2 km of Cretaceous to Cenozoic sediments that thin towards the Australian mainland; a rift shoulder to the Northern Carnarvon Basin (Geoscience Australia, 2014a). Some Silurian to Permian sequences are preserved in the Peedamullah Shelf

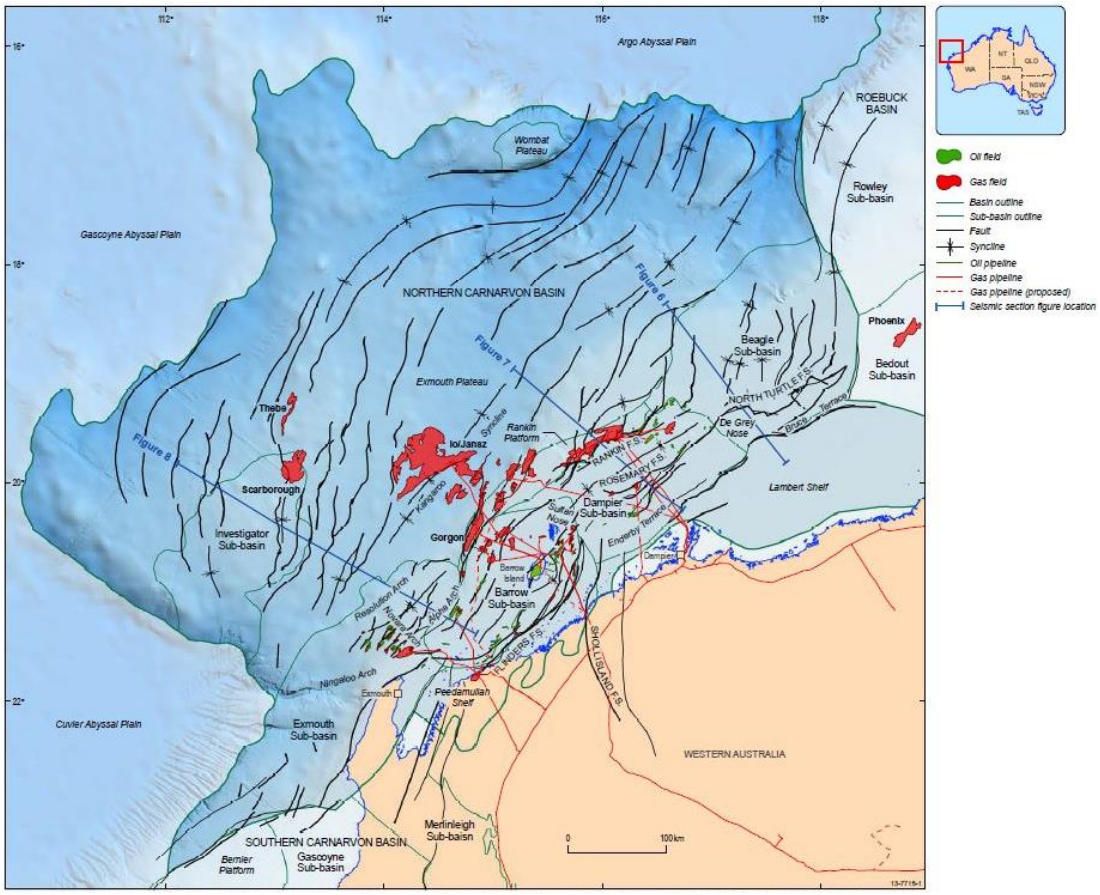

Figure 2.16 Prominent structural trends of the inboard Northern Carnarvon Sub-basins and significant hydrocarbon fields, from Geoscience Australia (2014a).

(Geoscience Australia, 2014a). In contrast to the rest of the Northern Carnarvon Basin, there is only a thin cover of Mesozoic strata (Hocking, 1990b). Etheridge and O'Brien (1994) and Hocking (1988, 1990a, 1990b) describe a north-south trend (i.e., Figure 2.8) as originating from the older Precambrian and Palaeozoic basement on the shelves.

2.2.3. INVERSION AND REACTIVATION

Structural inversion occurred periodically in the Northern Carnarvon Basin from the Cretaceous to the Neogene, primarily along major fault-bounded systems (Bradshaw et al., 1998; Cathro & Karner, 2006; Driscoll & Karner, 1996; Karner & Driscoll, 1999; Tindale et al., 1998). It formed many of the features described as “arches” in the Northern Carnarvon Basin, including the Exmouth Plateau Arch (Figure 1.11; Barber, 1988; Boyd et al., 1992; Cathro &

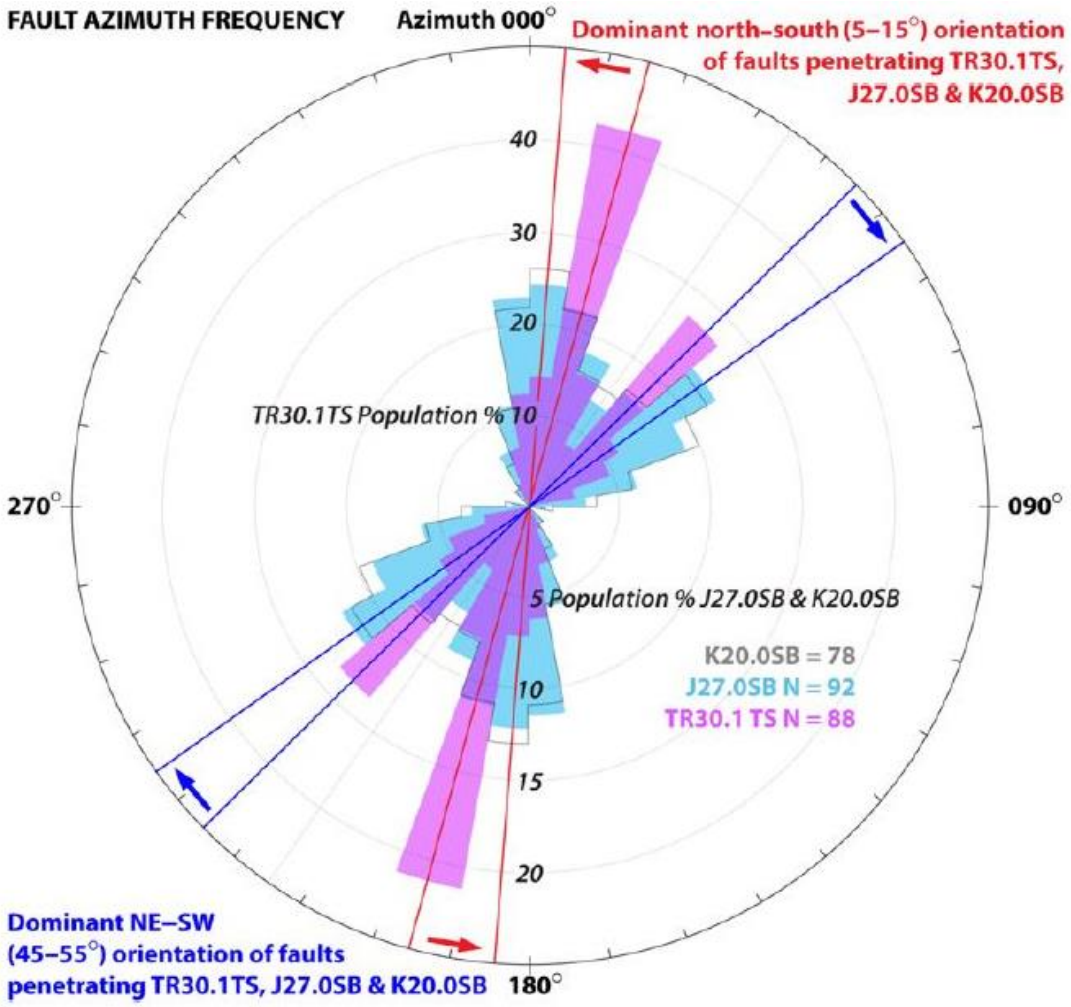

Figure 2.17 Key Mesozoic fault trends of the Beagle Sub-basin, Northern Carnarvon Basin, separated into pre-extension (purple), syn-extension I (blue) syn-extension II (grey), as per McCormack and McClay (2018).

Karner, 2006; Hearty et al., 2002; Jitmanhantakul & McClay, 2013; Keep et al., 1998; Tindale et al., 1998). Stagg and Colwell (1994) found that many of the major fault systems had undergone more than one episode of reactivation. Inversion is considered to be a leading cause in the trapping of hydrocarbons in the Northern Carnarvon Basin (Cathro & Karner, 2006).

Cathro & Karner (2006) noted that evidence of Cretaceous to Cenozoic inversion within the Dampier Sub-basin was predominantly available along the bounding fault systems, internal to the basin across roll-over anticlines of collapsed hanging wall blocks. In the Dampier Sub-basin, dominant inversion related structures are the Rosemary (Rosemary-Legendre) Trend and Barrow

Island (Figure 2.6; Bradshaw et al., 1998; Cathro & Karner, 2006; Driscoll & Karner, 1996; Karner & Driscoll, 1999; Tindale et al., 1998). Hocking (1988, 1990a, 1990b) describe many of the anticline features in the basin as the result of fault inversion. These inversion events occurred as early as the Cretaceous, but more commonly after the Miocene (Hocking, 1990a, 1990b).

Cretaceous aged inversion of the Dampier Sub-basin took place along the major bounding faults, the Madeleine, Rankin, Rosemary-Legendre, and Scholl Island fault systems (Figure 2.6), in a northeast to southwest orientation (Bentley, 1988; Cathro & Karner, 2006; Wulff & Barber, 1995). These Cretaceous inversions show up to 1,000 m of inversion (Cathro & Karner, 2006). Minor episodes of inversion are also identified in the region, such as a Turonian event recorded in the K50 deposits (Gearle Siltstone; Figure 2.18; Driscoll & Karner, 1998). In the Upper Cretaceous (Campanian) uplift and inversion due to rift activity on the southern margin took place in the southern reaches of the NWS (Bradshaw et al., 1998; Jitmanhantakul & McClay, 2013; Tindale et al., 1998) and fault block rotation and uplift occurred further to the north (Blevin et al., 1998a). Bradshaw et al., (1988) found that this Campanian inversion event impacted structures of the Exmouth Plateau.

Contrary to Cretaceous inversion, the Miocene inversion in the Dampier Sub-basin occurred adjacent to the northwestern extent of the Rosemary Fault Trend (Figure 2.6); these are also shorter in displacement, only reaching hundreds of metres of inversion (Cathro & Karner, 2006). In the Exmouth Sub-basin, a forced fold feature is attributed to inversion (Bradshaw et al., 1998; Cathro & Karner, 2006; Driscoll & Karner, 1996; Karner & Driscoll, 1999; Tindale et al., 1998). Late Paleogene to early Neogene inversion from continental collision formed many of the arch features through the Northern Carnarvon Basin, including the Exmouth Plateau Arch (Barber, 1988; Boyd et al., 1992; Cathro & Karner, 2006; Hearty et al., 2002; Jitmanhantakul & McClay, 2013; Keep et al., 1998; Tindale et al., 1998; Scarselli, 2014). Cainozoic inversion of the Rough Range, Paterson and Cape Range Faults (Figure 2.6) was identified by Hocking (1987).

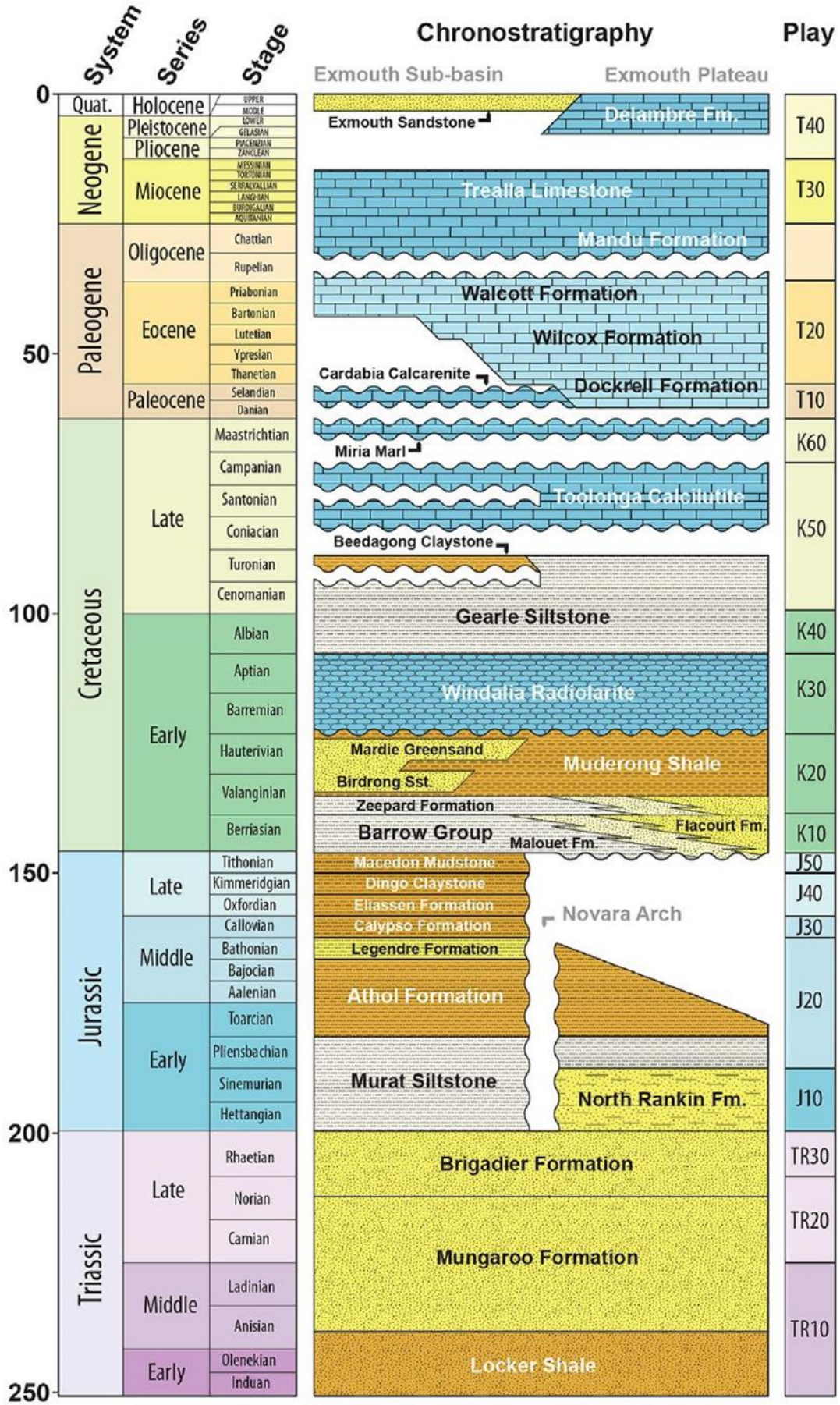
System
Series
Stage
Chronostratigraphy
Play
Exmouth Sub-basin
Exmouth Plateau
0
50
100
150
200
250
Quat.
Holocene
Pleistocene
Pliocene
Neogene
Miocene
Paleogene
Oligocene
Eocene
Paleocene
Cretaceous
Late
Early
Jurassic
Triassic
Middle
Chattian
Rupelian
Priabonian
Bartonian
Lutetian
Ypresian
Thanetian
Selandian
Danian
Maastrichtian
Campanian
Santonian
Coniacian
Turonian
Cenomanian
Albian
Aptian
Barremian
Hauterivian
Valanginian
Berriasian
Tithonian
Kimmeridgian
Oxfordian
Callovian
Bathonian
Bajocian
Aalenian
Toarcian
Pliensbachian
Sinemurian
Hettangian
Rhaetian
Norian
Carnian
Ladinian
Anisian
Olenekian
Induan
Exmouth Sandstone
Delambre Fm.
Trealla Limestone
Mandu Formation
Walcott Formation
Wilcox Formation
Cardabia Calcarenite
Dockrell Formation
Miria Marl
Toolonga Calcilutite
Beedagong Claystone
Gearle Siltstone
Windalia Radiolarite
Mardie Greensand
Muderong Shale
Birdrong Sst.
Zeepard Formation
Barrow Group
Flacourt Fm.
Malouet Fm.
Macedon Mudstone
Dingo Claystone
Eliassen Formation
Calypso Formation
Legendre Formation
Athol Formation
Murat Siltstone
Novara Arch
North Rankin Fm.
Brigadier Formation
Mungaroo Formation
Locker Shale
T40
T30
T20
T10
K60
K50
K40
K30
K20
K10
J50
J40
J30
J20
J10
TR30
TR20
TR10

Figure 2.18 Stratigraphic chart for the Exmouth Plateau and Sub-basin, displaying the stratigraphic packages as they correlate to geological time periods. Geological ages are also correlated to the Play intervals (right) of Marshall and Lang (2013). Image as per Black et al. (2017).

On previous page

There is no evidence of major crustal extension for the upper Permian, though some minor reactivation events did occur, such as the upper Permian Bedout Movement, the effects of which are mostly seen in the southern NWS (AGSO North West Shelf Study Group 1994; Etheridge & O'Brien, 1994; Forman & Wales 1981; Horstman & Purcell, 1988; Symonds et al., 1994).

Pryer et al. (2002) stated that the formation of the Barrow and Dampier sub-basins was a result of basement structures in both Paleozoic and Mesozoic times. Jitmahantakul and McClay (2013) found this was also the case with faults within the Exmouth Sub-basin, and Stagg and Colwell (1994) identified reactivation on deeper north-trending faults across the basin. Etheridge and O'Brien (1994) attributed the Upper Triassic to Lower Jurassic tectonic movement of structures in the Greater Carnarvon Basin to the reactivation of older Permo-Carboniferous (or Phanerozoic- Gartrell, 2000) structures. All the underlying basement structures reactivated during subsequent tectonic activity shaping the basins evolution (AGSO North West Shelf Study Group 1994; Pryer et al., 2002; Romine et al., 1997). Fault reactivation during the Upper Jurassic resulted in the erosion of material along the margins of the Exmouth Sub-basin (Tindale et al., 1998).

The intra-basin high axes, Madeleine Trend and Barrow Anticline (Figure 2.6) are likely reactivation structures, linked to a Permo-Carbonifeous detachment within the basement (Wulff & Barber, 1995). Driscoll and Karner (1998) identified broad basin-wide reactivation of faults occurred during the Tithonian to Valanginian separation event. The Rankin Trend (Figure 2.6) was also reactivated during this time (Hauterivian; Swift et al., 1988). Cretaceous reactivation has been identified in faults that were active between the Callovian and Oxfordian (Tindale et al., 1998). Bailey et al. (2016) identified Paleogene

reactivation in a series of Jurassic aged fracture networks within the Northern Carnarvon Basin. These reactivated fractures were most prominent in the marginal sub-basins (Bailey et al., 2016).

2.2.4. TECTONIC EVOLUTION OF THE EXMOUTH PLATEAU

The tectonic forces acting on the crust underlying the sedimentary basins of the NWS influenced the evolution of those basins (Etheridge et al., 1991; Pryer et al., 2002). Whilst all the basins of the NWS have been influenced by the same tectonic events, the style of response to these events varies widely (Stagg et al., 1999). The following section details the tectonic evolution of the Exmouth Plateau. Due to the limited number of in-depth studies of the plateau, literature often references the tectonic history of the Northern Carnarvon Basin and the larger NWS when describing the evolution of the Exmouth Plateau. As such the following section cannot be constrained specifically to the plateau, and reference will be made to the broader basin and margin when discussing its formation. The Mesozoic history represents the core of basin development, and this depositional history has been widely studied due to its economic importance (Figure 2.19).

The lower Palaeozoic, Cambro-Ordovician, portion of the NWS are deeply buried or absent (Longley et al., 2002) remaining unobserved and largely undescribed due to the depth at which it is buried; and due to its limited likelihood of it contributing to the hydrocarbon prospectively of the NWS (Figure 2.19; Longley et al., 2002). Above this, there is a Devonian to Permian section, which is related to the first main phase of Gondwanan breakup (for Gondwanan continent, see Figure 2.4; Longley et al., 2002; Metcalfe, 1999). The second and third phases occurred in the Mesozoic (Figure 2.1; Longley et al., 2002; Metcalfe, 1999). These phases form two syn-rift events and a period of sag that directly impact the infilling of the basins (Longley et al., 2002). In the Triassic, the NWS was originally a series of intra-continental basins (Figure 2.3c), but as a result of rift activities and seafloor spreading during the Jurassic and Lower Cretaceous, developed into a passive margin (Marshall & Lang, 2013). However, as identified by Hengesh and Whitney (2014) ongoing plate

Figure 2.19 Economic summary of divisions of the NWS, by age as identified by Rock-Eval screening, as per Longley et al. (2002).

migration and recent seismic activity are inconsistent with a true passive margin.

2.2.4.1. PRECAMBRIAN

Initial tectonic activity which formed the North West Shelf (NWS) is understood to have occurred between the mid and upper Mesoproterozoic, resulting in the assembly of the Proterozoic Australian continent as part of the Rodinia Supercontinent (Figure 2.20; Baillie et al., 1994; Hoffman, 1991; Myers et al., 1996). The northwest of Australia later experienced renewed and extensive continental breakup of Rodinia in the uppermost Precambrian (Figure 2.21; Baillie et al., 1994; Bond et al., 1984; Purcell & Purcell, 1988).

While not observable on seismic imaging it is thought that the NWS Megashear (see Section 2.2.1 Basement Structure) would have been a mobile belt formed through multiple extension and compression events between the Archean and Proterozoic (Pryer et al., 2002). The structuring of the NWS Megashear (NE-SW) was altered in the Proterozoic, first during the Barramundi Orogeny with the introduction of north trending features, and later the Pinjarra Orogeny

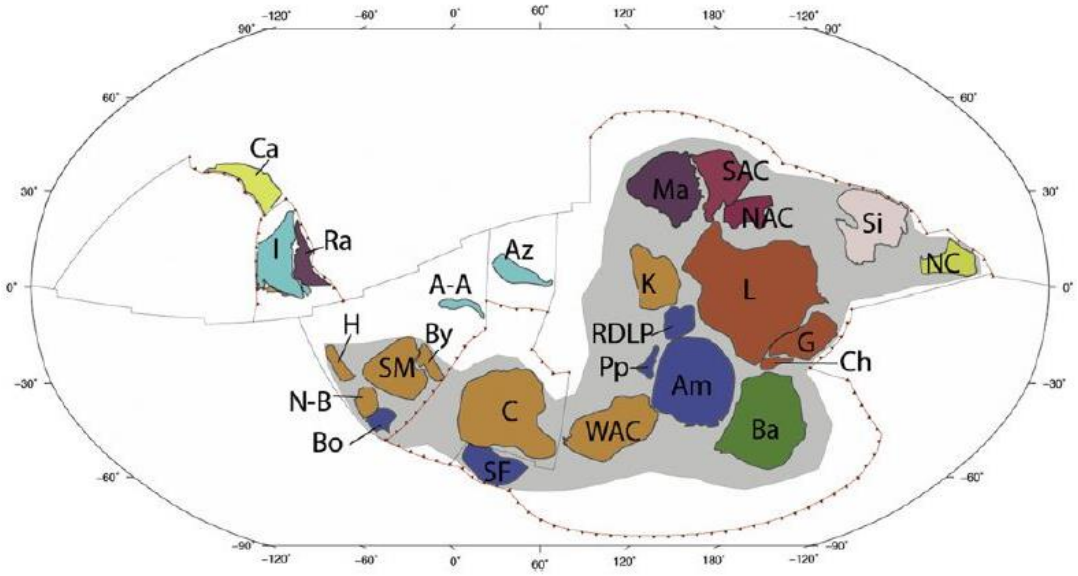

Figure 2.20 Tectonic geography of the Rodinian supercontinent (indicated by the shaded grey area) at the end of the Mesoproterozoic (1000 Ma), as per Merdith et al. (2017). A-A, Afif-Abas Terrane; Am, Amazonia; Az, Azania; Ba, Baltica; Bo, Borborema; By, Bayuda; Ca, Cathaysia (South China); C, Congo; Ch, Chortis; G, Greenland; H, Hoggar; I, India; K, Kalahari; L, Laurentia; Ma, Mawson; NAC, North Australian Craton; N-B, Nigeria-Benin; NC, North China; Pp, Paranapanema; Ra, Rayner (Antarctica); RDLP, Rio de la Plata; SAC, South Australian Craton; SF, São Francisco; Si, Siberia; SM, Sahara Metacraton; WAC,West African Craton. The longitude is arbitrary and unconstrained, and used as a guide. Cratonic crust is coloured by present day geography: North America, red; South America, dark blue; Baltica, green; Siberia, grey; India and the Middle East, light blue; China, yellow; Africa, orange; Australia, crimson; Antarctica, purple.

(Figure 2.22b) when the north trending features were reactivated altering the dominant northeast expression of the Barrow Sub-basin (Pryer et al., 2002), through structural inheritance and orientation of stress (Section 1.1.2.3. Resulting Architecture). From the mid-upper Neoproterozoic intracontinental dextral shear occurred along the Paterson-Peterman tectonic zone (Figure 2.5) impacting the NWS, and then continued until the close of the Precambrian (Baillie et al., 1994).

2.2.4.2. CAMBRIAN

The initial phase of Phanerozoic continental breakup began in the Cambrian (Figure 2.3a; Bond et al., 1984; Purcell & Purcell, 1988). It was this initial event that formed the greater Carnarvon Basin, along with the Bonaparte and Canning basins (Purcell & Purcell, 1988). Well developed, low angle detachment faults with a limited regional extent (Figure 2.23) are the oldest

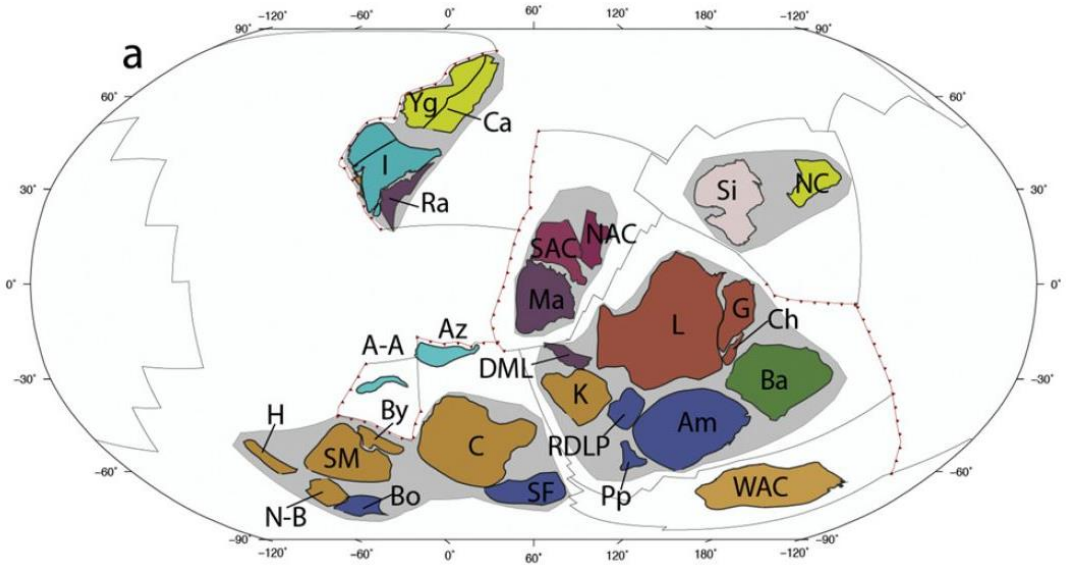

Figure 2.21 Tectonic geography showing the breakup of the Rodinian supercontinent (indicated by the shaded grey area) towards the end of the Precambrian (780 Ma), as modified from Merdith et al. (2017). A-A, Afif-Abas Terrane; Am, Amazonia; Az, Azania; Ba, Baltica; Bo, Borborema; By, Bayuda; Ca, Cathaysia (South China); C, Congo; Ch, Chortis; G, Greenland; H, Hoggar; I, India; K, Kalahari; L, Laurentia; Ma, Mawson; NAC, North Australian Craton; N-B, Nigeria-Benin; NC, North China; Pp, Paranapanema; Ra, Rayner (Antarctica); RDLP, Rio de la Plata; SAC, South Australian Craton; SF, São Francisco; Si, Siberia; SM, Sahara Metacraton; WAC,West African Craton. The longitude is arbitrary and unconstrained, and used as a guide. Cratonic crust is coloured by present day geography: North America, red; South America, dark blue; Baltica, green; Siberia, grey; India and the Middle East, light blue; China, yellow; Africa, orange; Australia, crimson; Antarctica, purple.

extensional features of the basin (Gartrell, 2000). The lower Paleozoic structures have a north-south orientation (McHarg, 2018). The Scholl Island Fault is an example of this (Figure 2.6; Gartrell, 2000; McHarg, 2018). Most detachment faults of this period sole out into shallow-dipping reflectors at depths between 10 and 15 km (Gartrell, 2000). They are potentially associated with the reactivation, or collapse, of a Proterozoic mobile belt (assumed to be in reference to the NWS Megashear; Gartrell, 2000) or Paleozoic extension (McHarg, 2018).

2.2.4.3. ORDOVICIAN TO LOWER CARBONIFEROUS

Baillie et al. (1994) make reference to a Lower Ordovician extensional event. This Lower Ordovician extension resulted in a northwards continuation of the Amadeus Basin (Figure 2.5), forming the early Canning and Roebuck basins (Figure 1.10; Baillie et al., 1994; Stagg et al., 1999). Following this, in the

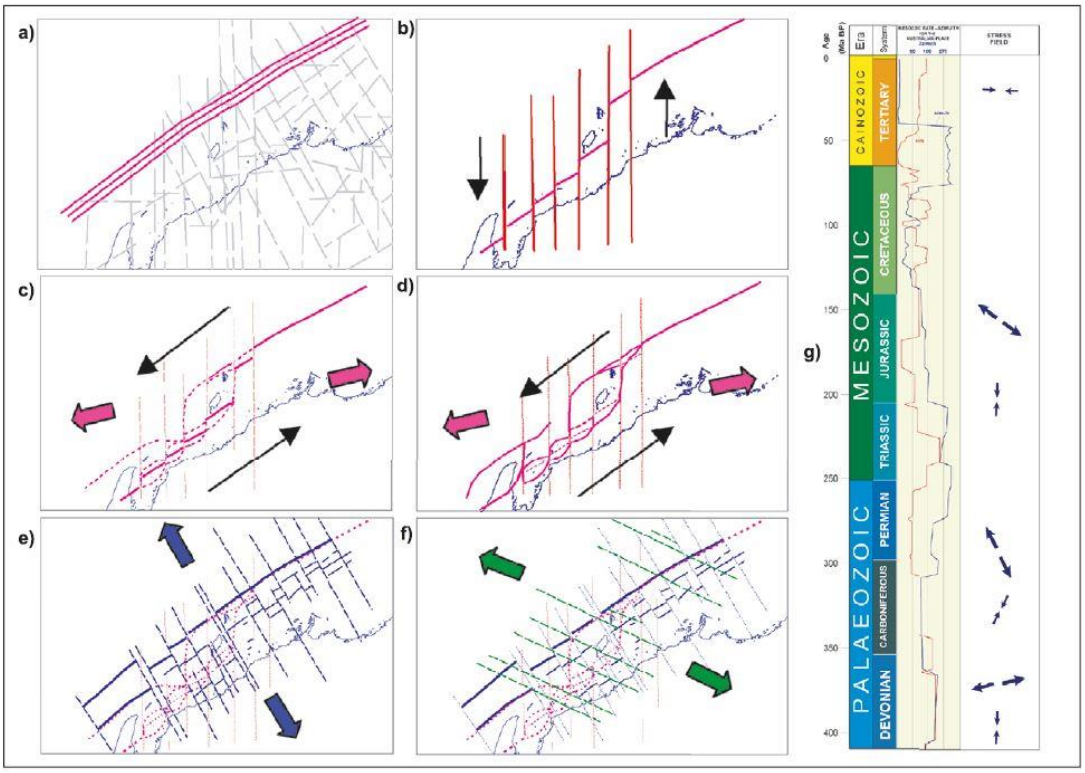

Figure 2.22 The NWS Megashear kinematics, a) Mesoproterozoic Megashear and pre-existing Precambrian reactive fabric; b) Megashear displacement during Pinjarra Orogeny; c) Upper Devonian reactivation of Megashear; Upper Devonian to early Carboniferous pull-apart basin system; e) late Carboniferous to early Permian extension; f) Incipient Cretaceous transfer structures and block rotation event; and g) major stress field changes through geological time; as per Pryer et al. (2002).

Middle Devonian an episode of northeast to southwest extension occurred (Baillie et al., 1994). This brought about the first major change to basin configuration, where the NWS (particularly the Roebuck Basin) was affected by a northeast to southwest extension (Baillie et al., 1994). At this time uplift also occurred over a broad area (Baillie & Jacobson, 1997).

Sometime between the Upper Devonian to lower Carboniferous extension occurred in a northeast orientation between the Pilbara, Kimberley and 'Darwin' blocks (Figure 2.5; AGSO North West Shelf Study Group, 1994; Baillie et al., 1994; Etheridge & O'Brien, 1994; Stagg et al., 1999). These early basin expressions were bound by regional sinistral strike-slip accommodation features, and to the north, the NWS Megashear (Figure 2.10; AGSO North West Shelf Study Group, 1994; Dooley & McClay, 1997; Pryer et al., 2002; Stagg et al., 1999). Pull-apart features formed along the megashear resulting

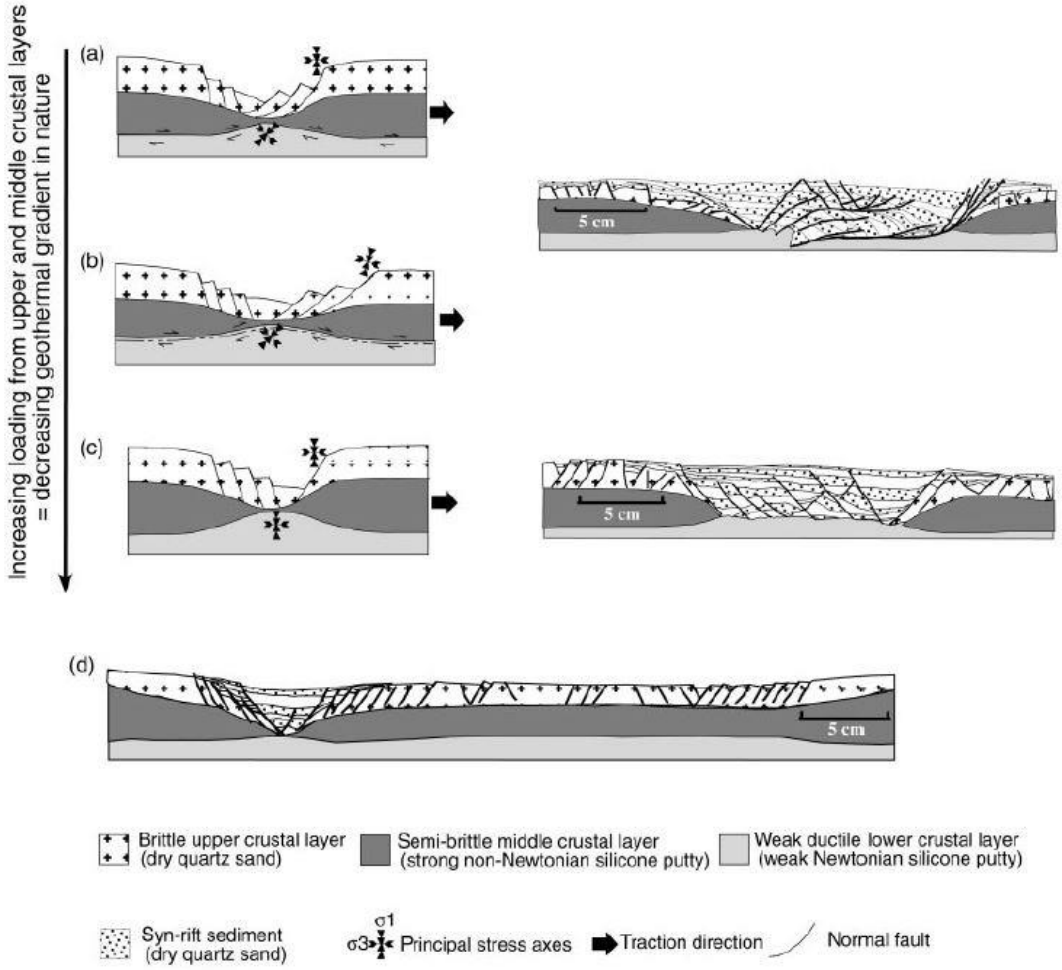

Figure 2.23 Low angle detachment faulting forming under thin and hot crustal conditions, with low angle normal faults forming later as per Mohr–Coulomb failure criteria, modified from Gartrell (2000).

in the later formation of some Barrow Sub-basin structures (Figure 2.22; Pryer et al., 2002). The NWS Megashear had significant control on the formation of many of the larger structures during the tectonic evolution of the NWS (Stagg et al., 1999). This extension event reactivated the northwest trending faults forming the Fitzroy Trough (Canning Basin), Petrel Sub-basin (Bonaparte Basin) and potentially the proto-Browse Basin (Figure 2.5; ASGO North West Shelf Study Group, 1994; Pryer et al., 2002). The formation of northwest and northeast trending accommodation zones in the Bonaparte Basin is linked to this event (Begg 1987; Drummond et al., 1991; O'Brien 1993; O'Brien et al., 1993; Pryer et al., 2002).

This northeast extension produced northwest trending fault bounded graben in the basement across areas of weakness formed in earlier stretching events (Chen, 2018), in particular impacting the Southern Carnarvon Basin, the Canning Basin and the Bonaparte Basin (Chen, 2018; Gunn, 1988; Iasky et al., 1998a, 1998b). This extension event, interpreted as transtension in the Northern Carnarvon Basin, was a prominent basin architecture controlling feature (Pryer et al., 2002). During this time the Northern Carnarvon Basin is observed to have undergone limited fault activity in the marginal areas (Hocking, 1988; Kingston et al., 1983). The northern structural trend of the more onshore portions of the greater Carnarvon Basin first developed in the Silurian, maturing through the Paleozoic (Hocking, 1990b).

2.2.4.4. MIDDLE CARBONIFEROUS TO PERMIAN

By the middle Carboniferous a global orogenic event related to the formation of Pangea (Figure 2.2) occurred, resulting in the uplift and deformation of the Australian Pacific margin, and extended into central Australia (Baillie et al., 1994; Powell & Veevers, 1987). Powell and Veevers (1987) have tentatively linked this to the formation of a major continental ice sheet over the southern Gondwana region in the mid-upper Carboniferous.

During the mid-upper Carboniferous rifting occurred once more when a continental sliver (Sibumasu; Figure 2.3b) separated from the Australian continent (AGSO North West Shelf Study Group, 1994; Bradshaw et al., 1988; Etheridge & O'Brien, 1994; Jablonski & Saitta, 2004; Marshall & Lang, 2013; Metcalfe, 1999, 2013; O'Brien et al., 1993; Pryer et al., 2002; Purcell & Purcell, 1988; Stagg et al., 1999; Veevers, 2006). During this Permo-Carboniferous extension the northeastern structural trend was developed (Figure 2.22e; Etheridge & O'Brien, 1994; Gartrell, 2000; McHarg, 2018) and reactivation occurred in the NWS Megashear in the Dampier Sub-basin (as invoked by Pryer et al., 2002). This event was a key basin shaping event in the Northern Carnarvon Basin (Pryer et al., 2002).

This event possibly occurred in two stages, initially in the lower-middle Carboniferous and a second time in the middle Carboniferous (Jablonski &

Saitta, 2004). Extension occurred in a northwest to southeast direction, orthogonal to the NWS Megashear (Pryer et al., 2002, 2014). Jablonski and Saitta (2004) found that this event initiated a broad period of subsidence, which continued into the Permian. In reference to the western margin, Etheridge and O'Brien (1994) found that the lithosphere was thinned from approximately 40 km to between 5 and 20 km (Figure 2.24; see Section 1.1.1.1. Domains and Their Phases, Necking Domain and Thinning Phase) in the NWS Megashear (ASGO North West Shelf Study Group, 1994; Stagg et al., 1999) during these events. This Carboniferous thinning impacted upon the lower crust (ASGO North West Shelf Study Group, 1994; Stagg et al., 1999).

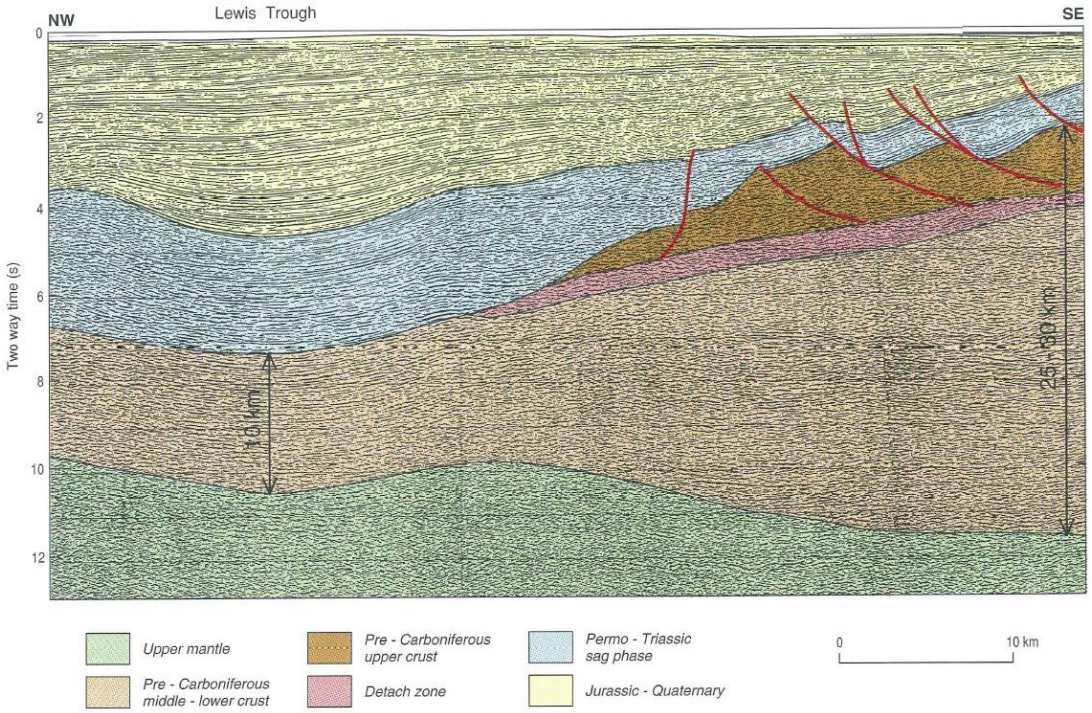

Figure 2.24 Extreme lithospheric thinning across the southern part of the North West Shelf. The interpretation is intended to demonstrate the relationship between the thinning and Permian extensional structures in the proximal part of the North West Shelf, deep seismic profile GSI 86/3185 as per Etheridge and O'Brien (1994).

The middle to upper Carboniferous events formed northeast to southwest faults while accommodation zones opened along north and northwest trends (AGSO North West Shelf Study Group, 1994; Etheridge & O'Brien, 1994; Jablonski & Saitta, 2004), influenced by the earlier structural grain of the Devonian aged Canning and Bonaparte rift system. The changes in basement

thickness caused by the Carboniferous to Permian extensions affected the later Mesozoic deformation events and the resulting structures, sub-basins and sediment supply points (Etheridge & O'Brien, 1994). The region most affected by Permo-Carboniferous extension was the Exmouth area (Pryer et al., 2014). Hocking (1990b) found that fault activity within the Northern Carnarvon Basin may have initiated as early as the upper Permian. McHarg (2018) later described Permian faults with a northeast trend.

Extension ceased in the lower, middle (Etheridge & O'Brien, 1994), or upper Permian (Chen, 2018), after which a regional phase of thermal subsidence (sag phase) occurred following the complete decay of a Pangean thermal anomaly (Etheridge & O'Brien, 1994; Falvey & Mutter, 1981; Jablonski & Saitta, 2004; Lister et al., 1986, 1991; McKenzie 1978; Veevers, 2000, 2006). This period of subsidence resulted in the deposition of thick late Permian to Triassic strata over much of the marginal areas (Figure 2.13; Etheridge & O'Brien, 1994; Stagg et al., 1999; Veevers, 2006). There is no evidence of major crustal extension for the remaining Permian, although some minor reactivation events did occur, such as the late Permian Bedout Movement, the effects of which are mostly seen in the southern NWS (AGSO North West Shelf Study Group 1994; Etheridge & O'Brien, 1994; Forman & Wales 1981; Horstman & Purcell, 1988; Symonds et al., 1994).

2.2.4.5. INDUAN – NORIAN (TRIASSIC)

Following the extensional events of the Paleozoic, thermal subsidence continued from the Permian into the Upper Triassic (Etheridge & O'Brien, 1994; Stagg et al., 1999; Veevers, 2006). This was briefly interrupted along the inboard margin by a major uplift and erosion event in the Norian (Forman & Wales, 1981; Longley et al., 2002; Marshall & Lang, 2013). This movement resulted in a series of structural highs and lows that formed isolation barriers between the Beagle and Dampier sub-basins (Blevin et al., 1994; Geoscience Australia, 2014a, 2019; Smith et al., 1999). In the Canning Basin (Figure 1.10) movement at this time is referred to as the Fitzroy movement (Etheridge & O'Brien, 1994; Forman et al., 1981). Other work tentatively links the Fitzroy

Movement to events in other NWS basins (Longley et al., 2002; O'Brien et al., 1993, 1996; Stagg et al., 1999) including in the Northern Carnarvon Basin, expressed as the Norian Unconformity (Forman & Wales, 1981; Longley et al., 2002; Marshall & Lang, 2013). However, this is in contrast to the original description of Forman et al. (1981) who regarded the Fitzroy Movement as only affecting the Fitzroy Graben (Figure 2.5). Drift of the Lhasa Block (Figure 2.3d) also occurred at this time, opening the Ceno-Tethys (Chen, 2018; Longley et al., 2002; Metcalfe, 1999; Metcalfe, 2013). Towards the end of the Norian, a section of the southern Exmouth Plateau subsided below sea-level (Jablonski & Saitta, 2004). Chen (2018) observed that Triassic fault activity is rare in the Northern Carnarvon Basin, with the exception of major tectonic development in the northern part of the plateau during the Mid-Upper Triassic.

2.2.4.6. UPPER TRIASSIC, RHAETIAN – LOWER CRETACEOUS

Rifting recommenced in the Uppermost Triassic or Lowermost Jurassic (Baillie et al., 1994; Blevin et al., 1994; Etheridge & O'Brien, 1994; Geoscience Australia, 2014a, 2019; Smith et al., 1999) with an E-W extension direction (Jitmahantakul & McClay, 2013). This event may correlate to the later episode of Metcalfe's (1996) Sibumasu rifting event. During this same time extension and flank uplift in the Dampier Sub-basin occurred (Figure 2.25; Driscoll & Karner, 1996, 1998). This Mesozoic rift activity developed the present-day structural elements and sub-basins (Baillie et al., 1994; Blevin et al., 1994; Etheridge & O'Brien, 1994; Geoscience Australia, 2014a, 2019; Smith et al., 1999). In the Lowermost Jurassic, a period of right-lateral wrenching affected the western and northwestern margins of Australia (Veevers, 2006). This resulted in Lower Jurassic subsidence over the margin (Jablonski & Saitta, 2004).

In the Triassic rifting and uplift recurred (Jitmahantakul & McClay, 2013; Purcell & Purcell, 1988). Jablonski (1997) interpreted the initiation of rifting as occurring in the Lower Triassic. More generally the event is referenced as

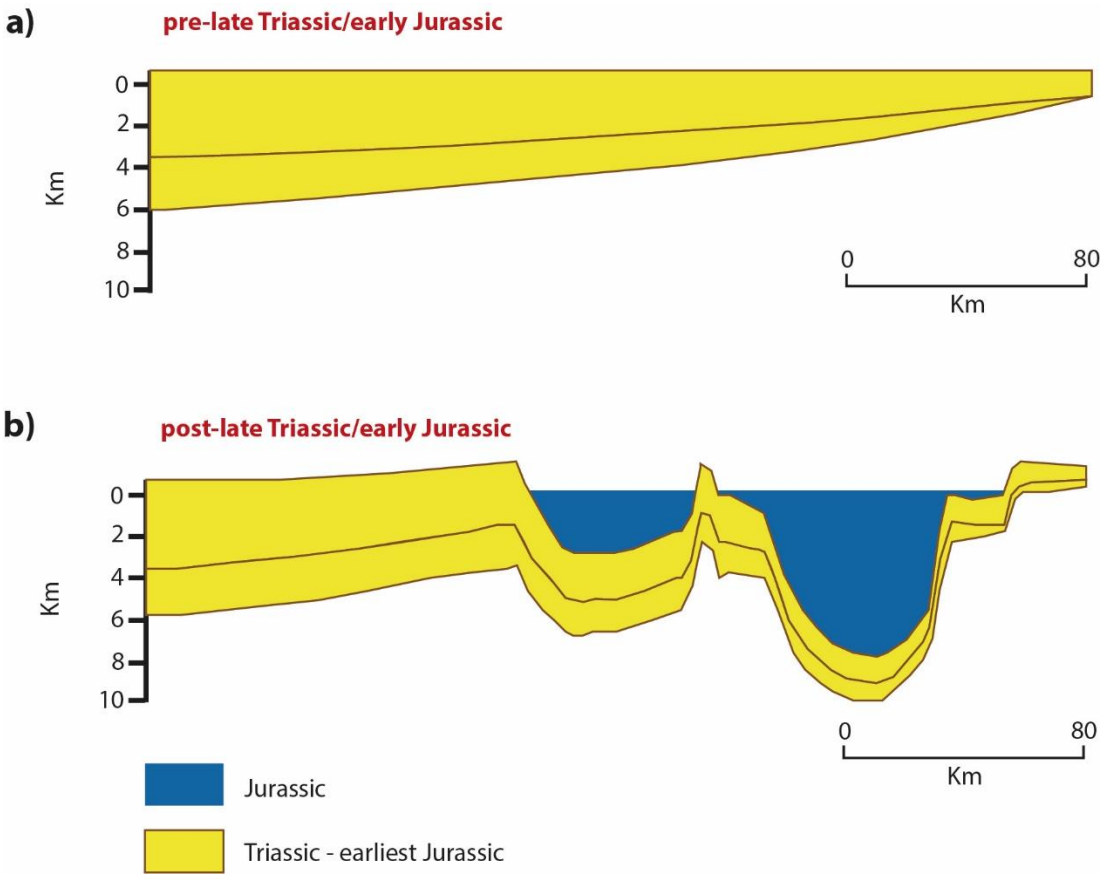

Figure 2.25 Flank uplift of the Dampier Sub-Basin as a result of east-west extension in the Uppermost Triassic to Lowermost Jurassic, modified from Driscoll and Karner (1998).

occurring between the Uppermost Triassic and Lowermost Jurassic (Baillie & Jacobson, 1997; Baillie et al., 1994; Blevin et al., 1994; Etheridge & O'Brien,1994; Geoscience Australia, 2014a, 2019; Rohrman, 2015; Smith et al., 1999). It is possible this discrepancy comes from the initial deformation in response to rifting not occurring uniformly across the basin (McHarg, 2018). The continuing Jurassic extension provided further accommodation space on the Exmouth Plateau (Rohrman, 2015) as the northern plateau also subsided below sea-level (Jablonski & Saitta, 2004). Normal faulting on the Exmouth Plateau at this time displays evidence of fault growth during sedimentation (Figure 2.14; Gartrell, 2000). Yeates et al. (1987) referred to this event as creating Rhaetian aged fault block uplift on the Exmouth Plateau Arch (Figure 2.14). Bilal et al. (2018) also identified rift onset through syn-kinematic strata at this time.

Seafloor spreading of the Argo (and Gascoyne) Abyssal Plain(s) (Figure 1.11) represent the rifting of continental fragments during the Upper Jurassic (Heine & Müller, 2005). These fragments are the Argoland or West Burma blocks (Figure 2.3; Heine & Müller, 2005; Metcalfe, 1996; Stagg et al., 1999). Longley et al. (2002) identified the separation of the West Burma blocks during the Sinemurian (Block I; Figure 2.3d), the Callovian (Block II; Figure 2.3d) and the Kimmeridgian-Tithonian (Block III; Figure 2.3d) in support of the broad timings described by Gradstien and Ludden (1992). The orientation of Argo seafloor spreading indicates that this phase of extension occurred in a north northwest to south southeast direction (Falvey & Mutter, 1981). This orientation is reflected in the Upper Jurassic normal faulting that occurred at this time in the NWS (Patillo & Nicholls, 1990). This resulted in the development of the Argo Abyssal Plain (Figure 1.11; Baillie et al., 1994; Heine & Müller, 2005; Marshall & Lang, 2013; Powell et al., 1988; Rohrman, 2015; Stagg et al., 1999; Veevers, 2006; Veevers et al., 1991). These drift events reactivated Palaeozoic structures forming northeast trending graben on the NWS (AGSO Group, 1994).

Plate divergence and seafloor-spreading of Jurassic age is a cause of the complex architecture of the north-western margin (Veevers, 1986), particularly in relation to the formation of marginal plateaus and abutting abyssal plains (Veevers, 1986). The seafloor spreading of the Argo Abyssal Plain may have resulted in areas of uplift, resulting in the accumulation of thin sequences (Bradshaw et al., 1998). Stagg et al. (2004) state that this uplift was thermally driven. Most uplift occurred on the margins of the plateau, and extensive faulting resulted (Stagg et al., 2004).

The potential impact of a mantle plume on the Exmouth Plateau and Exmouth Sub-basin occurred in the Upper Jurassic (Rohrman, 2015) to Lower Cretaceous (Figure 2.26; Veevers, 2006) and resulted in tectonic uplift of approximately 500 m of pre-late Jurassic strata (Rohrman, 2015; Veevers, 2006). This plume resulted in between 30 and 40 km of crustal thinning in the

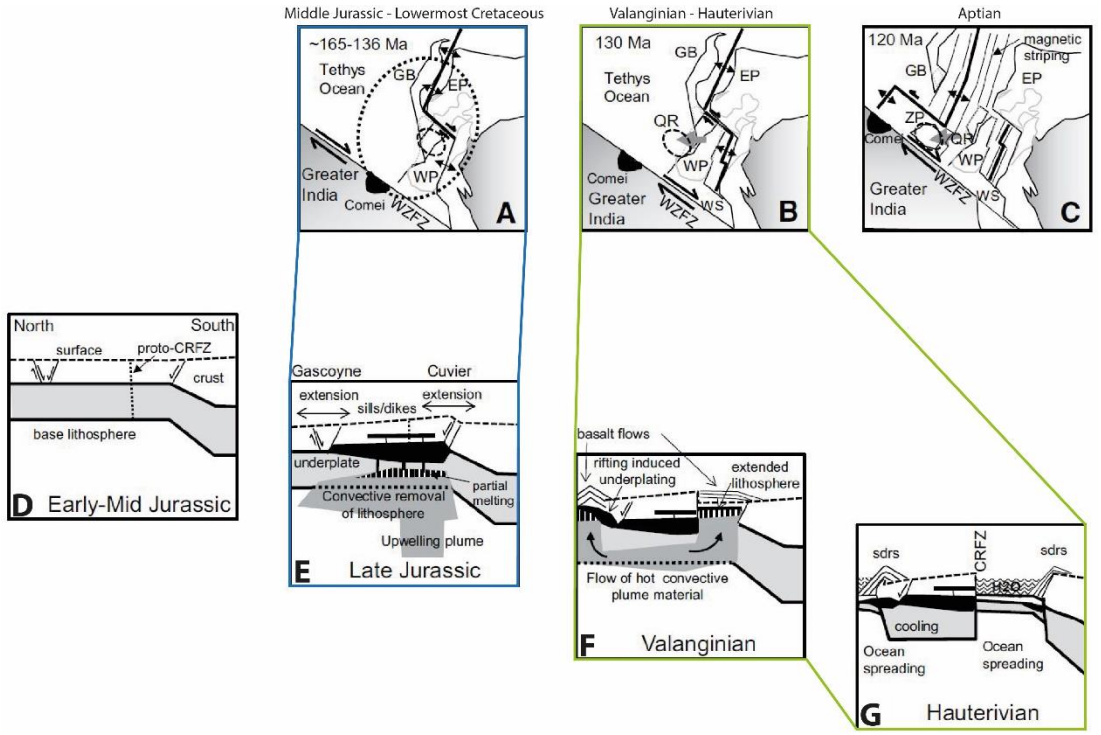

Figure 2.26 Mesozoic mantle plume activity associated with extensional events which formed the Exmouth Plateau, modified from Rohrman (2015).

GB-Gascoyne Block, EP-Exmouth Plateau, WP-Wallaby Plateau, QR-Quokka Rise, WS-Wallaby Saddle, WZFZ-Wallaby Zenith Fracture Zone, ZP-Zenith Plateau, CRFZ-Cape Range Fracture Zone, sdrs-Seaward dipping reflectors

Sonne Ridge-Sonja Ridge-Cape Range fracture zone (Figures 2.5 & 2.26; Rohrman, 2015). The emplacement of this mantle plume occurred prior to Cretaceous continental breakup (Rohrman, 2015). A related Upper Jurassic uplift event occurred in the Southern Carnarvon Basin (Wulff & Barber, 1995).

Seafloor spreading was reorganised in the Valanginian when the spreading centre shifted south (Figure 2.1; Gibbons et al., 2012, 2015). This event resulted in the formation of the Gascoyne and Cuvier Abyssal plains (Figure 1.11; Baillie & Jacobson, 1997; Baillie et al., 1994; Gibbons et al., 2012; Haq et al., 1992; Jablonski, 1997; Marshall & Lang, 2013; Powell et al., 1988; Purcell & Purcell, 1988; Rohrman, 2015; Stagg et al., 1999; Veevers et al., 1991; Veevers, 2006). This change in the location of spreading centres could be related to a mantel plume enhancing the yield strength of the Argo region

(Müller et al., 2002). Uplift then occurred and the region transitioned into a passive margin (Paumard et al., 2018).

Triassic and Jurassic tectonic activity is expressed in the northeastern structural trend of the Northern Carnarvon Basin (Figure 2.8; Hocking, 1990b) and was concentrated over the NWS Megashear (ASGO North West Shelf Study Group, 1994). Stagg and Colwell (1994) identified Triassic faults in the Northern Carnarvon Basin as the dominant structural features. Based on data available at the time, Stagg and Colwell (1994) interpreted three main types of faulting associated with this interval; extensional, transtensional and transpressional. The extensional faulting is evident in the outer Exmouth Plateau where faults sole out ocean wards near the base of the Triassic or in the pre-Triassic sequence, and beneath the Enderby Terrace (Figure 2.6) where the faults detach landwards in the basement (Stagg & Colwell, 1994). The transtensional faults, which could be the reactivation of deeper high angle fault zones, are found in the Exmouth Plateau with negative flower structures (Stagg & Colwell, 1994) which are not seen on 3D seismic data. Transpressional faults on the oceanward flank of the Exmouth Sub-basin and Rankin Platform, are associated with compressional anticlines, and coalesce at depth into narrow fault zones (Stagg & Colwell, 1994). More recently, these structures have been interpreted as fault propagation folds (McHarg et al., 2018). In the Northern Carnarvon Basin extension related to drifting is oblique to the earlier Permo-Carboniferous structures, forming north and northeast trends (Figure 2.8; Jimanhantakul & McClay, 2013; Elders et al, 2016; Black et al., 2017). The dominance of northerly trends suggests the east drifting Greater India had most impact on the Northern Carnarvon Basin (McHarg et al., 2018).

From the upper Tithonian to the lower Berriasian there was no-to limited fault movement and limited subsidence occurring in the Northern Carnarvon Basin (Hocking, 1990b; Paumard et al., 2018). The lack of fault activity during his time was also observed in the Dampier Sub-basin, though this was attributed to non-deposition (McHarg, 2018). This suddenly changed during the Berriasian (143.5 Ma) as active rifting events resulted in tectonic subsidence

and hinterland uplift (Paumard et al., 2018). This same event resulted in a shift of extension direction which is evident in Tithonian aged fault block rotation (Pryer et al., 2002).

2.2.4.7. UPPER CRETACEOUS TO PRESENT DAY

The Cenomanian marked a change in tectonic patterns for Australia (Baillie et al., 1994; Powell et al., 1988; Veevers et al., 1991). On the southern margin of Australia, the Southern Ocean underwent a slow stage of seafloor spreading, initiating in the Cenomanian and continuing until the Eocene global plate reorganisation when dominant seafloor spreading shifted from the Indian-Australian region to the Australia-Antarctica region (Figure 2.27; Baillie et al., 1994). A new east trending spreading ridge formed close to India in the Indian Ocean (Figure 2.1; Baillie et al., 1994). India continued to move north at a fast rate (19.5 cm/year) (Klootwijk et al., 1992). During this time, uplift and inversion (see Section 2.2.3. Inversion and Reactivation) due to southern margin rifting took place in the southern reaches of the NWS (Bradshaw et al., 1998; Jitmanhantakul & McClay, 2013; Tindale et al., 1998) and block rotation and uplift occurred further to the north (Blevin et al., 1998). This event impacted the structural evolution of the Exmouth Plateau (Bradhaw et al., 1998) and transpressional reactivation occurred (Longley et al., 2002). The NWS subsided through the Upper Cretaceous and Cenozoic as carbonate sediments accumulated across the shelf (Purcell & Purcell, 1988).

In the uppermost Paleogene to lower Neogene, the leading edge of Australia was approaching the area of the Banda Arc collision (Baillie et al, 1994; Keep et al., 2002; Powell & Johnson, 1980). The eventual collision of the Australian Plate and the Sunda Arc Subduction Zone in the middle Miocene resulted in sinistral torsion, leading to dextral shear of older fractures near the continent-ocean boundary and transforming former extensional basins on the Western Australian margin (Baillie et al., 1994). This collision resulted in the inversion of some faults in the NWS Megashear leading to the Cape Range and Barrow Anticlines (Figure 2.10c; Pryer et al., 2002). Late Miocene wrenching caused the rejuvenation of older structures, tightening some Cretaceous folds, and

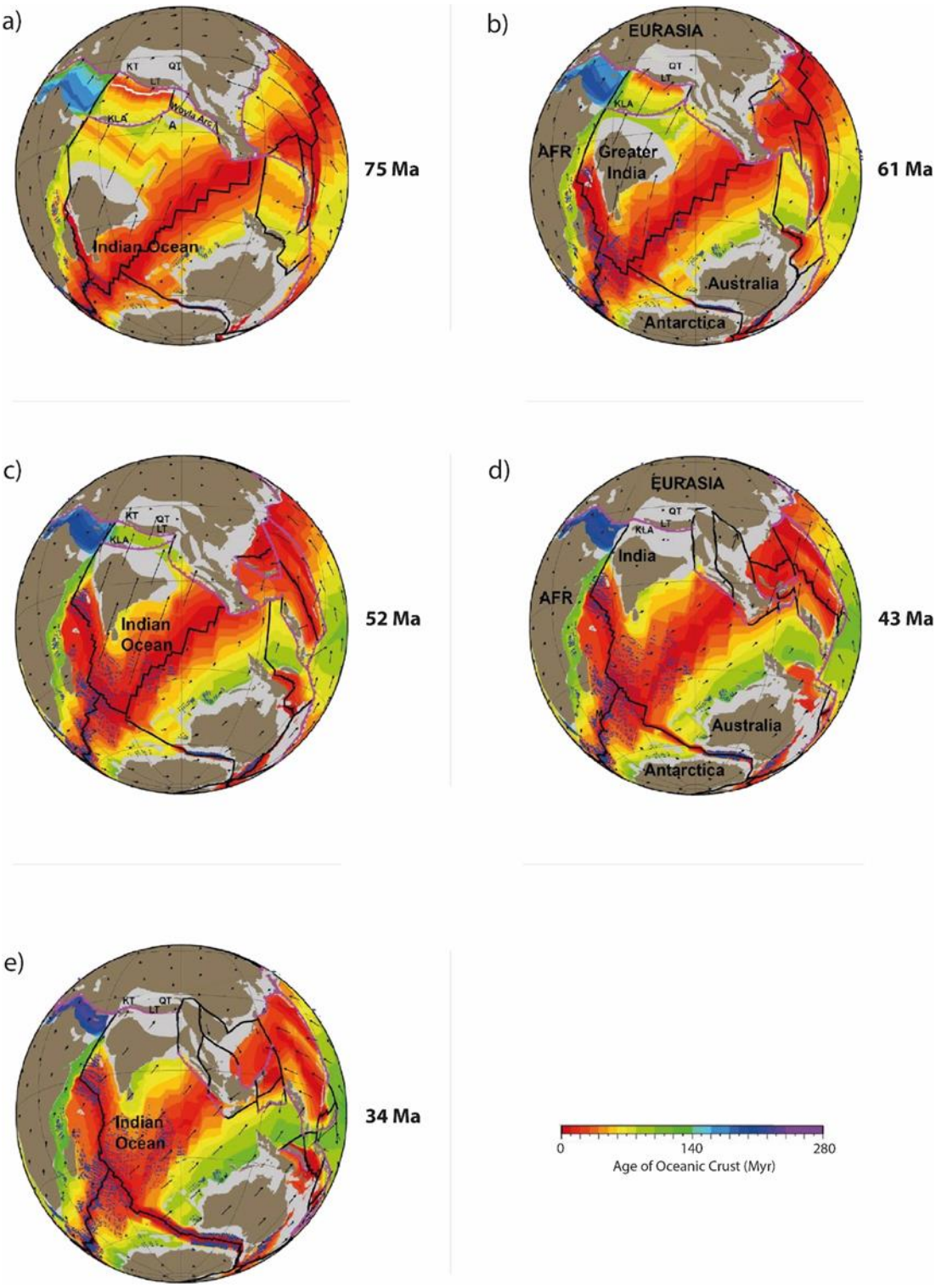

Figure 2.27 Seafloor spreading on the northwest margin of Western Australia, and on the southern Australian margin at the Australian – Antarctic plate boundaries, modified from Gibbons et al. (2015).

further faulting activity (Baillie & Jacobson, 1997; Jitmanhantakul & McClay, 2013). The margin also tilted to the west at this time (Tindale et al., 1998). The Timor-Banda Orogen is the product of this collision event (which occurred later, during the Neogene; Keep et al., 2002; Longley et al., 2002; Metcalfe, 1999). Neogene deformation within the Northern Carnarvon Basin was largely limited to the inboard, and had a limited impact (Keep et al., 2007). Ongoing northwards movement and collision of the Australian continent continues at the present day (Metcalfe, 2013).

2.2.5. STRATIGRAPHIC BASIN FILL

This section details the stratigraphic record of the Exmouth Plateau. The focus is on the Mesozoic aged stratigraphy. Many of the stratigraphic units recognised on the Exmouth Plateau (Figure 2.18) have more than one lithostratigraphic name. An effort has been made to condense the record by describing a single unit, as opposed to producing a section on all the stratigraphic units and equivalents separately. In addition, large volumes of literature have limited information of the depositional history of the Exmouth Plateau as an independent feature, and as such many of the following descriptions were derived from the broader Northern Carnarvon and greater Carnarvon basins. Additionally, many publications favour the division of the stratigraphy into a variety of packages based on the identified tectonic phases. However, as the tectonic phases of the Northern Carnarvon Basin are split in numerous ways by various authors, stratigraphic descriptions will be presented here in broad geological age ranges.

The complete sedimentary infill of the Northern Carnarvon Basin is estimated to be between 12 and 15 km (Figures 2.13 & 2.15; Geoscience Australia, 2014a; Hocking, 1990b; Stagg & Colwell, 1994), spanning from the Mesozoic to the Cainozoic (Hocking, 1990b). The earlier Paleozoic deposits were thinner, reaching thickness up to 5 km over the plateau (Felton et al., 1992). A widely accepted consensus is that stratigraphic development was a direct result of the episodic nature of seafloor spreading and rifting across the NWS (Marshall & Lang, 2013). Marshall and Lang (2013) noted that the stratigraphic

architecture was also closely related to tectonics, eustacy and sedimentation rates, and how these interact; resulting in changes to accommodation space. Cathro and Karner (2006) believed the deposition of sediments into the sub-basins was largely controlled by the Lower Cretaceous extension related topography.

2.2.5.1. PALEOZOIC

Little information of the oldest and deepest stratigraphical fill of the Northern Carnarvon Basin, and Exmouth Plateau, is know from direct observation. Due to the depths of the older strata deposits from the Southern Carnarvon Basin and near-shore portions of the Northern Carnarvon Basin are used as analogues (AGSO North West Shelf Study Group, 1994) for much of the older sequences.

The infill of the Northern Carnarvon Basin began in Ordovician to Silurian times, depositing a 4 km thick succession into the interior sag basin of the time (Baillie & Jacobson, 1997). Paleozoic sedimentation spanned terrestrial, fluvial and shallow marine environments (Figure 2.28; Hocking, 1988, 1990b). Sediment was occasionally contributed from the periodic faulting on the basin margin (Hocking, 1988). Devonian stratigraphy is described as a collection of thin sedimentary units (Hocking, 1988).

In the mid-Carboniferous, a period of major tectonic activity resulted in the folding and faulting of stratigraphy along a north trending axis (Hocking, 1988). Glacially influenced sedimentation began again in the late Carboniferous (Figure 2.29; Baillie & Jacobson., 1997; Hocking, 1988) and continued into the early Permian before ceasing (Hocking, 1988). Following this, non-glacial sedimentation recommenced and continued into the late Permian (Figure 2.28; Hocking, 1988). The AGSO North West Shelf Study Group (1994) described the Permian deposits as occurring during a sag phase.

2.2.5.2. TRIASSIC

The Triassic aged deposits in the Exmouth Plateau are thicker than in the inboard sub-basins (Figure 2.13; Exon & Willcox., 1978; Yeates et al., 1987).

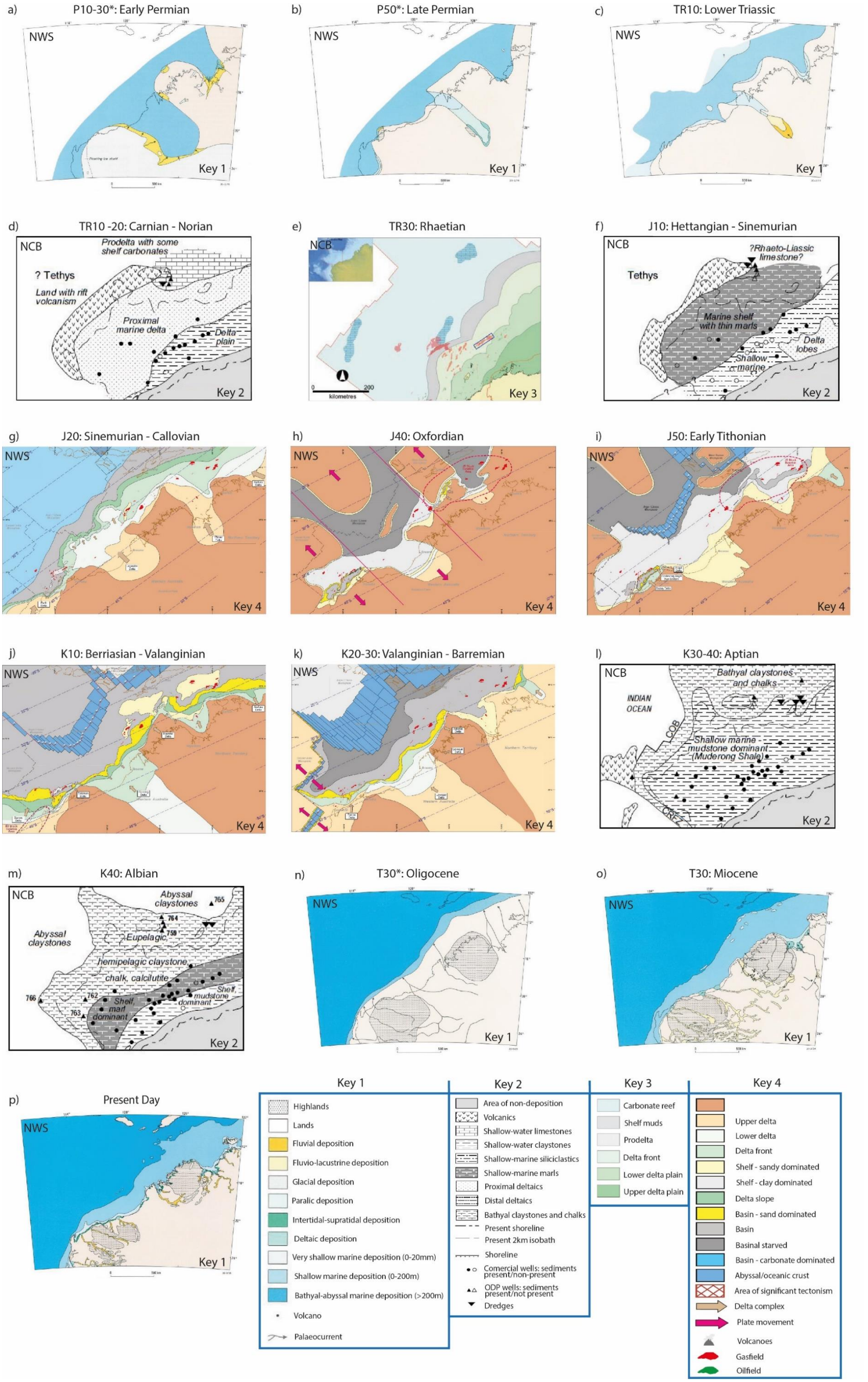

Figure 2.28 Paleogeography of the NWS of the Australian Continent over time, from the Early Permian until Present day. Modified from Adamson et al. (2013), Bradshaw et al. (1988); Stagg et al. (2004), and Longley et al. (2002).

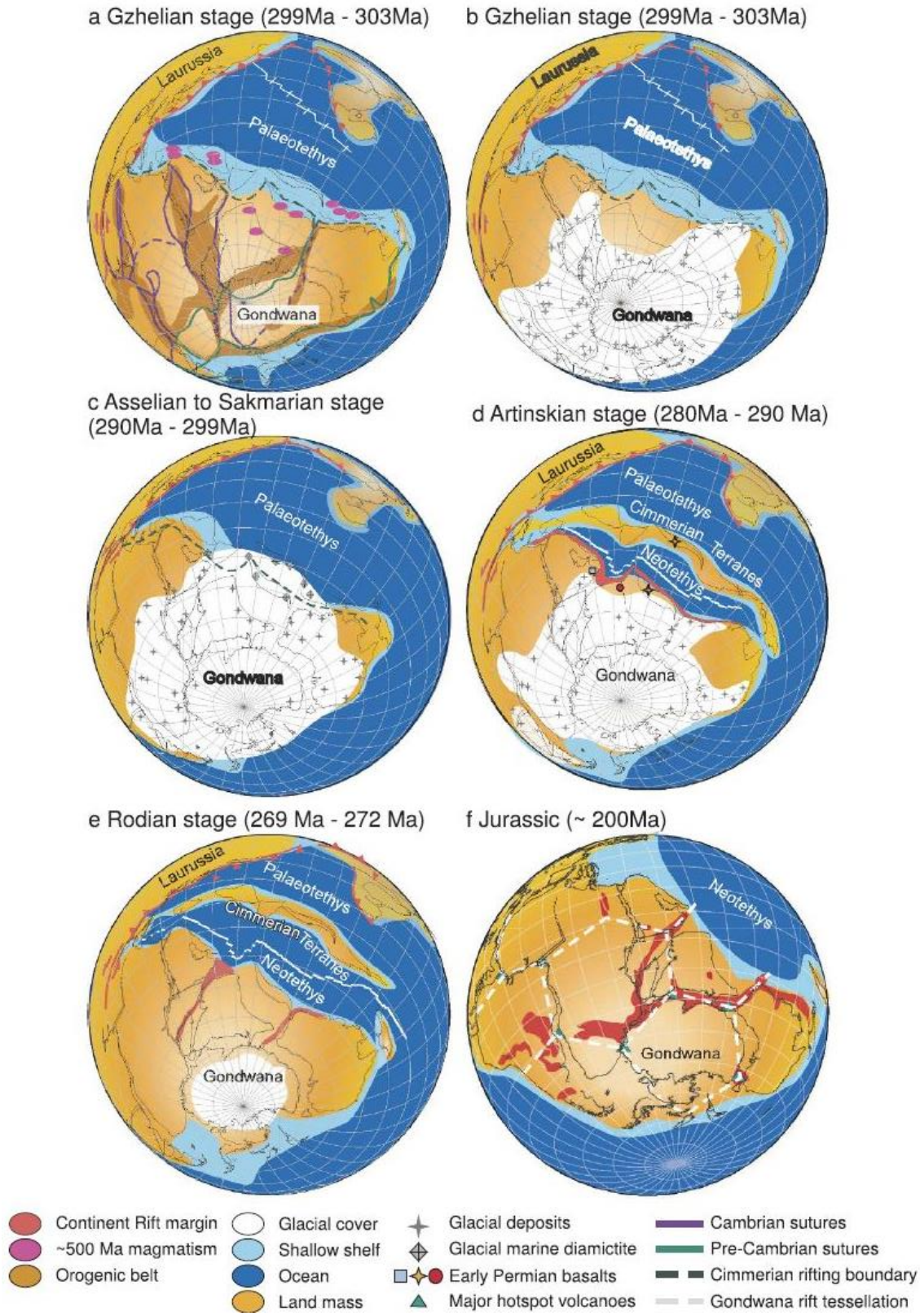

Figure 2.29 Glacial history of Pangea from the Permian to the Jurassic, as per Yeh and Shellnutt (2016).

Initial sedimentation at this time occurred in a broad subsiding basin (Adamson et al., 2013). Syn-rift deposition is identified in the outer Exmouth Plateau (AGSO North West Shelf Study Group, 1994). The sedimentation was highly varied across widespread deltaic systems, nearshore marine, and shelfal carbonates (Figure 2.28; Adamson et al., 2013). Large scale erosion of Triassic material has occurred along the Rankin and Gordon Platforms (Adamson et al., 2013).

Sedimentation is largely layer-cake (Figure 2.30; AGSO North West Shelf Study Group, 1994) due to deposition during a period of low to no tectonic activity (Adamson et al., 2013). Deposition occurs across three broad areas within the Northern Carnarvon Basin; the inboard, medial and outboard (Adamson et al., 2013). Seismic information suggests a thickness of up to 6 km in the Exmouth Plateau (Adamson et al., 2013; AGSO North West Shelf Study Group, 1994). The Exmouth Plateau corresponds to the medial and outboard areas of deposition (Adamson et al., 2013). In the north of the plateau, extending into the Roebuck Basin, a lava-flow which is of presumed Triassic age is observed (Chen, 2018).

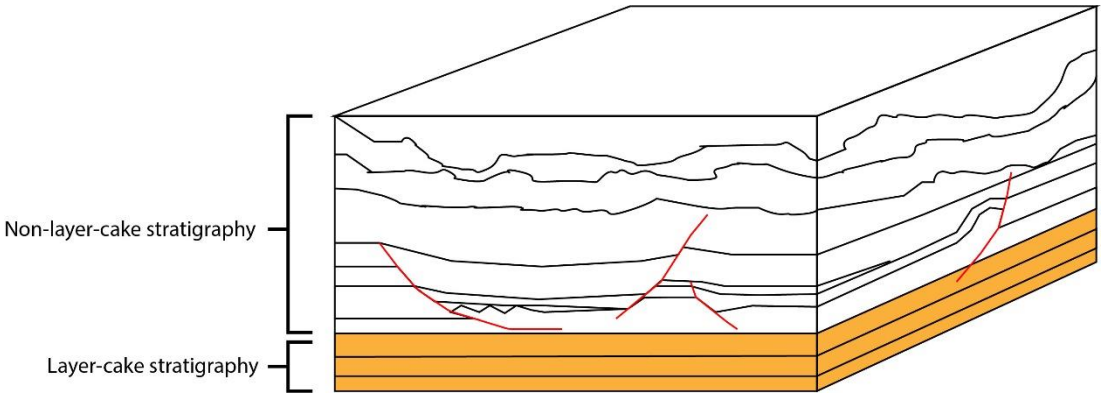

Figure 2.30 Block diagram showing the parallel stratigraphy of layer-cake style deposition.

2.2.5.3. JURASSIC

Jurassic deposits are thin, when compared to the underlying Triassic strata (Figure 2.13) or absent across the western Exmouth Plateau (Geoscience Australia, 2014a) and likely impacted by fault block formation (Exon & Willcox, 1978). Driscoll and Karner (1996) further describe syn-rift sediment wedges

that were deposited in the inboard basins, while the structurally higher Exmouth Plateau and Alpha Arch (Figure 2.6) were relatively sediment starved. Sedimentation was controlled by the transtensional basin collapse along the footwall of Paleozoic faults, which rapidly increased accommodation space (Baillie & Jacobson, 1997; Colwell et al., 1993; Wulff & Barber, 1995). Fault activity in the Exmouth Plateau during the Rhaetian resulted in thinner Jurassic aged deposits in comparison to the inboard depocentres (Exon & Willcox., 1978; Geoscience Australia, 2014a; Yeates et al., 1987) where deposits of the early to Middle Jurassic age are between 1 and 2 km thick (Stagg et al., 2004). The early to Middle Jurassic deposition on the Exmouth Plateau experienced a hiatus, likely relating to uplift (Figure 2.18; Felton et al., 1992). Stagg et al. (2004) also noted that Jurassic sedimentation on the plateau was absent, except in the northern plateau. Wulff & Barber (1995) theorised that large amounts of sediment deposited in the late Jurassic were transported into the rift system forming the inboard sub-basins, from the elevated footwall margins.

Deposition during the Callovian to Oxfordian times within the Barrow and Dampier Sub-basins was controlled by developing half-graben features (Wulff & Barber, 1995). The later Kimmeridgian and Tithonian deposits were much wider spread (Wulff & Barber, 1995). From the Oxfordian to the Valanginian, sediment deposition was controlled by the rifting of continental blocks and seafloor spreading (Longley et al., 2002). Higher sedimentation rates occur following the J10 (earliest Jurassic, Figure 2.18) and continue throughout the J20 (Lower to Middle Jurassic, Longley et al., 2002; Marshall & Lang, 2013). Spencer et al. (1995) found that the Plateau contained thin late Jurassic deposits and Haq et al. (1992) found that Jurassic strata were not deposited or preserved in some locations. This was contradicted by Longley et al. (2002) and Marshall and Lang (2013) who described the outboard sequences of this age as thick.

The continent-ocean boundary to the west of the Exmouth Plateau, is dominated by volcanic activity (AGSO North West Shelf Study Group, 1994). The volcanic systems in this region have also impacted on the infill history of

the Exmouth Plateau. The western edge of the plateau contains Triassic to Jurassic aged volcanic units, identified as flood basalts (Exon & Buffler, 1992). AGSO North West Shelf Study Group (1994) suggest that these volcanics likely extended along the outer margin of the plateau.

2.2.5.4. CRETACEOUS

Uplift in the Southern Carnarvon Basin occurred during the Upper Jurassic (Wulff & Barber, 1995). Also occurring at this time was volcanic activity associated with continental breakup (Figure 2.1; Exon & Buffler, 1992). The impact of a potential mantle plume into the Exmouth region (Figure 2.26; Exmouth Plateau and Sub-basin) along the Cape Range Fracture Zone (Figure 2.6) resulted in a change to the direction of sediment supply (Wulff & Barber, 1995). Previously supply had been from the eastern margin in the Jurassic (Wulff & Barber, 1995). Supply came from the south in the early Cretaceous (Wulff & Barber, 1995; Rohrman, 2015). The resulting depositional sequences of the early Cretaceous are thicker in the western part of the Exmouth Plateau, in comparison to the Jurassic (Bradshaw et al., 1998), but sediment supply was low supply across most of the Exmouth Plateau (Swift et al., 1988). Accommodation space in the Barrow and Dampier sub-basins at this time was a result of thermal subsidence (Cathro & Karner, 2006). Following this, a marine transgression occurred and a regionally significant shale (Figures 2.18, & 2.28, K20 Valanginian – Hauterivian deposition) was deposited over much of the Northern Carnarvon Basin. In the late Cretaceous an open marine setting prevailed on the passive continental margin (Figure 2.28; Cathro & Karner, 2006; Condon, 1967a; Geoscience Australia, 2014a).

2.2.5.5. CENOZOIC TO RECENT TIMES

The marine conditions from the later Cretaceous continued into the Cenozoic (Figure 2.28; Cathro & Karner, 2006; Condon, 1967a; Geoscience Australia, 2014a). Carbonate deposition was dominant in the early Cenozoic during the continued northward drift of the continent (Figure 2.18; Baillie et al., 1994; Cathro & Karner, 2006). Deposition of a prograding carbonate wedge takes place across the margin (Stagg et al., 1999).

2.2.6. HYDROCARBON POTENTIAL

The Northern Carnarvon Basin contains two petroleum systems (Geoscience Australia, 2019). These petroleum systems fall into the more regional petroleum supersystem framework of Bradshaw (1993) and Bradshaw et al. (1994, 1997). This framework for petroleum systems linked the Australian hydrocarbon basins by age, facies, tectonic evolution and the generation of hydrocarbons (Bradshaw 1993; Bradshaw et al., 1994, 1997). The internal petroleum systems are then defined by play elements and the impact of tectonic and/or climatic influences (Bradshaw 1993; Bradshaw et al., 1994, 1997; Geoscience Australia, 2019). The two supersystems of the Northern Carnarvon Basin are the Westralian 1 and Westralian 2 supersystems (Bradshaw et al., 1994; Spencer et al., 1993, 1994, 1995).

In the more widely known couplet source-reservoir nomenclature (Magoon & Dow, 1994) the two petroleum systems of the basin are the 'Locker/Mungaroo–Mungaroo/Barrow' petroleum system (Figures 2.18, & 2.31) and the 'Dingo–Mungaroo/Barrow' petroleum system (Figures 2.18, & 2.32; Bishop, 1999). As the couplet nomenclature highlights, the source rocks of these systems are the Triassic Mungaroo Formation and equivalents (Locker/Mungaroo–Mungaroo/Barrow), the Locker Shale (Locker/Mungaroo–Mungaroo/Barrow), and the Jurassic Dingo Claystone (Dingo–Mungaroo/Barrow; Figures 2.18, 2.31, & 2.32; Geoscience Australia, 2019). Other petroleum systems do exist within the basin (Figures 2.18, 2.19, 2.31, & 2.32), though these remain the dominant systems (Geoscience Australia, 2019; Summons et al., 1998). Some petroleum systems are known to occur outside of the Mesozoic stratigraphy (Figure 2.19; Baillie & Jacobson, 1997).

The 'Locker/Mungaroo–Mungaroo/Barrow' system is the more gas prone of the two major systems (Geoscience Australia, 2019). Covering a wide region of the basin this system extends on to the margins of the Exmouth Plateau (Geoscience Australia, 2019). This system sits within the Westralian 1 Petroleum Supersystem (Bradshaw et al., 1994; Edwards & Zumberge, 2005; Edwards et al., 2007). The 'Dingo–Mungaroo/Barrow' petroleum system is more oil-prone (Bishop, 1999), although this system is more localised,

occurring within the *en-echelon* sub-basins (Geoscience Australia, 2019). It is a part of the Westralian 2 Petroleum Supersystem (Bradshaw et al., 1994).

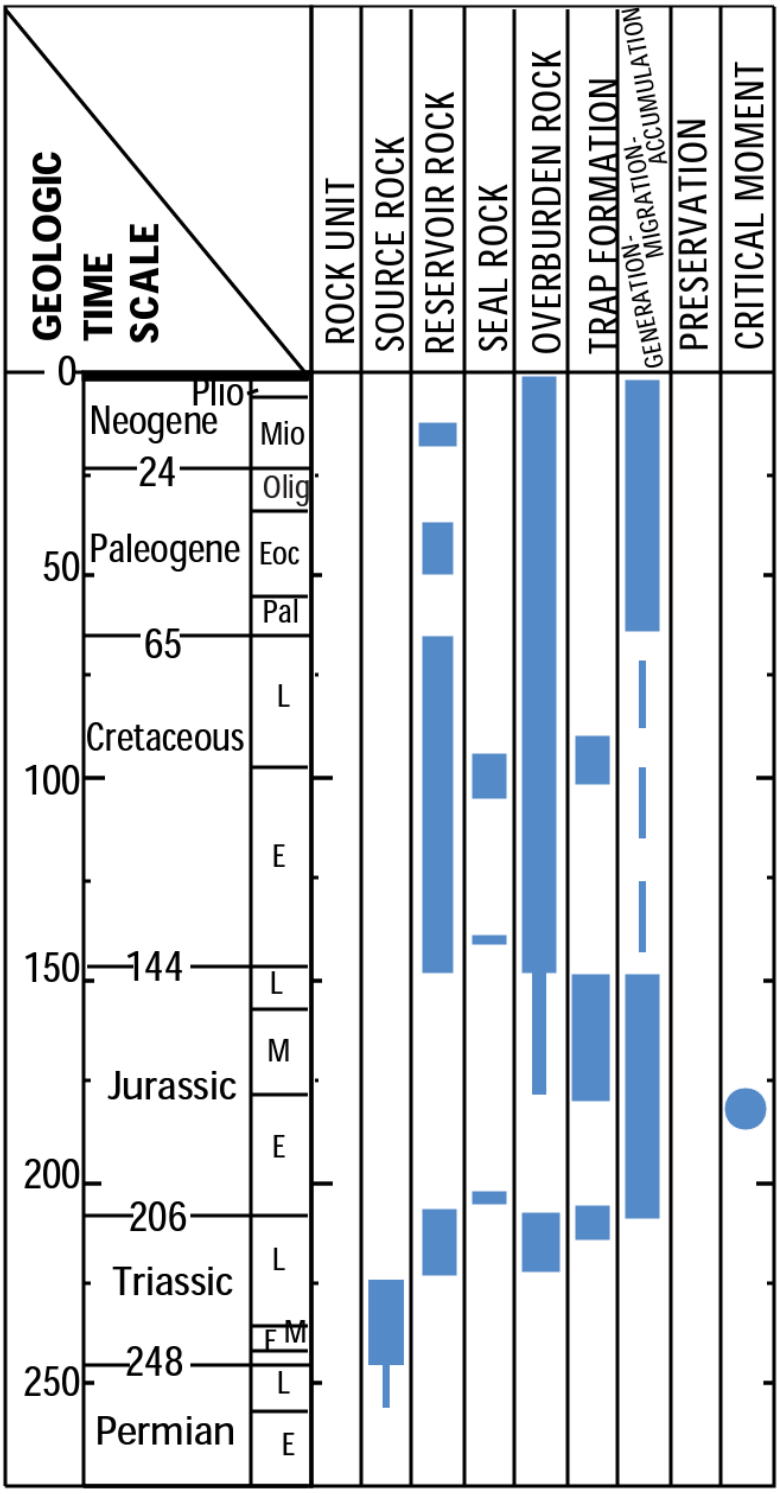

Figure 2.31 The Locker - Mungaroo/Barrow petroleum system of the North West Shelf Australia, as per Bishop (1999).

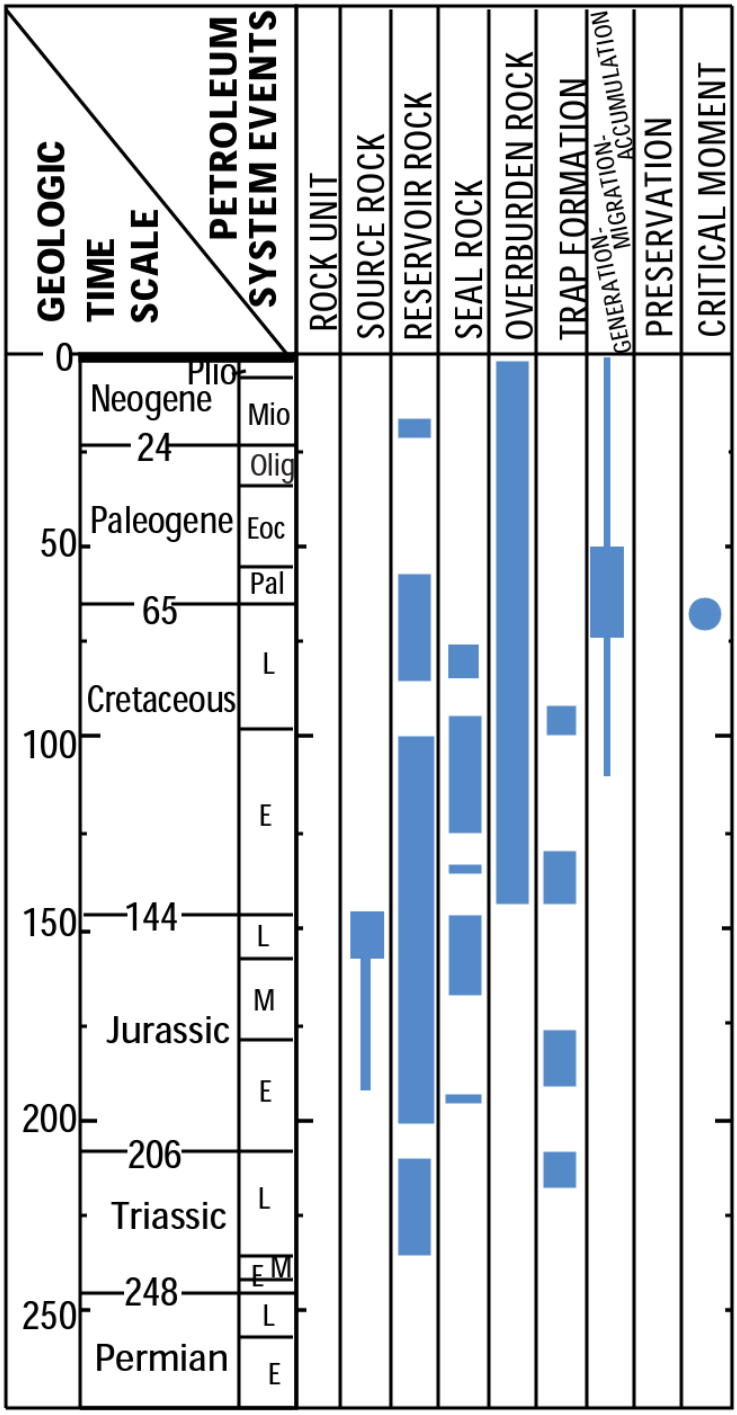

Figure 2.32 The Dingo - Mungaroo/Barrow petroleum system of the North West Shelf Australia, as per Bishop (1999).

3. Tectono-Stratigraphic Framework

The following describes the mega-sequences developed and identified as part of this study for the purposes of revealing a more detailed tectono-stratigraphic history of the Exmouth Plateau than is currently available. Current understanding of the evolution of the plateau is based on the combination of several key works. These provide a solid basis for understanding for the NWS (e.g., Etheridge & O'Brien, 1994; Longley et al., 2002; Marshall & Lang, 2013) and Northern Carnarvon Basin (e.g., Driscoll & Karner, 1998; Stagg & Colwell, 1994) as a whole. However, fine details of the evolution of specific areas, such as the Exmouth Plateau, are often obscured in these larger-scale studies due to the resolution of the investigation or are lost due to the broad nature of the definitions developed. Studies specific to the Exmouth Plateau are usually further limited by data availability at the time they were undertaken (e.g., Exon & Wilcox, 1978), or the application of results from a single region onto the broader plateau (e.g., Exon & Buffler, 1992; Exon et al., 1982; Jablonski, 1997; Jablonski & Saitta, 2004). The variation revealed by these more localised studies indicates that our understanding of the tectonic evolution of the Exmouth Plateau has remained limited.

A total of seven broad sequences were identified -as part of this research- in the Mesozoic strata (Figures 3.1, & 3.2) based on the interpretation and recognition of unconformities, onlap surfaces and regionally correlateable horizons that define packages of pre-, syn-, and post-kinematic sediments. These sequences have been further sub-divided; some of these sub-divisions can be recognised across the entire area of interest, others are limited to a part of the plateau, reflecting variation in fault activity. These mega-sequences are described in this chapter, along with a description of internal sub-divisions where appropriate. The seismic stratigraphic expression of the mega-sequences and their chrono-stratigraphic relationships are shown in the Figure 3.2. The mega-sequences are named according to their hierarchical stacking, and geological age, with reference to the widely adopted regional play intervals and picks developed by Marshall and Lang (2013). The mega-sequences

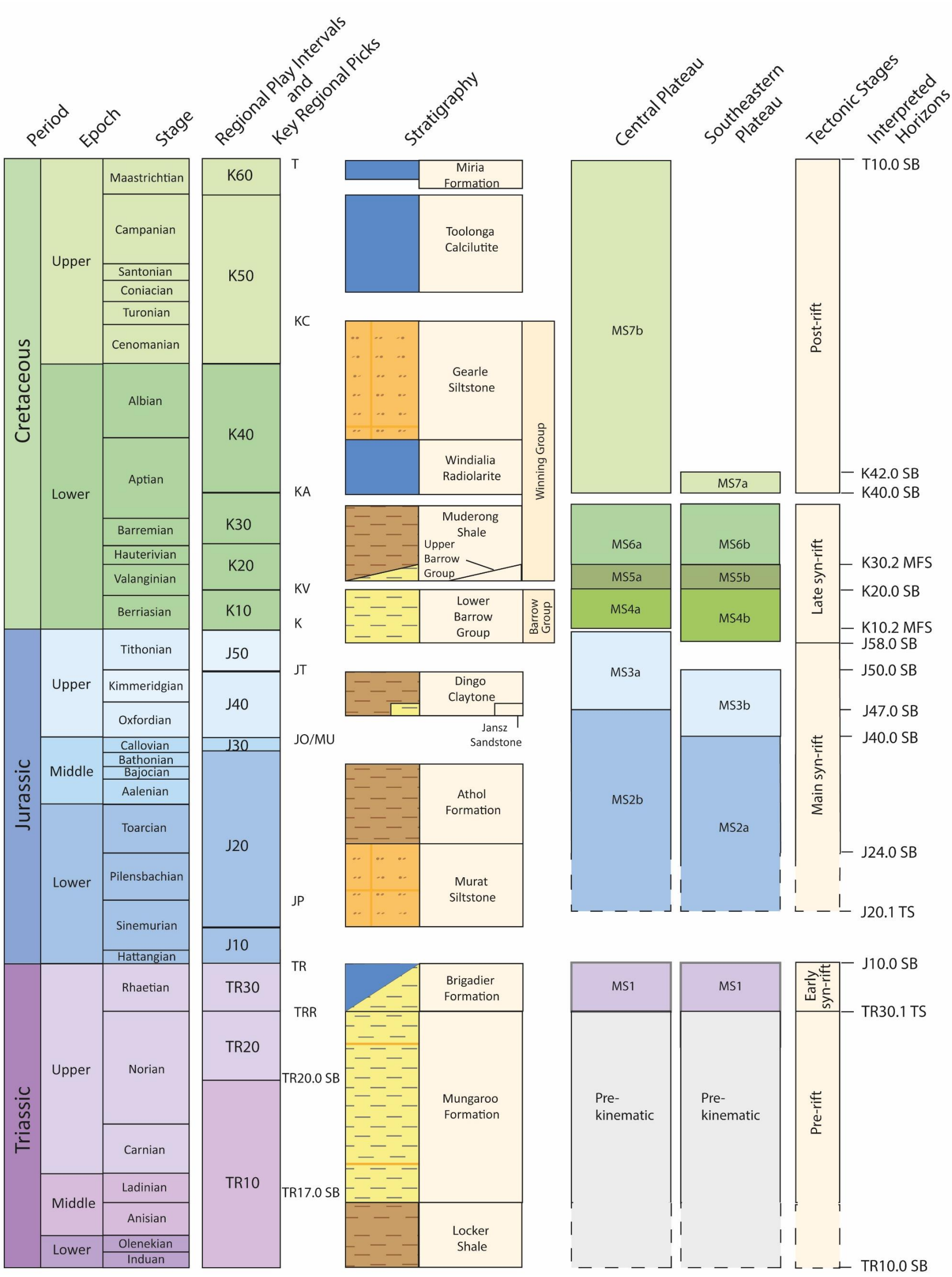

Figure 3.1 Stratigraphic chart of the Exmouth Plateau for this study, displaying the nomenclature used and the basin phases observed with the corresponding regional picks for key horizons based on the work of Marshall and Lang (2013).

a)

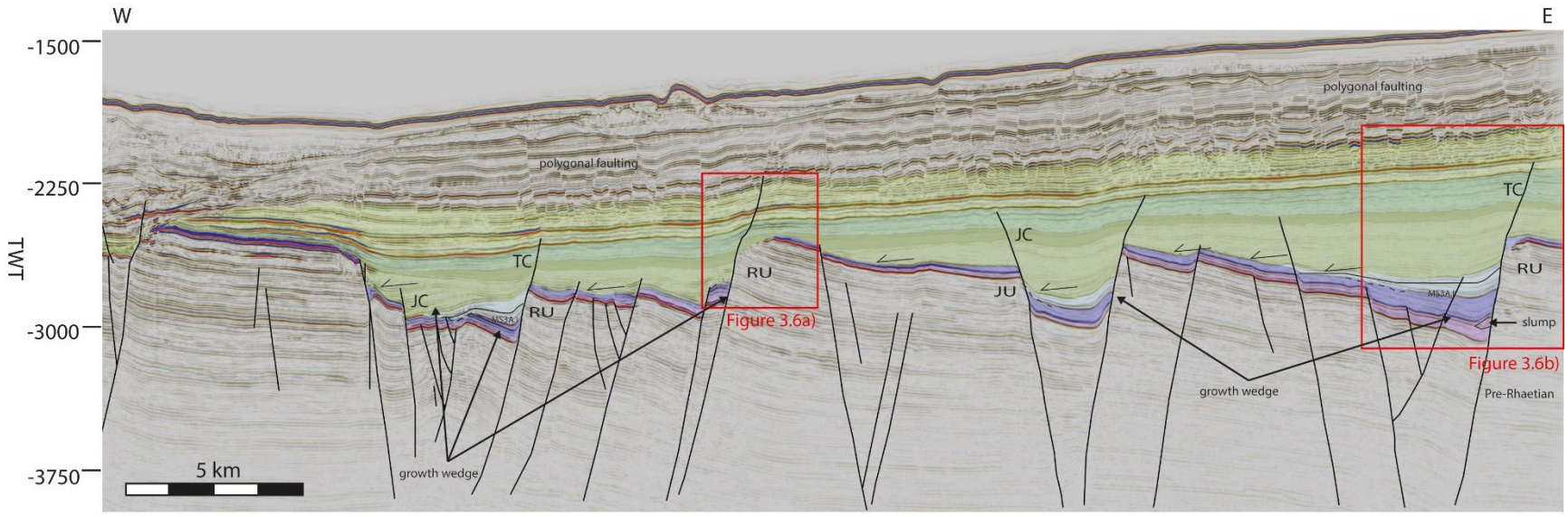

b)

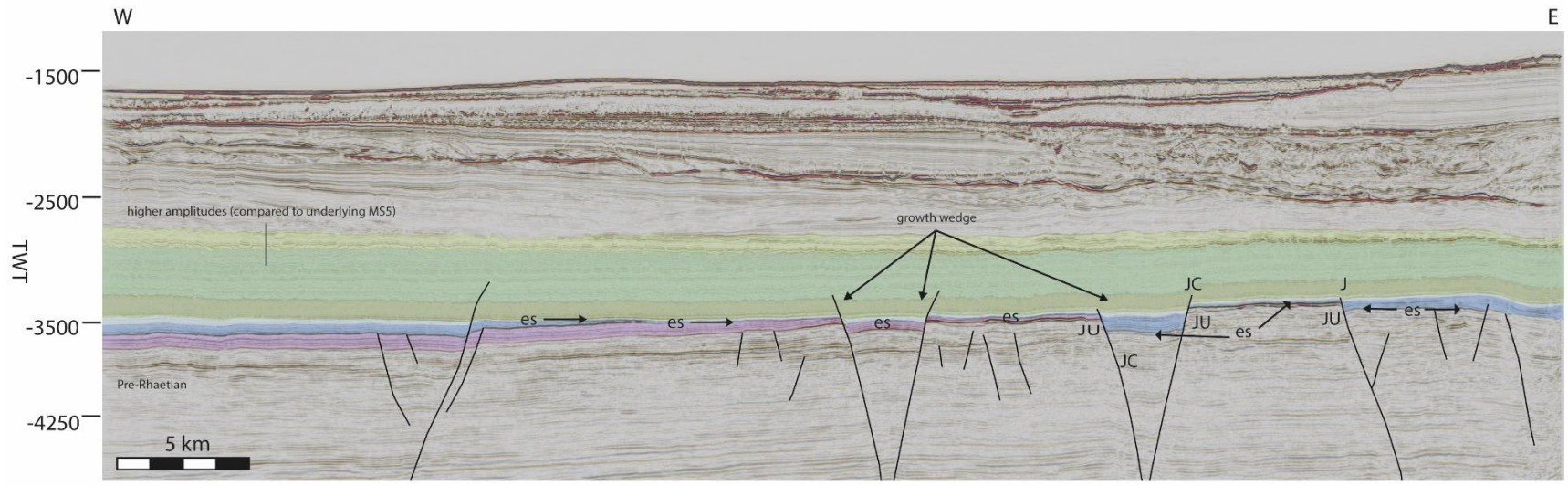

c)

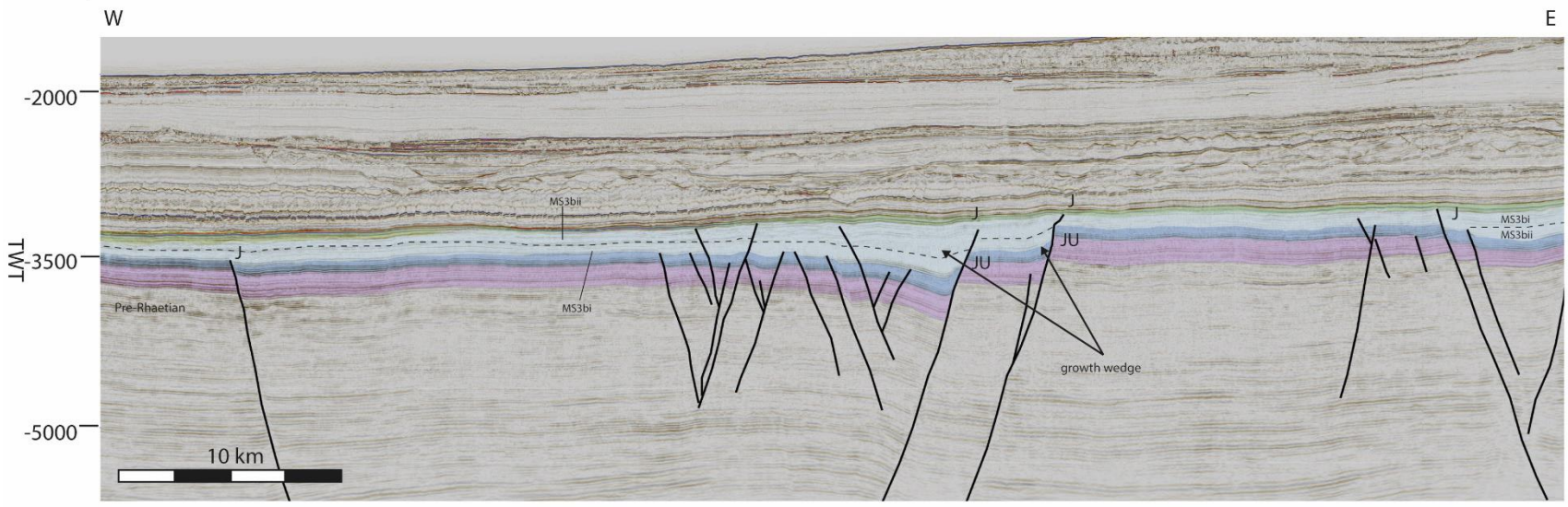

es	Major erossion surface	C	Cretaceous Fault Movement
RU	Triassic Uplift	J	Jurassic Fault Movement
JU	Jurassic Uplift	JC	Jurassic - Cretaceous Fault Movement
		TC	Triassic - Cretaceous Fault Movement

Triassic			Jurassic	Cretaceous		
MS1	MS2	MS3	MS4	MS5	MS6	MS7

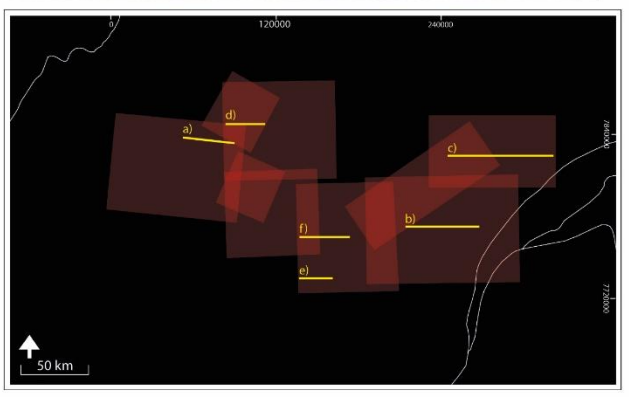

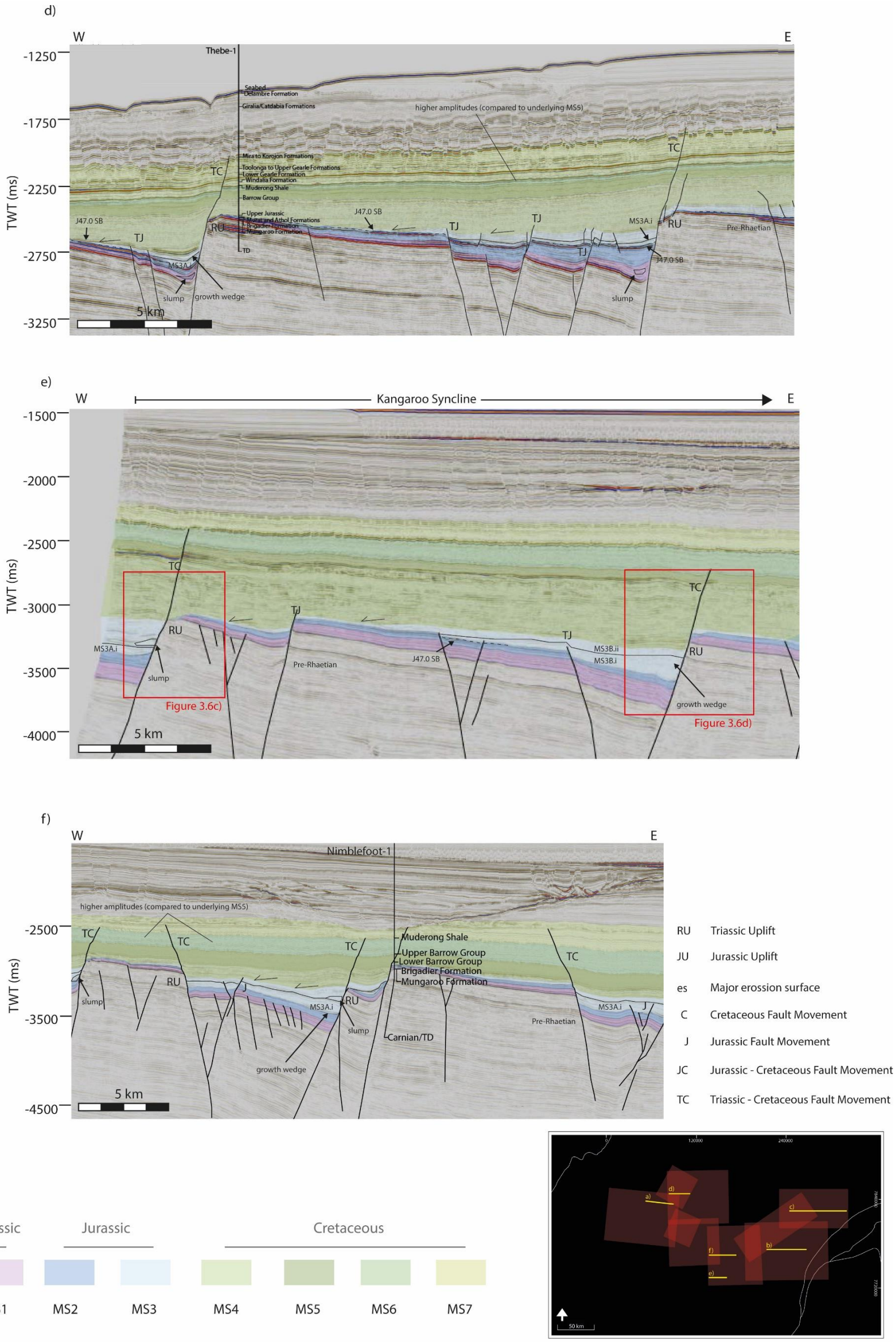

Figure 3.2 Seismic cross-sections through the area of interest displaying the identified mega-sequences, half-graben architecture, and eroded fault block crests. Red boxes highlighting the location of cross-sections in Figure 3.6.

names feature the regional play interval(s) that each mega-sequence covers, the numerical designation for the sequence, the geological age of the sequence and in brackets the top and base regional play interval picks for the sequence (Table 3.1).

Reference is made to the litho-stratigraphic units within each mega-sequence. However, a vast array of interpretations relating to the presence of certain units within the Exmouth Plateau occurs in both literature and industry reporting, i.e., the accepted stratigraphy for the Exmouth Plateau as per Geoscience Australia (2022; provided in Figure 3.1, as the Stratigraphy Column) includes the Dingo Claystone, Jansz Sandstone Athol Formation and Murat Siltstone in the Jurassic time, while the stratigraphic chart published by Black et al (2017; Figure 2.18) indicates that the Jurassic aged stratigraphy of the Exmouth Plateau was The Athol Formation, Calypso Formation, Murat Siltstone and North Rankin Formation. In addition, the North Rankin Formation itself is a topic of contention, labelled as early Jurassic by some (i.e., Black et al., 2017; Marshall & Lang, 2013) yet as late Triassic by others (i.e., Geoscience Australia, 2014a; Seggie et al., 2007). A third prominent stratigraphic mix-up or misunderstanding in the Northern Carnarvon Basin, is the Upper Barrow Group. The Upper Barrow Group (or Delta) is used to make reference to the deposition following the K20.0 SB event (final Australia-Greater India Separation in the Valanginian) and the onset of the Muderong Shale (i.e, Arditto, 1993; Cathro & Karner, 2006; Condon, 1967b; Geoscience Australia, 2014a; Hocking, 1988; Jitmanhantakul & McClay, 2013; Marshall & Lang, 2013; Paumard et al., 2018; Polomka & Lemon, 1996; Tindale et al., 1998) or to include the Muderong Shale (Longley et al., 2002; Marshall & Lang, 2013) depending on the authorship and/or company affiliation. For a full overview of the changing Barrow Group nomenclature over time, refer to Paumard et al. (2018).

This type of confusion or disagreement can be a shortcoming of any lithostratigraphic scheme where no set and agreed upon nomenclature for stratigraphic units exists. As the investigation of these differences is not pertinent to this research, not all units named in literature or well completion

Table 3.1 Nomenclature chart of the mega-sequences developed and used in this research to uncover the Mesozoic tectono-stratigraphic history of the Exmouth Plateau.

Full Name	Regional Play Interval(s)	Numerical Designation	Geological Age	Top Pick	Base Pick
K40 MS7a Aptian	K40	MS7a	Aptian	K42.0 SB	K40.0 SB
K40 - K60 MS7b Aptian - end Cretaceous	K60 K50 K40	MS7b	Aptian-Maastrachian	T10.0 SB	K40.0 SB
K30 MS6(a) Berriasian - Aptian	K30	MS6	Berriasian - Aptian	K40.0 SB	K30.2 MFS
K20 MS5(a) Valanginian Unconformity - Barremian	K20	MS5	Valanginian Unconformity - Barremian	K30.2 MFS	K20.0 SB
K10 MS4(a) Tithonian Unconformity - Valanginian Unconformity	K10	MS4	Tithonian Unconformity - Valanginian Unconformity	K20.0 SB	J50.0 SB
J40 MS3b Oxfordian Unconformity - Tithonian Unconformity	J40	MS3b	Oxfordian Unconformity - Tithonian Unconformity	J50.0 SB	J40.0 SB
J40 MS3a Kimmeridgian Unconformity - Tithonian Unconformity	J40	MS3a	Kimmeridgian Unconformity - Tithonian Unconformity	K10.2 MFS	J47.0 SB
J20 - J40 MS2a Pre-Oxfordian	J40 J30 J20	MS2a	Lower and Middle Jurassic	J40.0 SB	J24.0 SB
J20 - J40 MS2b Pre-Kimmeridgian	J40 J30 J20	MS2	Lower to Upper Jurassic	J47.0 SB	J24.0 SB
TR30 MS1 Rhaetian	TR30	MS1	Rhaetian	J10.0 SB	TR30.1 TS
TR10 - TR20 Pre-Kinematic	TR20 TR10	Pre-Kinematic	Triassic	TR30.1 TS	Unidentified

reports are used here. The true definition of these mega-sequences sits with the use of regional play interval picks (linked to Marshal & Lang, 2013 nomenclature) to outline specific intervals of geological time.

3.1. TR10 - TR20 Pre-Rhaetian (TR10.0 SB? - TR30.1 TS)

A thick mega-sequence composed of the broadly deposited Mungaroo Formation forms a series of parallel reflectors of medium amplitude and uniform thickness (Figure 3.2). The deposition of this sequence occurred in a fluvio-deltaic environment, likely in the more distal deltaic environment on the outboard Exmouth Plateau (Adamson et al., 2013). Later igneous intrusions have been emplaced in this sequence (Figure 3.3; Rohrman, 2013). The top of the sequence is defined by a reflector of high amplitude which is correlated to the TR30.1 TS regional pick. There has been erosion at the top of this mega-sequence (Chapter 5, Section 5.2) on uplifted fault blocks in the west of the study (Figure 3.3). In the area immediately adjacent to the Rankin Platform, widespread uplift has occurred and resulted in significant erosion of the Pre-kinematic sequence. The erosion is characterised by the widespread truncation of seismic reflectors (Figure 3.2b).

The base of this sequence is not observed in most of the data used in this study. No well penetrations occur to great enough depths and most seismic sections do not cover the whole of the interval. However, a prominent reflection is apparent at the base of the sequence on the Bart 2D regional line (Figure 3.4). As interpretation cannot be tied to any wells it remains unidentified, but is likely to correlate to one of Marshall and Lang's (2013) regional picks within the TR10 interval; most likely the TR10.0 SB pick. Early to Middle Triassic marine claystone and siltstone (Geoscience Australia, 2014a; Tortopoglu, 2015) of the Locker Shale is believed to have been deposited continuously from the inboard sub-basins to the outer part of the plateau. Faults also detach at this level indicating the presence of a regional detachment horizon.

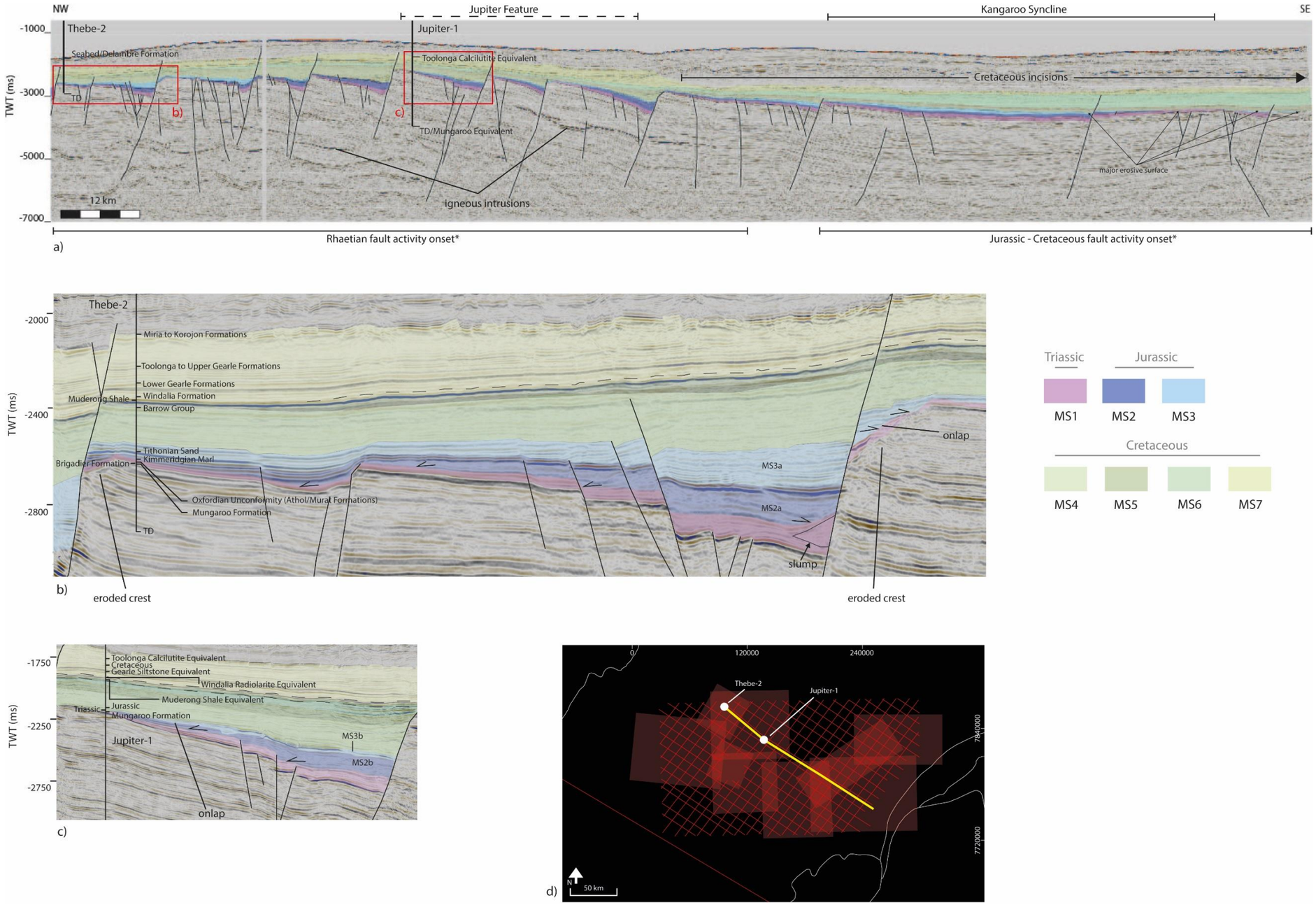

Figure 3.3 Regional cross-section through the study area displaying the mega-sequences as per this study. Cross-section a) showing the differences in structural architecture between the west and eastern plateau. The erosion of fault block crests, and timing indicators are captured in figure b) and the thinning of depositional packages over rotated fault blocks is shown in Figure c). The location of Figures b) and c) are highlighted on Figure a), the location of Figure a) is shown on the map (d), as are the two wells displayed in section a).

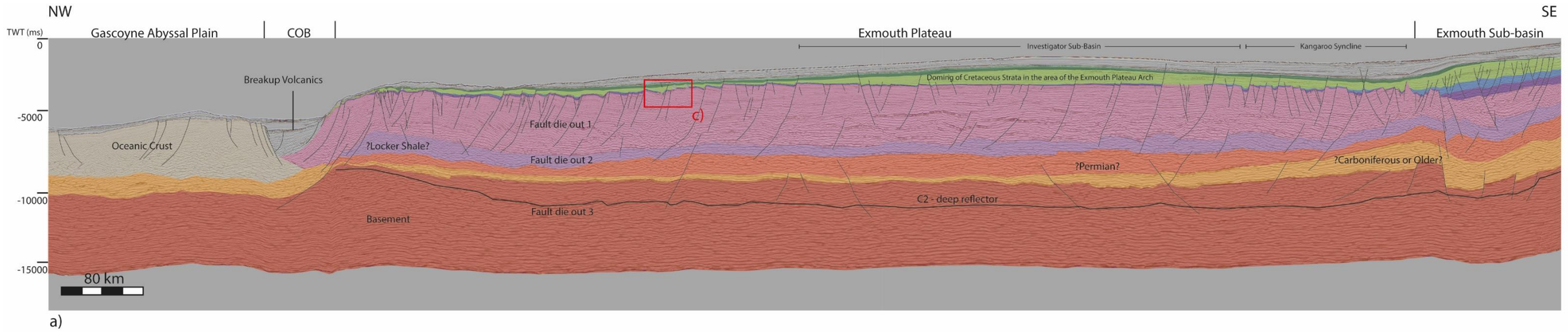

a)

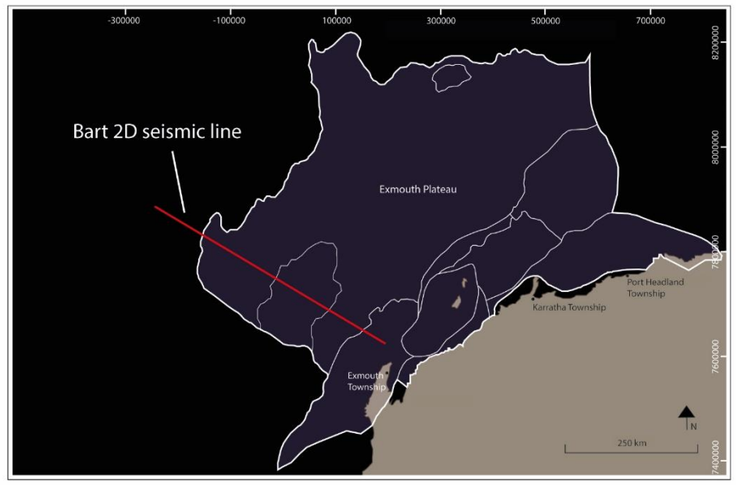

b)

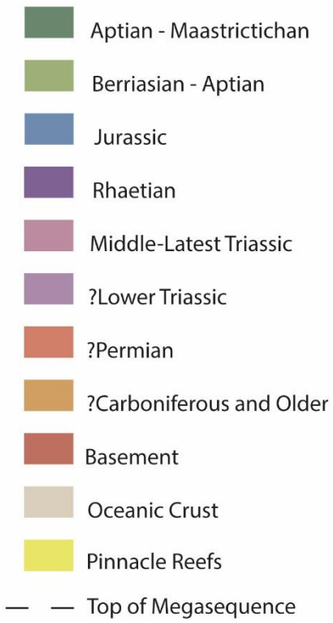

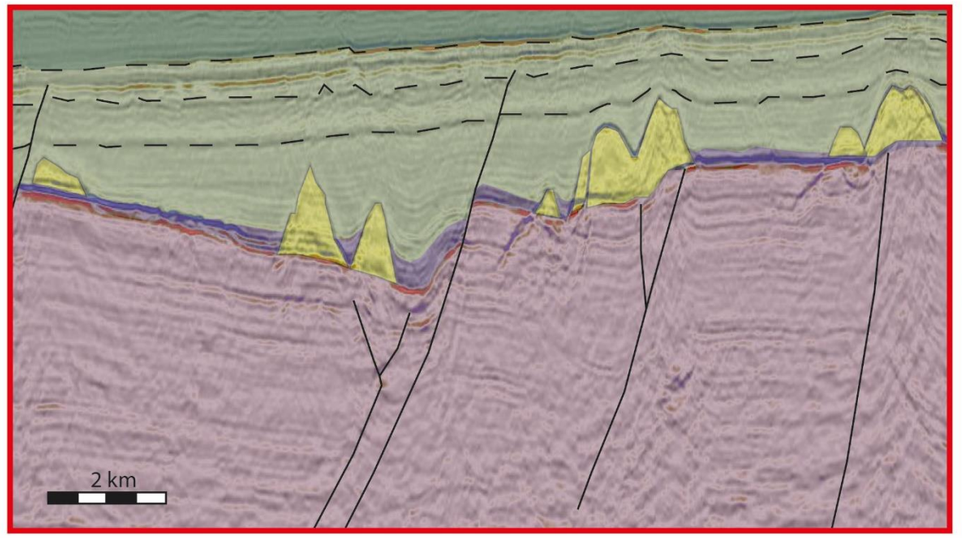

c)

Figure 3.4 Bart 2D regional seismic line (a) from the Nemo_Bart OBS seismic survey, displaying the broad Mega-sequences of this dissertation applied to the expanded regional context of the Exmouth Plateau. Location of Bart 2D line is indicated on map (b). Close up of Rhaetian Pinnacle Reefs is displayed as (c) with location highlighted on main cross-section by a red box.

The sequence is interpreted as post-rift in relation to the Permian aged rift activity (Etheridge & O'Brien, 1994; I'Anson et al., 2019), and pre-rift relative to the younger Mesozoic events discussed in this dissertation.

3.2. TR30 MS1 Rhaetian (TR30.1 TS - J10.0 SB)

The oldest mega-sequence to be mapped across the study area is a broad package of TR30 Rhaetian age (Figure 3.2) encompassing the Brigadier Formation, as intersected in wells such as Thebe-1 and Callirhoe-1. The TR30 (TR30.1 TS - J10.0 SB) sequence is thickest to the northeast and thins to the west (Figure 3.5). The gradual change from the distal deltaic environment of the underlying Mungaroo Formation to the more mixed delta front and plains resulted in deposition of the Brigadier Formation (Adamson et al., 2013; Marshall & Lang, 2013). A deepening environment resulted in the sedimentation of shelfal marine siltstone, claystone and marl (Geoscience Australia, 2014a; Tortopoglu, 2015) and the development of carbonate units (Adamson et al., 2013; Grain et al., 2013; Exon & von Rad, 1994).

Locally, the sequence increases in thickness into major faults and thins and pinches-out over uplifted or tilted fault blocks over the western and northeast portions of the area of interest. However, to the southeast, TR30 pre-dates faulting with no thinning over highs or growth into faults recognised (Figure 3.2b & c). Seismically the package is identified as a series of flat-lying to low angle reflectors, with some chaotic patterns in areas of substantial thickness changes; high amplitude reflectors often represent the very base of the package. Onlap of this package onto the underlying pre-kinematic stratigraphy is seen in the west of the study area. The top of this package is defined by a seismic reflector of high to medium amplitude, or by erosional unconformities in areas of uplift. In the eastern area, the amplitude of this top reflector decreases.

The chaotic seismic facies (as described in special publications, i.e., Emery and Meyers (1996) and workflow literature i.e., Mayall and Kneller, (2021))

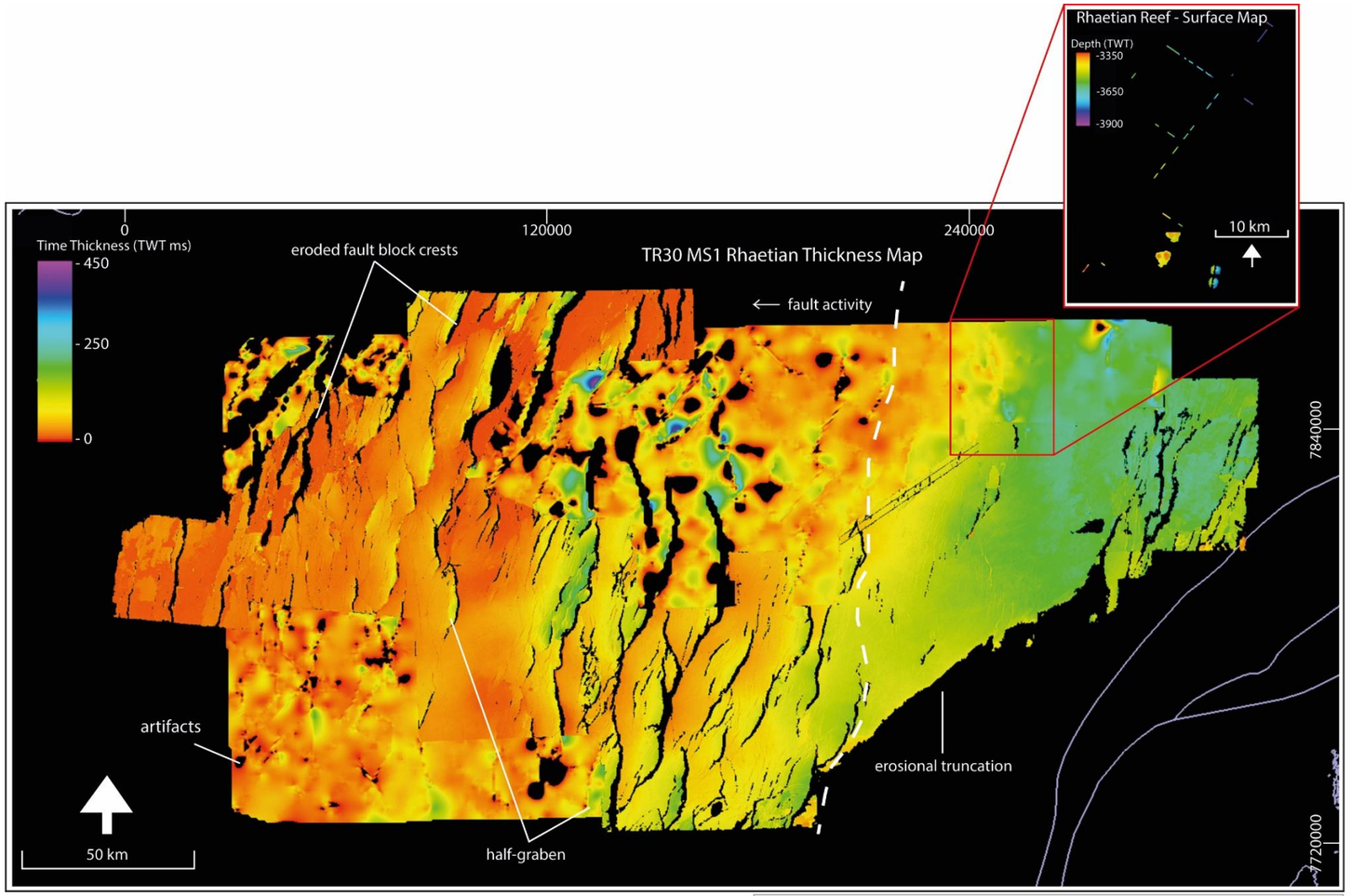

a)

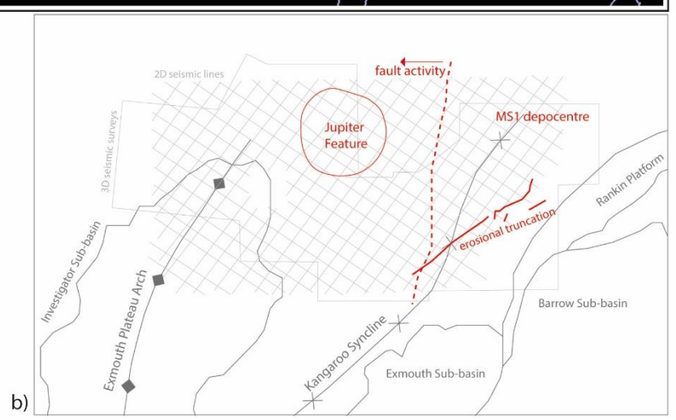

b)

Figure 3.5 Rhaetian (MS1) a) thickness map (TWT) over the Exmouth Plateau showing the eroded crests of uplifted fault blocks, half-graben structural architecture, and broad regional erosional truncation. Also observable on this thickness map is the Jupiter Feature, annotated on b) the supplement map.

commonly occur in the northwest of the study area in the upper part of the sequence, adjacent to eroded fault block crests (Figures 3.2, 3.3b, & 3.6e). These are interpreted as slumps (or base of scarp deposits as per Chiarella et al., 2021) that are the localised re-deposition of sediment from adjacent eroded fault block crests. In the southeast, this mega-sequence consists of a series of flat-lying reflectors, which are subject to broad-scale erosion adjacent to the Rankin Platform (Figure 3.5). To the northeast, pinnacle reefs are mapped within the TR30 Rhaetian strata (Figures 3.4, &3.7). This is part of the inboard reef trend identified by Grain et al. (2013).

3.3. J20 - J40 MS2 Early to Middle Jurassic (J20.1 TS - J47.0 SB)

The second oldest mega-sequence spans a large portion of the Jurassic (Figures 3.2, 3.3, & 3.8). The mega-sequence contains the shelfal to open marine sediments of the Athol Formation and Murat Siltstone, extending into the Dingo Claystone and their equivalents. Sediment is thickest to the northeast where the maximum thickness identified on seismic data is 710 m, thinning towards the western part of the plateau where it is below seismic resolution, or not deposited. Jurassic depositional sequences are found within the entire study area but are divided based on changes in sedimentation due to tectonic activity (Figure 3.9). Some of the individual packages within the J20-J40 mega-sequence, are present within specified areas and not across the whole area. This sequence contains many regionally recognised unconformities, some of which are not resolved in the seismic data due to the thin and condensed nature of the Jurassic sequence. The younger Jurassic strata (J10) are not identified on seismic or in well data.

3.3.1. J20 - J30 MS2A Pre-Oxfordian (J20.1 TS - J40.0 SB)

In the eastern portion of the study area the earlier Jurassic sequence is represented by a series of parallel reflectors, with the exception of some which

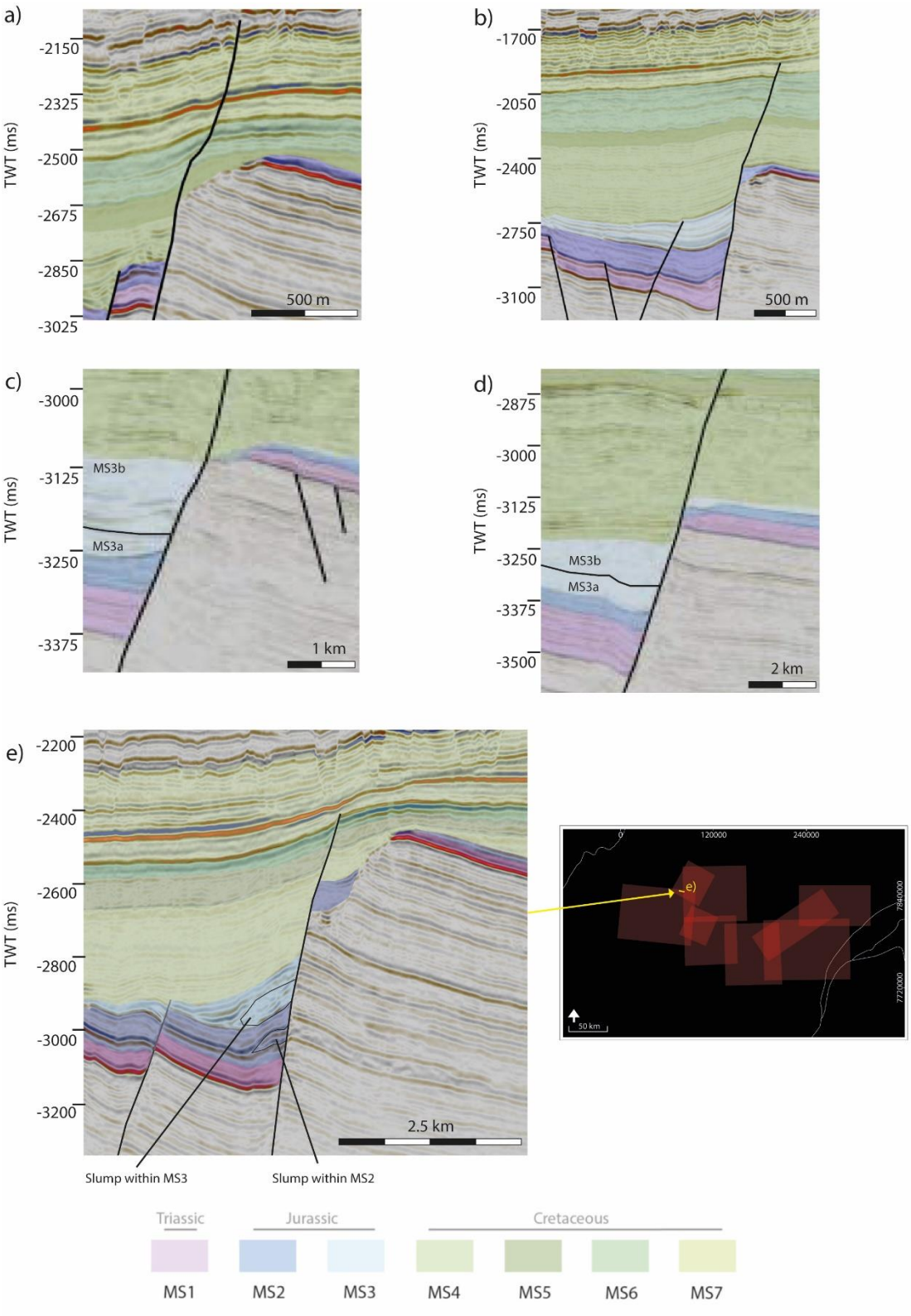

Figure 3.6 Several eroded crests in cross-section. Figures a) and b) are highlighted on Figure 3.2a, figures c) and d) are highlighted on Figure 3.2e. Location of Figure e) is highlighted on map. Two slump features are also identified in Figure e), which shows the chaotic nature of these features on seismic imaging.

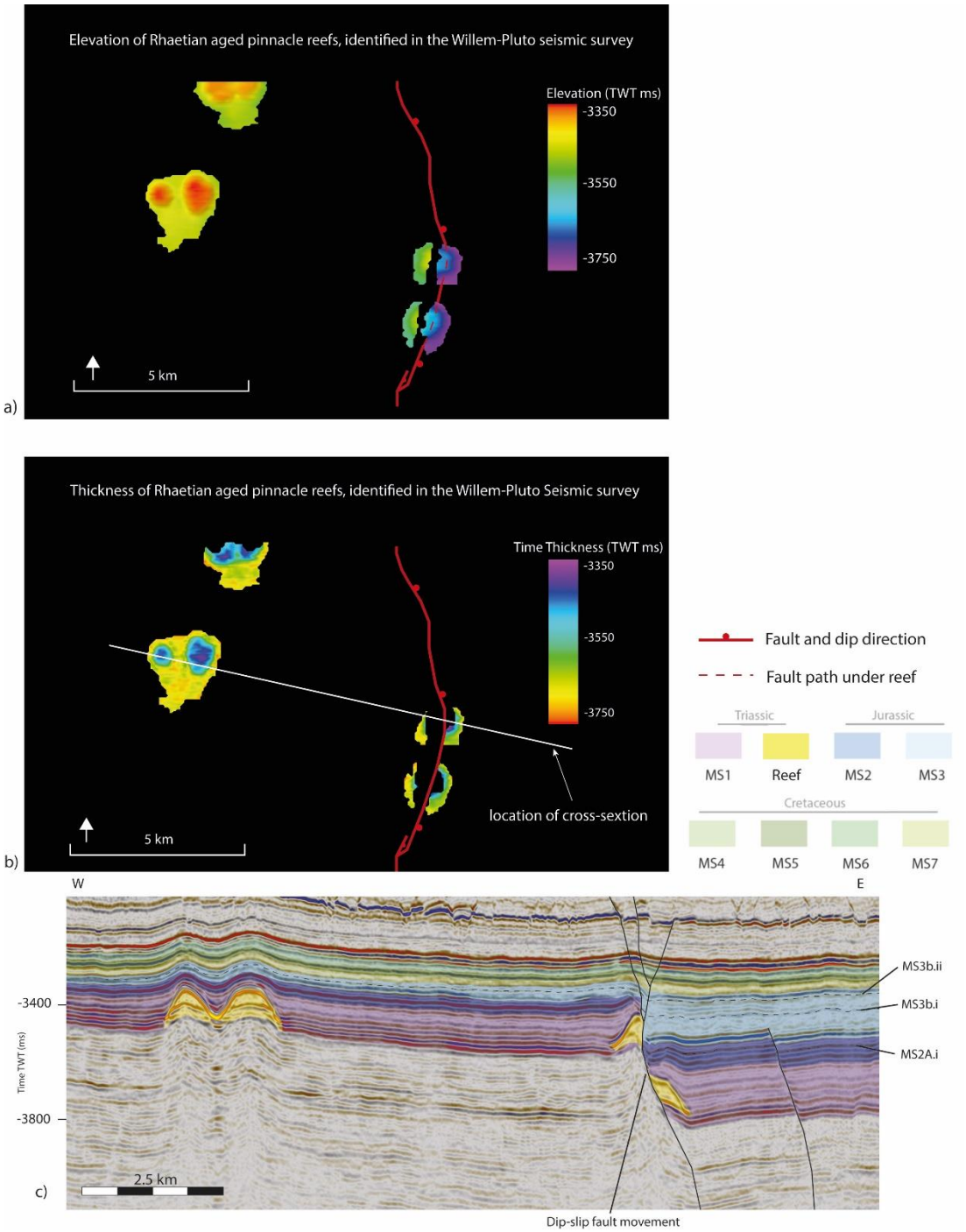

Figure 3.7 Close up of pinnacle reefs (observed on 3D seismic data) displaying the a) elevation, and b) thickness of pinnacle reefs. The pure dip-slip movement is observed in seismic c) cross-section in addition to the thickness map b).

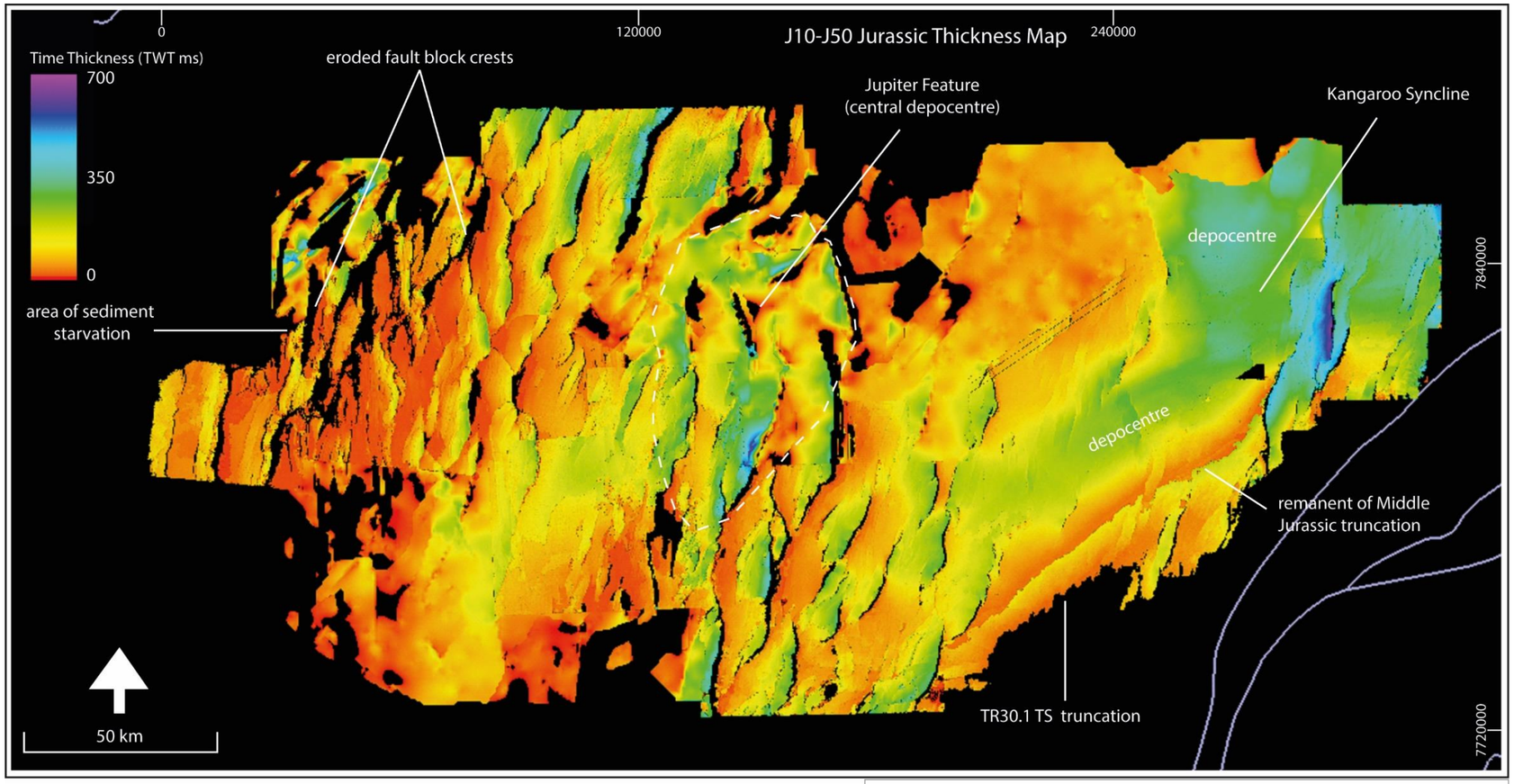

a)

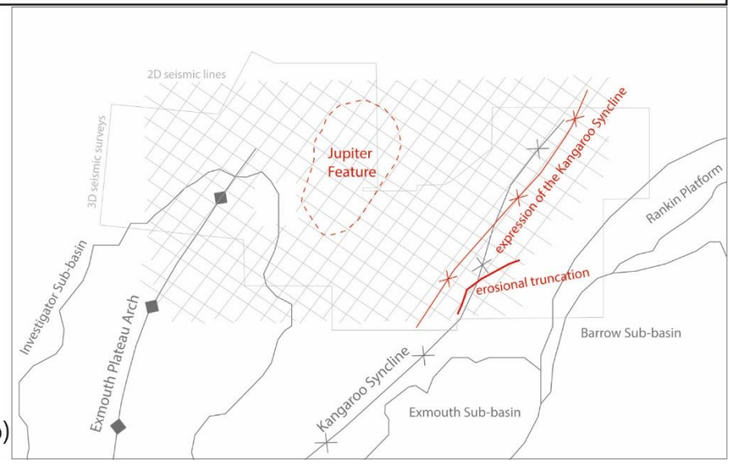

b)

Figure 3.8 a) Thickness map of the Jurassic sequences over the Exmouth Plateau, displaying the thinner nature of the Jurassic aged deposition. Additional annotation of observed features in b) annotated line map.

Mesozoic Chronostratigraphy of the Exmouth Plateau

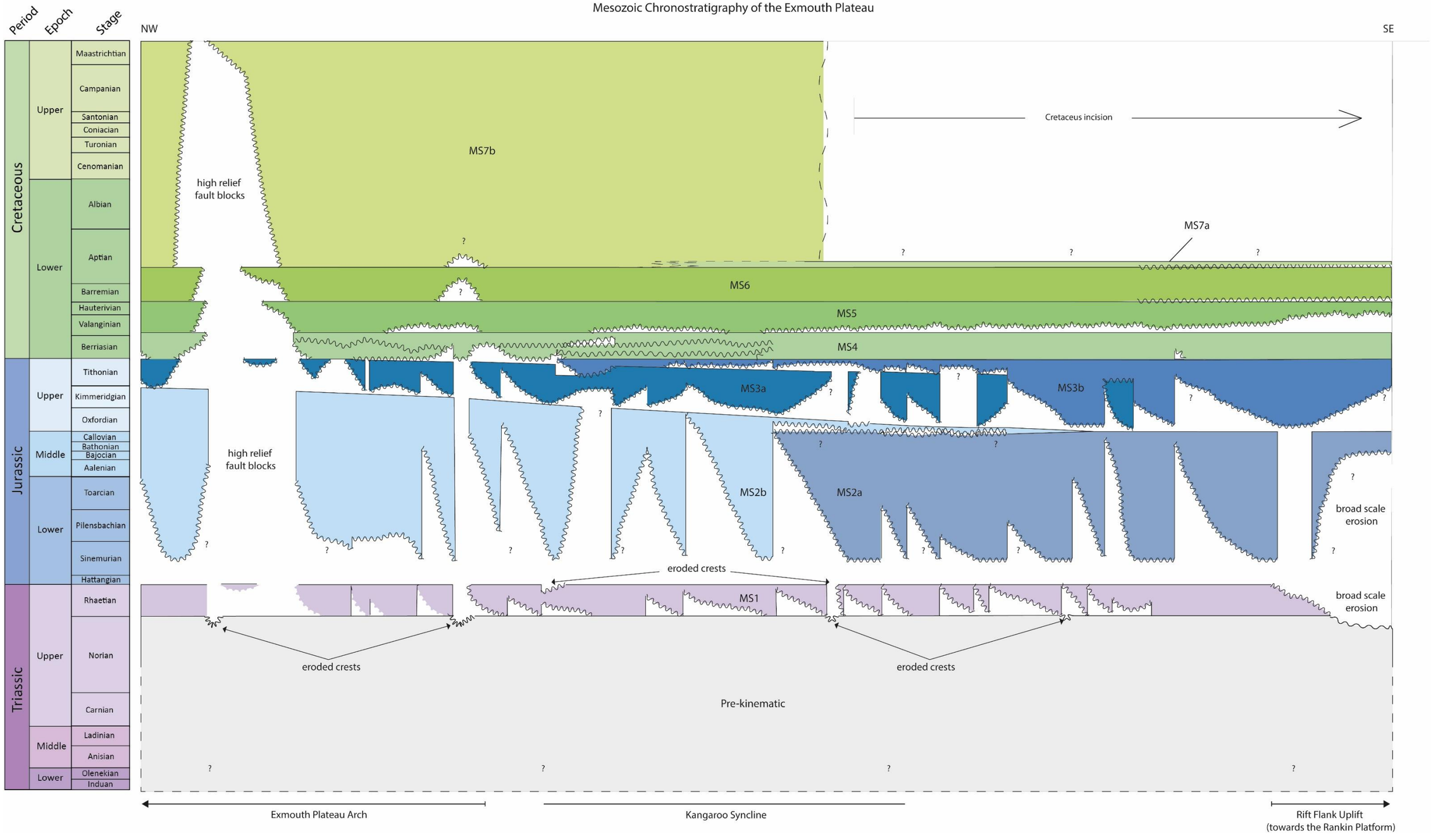

Figure 3.9 Chronostratigraphic chart of the Exmouth Plateau, displaying the largely generalized Mesozoic sedimentation, hiatus, and erosion, where some areas of erosion are the result of uplifted /rotated fault block crests being impacted by erosional processes and others are the onlap of these uplifted crests. Some areas are the result of uplifted fault block crests resulting in either erosion or non-deposition. The mega-sequences utilized here are the result of this body of research.

On previous page

converge in a thinning out pattern of reflectors to the northeast of the study area (Figure 3.10). The thinning out reflectors define a further sub-division (MS2a.i) discussed below (Figure 3.10). There is some thickening across faults within this unit, although thickening occurs to a lesser degree than is observed in the equivalent Jurassic sequences to the west. It is likely that this early to Middle Jurassic unit is evidence for the first fault movement in the eastern part of the study area during the Mesozoic. Within this sequence, a large uplift related erosional unconformity occurs in the extreme southeast, adjacent to the Rankin Platform (Figures 3.2b, & 3.3a). A small amount of this sequence is preserved on top of this erosional event.

An unconformity event, the Oxfordian Unconformity (J40.0 SB; Figure 3.10) forms the top, or near-top, of this mega-sequence. This unconformity is identified in seismic from the onlap of some reflectors in the overlying unit and the truncation, although limited, of MS2a at its top. The base of this sequence appears largely continuous with the underlying Triassic, except for a small portion of onlap and the formation of small growth wedges (Figure 3.10).

3.3.1.1. J20 MS2A.I (J20.1 TS - J24.0 SB)

The MS2a.i is represented by a series of parallel but thinning reflectors. This package of reflectors are thickest in the northeast and thin rapidly towards the southeast and central regions of the study area (Figure 3.10). As with sequence MS2a, there is some limited thickening of this package across faults, indicating that deposition occurred at a time of active fault movement.

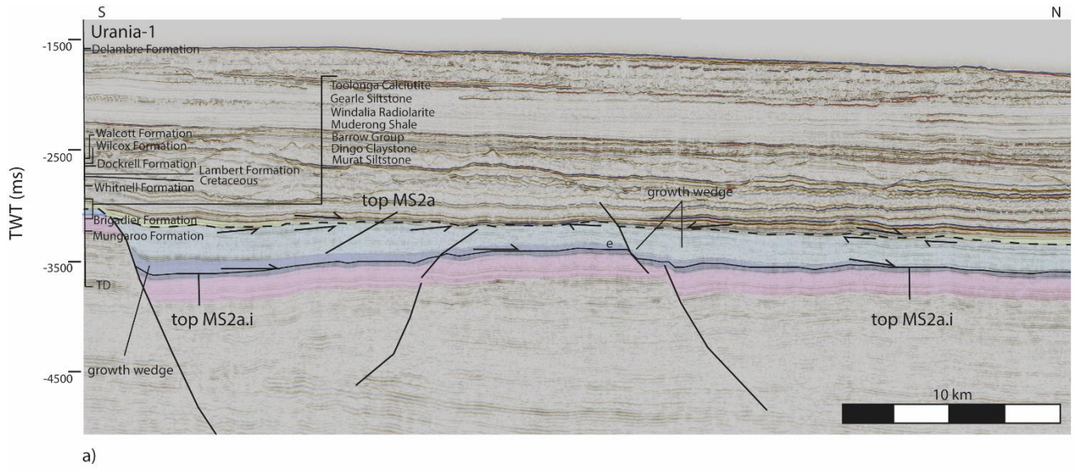

a)

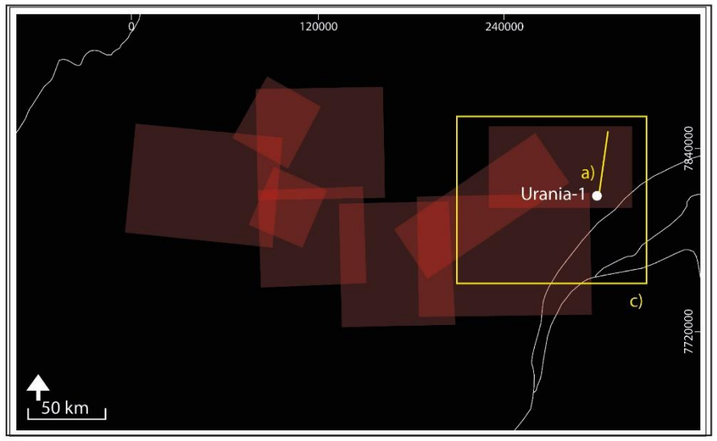

b)

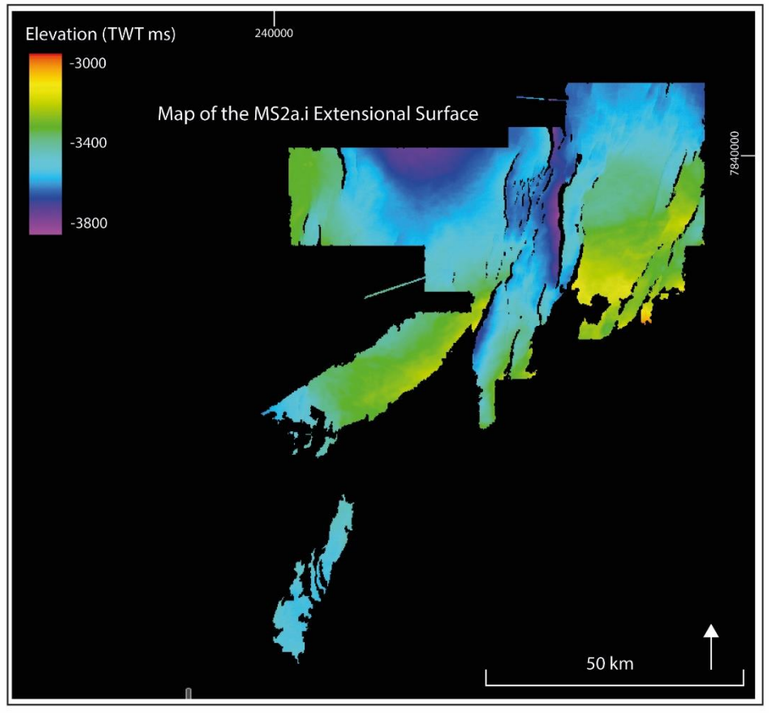

c)

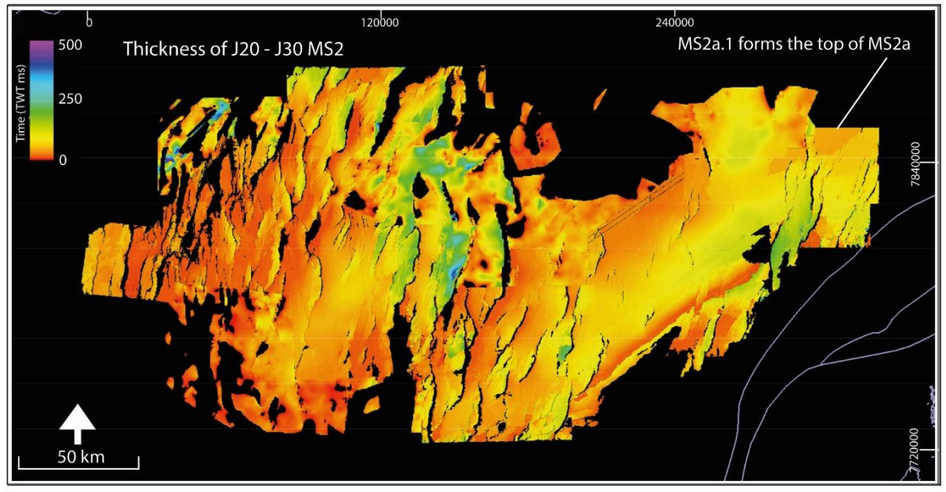

d)

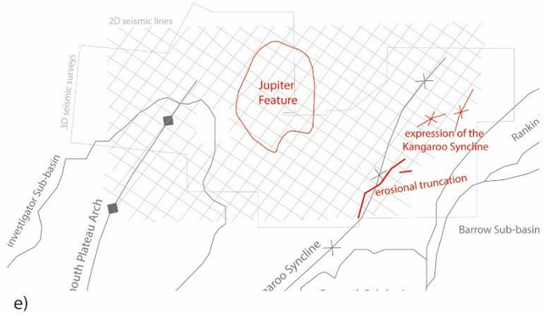

e)

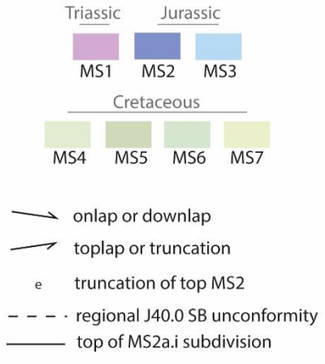

Figure 3.10 MS2a.i observed on a) cross-section in relation to the top of MS2, c) the complete distribution of the mapped surface, and d) how it completes the top of MS2 in the northeast. Further broad observations are provided in e) the annotation map, and the location of cross-section a) is provided in b) the location map.

However, no observed onlap of this package onto the underlying strata is observed. The top of this unit is readily identified in the northeast by an angular unconformity which cannot be confidently attributed to a regional pick from the currently available information (Figure 3.10). However, in investigating potential options, an event in the later Pliensbachian (J20) is a strong possibility. This event, correlated to the J24.0 SB and is recognised in the Exmouth Sub-basin by Jitmanhantakul and McClay (2013) as having tectonic significance. A second possibility is that this event correlates with the J20.2 MFS, but there is no regional tectonic activity to make this the more likely of the two possible options for the age of this unit.

This unconformity is formed where the MS2a.i reflectors thin out and/or are onlapped by the overlaying MS2a reflectors (Figure 3.10). Elsewhere, the interpretation of this division as a separate unit relied on the interpretation being carried from the northeast, as there is no visible change in character. This unit, like MS2a, was eroded due to a broad uplift event on the Rankin Platform in the Jurassic. The base of this unit is defined by the largely medium to low amplitude reflector which marks the top of the TR30 Rhaetian aged mega-sequence.

3.3.2. J20 - J40 MS2B Pre-Kimmeridgian (J20.1 TS - J47.0 SB)

In the west of the area, MS2b displays some gentle onlapping onto the underlying TR30 strata and it is occasionally truncated by the MS3a strata. On seismic data, the mega-sequence is characterised by a series of low and medium amplitude concordant reflectors, with minor chaotic reflectors occurring in the deepest downthrown half-graben. Growth wedges also formed within these half-graben (Figure 3.11). Sudden changes in the downlap and onlap angles of these growth features are evident in the more complete sections, indicating a break in sedimentation. This break could be linked to the J24.0 SB hiatus identified by Jitmanhantakul and McClay (2013), as above, or to a younger event (J20.1 TS). No further age constraints were available for the MS2b growth wedge formations. Chaotic seismic facies adjacent to eroded

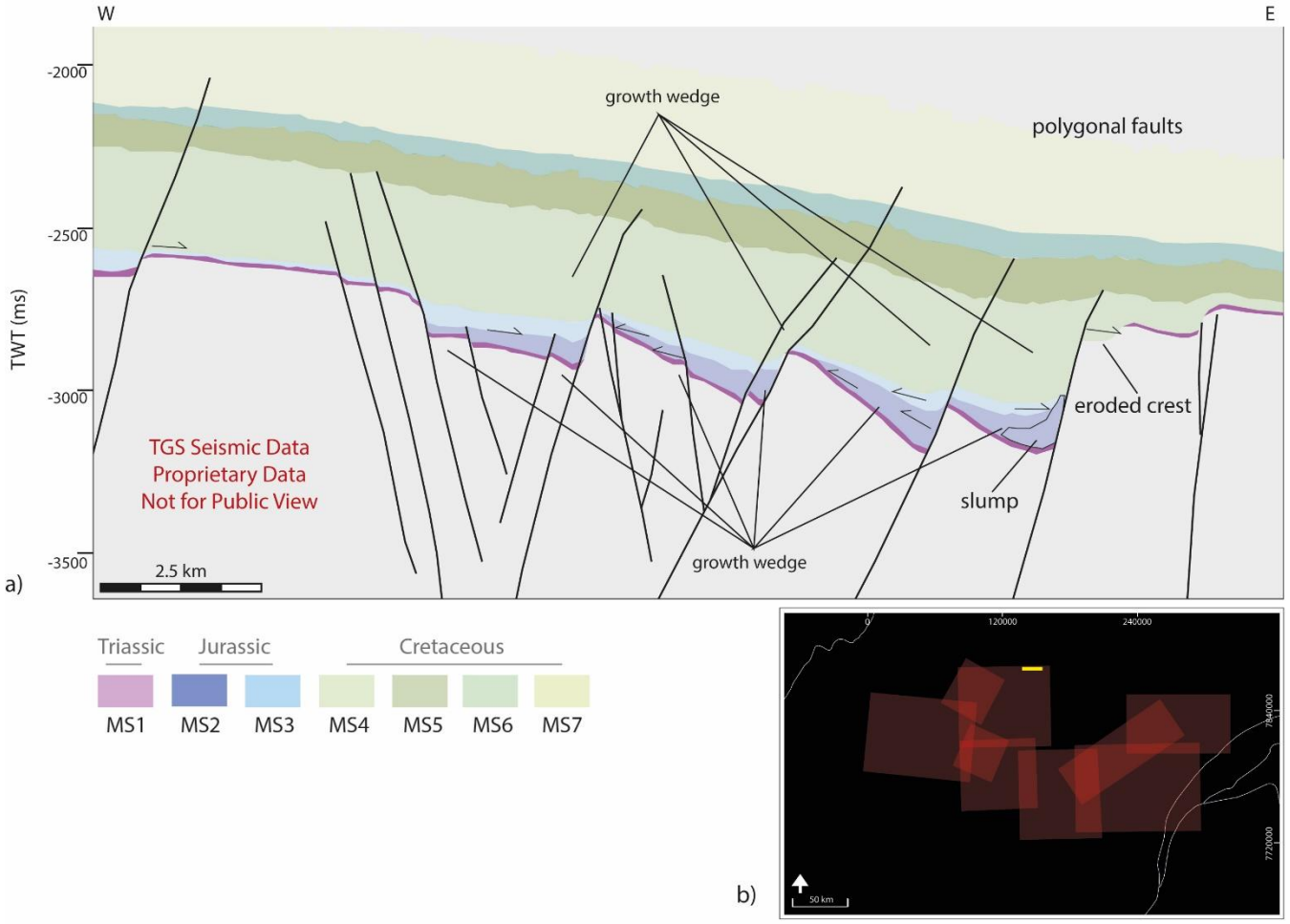

Figure 3.11 Growth wedge formation in MS2 and MS4 in the west of the study area. Seismic data used here is removed for final public version.

fault block crests are interpreted as slumps. These only occur in the more western parts of the study area.

The top of this mega-sequence is an unconformity (Figures 3.1, & 3.11), identified as the Kimmeridgian unconformity (J47.0 SB). The Kimmeridgian Unconformity can be recognised throughout the Bonaventure seismic survey area. In this same region, the Oxfordian Unconformity cannot be identified separately due to the condensed nature of the Jurassic sequence (and the limits of seismic resolution). The top of this sequence is a reflector of high amplitude. Erosion of the MS2b sequence has occurred widely on uplifted fault block crests (Figure 3.6a). At the base of this sequence, reflectors onlap and terminate onto the TR30 Rhaetian or TR20 Norian aged strata in areas of syn-depositional fault activity (Figure 3.11). Likewise, non-deposition occurs over some up-thrown fault blocks.

3.4. J40 - J50 MS3 Late Jurassic (J40.0 SB - 10.2 MFS)

The third mega-sequence to display the rift history of the Exmouth Plateau is the late Jurassic MS3 mega-sequence (Figures 3.2, & 3.12). This package contains stratigraphy which was deposited in the J40 Kimmeridgian and the J50 Tithonian. Some limited deposition from the earliest Cretaceous is also likely. There is no well-defined lithostratigraphic unit that can be assigned to this mega-sequence. Of the many wells that intersect this unit, a small number of Well Completion Reports in the west describe it as the precursor sediment gravity flows of the prograding Lower Barrow Group. However, due to the condensed nature - or absence - of this unit on upthrown highs, where drilling usually occurs, no clear conclusions can be drawn.

The late Jurassic sequence is thickest in the northeast, within the area of larger faults within the Willem-Pluto seismic survey. The late Jurassic mega-sequence is thinnest in the area of large-scale uplift adjacent to the Rankin Platform and within the Scarborough and Bonaventure seismic survey areas.

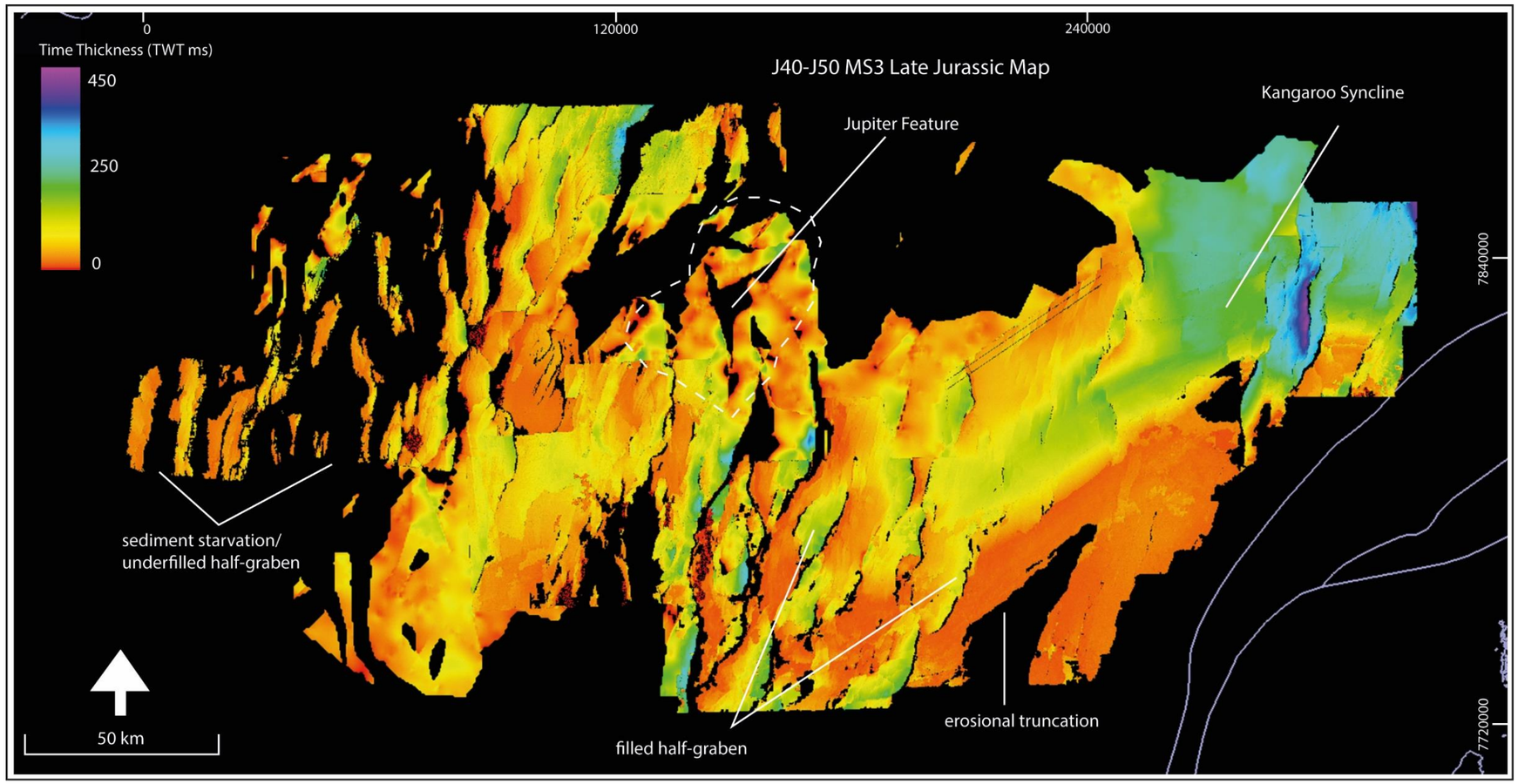

a)

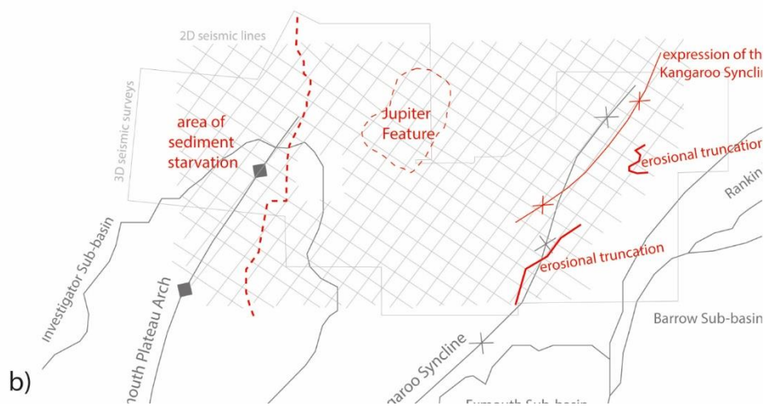

b)

Figure 3.12 Late Jurassic (MS3) a) thickness map (TWT) over the Exmouth Plateau showing the thickness of the Upper Jurassic deposition, with the underfilling, or sediment starvation, of half-graben in the western region highlighted. Additional observations are provided on the b) supplemental line map.

There are also large areas where late Jurassic sequences were not deposited or have been eroded (Figure 3.12). The following divisions within the mega-sequence can be recognised due to changes in the tectonic activity across the plateau.

3.4.1. J40 MS3A Kimmeridgian - Tithonian (J47.0 SB - K10.2 MFS)

Late Jurassic activity in the western plateau is recorded by the deposition of MS3a. It is identified on seismic data as a series of parallel to near-parallel reflectors that onlap the underlying pre-Oxfordian and pre-Kimmeridgian strata of the MS2 mega-sequence. The top of this package is easily identified by an angular unconformity surface across most of the western part of the area, where it is present (Figure 3.13). The amplitude of the corresponding reflector is highly variable. It is also a diachronous surface, identified as the K10.2 MFS regional pick in the west and a late Jurassic pick in the east.

This unit truncates the underlying MS2b, particularly in the western part of the study area; evidence of truncation is more limited towards the east. The seismic reflectors onlap the underlying strata at varied, but often high angles (Figure 3.11). The regional picks at the top and base of this mega-sequence are based on detailed investigation of this unit's age and the age of the surrounding unit. No well intersects a complete sequence of MS3a, and limited chronostratigraphic information is available.

The sequence occurs largely as, but is not limited to, the partial filling of half-graben as wedge-like features (Figures 3.2 & 3.3). This includes chaotic slump features of locally redistributed material. Sediment thickness decreases towards the south and west of the study area. In the central region MS3a is unconformably overlain by the MS3b unit, including some limited erosion of the top of MS3a (Figure 3.13). This interaction is of limited extent and further east the two units merge, becoming indistinguishable from one another. The sequence is thickest in the Thebe and Mary Rose Northern Extension survey areas.

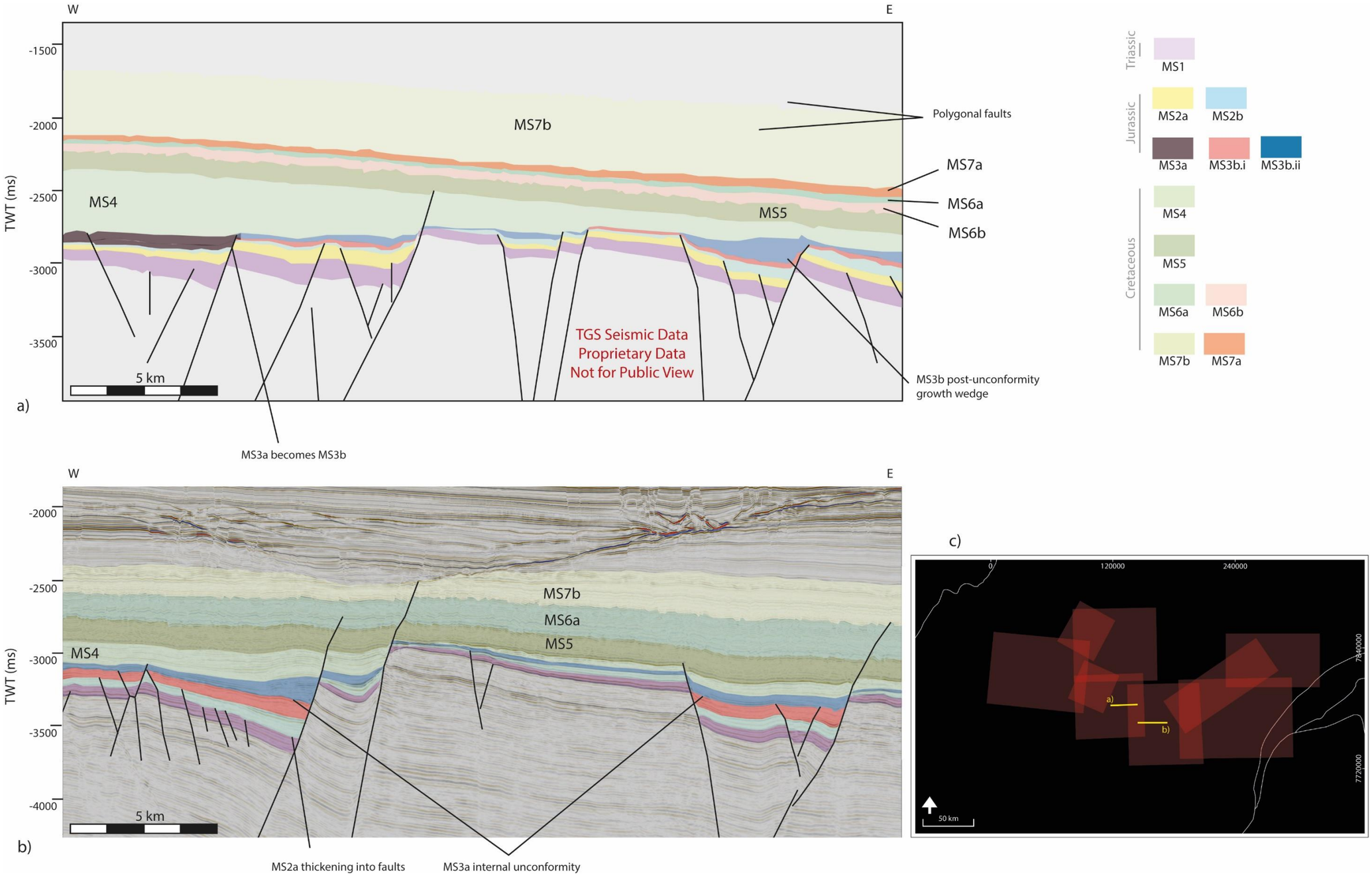

Figure 3.13 Cross-sections through the more western portion of the study area, highlighting the variation between internal divisions of the mega-sequences. Seismic data used here is removed for final public version.

3.4.2. J40 MS3B Oxfordian - Tithonian (J40.0 SB - J50.0 SB)

The second subdivision of MS3 records deposition after the Oxfordian Unconformity and prior to the Tithonian Unconformity (where the two unconformities are separate). The top seismic marker for this sequence is highly variable but is most commonly identified as the uppermost conformable reflector of low to medium amplitude, prior to a change in seismic facies to more chaotic facies, or to a series of higher amplitude reflectors (Figure 3.13). The base of the mega-sequence is a low angle unconformity, where a slight change in the angle of reflectors into downthrown half-graben or onto upthrown highs is observed (Figure 3.13).

This package displays an increase in thickness across faults, particularly in the uppermost strata in the Io-Jansz and Duyfken areas (Figure 3.12). A significant unconformity surface was identified within the MS3b sequence and extends into the west as the youngest Jurassic sequence (the MS3a mega-sequence). This division within the MS3 sequences was mapped in the Glencoe, Duyfken, and Honeycomb seismic surveys, though it does not occur extensively throughout any of these surveys (Figure 3.13). This is largely due to non-deposition over highs. In the Glencoe seismic survey, this unconformity predominantly occurs in the more western half and marks a sudden change in the formation of growth wedges against footwalls; i.e., following the unconformity, growth wedge formation is more pronounced (Figure 3.13). Reflectors onlap against these growth features. The occurrence of these seismic features continues into the west over the central region and is seen to cover a wide extent of the study area here.

Within the Willem-Pluto and Duyfken seismic surveys, two further unconformities were mapped within the late Jurassic strata. The older MS3b.v (Figure 3.14) is a seismic feature onto which overlying reflectors onlap. The younger MS3b.x (Figure 3.14) also has the same spatial extent as the MS3b.v unconformity, but in this case is a truncating unconformity surface. Neither of these unconformities can be correlated to the MS3a marker due to the difference in seismic character and distance.

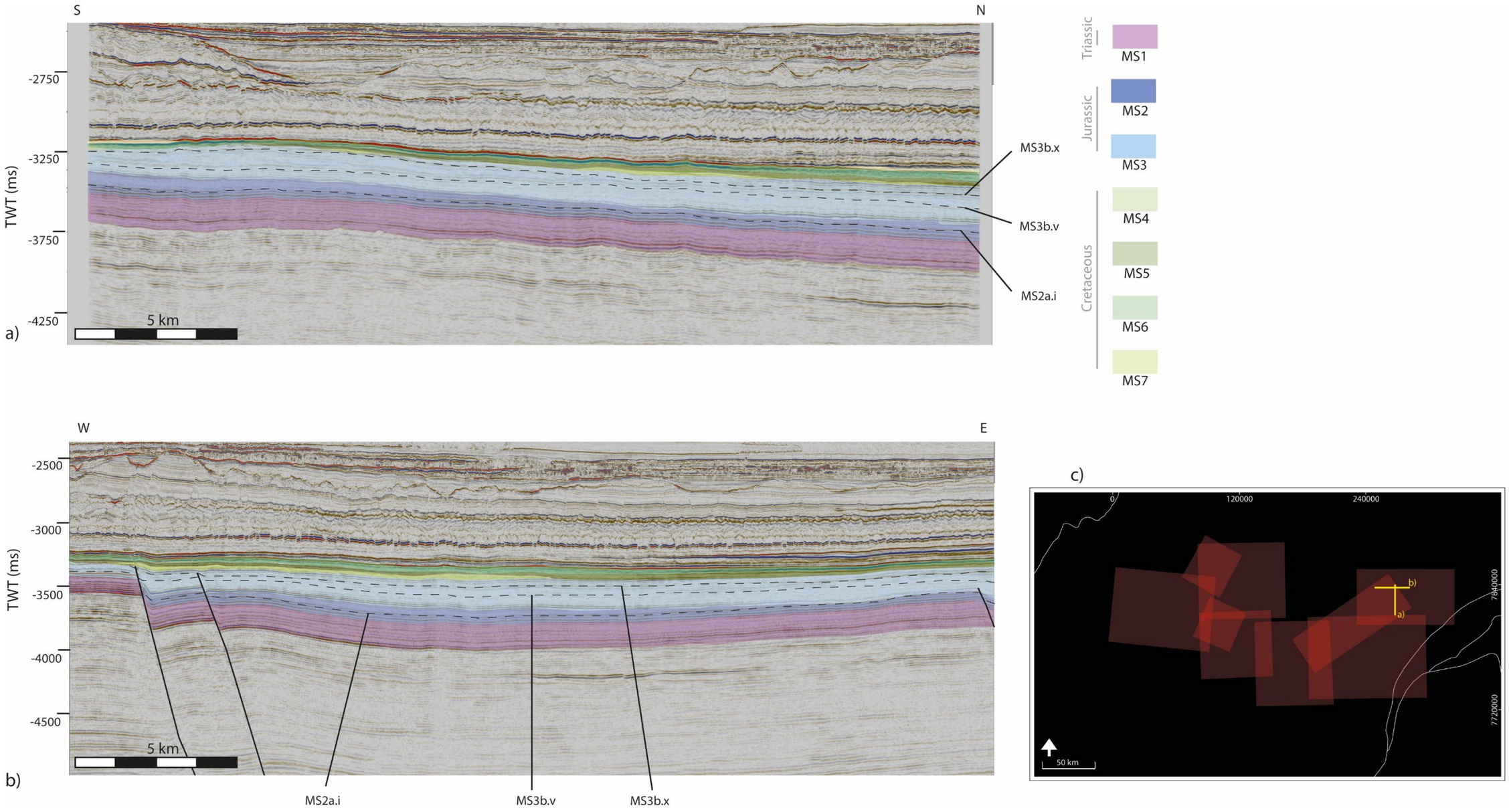

Figure 3.14 Internal divisions within MS2 and MS3 within the Willem-Pluto seismic survey area, located on the Wanthaya High.

3.5. K10 - K30 MS4 - MS6 Earliest Cretaceous (K10.2 MFS - K40.0 SB)

With a sudden change in the supply of sediment, the early Cretaceous package was supplied from the south (Wulff and Barber, 1995; Rohrman, 2015). This resulted in shallow shelf sediments prograding from the south over the Northern Carnarvon Basin. This progradation is represented as the northward migration of the shelf edge by the onset of Lower Barrow Group clinoforms. The already varied mega-sequence architecture resulted in a significantly different stratigraphic sub-division (Figure 3.1) on the Exmouth Plateau.

3.5.1. K10 MS4 Top Jurassic Unconformity - Valanginian Unconformity (K10.2 MFS - K20.0 SB)

This sudden change of sediment supply (see section 3.5) resulted in the deposition of the MS4 (K10.2 MFS - K20.0 SB), Lower Barrow Group (Figure 3.15), extending from the latest Jurassic into the earliest Cretaceous. The K10 Lower Barrow Group thins towards the northeast and is not deposited over a broad high in the area of the Willem-Pluto survey (Figure 3.16). Thickness changes across faults decline in the eastern part of the study area. The thickest sediment occurs in the southwest (Figure 3.16) where delta lobes migrated onto the plateau. Overall, the sequence thins northwards, and is generally thin in the east (Figures 3.2b, 3.2c & 3.2a). This unit is occasionally truncated at its top by the overlying MS5 and in places by MS6. In the west of the study area MS4 rapidly infills the previously starved half-graben features of the late Jurassic (Figure 3.2a). Fault activity is still high in the west as evidenced by the onlap of the K10 packages onto rotating fault blocks (Figure 3.2a). Some clinoforms are identified in the west. The onlap and downlap patterns are recognised in seismic data in the western extents of the study area. The MS4 sequence is represented by largely low to medium amplitude, concordant

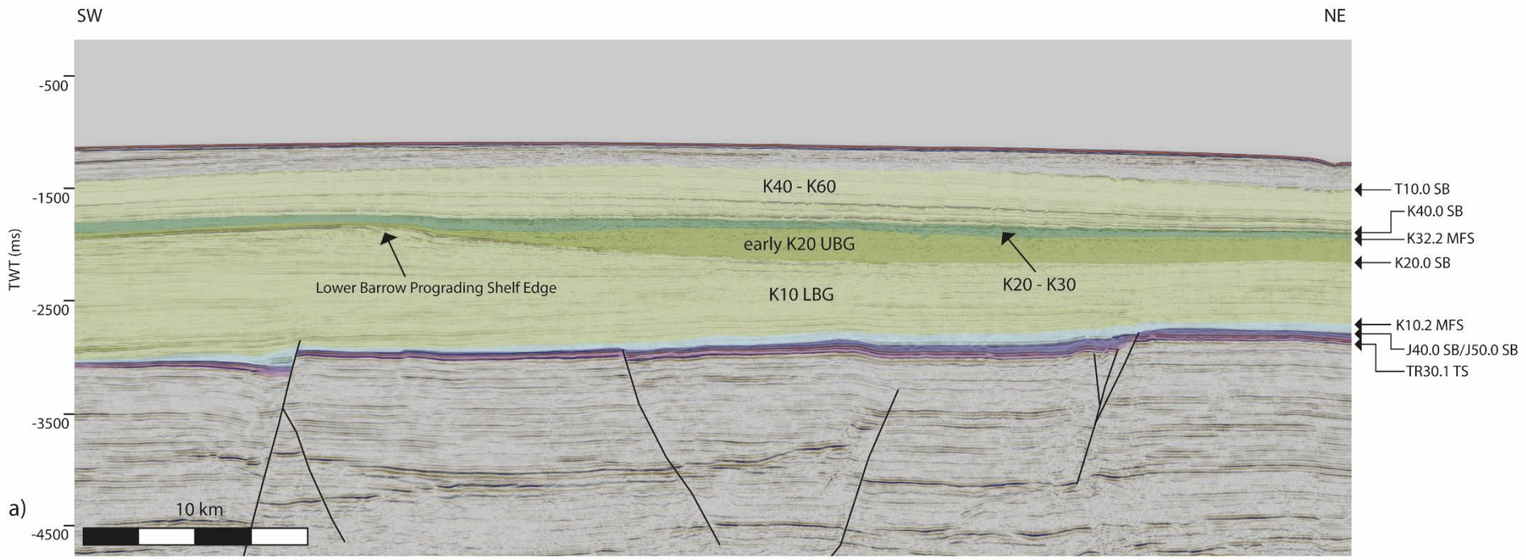

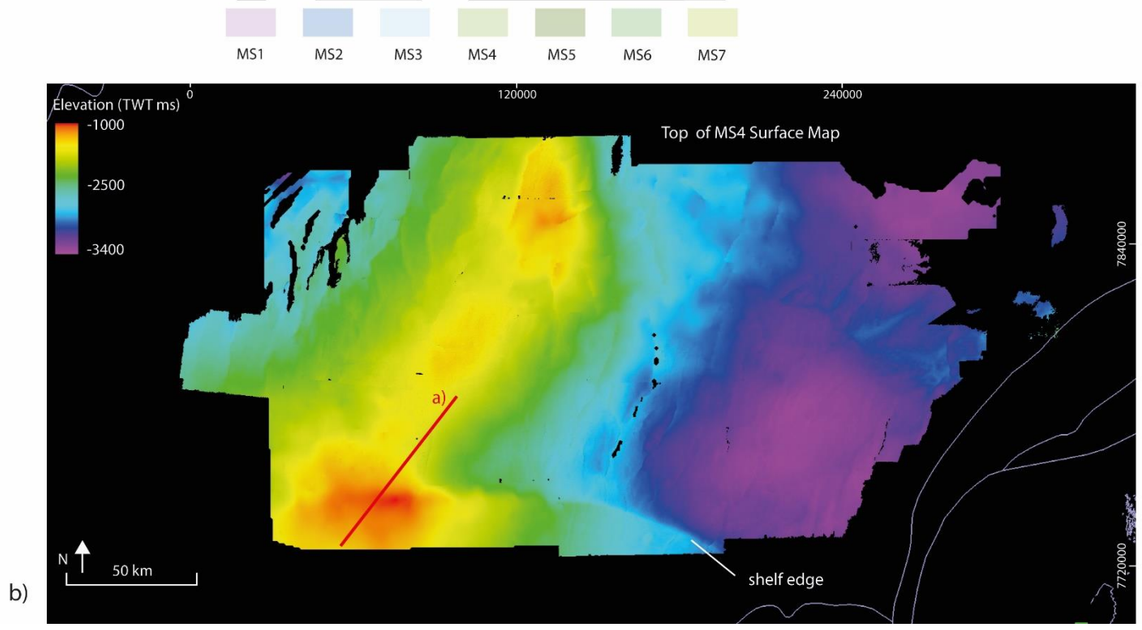

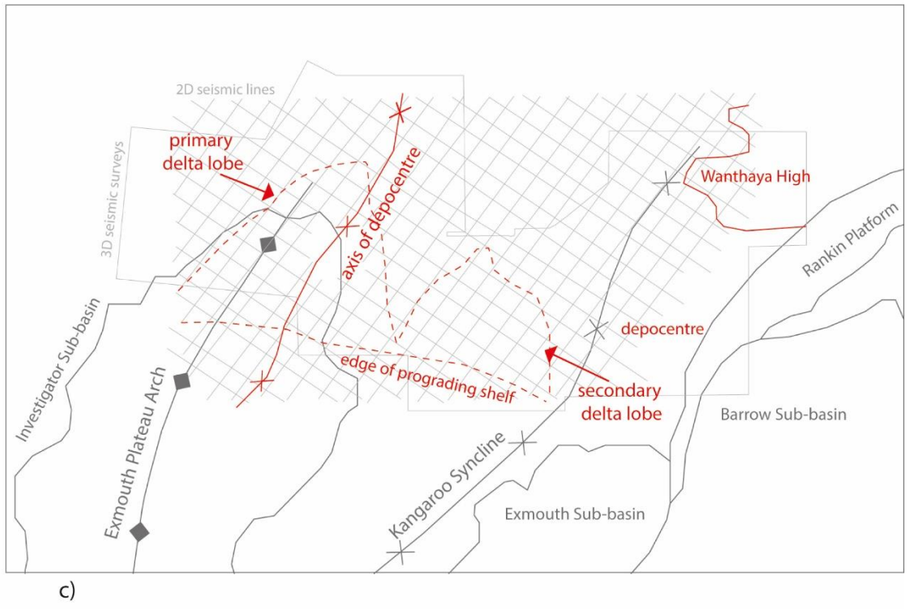

Figure 3.15 The prograded shelf edge of the Lower Barrow Group as observed in a) seismic cross-section, and b) an elevation map of the top surface. Key observations of structural and depositional feature are provided in c) the annotated line map of the Lower Cretaceous interval.

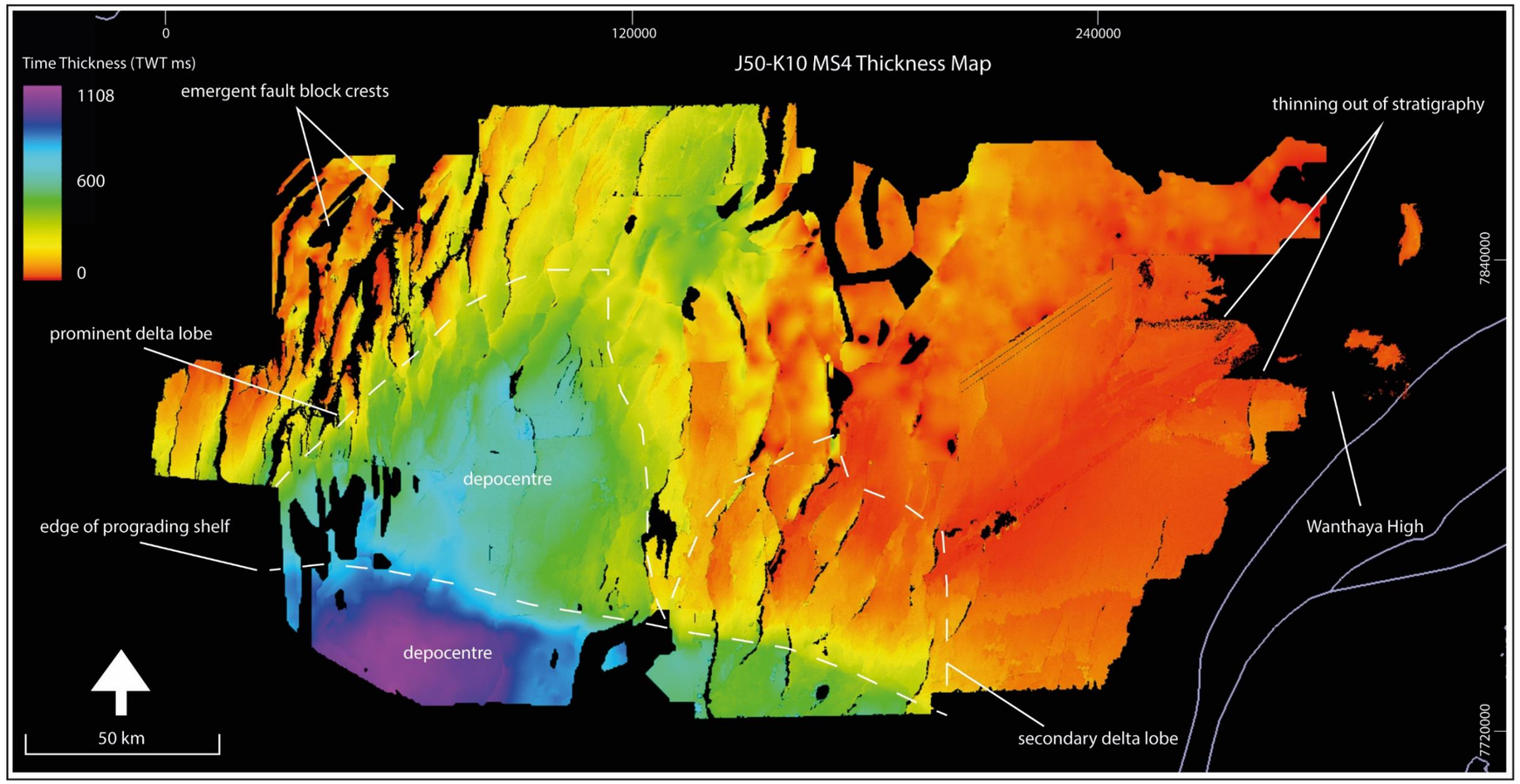

a)

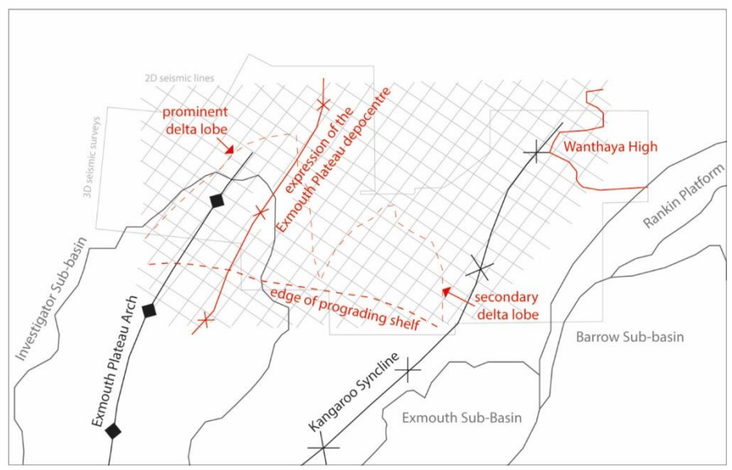

b)

Figure 3.16 Thickness map over the Exmouth Plateau showing the prograding shelf edge (southwest) moving into the plateau. The significant thinning and non-deposition of stratigraphy to the west revealing a new structural feature (see section 5.5.2 Wanthaya High) of the plateau. Annotated line map of features is shown in b).

reflectors. The reflectors within growth wedges are more chaotic in nature. Some high amplitude reflectors are also seen but there is no pattern to the location of these. Polygonal faulting occurs within this section (Figures 3.2a & 3.13a). In the east, thickening across faults at this time is limited to the sections which are more central to the study area (towards the west).

3.5.2. K20 MS5 Valanginian Unconformity - Barremian (K20.0 SB - K30.2 MFS)

After the Valanginian Unconformity (K20.0 SB), the shelfal marine earliest K20 Upper Barrow Group (MS5; K20.0 SB - K30.2 MFS) was deposited. Thickness of this sequence increases to the north of the shelf edge (Figures 3.15 & 3.17). The package then thins out in the northeast, over the topographically high Jurassic and MS4 strata (Figure 3.17). Here the MS5 reveals no thickening across faults. The K20 mega-sequence can be mapped across the entire study area as a complete package. In the west, there is a gradual decline of fault activity from the K10 - K20 Valanginian to the early K30 Barremian.

The MS5 sequence has a similar seismic character to the underlying MS4. It is represented by low to medium amplitude concordant reflectors, with some higher amplitudes present. This unit is affected by polygonal faulting.

3.5.3. K20 - K30 MS6 Barremian – Aptian (K30.2 MFS - K40.0 SB)

Following the deposition of the pre-breakup K20, the K20 to K30 shelfal marine Muderong Shale package was deposited in the mid-early Cretaceous. The pattern of deposition (Figure 3.18) in the east of the study is similar to that of the underlying MS5, where the sequence is thickest in the middle and thinnest in the south and north, where it onlaps onto a northeastern high (Figures 3.18, & 3.19). In the west, this sequence follows a similar pattern to the underlying MS5. There are limited thickness changes across faults, limited to the northwest. In seismic data, K30 is identified by higher amplitudes in

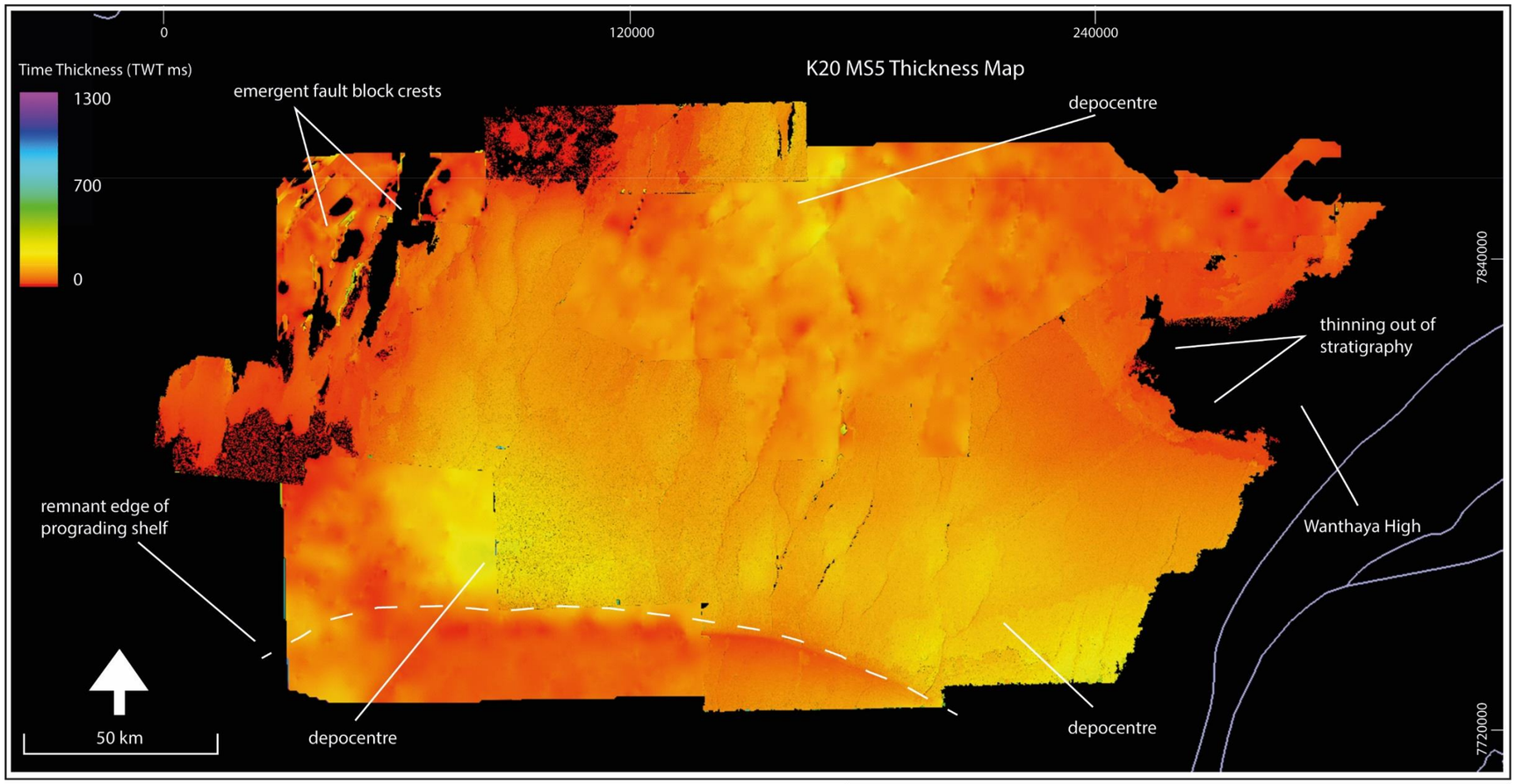

a)

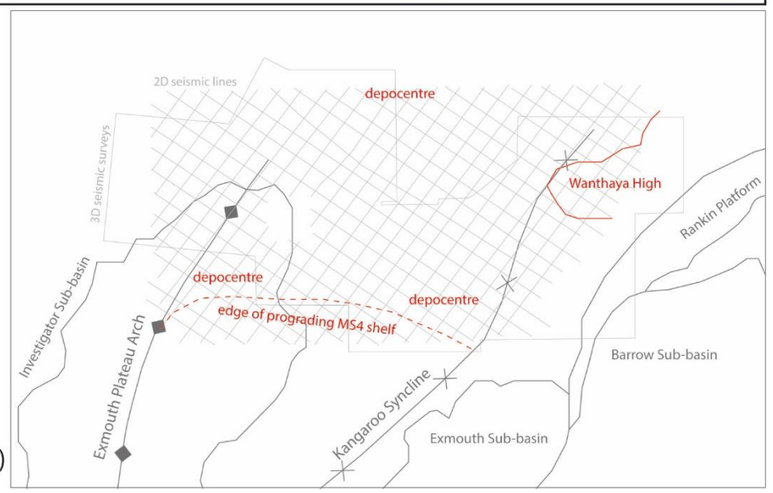

b)

Figure 3.17 a) Thickness (TWT) map of the K20 MS5 (K20.0SB - K30.2MFS), Upper Barrow Group over the Exmouth Plateau. The remnant shelf edge from the underlying Lower Barrow Group is a prominent feature of this interval as supply is carried over this feature and into the plateau, with deposition limited to the northeast. Annotated line map of key features shown in b).

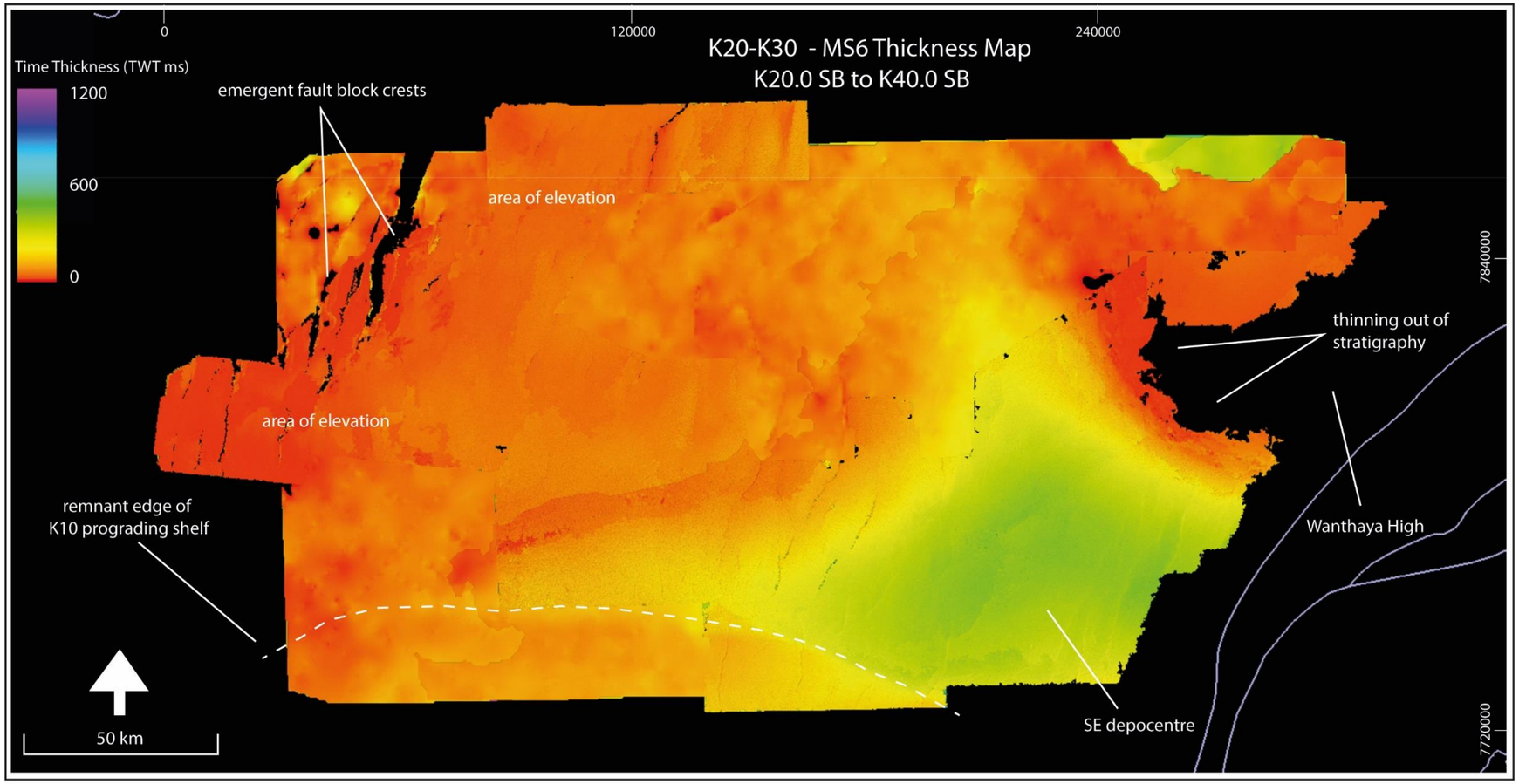

a)

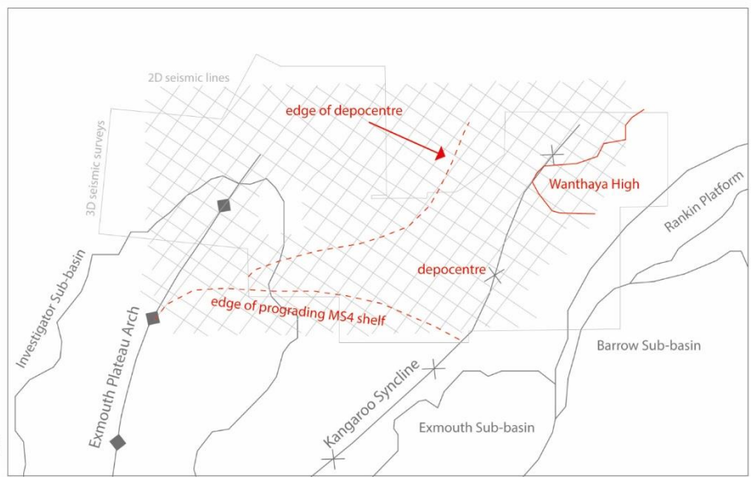

b)

Figure 3.18 a) Thickness (TWT) map of the K20-K30 MS6 (K30.2MFS - K40.0SB), Muderong Shale deposition over the Exmouth Plateau. The remnant shelf edge from the underlying Lower Barrow Group remains evident but is no longer the most prominent feature sedimentation is still limited in the northeast. Annotated line map shown in b).

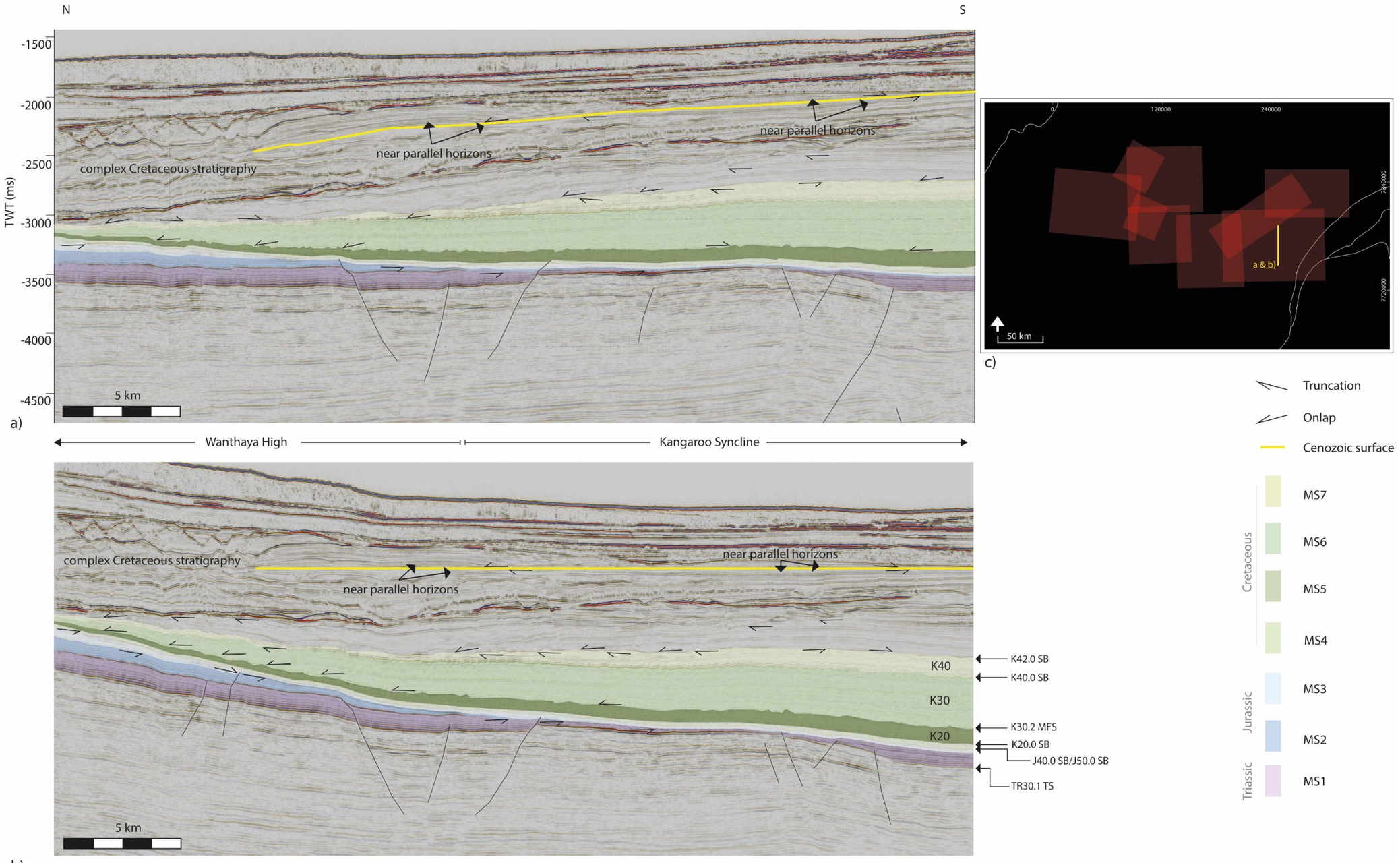

Figure 3.19 a) Cross-section of the Northeast High (Wanthaya High) in the northeast of the study, showing the onlap and truncation associated with this feature, and b) a 2D reconstruction of the potential elevation during the Cretaceous. The Cenozoic surface could not be identified by a narrower age range and was not identifiable for this studies scope across the whole line.

comparison to the underlying mega-sequences (Figure 3.2), particularly in the west. Onlap is a common feature in only the northeastern side of the study area, although no growth of the strata are observed. As such the fault system in the east is considered to be remnant during this time.

3.6. K40 - K60 MS7 Aptian - End Cretaceous (K40.0 SB - T10.0 SB)

The MS7 Aptian - End Cretaceous (Figure 3.20) mega-sequence encompasses the shallow marine K40 Windalia and K60 Miria Formations, K40 - K50 Gearle Siltstone, K50 Toolonga Calcilutite and temporal equivalents. The MS7 Aptian - End Cretaceous was sub-divided to distinguish where Cretaceous fault activity could be observed.

3.6.1. K40 MS7A Aptian (K40.0 SB - K42.0 SB)

In the east MS7a is highly incised by younger channel/canyon structures (Figure 3.3) and so is only interpreted within the Aptian. The upper pick for this interval is presumed to be the K42.0 SB, but biostratigraphic data would be required to a make a more accurate correlation. Further investigation of these incised Cretaceous aged structures is currently being undertaken by Curtin University - University of Aberdeen Doctoral Candidate, Mulky Winata. The MS7a package thins rapidly to the north (northeast) and is not deposited over much of the northeast high (Figure 3.20). It is thickest in the south where a broad sag occurs in the more central region (Figure 3.20) in the position of the Kangaroo Syncline.

In terms of seismic character, this Cretaceous package is characterised by relatively flat lying reflectors which are interrupted by polygonal faulting (Figure 3.2). The amplitude of these reflectors is low to medium and transparent. The top of this unit is represented by a medium amplitude reflector, which most often marks the end of polygonal fault networks. The base is a very low angle unconformity, as deposition prograded towards the north, and subtle onlapping occurred. No thickening is associated with movement along fault plains, making this sequence post-extensional in nature.

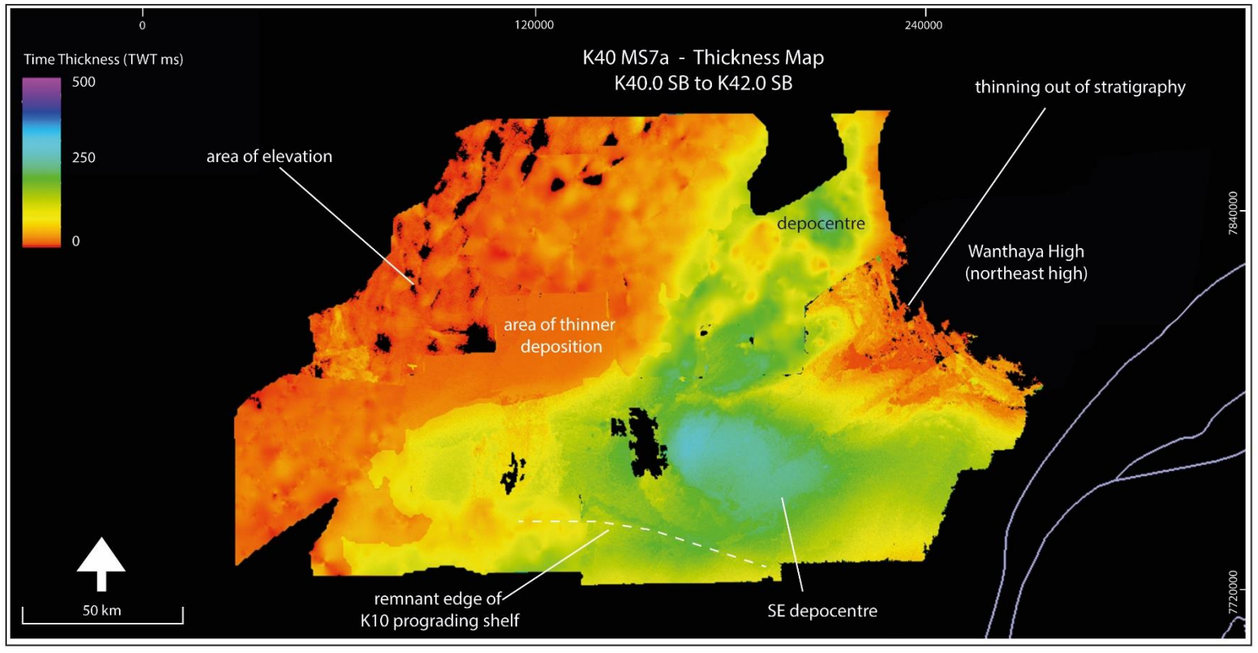

a)

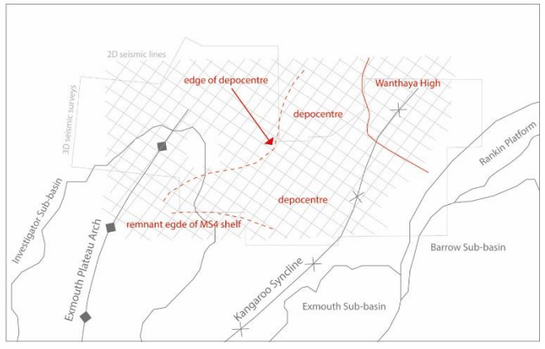

b)

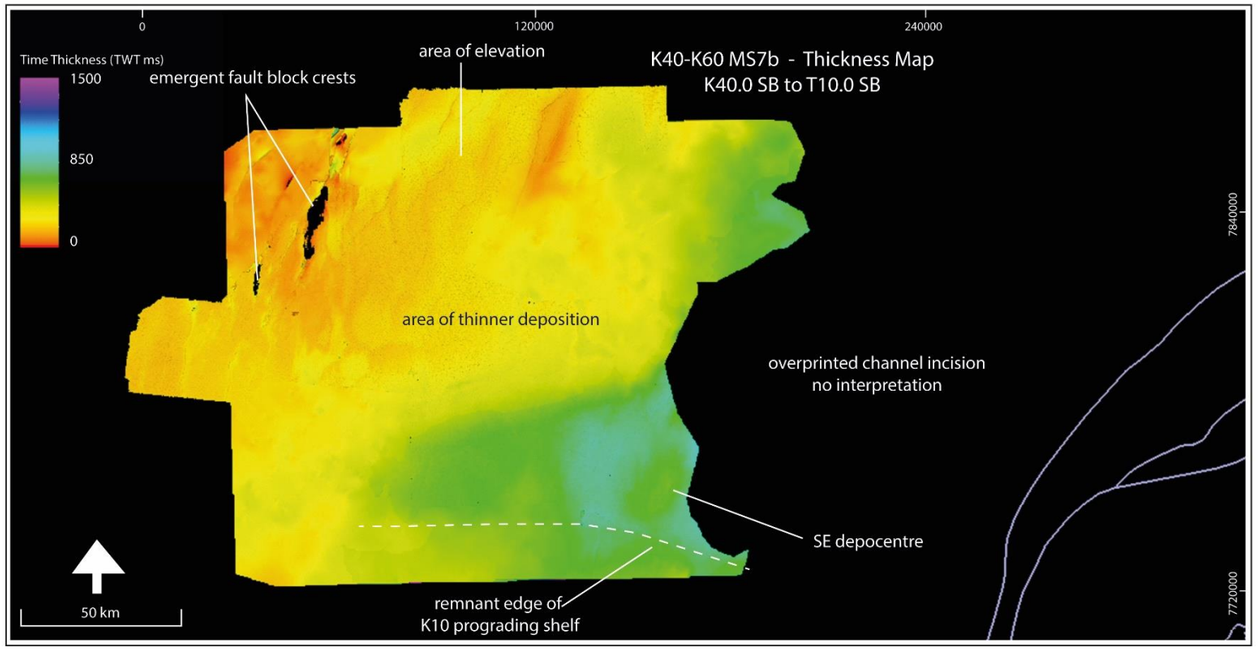

c)

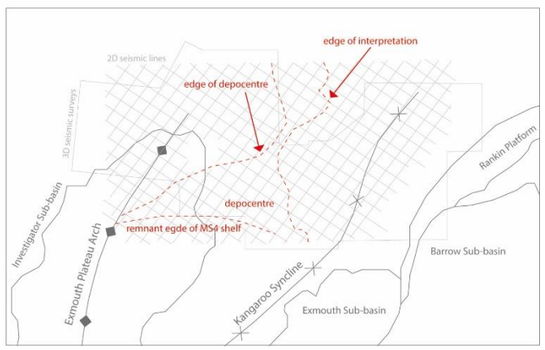

d)

Figure 3.20 Thickness (TWT) maps of the a) K40 MS7a showing the thickness of the Aptian aged package, deposited onto relative highs in the northeast and west, and b) the K40-K60 MS7b Aptian to end of Cretaceous aged packages showing still emergent fault block crests and a thinning out of strata in the west, c) annotation of prominent features also shown here.

3.6.2. K40 - K60 MS7B Post Aptian - End Cretaceous (K40.0 SB - T10.0 SB)

The MS7b mega-sequence in the west of the study area stretches to the very end of the Cretaceous (K40.0 SB - T10.0 SB; Figure 3.3). The strata are thickest over to the southeast (southern central region) of the interpreted area (Figure 3.20). With limited thickness changes on either side of major faults, the mega-sequence is largely post-rift, with very late stage syn-extension deposition observed to occur along a few larger faults. It is represented on seismic as a series of parallel reflectors of medium to high amplitude, with frequent polygonal faulting.

3.7. Chronostratigraphic History of The Exmouth Plateau

The broad mega-sequences defined in this study and described above were developed to enable correlation of events across the study area (Figure 3.21). The internal sub-divisions within the broader mega-sequences highlight variations in the timing and intensity of fault movement and sediment input. Further variations may apply to the mega-sequence framework in other parts of the Exmouth Plateau (Figure 3.4) due to the changing nature of tectonic and depositional activity. However, the broad division into pre-, syn, and post-rift sequences still applies, albeit with local variation. The chronostratigraphic chart (Figure 3.9) derived from the study area is most important for revealing the different periods of fault activity described in Chapter 4. The mega-sequence framework provides the basis for working out the timing of rift development and basin fill, and the lateral variations in these processes.

3.7.1. Pre-Mesozoic Rift (PRE TR30.1 TS)

As a prolonged period of thermal subsidence continued from the Permian into the Triassic (Etheridge & O'Brien, 1994; Jablonski & Saitta, 2004; Stagg et al., 1999; Veevers, 2006), thick layer-cake sequences were deposited (AGSO

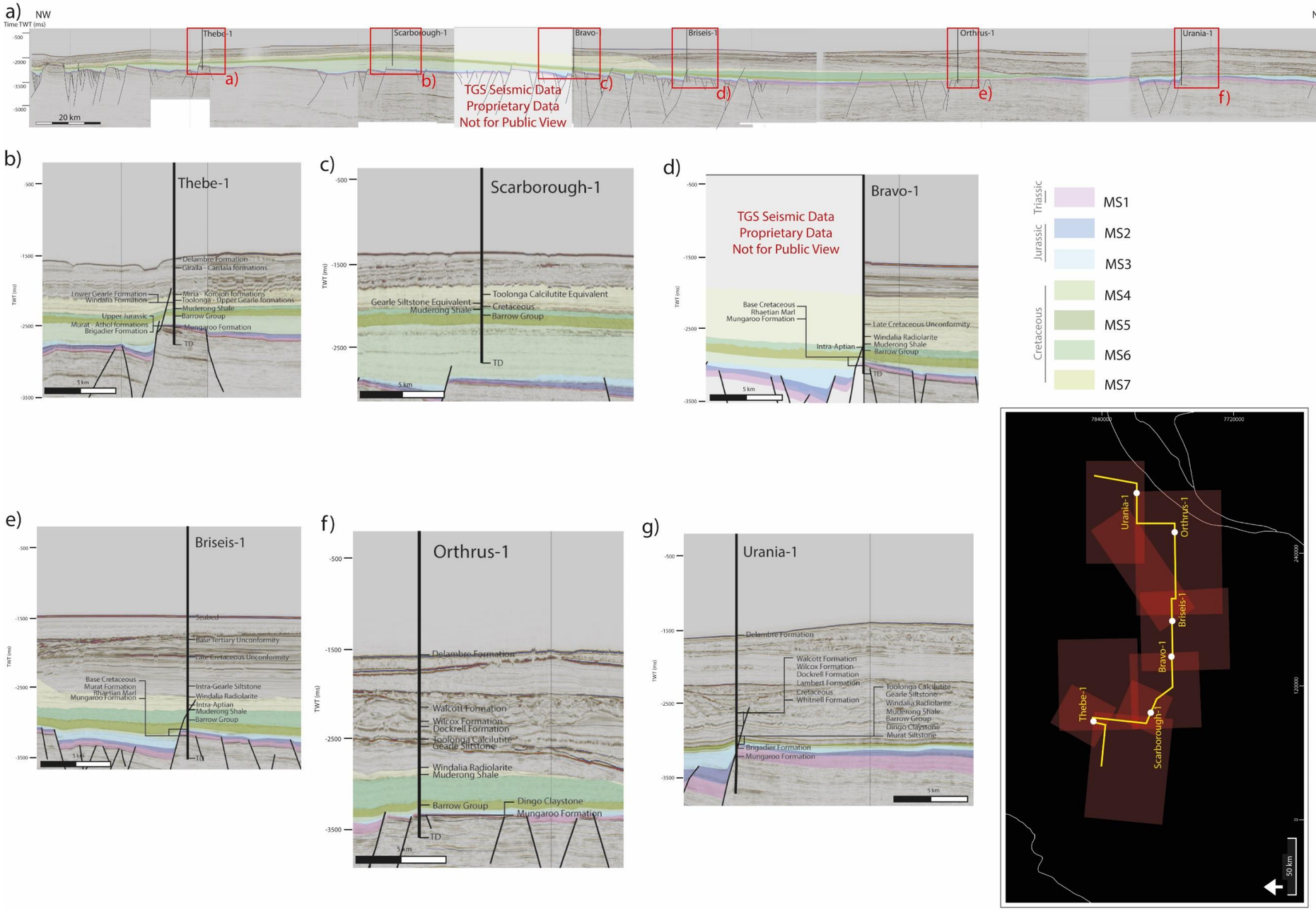

Figure 3.21 Composite cross-section through the study area displaying the variation in structural architecture and the relation of mega-sequences to this. Images b) to g) are inset from the composite line, with locations marked with red boxes, displaying close ups of prominent wells used for this research. Seismic data used here is removed for final public version.

North West Shelf Study Group, 1994) in a distal deltaic environment (Figure 3.22a; Adamson et al., 2013). Older stratigraphic units are observed in the regional Bart 2D seismic survey line (Figure 3.4). No evidence of movement is observed during the deposition of these older sequences on the Bart 2D seismic line. The age of these units is unconstrained by well penetrations. It is likely that the TR10 Triassic Locker Shale is present at depth across the Plateau, forming the basal portions of the pre-rift sequence of Mesozoic age.

3.7.2. Main Syn-Rift (TR30.1 TS - K10.2 MFS)

3.7.2.1. Top Norian Unconformity (TR30.1 TS)

Following the extended period of thermal sag and prolonged and uninterrupted deposition, rift activity began to affect the Exmouth Plateau in the Uppermost Triassic (Baillie et al., 1994; Blevin et al., 1994; Etheridge & O'Brien, 1994; Geoscience Australia, 2014a, 2019; Rohrman, 2015; Smith et al., 1999; Yeates et al., 1987). This resulted in an event recognised broadly in the western portion of the area of investigation, the Top Norian Unconformity (TR30.1 TS) which was earlier identified by Rad et al. (1992) in the northern plateau and the Ago Abyssal Plain. This is also evidenced along the southwestern region of the study, on the Bart 2D seismic line.

The latest Triassic sequence occurs across the area studied. In the west it is largely deposited within developing half-graben, whereas in the east, deposition remains layer-cake in nature (Figure 3.22b). Later localised uplift of fault blocks resulted in the small-scale erosion of the TR30 Rhaetian sediments from the crests of these fault blocks in the more western part of the study area. This uplift also resulted in the erosion of strata from the underlying pre-rift sequence, in line with evidence presented by Rad et al. (1992).

3.7.2.2. TOP TRIASSIC UNCONFORMITY (J10.0 SB)

At the end of the Triassic a prominent event is identified in the study area. It is best represented in the western regions by a sudden change in the angle of bedding between the Triassic and early to Middle Jurassic sequences. In the eastern regions this division is less clear, but the stratigraphy can be traced

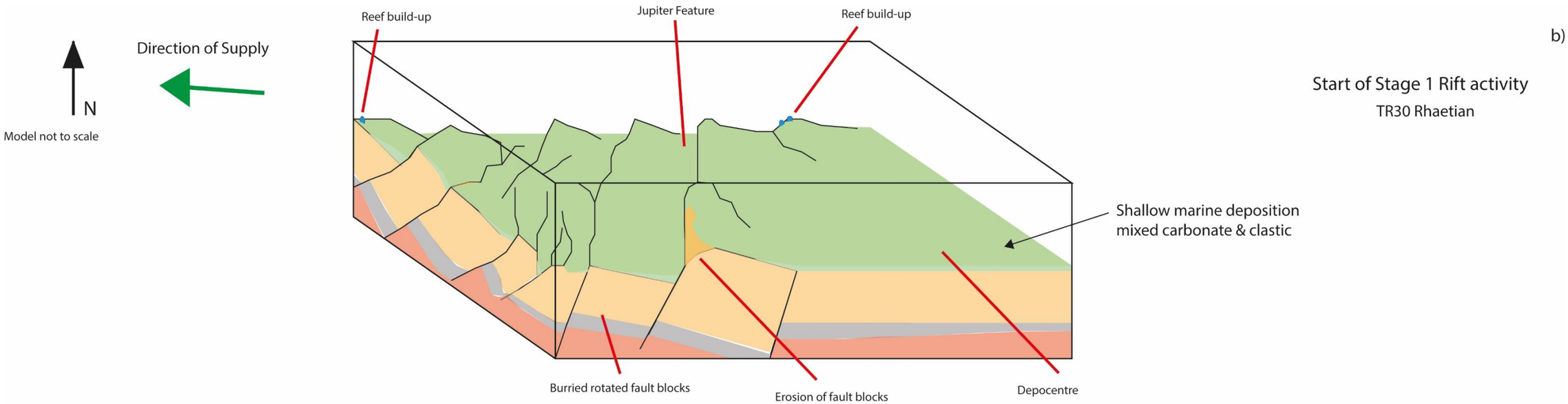

Figure 3.22 Conceptual sketch of cross-section of what the rift looked like during several stages of rift development. The Pre-kinematic Exmouth Plateau a) prior to Mesozoic rifting, and the b) initiation of rift activity in the TR30 Rhaetian.

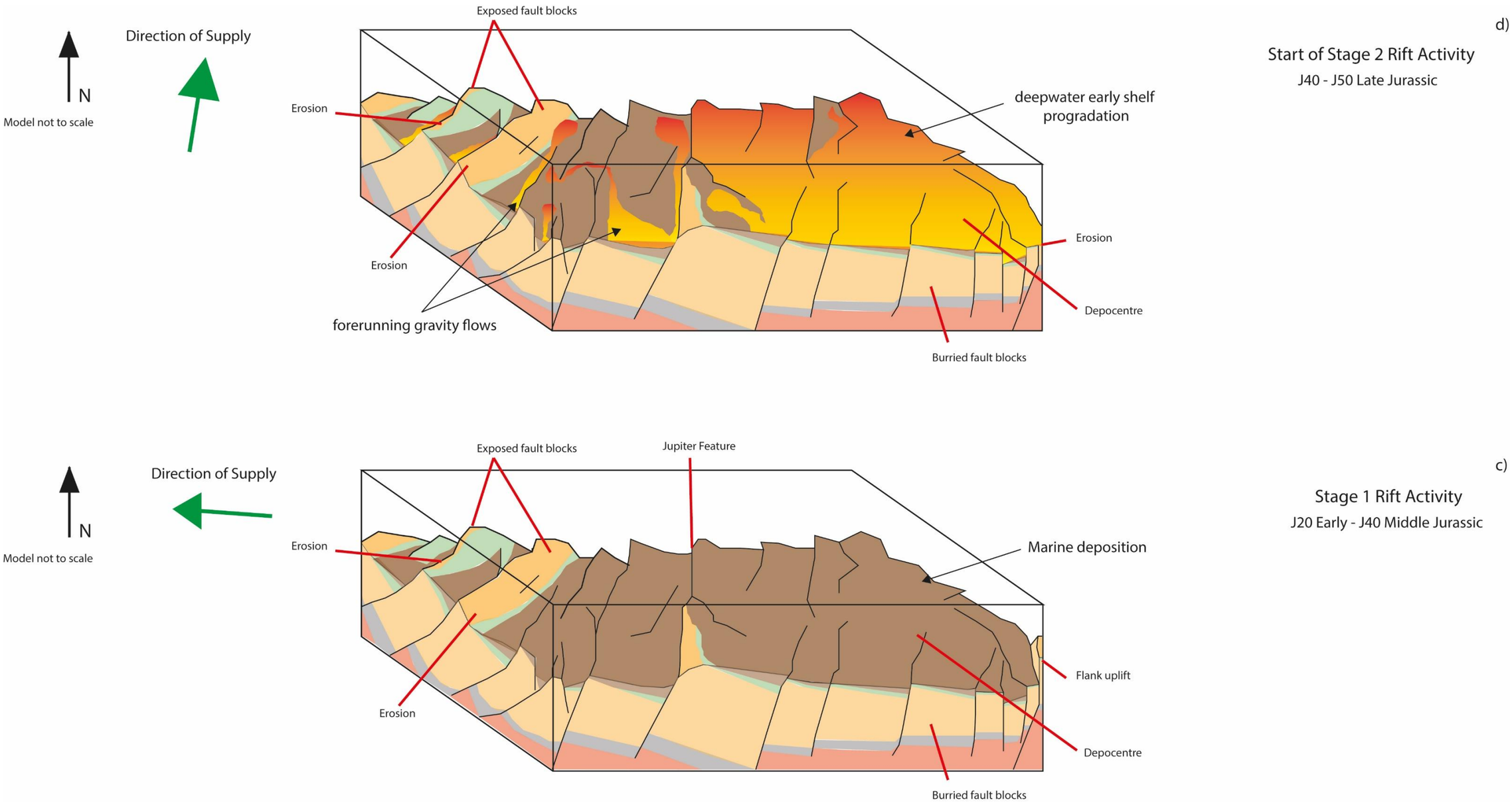

Figure 22 Conceptual sketch of cross-section of what the rift looked like during several stages of rift development. Lower Jurassic rift continuation c) and the Upper Jurassic rift development d).

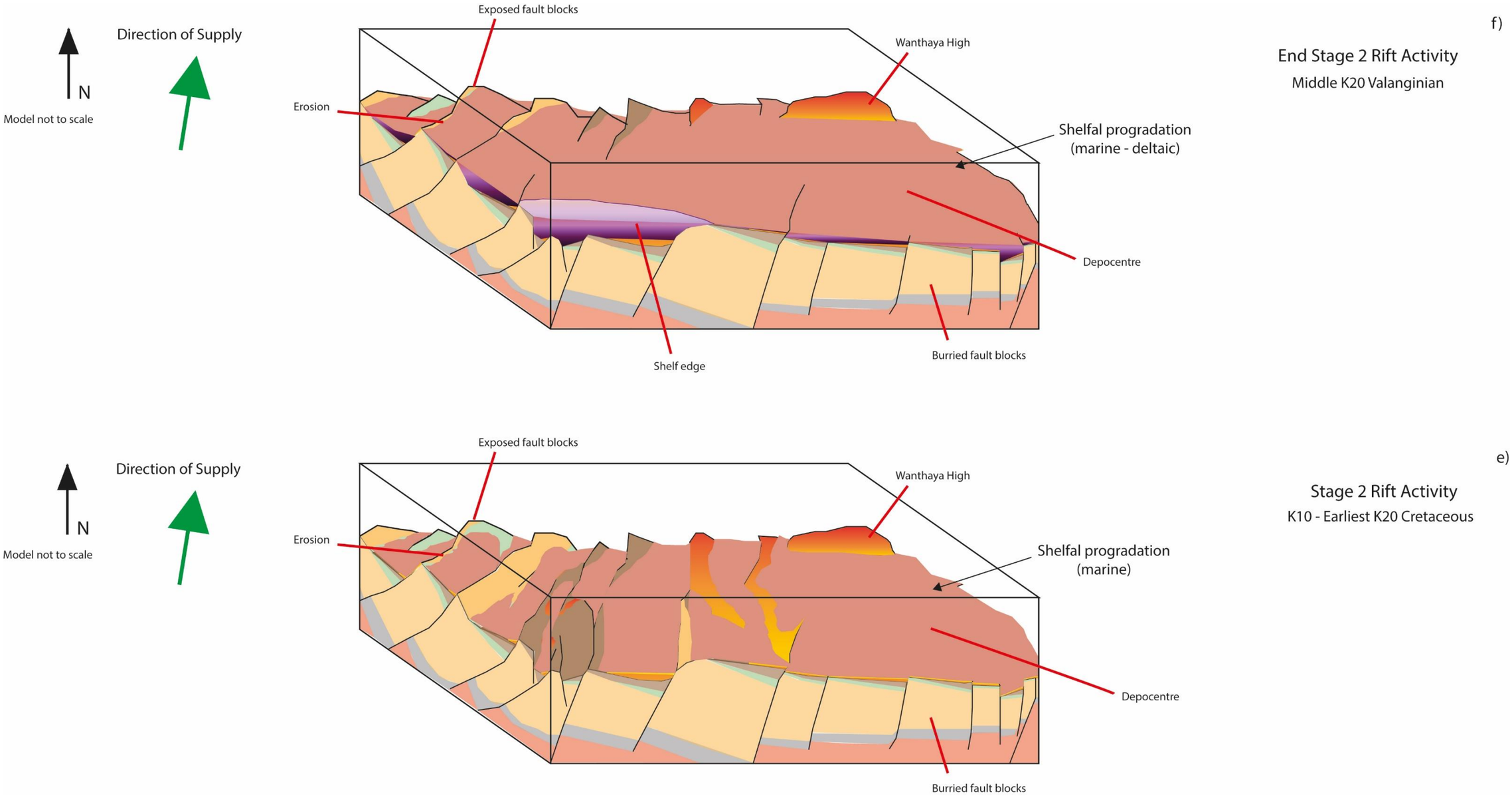

Figure 22 Conceptual sketch of cross-section of what the rift looked like during several stages of rift development. Initial onset of Lower Cretaceous rift activity e), and the end of rift activity f) in the mid-Valanginian.

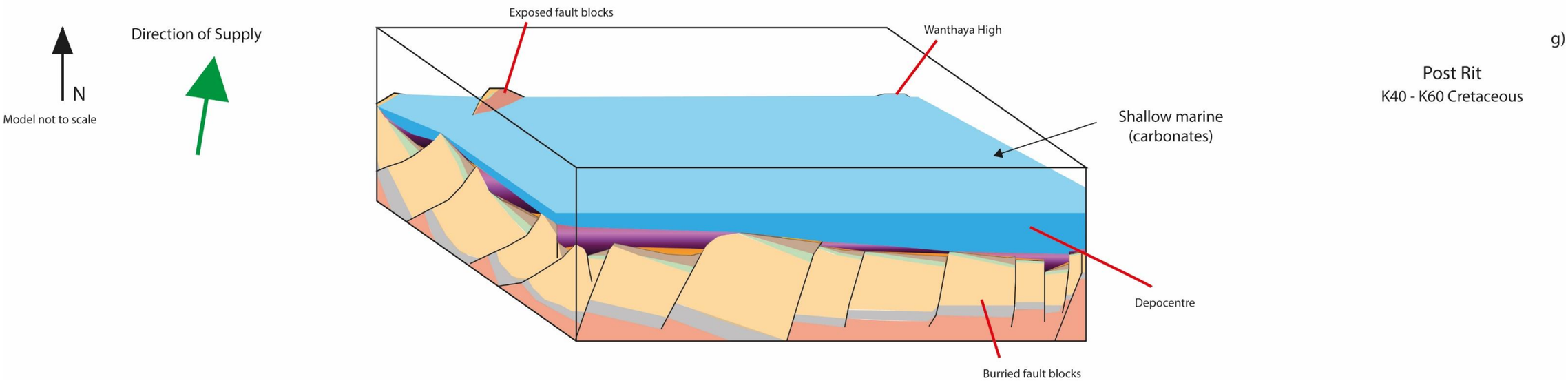

Figure 22 Conceptual sketch of cross-section of what the rift looked like during several stages of rift development. The end Cretaceous, post-rift, development of the Exmouth Plateau g).

through seismic reflectors as being of the same relative ages, even where no fault activity is indicated. It is also likely from the known stratigraphy of the region that there was a depositional hiatus or a period of limited sediment preservation in the earliest Jurassic. Following this, the marine sediments of the J20 Athol Formation, J20 Murat Siltstone and J40 Dingo Claystone were deposited. Ongoing fault movement explains the high angularity of this unconformity in the western regions of the study area. This hiatus could have ended as early as the J20 Sinemurian (J20.1 TS) or could be correlated to an event identified in the Exmouth Sub-basin during the J20 Pliensbachian - J24.0 SB (or JP; Jitmanhantakul & McClay, 2013). It is more likely tied into the tectonic activity associated with this later J24.0 SB event. Regardless of the exact timing, this period is known as a time of high accommodation space creation (Marshall & Lang, 2013).

Following on from this period of non-deposition or erosion, the accommodation space began to fill with marine sediments, largely fine grained in nature (Adamson et al., 2013). Some erosion continues on the uplifted and exposed fault block crests, further eroding previously deposited strata and the more recently deposited early Jurassic sequence. In addition, a broader erosional feature defines the southeastern edge of the study area, adjacent to the Rankin Platform. Much of the Triassic aged stratigraphy, the upper TR10 – TR20 Mungaroo Formation (pre-rift) and the TR30 Brigadier Formation (MS1) are eroded. In addition, a large portion of the early to Middle Jurassic sediments (MS2) are also eroded. This is tied into the extensional activity in the neighbouring Dampier Sub-basin and the associated rift flank uplift, producing the Rankin Platform (Figure 3.22c; Cathro & Karner, 2006; Driscoll & Karner, 1996, 1998).

3.7.2.3. MIDDLE JURASSIC UNCONFORMITY (J40.0 SB)

The prominent Middle Jurassic Unconformity (J40.0 SB) marks the formation of the Argo Abyssal Plain (but not the end of extension) and can be observed in many places on the Exmouth Plateau. However, due to the condensed nature of the Jurassic sequence, this event is not clearly separated from the

later Kimmeridgian Unconformity (J47.0 SB) or, in places, the Tithonian Unconformity (J50.0 SB). The amalgamated nature of these unconformities, as represented on seismic data, leads to the many different descriptions in literature of late Jurassic stratigraphic events across the NWS (Geoscience Australia, 2014a, 2015, 2019; Heine & Müller, 2005; Marshall & Lang, 2013; Stagg et al., 2004; Whittam et al., 1996).

The sediments that were deposited following the J40.0 SB Middle Jurassic event are limited in thickness, as is their description from well completion reports. In the west this mega-sequence (MS3a) is largely underfilling half-graben which are sediment starved (Figure 3.22d). In this same area, the erosion of material from higher relief upthrown fault block crest also occurs, but to a lesser degree than in the underlying early to Middle Jurassic examples. To the east the unit (MS3b) is much more flat-lying over the limited topography but does show evidence of syn-kinematic deposition.

3.7.3. Late Syn-Rift (K10.2 MFS - K40.0 SB)

3.7.3.1. Berriasian Unconformity (K10.2 MFS)

Following on from the latest Jurassic, a significant change occurred on the Exmouth Plateau. This is largely related to the northwards progradation of a shallow marine shelf in the form of the K10 Lower Barrow Group (Figures 3.22e & 3.22f). There is a recognised erosional unconformity in the neighbouring Exmouth Sub-basin at this time (Jitmanhantakul & McClay, 2013). While no significant erosion is evidenced on seismic data on the Exmouth Plateau, there are onlapping reflectors between the pre- and post-K10.2 MFS surface (Figure 3.2). This mega-sequence thins out as it prograded northwards across the plateau. This time is also the end of fault activity in the eastern portion of the study area, whilst the movement along faults continues in the west. There are indications that erosion of uplifted fault blocks occurred during the deposition of the K10 Lower Barrow Group, but no clear evidence of the K10 Lower Barrow Group being eroded in this manner.

3.7.3.2. Valanginian Unconformity (K20.0 SB)

Following on from the Valanginian final separation event (K20.0 SB; Geoscience Australia, 2014a, 2019; Marshall & Lang, 2013), fault activity began to decrease in the western regions. Accommodation space was still available and being created, although at a lower rate than during the deposition of the K10 Lower Barrow Group. The strata of the marine earliest K20 Upper Barrow Group and the K20 - K30 Muderong Shale began to fill in the available space.

3.7.4. Post Rift (K40.0 SB - T10.0 SB)

3.7.4.1. Aptian Unconformity (K40.0 SB)

Following the K40.0 SB Aptian event and continuing up to the end of the Cretaceous, thick sequences were deposited and sedimentation controls the architecture of the plateau except for in the west, there are several prominent fault blocks on which movement continued into middle Cretaceous (Figure 3.22g). These fault blocks remain unburied by the later Cretaceous sediment. Polygonal faulting is also a prominent feature in the northwest but is post-depositional. In the east sediments are largely recycled by erosion through large scale and high-density channel incisions. This made interpretation of the strata from K42.0 SB to T10.0 SB challenging, and it now forms the basis for a separate doctoral research project (undertaken by Mulky Winata).

4. Structural Architecture of the Exmouth Plateau

A variety of extensional features form the Exmouth Plateau, of these an extensive network of normal faults is the primary feature. Faults across the plateau formed in a variety of orientations, the most prominent being NNE-SSW and NE-SW (Figures 4.1, & 4.2). Additional displacement occurred along NW-SE orientated faults (Figures 4.1, & 4.2) and a limited number of faults formed in an E-W orientation (Figure 4.2). The dip of these faults is predominantly N, NW, and W, meaning that the faults dip seaward and the rotated fault blocks dip southeast and east; towards the Australian mainland (Figures 3.2, & 4.2). Many of the faults are simple extensional faults with varying degrees of displacement. Fault block rotation has resulted in the formation of half-graben across much of the plateau. A limited number of landward dipping faults have formed symmetrical graben. In addition to the uplift of individual footwall fault blocks, the plateau has experienced broader scale uplift. The extent of this uplift varies spatially. However, a clear structural high formed from the regional uplift is present in the western parts of the study area (Figures 4.1, & 4.2), corresponding in position to the Exmouth Arch (Figure 4.2). Uplift and erosion of Jurassic sequences by a Middle to Upper Jurassic unconformity (see section 3.7.2.3 Middle Jurassic Unconformity (J40.0 SB)) is evident on the flank of the Dampier Sub-basin (Figures 3.2b, 3.3a, 3.5a, & 3.8a). In regions exposed to greater fault block uplift or rotation, the crests of the rotated fault blocks have been eroded (Figures 3.2a, & 4.1).

Fault traces are variable in map view (Figure 4.2). Faults with a curved fault trace are often associated with well-developed syn kinematic sequences. These curved fault traces are a result of stress transfer at their tips, causing faults to bend towards one another and link across accommodation and transfer zones (Figure 4.1). In contrast, many of the faults which display little to no syn-kinematic growth form straight fault traces. The majority of faults which display observable displacement across periods of rifting (main faults), extend to depths of 5.5 km (Figure 3.4, as fault die out zone 1) intersecting

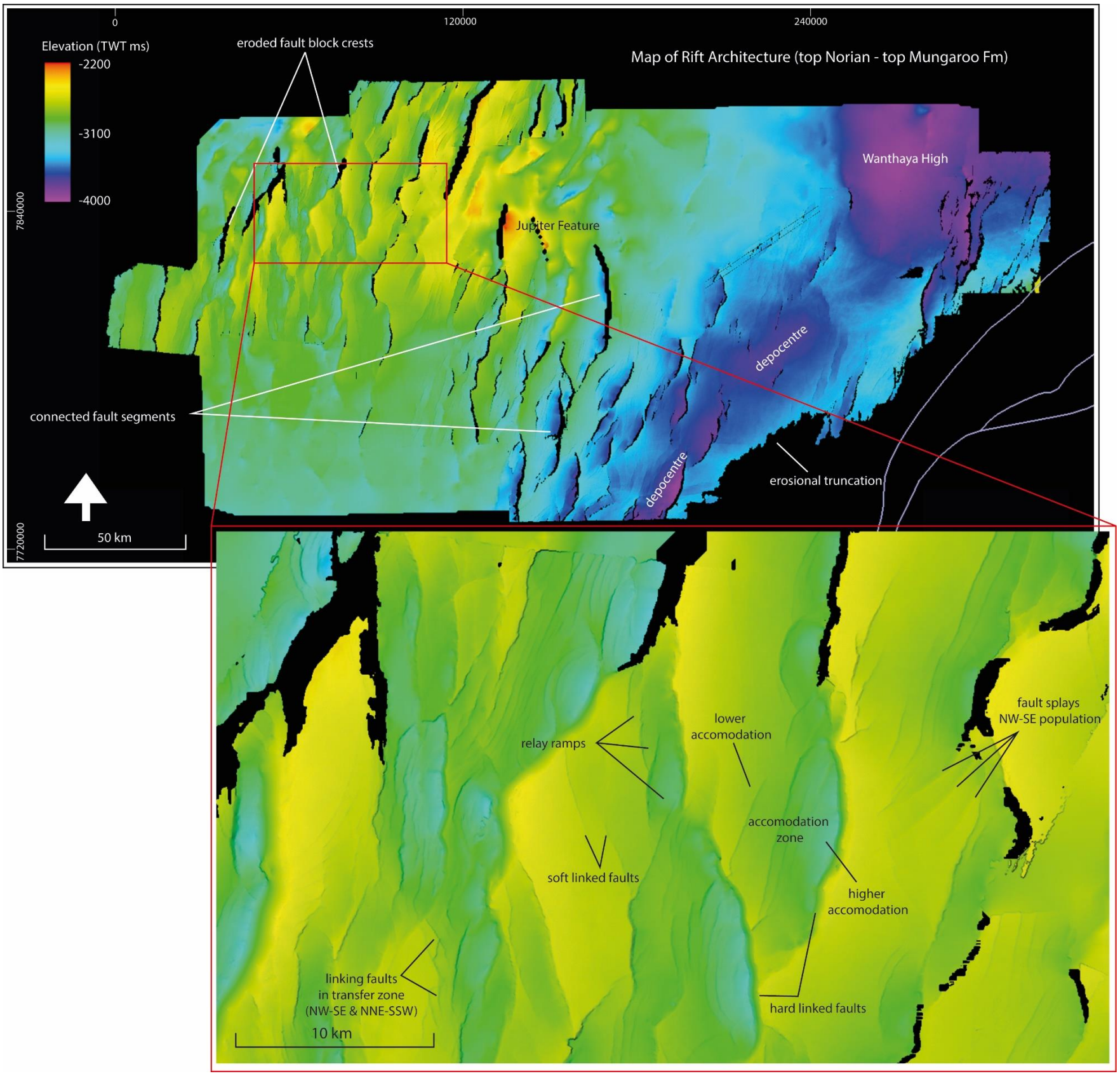

Figure 4.1 Rift architecture displayed on a surface map of the TR30.0 SB (top Norian) horizon sequences over the Exmouth Plateau. Inset showing some of the typical relationships of faults to one another, shown on a small section of the western plateau.

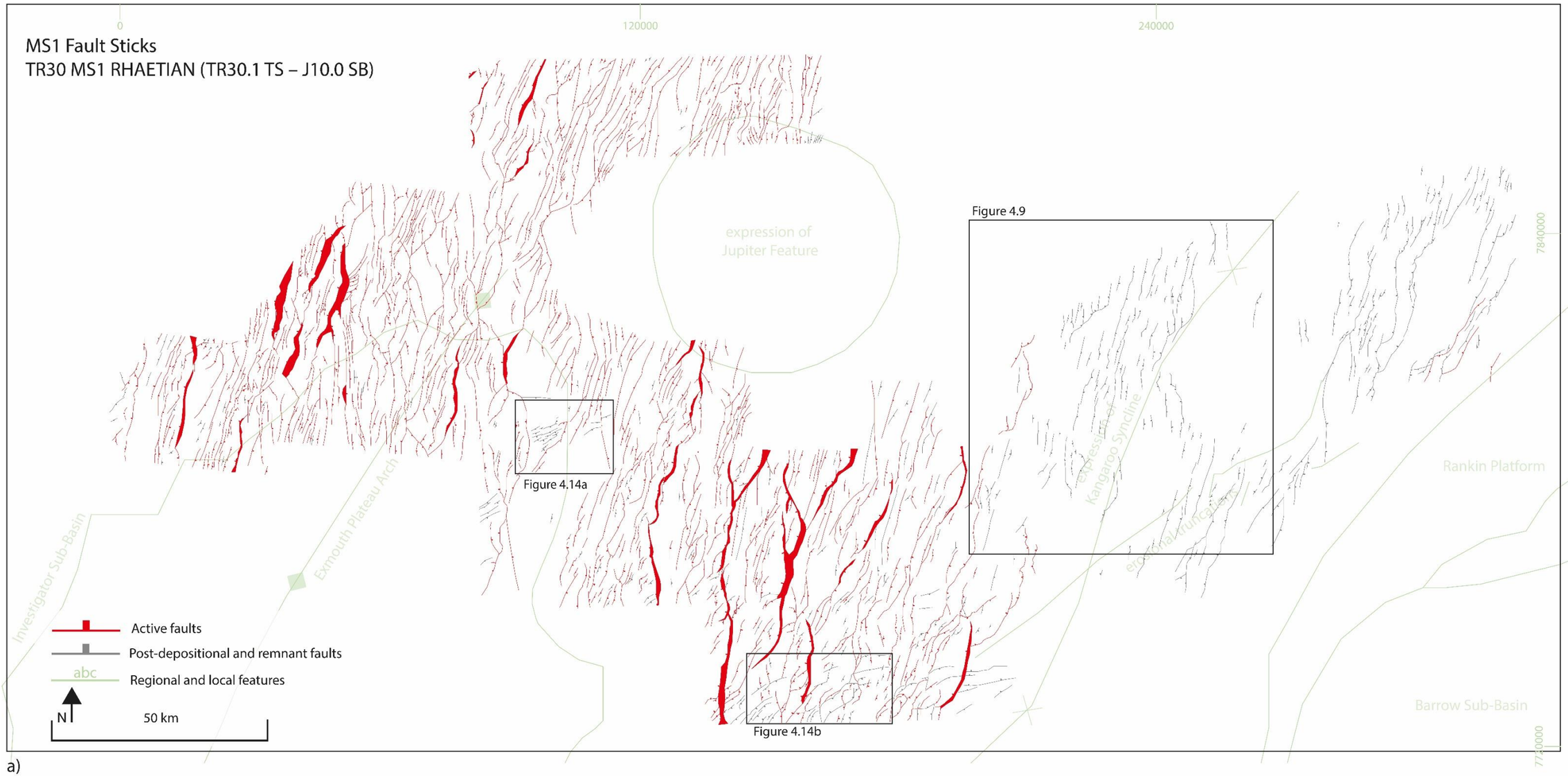

Figure 4.2a Fault stick maps of fault traces as mapped from 3D seismic data. Rhaetian (TR30 MS1) age fault activity (red) and faults which penetrate the Rhaetian aged stratigraphy following deposition (grey). The fault sticks showing significant fault activity in the west of the study area, as well as a higher frequency of faults and fault networks in this area. Note also the more east to east-north-east orientated faults in the southernmost survey area (Glencoe survey) and to the northwest of this location (Scarborough and Honeycomb surveys). Note that regional scale features are provided in the green underlay, this includes the expression of some features during time frame displayed.

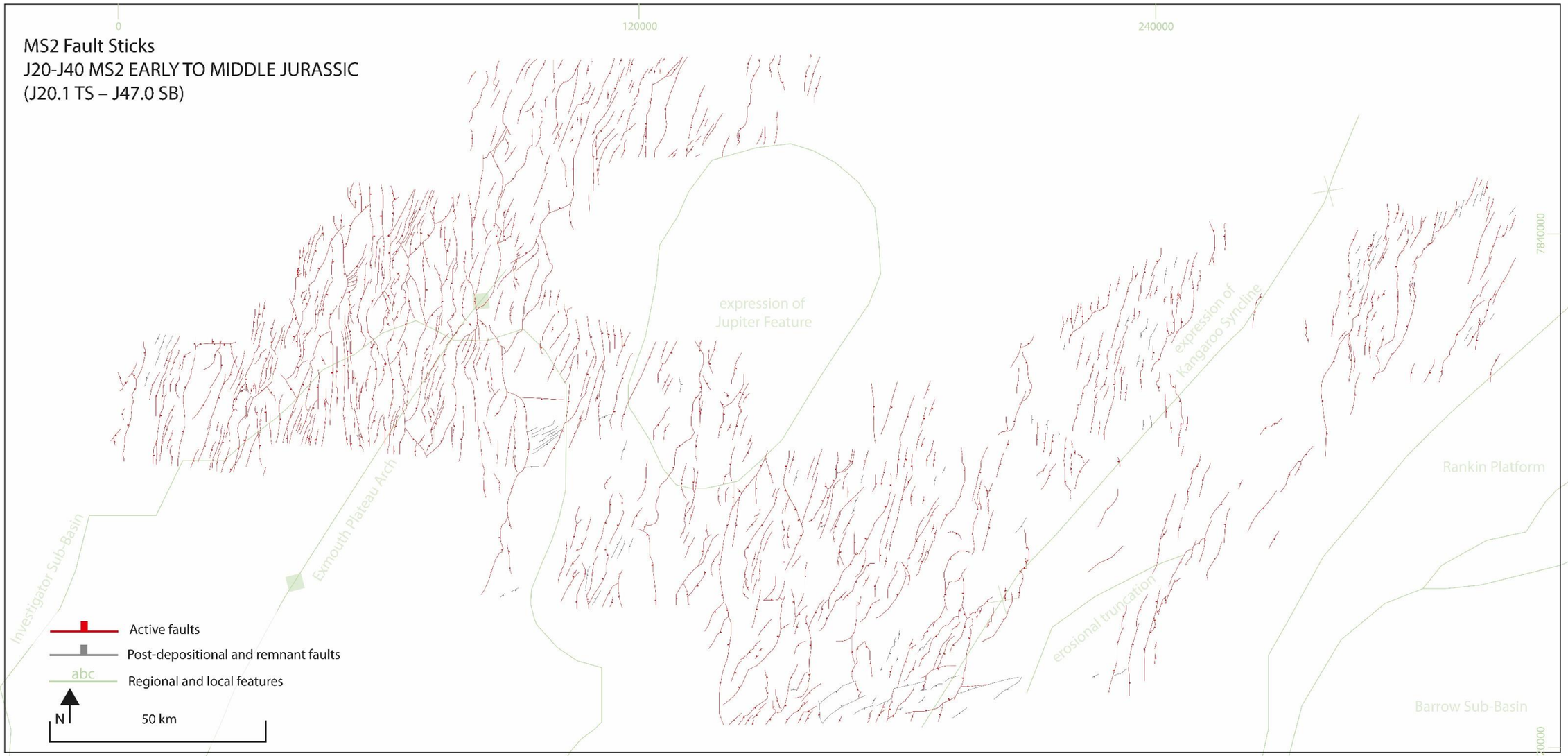

b)

Figure 4.2b Fault stick maps of fault traces as mapped from 3D seismic data. Lower to Middle Jurassic (J20 – J40) fault activity (red) and post-depositional (grey) faults which penetrate the Lower and Middle stratigraphy. The fault sticks showing significant fault activity in the west of the study area, as well as a higher frequency of faults and fault networks in this area. The eastern area of the study area which had limited fault activity during the Rhaetian (TR30) (a) now shows most of the faults to be active. The east to east-north-east orientated faults continues through the strata of the J20-J40 MS2 mega-sequence (Lower and Middle Jurassic). Note the reduced intensity/frequency of fault activity during and following Jurassic deposition in comparison to the a) Rhaetian (TR30) fault activity map. Note that regional scale features are provided in the green underlay, this includes the expression of some features during time period displayed.

Figure 4.2c Fault stick maps of fault traces as mapped from 3D seismic data. Upper Jurassic to earliest Cretaceous (J40 - K10) age fault activity (red) and faults which penetrate the J40-J50 MS3 stratigraphy following deposition (grey). Fault activity and frequency remains higher in the west of the study area. Note some faults in the east of the study area are now inactive during the deposition of MS3 J50 - K10, after being active for on the deposition of MS2; J20 - J40 (b). Note that regional scale features are provided in the green underlay, this includes the expression of some features during time frame displayed.

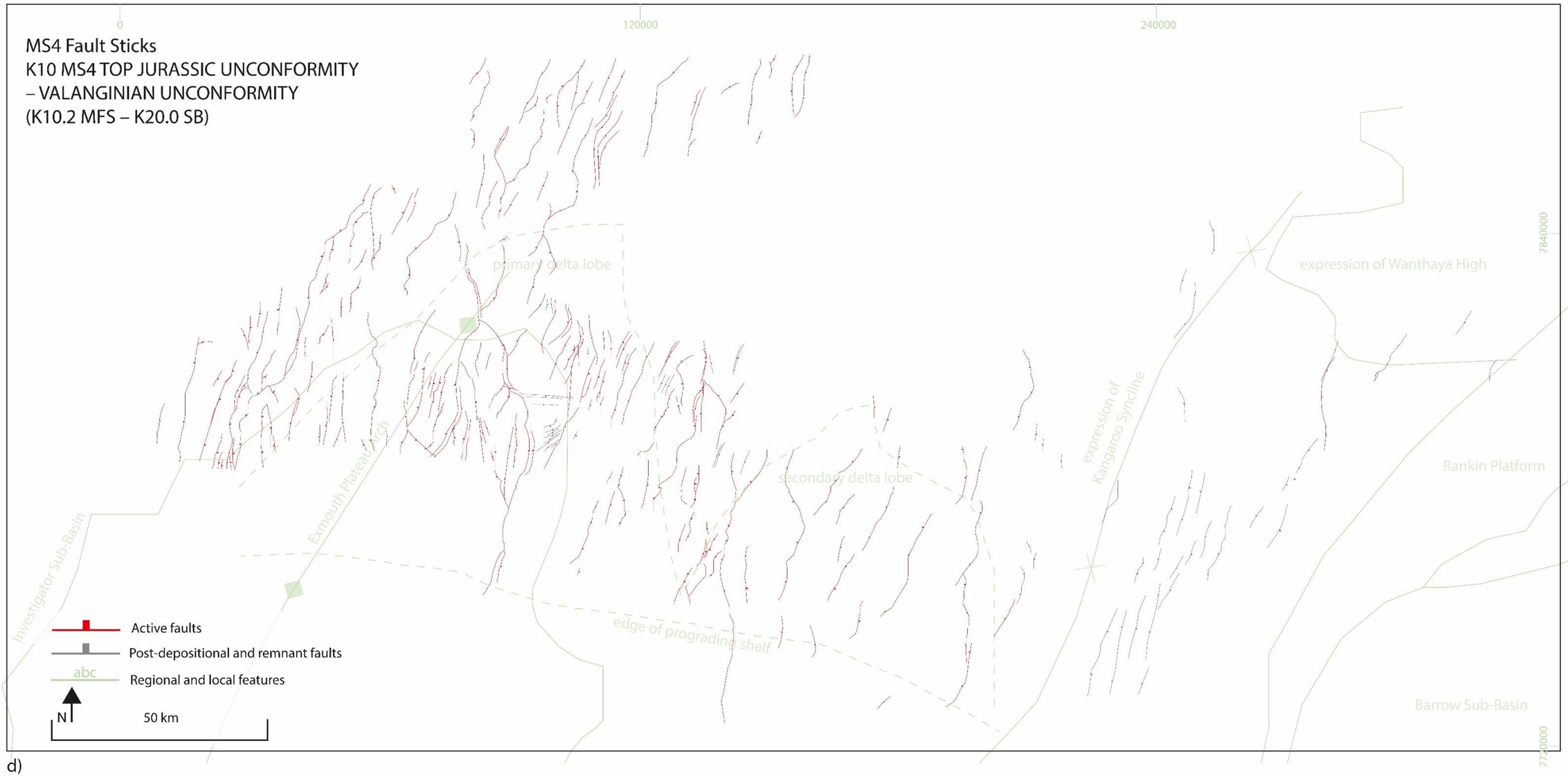

d)

Figure 4.2d Fault stick maps of fault traces as mapped from 3D seismic data. Fault activity during deposition (red) of the K10 MS4 mega-sequence during the Berriasian and Valanginian (K10 time only, no K20) and faults which penetrated the K10 MS4 strata as a post-depositional feature (grey) are displayed here. Note the low volume of active faults in the east of the study area by this time, while the western region experienced ongoing fault activity. Note that regional scale features are provided in the green underlay, this includes the expression of some features during the time frame displayed.

e)

Figure 4.2e Fault stick maps of fault traces as mapped from 3D seismic data. Valanginian (K20, no K10) fault activity is post-depositional penetration of faults through the K20 MS5 strata, with a reduced frequency of faults in the east compared to the west of the study. In the northwest there are a few limited faults where movement is still occurring. Note that regional scale features are provided in the green underlay, this includes the expression of some features during time frame displayed.

f)

Figure 4.2f Fault stick maps of fault traces as mapped from 3D seismic data. Barremian to mid-Aptian K20-K30 MS6 is intersected by a scattering of faults, where faults largely penetrated the strata after deposition, except in the northwest where some continued movement has been observed. Note that regional scale features are provided in the green underlay, this includes the expression of some features during time frame displayed.

g)

Figure 4.2g Fault stick maps of fault traces as mapped from 3D seismic data. The post mid-Aptian faults which have intersected the strata following deposition of the K40-K60 MS7 mega-sequence. Interpretation of MS7 in the east of the study area is limited to the mid-Aptian (~K40) only. Note that regional scale features are provided in the green underlay, this includes the expression of some features during time frame displayed.

only the Mesozoic sediments. Some faults are listric in cross-section, and these penetrate parts of the stratigraphy for which there is no stratigraphic age constraint (as provided by well intersection), reaching depths of 9 km (Figure 3.4, as fault die out zone 2). The majority of listric faults detach on a weak stratigraphic layer (Figure 3.4, as fault die out zone 2), which is likely to be the Locker Shale of early to Middle Triassic age (TR10) – in-line with observations made by previous authors i.e., AGSO North West Shelf Study Group (1994) and Gartrell (2000). Few faults can be interpreted as continuing past this ductile layer (Figure 3.4).

Fault-related folding is commonly associated with faults over the Exmouth Plateau. Breached fault propagation folds (Figure 4.3) occur over much of the area and are the most common type of fault-related fold. Most are characterised by small scale monocline folds (Figure 4.4a) that form in Mesozoic strata (Figure 4.4b). No fold structures were identified in the Scarborough or Duyfken seismic surveys, potentially due to erosion in these areas.

A single anticline formed by a fault propagation fold (Figure 4.5) is observed in the northwest of the study area. The fold is small in size, measuring less than 1 km in length with active folding affecting strata over 250 m. The trishear angle defined by this fold is tight, resulting in a highly angular fold structure. The folded strata are of latest Triassic to earliest Cretaceous age (Figure 4.5). The younger sediment of early Cretaceous age drape over the fault propagation fold with onlap onto limbs lower in the sequence, indicating the cessation of fold growth in the earliest Cretaceous. Other fault propagation folds in the area studied have limited impact on stratigraphy by comparison and show no anticline formation in the overlying strata.

4.1. Fault Populations

The top of the pre-kinematic sequences (Figure 4.1) shows the deformation from Mesozoic rift activities. The most prominent faults span entire 3D surveys and are often mapped across several surveys. They typically comprise a series

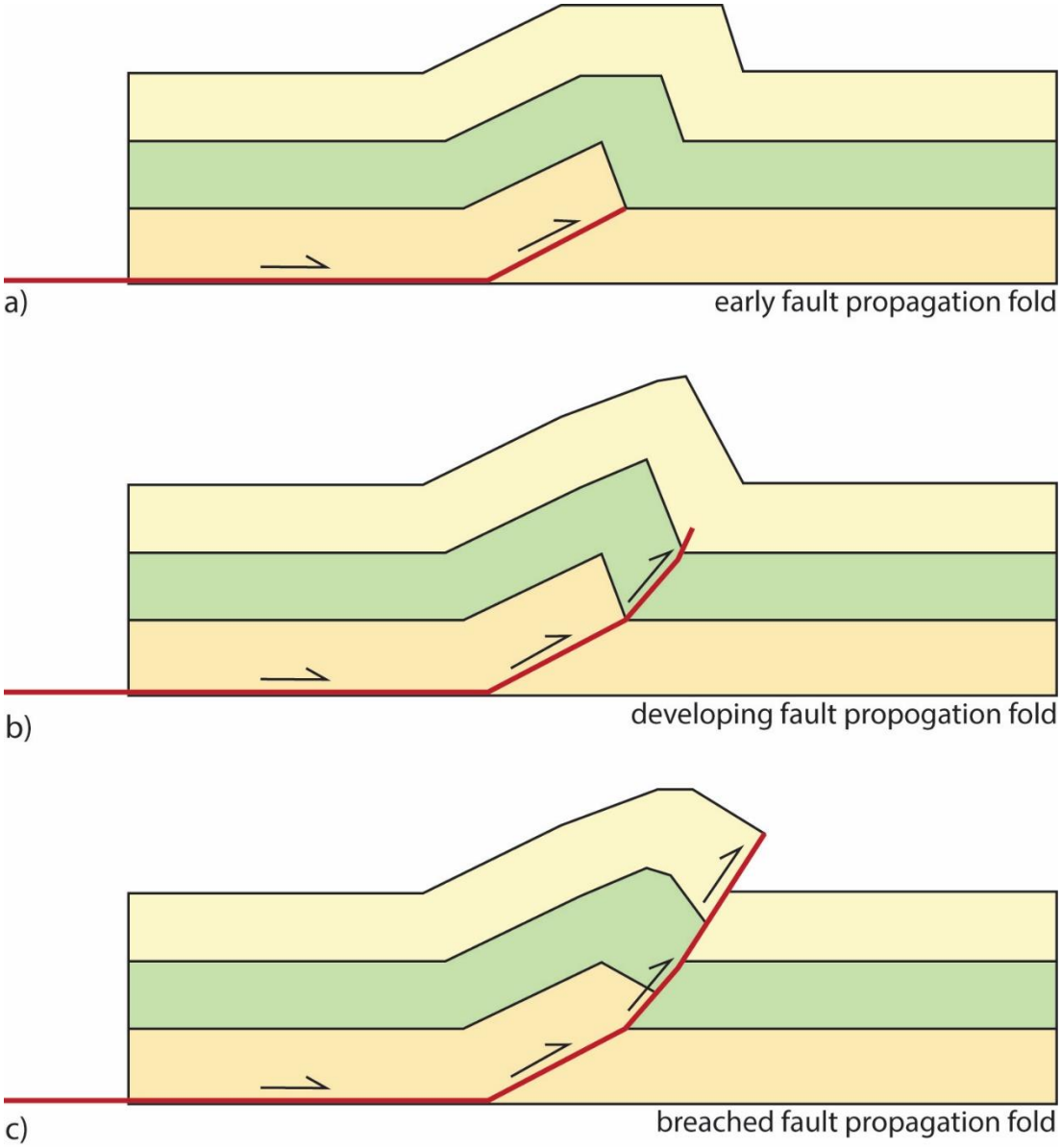

Figure 4.3 Fault propagation fold development from a) initial fold development ahead of fault tip, into b) further development and c) breaching of the fold by the fault tip, after Bernard et al. (2007), Brandes and Tanner (2014), Chester and Chester (1990), Erslev (1991), Hughes and Shaw (2015), Storti and Poblet (1997), Suppe (1983), and Suppe and Medwedeff (1990).

of connected fault segments (Figures 4.1, & 4.2). The minor variation of strike along many of these faults is characteristic of this style of growth (Cartwright et al., 1995). Where growth occurred along the strike of a single fault, and where other faults of similar orientation are located nearby, isolated faults are

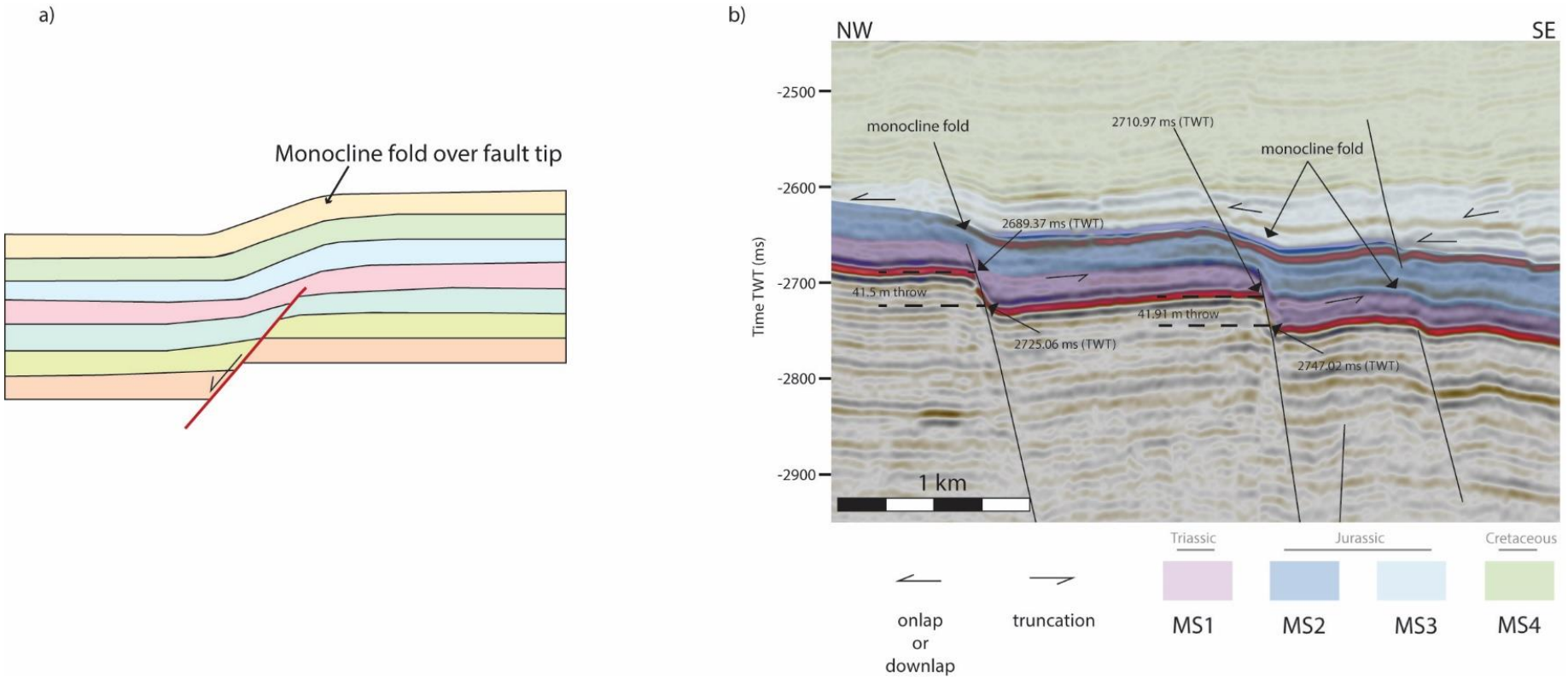

Figure 4.4 Monocline folds forming bended layers of strata over a fault tip, where the strata remain relatively even in thickness on both sides of the fault plane but do thin over the tip as part of a stretching. Image a) shows a diagram with stratigraphy on either side of the fault and overlaying the fault tip, after Brandes and Tanner (2014), Chester and Chester (1990), Erslev (1991), and Fossen and Rotevatn (2016). Image b) is an example from this study, showing monoclines forming over faults in the latest Triassic to Jurassic stratigraphy, this formation is readily identified across much of the area investigated. The throw these faults is annotated with the TWT for two locations showing the throw at the base of the TR30 Rhaetian, location of the cross-section is shown on Figure 4.5b).

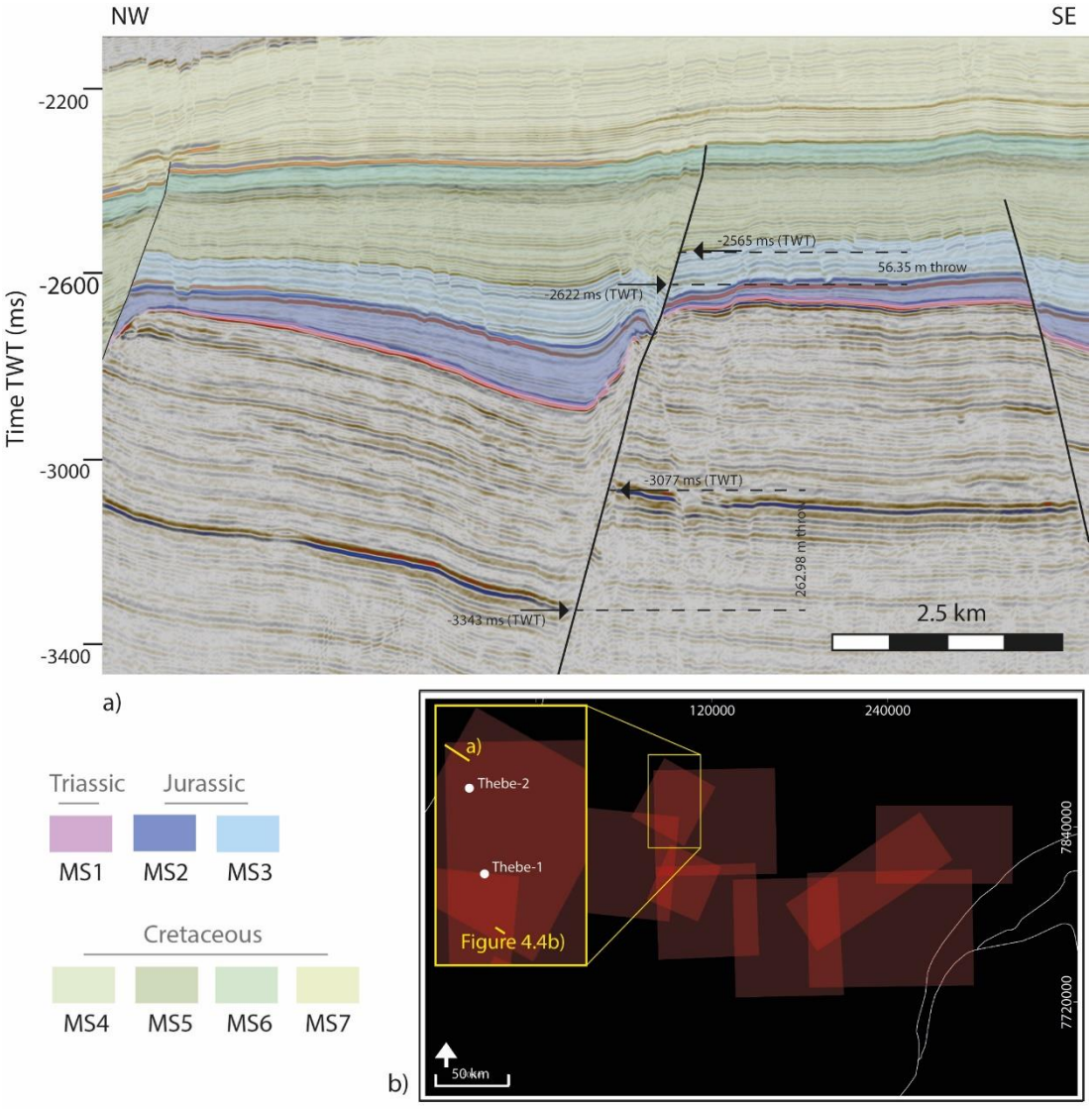

Figure 4.5 Breached fault propagation fold (centre of seismic line a) located in the Mary Rose Northern Extension and Thebe seismic surveys. This feature shows the fault propagated through the latest Triassic (TR30 Rhaetian, thin but present), Jurassic J20 - J50 and earliest Cretaceous K10 strata, with the younger early Cretaceous deposition forming a drape style anticline over the top of the now breached fold. The throw as calculated by the candidate is annotated along two sections of the fault, with the time of the points used also provided (note, this used the interval velocity of the Thebe-2 well). Figure b) provided the location of the provided seismic cross-section, and the location of the cross-section for Figure 4.4b).

linked with other faults across accommodation zones. In most incidents of segment linkage, hard linkages are formed in the accommodation zone (Figures 4.1, 4.6, & 4.7). Hard linked faults are connected by faults with less significant throw (Figure 4.8). Soft linkages occur to a lesser degree (Figures 4.1, 4.6, 4.7, & 4.8). These linkages occur as relay ramps, including single and

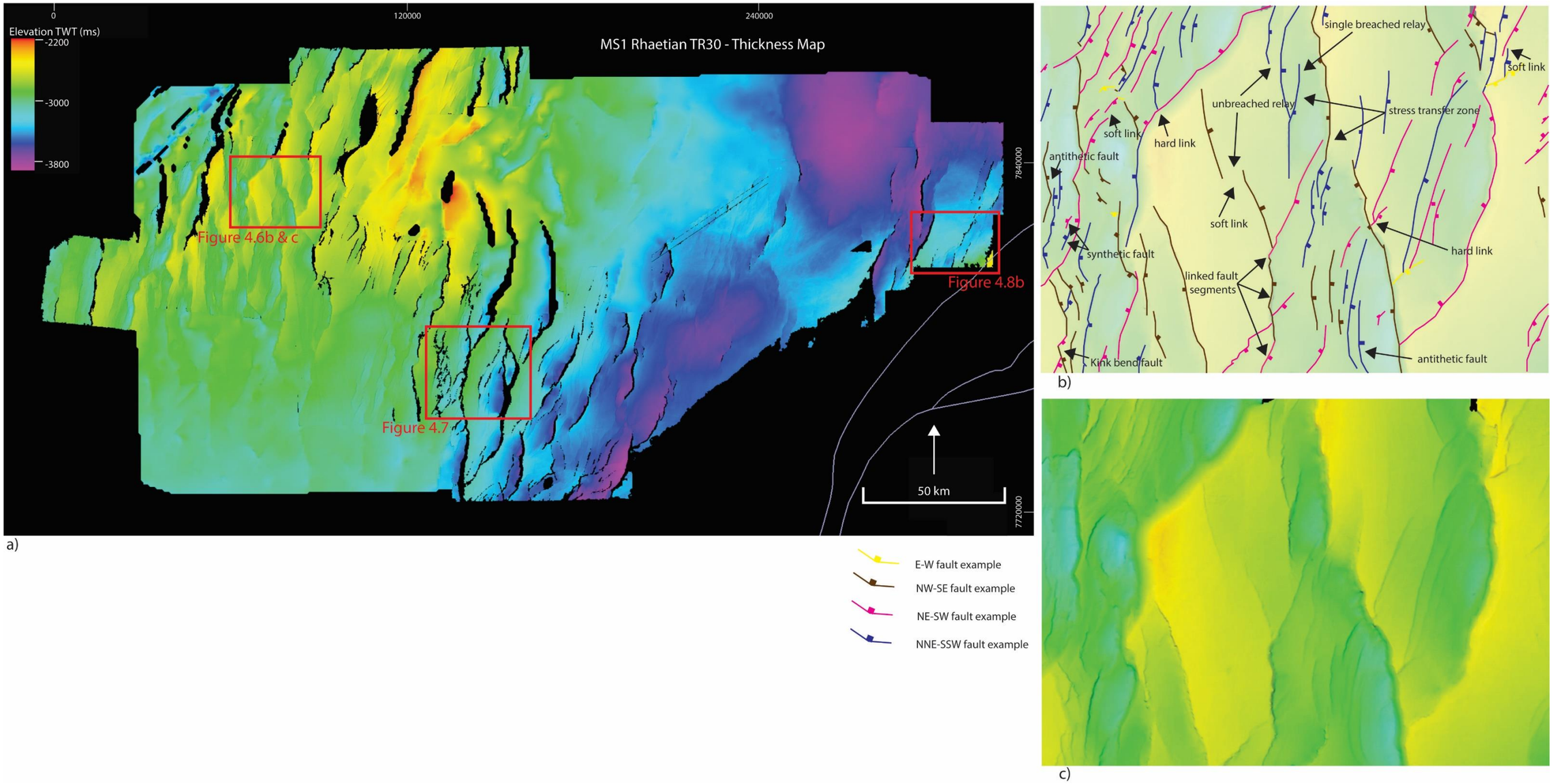

Figure 4.6 Examples of various fault characteristics over the various fault populations, with the annotated fault traces being showing in b) which is visible unannotated in c) with the location of the close up shown on a).

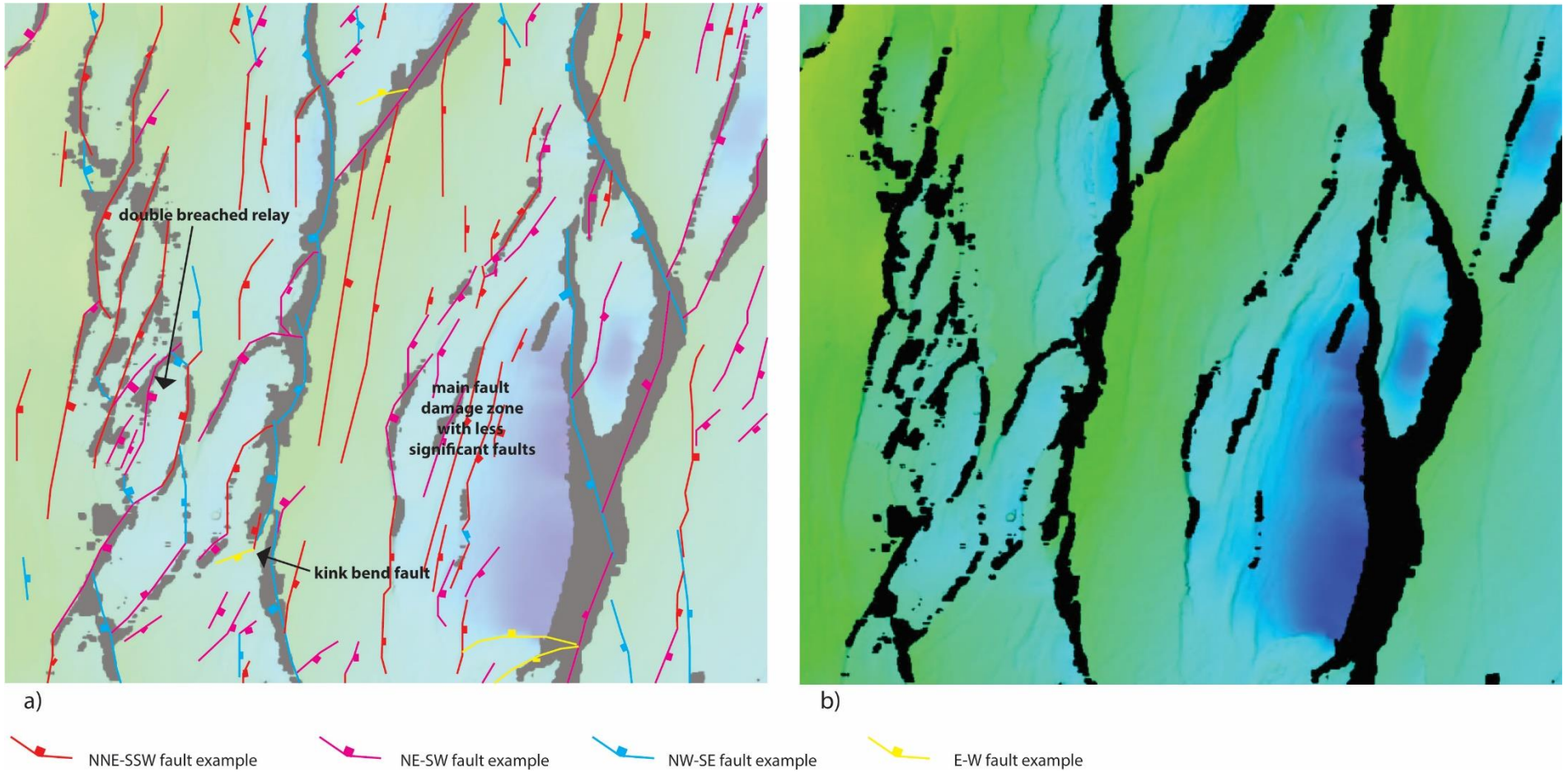

Figure 4.7 Examples of various fault characteristics over the various fault populations, with the annotated fault traces being showing in a) which is visible unannotated in b) with the location of this image shown on Figure 4.6a).

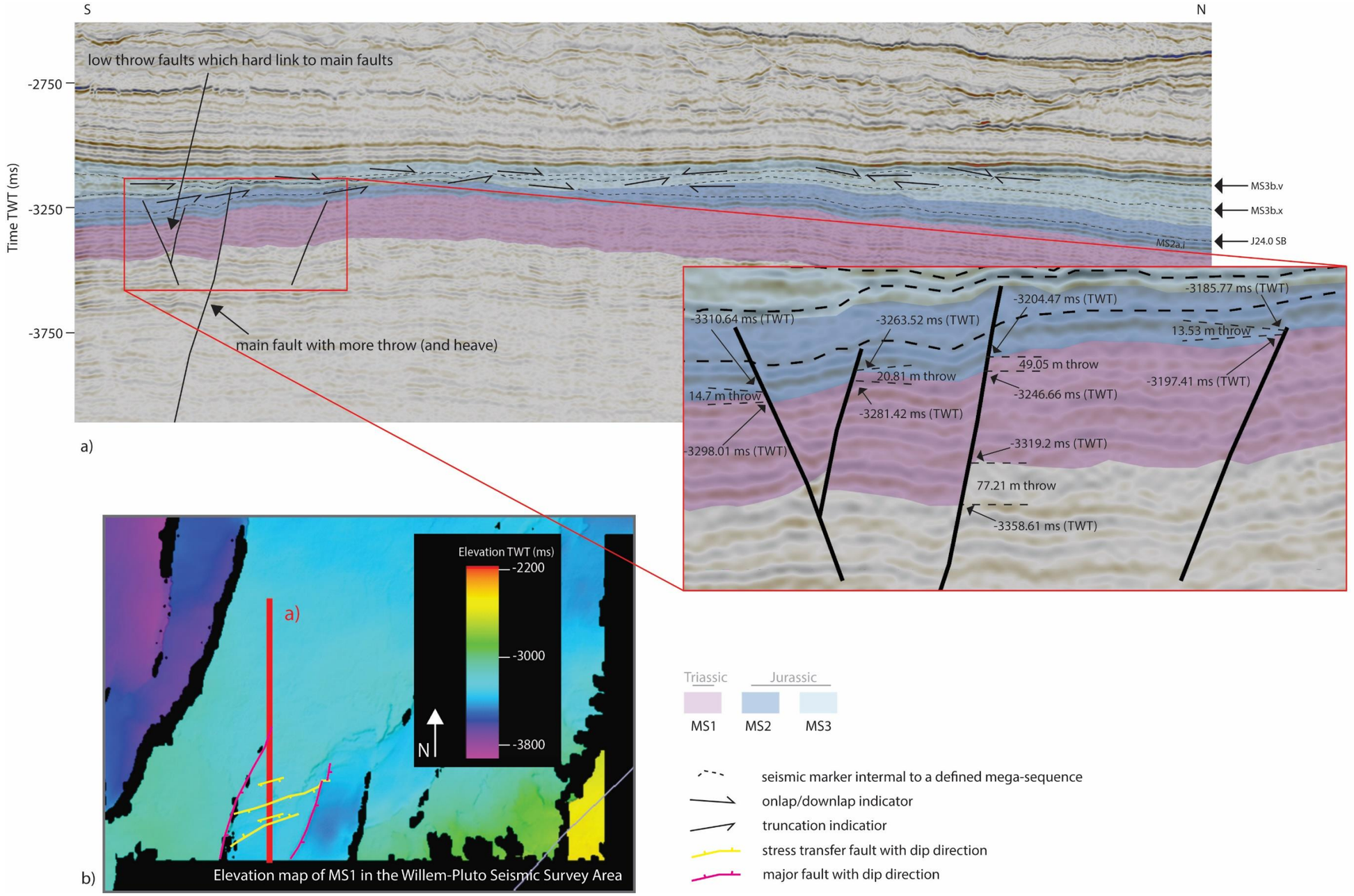

Figure 4.8 Hard linkages between faults in the Willem-Pluto seismic survey, as shown a) these faults display less throw than the main fault (inset) to which they hard link. Location of seismic cross-section shown on surface map of part of the Willem-Pluto survey, location of this map is identified on Figure 4.6a).

double breached relay structures and un-breached relays (Figures 4.6, & 4.7). There are several smaller-scale faults that occur a) in accommodation zones between larger faults (Figure 4.1), b) in *en-echelon* arrays (Figure 4.9), and c) as antithetic and synthetic faults in the hangingwalls (and occasionally footwalls) of larger faults (Figures 4.6, & 4.7). These smaller-scale faults display significantly less throw than the larger linked faults.

Faults on the Exmouth Plateau are divided into populations based on their strike. These populations are NNE-SSW (0º - 20º), NE-SW (20º - 50º), NW-SE (100º - 180º) and E-W (50º - 100º; Figures 4.2 & 4.10). The greatest number of faults occur in the NNE-SSW and NE-SW populations (Figure 4.10). The NW-SE and E-W populations contain far fewer faults than the NNE-SSW and NE-SW populations (Figure 4.10).

4.1.1. NNE-SSW POPULATION

The main orientation in which faults formed is NNE-SSW (Figure 4.10). This population of faults includes a large number of faults formed during and after the deposition of Mesozoic sediments. The largest faults in this population are made up of linked fault segments (i.e., Figure 4.6). These faults most commonly display hard linkages across transfer zones (i.e., Figure 4.6). Hard linkages are either single or double tip breaches (i.e., Figures 4.6, & 4.7).

These faults display significant throws, which are variable across the study area (Figures 4.5a, 4.11a & 4.12b). The largest number of faults within the NNE-SSW population occur towards the west, specifically in the Bonaventure, Glencoe and Thebe surveys. They also occur in the northeastern portions of the area of interest (the eastern extent of both Willem-Pluto and Duyfken surveys). Throw varies in the Thebe survey from between 244 to 720 m (i.e., Figure 4.5a, and similar to examples in Figure 4.11a). It reaches an average in the north of the Bonaventure survey of 697 m which decreases south to 441 m. In the Glencoe survey, these faults also display a decrease in throw to the south, with an average of 633 m compared to 709 m in the north. NNE-SSW orientated faults are largely absent from the Io-Jansz, Duyfken and western

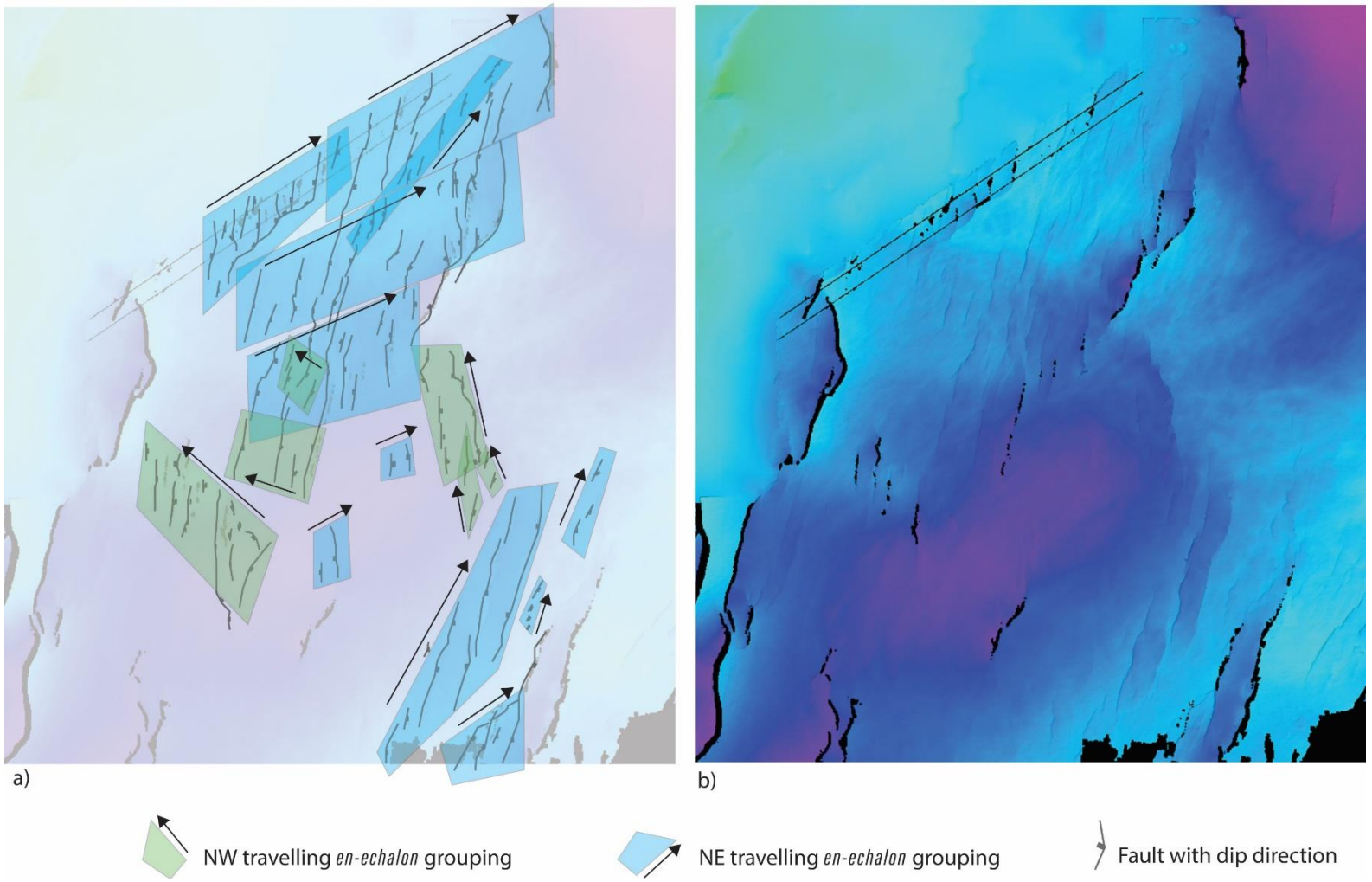

Figure 4.9 Examples of en-echelon faults over the various fault populations, with the annotated fault traces being showing in a) which is visible unannotated in b) with the location of the close up shown on Figure 4.2a. Several en-echelon faults are identified here, some more obvious that others, occurring within the NNE-SSW (largely) fault population and stepping in (travelling in) a NW or NE direction.

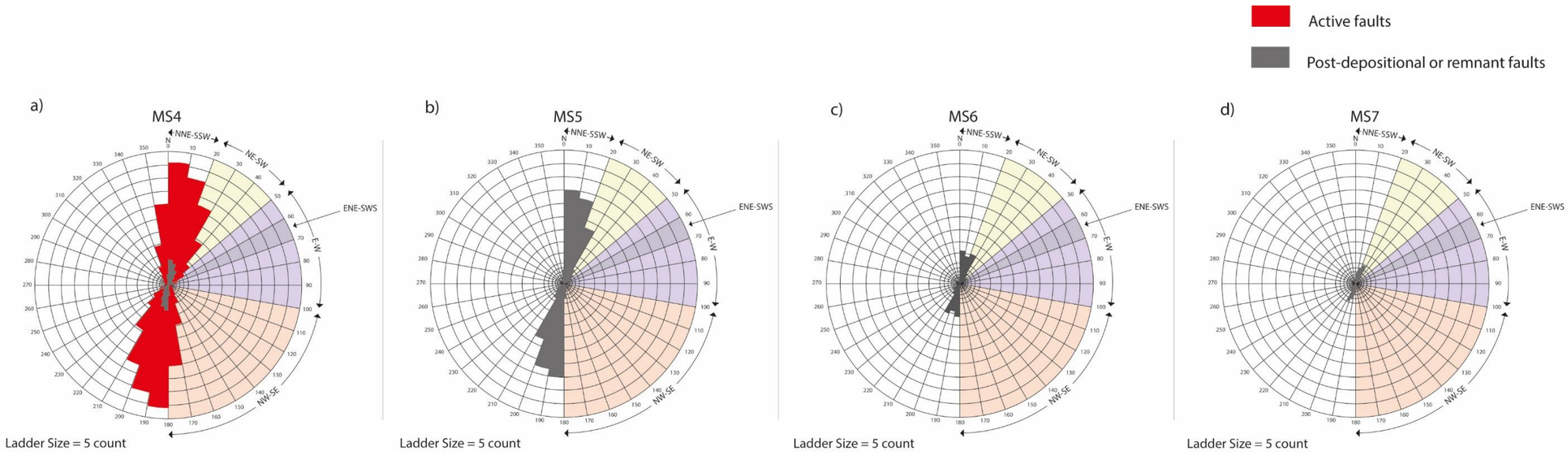

Figure 4.10 Rose diagrams displaying the orientation of faults which were active, post-depositional, and remnant, as identified within each of the mega-sequences. These rose diagrams display the count (number) of faults identified within each 10º increment as the radiating ladder circles, with the various fault populations identified on the base of the rose diagrams.

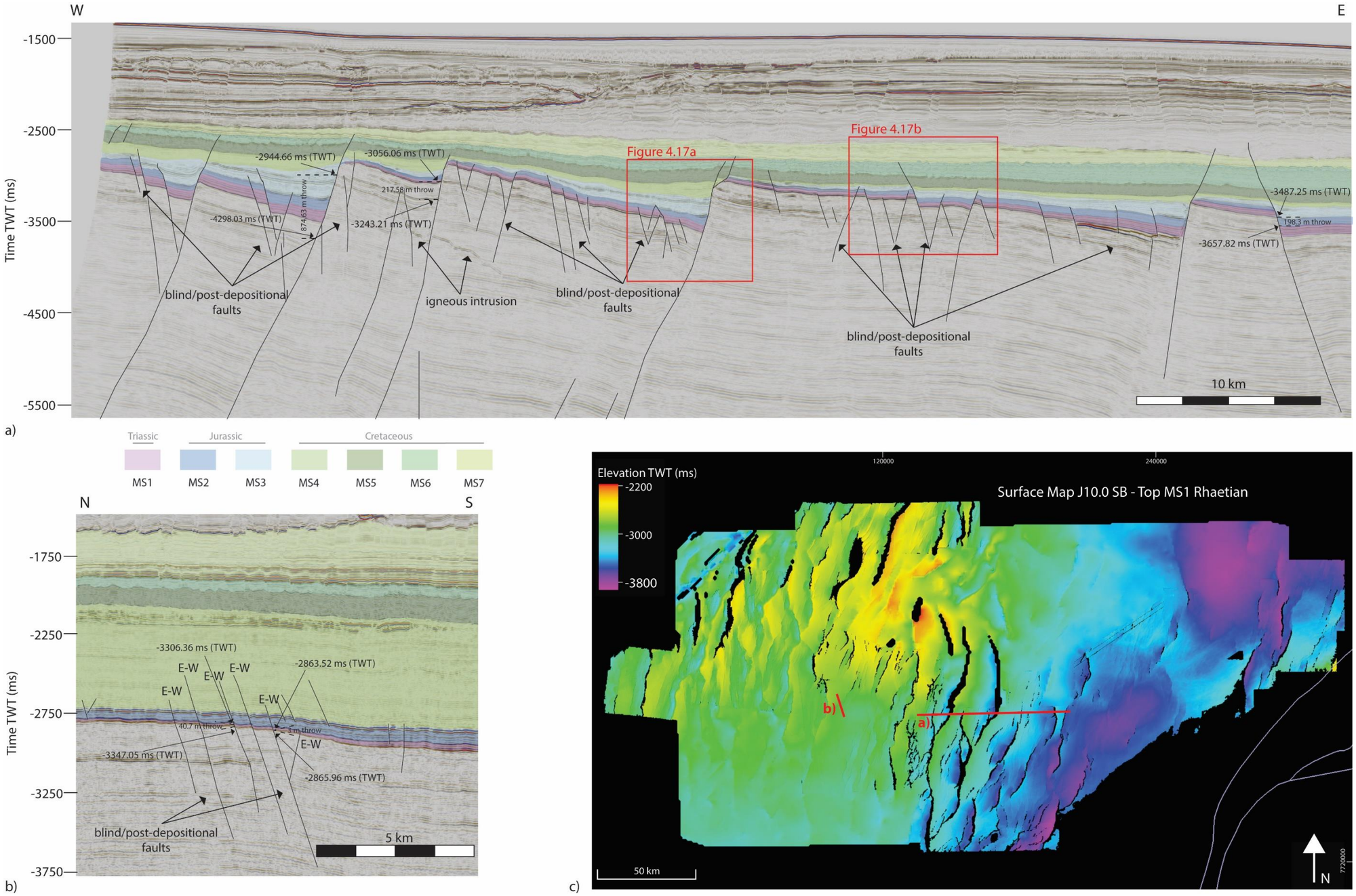

Figure 4.11 Post-depositional, or blind, faults within the study area with a) NE-SW and NNE-SSW populations and an associated igneous intrusion, and b) the E-W populations. Location of seismic cross-sections shown in c).

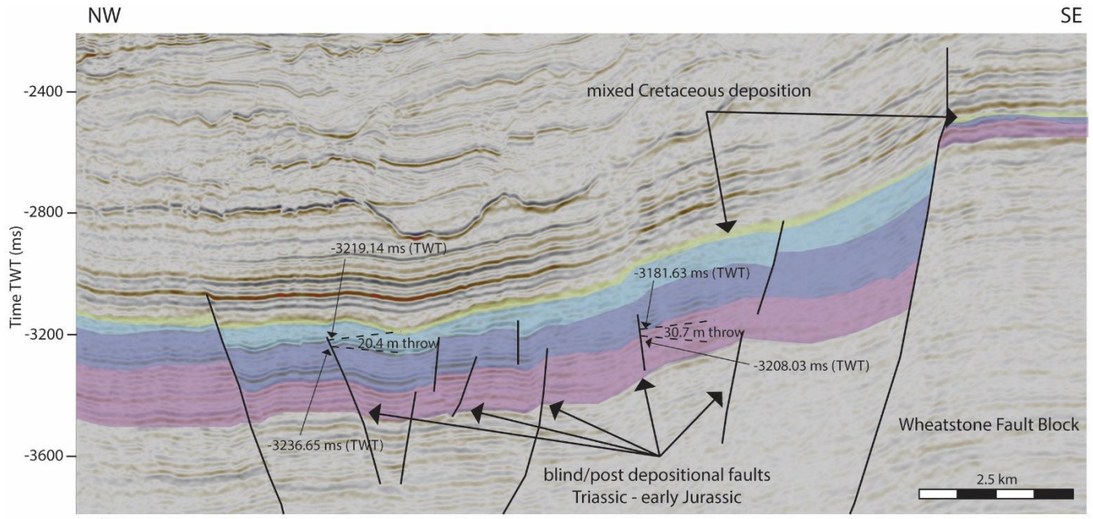

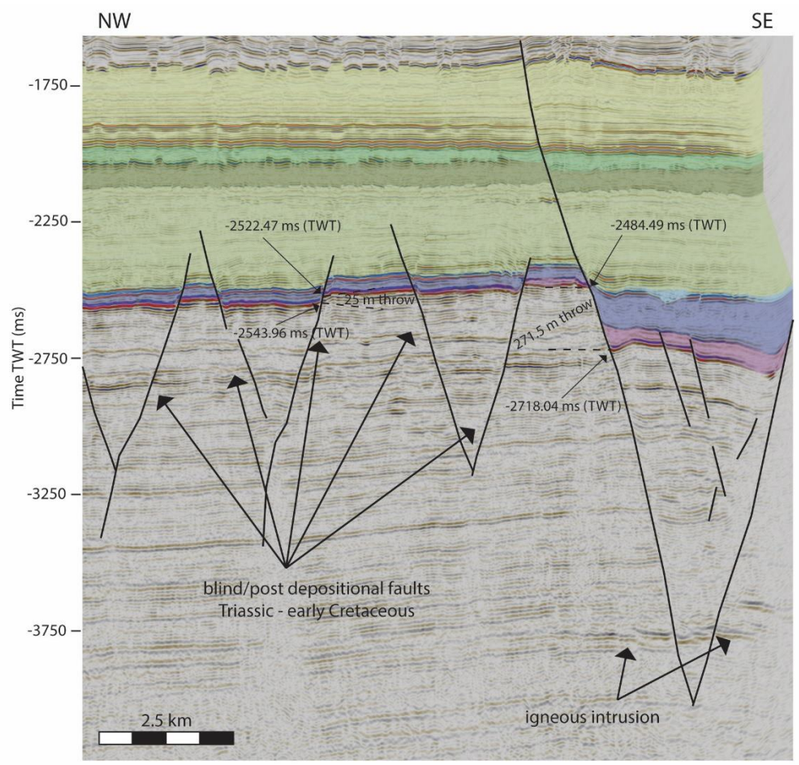

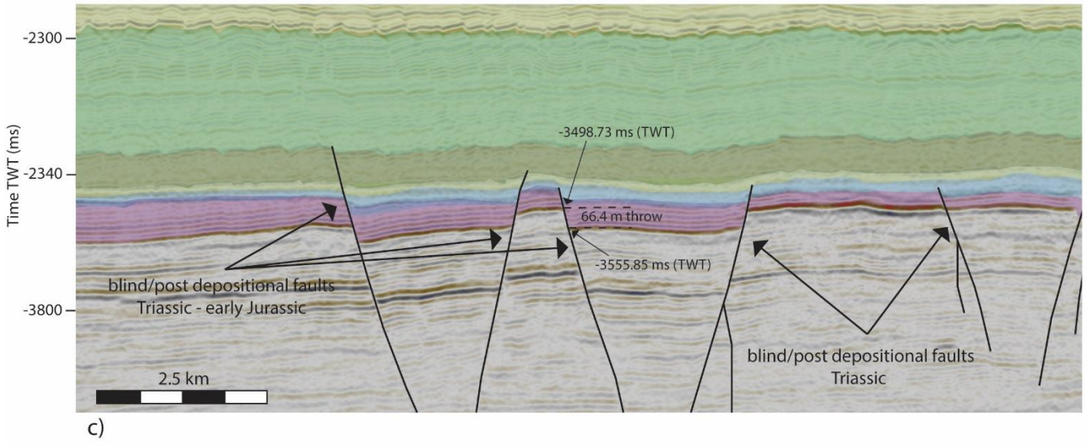

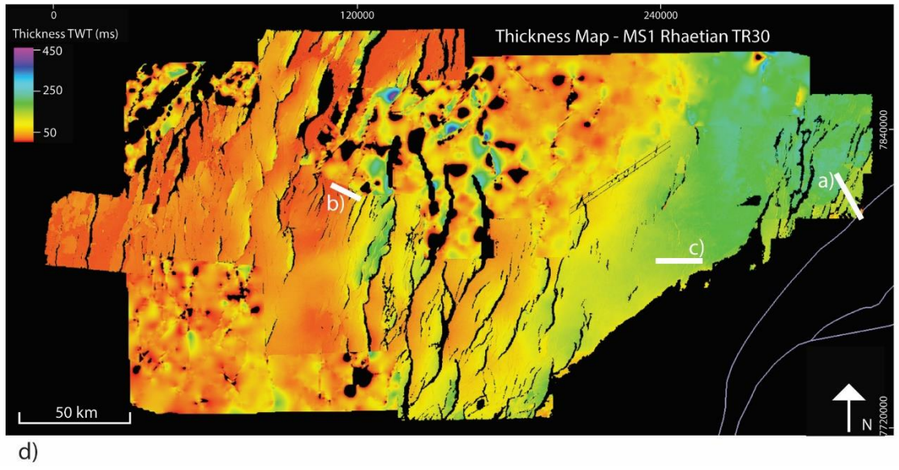

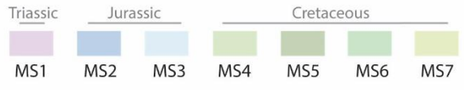

Figure 4.12 Specific Post-depositional faults a) intersecting the Triassic and Jurassic from the Willem-Pluto area, specifically the area to the north of the Wheatstone Fault Block/Petroleum Field, b) the Scarborough survey showing some post-depositional faults intersecting strata following deposition of the Cretaceous, with igneous intrusions, and c) examples from the Duyfken survey which are post-depositional for the Triassic and some of the Jurassic. Location of cross-sections shown on d).

Willem-Pluto survey areas (Figure 4.2). When this orientation of fault is observed in the eastern Duyfken and Willem-Pluto region, they display throws of 639 and 523 m respectively. Linked fault segments could not be mapped in the Scarborough survey, though the appearance of some faults indicates that they are part of a linked network which continues out of the survey area (Figure 4.6). The potential linked faults in Scarborough have throws in the order of 250 to 320 m (i.e., Figure 4.12b). These present as either a kinked fault when linked with another fault population, or a single fault segment (Figures 4.6, & 4.7).

Several small, isolated faults also occur within this population. These faults tend to have more limited throws, ranging from between 11 and 46 m (similar to examples shown in Figure 4.12a). Most examples of faults with limited throws in this population were active after the deposition of the Mesozoic strata through which they cut (Figure 4.11). The limited throw faults within this population occur largely as splays at the tips of faults or as minor faults in accommodation zones between overlapping tips. Limited throw faults within the NNE-SSW population may also form separately from a linked fault network. These faults are particularly evident in the Duyfken and Io-Jansz surveys, the westernmost extent of the Willem-Pluto survey and in the southeast of the Glencoe survey. Here a series of NNE-SSW faults form *en-echelon* arrays oriented both NE and NW (Figure 4.9).

The length of these faults is highly variable. Measured as individual fault segments, these faults are longest in the Thebe, Bonaventure and Glencoe surveys, measuring between 16 and 5 km in length, where the more prominent throws are found. The length of these faults decreases with throw. Faults with more limited throws are usually between 7 and 4 km in length, where the entire fault has been captured in seismic data.

4.1.2. NE-SW POPULATION

The second most prominent orientation of faults is NE-SW (Figure 4.10). This population contains faults which were active both during and after the deposition of Mesozoic strata. These faults connect with other faults across accommodation zones within this trend to form linked fault systems (Figures

4.6, & 4.7). Linked faults within this population are predominantly soft linked (Figures 4.6, & 4.7). Hard linkages between faults do occur, particularly if the linking faults within the accommodation zone show limited displacement (Figures 4.6, & 4.7).

These faults display the greatest throw in the central area of the plateau. Here the highest throw along these faults is 930 m in the northwest of the Bonaventure survey where the most pronounced structural relief is also observed. Throw decreases to an average of 500 m in the more central areas of the Bonaventure survey (i.e, Figure 4.13b), decreasing again to the south. Throws in the Scarborough and southern Bonaventure surveys are 230 - 300 m (i.e., Figure 4.12b). To the north (Thebe survey) the throws are slightly less than in the central Bonaventure survey, at 348 m. In this area, the NE-SW population are predominantly hard linked.

Fault throws within the Glencoe survey generally fall between 523 to 870 m (Figure 4.11a). Faults within this population identified within the Glencoe Seismic Survey area, are only identified in the eastern portion of the Glencoe survey area; other populations are present in the western half. Fault throws in the NE-SW population decrease significantly to the east of the Glencoe survey (similar to examples in Figure 4.12c). Continuing north from the Glencoe survey, a linked fault on the western edge of the Io-Jansz survey has a maximum throw of 406 m. On the western edge of the Duyfken survey throws reach a maximum of 174 m. This set of the population is mostly soft linked across accommodation zones (Figures 4.6, & 4.7). No other faults which were active at the time of deposition occur within the Io-Jansz or Duyfken surveys. A few of these faults occur in the eastern section of the Willem-Pluto survey and have hard linkages (Figures 4.8, & 4.12), they have lower throws of 104 m. Hard linkages are either single or double tip breaches of the accommodation zone (Figures 4.6, & 4.7).

Faults which were active after the deposition of early Cretaceous sediments also occur within this trend and display limited throw (similar to examples in Figure 4.12). These are limited to the Glencoe survey and the western edges of both the Io-Jansz and Duyfken surveys. The throw on these faults range

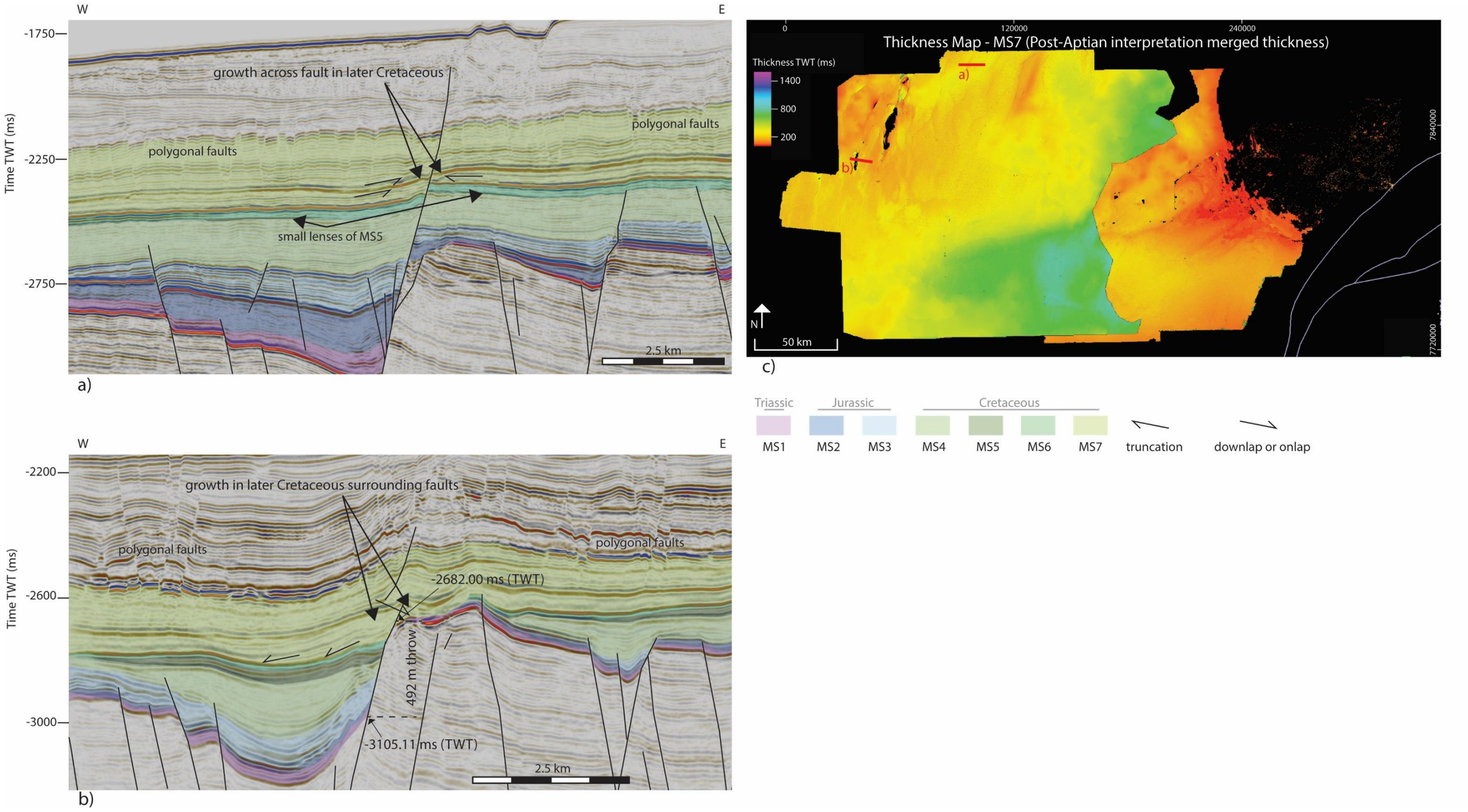

Figure 4.13 Post-Cretaceous fault activity, or remnant fill, over limited major faults in the north to northwest of the studied area. Cross-sections display a) some indication of thickening across a major fault in the MS7 K40 – K60 strata, and b) growth across a major fault in the MS7 K40 strata. Location of cross-sections shown on c).

from 11 to 58 m. Here faults are mainly part of the damage zone of larger faults, forming antithetic and synthetic faults in the hanging walls or splays from the tips of larger faults (Figures 4.6, & 4.7). They also form kinked fault traces in a few cases (Figures 4.6, & 4.7).

The larger faults in this population are up to 17 km in length as measures on individual fault segments in the Thebe, Bonaventure, Glencoe, and Willem-Pluto seismic surveys. These are the faults with the highest throws and have a minimum length of 7 km. Where faults in this population have limited throws, the lengths vary from between 2 to 4.5 km.

4.1.3. NW-SE POPULATION

A limited number of faults form in a NW-SE orientation (Figures 4.6, 4.7, & 4.10). Most of this population occurs as faults which were active after the deposition of the Mesozoic strata through which they cut (Figure 4.11). Faults within this population which have larger throws are restricted to the more western plateau area (the Bonaventure, Scarborough, Thebe and western Glencoe surveys; Figure 4.11a, 4.11c). In these instances, the faults are always associated with other populations, forming a segment of a larger linked fault network on a more prominent trend or a kinked fault formation (Figures 4.6, & 4.7). Connection with other faults across accommodation zones is always a single tip breach, forming a hard link (Figures 4.6, & 4.7).

The throw variation of these faults reflects the same pattern as seen in the more prominent fault populations. In the northernmost area (Thebe survey) faults display throws of 116 m. In the more western area of the Bonaventure survey these faults have throws of 348 m which decreases into the central area to between 174 and 325 m. Moving south to the Scarborough survey throws are 232 m. The single example within the western Glencoe survey has a throw of 348 m.

Faults which were active after the deposition of Mesozoic stratigraphy (Figure 4.2) occur as a) synthetic/antithetic faults within the hanging and footwall of larger faults (Figures 4.6, & 4.7), b) fault splays at the tips of larger faults (Figures 4.6, & 4.7), c) linking faults across accommodation zones (Figures

4.6, & 4.7), or as d) kinked faults with other fault populations (Figures 4.6, & 4.7). Kinked faults form only within the southeast of the Glencoe survey and have limited throws of 10 to 15 m (Figures 4.6, & 4.7). No NW-SE faults formed east of the Glencoe survey. These NW-SE faults occasionally occur in the more western surveys and have throws of between 20-58 m.

Faults with the large throws (i.e., Figure 4.13) in the Thebe, Bonaventure and Scarborough seismic survey are between 5 and 9 km in length. This increases in the single fault of this orientation from the Glencoe seismic survey which has a length of 12 km. In the southern Glencoe survey area, faults with more limited throws (Figure 4.11a) have lengths of between 1.5 and 5 km. Length ranges for these faults change to between 1.5 and 2.1 km in the northern Glencoe survey and more western survey areas.

4.1.4. E-W POPULATION

This fault population has the smallest number of faults out of all the identified populations. Most faults within this population display no evidence of fault activity occurring during the deposition of the Mesozoic stratigraphy (i.e., Figure 4.11). These post-depositional faults are only identified within the Scarborough, Glencoe, Duyfken, and the southeast of the Willem-Pluto seismic surveys (Figures 4.2, & 4.14). An E-W fault sub-population occurs within the Glencoe and Scarborough surveys where it forms a more ENE-WSW orientation (60º - 70º; Figure 4.14). In this southern area of the Glencoe seismic survey, igneous sills are readily identified (i.e., Rohrman, 2013; Figure 3.3a) and faulting may be related to this. In this area, this population links with other populations to form rectangular fault geometries (Figure 4.14). In the Scarborough survey, they form a fan of splay faults in the damage zone of a larger fault (Figure 4.14).

These faults intersect different stratigraphic units in different areas. All of the faults identified within the Scarborough survey are observed to be present within Jurassic and early Cretaceous strata (Figure 4.12). In the Glencoe and Duyfken surveys, faults occur within Triassic and Jurassic strata (Figure 4.12).

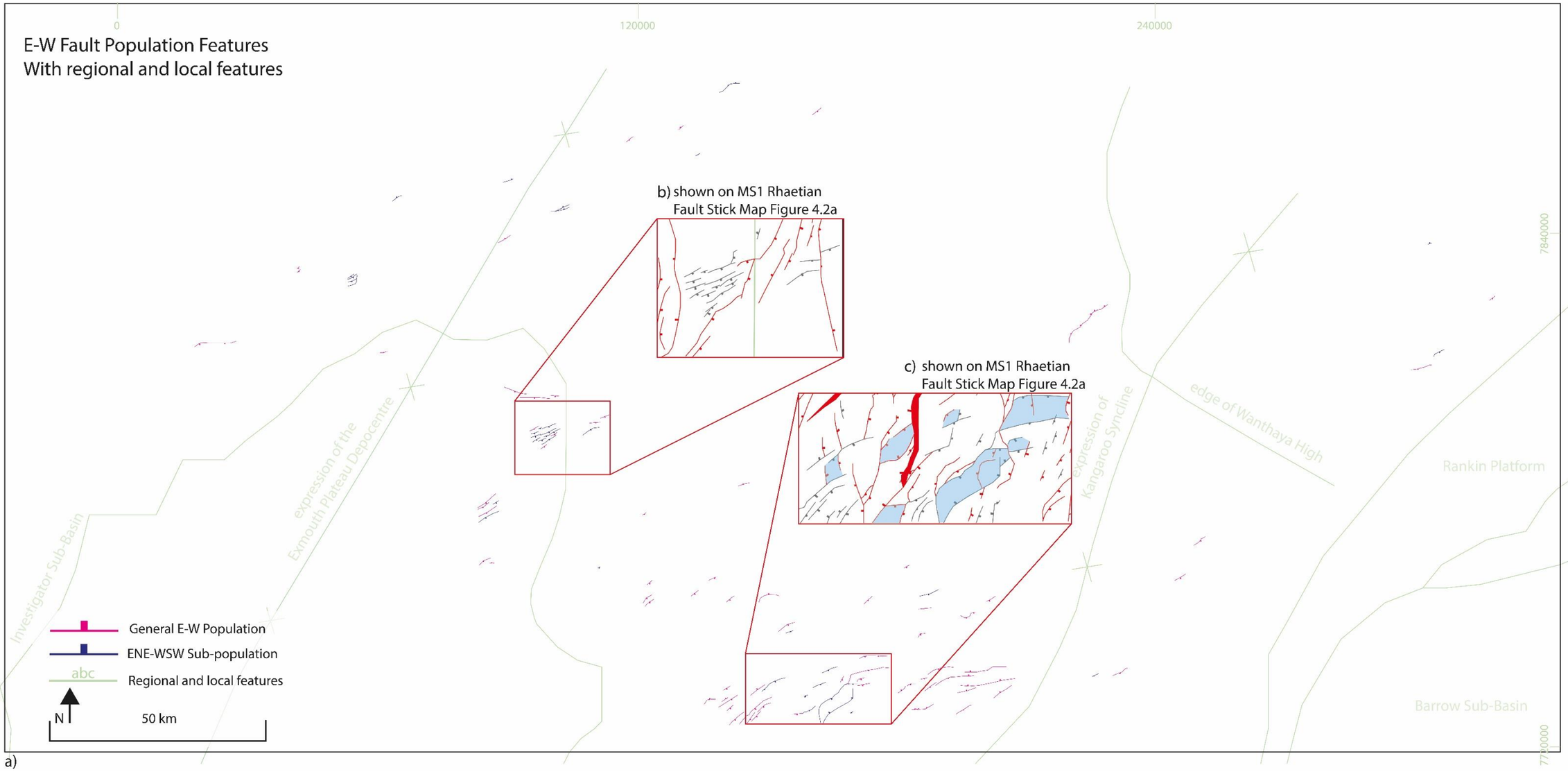

Figure 4.14 The E-W fault population a) displayed to highlight the ENE-WSW sub-population (blue) in comparison to the remaining E-W population (pink). With insets b) showing the E-W population as a splay type of formation in the damage zone of larger faults, and c) where the E-W population forms rectangular type geometries (blue fill) with other fault populations. The location of these insets is also shown on Figure 4.2a.

In the Willem-Pluto survey, these faults occur near to the uplifted block of the Wheatstone Field, where they are present in the stratigraphy from the Triassic to the late Jurassic (Figure 4.12).

Additionally, some movement - though limited - does occur on some faults within the E-W fault population (Figure 4.15). This is observed in the Duyfken, Glencoe, Honeycomb, Scarborough, Bonaventure, Thebe, and Marie Rose Northern Extension. In these instances, movement commonly occurs on the fault as a stress transfer mechanism between two larger faults within the more prominent fault populations (Figure 4.2). In the southern Glencoe survey, some faults of this population occur independently of larger faults, forming in conjunction with the no-to-limited throw faults of the same population, where igneous sills are identified (Figures 4.2 & 4.15). Activity on these faults is most prominent in the latest Triassic and earliest Jurassic (TR30-J20) but can extend into the later Jurassic (Figure 4.2).

Faults within the ENE-WSW sub-population display throws of 116 m in the south of the Glencoe seismic survey and 232 m in the Duyfken seismic survey, in the area adjacent to the southern Glencoe seismic survey. This is much smaller in the Scarborough survey, where throws are in the order of 23 to 40 m (Figure 4.11b). Most of the remaining faults in the E-W population display throws of 23 to 34 m. Throws in the Glencoe seismic survey tend to be towards the lower end of this range. These throws increase to 34 m across the Duyfken seismic survey and into the Willem-Pluto seismic survey. This population has the least throw in the Scarborough seismic survey, at a consistent measurement of less than 10 m (Figure 4.11b).

The length of the E-W faults is highly dependent on their location. Those faults identified in the Scarborough seismic survey display lengths of between 8 and 10 km, except in the case of the ENE-WSW sub-population which show individual fault segments of between 1.4 and 4 km linking to form larger fault networks of limited throw. In the southern portion of the Glencoe survey, the individual ENE-WSW fault segments are also smaller, with lengths between 1.5 and 4 km.

Figure 4.15 Fault sticks of the E-W population – including the ENE-WSW sub-population – with the regional and local features underlain, and the Upper Cretaceous K40-K60 expression of the Wanthaya High. With those faults with any evidence of syn-kinematic deposition during the Mesozoic coloured as active faults (in red) and those that show no evidence of syn-kinematic timing coloured in grey.

4.2. Timing of Mesozoic Fault Activity

Fault activity is identified as having occurred throughout the Mesozoic and can be divided into Main Syn-Rift and Late Syn-Rift with a further period of development in the Post-Rift. Movement on faults did not occur synchronously across the plateau during the identified Mesozoic rift activity. Key differences have been observed in the onset of fault activity, longevity of movement, and the cessation of fault activity. These variations in the timing of fault activity is described below, with reference to the mega-sequences defined in Chapter 3 (Figure 3.1).

4.2.1. PRE-MESOZOIC RIFT (PRE TR30.1)

4.2.1.1. TR20 AND OLDER (OR PRE-TR30.1 TS)

The deepest parts of the seismic data reveal a series of rotated fault blocks containing Norian (Triassic) aged stratigraphy. This is interpreted as being the middle part of the Mungaroo Formation (the shallower units of which are intersected in numerous wells across the plateau; Figure 3.21). This Pre-Kinematic sequence is discussed in Chapter 3 as displaying parallel reflectors (Figure 3.2), representing deposition which occurred before the initiation of fault activity. No evidence of fault activity is seen across the entire area of investigation during this time (Figure 3.2). There is no indication of depositional sequences thickening in footwalls or across fault block. Likewise, there are no incidences of strata thinning out over highs, except in cases where this is attributed to later erosion (Figure 3.2). All faults interpreted within the TR20 or older strata are considered to have formed after the deposition of the regional and economically important TR20 – TR10 (Mungaroo Formation; Figures 2.19 and 3.1) and older strata.

4.2.2. MAIN SYN-RIFT (TR30.1 TS - K10.2 MFS)

4.2.2.1. TR30 RHAETIAN (TR30.1 TS - J10.0 SB)

The first evidence of fault movement occurs during Rhaetian times. As described in Chapter 3, Section 3.2, the TR30 MS1 sequence displays thickening into footwalls and thinning out over highs (Figure 3.2). However, movement during the Rhaetian is not universal within the study area. As described in Chapter 3 (Tectono-Stratigraphic Framework), evidence of movement within the Rhaetian is only observed within the Thebe, Bonaventure, Scarborough, Marie-Rose Northern Extension, Honeycomb and Glencoe 3D seismic surveys, the Ja95 2D seismic survey and the Bart 2D seismic line (Figures 3.4, & 4.2a). Here fault activity is dominated by the NNE-SSW population, although a significant movement is also seen on the NE-SW population (Figure 4.10). Minor movement also occurs in NW-SE population (Figure 4.10). The TR30 MS1 sequence remains unaffected by any fault activity in the remainder of the study area to the east (Figure 3.5), where reflectors remain parallel (Figure 3.2). This highlights a separation within the plateau, in terms of the response to rift-activity (i.e., Figure 3.5).

4.2.2.2. J20 TO J30 PLIENSBACHIAN - OXFORDIAN (J24.0 SB - J40.0 SB)

In the west of the study area (this research), fault activity continued from the latest Triassic into the Jurassic. Pronounced growth wedge formation (Figures 3.3, & 3.11) and thinning (Figure 3.2) out over the uplifted and rotated fault blocks occur extensively within MS2b (J24.0 SB – J47.0 SB) mega-sequence (Figure 3.2). There are a limited number of fault blocks in the western part of the study area on which no growth wedges occur, but this is rare. In addition to the formation of growth wedges, movement of faults in the Lower-Middle Jurassic is demonstrated by the onlap of seismic reflectors against the underlying Rhaetian sequences (Figure 3.3). This onlap of strata onto the underlying sequences occurs exclusively within the Thebe, Bonaventure, Scarborough, Mary-Rose Northern Extension, Honeycomb and Glencoe 3D

seismic surveys, the Ja95 2D seismic survey and the Bart 2D seismic line (Figure 1.13), or within the western part of the study area.

In the eastern portion of the study area, something different is observed. Here fault activity initiated during the Lower Jurassic- as there is no evidence of Rhaetian fault activity (Figures 3.5, & 4.2a). Early Jurassic strata (MS2a (J24.0SB-J40.0SB)) show a small amount of thickening across faults (Figures 3.2, & 4.16). This occurs to a significantly lesser extent than on active faults of the same age in the west (Figures 3.6c, 3.6e, & 4.17). In addition, broad-scale uplift and erosion in the southeast occurred by the time of the Oxfordian Unconformity (J40.0 SB; see Chapter 5; Figures 3.2b, & 3.3a). This event removed a large portion of the early-Middle Jurassic depositional evidence (Figures 3.2b, & 3.3a) for potential fault movement.

Fault movement at this time is dominated by faults from the NNE-SSW and NE-SW populations (Figures 4.2b, & 4.10). Movement also occurs on faults from the NW-SE population, but to a significantly lesser extent (Figures 4.2b, & 4.10). Active fault populations are also spatially restricted (Figure 4.2b). In the eastern region, the dominant activity occurs in the NE-SW population, but this is still less than the magnitude of fault activity that occurs on NNE-SSW faults in the area as a whole (Figures 4.2b, & 4.10).

4.2.3. LATE SYN-RIFT (TR30.1 TS - K10.2 MFS)

4.2.3.1. J40 TO J50 OXFORDIAN - BERRIASIAN (J40.0 SB - K10.2 MFS)

Fault movement occurs across the Exmouth Plateau during the Upper Jurassic (Figure 4.2c), with the pattern of fault movement revealed by the deposition of MS3 (J40.0 SB-K10.2 MFS; Figures 3.2, & 3.12). Following the initiation of sea-floor spreading in the Argo Abyssal Plain during the Oxfordian (Figure 2.1), fault activity increased and thickness changes across faults became a dominant characteristic of the more prominent faults in the southeast of the study area (Figure 3.2). There is no evidence to suggest a similar change in

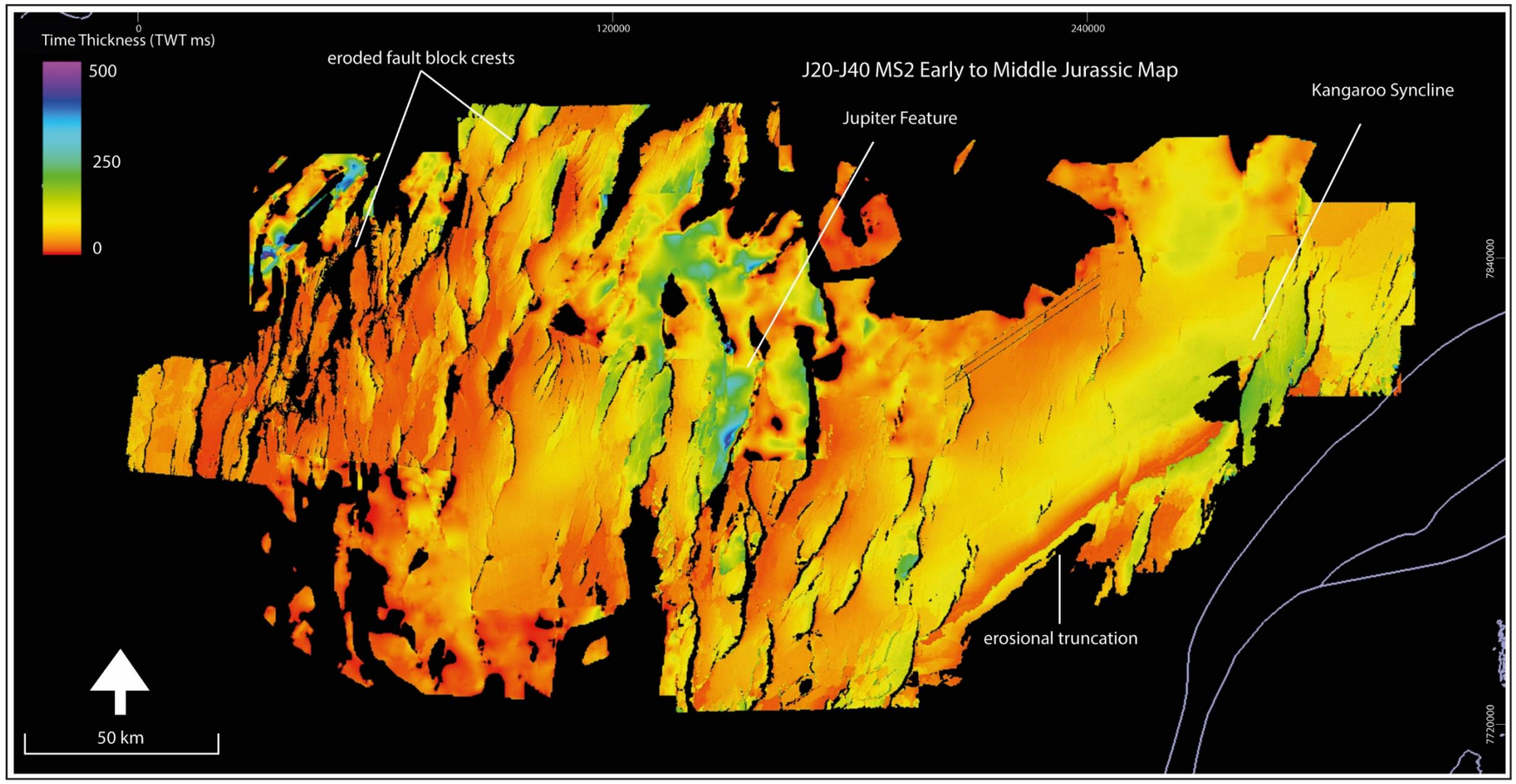

a)

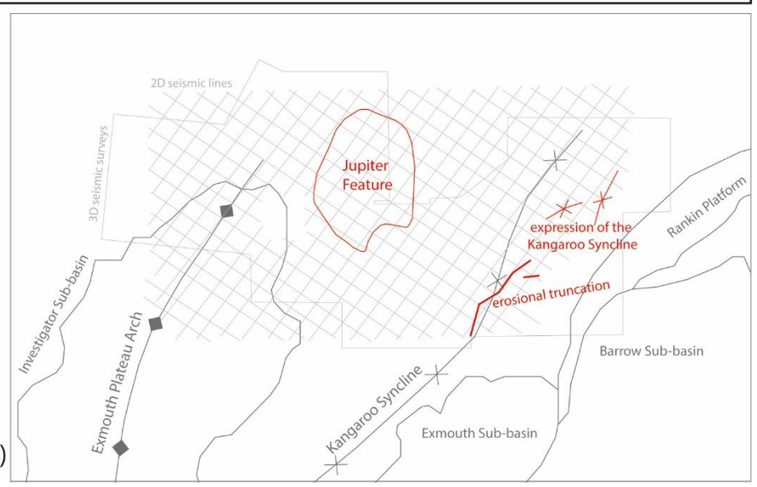

b)

Figure 4.16 a) Time thickness map of the early to Middle Jurassic (J20 – J40 MS2) over the Exmouth Plateau showing the thickness of the MS2 deposition, and line map of key features in b).

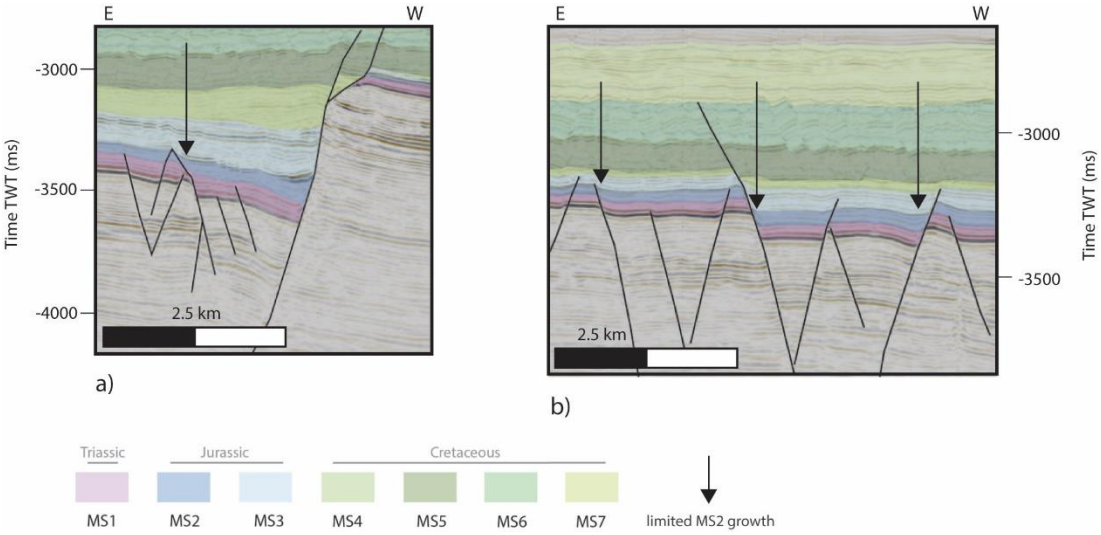

Figure 4.17 Growth wedge formation in the western portion of the studied area, displaying limited growth in the MS2 package across some faults. Location of cross-sections is available on Figures 4.11a).

fault activity in the west where growth wedges continued to form (Figure 3.2), as they had previously, indicating the continuation of fault movement.

Another indication of fault activity during this time in the northwest is a period of sediment starvation (Figure 3.12). The extreme underfilling of the accommodation space in this area, compared to elsewhere at this time, implies that significant structural relief of faults impacted sediment supply. This structural relief inhibited the delivery of sediments into the west of the area studied, likely due to the emergence of fault blocks above the delivery pathways. This resulted in restricted deposition and the above mentioned underfilling of accommodation space (Figures 3.12, & 3.22d). Due to this period of sediment starvation, the depositional record of fault movement is not complete in the northwest, although it is likely to be ongoing. Faults from the NNE-SSW, NE-SW, and NW-SE populations are all active during the Upper Jurassic (Figures 4.2c, & 4.10). Activity on the NNE-SSW and NE-SW trends was most prominent at this time (Figure 4.10).

4.2.3.2. K10 BERRIASIAN - VALANGINIAN (K10.2 MFS - K20.0 SB)

The early Lower Cretaceous brought about a decline of fault activity in the east of the region (Figures 3.16, & 4.2d), where fault movement stops just prior to the Valanginian (Figures 3.2b, 3.3a, & 3.19). This is seen in the steady reduction of thickening into faults and thinning over highs during the deposition of MS4 (K10.2 MFS -K20.0SB; Figures 3.2a, 3.2b, 3.3b & 3.16).

In the west, fault activity continued during the deposition of MS4 (K10.2 MFS - K20.0SB). At the start of this interval half-graben infilling was still occurring (Figures 3.2, 3.3, 3.6, 3.11, & 3.13a). This is evidenced in the prominent formation of growth wedges against footwall fault blocks (Figures 3.2, 3.3, 3.6, & 3.11). These growth wedges begin to reduce in magnitude over the course of the K10 (Berriasian – early Valanginian) time interval (Figures 3.2, 3.3, 3.6, & 3.11). By the end of the Valanginian seismic reflection evidence indicates a decreased magnitude of displacement on most faults in the west (Figures 3.2, 3.3, & 3.11), with the exception of a few faults in the northwest that exhibit extreme relief (Figure 3.16).

Fault movement at this time primarily occurs on NE-SW orientated faults, with the NW-SE fault population now the second most important (Figure 4.10). Limited movement occurs within the NNE-SSW fault population (Figure 4.10). This change in the trend of fault activity coincides with the separation of the Australian and Greater Indian.

4.2.4. POST-RIFT (K40.0 SB - T10.0 SB)

4.2.4.1. K10 TO K20 VALANGINIAN - BARREMIAN (K20.0 SB - K30.2 MFS)

Following the Valanginian event, no further fault movement is evident in the eastern portions of the study area (Figure 4.2e). To the west, thickening into footwall fault block and thinning over highs highlights that fault activity maybe ongoing during the K10 and K20 intervals (Figure 3.2a, 3.6a, & 3.6e). Alternatively, fault propagation at this time could be the result of differential

compaction between hanging walls and footwalls (Figures 3.2 & 3.17). Thickening into footwalls no longer creates the prominent growth wedge geometry seen in the Jurassic and earliest Cretaceous, but thickening is still observed (Figures 3.6, & 3.11). The dominant fault population on which movement occurs during this time is the NE-SW population (Figure 4.10). Some movement also occurs on the NNE-SSW population (Figure 4.10). Limited movement on the NW-SE population also occurs during this interval (Figure 4.10).

4.2.4.2. K30 BARREMIAN - MID-APTIAN (K30.2 MFS - K40.0 SB)

To the west, movement is ongoing during the deposition of MS6 (K30.2 MFS-K40.0SB). In seismic cross-section (Figure 3.2) thickening of strata into footwall fault blocks is limited during the deposition of the K20 to K30 strata as MS6 (the Muderong Shale) and occurs in the northwest and in the region north of the Glencoe 3D seismic survey, within the Ja95 2D seismic survey (Figures 3.2, & 3.13). Here the faults that remain active are from the NNE-SSW population (Figure 4.10). Some fault movement on the NE-SW and NW-SE populations occur around the active NNE-SSW faults (Figures 4.2f, & 4.10).

4.2.4.3. K40 TO K60 MID APTIAN - END OF CRETACEOUS (K40.0 SB - T10.0 SB)

Following the mid-Aptian, some movement on major faults in the northwestern portion of the study area occurred but was limited and short-lived. Evidence for this movement is seen in the thickening of the K40 to K60 stratigraphy into footwall fault blocks and the thinning-out over the upthrown fault blocks (Figures 3.2a & 3.20). The ongoing movement occurred exclusively on faults from the NE-SW population (Figures 4.2g, & 4.10). Mesozoic fault movement had ceased prior to the end of the Cretaceous.

4.2.5. BLIND FAULTS

There are some instances in which the precise age of fault activity cannot be quantified. This is due to the faults occurring after deposition of the stratigraphy through which they penetrate (Figures 4.11, & 4.12). It is possible that some, or all, of these faults have syn-depositional features which are not captured at the available seismic resolution. Short of examining these faults in outcrop, which is certainly not possible, no further conclusions can be made about the timing of activity relative to deposition. For this dissertation, it is assumed that these faults nucleated after the deposition of the adjacent stratigraphy, and propagated blind without reaching the surface.

Most faults from the E-W population lack any associated kinematic sequences (Figures 4.2, & 4.15). As these faults cut strata of various ages (Triassic-Jurassic and Jurassic-Cretaceous; Section 4.1, this Chapter) they are not linked to any single event. It is likely that those faults that do not penetrate Cretaceous stratigraphy (Figures 4.2, & 4.12) are a result of extension events in the late Upper Triassic or early Lower Cretaceous and associated igneous intrusions (Figures 4.11, & 4.12). For those faults which are identified as cutting the early Cretaceous stratigraphy (Figure 4.12), no faults are identified after the Valanginian Unconformity. Making the Valanginian separation event (see Chapter 2, Section 2.2.4.6) the source of the E-W trending faults which intercept the Cretaceous strata.

Faults with these characteristics also occur in the NW-SE population (Figures 4.2, & 4.10). Most of this population occurs as blind faults, forming after the deposition of the Mesozoic aged strata through which they penetrate (Figures 4.11, & 4.12). They are largely limited to the southern part of the study area, forming key components of fault damage and transfer zones. Blind faults within the NNE-SSW population occur largely within the damage zones of larger fault networks (Figure 4.2). They are considered to have formed as a result of stress transfer from these larger faults. This would have occurred in the uppermost Triassic (eastern portion of the study area) and the Lower Cretaceous (western portion of the study area), when the larger faults were growing. Faults from the NE-SW population, without syn-kinematic sequences within the Jurassic and

Lower Cretaceous strata (Figure 4.2) also form key features associated with stress transfer in the damage zone of larger faults.

Several polygonal fault networks also occur within the study area (i.e., Figures 3.2, & 3.13). These are post-depositional features and are not gravity driven. They occur in the Upper Jurassic and Cretaceous stratigraphic units (i.e., Figures 3.2, & 3.13). Polygonal faulting has not been investigated at length as part of this research due to their development as post-depositional, dewatering features.

4.3. Summary

The Exmouth Plateau has been widely impacted by simple extension along normal faults. These faults have formed in a wide variety of fault orientations and can be grouped into four fault populations. The most prominent of these fault populations are the NNE-SSW and NE-SW populations (Figure 4.10). Displacement along these faults is highly variable, causing significant changes in structural relief across the plateau. Fault activity has formed the main structural elements in the Exmouth Plateau, in the form of rotated fault blocks (Figure 3.2). The rotation of these fault blocks and associated syn-kinematic sediments has provided age constraints for the timing of fault movement on the plateau. Critical differences in the timing of fault initiation and cessation are observed. The earliest fault activity occurred to the west during the Rhaetian where movement continued into the Lower Cretaceous (Figures 3.2, & 4.2). To the east, fault activity began later during the Lower to Middle Jurassic (Figures 3.2, & 4.2). In addition, displacement along faults in the east ended in the lowermost Cretaceous at the latest, well before movement was completed in the west (Figures 3.2, & 4.2).

There are also distinct differences in the intensity of faulting across of the area, with a greater density of faults with larger displacements in the west compared to the east (i.e, Figure 4.8a, 4.11a, 4.12, & 4.13). This reasons for this are not apparent but could relate to rheological changes in the Palaeozoic basement (Gartrell, 2000; Handy, 1989; Mondy, 2019; Weissel & Karner 1989), the strength of the lithosphere adjacent to the rift-flank uplift (Chery et al., 1992;

Figures 3.2b, 3.3a, & 3.22c) and associated changes in flexure and geothermal gradients (Handy, 1989).

Much is known about the plate boundaries and the predicted stress orientations that existed in northwestern Australia during the Mesozoic. This is based on in-depth plate tectonic reconstructions, and the subsequent breakup of the Gondwanan supercontinent (Gibbons et al., 2012; 2013; 2015; Muller et al., 2019). During Lower to Middle Jurassic rifting, plate orientation and sea-floor spreading centres indicate that the area near the Argo Abyssal Plain most likely experienced NW-SE oriented extension (Figure 2.1), which should result in the preferential development of NE-SW oriented faults. However, the most significant set of faults identified in the study area during this period of time are oriented NNE-SSW (Figures 4.2, & 4.10). Although other faults were also active at this time (NE-SW and NW-SE; Figures 4.2, & 4.10), there is an apparent mismatch with the expected extension direction. This is considered further in the discussion (Chapter 6).

After the formation of the Argo Abyssal Plain, rift activity switched to the western margin of Australia (Figure 2.1). Sea-floor spreading centres associated with the Cuvier and Gascoyne Abyssal planes indicate a WNW-ESE extension direction (Figure 2.1). This is consistent with activity on NNE-SSW oriented fault and suggest that stresses associated with this margin may also have had a significant influence during the Lower and Middle Jurassic. Activity on and NE-SW fault populations remained significant until the Berriasian (Figures 4.2, & 4.10) when there was a change in the orientation of prominent fault activity to the NW-SE population, further reflecting the plate organisation that occurred at this time.

5. Rift-Related Morphology of The Exmouth Plateau

The morphology of the Mesozoic rift on the Exmouth Plateau developed from the Upper Triassic to the Lower Cretaceous (Figure 5.1). Rift-related morphology is defined by the elevation of the pre-rift section relative to an arbitrary datum. In the earlier part of the Triassic, a prolonged phase of thermal subsidence (See Section 2.2.4 Tectonic Evolution of the Exmouth Plateau; Etheridge & O'Brien, 1994; Falvey & Mutter, 1981; Jablonski & Saitta, 2004; Lister et al., 1986, 1991; McKenzie 1978; Playford et al., 1976; Veevers, 2000, 2006; Yeates et al., 1987) resulted in a thick succession of pre-kinematic stratigraphy (i.e., Figure 3.4a, the Middle-Latest Triassic). Following this phase of ongoing subsidence and deposition, fault activity began in the Uppermost Triassic, at the end of the TR20 Norian or start of the TR30 Rhaetian (Chapter 4). Rift activity continued into the Middle to Upper Jurassic when seafloor spreading in the Argo Abyssal Plain was initiated (as per Gradstien & Ludden, 1992; Heine & Müller, 2005; Metcalfe, 1996; Stagg et al., 1999; Veevers, 2006; Veevers et al., 1991). Changes in the expression of rift activity (Chapter 4) occurred after this, with fault activity continuing into the Cretaceous. Fault activity across the entire area under investigation was not continuous throughout the Mesozoic rift events (Chapter 4). The morphological development of the rift mirrors the division of timing observed in the formation of faults (Chapter 4) on the Exmouth Plateau.

Rift-related morphology comprises four different components. The first component is isostatic uplift along fault planes with large displacements (particularly on the margins of fault bounded basins) which may result in the removal of sequences from hangingwalls by erosion. The second component is the thermal effects, related to elevated lithospheric heat flow and subsequent cooling. The loading of sediments (and other material) also impacts the topographic expression of a rift and is the third component of rift-related morphology. The fourth component is the rotation of individual fault blocks. The contribution of these factors changes over time and may be

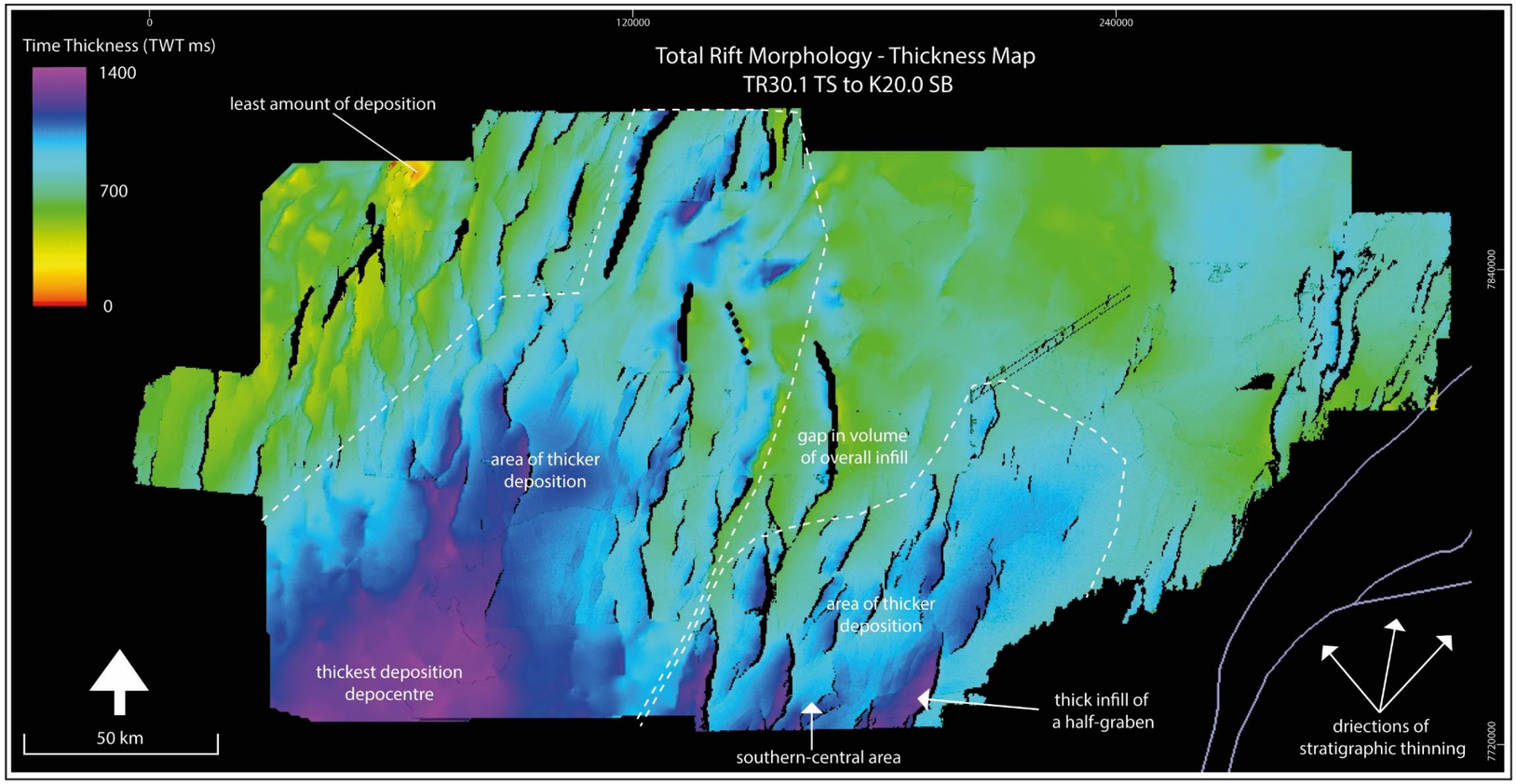

a)

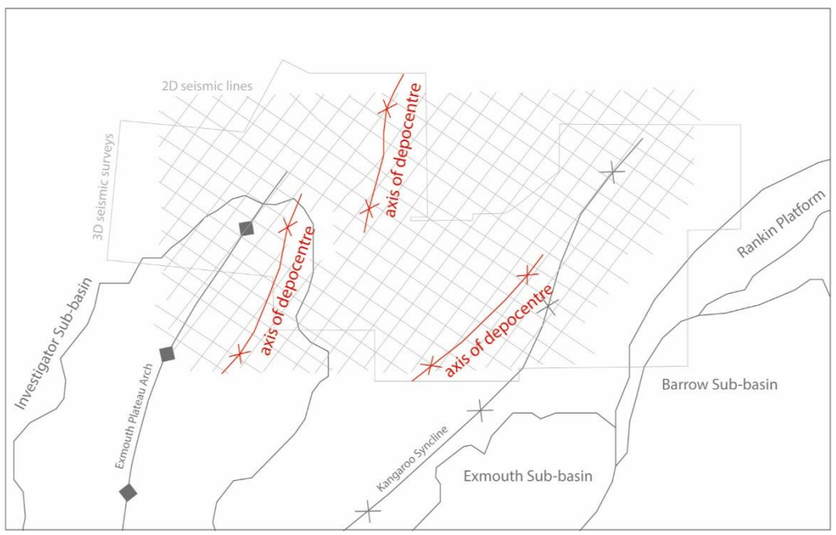

b)

Figure 5.1 a) Time thickness map displaying the total rift-related morphology of the Exmouth Plateau, from the onset of rift-related activity in the Rhaetian to the end of active rifting in the Valanginian (K20), b) regional structures (grey) and key features formed during the rift period (red) of the Exmouth Plateau.

temporary or longer lasting. These rift components may occur regionally, or locally. The thermal component is most likely to be temporary, as heat flow declines following the cessation of rift activity (see Section 1.1.2.1 Thermal Subsidence; Boillot, 1979; Chenin et al., 2018, 2022; Falvey, 1974; Grasemann & Stuwe, 2011; Kearey et al., 2009; Li et al., 2004; Manatschal et al., 2021, 2022; McKenzie, 1978; Martins-Neto & Catuneanu, 2010; Péron-Pinvidic et al., 2013; Ruppel, 1995). Due to the fluctuations of these contributions - in broad terms, the Mesozoic thermal contributions continued from the Permian into the Upper Triassic (Etheridge & O'Brien, 1994; Stagg et al., 1999; Veevers, 2006), then further rift events from the Upper Triassic to the Lower Cretaceous resulting in further thermal changes and related compensation on the margin (Baillie et al., 1994; Blevin et al., 1994; Etheridge & O'Brien, 1994; Geoscience Australia, 2014a, 2019; Metcalfe, 1996; Rohrman, 2013, 2015; Smith et al., 1999; Veevers, 2006) - the present-day morphology will not fully define the topography that existed during rifting. Combined with fluctuations in sea-level these processes are also responsible for the creation of accommodation space. The actual topography or bathymetry of a rift will depend upon the extent to which it is filled by sediment. Consequently, if available accommodation space is filled, thickness maps can be used as a proxy for the morphology of the rift that existed during that time interval. Where the accommodation space is not completely filled these observations reveal the distribution of sediments and the apparent topographic or bathymetric influence of the rift on these processes.

This chapter uses the observation of thickness variations observed between the main phases of rift activity. These phases are separated by the sea-floor spreading events of the Middle to Upper (J40.0 SB) Jurassic and the later Valanginian separation event (K20.0 SB). A representative Exmouth Plateau Wheeler Diagram is presented in Figure 3.9.

5.1. Total Rift-Related Morphology

The total morphology generated by Triassic to Cretaceous rift events (Figure 5.1) can be estimated by the thickness of sediments preserved between the

top of the last pre-rift sequence (Pre TR30.1 TS, the Mungaroo Formation) and the top of the early post-rift (Post K40.0 SB, the Muderong Shale). Due to its deposition during a marine transgression, the K20 - K30 Muderong Shale was used as it is a wide-spread, regionally occurring sequence which can be considered to be close to a paleohorizontal, or with a low angle of dip on a regional scale, despite local remnant bathymetry. The underlying packages do not occur as widely or as uniformly as the Cretaceous aged shale unit and hence are less useful. It is also the first post-rift sequence to have been deposited after the Valanginian end-rift event (the K20.0 SB), and prior to significant post-rift subsidence. Both of these factors make the K40.0 SB Top Muderong Shale pick a reasonable datum from which to estimate the total rift morphology. Limitations do exist with this method due to the ongoing chance of tectonic activity, erosion as well as the potential that deposition was low at the time; all factors that could limit the horizons' ability to divulge the past.

The total rift morphology map (Figure 5.1) shows a number of significant features that formed within the study area during the Mesozoic. There is a significant amount of thinning shown in the sedimentary packages to the northeast (Figure 5.1). Early Cretaceous stratigraphy thins out or was not deposited over this feature (Figures 5.2 & 5.5). Tectonic movements in this area are limited, and the deposited stratigraphy are thin (c.450m in the Urania-1 well area vs. c. 1400 m in the Scarborough area; see Figure 3.21a for comparison of stratal thicknesses), making the exact origin of this feature unclear. Further thickness comparisons are available on Figures 5.2, 5.3, & 5.4. The southeast displays an overall thickening relative to the adjacent regions to the north of thinner stratigraphy (Figure 5.1) and was a consistent feature throughout the formation of the rift (Sections 5.2 & 5.3). The observed orientation of this feature is NE-SW and maximum thickness occurs along the downthrown side of half-graben towards the more central (southern-central) region (Figures 5.1, & 5.3a). The thickest preserved succession of sedimentary packages is observed in the southwest (Figures 5.1, & 5.4). This feature forms a broad depocentre which trends to the NW and developed in the second stage of rifting (Section 5.3). In the northwest, relative elevation rises. The erosion of

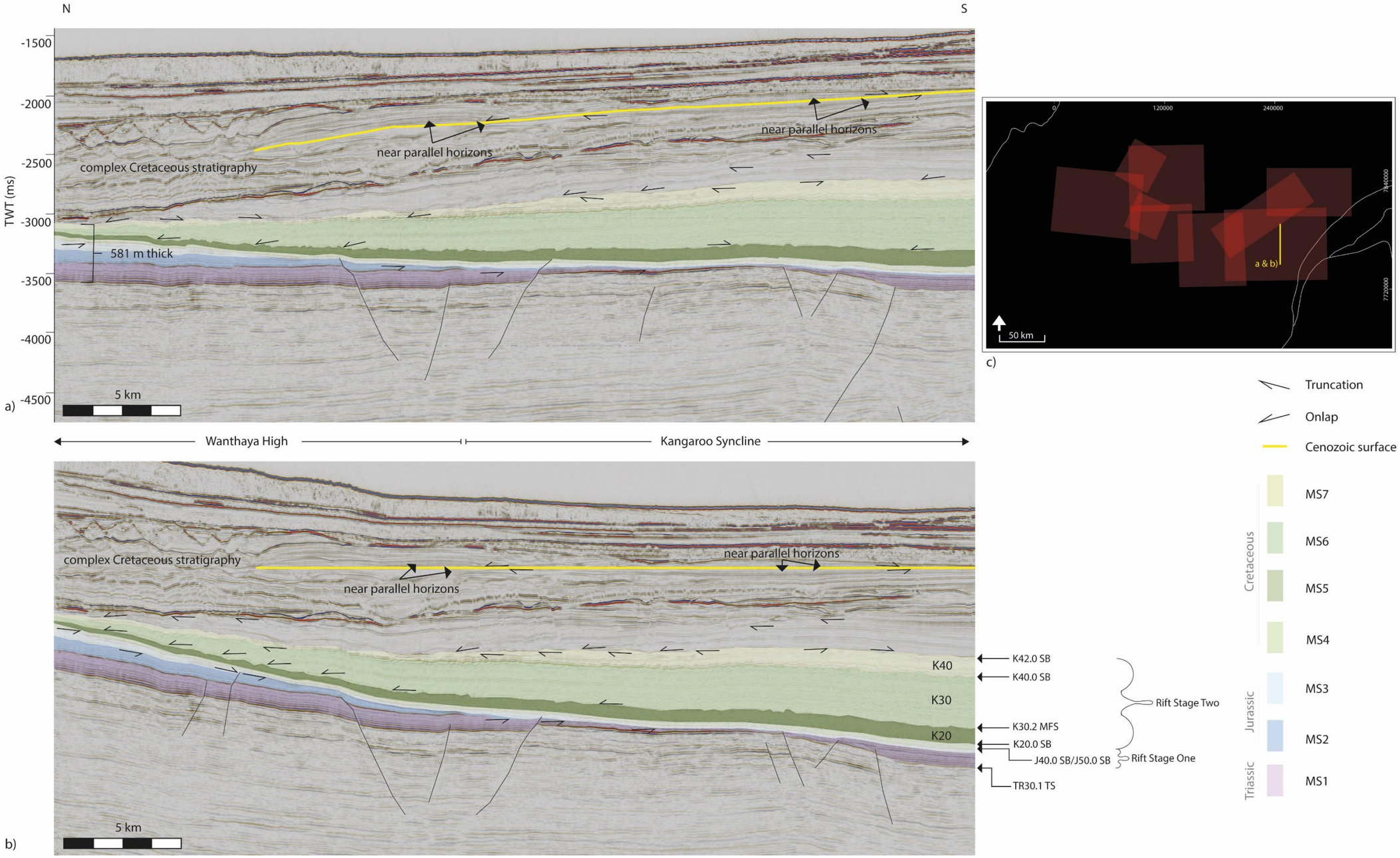

Figure 5.2 Cross-section of the Northeast High (Wanthaya High) in the northeast of the study, showing the onlap and truncation associated with this feature, and b) a 2D reconstruction of the potential elevation during the Cretaceous. The Cenozoic surface could not be identified by a narrower age range and was not identifiable for this studies scope across the whole line.

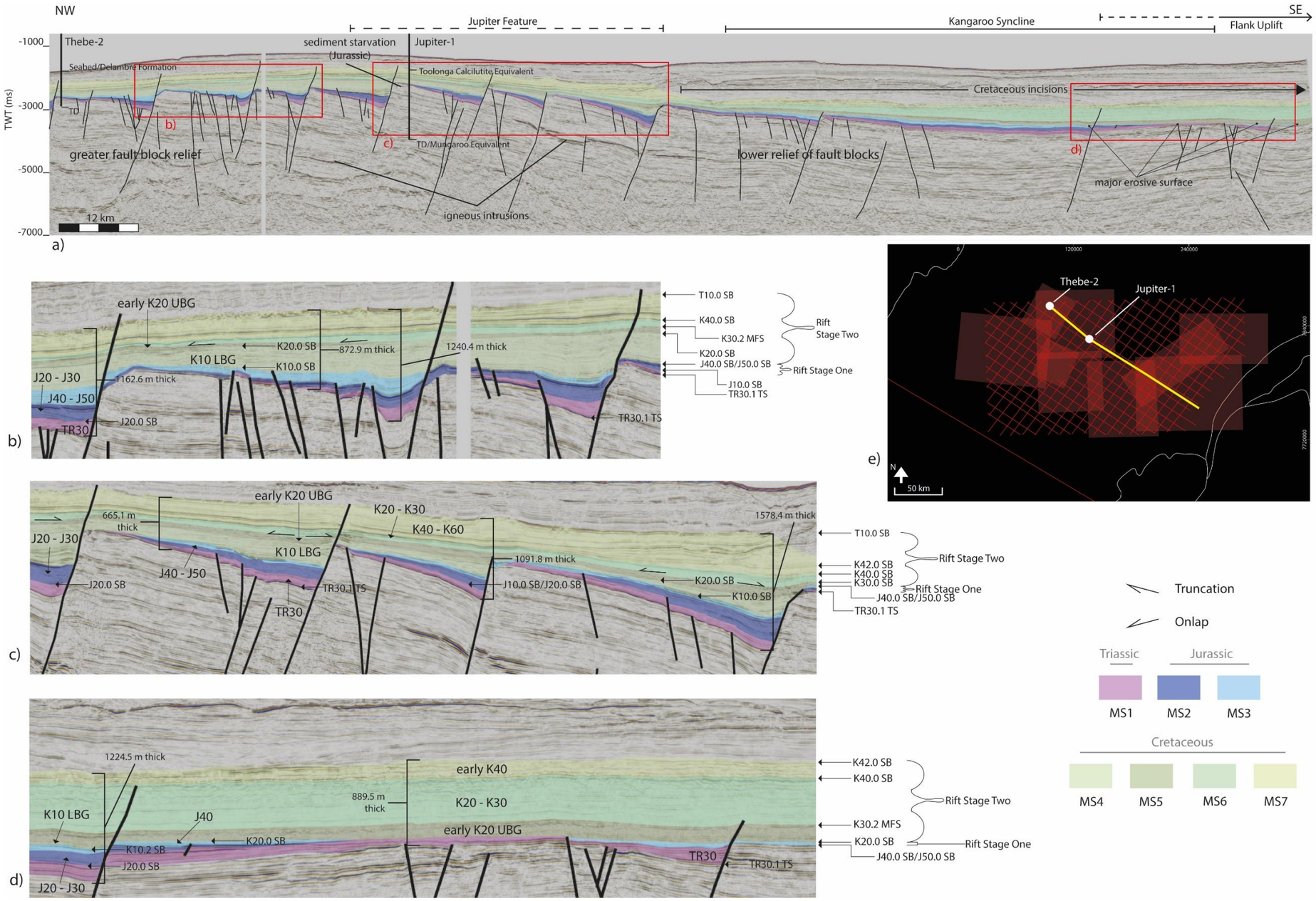

Figure 5.3 Regional cross-section through the study area displaying the mega-sequences as per this study. Cross-section a) showing the differences in structural architecture between the west and eastern plateau. The erosion of fault block crests is, and timing indicators are captured in figure b) and the thinning of depositional packages over rotated fault blocks is shown in Figure c). The location of Figures b) and c) are highlighted on Figure a), the location of Figure a) is shown on the map (d), as are the two wells displayed in section a).

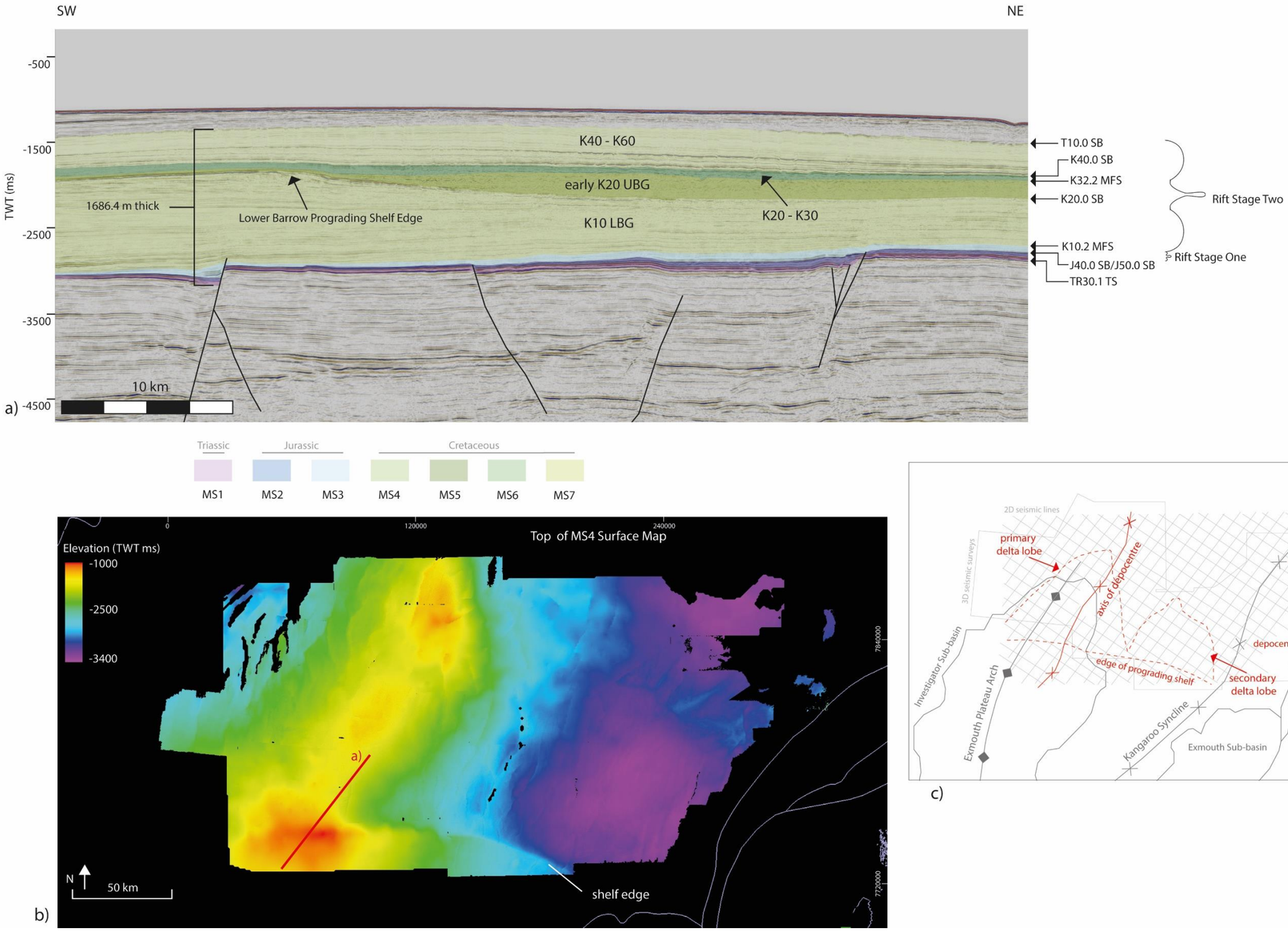

Figure 5.4 The prograded shelf edge of the Lower Barrow Group as observed in a) seismic cross-section, and b) an elevation map of the top surface. Key observations of structural and depositional feature are provided in c) the annotated line map of the Lower Cretaceous interval.

MS1 Thickness Map

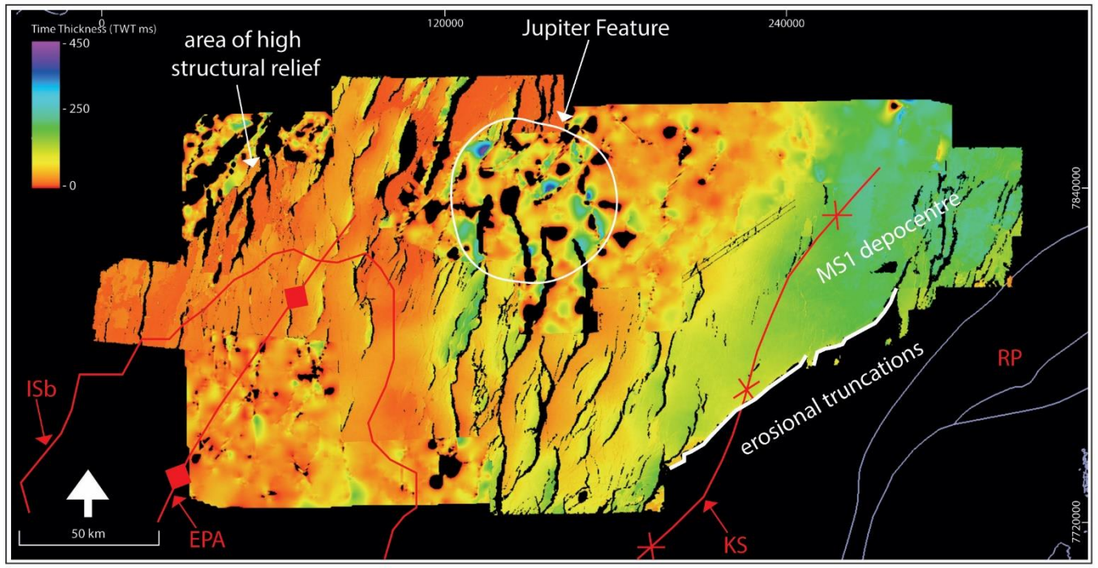

a)

MS2 Thickness Map

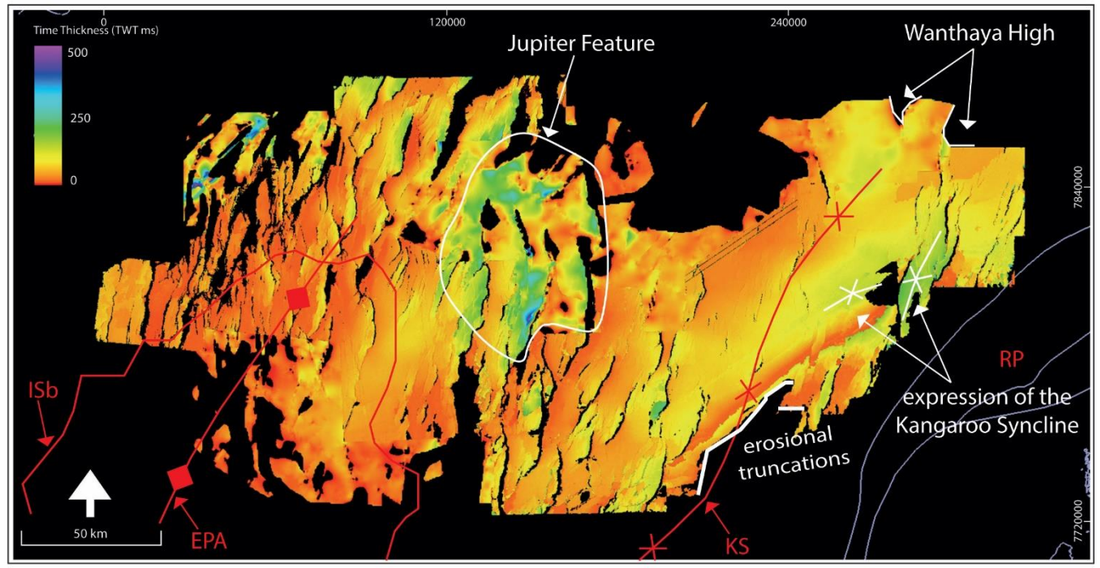

b)

MS3 Thickness Map

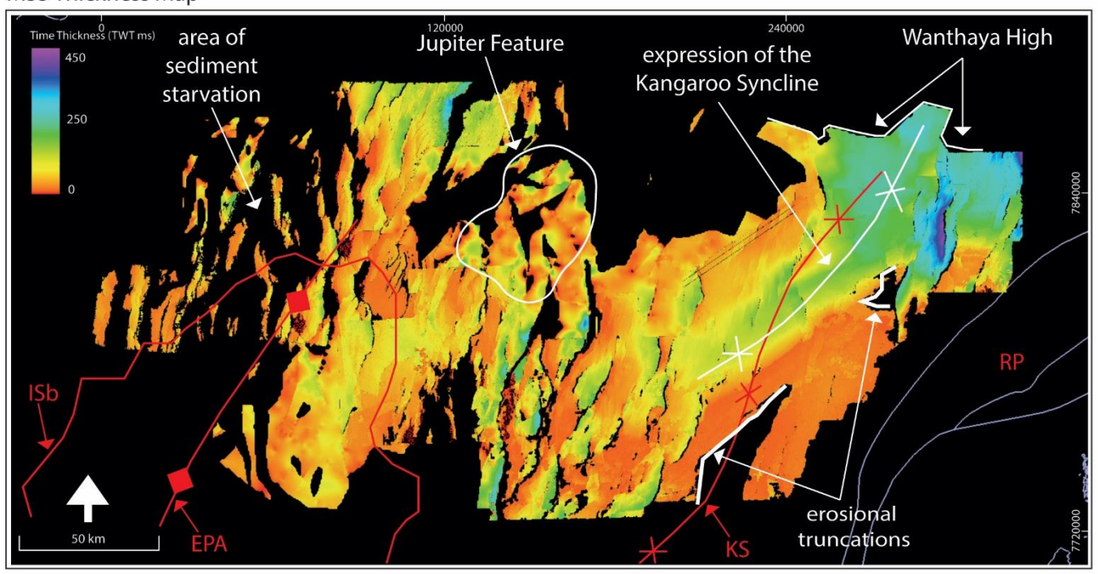

c)

MS4 Thickness Map

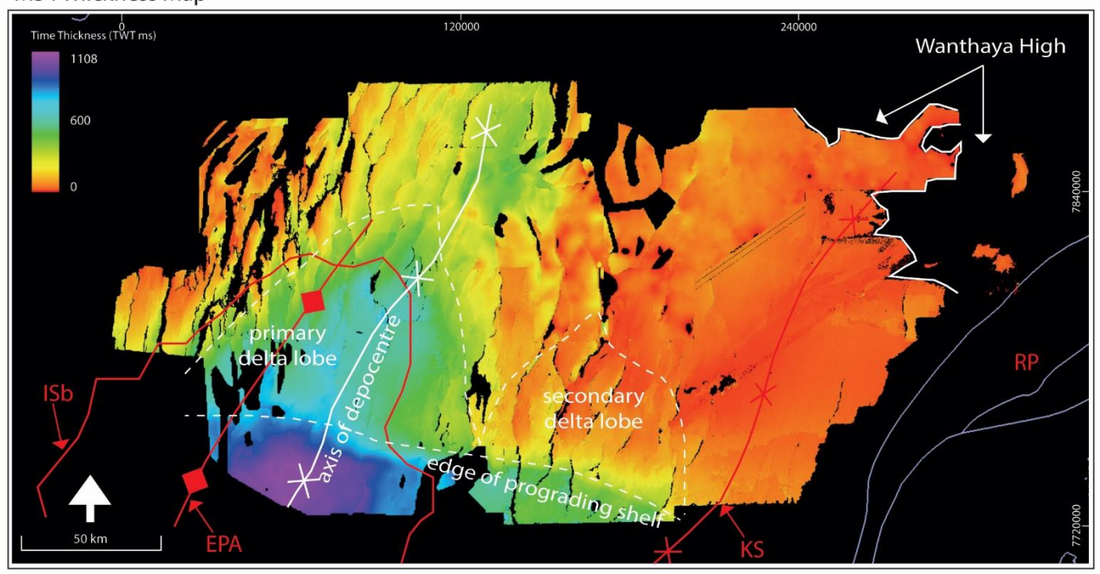

d)

MS5 Thickness Map

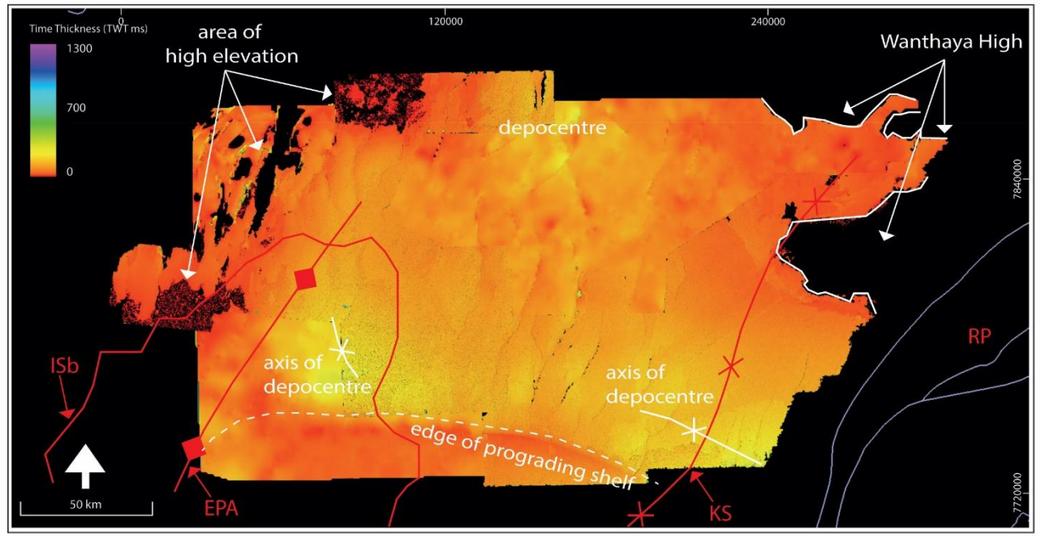

e)

MS6 Thickness Map

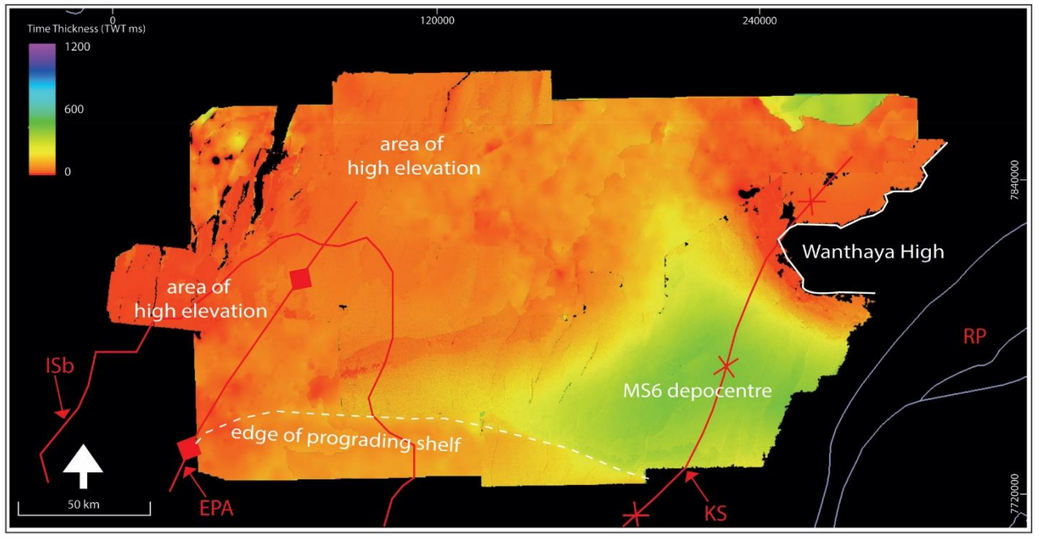

f)

MS7a Thickness Map

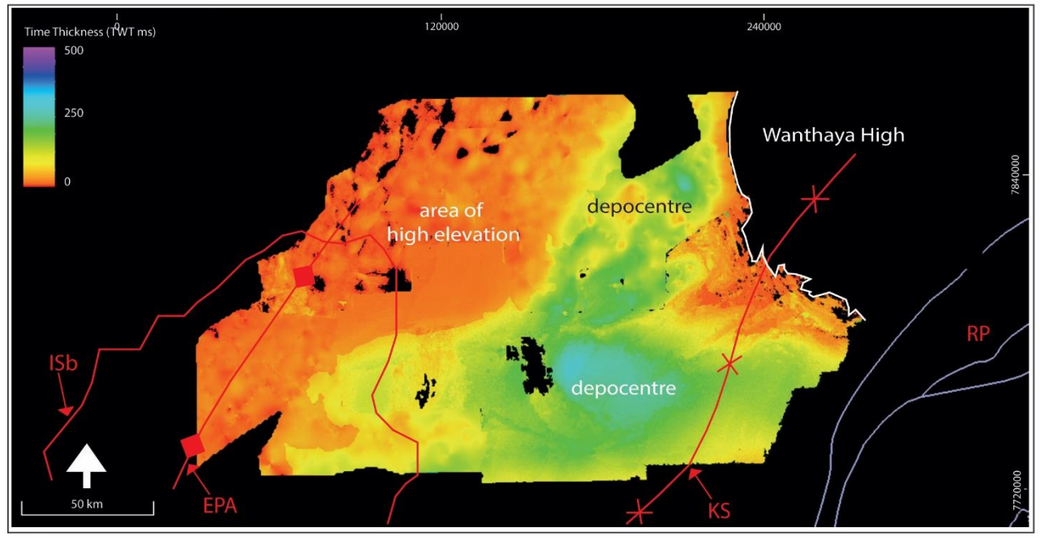

g)

MS7b Thickness Map

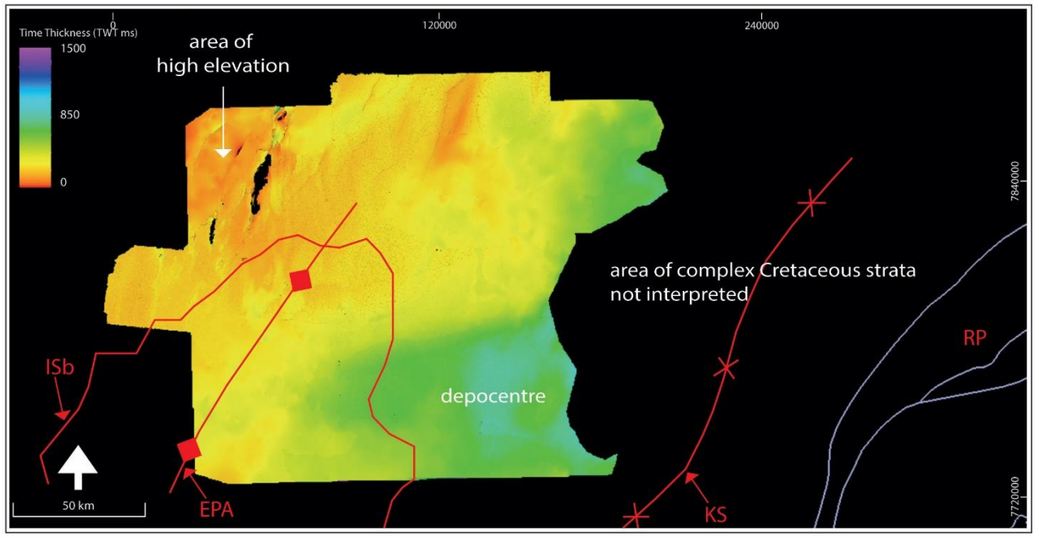

h)

Figure 5.5 Thickness maps of individual mega-sequences (as per this study) displaying the changes over time of the depocentre in the area of the Kangaroo Syncline (southeast depocentre), Exmouth Plateau Depocentre (southwest depocentre), Jupiter Feature, Wanthaya High (northeast high) and areas of high elevation. Regional structural features (red) and mega-sequence relevant features (white) annotated on the individual maps.

fault block crests are a prominent feature, and onlap of exposed fault blocks by the K20 - K30 Muderong Shale is observed (Figure 5.6g). Fault blocks in the northwest display greater overall uplift than fault blocks within the eastern areas (Figure 5.3). This pattern of increased uplift to the northwest could be evidence of increased uplift towards the continent-ocean boundary due to isostatic response (see Section 1.1.2.1 Thermal Subsidence). In the central region of the study area lower volumes of infill over some NNE-SSW and NE-SW trending faults are observed (Figure 5.1, & 5.3). The thinner sequences here occurred after the Middle Jurassic; prior to this, this area was a depocentre.

These patterns are the combination of several events which impacted the development of the Exmouth Plateau. These events can be broadly divided into two episodes of rift activity: the pre- and post- Middle Jurassic Unconformity rift stages, with a subsequent phase of modification occurring post-breakup. Each rift stage experienced different episodes of uplift and subsidence and helped to develop the structural architecture of the plateau. The morphological evolution of the rift during each of these stages is analysed in the following sections.

5.2. First Stage of Rift Development

The first stage of rift activity extends from the onset of extensional activity on the plateau in the Uppermost Triassic up to the initiation of Argo seafloor spreading in the Middle Jurassic. The morphology of this initial phase of rifting has been analysed by investigating the changes in deposition between TR30.1 TS (Top Norian) and J40.0 SB-J50.0 SB (Middle Jurassic Unconformity (MJU)-Tithonian Unconformity; Figures 5.2, 5.3, & 5.4). However, the Upper Triassic to Jurassic rift is not completely infilled by sediment, so thickness maps do not record absolute morphology. The MJU is unlikely to represent a paleo-horizontal surface due to tectonic activity and erosion, as well as the low rates of sedimentation (particularly in the northwest of the studied area, Figures 5.2, 5.5c) and the difficulty of recognising the unconformity in condensed sequences, due to either the limitations of seismic visualisation or the

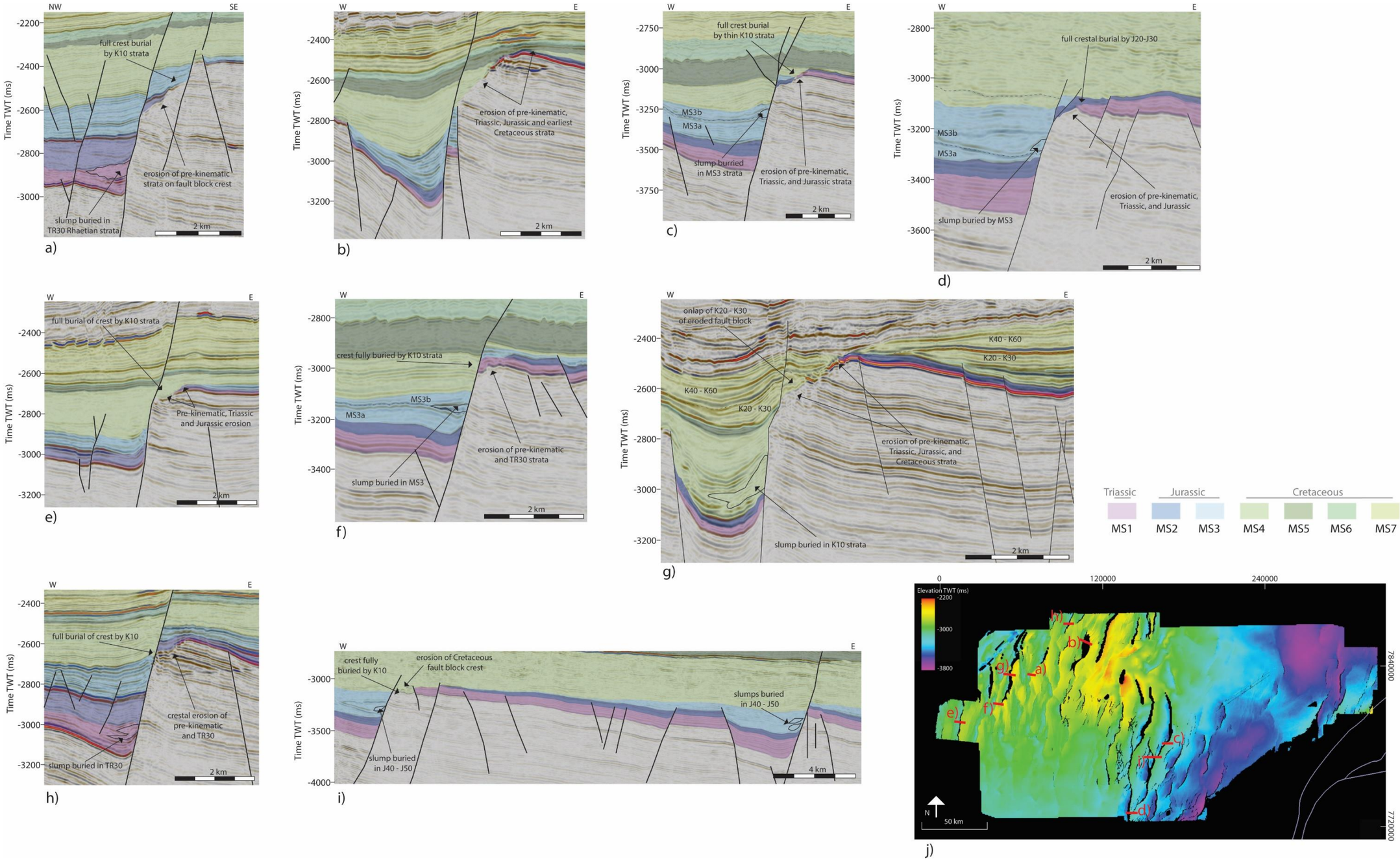

Figure 5.6 Fault block crest erosion over various location in the area studied, displaying various timings of erosion, burial of the redistributed slump material (when present) and the final full burial of the eroded fault block crest.

presence of the unconformities in an incomplete stratigraphical record. The top TR20 (TR30.1 TS, top Mungaroo Formation) to MJU (J40.0 SB - J50.0 SB) thickness map (Figure 5.7) is still useful for inferring rift morphology, as it can yield information about the distribution of sediments and eroded fault block crests as well as indicating areas of relative uplift. The change in thickness of the early to Middle Jurassic sequence is the combination of changes in elevation, preservation of stratigraphic packages and sediment supply. This enables some significant observations to be drawn in relation to the morphology of the plateau at this time.

The depositional environment on the plateau during this stage of rifting was dominantly marine, evolving from fluvio-deltatic initially shallow to deep marine, mass-flow over this period (Adamson et al., 2013; Longley et al., 2002; Marshall & Lang, 2013). This included the initial development of carbonate facies (discussed in detail by Grain et al., 2013), including reef build ups identified within the study area during the Rhaetian - TR30 (Figure 5.8). Grain et al. (2013) concluded that the presence of these reef build ups and other carbonate sedimentation on the plateau during the Rhaetian - TR30 would have required the water to be no deeper than 50 m. Carbonate sedimentation declined as relative sea-level increased at the end of the Triassic (J10.0 SB) and a clastic influx occurred (Grain et al., 2013). There is no indication that the Lengenre prograde made it as far west as the area of interest to this research.

5.2.1. REGIONAL MORPHOLOGY

A significant removal and thinning of Triassic and Jurassic stratigraphy occurred in the southeast of the study area (Figures 5.3a, 5.3d, 5.5a-c, & 5.7), culminating in the sub-crop of the TR20 (Mungaroo Formation) beneath the J40.0 SB (Oxfordian Unconformity). The broad erosional feature is orientated NE-SW (Figure 5.7) and defines the Rankin Platform. This is associated with uplift of the rift flank on the edge of the Dampier Sub-basin which developed during this period. To the northwest of this erosional feature, there is a prominent NW-SE trending zone of thicker sediments (a depocentre), which form the most prominent feature of this stage of morphological evolution of the

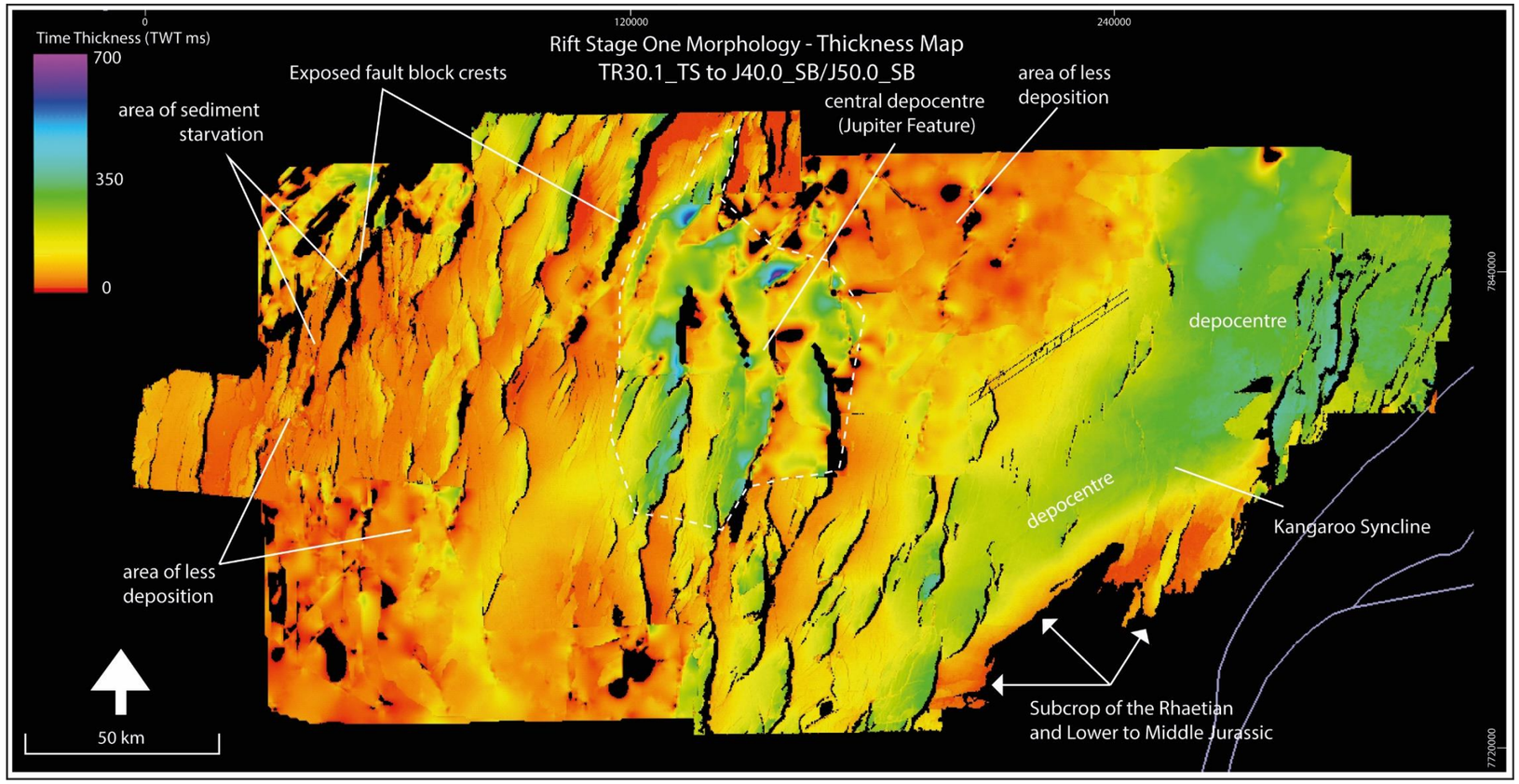

a)

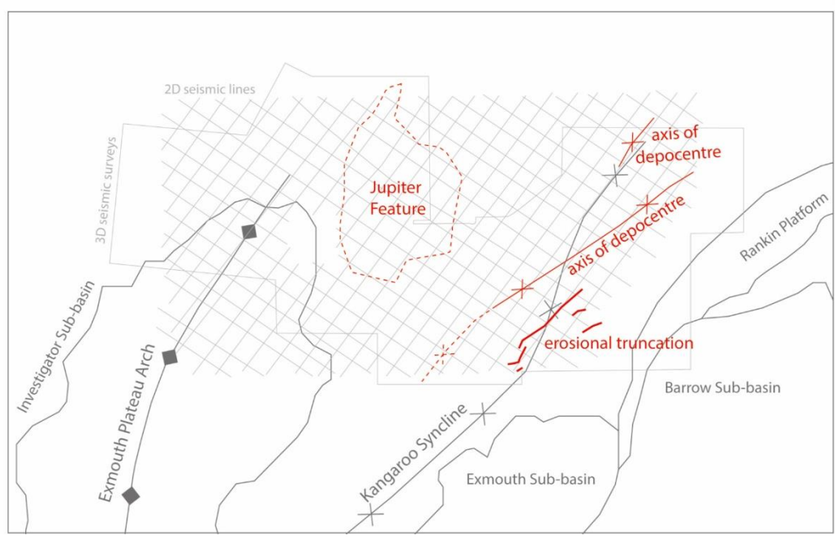

b)

Figure 5.7 a) Rift morphology map (displayed in time thickness) of the first stage of rift history, TR30.1 TS Rhaetian to J40.0 SB/J50.0 SB Middle - Upper Jurassic, b) regional structures (grey) and key features formed during the rift period (red) of the Exmouth Plateau.

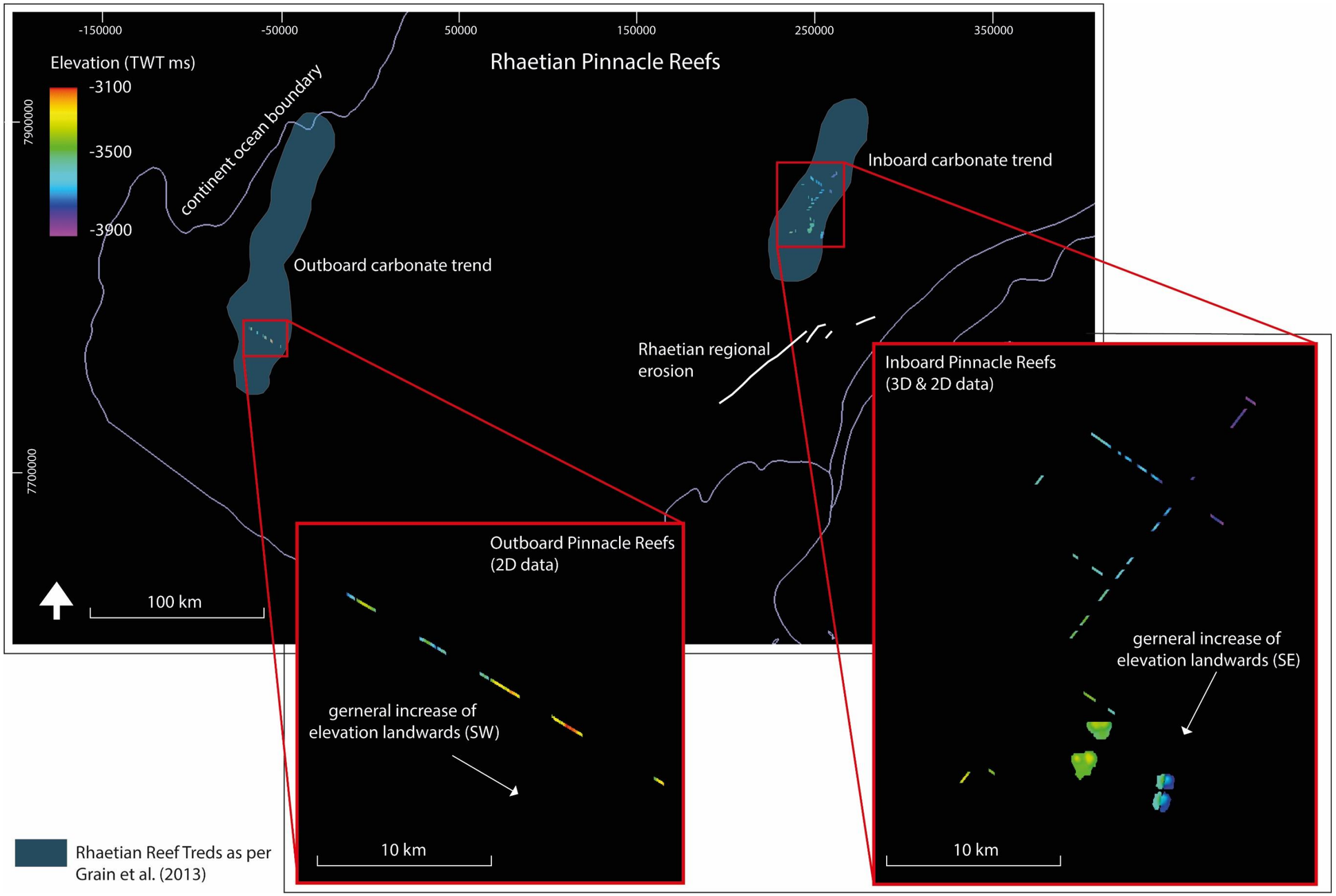

Figure 5.8 Rhaetian aged pinnacle reefs identified in this study in relation to the Rhaetian reef trends identified and described by Grain et al. (2013). Elevation of the trends are annotated on the inset maps for both the inboard and outboard trends.

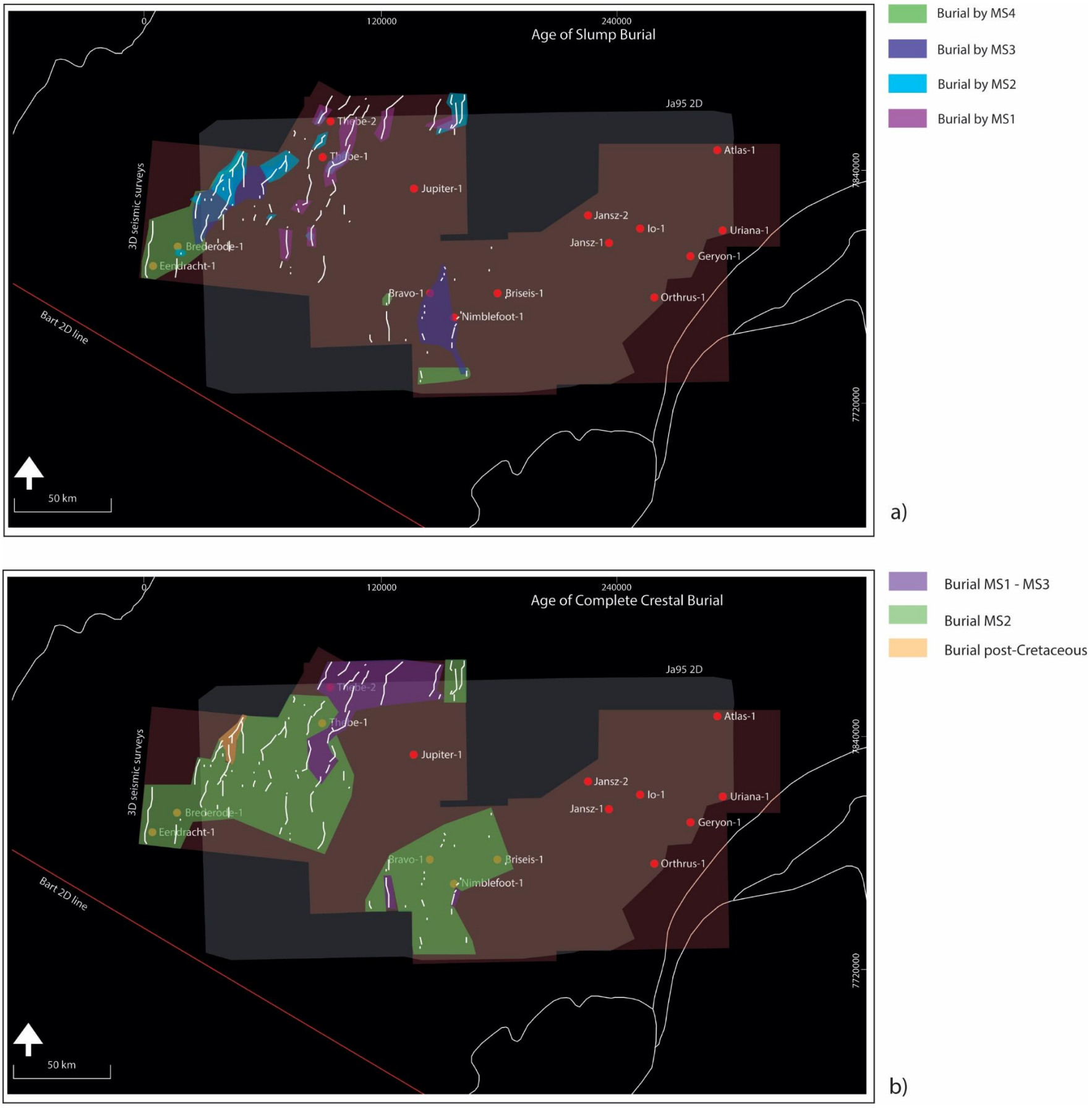

Figure 5.9 Map displaying the age of eroded crests as per the age of a) slump burial, and b) age of complete fault block crest burial.

rift (Figures 5.3a, 5.3d, 5.5a-c, & 5.7). Sedimentary packages within this feature are thicker, and the succession is more complete than in the surrounding relative highs (Figures 5.3a, & 5.7). The thickness maps of individual mega-sequences (Figure 5.5) within this feature show limited evidence of the depocentre due to the thin nature of the preserved stratigraphy in this area. However, it is more prominent during Lower and Middle Jurassic rifting than during Upper Jurassic-Lower Cretaceous rifting. This major feature corresponds to the position of the Kangaroo Syncline (Figure 5.7).

Relative to this depocentre (correlated to the Kangaroo Syncline), the elevation increases from east to west (Figure 5.7). A large area of thin sediment in the northwest of the region corresponds to an area of sediment starvation (Figure 5.7) evidenced by eroded fault block crests and onlap of sediments onto the fault blocks (Figure 5.6). Thickness maps do not represent absolute structural relief but the onlap and erosion of crests in this area implies a relative high. Sediment starvation (Figures 5.5c, & 5.7) could indicate a physical barrier to sediment supply, or limited sediment supply. The half-graben in the west of the study area were largely underfilled during this stage of rift activity (Figures 5.5a-c, & 5.7), indicating the structural features in this area formed barriers to the delivery of sediment. However, without further evidence, it is not clear how much of the thickness variation is due to uplift as opposed to sediment starvation.

During this period of time, the central area was also a depocentre (Figures 5.3a, 5.3c, & 5.7), referred to as the Jupiter Feature in this dissertation. During this early stage of rifting this feature is expressed over a series of faults which contain thicker sedimentary sequences than the surrounding relative highs (Figures 5.3a, & 5.3c). These sedimentary sequences thicken into the footwalls of the half-graben (Figures 5.3a, & 5.3c). This feature is separated from the NE-SW trending regional depocentre which correlated to the Kangaroo Syncline and appears to be controlled by the throw of the impacted faults.

5.2.2. LOCAL FAULT-RELATED MORPHOLOGY

Uplift of fault blocks during this first stage of rift development (TR30.1 TS to J40.0 SB-J50.0 SB) is relatively widespread (Chapter 5). The density of faulting across the plateau is highly varied (see Chapter 4). A larger number of faults are identified in the west and central areas while the density of faults decreases in the eastern regions. From the deformation map of the first stage of rifting (Figure 5.7) it can be observed that the most prominent footwall uplift and/or hangingwall subsidence occurred in the central area on the more northeast orientated faults.

5.2.3. DISTRIBUTION OF EROSION

The uplift of fault blocks during the initial stage of rifting resulted in the removal of material from fault block crests (Figures 3.2, 3.3, 3.6, & 5.6). These crests can be mapped extensively in the western part of the area during the initial stage of rifting (Figure 5.9). They can be mapped through both the erosional unconformity that remains on the uplifted fault block crests following the removal of material, and through the chaotic slump facies deposited adjacent to these crests (Figure 5.6) which have been interpreted as the redistribution of eroded material (Chapter 3). The material which has been removed from the eroded crests is of variable age, beginning from the pre-kinematic Mesozoic strata (Figures 5.6), and extending into the early Cretaceous, where material was removed from the earliest sections of J50-K10 (MS4) packages. These crests occur across two areas, the northwest (Mary Rose Northern Extension, Thebe, and Bonaventure seismic surveys) and the south, south-central areas (Honeycomb, Glencoe, and Ja95).

The elevation of the eroded crests relative to the Middle Jurassic Unconformity (MJU, J40.0 SB - J50.0 SB) shows that some uplifted crests remain exposed and subject to erosion at the close of the first stage of rifting (Figure 5.10). Erosion of fault block crests was initiated in the more northern area, where slump features are buried within TR30 Rhaetian aged sediments (Figures 5.6, & 5.10). Erosion then migrates to the south into the area of the Bonaventure seismic survey by the later Jurassic (Figures 5.6, 5.10). Erosion of the southern

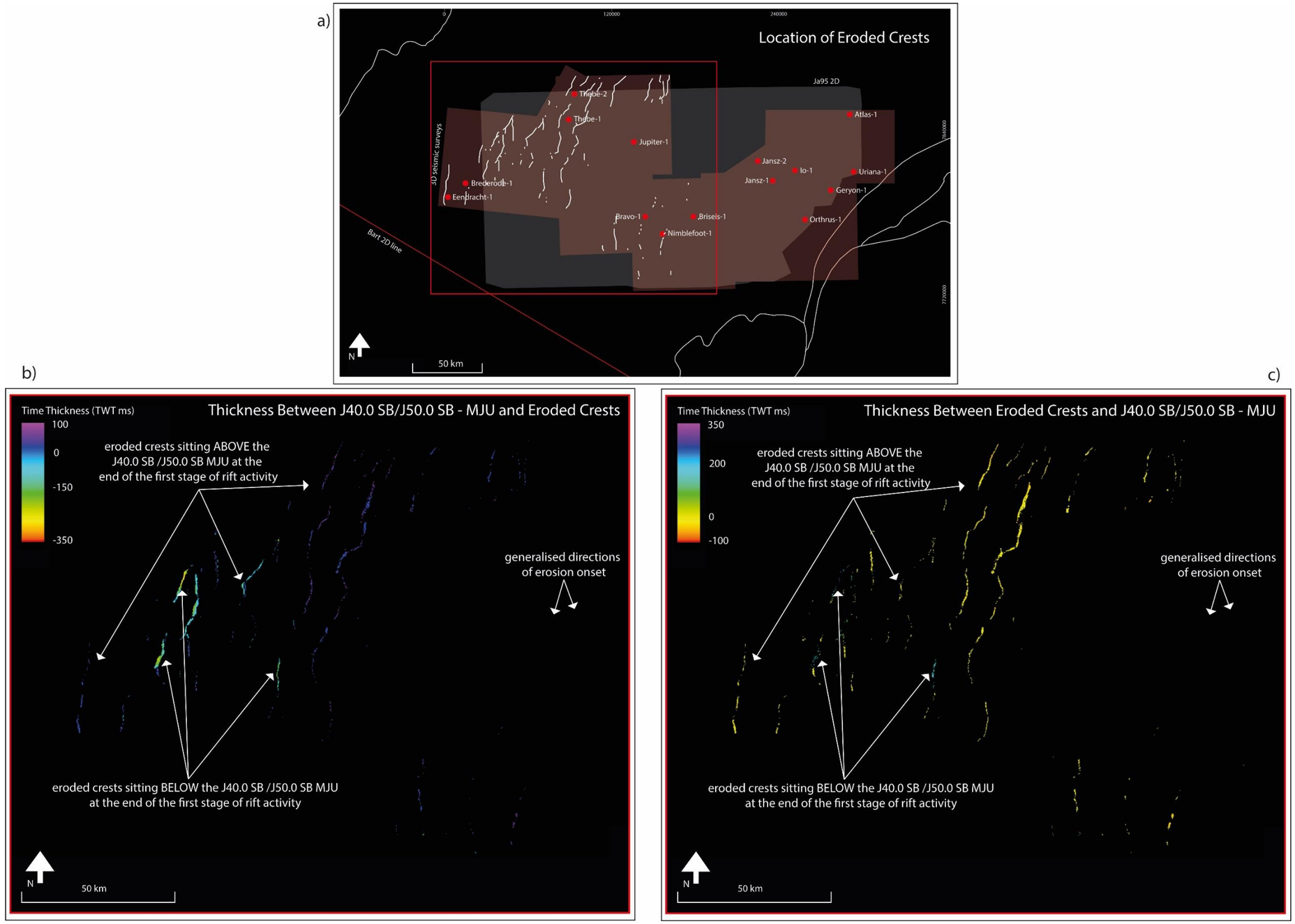

Figure 5.10 a) Location of eroded crests with the b & c) timing of burial of these crests relative to the Middle Jurassic Unconformity (J40.0 SB - J50.0 SB) as revealed by thickness maps.

crests did not begin until the later Jurassic (Figures 5.6, 5.10) and does not continue into the second stage of rifting.

A large volume of material was also eroded from the area adjacent to the Rankin Platform (Figures 5.7, 5.3a, & 5.5a-c).

5.3. Second Stage of Rift Development

The change in thickness of the late Jurassic (J40.0 SB - J50.0 SB) to early Cretaceous (K20.0 SB) sequence is shown in Figure 5.11. This represents the combination of variation in elevation, variation in sedimentary fill and preservation of stratigraphic packages during the second rift stage. This stage was dominated by sediment supply, in which large parts of the rift were filled by early Cretaceous sediment (Figures 5.3, & 5.6).

The second stage of rift activity extends from the amalgamated unconformities, here referenced as the MJU (Middle Jurassic Unconformity), representing the initiation of Argo seafloor spreading in the Middle Jurassic. The rift-related morphology of this phase of rifting has been analysed, as above, by investigating the changes in thickness between J40.0 SB-J50.0 SB (Middle Jurassic Unconformity (MJU)-Tithonian Unconformity, where the two unconformities are separate) and the K20.0 SB (Valanginian Unconformity). The environment at this time varied across the area from deep water to shallow marine (as per Bradshaw et al., 1998; Cathro & Karner, 2006; Condon, 1967b; Geoscience Australia, 2014a), filling much of the available accommodation space to the south as the shelf edge of the K10 (Lower Barrow Group) prograded northwards (Figure 5.4).

5.3.1. REGIONAL MORPHOLOGY

During the second rift stage (J40.0 SB - J50.0 SB to K20.0 SB), regional uplift and subsidence in the Uppermost Jurassic to Lowermost Cretaceous (Hocking, 1990b; Paumard et al., 2018; Rohrman, 2015; Veevers, 2006) was more significant that displacement on individual faults in controlling morphology. Observed thickness anomalies are prominent in the southwest, southeast, northwest and northeast. These changes are markedly different

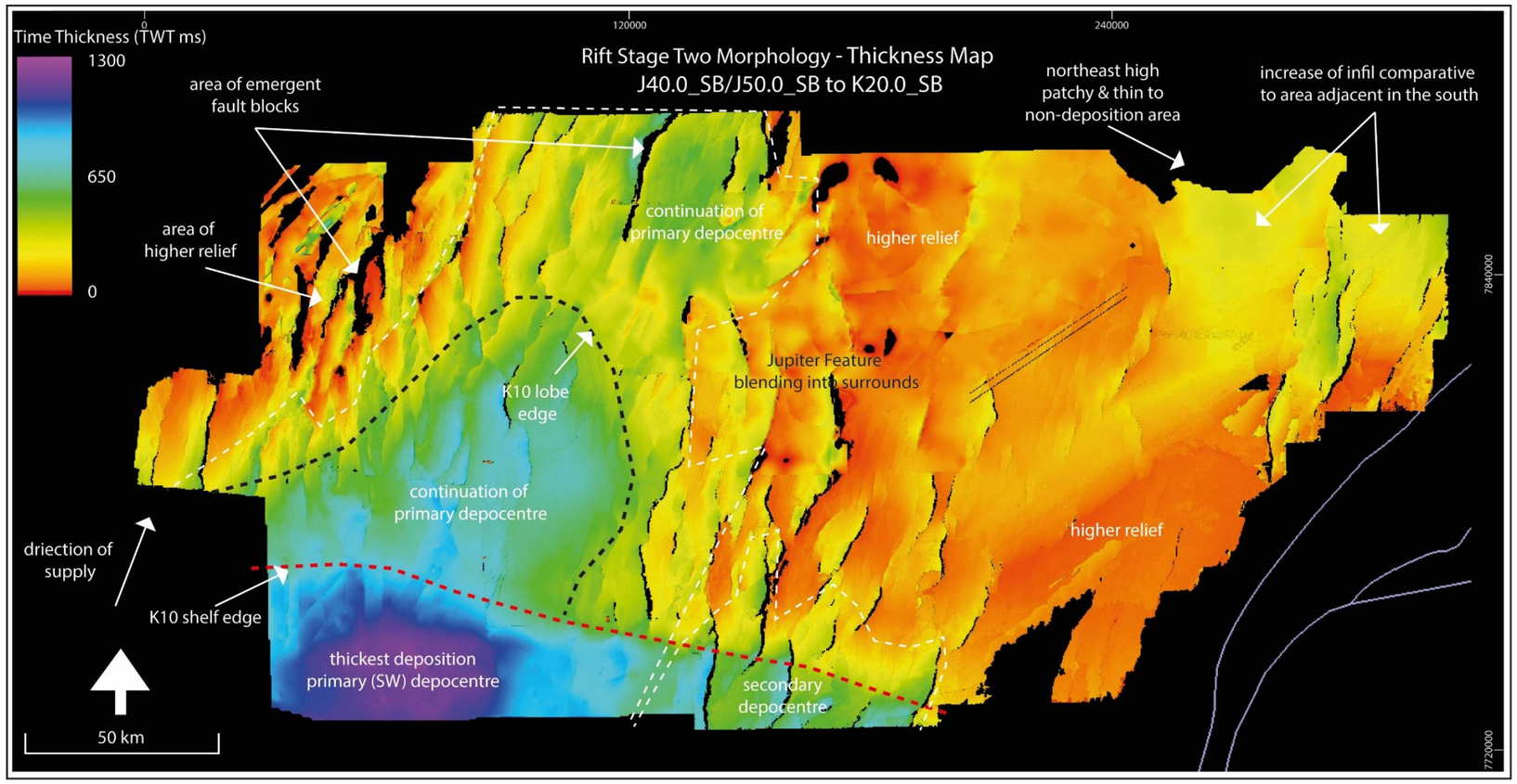

a)

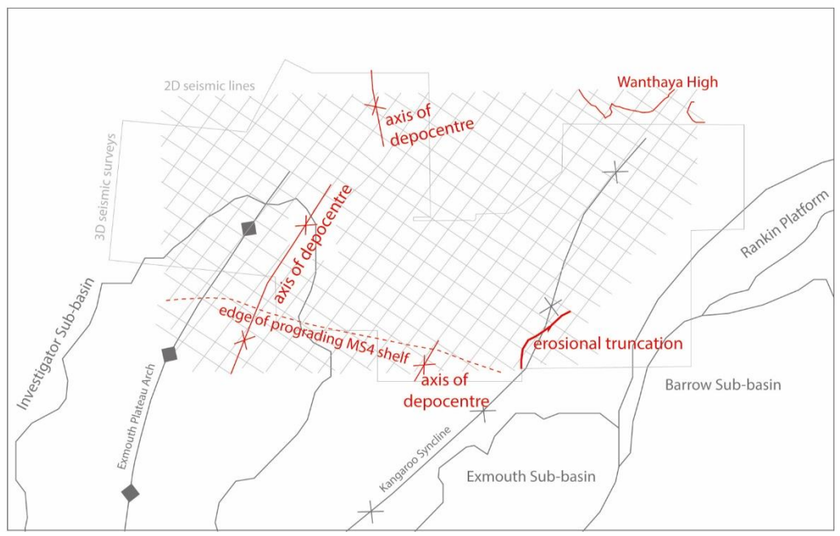

b)

Figure 5.11 a) Rift morphology map (displayed in time thickness) of the second stage of rift history, J40.0 SB/J50.0 SB Middle - Upper Jurassic to K20.0 SB Valanginian, b) regional structures (grey) and key features formed during the rift period (red) of the Exmouth Plateau.

from the morphology observed in the initial stage of rifting (Figures 3.22a-c, & 5.7). In the southeast, subsidence continues following the earlier development of a regional depocentre (Figure 5.7) though the infill here is significantly reduced compared to the fill of stage one (Figures 5.7, & 5.11). In the northwest, there is a small area displaying higher relief than the surrounding region (Figure 5.11). Higher structural relief is also observed in the centre of the study area.

The southwestern depocentre is the most prominent feature identified in this interval. It results from the progradation of the K10 (Lower Barrow Group, LBG) from the south forming a shelf edge during the latest Jurassic to earliest Cretaceous with a lobate feature extending to the north of this (Figures 3.15, & 5.11). The K10 LBG sediments infill the accommodation space to the south, while in the northwest the accommodation space is only partially filled (Figures 5.3, & 5.5d). In the west of the study area, half-graben infill (by the K10 LBG) exhibits prominent growth wedge geometry against fault planes indicating that fault activity was still ongoing (Figure 5.3). The K10 (LBG) sediments were also fed into the east of the region, but limited to no growth of the strata occurs across faults planes in this area (Figure 5.3). South of the prograding shelf edge (Figures 3.15, & 5.11) the depocentre contains thick deltaic successions. To the north of the shelf edge, well data shows that the depocentre is largely filled by gravity flow deposits. Additional K10 gravity flows are seen in the southern area adjacent to the primary depocentre, along the downthrown sections of half-graben within the broad depocentre in the area of the Glencoe seismic survey (Figure 5.11, secondary depocentre).

During this stage of rifting sediment was either not deposited or not preserved in the northeast of the area (Figure 5.11). The thin nature of preserved stratigraphic units in the northeast (Figures 5.2, & 5.5d-f) hampers the seismic interpretation. Fault activity is limited in the northeast and there is no strong evidence for fault movement (see Chapter 4) here during this second rift stage. There is no evidence that sediment supply to the area was restricted due to fault block uplift to the south of this feature. To the north of this feature

deposition is continuous but thin, and patchy (Figure 5.11), indicating a relative high with limited deposition.

The supply of K10 (LBG) sediment into the far northwest was restricted by an area of prominent structural relief (Figure 5.11). Fault blocks remain emergent along a NE-SW structural trend (Figures 5.5d-f, & 5.11). It formed significant structural relief in the Lower to Middle Jurassic and remained a prominent feature as a result of continued fault movement in this part of the Exmouth Plateau. In the central region, the Jupiter Feature sits higher than the surrounding regions (Figure 5.11). This feature is less prominent during the second stage of rifting following reactivation of fault activity, seemingly blending into the surrounding structural relief (Figure 5.11). This has resulted from the reduction of fault activity to the east and increased supply to infill available accommodation space.

5.3.2. DISTRIBUTION OF EROSION

As with the first stage of rift induced uplift, the second stage of rift activity resulted in the uplift and erosion of fault blocks (Figure 5.6). It is inferred that the same erosional processes which altered the architecture of fault blocks in the initial rift stage continued into the second rift stage. However, due to burial of some of these eroded fault blocks their distribution is less extensive compared to the early rift stage (Figures 5.9, & 5.12) and they are now restricted to in the northwest of the study area (Figures 5.9, & 5.12; Mary Rose Northern Extension, Thebe, and Bonaventure seismic surveys).

The pattern is confirmed by the elevation of the eroded crests relative to the K40.0 SB (top Muderong Shale) datum (Figure 5.12). This shows that greater elevation occurred in the northern region, specifically the northwest, than in the south (Figure 5.12). This is consistent with the observation of slump facies in the north which indicate that erosion and reposition of eroded material continued into the earliest Cretaceous (Figures 5.9, & 5.12) while there is no indication of continued exposure and erosion in the south.

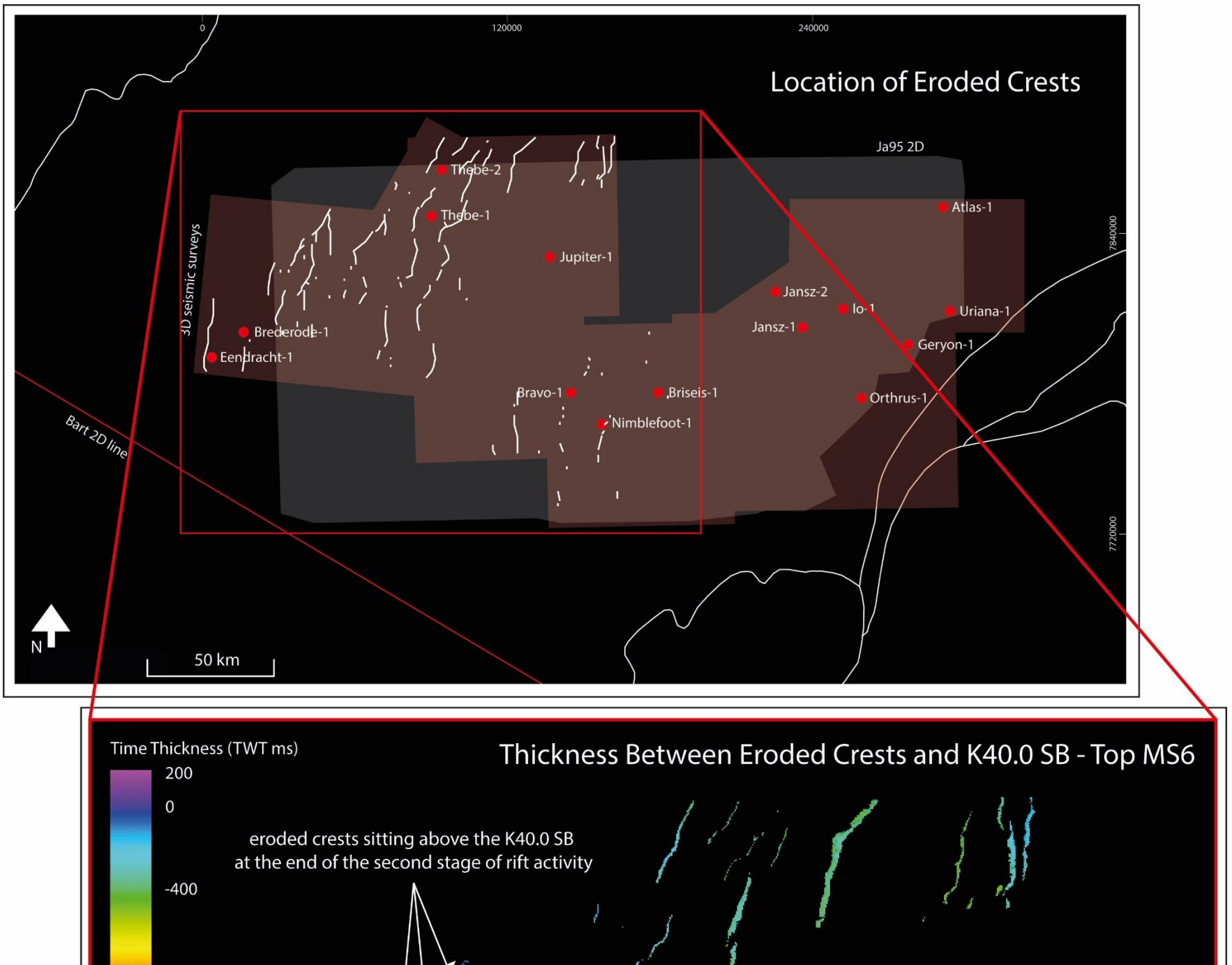

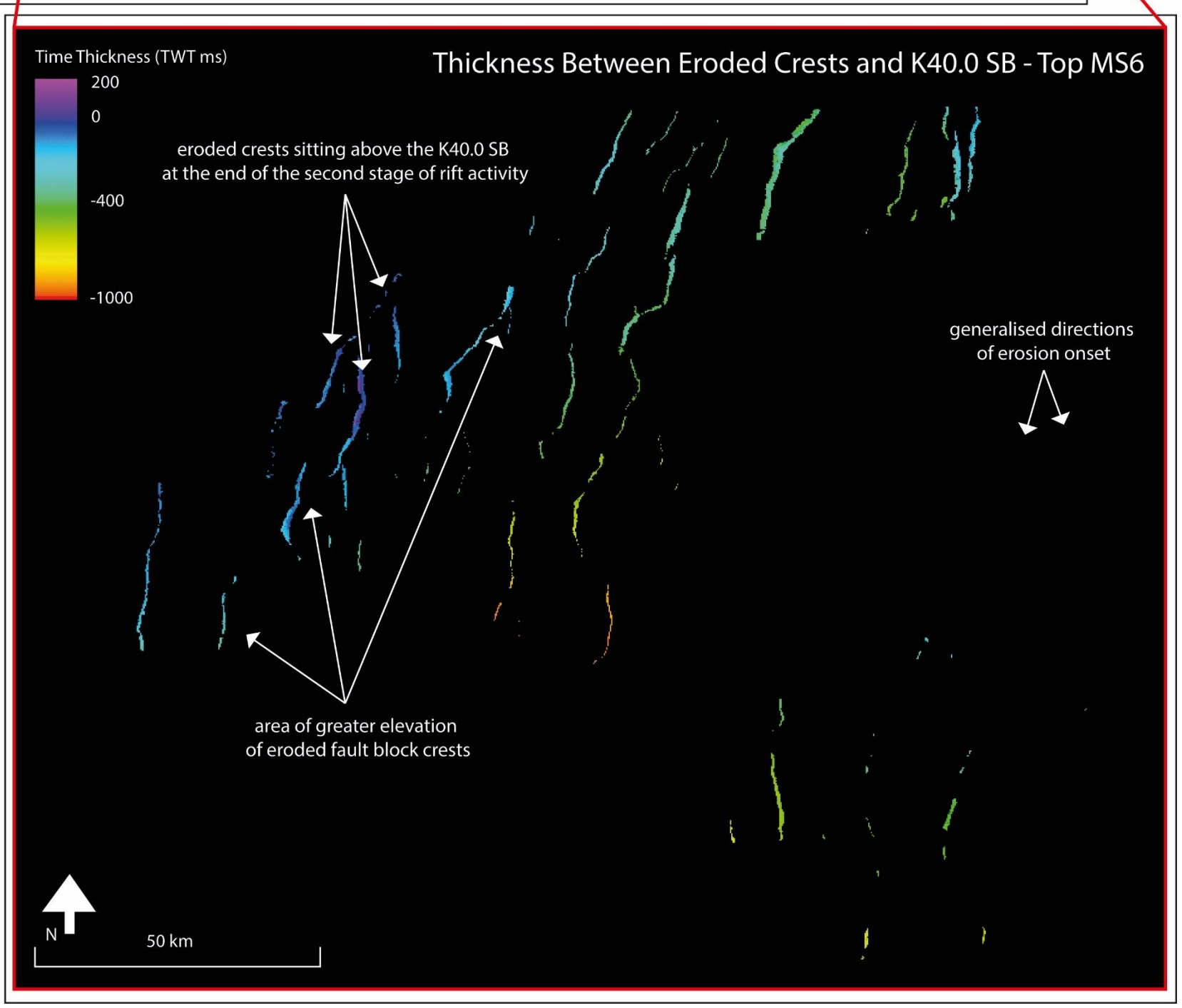

Figure 5.12 Map displaying the thickness between eroded crests observed on 3D seismic surveys and the end rift activity, K40.0 SB (top MS6, Muderong Shale). Where thickness displayed in negative numbers are eroded crests which were buried by the end of the deposition of the K30 Muderong Shale.

5.4. Post-Rift Stage

5.4.1. EARLY POST-RIFT

The variation in thickness of the Valanginian to the middle Aptian (K20.0 SB – 40.0 SB) sequence is expressed in the maps of the post-rift interval (Figures 5.13, & 5.14). Due to the complex seismic stratigraphy in the later Cretaceous there is no single horizon which would suitably represent a paleohorizontal surface. For this reason, the maps were split to more accurately display changes in the post-rift successions.

In the first map (Figure 5.13) the thickness of the K20 and K30 intervals are displayed. The base of K20 (K20.0 SB) clearly shows the Barrow shelf edge and is thus not a paleohorizontal surface, but the uppermost sediments/strata of the K30 (K40.0 SB) is a reasonable datum, having been deposited broadly and as a relatively horizontal surface.

5.4.1.1. REGIONAL MORPHOLOGY

Most changes to the topography of the studied area after the Valanginian separation event (K20.0 SB) are of regional scale. A prominent feature at this time is the continued formation of a sizeable depocentre in the southeast (Figure 5.13). This feature continued into the Upper Cretaceous, as subsidence continued following the K20.0 SB Valanginian breakup event. Stratigraphic thickness is greater in this region, with stratigraphic features such as downlap, onlap and the formation of growth packages indicating this area sat at a lower elevation than the surrounding relative highs (Figures 5.2, & 5.3a).

The earliest K20 deposition (MS5, Upper Barrow Group) was deposited directly over the K10 (LBG) in the south of the studied region (Figure 5.4). The K10 (LBG) shelf edge is observed in the image displaying the early K20 Upper Barrow Group (UBG) (Figure 5.4). The K10 (LBG) shelf edge is preserved as the younger sequence is thin on top of it, but then thickens to fill the accommodation space in front of it (Figure 5.4). The Upper Barrow Group also

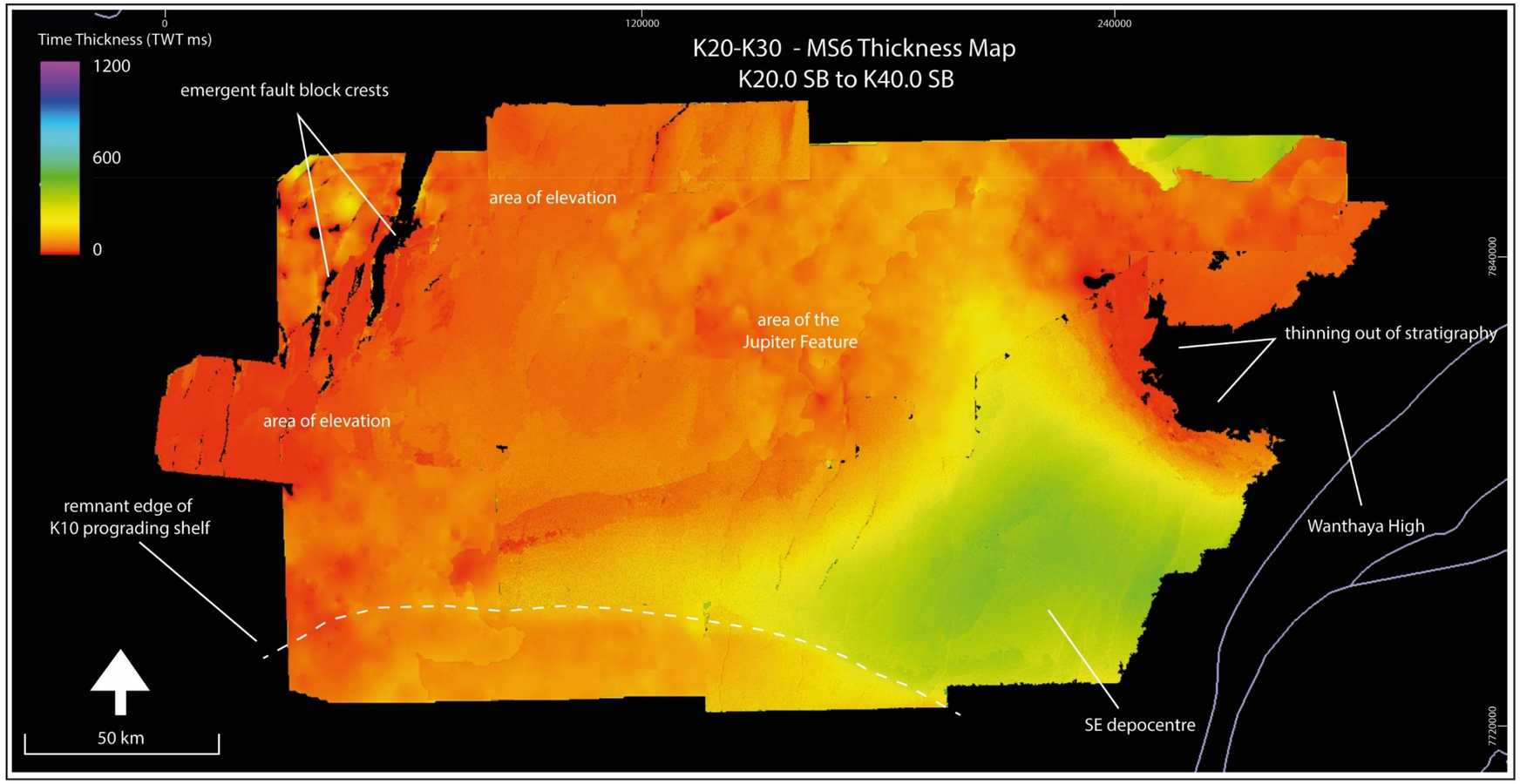

a)

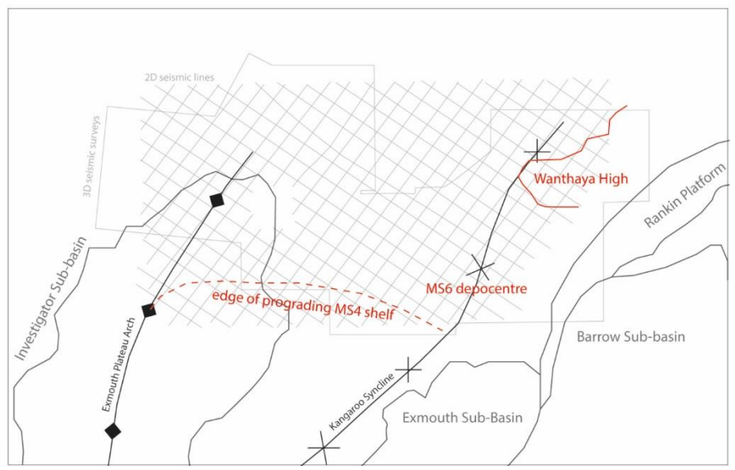

b)

Figure 5.13 Early post-rift maps of the Exmouth Plateau. The thickness map a) shows the preserved depositional history of the area studied with the key features annotated. Line map b) shows the major regional features and the key features ot the area srudied between the K20.0 SB and the K40.0 SB.

largely infilled the remnant bathymetry created by half-graben structures (Figures 5.3, & 5.6).

The northeast high continues to develop after the K20.0 SB Valanginian event, with strata thinning out and not being deposited (Figure 5.13). There is no indication that this feature is fault controlled, however stratigraphic evidence for the nature of this feature is limited. Downlapping reflectors can be identified in the K20-K30 (MS6) packages (Figure 5.2) surrounding it. Several angles of downlap are identified (Figure 5.2) in the packages which overlie the T10.0 SB (top Cretaceous), indicating that the area was likely experiencing a change in relief, or a change in the direction of sediment supply during this time. Some truncation has also been identified K20-K30 (MS6) packages (Figure 5.2).

The west of the study area was elevated at this time (Figure 5.13). There are no clear indications of this high representing the Exmouth Plateau Arch as it is more regional in extent. The relative high starts to the southwest and continues northeast to finish to the east of the central study area (Figure 5.13). All of the area to the north and west of this SW-NE feature are significantly topographically higher than the broad synclinal depression of the southeast (Figure 5.13). The combination of the previously underfilled half-graben and still active faults limited the accumulation of sediment in this area (i.e., Figure 5.6g), though the number of emergent fault blocks had reduced by this time.

The Jupiter Feature is indistinguishable from this broad north-northwestern high following the K20.0 SB Valanginian event (Figure 5.13). In cross-section (Figures 5.3a, & 5.3c) the MS5 K20 (UBG) was deposited in the previously underfilled half-graben and infilled them. The K20-K30 (Muderong Shale) then thins over the feature (Figure 5.13), indicating the area was now bathymetrically higher than the surrounding areas when the marine shale was being deposited.

5.4.1.2. LOCAL FAULT-RELATED MORPHOLOGY

In a few locations to the north and northwest, faults continue to experience movement even after the K20.0 SB Valanginian break-up event (Figure 4.13). This is seen where stratigraphy of this age is draped over the fault planes and

some minor thickening occurs. All of these faults are NNE-SSW orientated. In the northwest not all areas which are dominated by the underfilling of half-graben display evidence of continued fault activity and are interpreted to be the infilling of remnant bathymetry.

5.4.2. LATE POST-RIFT

Following deposition of the K20-K30 (Muderong Shale), two maps display sediment distribution on the subsiding passive margin between K40.0 SB and K42.0 SB in the Cretaceous (Figure 5.14a) and between K40.0 SB and T10.0 SB (Figure 5.14c). The two sequences were separated due to the complex seismic stratigraphy following the Aptian events. Care must still be taken when making inferences from these maps.

5.4.2.1. REGIONAL MORPHOLOGY

The variation in elevation during the Lower Cretaceous continues into the Upper Cretaceous as seen in the sequential maps (Figure 5.14). In the post-rift packages the broad area of limited sedimentation that dominated the western areas during the initial post rift period continues into the later Cretaceous (Figure 5.14c).

Most changes to the bathymetry and topography of the study area after the K40.0 SB Aptian unconformity are of regional scale. The most prominent of these features is the continued formation of the depocentre in the southeast (Figure 5.14). In the post-rift, this depocentre forms an ‘L’ shape around the area to the northeast where strata thin out (Figure 5.14a). The depocentre is abutted to the west by another area of limited sediment deposition (Figure 5.14a).

The northeast high (see Section 5.4.1 Early Post-Rift for initial indications of feature) continues to develop into the Aptian, with strata thinning out and not being deposited (Figure 5.14a). Some deposition does begin to extend back over this feature at this time, where deposition and preservation resulted in patchy deposition of Aptian aged stratigraphy (Figures 5.2, & 5.14a). No indication of fault-controlled movement occurs at this time. Further analysis

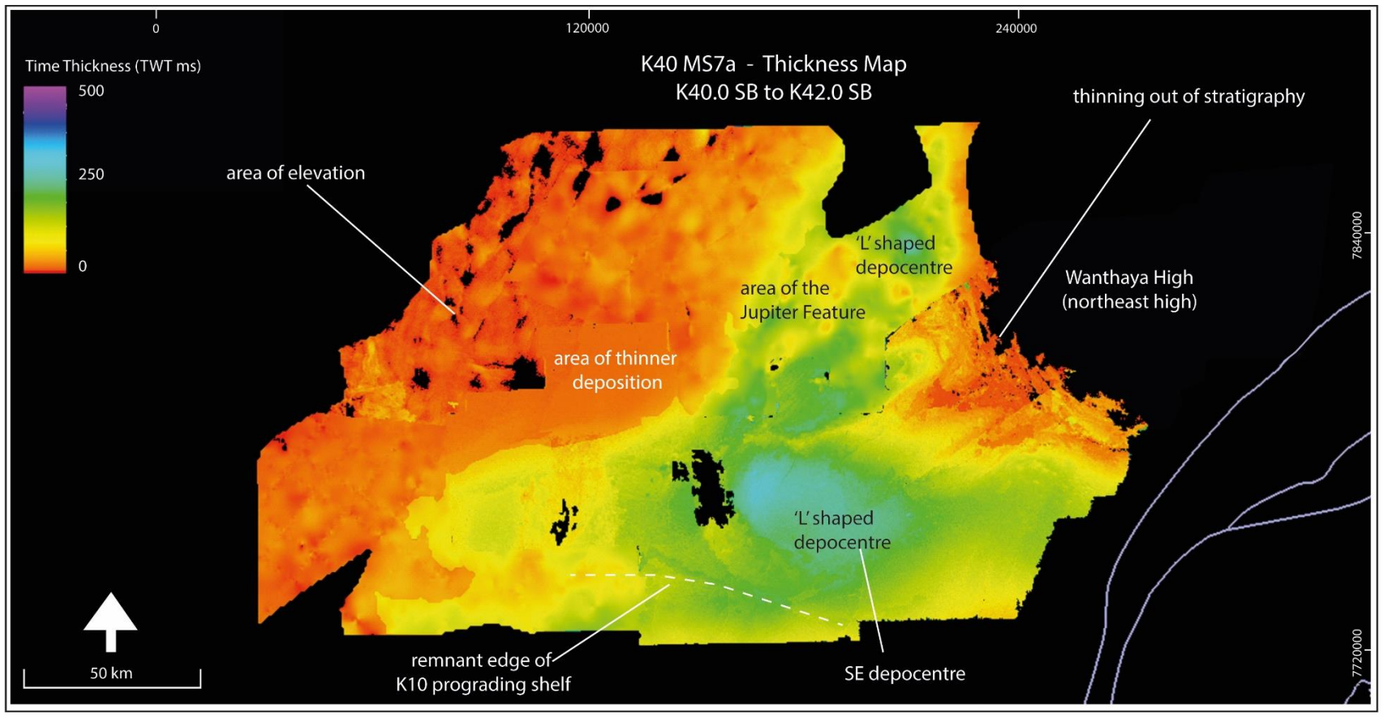
0
120000
240000
Time Thickness (TWT ms)
500
250
0
K40 MS7a - Thickness Map
K40.0 SB to K42.0 SB
thinning out of stratigraphy
area of elevation
'L' shaped
depocentre
area of the
Jupiter Feature
Wanthaya High
(northeast high)
area of thinner
deposition
'L' shaped
depocentre
7840000
7720000
50 km
remnant edge of
K10 prograding shelf
SE depocentre

a)

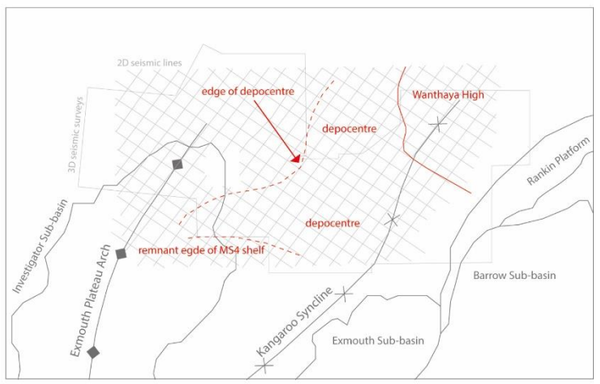
2D seismic lines
3D seismic surveys
edge of depocentre
depocentre
Wanthaya High
Rankin Platform
depocentre
remnant egde of MS4 shelf
Investigator Sub-basin
Exmouth Plateau Arch
Barrow Sub-basin
Kangaroo Syncline
Exmouth Sub-basin

b)

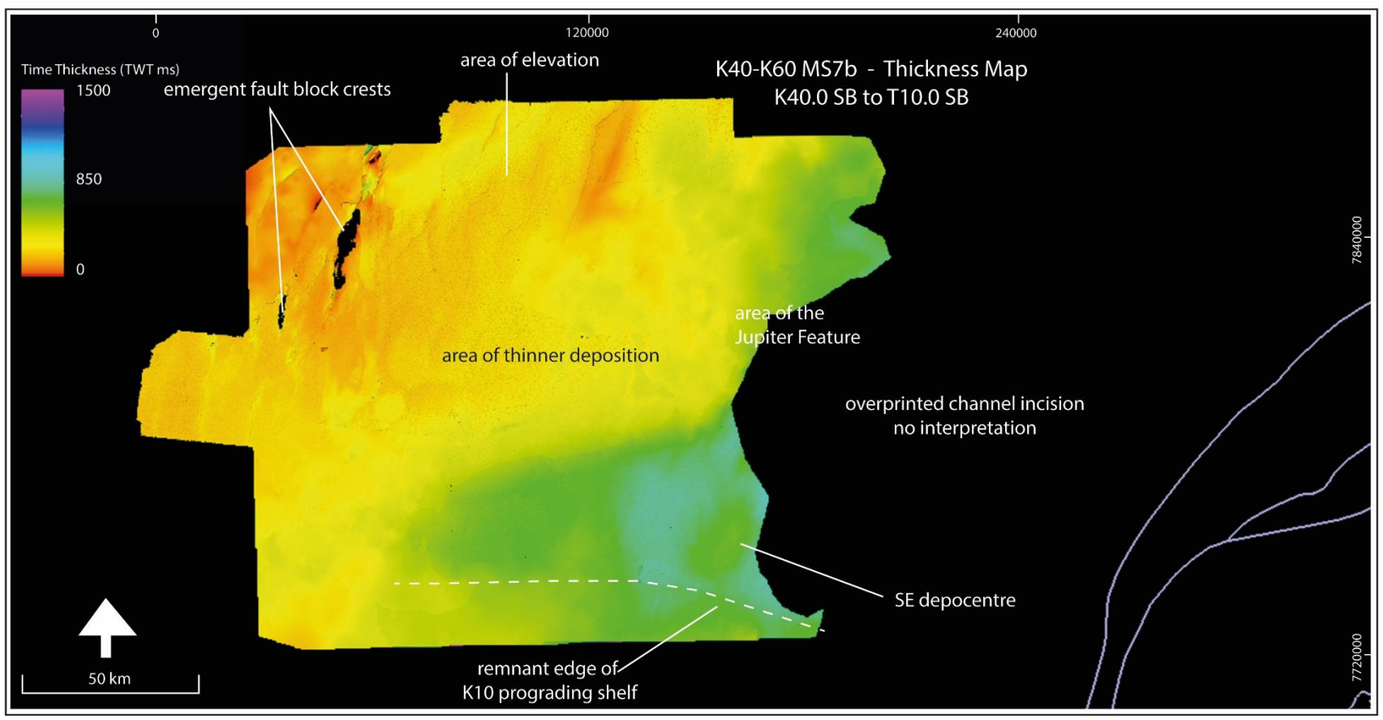
0
120000
240000
Time Thickness (TWT ms)
1500
850
0
area of elevation
emergent fault block crests
K40-K60 MS7b - Thickness Map
K40.0 SB to T10.0 SB
area of the
Jupiter Feature
area of thinner deposition
overprinted channel incision
no interpretation
7840000
7720000
SE depocentre
50 km
remnant edge of
K10 prograding shelf

c)

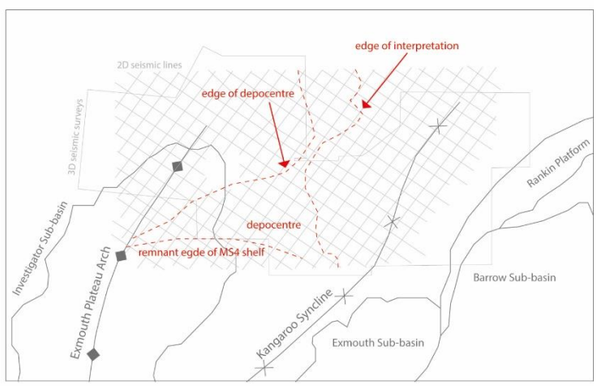
edge of interpretation
2D seismic lines
edge of depocentre
3D seismic surveys
Rankin Platform
depocentre
remnant egde of MS4 shelf
Investigator Sub-basin
Exmouth Plateau Arch
Barrow Sub-basin
Kangaroo Syncline
Exmouth Sub-basin

d)

Figure 5.14 Post-rift thickness maps of the a) MS7a, from the K40.0 SB to K42.0 SB and line map b). The c) K40.0 SB to T10.0 SB history and accompanying line map d).

On previous page

was conducted to determine the origin of this feature. In the areas available for analysis, it appears to be continuous with the depocentre to its south and west, except the sedimentary sequences thin significantly (Figures 5.2, 5.5g-h, & 5.14a). More detailed summary on this feature is available in Section 5.5.2 Wanthaya High.

Initial observations identified sedimentary packages to be thickening away from or thinning towards this feature (Figures 5.2, & 5.14a). This change in the thickness of sedimentary packages is observed to the west and south of the high (Figures 5.2, & 5.14a). This is a pattern that is replicated in the overlying later Cretaceous to Holocene (as identified in Jansz-1) strata (Figures 5.2, & 5.14a). The early Cretaceous strata which thin towards this feature display a series of angular downlap patterns (Figures 5.2). These downlap features occur across a variety of angles (Figures 5.2), to both the south and west of the feature. In addition, some truncation was also observed in the early Cretaceous strata (Figures 5.2), implying tilting and erosion. The overlaying stratigraphy is complex due to abundant channel and valley incisions (see Winata et al., 2021) but parts of the sequence contain undisturbed and clearly imaged uniform reflectors that dip steeply (Figures 5.2). The uniform and parallel nature of these reflectors imply a low angle of deposition. A selected reflector in this post-Cretaceous package was mapped as far as possible on the surrounding 3D seismic surveys (Figures 5.2) and extrapolated to extend the interpretation across the eroded part of the sequence. This reflector is unable to be given further context in terms of age due to its location from wells and its presence within the overlaying complex strata. As it falls outside of the Mesozoic it is effectively out-of-scope for this study, and as such is termed “the or a Cenozoic surface”. When flattened, this suggests that the underlying sequences did thin on to a high and that the present-day elevation is a result

of latter tilting (Figures 5.2). In addition, the observed downlaps become onlaps against a feature of bathymetric relief (Figures 5.2).

The persistent pattern of thinning (Figures 5.2, & 5.5) indicates the presence of a longer-lived feature. The high has been observed in this study to be a consistent feature since the Upper Jurassic, straddling several phases of rift-related basin development. The persistence of this feature over time, in conjunction with the presence of truncation and the evidence of later tilting provide strong evidence that this feature is of bathymetric origin and not likely to be the product of depositional processes.

The elevated western extent of the study area continued to be sediment starved (Figures 5.3, 5.5, & 5.14). The relative high starts to the southwest and continues on a broad diagonal trend to finish to the east of the central study area (Figure 5.14). All of the area to the north and west of this diagonal feature is significantly topographically higher than the broad synclinal depression of the southeast (Figure 5.14).

5.4.3. DISTRIBUTION OF EROSION

Although there are exposed fault block crests in the post-rift stage, there is no evidence of continued erosion of these features observed on seismic data. Widespread erosion of sediment from the topographical highs was possible but no strong indications for this has been observed in the thinly preserved stratigraphic sequences.

The relative elevation of uplifted fault block crests displays limited change between the end of the rifting (Section 5.3; Figure 5.12) and the end of the Cretaceous (Figures 5.15 & 5.16). Complete burial of the crests not achieved by this time, but the remaining exposed crests are located in the northwest only (Figure 4.13). Unlike the previous stage (Section 5.3) the elevation of all eroded crests are aligned in a landward regional tilting of the Exmouth Plateau (Figure 5.16).

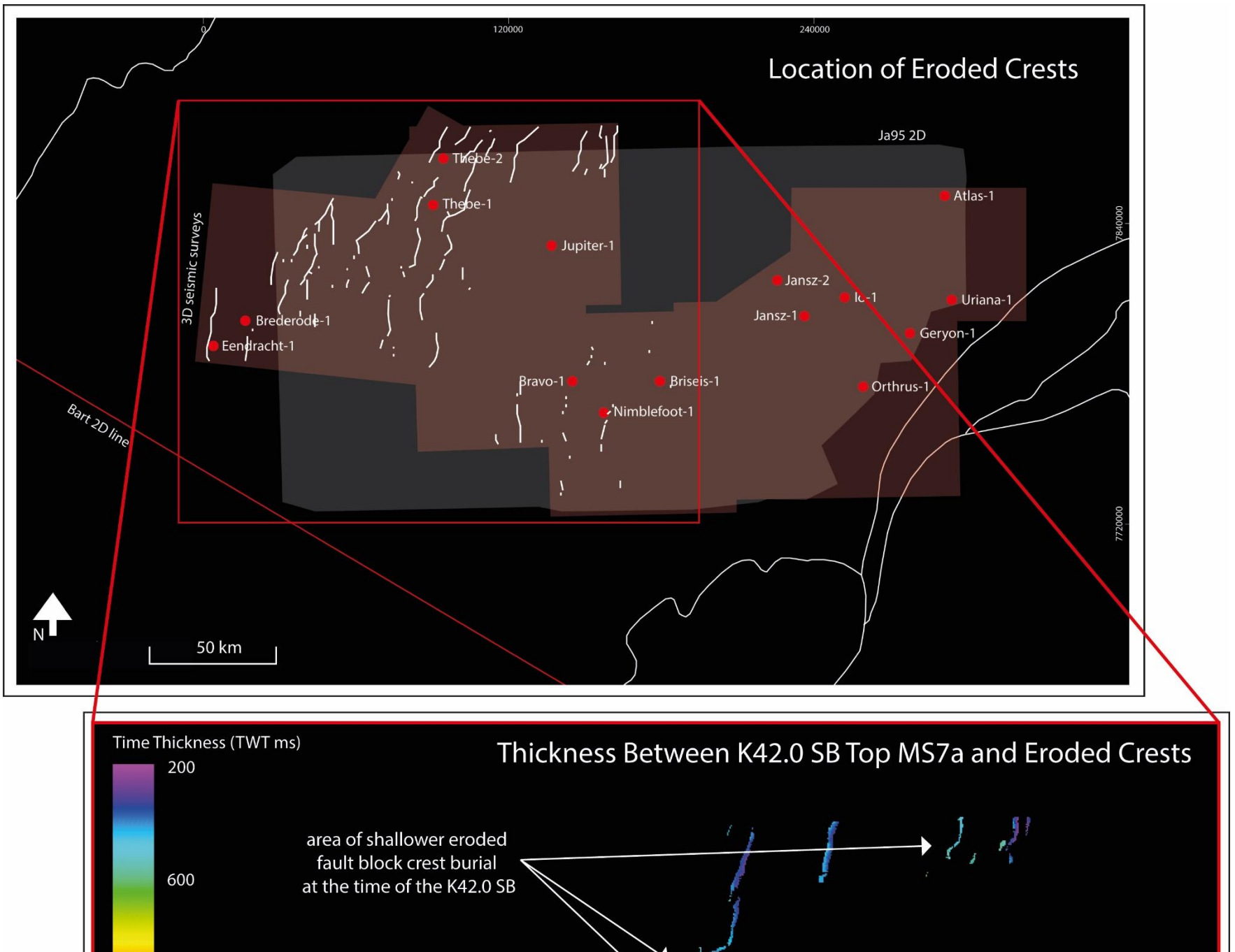

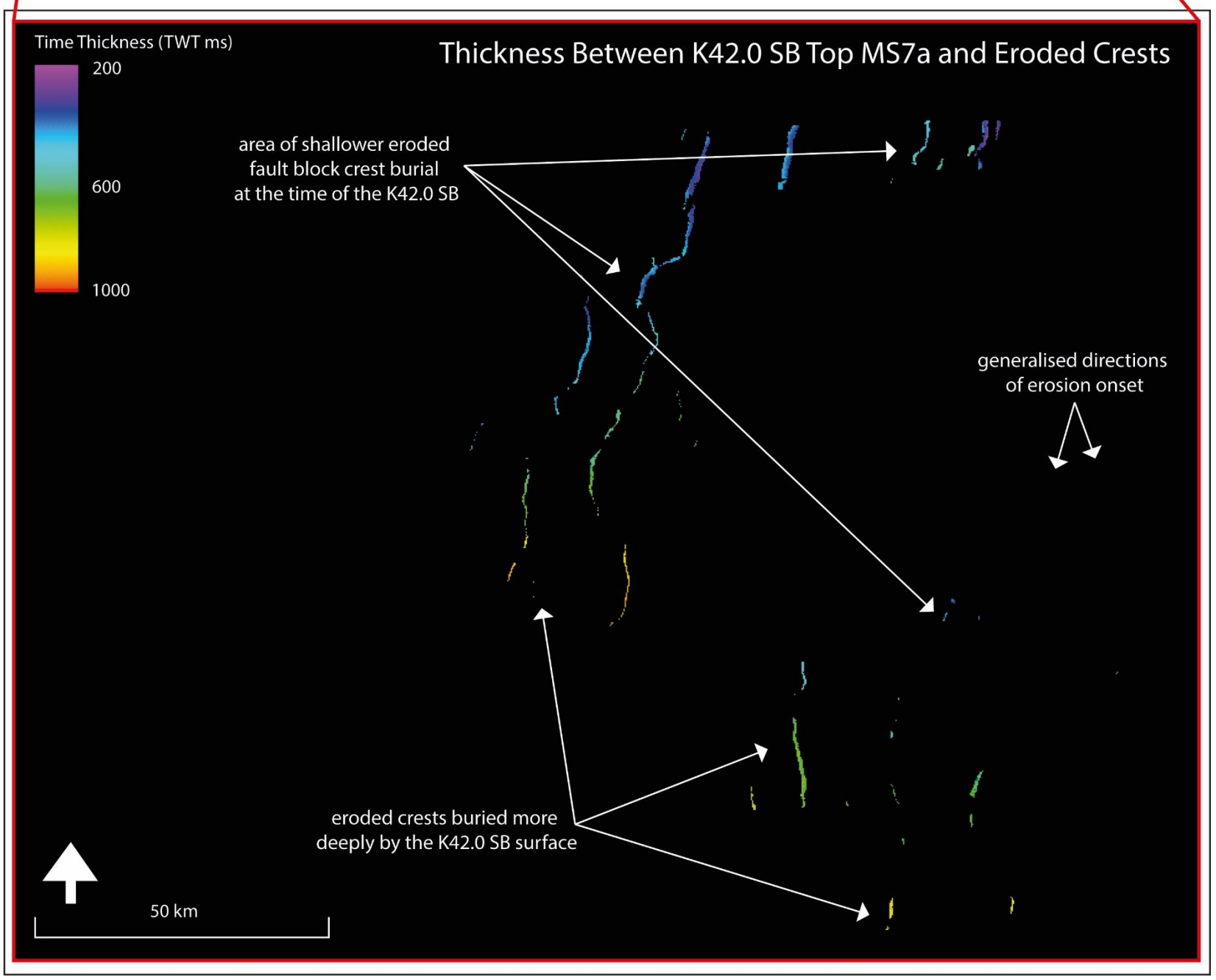

Figure 5.15 Map displaying the thickness between eroded crests observed on 3D seismic surveys and the after the of rift activity, K42.0 SB (top MS7a), intra-Aptian.

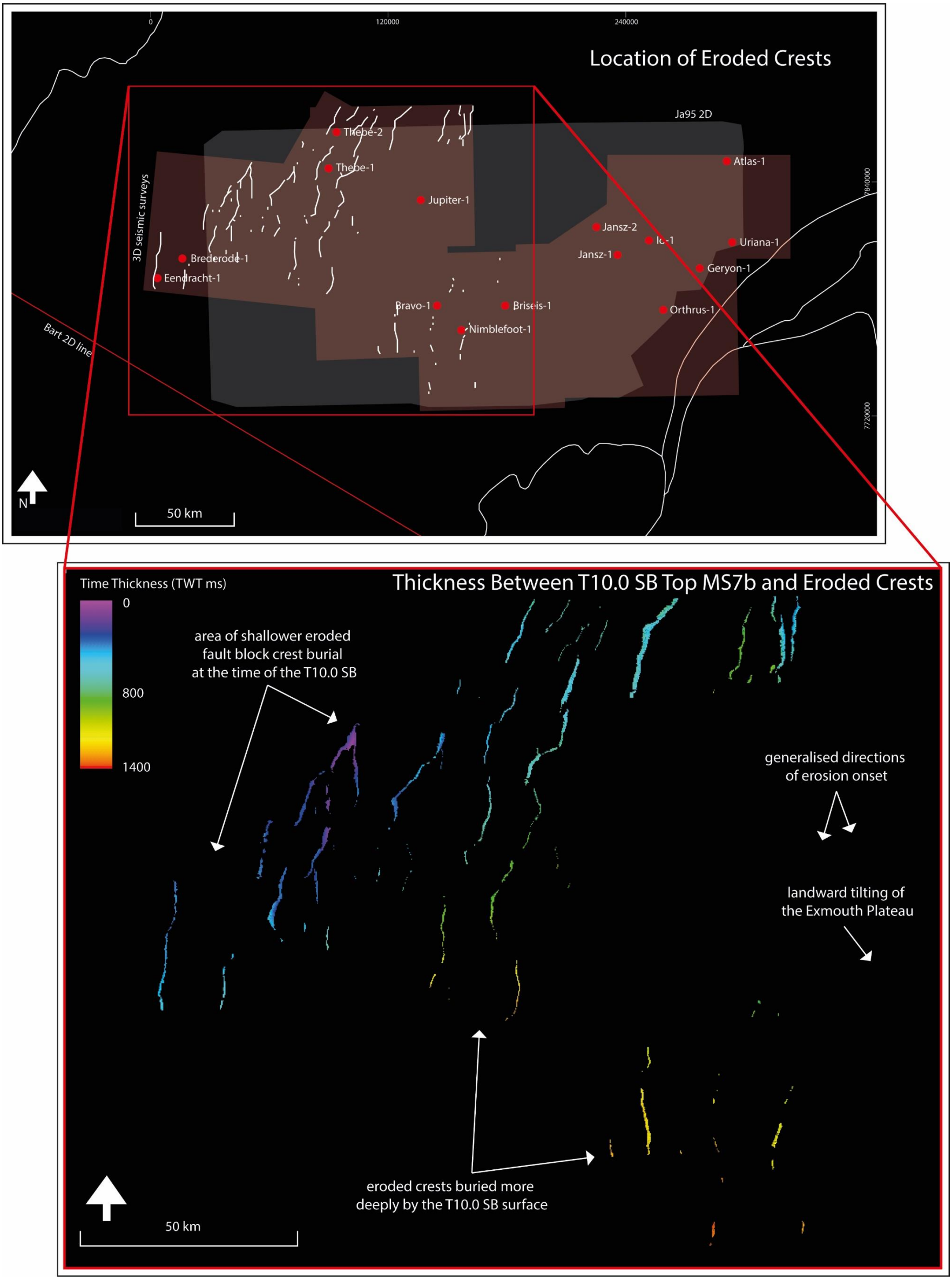

Figure 5.16Map displaying the thickness between eroded crests observed on 3D seismic surveys and the end rift activity, T10.0 SB (top MS7b). Where thickness displayed as 0 are eroded crests which were buried after the end of the deposition of the Maastrichtian (T10.0 SB).

5.5. Morphological Evolution of The Rift

In the first stage of rift formation there is uplift of individual fault blocks and removal of material from them by erosion (Figure 3.22). The uplift of fault blocks during this time is main component of bathymetric variation and the supply of sediments to the region is limited. Rift flank uplift from the Dampier Sub-basin resulted in the removal of large volumes of sedimentary packages in the southeast (Figures 5.7, 5.3a, 5.3c, & 5.5a-c). The second rift stage is dominated by the incursion of sediment from the south (Figure 3.22). Erosion of fault blocks continues to occur into the early Cretaceous. In the post-rift stage major bathymetric changes occur in relation to the broad depocentre in the southeast and the persistence of an expansive high extending across the northwest (Figures 5.13, & 5.14).

5.5.1. SOUTHEASTERN DEPOCENTRE - THE KANGAROO SYNCLINE

The formation of a broad depression containing thicker and more complete packages of sedimentary sequences occurred in the Upper Triassic between later uplifted flank of the Dampier Sub-basin and the area of elevated fault blocks to the NW (Figures 5.5a-c, & 5.7). The feature is prominent throughout the Jurassic as an elongate depocentre with a northeast-southwest orientation, corresponding to the Kangaroo Syncline in the first stage of rifting (Figure 5.5a-c, & 5.7). It remains the location of continued deposition in the post-rift interval, with a different orientation to the original feature (Figure 5.5d-h). This change in orientation occurs with the emergence of the northeast relative high (Figures 5.2, & 5.7).

5.5.2. NORTHEAST HIGH - THE WANTHAYA HIGH

The relative high in the northeast is evident from the Upper Jurassic through the Cretaceous (Figures 5.2, 5.5, & 5.11). The persistence of this feature over several rift intervals, despite changes in sediment regime, indicates it is likely a bathymetric high and not an area of sediment starvation. This is substantiated by the observation that deposition occurs around this feature

during the second stage of rifting and in the early post-rift, indicating that sediment supply to this site is restricted (Figures 5.2, 5.5, & 5.11). As no evidence of uplifted fault blocks correspond to this zone of thin stratigraphy, which could act as barrier to sediment supply, it is reasonable to conclude that the area was higher than the surrounding regions during these rift stages. The third piece of compelling evidence for this feature being bathymetrically higher is the presence of angular unconformities in the surrounding areas which show truncation surfaces within the sequences surrounding the feature (Figures 5.2, & 5.5), which are accompanied by downlapping reflectors of various angles. The combination of these observations indicate that this feature was higher than the surrounding sediments during the later Cretaceous. A fourth piece of supporting evidence for a high is the overlying Cenozoic strata of uniform and shallow dipping reflectors, which imply later tilting on a regional scale. When the later tilt is removed (flattening of the Cenozoic strata) the observed downlap become onlap against a relief feature (Figure 5.2). This feature will be referred to as the Wanthaya High for the remainder of this dissertation. Wanthaya is Thalanyji for welcome or hello – Thalanyji are the Indigenous or Aboriginal Peoples of the land and sea in the Exmouth Region.

5.5.3. JUPITER FEATURE

The Jupiter Feature initially started out as a depocentre in the first stage of rift development as faults in the area were active during deposition creating half-graben filled with sedimentary packages (Figures 5.3a, & 5.3c). The later K10 - earliest K20 (Barrow Group) infilled all of these features and the area was uplifted, relative to the surrounding regions during the early Cretaceous deposition of the K20 - K30 Muderong Shale (Figures 5.3a, & 5.3c). This uplift is evidenced by the onlap of the Muderong Shale onto the early K20 Upper Barrow sediments (Figures 5.3c).

5.5.4. EXMOUTH PLATEAU ARCH & DEPOCENTRE

The presence of the depocentre formed by the K10 (LBG) during the Lower Cretaceous corresponds to the location of the Exmouth Plateau Arch, a prominent bathymetric feature at the present day (Figure 5.11). However, as

this is an area of subsidence, with limited bathymetric expression, it is clear that the Exmouth Plateau Arch did not exist at this time. There is no observation to indicate any feature which could correlate to the arch during the Triassic or Jurassic (Figures 5.7 & 5.11) although the thickness of preserved stratigraphy, particularly during the Jurassic (Figures 5.3a-b, & 5.5) may impact on the identification of any larger scale features in the western areas of the study. There is no evidence of this feature having formed in the Cretaceous intervals. These observations indicate that the Exmouth Plateau Arch formed later than the Cretaceous, doming the existing stratigraphy (Figure 3.4a). A more relevant name for the area during the Mesozoic would be the Exmouth Plateau Depocentre.

5.5.5. REGIONAL EROSION

The broad scale of erosion in the southeast (from rift-flank uplift) removed large volumes of material from this area, eroding down to the pre-kinematic strata (Figures 5.3a, & 5.5a-c). This occurred near the end of the Oxfordian (J47.0 SB) and it is possible that erosion removed evidence for the relative elevation of the area during the Upper Triassic and Lower to Middle Jurassic. Sediment supply into the plateau was also likely impacted by this. As supply was delivered into the Exmouth Plateau during this time from the east (Adamson et al., 2013; Chen, 2018) any significant uplift along a supply pathway would have impacted the transport (Watts, 2001) into the plateau. This alteration to supply pathways could have resulted in the dispersal of sediments to the south (Dampier Sub-basin) or to the north (onto the Exmouth Plateau) rather than in the previous westerly direction.

The removal of material from uplifted fault block crests yields information about the palaeo environment and of later modification to the elevation of the plateau. Crestal erosion began in the TR30 Rhaetian (Figure 5.9). As the formation of pinnacle reefs at this time indicate a relatively shallow marine environment (≤50 m; Grain et al., 2013), it is likely that the crests of fault blocks were sub-aerially exposed, given that fault displacements are of greater magnitude (Chapter 4). Following the TR30 Rhaetian, the erosion of fault block crests can

no longer be associated to with subaerial erosion as the environment during this time was deep marine. The eroded fault blocks show variable elevation relative to the K20 - K30 Muderong shale (Figure 5.12), so it is unlikely that they represent erosion by wave action. It is most likely that they are a result of submarine mass wasting processes (Barrett et al., 2021; Bilal et al., 2018).

The diachronous nature of erosion occurring on the uplifted fault block crests displays the Mesozoic tilting of the Exmouth Plateau. The later occurring post-rift tilting to the elevation of eroded fault block crests occurred following the main stage of rifting, indicating landward tilting of the Exmouth Plateau occurred, both before and after the continental break-up events (Figures 5.12, & 5.7).

6. Tectono-Stratigraphic Evolution of The Exmouth Plateau

The following chapter is a synthesis of the observations presented and discussed in previous chapters. These observations seek to tie together the deformation history, uplift history and sediment patterns to determine sedimentary response to rifting of the NWS as it pertains to the Exmouth Plateau.

6.1. Synthesis Of Tectono-Stratigraphic Evolution of The Exmouth Plateau

6.1.1. PRE-KINEMATIC STAGE OF MESOZOIC RIFT DEVELOPMENT

There is no evidence of fault activity on the Exmouth Plateau during the bulk of the Triassic (Figure 6.1). During this period a phase of subsidence continued following the older Permo-Carboniferous rifting (Chapter 3; Section 3.1). This stage of subsidence meets the post-rift subsidence of the earlier Permo-Carboniferous rift activity as the rift cools (see Boillot, 1979; Grasemann & Stuwe, 2011; Manatschal et al., 2021), and as a pre-rift thermal response (i.e., Falvey, 1974; Kearey et al., 2009) to rift activity for the Mesozoic rifting. The only modification to the Triassic pre-rift sequences is the subsequent removal of material by erosion during the regionally significant Middle Jurassic uplift of the Dampier rift flank and the removal of material from individual uplifted fault block crests (Chapter 5; Figure 6.2) and post-depositional fault emplacement (Chapter 4).

6.1.2. FIRST STAGE OF MESOZOIC RIFT DEVELOPMENT

Growth wedges first occur in the west of the plateau in the Rhaetian and indicate that extension began at this time (Figure 6.3; Chapter 3; Section 3.2). Sequences in the east of the study area first display angular downlap and onlap as part of growth wedge formation against hangingwalls during the early

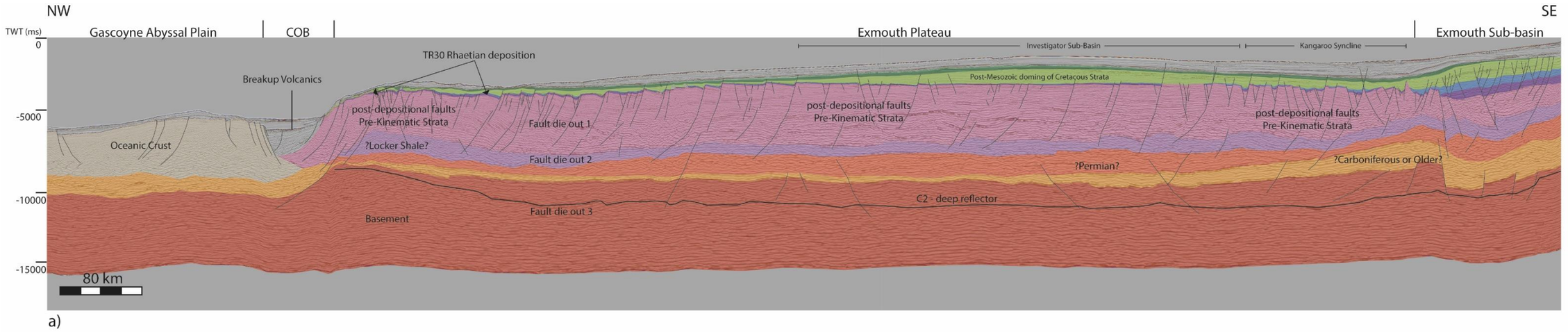

a)

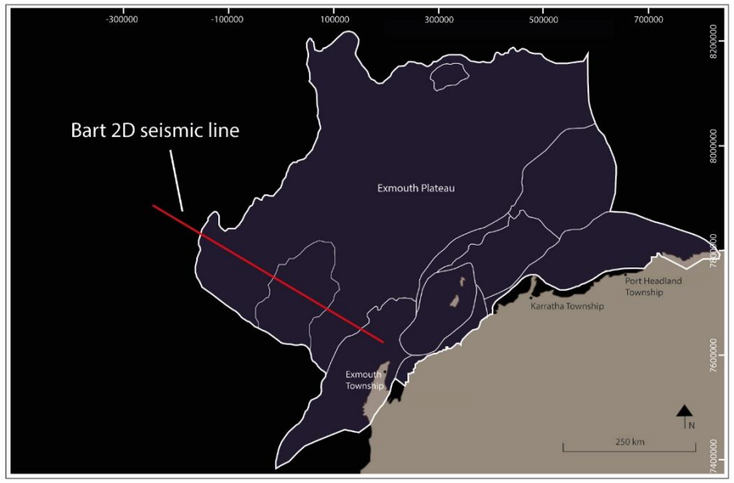

b)

- Aptian - Maastrictichan
- Berriasian - Aptian
- Jurassic
- Rhaetian
- Middle-Latest Triassic
- ?Lower Triassic
- ?Permian
- ?Carboniferous and Older
- Basement
- Oceanic Crust

Figure 6.1 Interpreted Bart 2D seismic line, transecting the Exmouth Plateau, displaying broad mega-sequence deposition as per this study. Limited deposition on the outer margin following the onset of Mesozoic rift activity, post-depositional doming forming the Exmouth Plateau Arch, fault termination depths, and the C2 reflector as interpreted by AGSO North West Shelf Study Group (1994), Gartrell (2000), and Mutter & Larson (1989) are highlighted on this seismic cross-section.

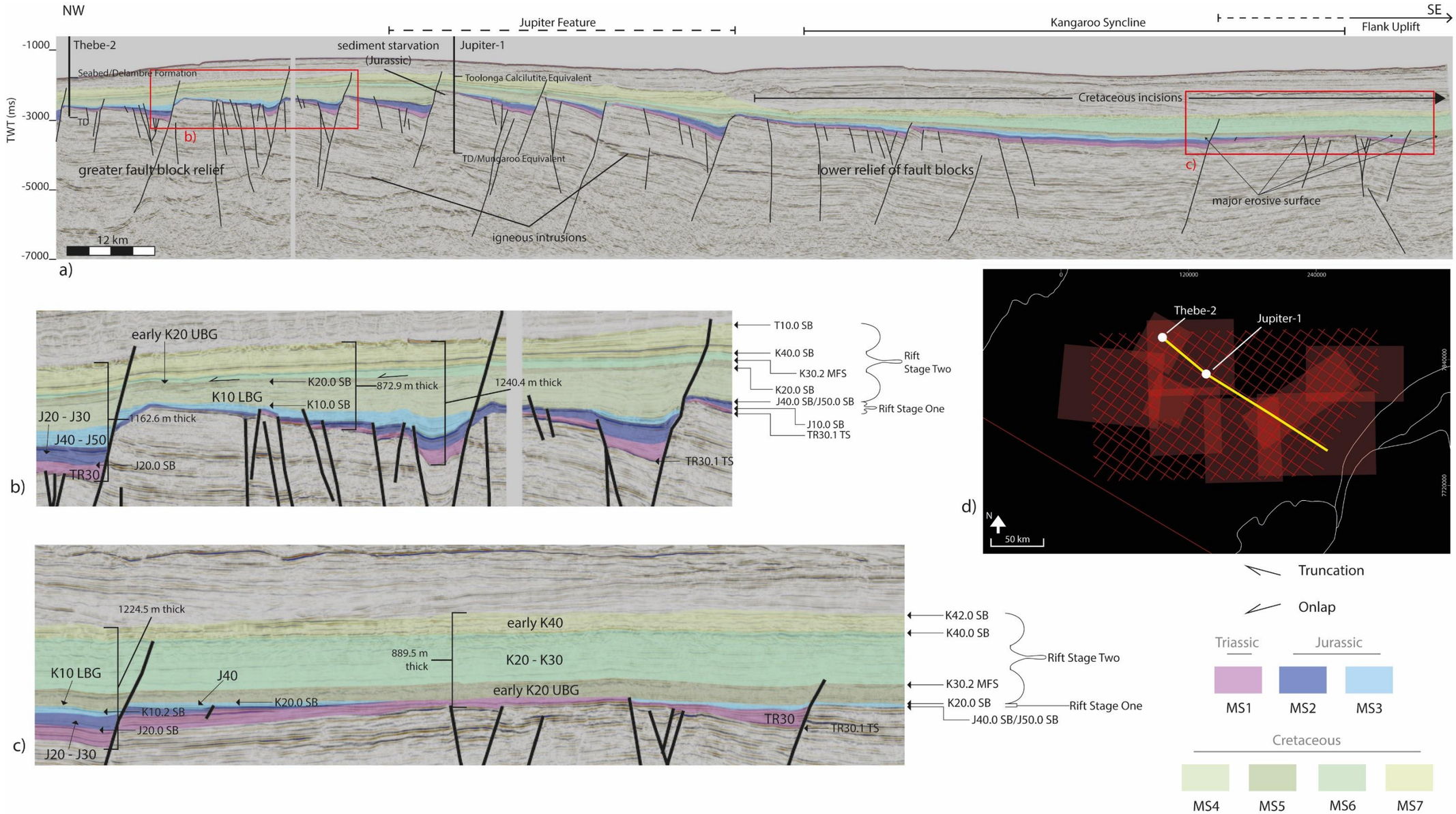

Figure 6.2 Regional cross-section through the study area displaying the mega-sequences as per this study. Cross-section a) showing the differences in structural architecture between the west and eastern plateau. The erosion of fault block crests is, and timing indicators are captured in figure b) and the thinning of depositional packages over rotated fault blocks is shown in Figure c). The location of Figures b) and c) are highlighted on Figure a), the location of Figure a) is shown on the map (d), as are the two wells displayed in section a).

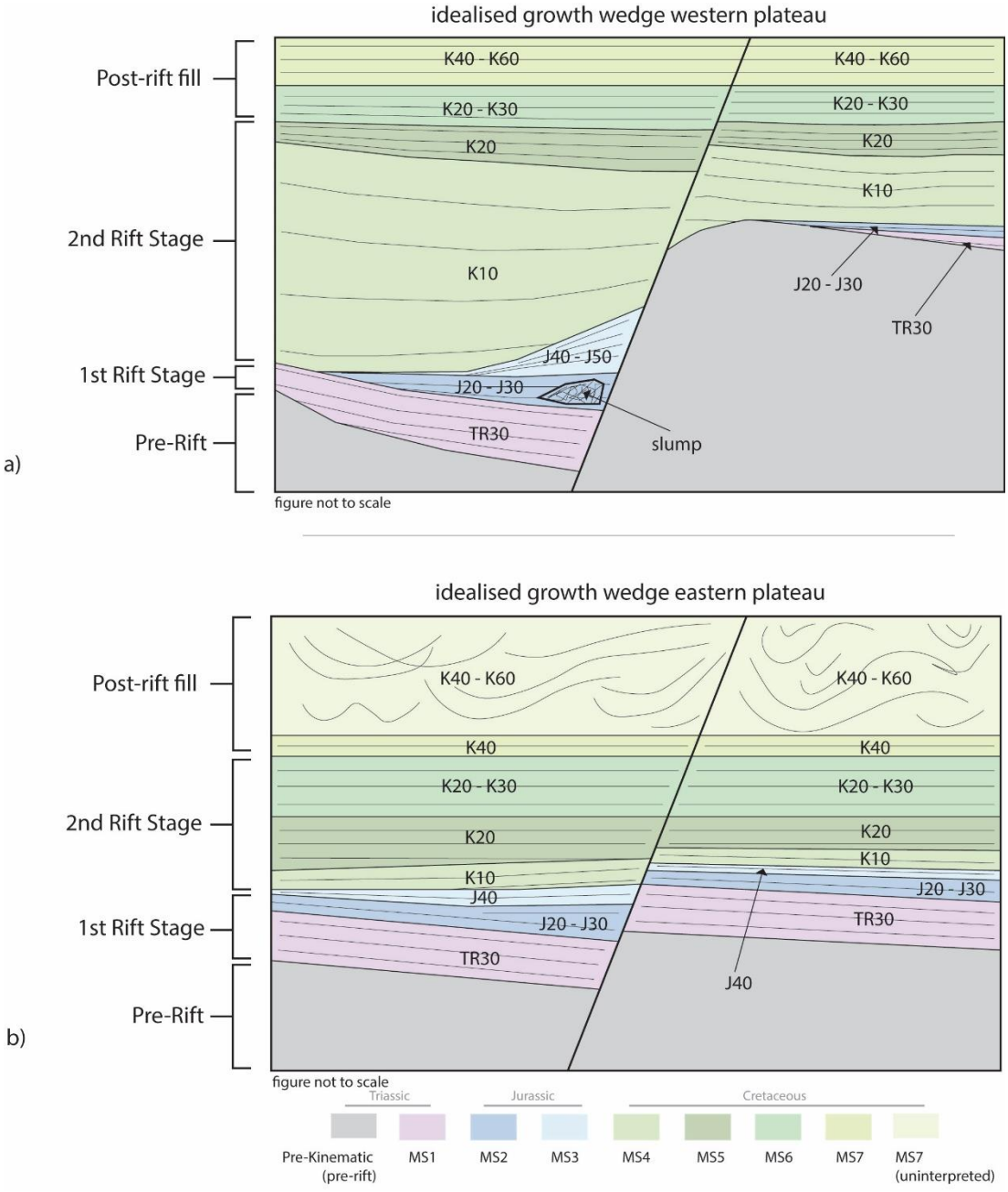

Figure 6.3 Idealised growth wedges of the studied area, showing the a) prominent expression of growth wedge formation in the western region and b) the more limited growth wedge formation typical of the eastern region.

Jurassic (Figure 6.3). The later initiation of growth wedge formation highlights the variability in the timing of the onset of rifting across the plateau (Figure 6.4). This separation in the start of activity also corresponds to differences in the elevation of the plateau at this time (Chapter 5; Section 5.2), with elevation greatest where fault activity is most prominent in the north and west of the area study area and limited to the east (Figure 6.5).

The plateau formed a mixed carbonate and clastic shelf during the Rhaetian (see Grain et al., 2013), but deposition quickly transitioned to a deeper marine environment in the Jurassic (Chapter 3; Section 3.3). The preserved Jurassic sequences are comparably thin (Chapter 3 & 5), mainly where the elevation was greater, in the west. The regional unconformities are thus difficult to distinguish in this part of the Plateau. The most complete sedimentary packages from this period are located within the NE trending Kangaroo Syncline (Figure 6.2). Further complicating the depositional record of the area is the later removal of large volumes of material. This material was removed and recycled from the uplifted crests of fault blocks in the regions of greater relief (Figure 6.2; Chapter 5). Erosion also took place in the southeast, where the uplift of the Dampier rift-flank resulted in the widespread removal of the pre-Oxfordian (J40.0 SB) Mesozoic strata (Figures 6.2, & 6.4; Chapter 5; Section 5.2).

6.1.3. SECOND STAGE OF MESOZOIC RIFT DEVELOPMENT

Movement along faults continues across the region into the Upper Jurassic and Lower Cretaceous (Figures 6.2, & 6.3). This continuation of fault activity contributed to the sediment starvation in the northwest, where ongoing fault activity (Chapter 4; Section 4.2.3) combined with relative bathymetric relief (Chapter 5; Section 5.3) resulted in limited supply to this area (Figures 6.4, & 6.5). In the Lower Cretaceous fault activity was most dominant along NE-SW and NW-SE trends in the western part of the plateau. The removal of material from uplifted fault block crests continued into the early Cretaceous, but this was limited to the more northwestern regions (Figures 6.2, & 6.4; Chapter 5; Section 5.3). The continuing fault activity was not as widespread during the

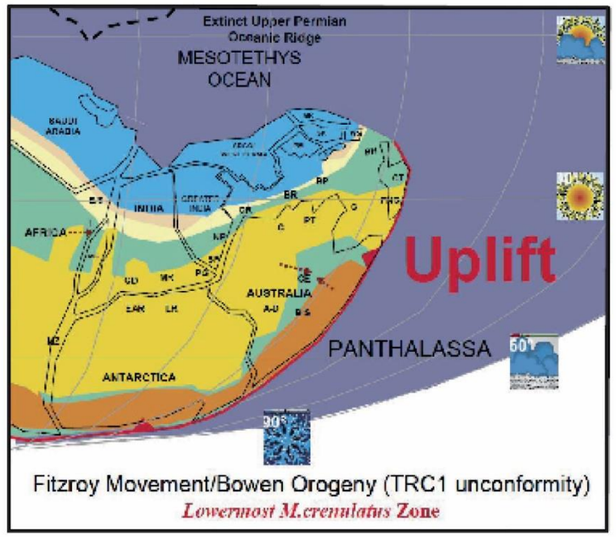

a) Middle Triassic (TR10 Carnian) Pre-Mesozoic rift plate tectonic reconstruction.

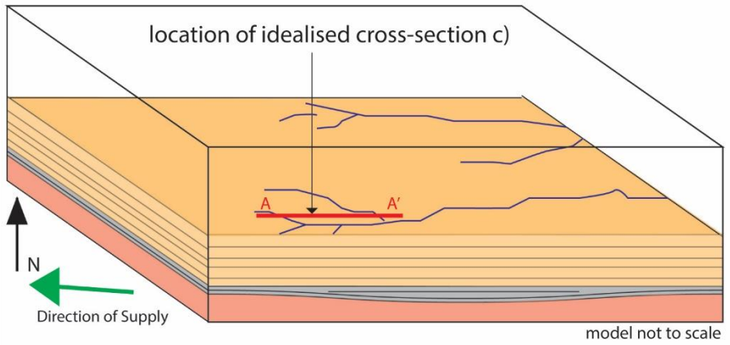

b) Block model (simplified) of Post-Permo-Carboniferous post-rift sag.

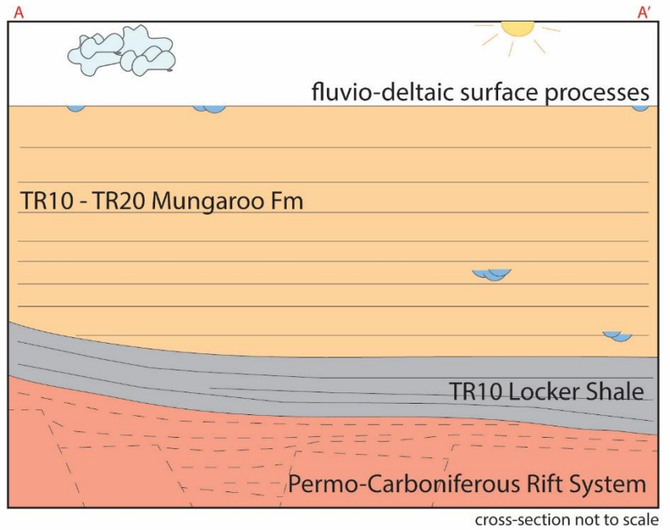

c) Post-Permo-Carboniferous rift sag idealised cross-section. Location of cross-ection on block model in Figure b).

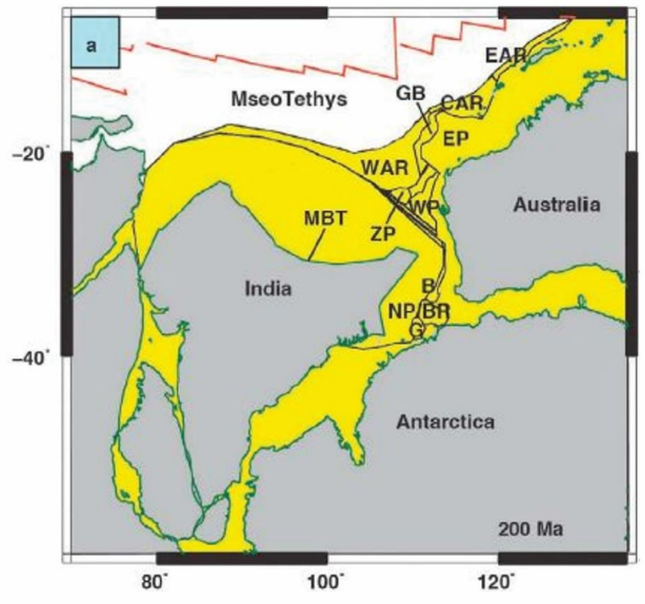

d) Latest Triassic - TR30 Rhaetian, onset of Mesozoic rift activity (reconstruction displaying early Jurassic).

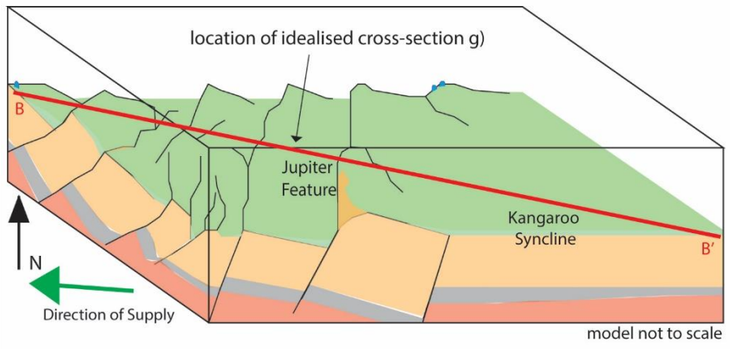

e) Simplified block model for the TR30 Rhaetian onset of mesozoic rift activity.

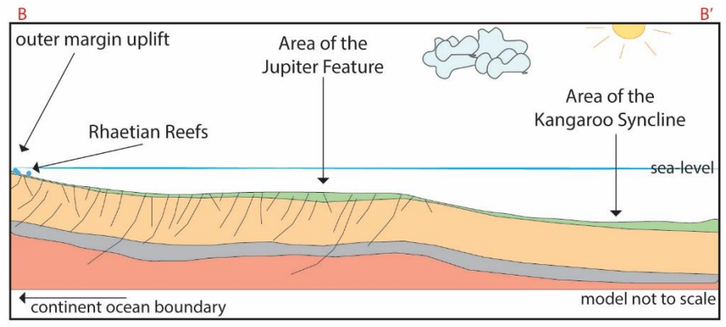

f) Idealised cross-section of the Exmouth Plateau in the latest Triassic (TR30 Rhaetian). Location of idealised cross-section on block model in Figure e) and on thickness map in Figure 6.5a).

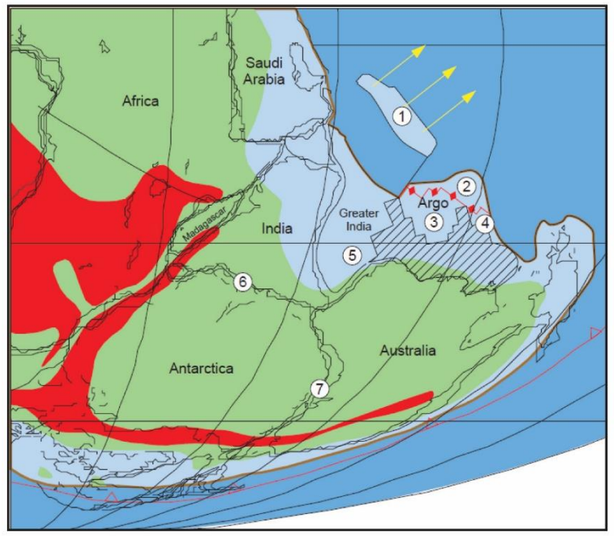

g) Lower Jurassic (J20 Pilensbachian) Mesozoic rift plate tectonic reconstruction.

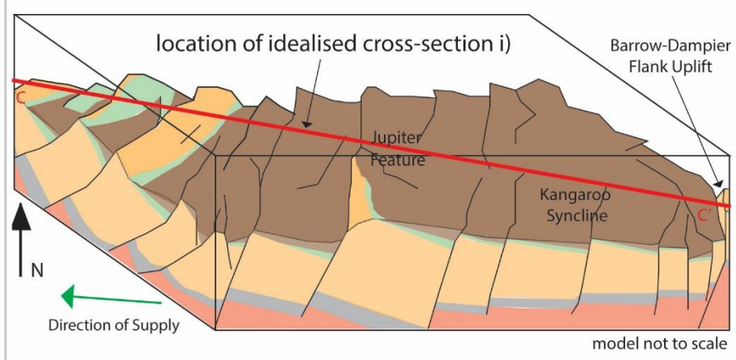

h) Simplified block model of J20 Early Jurassic to J40 Middle Jurassic Mesozoic rift activity.

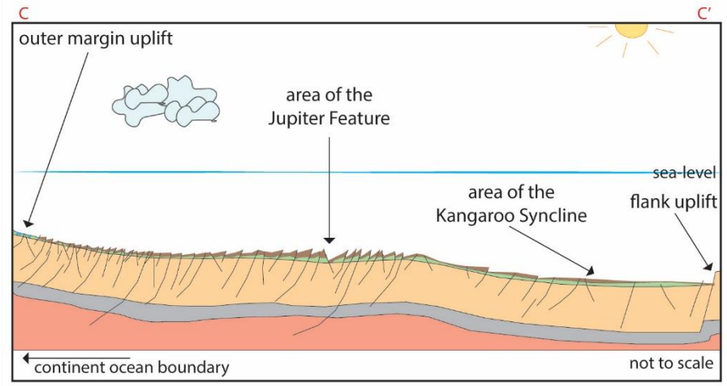

i) Idealised cross-section of the Exmouth Plateau in the Lower to Middle Jurassic (J20 - J40). Location of idealised cross-section on block model in Figure h) and on thickness map in Figure 6.5b).

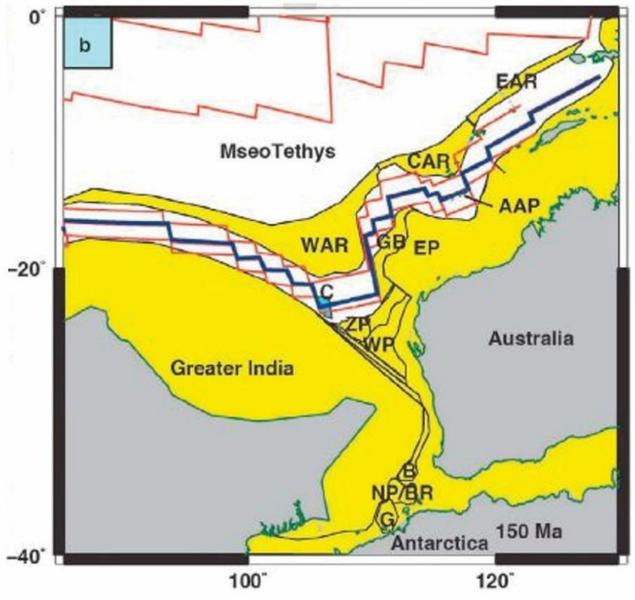

j) Upper Jurassic - J40 - J50 - Mesozoic rift activity reconstruction.

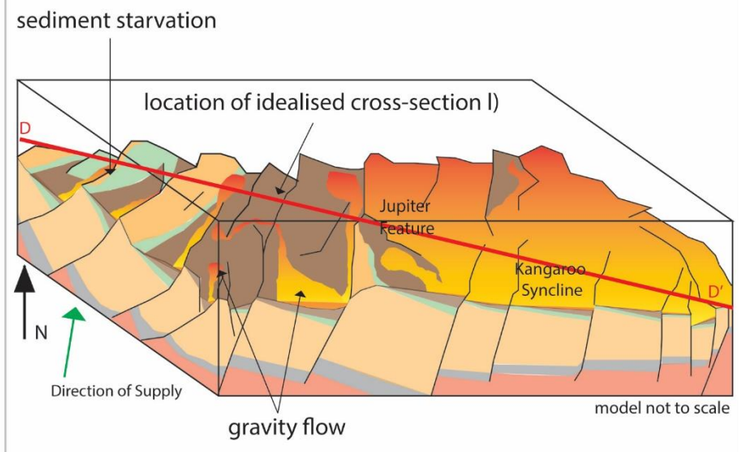

k) Block model (simplified) for the Upper Jurassic (J40 - J50) rift activity on the Exmouth Plateau.

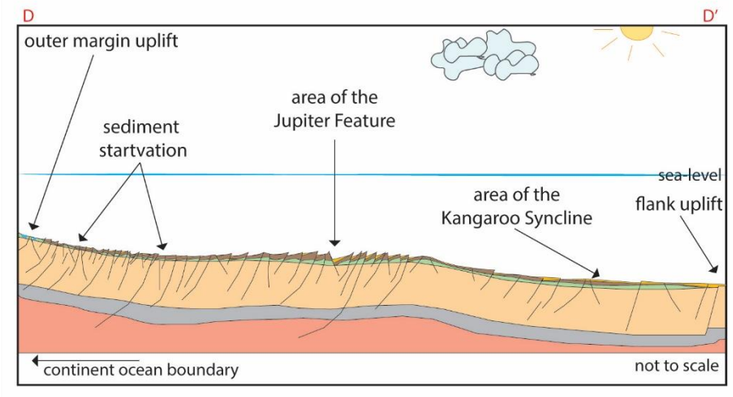

l) Idealised cross-section of the Exmouth Plateau in the Upper Jurassic (J40 - J50). Location of idealised cross-section on block model in Figure k) and on thickness map in Figure 6.5c).

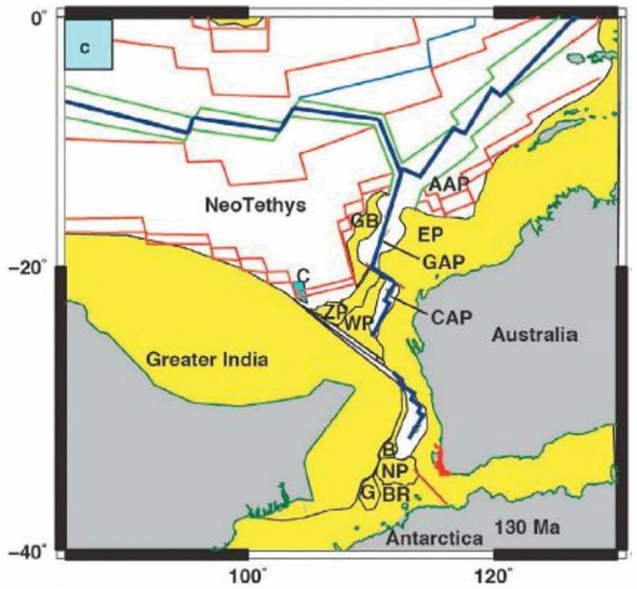

m) Lower Cretaceous (K10 Berriasian) Mesozoic rift plate tectonic reconstruction.

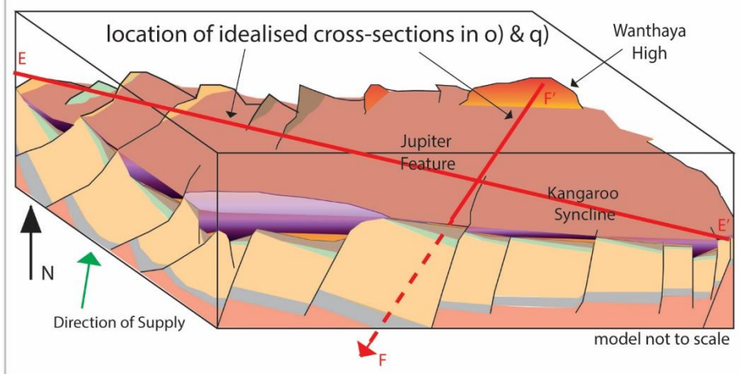

n) Simplified block model of K10 - earliest K20 Lower Cretaceous Mesozoic rift activity.

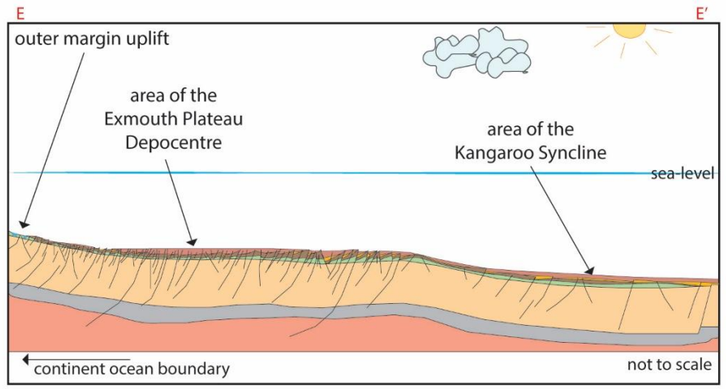

o) Idealised cross-section of the Exmouth Plateau in the Lowermost Cretaceous (K10 - early K20). Location of idealised cross-section on block model in Figure n) and on thickness map in Figure 6.5d).

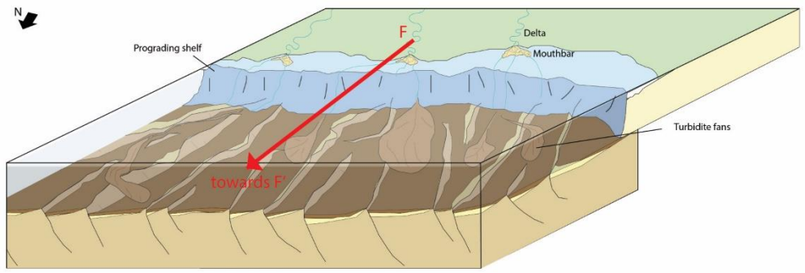

p) Block model of prograding K10 - early K20, Lowermost Cretaceous shelf edge.

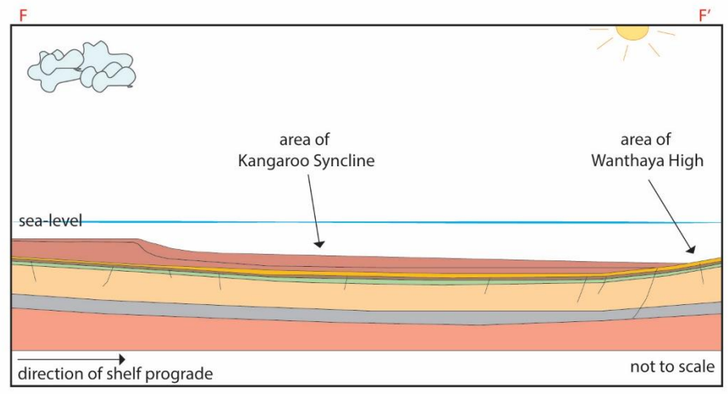

q) Idealised cross-section of the Exmouth Plateau in the Lowermost Cretaceous (K10 - early K20). Location of idealised cross-section on block model in Figure n) and on thickness map in Figure 6.5d).

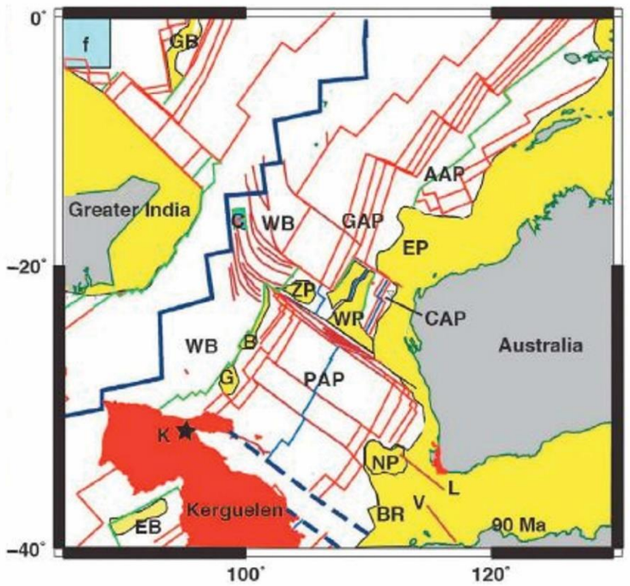

r) Upper Cretaceous Mesozoic rift plate tectonic reconstruction (image of K50 Turonian).

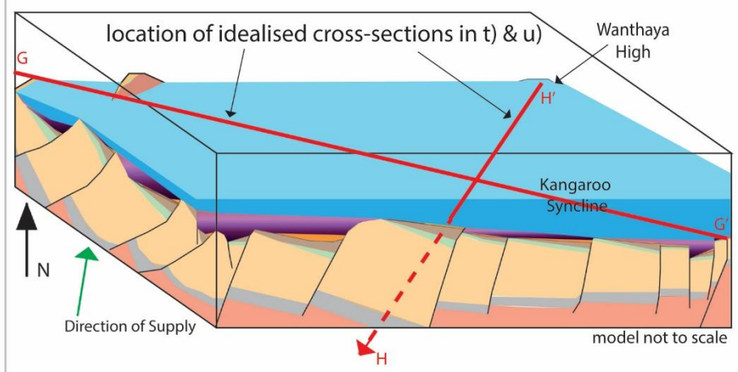

s) Simplified block model of K40 to Upper Cretaceous (K60) Mesozoic rift activity.

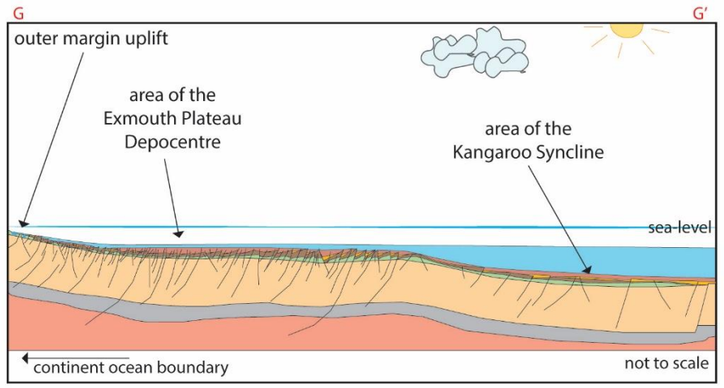

t) Idealised cross-section of the Exmouth Plateau in the Upper Cretaceous (K60). Location of idealised cross-section on block model in Figure s) and on thickness map in Figure 6.5f).

Figure 6.4 Summary of tectonic history of Mesozoic rift history of the North West Shelf, with idealised block models and cross-sections of the formation of the Exmouth Plateau. Images a) to c) show the Exmouth Plateau as defined between the Permo-Carboniferous and Mesozoic rifts. Figures d) to f) display the onset of Mesozoic rift activity on the plateau in the TR30 Rhaetian. Items g) to i) show the developing rift in the Lower to Middle Jurassic, with the Upper Jurassic shown in images j) to l). The last stage of Mesozoic rift activity is shown in m) to q) in the Lowermost Cretaceous. Then the post-rift Upper Cretaceous is displayed in figures r) to u). Tectonic reconstructions shown are modified from a) Jablonski and Saitta, (2004); d), j), m), and r) Gibbons et al. (20012); and g) Longley et al. (2002). Block model in p) is modified from Rohead-O'Brien et al. (2018) and the remaining images are the result of this body of work.

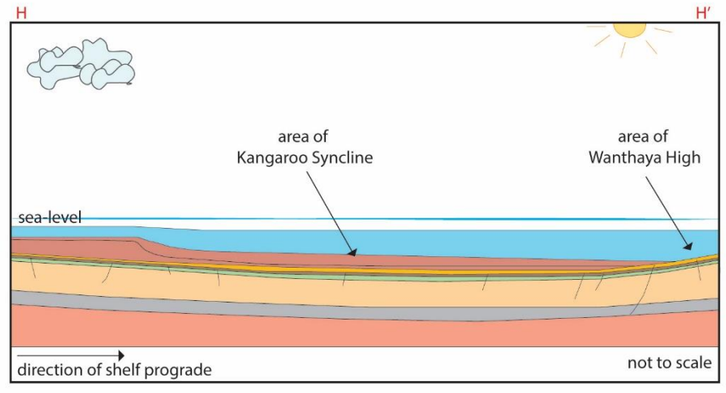

u) Idealised cross-section of the Exmouth Plateau in the Upper Cretaceous (K60). Location of idealised cross-section on block model in Figure s) and on thickness map in Figure 6.5f).

MS1 Thickness Map

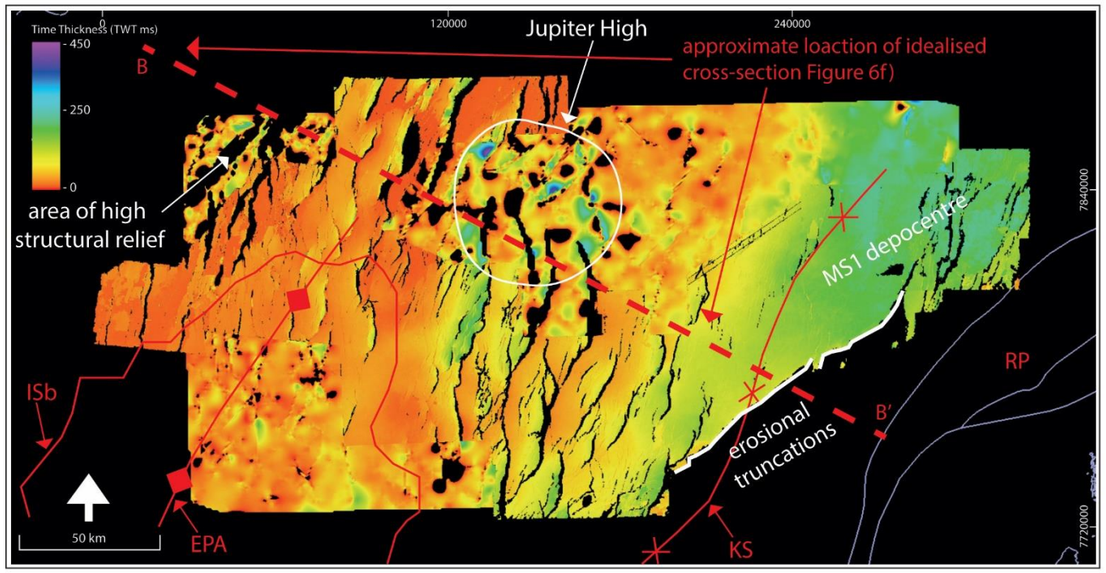

a)

MS2 Thickness Map

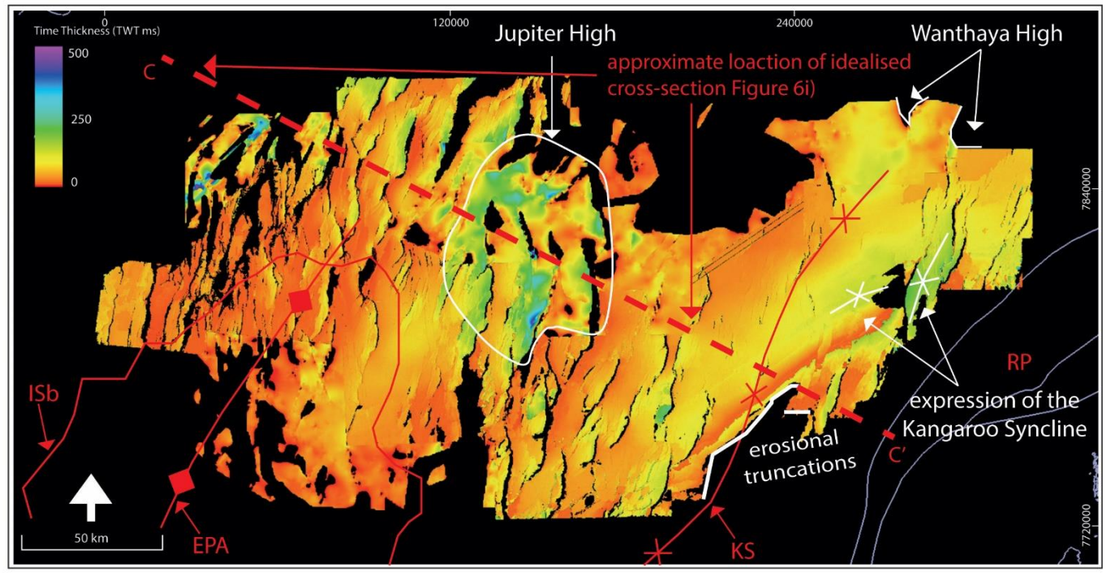

b)

MS3 Thickness Map

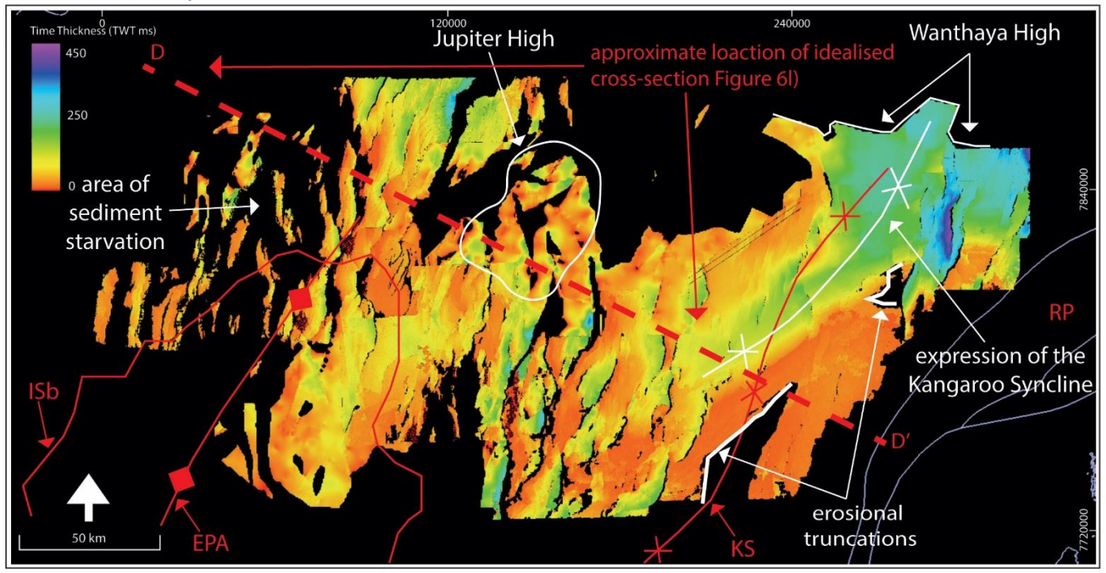

c)

MS4 Thickness Map

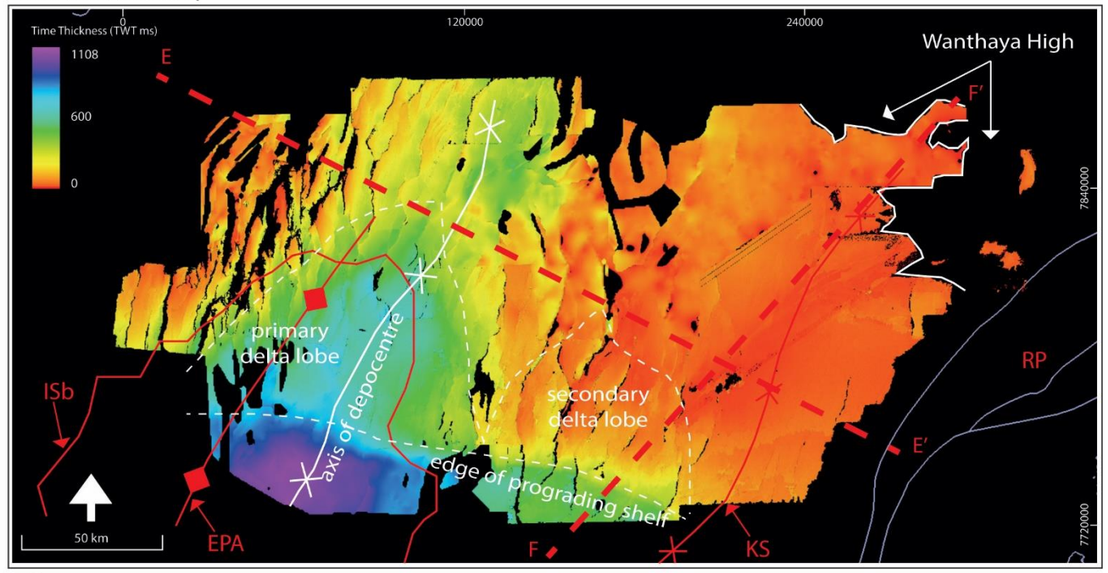

d)

MS5 Thickness Map

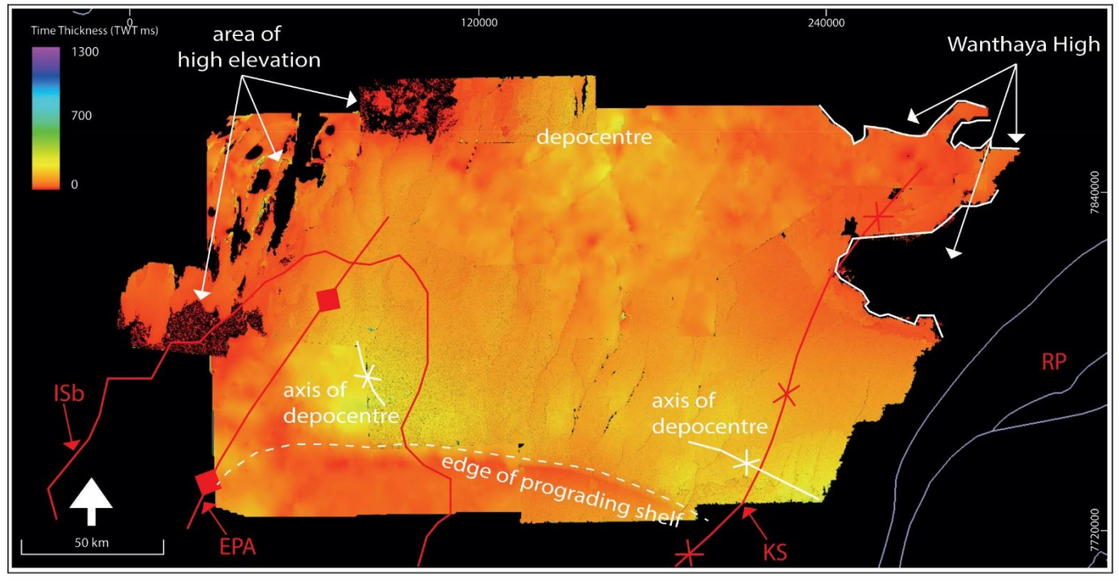

e)

MS6 Thickness Map

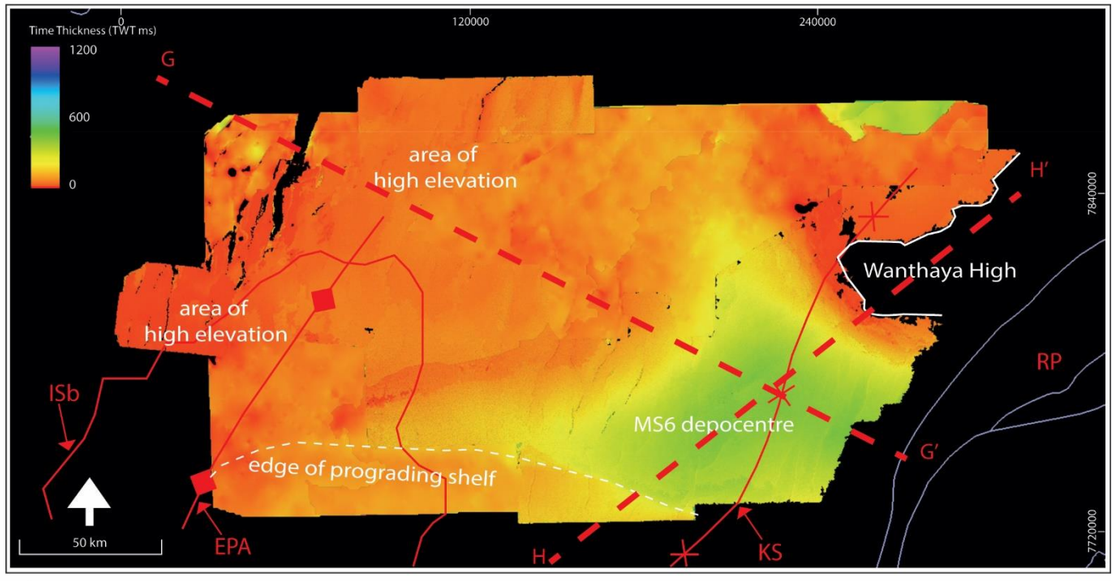

f)

MS7a Thickness Map

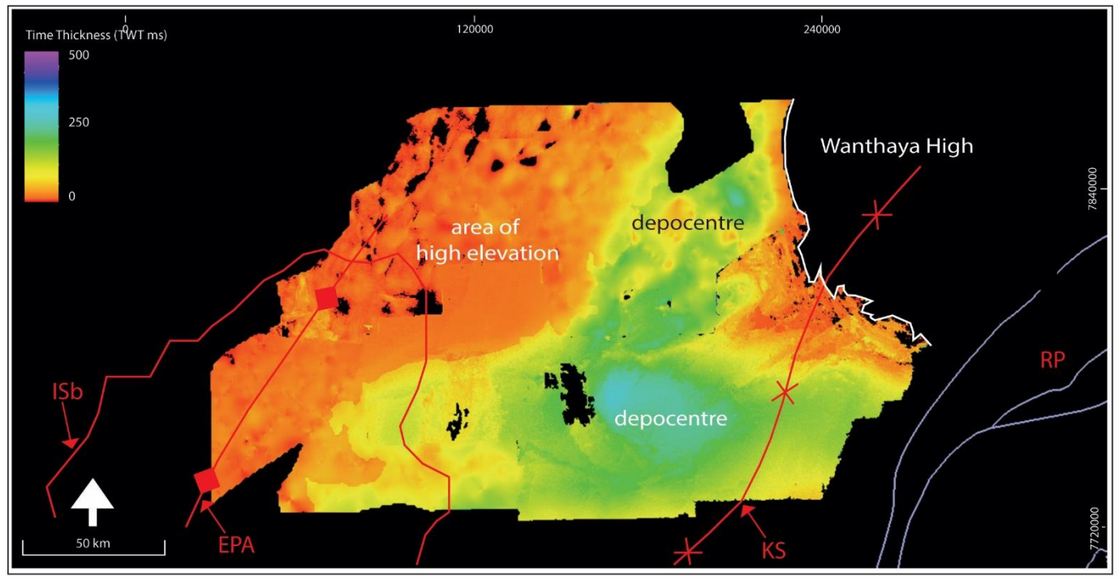

g)

MS7b Thickness Map

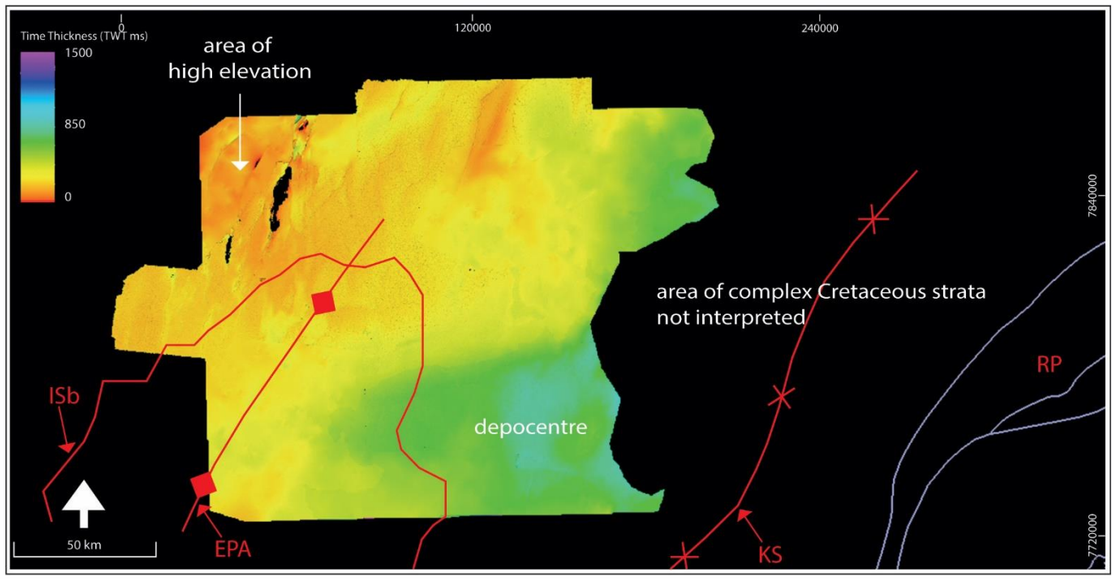

h)

Figure 6.5 Thickness maps of individual mega-sequences (as per this study) displaying the changes over time of the depocentre in the area of the Kangaroo Syncline, Jupiter Feature, Wanthaya High (northeast high) and areas of high elevation. Regional structural features (red) and mega-sequence relevant features (white) annotated on the individual maps.

On previous pages

second stage of rifting as fault activity ceased in the Lowermost Cretaceous in the east (Figures 6.4, & 6.5). However, the presence of a persistent high (the Wanthaya High) in the northeast is evident following the broader cessation of fault movement in this area (Figures 6.4, & 6.5; Chapter 5; Section 5.5).

The onset of sedimentation associated with the K10 Lower Barrow system occurred in the latest J50 Tithonian marked by the deposition of gravity flows in advance of the prograding shelf. These flows were primarily deposited in downthrown half-graben (Figures 6.2, 6.3, & 6.4). As sediment supply reached further north, the previously starved half-graben were infilled (Figures 6.2, & 6.3), while limited to no sedimentation occurred over the Wanthaya High (Figures 6.4, 6.5; Chapters 3 & 5). The deposits formed a large lobe in the southwest, north of the prograding shelf edge, creating a focused load-driven depocentre (Figures 6.4, & 6.5). The western and northwestern extent of this depocentre was controlled by the plateau's increasing elevation towards the continent-ocean boundary (Figure 6.5). Some of these early gravity flows also travelled in a north-easterly direction, forming a minor lobe feature in the southern end of the broad synclinal feature to the east (Figure 6.5; Chapter 5; Section 5.3).

Fault activity decreased significantly during the Lower Cretaceous (Figures 6.1, 6.2, & 6.4; Chapter 4; Section 4.2.3). Growth wedge development in the west began to decline before the K20 Valanginian separation event (K20.0 SB). Following this event, the development of fault-related growth wedges was markedly reduced. Further reduction of syn-kinematic deposition occurred until the K40.0 SB - mid-Aptian.

6.1.4. POST-RIFT EVOLUTION

As the plateau entered a passive phase of evolution, only minor movement occurred along a limited number of NE-SW trending faults (Chapter 4; Section 4.2.4). The long-lived relative elevation of the northwest continued through this stage, as did the elevation of the Wanthaya High (Figures 6.4, & 6.5). However, the high to the northeast underwent later subsidence in the Cenozoic related to an oceanward tilting of that region. Latter tilting may also have occurred in the area of the southern seismic surveys (Honeycomb and Glencoe), where a post-rift tilting is observed in the elevation of previously eroded fault block crests (Figure 6.5; Chapter 5; Section 5.4). The ongoing development of a depocentre in the southeast continues into the post-rift, which expanded to the north (north-central) area (Figures 6.4, & 6.5).

6.2. Implications

6.2.1. PLATE KINEMATICS AND FAULT ORIENTATIONS

This study has identified two cycles of rift activity, followed by a cycle of subsidence and post-rift modification, which is not dissimilar to the Mesozoic stages first identified by Metcalfe (1999) and developed by Longley et al. (2002). However, the detailed chronology and associated rift-related deformation of these stages are more complex on the Exmouth Plateau, as detailed here.

6.2.1.1. ONSET OF RIFTING

The observations made in this body of work did not identify any evidence of fault movement occurring in the Triassic aged deposits on the Exmouth Plateau until the TR30 Rhaetian. Different authors have inferred different timings for the onset of rift activity in the Northern Carnarvon Basin (i.e., Baillie et al., 1994; Blevin et al., 1994; Chen, 2018; Etheridge & O'Brien, 1994; Geoscience Australia, 2014a, 2019; McHarg, 2018; Smith et al., 1999). In the area studied here, the Triassic phase of subsidence continued following the older Permo-Carboniferous rift activities (Etheridge & O'Brien, 1994; Stagg et

al., 1999; Veevers, 2006). The pre-rift deposition of the thick TR10 - TR20 Mungaroo Formation continued beyond the TR20.0 SB - mid-Norian uplift which is recorded in the inboard Northern Carnarvon Basin and the Canning Basin (Forman & Wales, 1981; Rad et al., 1992). While faults do penetrate strata of this age, there is no indication that these faults were active during deposition (Figures 6.1, & 6.2). There is no evidence from the TR10 - TR20 Mungaroo Formation in the Exmouth Plateau to suggest any deformation linked to the hotly debated Fitzroy Movement, identified in the Canning Basin during the TR10 - TR20 Norian (TR20.0 SB; Forman et al., 1981), or the earlier deformation identified in the northeast of the Northern Carnarvon and Roebuck basins (i.e., Chen, 2018).

Evidence of fault movement on the plateau first occurs in the latest Triassic (Figures 6.2, & 6.4). In the more western part of the study area, initial fault movement occurs in the TR30 Rhaetian (Figure 6.2), which is younger than that identified inboard (Longley et al., 2002; Marshall & Lang, 2013) and older than that observed on the northern margin of the plateau (Chen, 2018). This is consistent with observations of Black et al. (2017), Bauer et al. (1994), Jitmahantakul and McClay (2013) and Stagg et al. (2004) for the Exmouth Plateau and Sub-Basin. However, the areas in the east of the region studied here show a more delayed response to rift activity, with the onset of fault movement occurring in the Jurassic, more in-line with rift initiation observed in the north of the plateau by Chen (2018). The angularity of downlap and onlap in the hangingwall growth wedges increases from the Triassic to the Jurassic. This corresponds to similar observations by Jitmanhantakul and McClay (2013) in the Exmouth Sub-Basin, indicating the presence of an early Jurassic hiatus (as the JP unconformity), where Hettangian and Sinemurian sequences are not preserved in the stratigraphic record. This could be due to the later removal of strata or to non-deposition following the onset of rifting on the plateau, as fault blocks formed high relief features. The precise age of the early Jurassic unconformities is difficult to establish due to their thin nature or lack of preservation and they may correspond to either the J20.1 TS or the J24.0 SB (Figure 3.1) regional events. The eastern region of the plateau does not

display active faulting until the Lower Jurassic, which is consistent with the observations of Etheridge and O'Brien (1994; Figures 6.2, 6.3, & 6.4). Additionally, sequences in the east of the study area first display angular downlap and onlap as part of growth wedge formation against hangingwalls during the early Jurassic (Figures 6.2, 6.3, & 6.4).

This study demonstrates that the onset of fault activity on the plateau, is in fact variable (Figure 6.4), as initially suggested by McHarg (2018), and hence resolves the differences between different authors, whose inferences for the whole of the basin are often based on observations from only one part of it.

6.2.1.2. FIRST PHASE OF MESOZOIC RIFTING

Rift-related activity on the Exmouth Plateau is marked by the appearance of faults across three critical orientations (NNE-SSW, NE-SW and NW-SE; Figures 4.2, & 4.10). Faults occur either independently or as linked fault systems, largely on NNE to NE trends. Fault throw is highly variable, but a generalised pattern of throw increasing to the north/northwest is evident in all of these fault populations. Later development of a fourth (E-W) post-depositional fault population occurs but is largely limited to two areas (Figure 4.14). The throw on this population primarily increases eastwards, but the trend is less evident.

During the first stage of rift activity the fault movement is most prominent across the NNE-SSW and NE-SW orientated populations (Figures 4.2, & 4.10). The NNE-SSW population of faults occur as long, straight features, implying they are a result of orthogonal extension (McClay & White, 1995). The growth of pinnacle reefs on fault blocks from this populations (Figure 3.7) displays no lateral offset and provides evidence that movement on faults during this stage of rift-related activity was purely dip-slip. Pure dip-slip movement is a clear indication that extension was orthogonal to the strike of these faults and hence has a WNW-ESE orientation (Figure 6.5).

Further support for a WNW orientated extension event during this time is the trend of the second most prominent fault population at this time. The NE-SW population display curved fault traces, and often extended to greater depths

(Figure 6.1). These curved traces also often form *en-echelon* fault arrays which are also NE-SW trending (Figures 4.2, 4.9, & 4.10). Modelling by McClay and White (1995) found that curved faults forming *en-echelon* patterns formed as a result of reactivation of underlying fault systems during oblique extension. This type of faulting has been previously observed on the Rankin Platform (l'Anson, 2019; McHarg; 2018) near to the key *en-echelon* fault systems identified in this study (Figure 4.9). There is an underlying NE-SW structural grain in the Northern Carnarvon Basin related to Permian extension (l'Anson et al., 2019; Jitmahantakul & McClay, 2013; Pryer et al., 2002; Stagg & Colwell, 1994) and these Mesozoic aged NE-SW orientated faults are the result of the oblique reactivation and new nucleation (Clifton et al., 2000; Etheridge et al., 1991; Henza et al., 2010; Pryer et al., 2002) of those earlier Permian structures which was also identified by McHarg (2018) in the innermost area of the plateau.

This evidence for WNW-ESE extension appears inconsistent with the direction of sea-floor spreading (Falvey, 1974; Veevers, 1988) in the Argo Abyssal Plain which occurred in a north-westerly direction. While most investigations into of the development of the Exmouth Plateau and Northern Carnarvon Basin (i.e., AGSO North West Shelf Study Group, 2004; Barber, 1988; Bradshaw et al., 1988; Cathro & Karner, 2006; Driscoll & Karner, 1996; Exon & Wilcox, 1978, 1980; Exon et al., 1982; Gartrell, 2000; Hocking, 1990b; Jablonski & Saitta, 2004; Longley et al., 2002; Stagg et al., 2004; Veevers, 1988; Yeates et al., 1987; and others) describe the separation of Argoland as the key extensional event during the Jurassic. Observations made during the course of this study are at odds with our current understanding of the plate movement which generated the North West Shelf. The orientations indicate that the greater extensional stresses were being generated on the western margin, not the northern margin during the latest Triassic to Middle Jurassic (Figure 6.5).

The onset of fault activity occurs later in the Triassic than the activity identified by Chen (2018) in the northern reaches of the Exmouth Plateau and Bedout Basin, indicating that there is no connection to the debated and often invoked Fitzroy Movement initiating fault activity at the southern end of the plateau.

Instead, the Triassic initiation in the southern portion of the Exmouth Plateau is more in line with the later rifting of Sibumasu as per Metcalfe (1996). The initiation in the Upper Triassic here is also earlier than the Barrow-Dampier extension and flank uplift of the Rankin Platform identified as Jurassic in origin (Driscoll & Karner, 1996, 1998), the timing of which is Middle Jurassic as defined by this body of work.

Similar to the formation of faults in the Beagle Sub-basin (Chen, 2018), Jurassic aged fault nucleation occurs on the plateau, however the throw and length of these fault is more significant than in the Beagle Sub-basin. Fault movement is evident in the Jurassic strata observed on the Plateau with Jurassic packages displaying evidence of growth across faults (Figures 6.1, 6.2, & 6.3). However, no seismic observation of the earliest Jurassic (J10 Hettangian to J10 - J20 Sinemurian; or J20 Pilensbachian) stratigraphy has been possible in the area studied here due to the very thin, or absent, nature of it in the area impacting to history that can be learned from those packages. So, no certainty can be applied to statements limiting the initiation of these faults to have started in the Lowermost Jurassic. In the first phase of rifting identified in this body of work, the rifting of the Argoland fragment to open the Argo Abyssal Plain occurred in the Middle to Upper Jurassic. This timing is in agreement with many previous works for the opening of the Argo region (i.e., Heine and Müller, 2005 – as the West Burma Block; Li & Powell, 2001; Metcalfe, 1996 - as Lhasa). However, the rifting of Argoland was most likely not the first rift-related tectonic stress induced on the Exmouth Plateau during the Mesozoic rift history.

The continued uplift of the outer margin (Section 6.2.3) in the first stage of rifting is likely connected to the limited load already occurring on the outer margin, the limited new load being deposited during the latest Triassic and Jurassic. However, this neglects the prolonged period of extreme relief identified (Chapter 5) in the outermost area of the margin. The relief on the outer margin is more spatially complex compared to the well know Dampier flank uplift of the Rankin Platform. Given the accepted process of flank uplift occurring in the build up to and during rifting in response to thermal processes,

this outer margin uplift indicates that geoscientists are still missing a crucial piece of the puzzle when reconstructing the breakup of the Gondwanan Supercontinent and the evolution of the North West Shelf.

6.2.1.3. SECOND PHASE OF MESOZOIC RIFTING

The third orientation of faults, NW-SE, occur from the TR30 Rhaetian but are particularly prominent during the Lowermost Cretaceous, where extension is attributed to the Greater India separation event (Figure 4.10). As identified by McHarg (2018) in the Dampier Sub-basin, these faults are most likely strongly controlled by the interactions between the two continental plates, as is implied by their increase in significance towards the western margin of the Exmouth Plateau (Figure 6.5). The rise in the dominance of the NW-SE fault population occurs as plate reorganisation causes a change in the directional stress regime as India and Australia separated. Faults do decrease from the Middle Jurassic J40.0 SB during the deposition of the K10 MS4 strata (Figure 4.10) indicating a clear connection to the Argo Sea-floor spreading the Valanginian Separation similar to the fault timing identified to the north by Chen (2018). This agrees with observation from the inboard sub-basins made by Hocking (1990b) and Paumard et al. (2018). McHarg (2018) also identified this drop-in fault activity, but this was linked to a period of non-deposition. While this time period on the plateau exhibits a reduced period of deposition or preservation (in comparison to the earlier and later strata) there is evidence of fault movement available, particularly after the southern supply of the K10 Lower Barrow Group arrived.

Uplift of the outer margin remains into this stage of rift history, with parts of the northwestern area remaining elevated so that the larger fault blocks remain exposed at the close of activity in the early K20 Valanginian, and at the end of the K30 early Aptian. The uplift of the outer margin during the second stage of rift activity indicates that there was continued thermal and load driven geodynamics at play on the western margin. The extreme uplift limited the potential for load to be delivered into the outer region, creating a barrier to deposition that further fed into the Exmouth Plateau Depocenter (Chapter 5;

Section 5.5.4). Instead, the Exmouth Plateau Depocenter was being infilled during the early Cretaceous, and the long-lived Kangaroo Syncline was receiving infill from the south-southeast. The bathymetrically elevated Wanthaya High was also receiving limited supply at this time.

6.2.1.4. MISSING PUZZLE PIECE SUMMARY

This research points to an extensional event on the western margin would have occurred as early as the onset of the TR30 Rhaetian (~208MY) and continued up until the end of the Middle Jurassic (J30; ~163MY) at the Middle Jurassic Unconformity - J40.0 SB. Additional Upper Triassic activity has also been recorded by von Rad and Exon (1983) and von Rad et al. (1992) on the Wombat Plateau in the form of volcanics, which have not yet been suitably linked to the later Jurassic rift initiation events (Zahirovic et al., 2016).

It is possible that the fault orientations and outer margin uplift indicate that the separation of the India - Australian plates began much earlier than previously identified by current tectonic reconstructions. Initial tension through the plates could have started well before the final continental separation (Kearey et al., 2009; Powell et al, 1987) in the areas of the Cuvier and Gascoyne abyssal plains. Then in the J40 Oxfordian plate stress shifted northwards to the loci of sea-floor spreading in the Argo Abyssal Plain (Muller et al., 2000). Once the successful separation of the Argoland fragment occurred in the Upper Jurassic to Lower Cretaceous (Muller et al., 2000; Powell et al., 1987), rifting would have then shifted back to the western side of the plateau boundary (c.131.9MY Muller et al., 2000), forming the Cuvier and Gascoyne abyssal plains in the Lower Cretaceous, in line with agreed timing (as per Johnson et al., 1976, 1980; Falvey & Mutter, 1981; Powell et al., 1988; Müller et al., 1998; and others). The suggestion of a step or pause in rift nucleation (concepts loosely identified by Taylor et al., 1999) from the west of the plateau in the vicinity of the Indian plate in the Upper Triassic to Middle Jurassic to the north and east at the Argo region has not yet been included in widely accepted reconstructions of the region. Yet the evidence presented to here and in other studies (i.e., McHarg, 2018; von Rad & Exon, 1983; von Rad et al, 1992) show

ample evidence of an earlier initiation of rifting stress on the western margin with no currently accepted source for this activity.

At the very least, the variation identified on the Exmouth Plateau, in this research and in earlier works (i.e., Chen, 2018; McHarg, 2018) indicates a plateau segmented in its response to the impacts of continental breakup, OR, that there remains a crucial part of the margins history not yet fully recognised in reconstructions.

6.2.2. RIFT FLANK UPLIFT – INBOARD BASINS

A dominant feature that occurs during the first stage of rifting is the uplift of the rift-flank of the failed Barrow-Dampier rift system. Here it resulted in the erosion of a significant volume of Triassic sediments, and erosion or non-deposition of early and Middle Jurassic sediments (Figure 6.2). The uplift of rift-flanks is a common and important feature of rifts (Watts, 2001; Weissel & Karner, 1989) which involves many processes (Daradich et al., 2003). Rift-flank uplift occurs in many large-scale rift basins such as the East African Rift System (Veevers, 1977; Veevers & Cotterill, 1976) and the Gulf of Suez (Morag et al., 2019). Flank uplift occurs when the lithosphere is heated, and the buoyancy forces begin to respond by thermal uplift (Braun & Beaumont, 1989; Driscoll & Karner, 1998; Watts, 2001) at the onset of rifting (Weissel & Karner, 1989). The uplift can then result in the removal of material by erosion, creating an isostatic (load) based uplift in addition to the thermal uplift (Braun & Beaumont, 1989; Dewey & Bird, 1970; Driscoll & Karner, 1998; Falvey, 1974; Mondy, 2019). Some authors (such as Zuber & Parmentier, 1986; Parmentier, 1987) suggest that the uplift of flanks could be purely the result of sudden lithospheric thinning or shear stress generated by the extension. In the meantime, the broad pattern of isostasy from the uplift results in an overdeepening of the region adjacent to the flank (away from the rift centre; Braun & Beaumont, 1989; Mondy, 2019; White & McKenzie, 1988). The development of this feature is likely to indicate variation with depth in the strength of the lithosphere (Braun and Beaumont, 1989) due to composition changes (Bott, 1971; Chery et al., 1992; Mondy,

2019; Weissel & Karner, 1989), or deep detachments (Weissel & Karner, 1989).

The flanks may remain elevated for more than 50 million years after the cessation of rifting (Weissel & Karner, 1989). However, they may also be relatively short-lived if the extension of the lithosphere is depth-dependent (Royden & Keen, 1980), due to lateral transfer of heat into the flanks (Steckler, 1985; Cochran, 1983), or if extension results in localised convection (Buck, 1986; Keen, 1985; Steckler, 1985). When the thermal effects begin to reduce, the uplifted flank will cool and subside rapidly (Driscoll & Karner, 1998; White & McKenzie, 1988). While load removal may increase the uplift through buoyancy, it can also expedite the cooling and subsidence of the rift-flank (Driscoll & Karner, 1998). Sedimentation during or after a rifting event will increase the load related subsidence, ending the uplift (Braun & Beaumont, 1989; Driscoll & Karner, 1998).

The uplift of the inner rift-flank of the Exmouth Plateau occurred after early and Middle Jurassic sedimentation (Figure 6.2). Widespread erosion of the Triassic and Jurassic sediments occurred during the flank-uplift but the deposits of this age (MS1 & MS2) are parallel and layer-cake in this area and hence there is no indication of the flank having been uplifted prior to or during their deposition (Figure 6.2). Following the erosion, deposition occurred once again in the J40 Oxfordian, just prior to the regional Middle Jurassic Unconformity (MJU/J40.0 SB). No syn-kinematic sediments were observed in the late Jurassic strata to indicate that the uplifted flank then underwent a gradual period of subsidence (Figure 6.2). Instead, the sedimentary records shows that the event was short lived, occurring and completing within 11 MY (from the start of the Middle Jurassic (~174.1MY) to the J40 Oxfordian sea-floor spreading (~163.5MY)).

The scale of this uplift is smaller than other widely observed episodes of rift-related uplift (Morag et al., 2019; Veevers, 1977; Veevers & Cotterill, 1976) associated with rifting centres. The magnitude of the uplift can be approximated by extending the interpretation of the TR30.1 TS (Top Norian) horizon over the rift-flank region and comparing the time difference between it and the J40.0 SB surface (Oxfordian Unconformity); then converting the time

thickness into metres as per Equation 1.2 (Chapter 1, Section 1.5). This suggests that the flank of the Barrow-Dampier rift was uplifted by c. 715 m, which is significantly lower than the 1-2 km identified by Braun and Beaumont (1989). As the magnitude the flank-uplift depends on the scale of rifting, and the Barrow-Dampier rift sits at the lower end of the scale of rift-flank uplift. The reduced volume of uplift to comparative rifts may be due to the failure of the Barrow-Dampier rift system, as well as being the result of the above-mentioned shorter duration of rift-flank uplift.

The duration of uplift was also shorter than larger rift systems (i.e., Suez Rift, East African Rift) where flank-uplift occurs at the onset of rifting and then remains elevated for a prolonged period after the cessation of rift activity (Weissel & Karner, 1989). Most rift-flanks are uplifted, eroded, and subsided over a period of 60MY (Weissel & Karner, 1989). Previous estimates for Dampier-Barrow flank-uplift are closer to that at 40 MY (Veevers, 1988) or 50 MY (Falvey, 1974). These observations are also more consistent with the predicted timing of uplift relative to rift activity, where the flank of a rift should begin to uplift just prior to, or at the commencement of, rift activity (Braun & Beaumont, 1989; Driscoll & Karner, 1998; Watts, 2001); assuming that the Barrow-Dampier rift activity occurred during the Pliensbachian and Toarcian (early to mid J20; Veevers, 1988). The uplift of the Dampier rift-flank occurred later, in the Middle-Upper Jurassic indicating that the more significant period of Barrow-Dampier extension occurred later than previously suggested - Lower Jurassic, Veevers (1977). The subsequent prolonged period of subsidence of the uplifted flank appears absent in the area investigated. Indicating that the subsidence was likely rapid in response to the cooling of the rift and/or the removal of load, with load removal further decreasing the length of flank uplift.

The uplift of the Barrow-Dampier rift-flank resulted in the development of an over -deepened feature in the region adjacent to the flank, the prominent NE-SW orientated syncline referred to as the Kangaroo Syncline (Figures 5.5, 6.2, & 6.5). The observed low sedimentation rates coincident the early formation of the Kangaroo Syncline (Exon & Wilcox, 1978) point to a geodynamic mechanism other than pure loading. Relative elevation of the region show that

it forms a morphological low between the uplifted Barrow-Dampier rift flank to the SE and the uplifted external part of the Exmouth plateau to the NW (Figure 6.5). This resulted in the formation of the Kangaroo Syncline as a depocentre as described by the “rim basin” concept of Veevers (1977). Later loading of the feature drove further subsidence, resulting in a depression in the area of the Kangaroo Syncline that persisted over time (Figure 6.5).

The extent and volume of uplift on the inner margin or inner rift flank uplift, indicate that the influence of the underlying geodynamic processes in that area were minimal (Chenin et al., 2022; Grasemann & Stuwe, 2011) in comparison to other examples of rift flank uplift (see Morag et al., 2019; Veevers, 1977; Veevers & Cotterill, 1976; Weissel & Karner, 1989). The isostatic response to load became the key driver of subsidence (Cloetingh et al., 2013).) in the Kangaroo Syncline as evidence points to a fast return of thermal equilibrium to the inner flank uplift.

6.2.3. MARGIN UPLIFT

The relative elevation of the outer margin during Mesozoic rift events was greater than the inner plateau (south and southeast). Bathymetric indications (Chapter 5) show that these areas were elevated from the onset of extension activity in the TR30 Rhaetian. The Rhaetian reef trends on the southern plateau, as identified by Grain et al. (2013), and the erosion of fault block crests at this time highlight the relative elevation of the outer flank during the Rhaetian (Figure 5.8). The erosion of fault block crests was also initiated at this time and continued during the Jurassic and into the Cretaceous. The onset of erosion of fault blocks crests migrated to the south or southeast over time (Chapter 5). This indicates that relative elevation was increasing during the Mesozoic, uplifting fault blocks above the sediment-water interface as the elevation of the outer margin increased (Figures 5.8, & 6.5).

The greater relative elevation of the outer margin continued on the Exmouth Plateau during the first stage of Mesozoic rift activity (Figures 6.1, & 6.5). This resulted in a substantial shift in the supply of sediment to the margin. The Triassic deposition was thick and uniform in thickness (Figures 6.1, & 6.2).

With the onset of rift activity, the rotation of fault blocks began to impact the outer margin and limited sedimentation of the TR30 Rhaetian aged strata occurred (Figure 6.1). The increased elevation resulted in a depositional hiatus in the early Jurassic (J10 - early J20), which was then followed with a reduction in the volume of sediment supply. The limited supply was confined to selected pathways (Section 6.2.4) and deposits on the outer margin remained low.

Further tilting occurs in the west/northwest after the Argo sea-floor spreading and into the Lowermost Cretaceous (Figures 5.14, 5.16, & 6.5). Erosion of fault block crests continues during the early sedimentation of the K10 Lower Barrow Group (Chapter 5) before many of the remaining crests were buried. Elevation is observed to persist during the Cretaceous.

No regional erosional unconformity was developed over this outer flank-uplift. White and McKenzie (1988) argue that this is not evidence against the existence of a flank-uplift, rather that the ongoing elevation of the outer margin was lower than the forces controlling erosion (Watts, 2001) – consistent with the submarine setting of the Exmouth Plateau from the TR30 Rhaetian onwards. Given the reducing volume of supply reaching the outer margin, regional unconformities are likely to not be recognised in seismic data. The pattern of increasing elevation (Chapter 5) towards the oceanward margin indicates that the uplift of the outer margin was much more widespread than that of the inner rift-flank, but due to reduced deposition the volume of uplift is unable to be calculated with any level of confidence.

Uplift on other parts of the margin of the NWS have also been investigated to reveal the morphology of the margin as associated with sea-floor spreading. Lorenzo et al. (1991) and Veevers (1988) found that the southern margins of the Exmouth Plateau had likely undergone uplift as a result of spreading of the Cuvier and Gascoyne Abyssal Plains expressed by the prominent Valanginian unconformity (K20.0 SB) observed in the Exmouth Sub-basin, and further to the south in the Gascoyne platform and northern Perth Basin. Uplift of the southern part of the margin occurred immediately after the initiation of spreading and influenced the formation of syn-kinematic strata by restricting supply of the K10 to early K20 Barrow Group sediments (Lorenzo et al., 1991)

to the north and west. However, observations made in this study highlight that the outer margins (abutting the Cuvier in the south and the Gascoyne in the southwest) were uplifted prior to the K20 Valanginian. The sustained elevation of the outer margin likely lasted from the TR30 Rhaetian into the K50 - K60 Upper Cretaceous, some ~140 MY. The margin uplift is also consistent with the formation of faults which also developed from the TR30 Rhaetian. These faults imply WNW extension which is consistent with the pattern of elevation increasing to the east at this time (Figure 5.11), indicating that the outer margin was uplifted as a result of extension relating to the separation of Greater India and not Argoland. This reinforces the interpretation based on fault orientations that extension on the western margin had a significant control from the Uppermost Triassic.

The restricted deposition on the northern or northwestern margins also indicates that the outer margin was uplifted for an extended period. During the Jurassic deposition was limited on the outer margins but sediment was being supplied to the region, as evidenced by the Kangaroo Syncline, Jupiter Feature, and the Exmouth Plateau Depocentre (Chapter 5, Section 5.5). These form, and develop on, the intrabasianal depocentre of Exmouth Plateau as described by Veevers (1977, 1988) and also been identified in other NWS basins (Veevers, 1974) as a rift-related response and as flexure induced by loading (Rouby et al., 2013; White & McKenzie, 1988). The relative relief of the outer margin can be tracked into the Cretaceous with the emplacement of the K10 Barrow Lobe, as it preceded the arrival of the prograding shelf edge (Figure 5.11). K10 to earliest K20 Barrow Group sedimentation is limited to the north and northwest. At first this was due to a sediment starved system creating barriers through uplifted fault blocks, but as they were infilled, sedimentation was still limited towards the continent ocean boundary. The limiting of supply into regions is a prominent feature displayed by most uplifted flanks (Watts, 2001).

Thermal implications of rift activity cause uplift (Keen, 1979; Turcotte & Emerman, 1983) and cooling results in the subsidence of the uplifted regions (Karner et al., 2004; Keen, 1979; Keen & Boutilier, 1990; McKenzie, 1978;

Moore et al., 1986; Pitman & Andrews, 1985; Manatschal et al., 2022). Loading of the crust in the areas of the Kangaroo Syncline and the Exmouth Plateau Depocentre, result in isostatic subsidence amplifying the flexure of the crust (Burov & Cloetingh, 1997; Gilchrist & Summerfield, 1994; Kooi & Beaumont, 1994; Sandiford et al., 1998; Van der Beek et al., 1994, 1995; Watts, 1989; Watts et al., 1982; Rouby et al., 2013). Increased thermal input may well have resulted in the prolonged uplift (Alves et al., 2021; Bai et al., 2020) of the outer margin. The critical nature of thermal history on rifted margins (Grasemann & Stuwe, 2011; Hu et al., 2001) in conjunction with the earlier onset of rifting on the southern plateau and prolonged time of marginal uplift leave us with clear knowledge about how much we didn't know we didn't know.

6.2.4. SEDIMENTARY SYSTEMS IN A SUB-MARINE RIFT

6.2.4.1. BATHYMETRIC INDICATIONS OF SEA-LEVEL

Bathymetry during the TR30 Rhaetian can be inferred from the presence of carbonate build ups (Chapter 5) identified by Grain et al. (2013). This reef trend provides insight into the relative sea-level during the TR30 Rhaetian as they indicate deposition was occurring close to sea-level; in water depths of 50 m or less (Grain et al., 2013). This is consistent with the transgression that occurred towards the end of the TR20 Norian which resulted in flooding of the southern portion of the plateau (Jablonski and Saitta, 2004). The reef trends (Figure 5.8; Grain et al., 2013) occur over areas which may imply bathymetric elevation of the outer margin and more central plateau was greater than the area in between, where pinnacle reef formation did not occur. In addition to this, eroded fault block crests coincide with areas of carbonate formation. The uplift of fault block crests in such shallow water would likely have resulted in subaerial exposure leading to erosion (Figures 3.22, & 6.4). It is also of interest to note that the reef trends are oriented NNW-ESE (Figure 5.8), consistent with the general pattern of uplift noted above.

Following the TR30 Rhaetian, a sudden rise in relative sea-level resulted in the cessation of patch reef growth (Grain et al., 2013). Consequently, the subsequent erosion of fault block crests was most likely occurring in a

submarine environment. This is consistent with the early Jurassic stratigraphy of the plateau which indicates a deep-water environment. However, this evidence is not absolute due to the reduced preservation of Jurassic stratigraphy. The mechanism of later removal of material from uplifted crests is difficult to establish. This part of the plateau was distal to the sediment supply which was from the east or northeast (Figure 6.6) where fault activity was minimal in comparison. The distal nature of the deep marine depositional environment resulted in the restriction of sedimentation to the down thrown half-graben (Chen et al., 2021 – Dampier Sub-basin; Cullen et al., 2020 – Gulf of Corinth). The successive emplacement of several layers of sedimentary packages in this manner resulted in localised unconformities within half-graben as the crests of fault blocks remained above the sediment-water interface in the manner described by Cullen et al. (2020) in the Gulf of Corinth. Sediment supply to the outer margin was limited during the Jurassic (Figure 3.4) and exposure above areas of sediment accumulation was occurring, which resulted in crestal erosion. The progressive southward migration of crestal erosion highlights the continued development of uplift of the outer margin during rift activities.

In the earliest Cretaceous turbidites were being deposited in front of the prograding K10 to early K20 Barrow Group in underfilled half-graben, and erosion of the uplifted fault block crests at this time is evident (Figures 3.22, & 6.4). This indicates that the fault block crests remain emergent above the level of sedimentation in the earliest Cretaceous. Evidence for erosion of fault block crests during K10 Lower Barrow Group sedimentation is only apparent in the lowermost part of this sequence, and no indication of crests being exposed above the sediment-water interface or sea-level occurred during the K20 Valanginian, at the top of the K10 Lower Barrow Group.

6.2.4.2. PATHWAYS OF DEPOSITION

Regional deposition during rift activity is controlled by structure, erosion and uplift (Blaich et al., 2011; Gernigon et al., 2014). The Exmouth Plateau displays

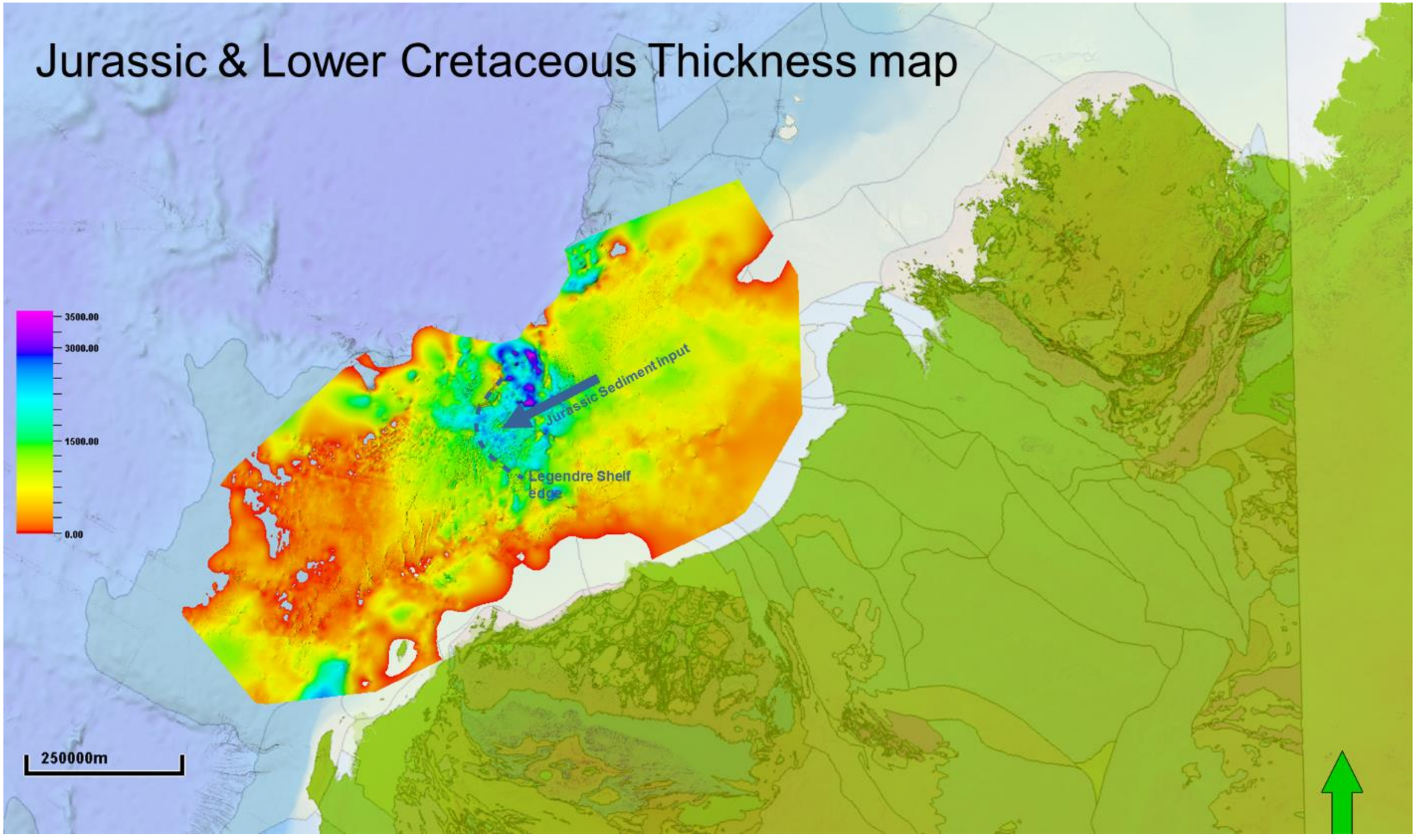

Figure 6.6 Jurassic and Lower Cretaceous thickness map displaying the prograding Legendre shelf edge. Regional map complied by C. Elders (2021).

variations in extension related faulting, uplift, and erosion all of which impact on the deposition of Mesozoic strata.

Following the onset of fault activity on the Exmouth Plateau sediment deposition of became less layer-cake in nature and geometries formed during deposition as a result of the presence of faults and ongoing fault movement. Supply during the latest Triassic was sourced from the east and fed onto the Exmouth Plateau. By the Jurassic the supply transitioned into the distal portion of the west-southwest prograding Legendre shelf system (Figure 6.6; Chen, 2018). This system prograded over an area of the plateau with comparably limited fault activity, where deposition remained layer-cake in nature (Chen, 2018). However, no evidence of a distal deltaic Lengendre system has been observed in the area studied for this body of work, meaning the Legendre system became restricted before reaching the more western side of the plateau. Restriction of this westward prograding system could have been hampered by the eastern extent Wanthaya High, which sits outside of the studied area. Sediment was diverted onto the more northwestern plateau and into the inboard sub-basins by Jurassic uplift. The limited volume of sediment supply at this time resulted in a lower sedimentation rate which coincided with the formation of accommodation in down thrown half-graben to form successive fan deposits (Chen et al., 2020). These fans often onlap the rotating fault blocks but the limited supply left fault blocks unburied.

Sea-floor spreading in the Argo oceanic basin in the J40 Oxfordian signalled a change in processes which impacted the plateau during the Upper Jurassic and into the Cretaceous. Coinciding with a reduction in supply from the east, uplift occurred to the south and supplied sediment to a shallow marine shelf, the edge of which began to migrate northwards. In the latest Jurassic, the K10 Lower Barrow Group had begun to prograde onto the Exmouth Plateau from the south (Figure 6.7). The first evidence of this change in supply is the deposition of basin floor fans which began to infill half-graben developed in the Lower and Middle Jurassic (Figures 3.22, & 6.4) but which are deposited successively. This pattern of supply occurred progressively towards the north

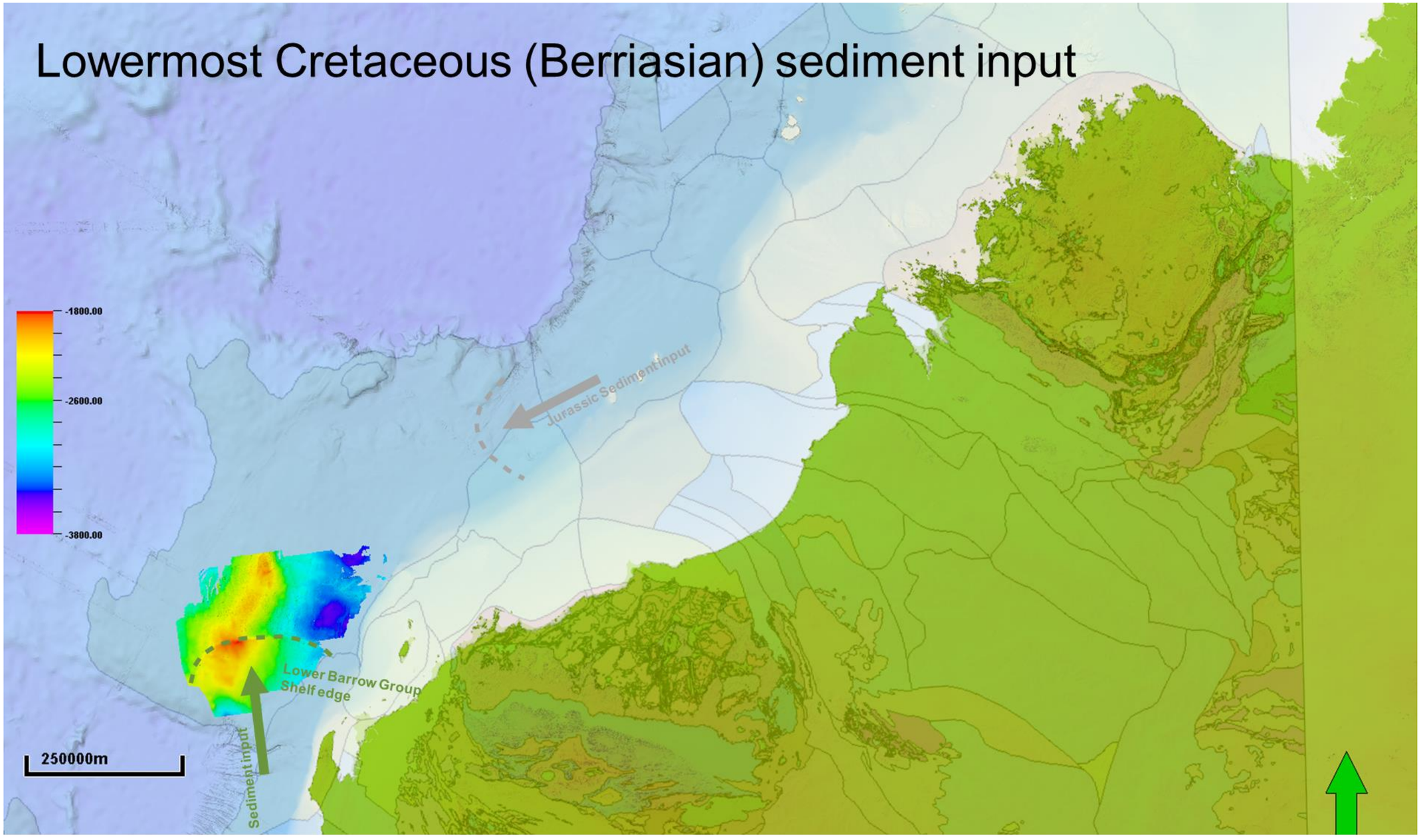

Figure 6.7 Berriasian thickness map displaying the prograding K10 Lower Barrow Group shelf edge. Regional map complied by C. Elders (2021).

along the downthrown fault blocks, which resulted in fan geometries. Sediment pathways were focused along downthrown half-graben adjacent to these uplifted fault blocks (Emery, 1980) and in relay structures (Sakai et al., 2013) or successive fan build-ups (i.e., Cullen et al., 2020 in Greece) until supply bypassed the fault blocks. The succession of fan style deposition is noted in the angular unconformities observed in many of the half-graben during the Upper Jurassic and Lowermost Cretaceous. This pattern of supply is particularly important to the area of the K10 Lower Barrow Lobe. However, the west to northwest migration of this lobe was also controlled by the increase in elevation of the outer margin (Section 6.2.3). The previously starved half-graben were successively infilled and bypassed from south to north/northeast. Infill of the eastern region was limited at this time as the mechanism for supply relied on the pathways formed by the north to northeast orientated fault blocks.

The depositional pathways of north and northeast trending fault blocks were largely infilled by the end of extensional activity. This infilling allowed the post-rift supply to bypass the strict control of the fault pathways of the underlying strata and infill the subsiding depocentre to the southeast, as well as infilling remnant topography in the west.

6.2.5. FORMATION OF A RIFTED MARGIN

6.2.5.1. RIFT DOMAINS OF THE EXMOUTH PLATEAU

The Exmouth Plateau sits close to a rifting centre, and to a failed rift, making it a mix of rifting domains, as described by (Chenin et al., 2022; Nabliboff et al., 2017; Péron-Pinvidic & Manatschal, 2010). This proximity means that the underlying thermal and magmatic processes of tectonic movement (see Manatschal et al., 2021) cannot be ignored in discussing the formation of the regions rift history. Alves et al. (2021) have discussed the complexity of magma rich rift zones. However, architecture and tectono-stratigraphic evolution of the studied portion of the plateau indicate the region is more aligned with both a proximal domain on the more inboard region and a necking domain further to the continental boundary, corresponding approximately to the area of the Investigator Sub-basin covered in this study.

The sub-horizontal nature of the basement on the more inboard plateau (AGSO North West Shelf Study Group, 1994) is in-line with the proximal domain formed in the initial stretching phase of rifted margins (Chenin et al., 2022; Nabliboff et al., 2017). The moho trend identified in the proximal to necking (distal) domains (Chenin et al., 2022; Péron-Pinvidic et al., 2013) from the inboard to outboard respectively of the general sections of the AGSO North West Shelf Study Group (1994) or to the rheology changes suggested by Gartrell (2000). The presence of magmatic input (intrusions or flows) varies across the area and are likely to impact on the resulting expression of rift domains (Alves et al., 2021; Péron-Pinvidic et al., 2013).

The highly faulted nature of the western, more oceanward, portion of the area studied (Chapter 4) support the assignment of a necking domain (Péron-Pinvidic et al., 2013). With new faults forming in the area (Nabliboff et al., 2017), and a reactivation of older structures signalling necking. The outboard margin is also uplifted on the plateau with loading driving mechanical subsidence inboard of this (Chapter 5) are suggestive of a necking domain as per Chenin et al. (2018), Manatschal et al. (2021, 2022), and McKenzie (1978). The prominence of half-graben architecture over the more western portion of the study area (Chapter 4) is in line with the characteristics of a more proximal domain (Manatschal et al., 2021, 2022; Nabliboff et al., 2017; Péron-Pinvidic et al., 2013). The relatively thin infill of Jurassic aged strata (Chapter 3) is also in line with a proximal domain (Chenin et al., 2022; Manatschal et al., 2021, 2022), although this is usually due to the reduced volume of accommodation space relative to other rifted domains. Further evidence for the proximal domain is the formation of faults to mid-depths, with some deeper (Chapter 4; Péron-Pinvidic et al., 2013). Both Uplift and subsidence continue to occur (Chapter 5) as the rift activity continues (Péron-Pinvidic et al., 2013).

7. Conclusions

The development of the Exmouth Plateau is divided into three stages; two phases of rift activity and a later phase of post-rift modification. Initial rifting commenced in the latest Triassic (TR30 Rhaetian) closer to the continent-ocean boundary and in the early Jurassic (J20 Pliensbachian) on the inboard closer to the Barrow-Dampier failed rift. This stage continued into the Middle to Upper Jurassic when rift-related activity on the plateau altered, continuing into the Lower Cretaceous. Sedimentation during the interval of rifting evolved from shallow marine carbonate shelf in the TR30 Rhaetian, into a mass-flow deep marine system in the Jurassic, with sheet-like gravity flows the half-graben formed during rift activity deposited in the uppermost Jurassic. Influx of sediments come from the south as the progradation of the continental shelf in the early Cretaceous infilling the previously starved rift architecture. The post-rift interval began in the Aptian and continued until at least the close of the Cretaceous. The onset of rifting in the TR30 Rhaetian resulted in the uplift of the outer margin, which remained elevated into the post-rift. Additional regional uplift occurred in the Lower to Middle Jurassic on the inboard portion of the plateau, adjacent to the Barrow-Dampier Rift, but was short-lived.

The aims of this study were to identify the timing of rift-related activity and their relation to geodynamics on the Exmouth Plateau, with a view to describe the sedimentary response to deep-sea rifting. The conclusions of this research are presented below and form new work, highlighting the importance of the Exmouth Plateau to uncovering the margins full tectonic history and how little we currently know of the formation of the Exmouth Plateau. In addition, this body of research highlights the implications of regional scale uplift on the formation of rifted margins.

- Faults formed on the plateau in four key orientations. The most prominent are NNE-SSW and NE-SW oriented and were active across a large proportion of the region in each of the rift stages. The NW-SE population were more limited in distribution and the E-W population only occurred as transfer faults between other populations or as a post-

depositional structure. The development of Mesozoic faults initiated as early as the TR30 Rhaetian and continued into the Cretaceous, to the time of continental separation (K20.0 SB). Some movement may have continued on a small number of faults but by this time the thickening across faults was largely related to infilling remnant topography. The orientations and timing of fault activity highlight the variation to most previous research, aligning with the statements of McHarg (2018) on the variability of fault activity in the Dampier Sub-Basin.

- Rift activity initiated much earlier than previously described by many studies, and the orientation of this activity indicates that plate motion occurred in a WNW-ESE direction rather than the NW-SE direction that is widely accepted.
    - The onset of rifting is variable across the Exmouth Plateau. Extension started in the Upper Triassic in the west –or more outboard region- of the plateau and in the Lower Jurassic further to the east.
    - Extension also continued for longer in the west, continuing on some major faults until Aptian while it ceased in the lowermost Cretaceous in the east. Greater throws are also observed towards the western margin of the plateau, decreasing landward.
    - The onset of activity is linked to the stretching of the lithosphere in the lead up to the initiation of sea-floor spreading event, but the orientation of key fault populations does not support the current model for the direction extension related to the opening of the Argo Abyssal Plain.
    - The later stage of activity (Upper Jurassic to Valanginian) represents the onset and build-up of activity in relation to the separation of Australia and Greater India.
- A key piece of basin architecture is the Jurassic aged rift flank-uplift which is associated to the Jurassic aged, failed rift of the Barrow-Dampier system. This research suggested that the development of the

rift-flank occurred during the Middle Jurassic and not during the Lower Jurassic as previously described.

  - The uplift of the Barrow-Dampier rift-flank was crucial for supply into the plateau and the development of a major depocentre, the Kangaroo-Syncline.
  - Of further interest is the limited nature of the uplift of the rift flank in comparison to other margins. The uplift on the Barrow-Dampier rift flank has been identified here as being relatively short lived (11 million years) and to reduced heights compared to other rifts (less than 1 km).
    - This suggests the failed Barrow-Dampier rift resulted in less thermal alteration to the crust and/or mantle upwelling than originally predicted.

- A second regional uplift occurred along the ocean margin to the northwest of the area studied where the Exmouth Plateau meets the Gascoyne Abyssal Plain. This uplift was long-lived, extending from the Upper Triassic to at least the end of the Cretaceous. This uplift would have contributed to the formation of the Kangaroo Syncline and the later overlying depocentre, as well as to the depocentre in the area that later became the Exmouth Plateau Arch, the Exmouth Plateau Depocentre as per this research.
  - Prolonged outer margin uplift in the area studied here, indicates that the initial mechanisms of rifting along the northwestern margin are not yet fully understood.
  - Deformation of the continent-ocean-boundary was initiated along the early spreading centres of the Gascoyne and Cuvier abyssal plains prior to the onset of sea-floor spreading in the Argo Abyssal Plain.
- Flexure of the margin was key to the formation of the primary depocentres during the poly-phase rift history.
  - Barrow-Dampier rift flank and outer margin uplift resulted in the formation of key depocentres and depositional barriers.

- A new feature, the Wanthaya High, has been identified and described in this research. Extending from the latest Jurassic into at least the Lower Cretaceous.

7.1. Further Work

As there are ample high-quality 3D and deep 2D seismic surveys available on the Exmouth Plateau there are further investigations which could continue to develop the history and understanding of this expansive region. Potential paths of investigation are listed below.

- Extension of tectono-stratigraphic framework developed in this study to other regions of the Exmouth Plateau.
- Full scale source-to-sink analysis of the region (similar to Chen et al., 2020 and Cullen et al., 2020) with particular focus on the recycling of material during key hydrocarbon source and reservoir intervals (see Chapter 2; Section 2.2.6 Hydrocarbon Potential) and the redistribution (Mondy, 2019) of the material removed during the rift-flank uplift. Examining the individual accommodation zones and the plateau as a whole.
- Analysis of the pre-Mesozoic tectonic evolution of the plateau.
    - Study of the basement terrain(s), specifically to any major lateral changes to the composition and structural expression.
- Analysis of the rift-flank uplift related to the Barrow-Dampier rift events, which would include gravity and numerical modelling to determine the timing of flank-uplift and later subsidence as well as the mechanisms of uplift.
- Analysis of the outer margin uplift and the implications this provided for the evolution of the margin.
- Complete analysis focused on a feature identified in this study; Wanthaya High. This should include a detailed interpretation of the time of formation, depositional infill, and later tilting.

- Detailed core study to identify the various Middle and Upper Jurassic events and provide greater detail of sedimentary processes and environments of deposition during this important geological interval.
    - Ideally accompanied by a detailed depositional seismic study using PaleoScan software or similar.
- Numerical modelling to better understand geodynamic controls on uplift and application of this to other rifted continental margins.
    - Including in-depth modelling of the short-lived Barrow-Dampier rift flank, and the persistent uplift of the outer margin.
- In-depth fault throw, heave, and dip study over the plateau.
- Investigation on the limitation of the progression of the Legendre system into the area studied here, from its source in the east.

8. References

Adamson, K.R., Lang, S.C., Marshall, N.G., Seggie, R.J., Adamson, N.J., & Bann, K.L. (2013). *Understanding the Late Triassic Mungaroo and Brigadier Deltas of the Northern Carnarvon Basin, North West Shelf, Australia* [Paper presentation]. West Australian Basins Symposium, Perth, Western Australia.

Aanyu, K., & Koehn, D. (2011). Influence of pre-existing fabrics on fault kinematics and rift geometry of interacting segments: analogue models based on the Albertine Rift (Uganda), Western Branch-East African Rift System. *Journal of African Earth Sciences*, 59(2-3), 168-184.

AGSO North West Shelf Study Group. (1994). *Deep reflections on the North West Shelf: changing perceptions of basin formation.* In The Sedimentary Basins of Western Australia, Proceedings of Petroleum Exploration Society of Australia Symposium, Perth.

Allen, P.A. (2008). From landscapes into geological history. *Nature* 451 (7176), 274–276.

Allen, P.A., & Allen, J.R. (2013). *Basin analysis: Principles and applications*. Third ed. Blackwell Science Ltd., Oxford.

Alves, T., Fetter, M., Busby, C., Gontijo, R., Cunha, T.A., & Mattos, N.H. (2020). A tectono-stratigraphic review of continental breakup on intraplate continental margins and its impact on resultant hydrocarbon systems. *Marine and Petroleum Geology*, 117, 104341.

Alves, T.M., Tugend, J., Holford, S., Bertoni, C., & Li, W. (2021). Continental margins unleashed-From their early inception to continental breakup. *Marine and Petroleum Geology*, 129, 105097.

Anfiloff, V. (1988). *Polycyclic rifting-an interpretation of gravity and magnetics in the North West Shelf* [Paper presentation]. The Sedimentary Basins of Western Australia, Petroleum Exploration Society of Australia Symposium, Perth.

Angelier, J. (1984). Tectonic analysis of fault slip data sets. J. Geophys. Res. Solid Earth 89 (B7), 5835–5848.

Arditto, P.A. (1993). Depositional sequence model for the post-Barrow Group Neocomian succession, Barrow and Exmouth sub-basins, Western Australia. *The APPEA Journal,* 33(1), 151-160.

Audley-Charles, M.G. (1988). *Evolution of the southern margin of Tethys (North Australian region) from early Permian to late Cretaceous.* Geological Society of London, Special Publication 37 (1), 79-100.

Bagas, L. (2004). Proterozoic evolution and tectonic setting of the northwest Paterson Orogen, Western Australia. *Precambrian Research*, 128(3-4), 475-496.

Bai, Y., Wang, X., Dong, D., Brune, S., Wu, S., & Wang, Z. (2020). Symmetry of the South China Sea conjugate margins in a rifting, drifting and collision context. *Marine and Petroleum Geology*, 117, 104397.

Bailey, A.H., King, R.C., Holford, S.P., & Hand, M. (2016). Extending interpretations of natural fractures from the wellbore using 3D attributes: The Carnarvon Basin, Australia. *Interpretation*, 4(1), SB107-SB129.

Baillie, P.W., & Jacobson, E.P. (1997). Prospectivity and exploration history of the Barrow Sub-basin, Western Australia. *The APPEA Journal*, 37(1), 117-135.

Baillie, P.W., Powell, C.M., Li, Z.X., & Ryall, A.M. (1994). *The tectonic framework of Western Australia's Neoproterozoic to Recent sedimentary basins* [Paper presentation]. The Sedimentary Basins of Western Australia: Proceedings of the Petroleum Exploration Society of Australia Symposium, Perth.

Barber, P. (1988). *The Exmouth Plateau Deepwater Frontier* [Paper presentation]. Proceedings of the Petroleum Exploration Society of Australia Symposium, Perth.

Barrett, B.J., Hodgson, D.M., Jackson, C.A.L., Lloyd, C., Casagrande, J., & Collier, R.E.L. (2021). Quantitative analysis of a footwall-scarp

degradation complex and syn-rift stratigraphic architecture, Exmouth Plateau, NW Shelf, offshore Australia. *Basin Research,* 33(2), 1135-1169.

Bastia, R., & Radhakrishna, M. (2012). Basin evolution and petroleum prospectivity of the continental margins of India, *Newnes* 59.

Bauer, J.A., Hooper, E.C.D., & Crowley, J. (1994). *The Leatherback Discovery, Carnarvon Basin*.

Beaumont, C., & Ings, S. J. (2012). Effect of depleted continental lithosphere counterflow and inherited crustal weakness on rifting of the continental lithosphere: General results. *Journal of Geophysical Research: Solid Earth*, 117(B8).

Beaumont, C., Keen, C.E., & Boutilier, R. (1982). On the evolution of rifted continental margins: Comparison of models and observations for the Nova Scotian margin: *Royal Astronomical Society Geophysical Journal*, 70, 667-715.

Begg, J. (1987), Structuring and controls on Devonian reef development on the northwest Barbwire and adjacent terraces, Canning Basin. *The APEA Journal*, 27(1).137-51.

Belgarde, C., Manatschal, G., Kusznir, N., Scarselli, S., & Ruder, M. (2015). Rift processes in the Westralian Superbasin, North West Shelf, Australia: insights from 2D deep reflection seismic interpretation and potential fields modelling. *The APPEA Journal*, 55(2), 400-400.

Bentley, J. (1988). *The Candace Terrace-a geological perspective*.

Bernard , S., Avouac, J.P., Dominguez, S., & Simoes, M. (2007). Kinematics of fault-related folding derived from a sandbox experiment. Journal of Geophysical Research: *Solid Earth*, 112(B3).

Bhattacharya, J.P., Copeland, P., Lawton, T.F., & Holbrook, J. (2016). Estimation of source area, river paleo-discharge, paleoslope, and sediment budgets of linked deep-time depositional systems and

implications for hydrocarbon potential. *Earth Science Review*, 153, 77-110.

Bilal, A., & McClay, K. (2022). Tectonic and stratigraphic evolution of the central Exmouth Plateau, NW Shelf of Australia. *Marine and Petroleum Geology* 136, 105447.

Bilal, A., McClay, K., & Scarselli, N. (2018). *Fault-scarp degradation in the central Exmouth Plateau, North West Shelf, Australia*. Geological Society, London, Special Publications, 476(1), 231-257.

Bishop, M.G. (1999). *Total Petroleum Systems of the Northwest Shelf, Australia: The Dingo-Mungaroo/Barrow and the Locker-Mungaroo/Barrow* (No. 99-50-E). Geological Survey (US).

Black, M., McCormack, K.D., Elders, C., & Robertson, D. (2017). Extensional fault evolution within the Exmouth Sub-basin, North West Shelf, Australia. *Marine and Petroleum Geology*, 85, 301-315.

Blaich, O.A., Faleide, J.I., & Tsikalas, F. (2011). Crustal breakup and continent-ocean transition at South Atlantic conjugate margins. *Journal of Geophysical Research: Solid Earth*, 116(B1).

Blevin, J.E., Stephenson, A.E., & West, B.G. (1994). *Mesozoic structural development of the Beagle Sub-basin—implications for the petroleum potential of the Northern Carnarvon Basin* [Paper presentation]. The Sedimentary Basins of Western Australia 1: Proceedings of the Petroleum Exploration Society of Australia Symposium, Perth.

Blevin, J.E., Struckmeyer, H.I.M., Cathro, D.L., Totterdell, J.M., Boreham, C.J., Romine, K.K., Loutit, T.S., & Sayers, J. (1998). *Tectonostratigraphic framework and petroleum systems of the Browse Basin, North West Shelf*. In Purcell, P.G., & Purcell, R.R., (Eds), The Sedimentary Basins of Western Australia 2: Proceedings of the Petroleum Exploration Society of Australia, Perth.

Bulnes, M., & McClay, K.R. (1998). Structural analysis and kinematic evolution of the inverted central South Celtic Sea Basin. *Marine and Petroleum Geology*, 15(7), 667-687.

Boillot, G. (1979). *Geology of continental margins*. Masson.

Bonali, F.L., Tibaldi, A., Mariotto, F.P., & Russo, E. (2018). Interplay between inherited rift faults and strike-slip structures: Insights from analogue models and field data from Iceland. *Global and Planetary Change*, 171, 88-109.

Bonali, F.L., Tibaldi, A., Mariotto, F.P., Saviano, D., Meloni, A., & Sajovitz, P. (2019). Geometry, oblique kinematics and extensional strain variation along a diverging plate boundary: The example of the northern Theistareykir Fissure Swarm, NE Iceland. *Tectonophysics*, 756, 57-72.

Bond, G.C., Nickeson, P.A., & Kominz, M.A. (1984). Breakup of a supercontinent between 625 Ma and 555 Ma: new evidence and implications for continental histories. *Earth and Planetary Science Letters*, 70(2), 325-345.

Bosworth, W. (1985), Geometry of propagating continental rifts: *Nature*, v. 315, p. 625-627.

Bott, M.H.P. (1971). Evolution of young continental margins and formation of shelf basins. *Tectonophysics*, 11(5), 319-327.

Bott, M.H.P. (1993). Modelling the plate-driving mechanism. *Journal of the Geological Society* 150, 941–951.

Boyd, R., Ruming, K., Goodwin, I., Sandstrom, M., & Schröder-Adams, C. (2008). Highstand transport of coastal sand to the deep ocean: a case study from Fraser Island, southeast Australia. *Geology* (Boulder) 36 (1), 15–18.

Boyd, R., Williamson, P., & Haq, B.U. (1992). *Seismic stratigraphy and passive-margin evolution of the southern Exmouth Plateau* [Paper presentation]. Proceedings of the ODP, Science Results: Ocean Drilling Program, College Station, Texas.

Brownfield, M.E., & Charpentier, R.R. (2006). *Geology and Total Petroleum Systems of the West-Central Coastal Province (7203), West Africa.* U.S. Geological Survey Bulletin 2207-B.

Buck, W.R. (1986). Small-scale convection induced by passive rifting: the cause for uplift of rift shoulders. *Earth and Planetary Science Letters*, 77 (3–4), 362–372.

Bulnes, M., & McClay, K.R. (1998). Structural analysis and kinematic evolution of the inverted central South Celtic Sea Basin. *Marine and Petroleum Geology*, 15(7), 667-687.

Burke, K., & J.F. Dewey. (1973). Plume-generated triple junctions: Key indicators in applying plate tectonics to old rocks, *Journal of Geology*, 81, 406–433.

Bradshaw, M. (1993). Australian petroleum systems. *PESA Journal*, 21, 43–53.

Bradshaw, M.T., Bradshaw, J., Murray, A.P., Needham, D. J., Spencer, L., Summons, R.E., Wilmot, J., & Winn, S. (1994). *Petroleum systems in West Australian basins* [Paper presentations]. The sedimentary basins of Western Australia. Proceedings of a PESA Symposium, Perth, Western Australia.

Bradshaw, M., Edwards, D., Bradshaw, J., Foster, C., Loutit, T., McConachie, B., Moore, A., Murray, A.P., & Summons, R. (1997). *Australian and Eastern Indonesian petroleum systems* [Paper presentation]. Proceedings of the Conference on Petroleum Systems of SE Asia and Australasia, Indonesian Petroleum Association, Jakarta, Indonesia.

Bradshaw, J., Sayers, J., Bradshaw, M., Kneale, R., Ford, C., Spencer, L., & Lisk, M. (1998). *Palaeogeography and its impact on the petroleum systems of the North West Shelf, Australia* [Paper presentation]. The Sedimentary Basins of Western Australia 2: Proceedings of West Australian Basins Symposium, Perth, Western Australia.

Bradshaw, M.T., Yeates, A.N., Beynon, R.M., Brakel, A.T., & Langford, R.P. (1988). *Paleogeographic evolution of the North West Shelf region* [Paper presentation]. The Sedimentary Basins of Western Australia 2: Proceedings of West Australian Basins Symposium, Perth, Western Australia.

Brandes, C., & Tanner, D.C. (2014). Fault-related folding: A review of kinematic models and their application. *Earth-Science Reviews*, 138, 352-370.

Braun, J., & Beaumont, C. (1989). A physical explanation of the relation between flank uplifts and the breakup unconformity at rifted continental margins. *Geology*, 17(8), 760-764.

Brune, S., Heine, C., Pérez-Gussinyé, M., & Sobolev, S.V. (2014). Rift migration explains continental margin asymmetry and crustal hyper-extension. *Nature Communications* 5.

Brune, S., Popov, A.A., Sobolev, S.V. (2012). Modeling suggests that oblique extension facilitates rifting and continental break-up. *Journal of Geophysical Research: Solid Earth* 117.

Burov, E., & Cloetingh, S.A.P.L. (1997). Erosion and rift dynamics: new thermomechanical aspects of post-rift evolution of extensional basins. *Earth and Planetary Science Letters* 150, 7–26.

Cameron, N., Bate, R., Clure, V., & Benton, J. (1999). *Oil and gas habitats of the South Atlantic: Introduction.* Geological Society, London, Special Publications 153, 1–9.

Cartwright, J.A. (1987). *Transverse structural zones in continental rifts-an example from the Danish Sector of the North Sea.* In Conference on petroleum geology of North West Europe. 3.

Cartwright, J.A., Trudgill, B.D., Mansfield, C.S. (1995). Fault growth by segment linkage: an explanation for scatter in maximum displacement and trace length data from the Canyonlands Grabens of SE Utah. *Structural Geology*, 17(9), 1319-1326.

Carvajal, C., & Steel, R. (2009). Shelf-Edge architecture and bypass of sand to deep water: influence of shelf-edge processes, sea level, and sediment supply. *Journal of Sedimentary Research*, 79 (9), 652–672.

Cathro, D.L., & Karner, G.D. (2006). Cretaceous–Tertiary inversion history of the Dampier Sub-Basin, Northwest Australia: insights from quantitative basin modelling. *Marine and Petroleum Geology*, 23(4), 503-526.

Chalmers, J.A., Pulvertaft, T.C.R., Christiansen, F.G., Larsen, H.C., Laursen, K.H., & Ottesen, T.G. (1993). *The southern West Greenland continental margin: rifting history, basin development, and petroleum potential.* In Geological Society, London, Petroleum Geology Conference series, 4(1), Geological Society of London.

Chapin, C.E., Chamberlin, R.M., Osburn, G.R., White, D.W., & Sanford, A.R. (1978). *Exploration framework of the Socorro geothermal area, New Mexico. Field guide to selected cauldrons and mining districts of the Datil–Mogollon volcanic field, New Mexico*: New Mexico Geological Society, Special Publication, 7, 115-129.

Chen, P. (2018). *Tectonostratigraphic Evolution of the Roebuck Basin and the northeast area of the Northern Carnarvon Basin, North West Shelf, Australia* [Doctoral dissertation, Curtin University].

Chen, H., Wood, L.J., & Gawthorpe, R.L. (2021). Sediment dispersal and redistributive processes in axial and transverse deep-time source-to-sink systems of marine rift basins: Dampier Sub-basin, Northwest Shelf, Australia. *Basin Research*, 33(1), 227-249.

Chenin, P., Manatschal, G., Ghienne, J.F., & Chao, P. (2022). The syn-rift tectono-stratigraphic record of rifted margins (Part II): A new model to break through the proximal/distal interpretation frontier. *Basin Research*, 34(2), 489-532.

Chenin, P., Manatschal, G., Picazo, S., Müntener, O., Karner, G., Johnson, C., & Ulrich, M. (2017). Influence of the architecture of magma-poor

hyperextended rifted margins on orogens produced by the closure of narrow versus wide oceans. *Geosphere*, 13(2), 559-576.

Chenin, P., Schmalholz, S.M., Manatschal, G., & Karner, G.D. (2018). Necking of the lithosphere: A reappraisal of basic concepts with thermo-mechanical numerical modeling. *Journal of Geophysical Research: Solid Earth*, 123(6), 5279-5299.

Chery, J., Lucazeau, F., Daignieres, M., & Vilotte, J.P. (1992). Large uplift of rift flanks: A genetic link with lithospheric rigidity? *Earth and Planetary Science Letters*, 112(1-4), 195-211.

Chester, J.S., & Chester, F.M. (1990). Fault-propagation folds above thrusts with constant dip. *Journal of Structural Geology*, 12(7), 903-910.

Chiarella, D., Capella, W., Longhitano, S.G., & Muto, F. (2021). Fault-controlled base-of-scarp deposits. *Basin Research,* 33(2), 1056-1075.

Clerc, C., Ringenbach, J.C., Jolivet, L., & Ballard, J.F. (2018). Rifted margins: ductile deformation, boudinage, continentward-dipping normal faults and the role of the weak lower crust. *Gondwana Research*, 53, 20–40.

Clifton, A.E., Schlische, R.W., Withjack, M.O., Ackermann, R.V. (2000). Influence of rift obliquity on fault-population systematics: results of experimental clay models. *Journal of Structural Geology*, 22, 1491–1509.

Cloetingh, S., Burov, E., Matenco, L., Beekman, F., Roure, F., & Ziegler, P.A. (2013). The Moho in extensional tectonic settings: Insights from thermo-mechanical models. *Tectonophysics*, 609, 558-604.

Cochran, J.R. (1983). Effects of finite rifting times on the development of sedimentary basins. *Earth and Planetary Science Letters,* 66, 289-302.

Colwell, E.B., Exon, N.F., Hill, R.J., O'Brien, G.W., Pigrim, C.J., Ramsey, D.C., Stagg, H.M.J., Struckmeyer, H.I.M., Symonds, P.S. & Willcox, J.B. (1993). *Regional deep seismic of the North West Shelf* [Paper presentation]. Second Australian Geological Survey Organisation

Petroleum Group Seminar, Australian Geological Survey Organisation Record no. 1993/83.

Cohen, K.M., Finney, S.M., Gibbard, P.L., & Fan, J.-X. (2013). The ICS International Chronostratigraphic Chart. *Episodes* 36, 199-204.

Cohen, K.M., Harper, D.A.T., & Gibbard, P.L. (2022). *ICS International Chronostratigraphic Chart 2022/10*. International Commission on Stratigraphy, IUGS.

Condon, M.A. (1967a). The Geology of the Carnarvon Basin, Western Australia, Part 2: Permian stratigraphy: *Australia Bureau of Mineral Resources, Bulletin*, 77

Condon, M.A. (1967b). The Geology of the Carnarvon Basin, Western Australia, Part 3: Post-Permian stratigraphy; structure; economic geology: *Australia Bureau of Mineral Resources, Bulletin*, 77.

Cook, P.J., & Carleton, C.M. (2000). *Continental Shelf Limits: the Scientific and Legal Interface.* Oxford University Press, Oxford, New York, pp. 1–324.

Corti, G. (2009). Continental rift evolution: from rift initiation to incipient break-up in the Main Ethiopian Rift, East Africa. *Earth-Science Reviews*, 96(1-2), 1-53.

Corti, G. (2012). Evolution and characteristics of continental rifting: Analog modeling-inspired view and comparison with examples from the East African Rift System. *Tectonophysics* 522–523.

Crossley, R. (1979). The Cenozoic stratigraphy and structure of the western part of the Rift Valley in southern Kenya. *Journal of the Geological Society*, 136(4), 393-405.

Cullen, T.M., Collier, R.E.L., Gawthorpe, R.L., Hodgson, D.M., & Barrett, B.J. (2020). Axial and transverse deep-water sediment supply to syn-rift fault terraces: Insights from the West Xylokastro Fault Block, Gulf of Corinth, Greece. *Basin Research*, 32(5), 1115-1149.

Czarnota, K. (2009). *Tectonostratigraphic history of the Western Exmouth Sub-basin, NW Shelf, Western Australia* [Doctoral dissertation, Royal Holloway, University of London].

Daradich, A., Mitrovica, J.X., Pysklywec, R.N., Willett, S.D., & Forte, A.M. (2003). Mantle flow, dynamic topography, and rift-flank uplift of Arabia. *Geology*, 31(10), 901-904.

Davis, M., & Kusznir, N. (2004). 4. *Depth-dependent lithospheric stretching at rifted continental margins.* In: Rheology and Deformation of the Lithosphere at Continental Margins. Columbia University Press, pp. 92–137.

Davis, J.K., & Lavier, L.L. (2017). Influences on the development of volcanic and magmapoor morphologies during passive continental rifting. *Geosphere* 13, 1524–1540.

de Gromard, R.Q., Kirkland, C.L., Howard, H.M., Wingate, M.T., Jourdan, F., McInnes, B.I., Danišík, M., Evans N.J., McDonald, B.J., & Smithies, R.H. (2019). When will it end? Long-lived intracontinental reactivation in central Australia. *Geoscience Frontiers*, 10(1), 149-164.

Dewey, J.F., & Bird, J. M. (1970). Mountain belts and the new global tectonics. *Journal of Geophysical Research*, 75(14), 2625-2647.

Dooley, T., & McClay, K. (1997). Analog modeling of pull-apart basins. *AAPG Bulletin*, 81(11), 1804-1826.

Driscoll, N., & Karner, G.D. (1996). *Tectonic and stratigraphic evolution of the Carnarvon Basin, northwest Australia.* Minerals and Energy Research Institute of Western Australia.

Driscoll, N.W., & Karner, G.D. (1998). Lower crustal extension across the Northern Carnarvon basin, Australia: Evidence for an eastward dipping detachment. *Journal of Geophysical Research: Solid Earth*, 103(B3), 4975-4991.

Drummond, B.J., Sexton, M.J., Barton, T.J. & Shaw, R.D. (1991). The nature of faulting along the margins of the Fitzroy Trough, Canning Basin, and

implications for the tectonic development of the trough. *Exploration Geophysics*, 22, lll-16.

Duncan, R.A., Larsen, H.C., Allan, & J.F. Editors (1996). *Proceedings of the Ocean Drilling Program. Ocean Drilling Program,* Texas A and M University, College Station, TX.

Edwards, D.S., & Zumberge, J.E. (2005). *The Oils of Western Australia II. Regional Petroleum Geochemistry and Correlation of Crude Oils and Condensates from Western Australia and Papua New Guinea.* Geoscience Australia, Canberra and GeoMark Research Ltd, Houston. Geoscience Australia Report, 37512.

Edwards, D.S., Zumberge, J.E., Boreham, C., Kennard, A.B., & Bradshaw, M.T. (2007). *Petroleum systems and supersystems of the Australian Northwest Shelf: a geochemical approach* [Paper presentation]. International conference on Emerging plays in Australasia, London, United Kingdom.

Elders, C., Morón, S., Zahirovic, S., Müller, D., Rey, P., l'Anson, A., Chen, P., Rohead-O'Brien, H., McHarg, S., Fletcher, Z., Abbott, S., Nicholson, C., Orlov, C., & Rollett, N. (Unpublished). Continental margin response to polyphase rifting: the North West Shelf of Australia.

Elders, C., McHarg, S., & l'Anson, A. (2016). Fault geometry and deformation history, Northern Carnarvon Basin. *ASEG Extended Abstracts*, (1), 1-3.

Eldholm, O., Thiede, J., & Taylor, E. (1989). *Evolution of the vøring volcanic margin.* In: Proceedings of the Ocean Drilling Program. Scientific Results, vol. 104. Ocean Drilling Program, Texas A and M University, College Station, TX.

Erslev, E.A. (1991). Trishear fault-propagation folding. *Geology* 19, 617–620.

Emery, K.O. (1980). Continental margins—classification and petroleum prospects. *AAPG Bulletin*, 64(3), 297-315.

Emery, D., & Myers, K. (Eds.). (2009). *Sequence stratigraphy.* John Wiley & Sons.

Etheridge, M.A., & O'Brien, G.W. (1994). Structural and tectonic evolution of the Western Australian margin basin system. *PESA Journal*, 22, 45-63.

Etheridge, M.A., McQueen, H. & Lambeck, K. (1991). The role of intraplate stress in Tertiary (and Mesozoic) deformation of the Australian continent and its margins: a key factor in petroleum trap formation. *Exploration Geophysics,* 22, 123-28.

Etheridge, M.A., & Wall, V. (1994). *Tectonic and structural evolution of the Australian Proterozoic* [Paper Presentation]. Geological Society of Australia Abstracts, 37.

Exon, N.F., & Buffler, R.T. (1992). *Mesozoic seismic stratigraphy and tectonic evolution of the western Exmouth Plateau* [Paper presentation]. Proceedings of the Ocean Drilling Program (ODP), Scientific Results 122.

Exon, N.F., Von Rad, U., & Von Stackelberg, U. (1982). The geological development of the passive margins of the Exmouth Plateau off northwest Australia. *Marine Geology*, 47(1-2), 131-152.

Exon, N.F., & Von Rad, U. (1994). *The Mesozoic and Cainozoic sequences of the northwest Australian margin*, *as revealed by ODP core drilling and related studies.*

Exon, N.F., & Willcox, J.B. (1978). Geology and petroleum potential of Exmouth Plateau area off Western Australia. *AAPG Bulletin*, 62(1), 40-72.

Exon, N.F. & Willcox, J.B. (1980). *The Exmouth Plateau: Stratigraphy, structure and petroleum potential.* Bureau of Mineral Resources Bulletin, 199.

Falvey, D.A. (1974). The development of continental margins in plate tectonic theory. The APPEA Journal, 14(1), 95-106.

Falvey, D.A., & Mutter, J. C. (1981). Regional plate tectonics and the evolution of Australia's passive continental margins. *BMR Journal of Australian Geology and Geophysics*, 6(1), 1-29.

Felton, E.A., Miyazaki, S., Dowling, L., Pain, L., Vuckovic, V., & le Poidevin, S.R. (1992). *Carnarvon basin.* Bureau of Resource Sciences, Australian Petroleum Accumulations Report 8.

Fletcher, R.C., & Hallet, B. (1983). Unstable extension of the lithosphere: A mechanical model for basin-and-range structure. *Journal of Geophysical Research: Solid Earth*, 88(B9), 7457-7466.

Fontes, S.L., Benevides, A., Panetto, L., Maurya, V.P., La Terra, E.F., & Padilha, A. (2022). *Deep images of electrical conductivity in Parnaiba basin-NE Brazil* (No. EGU22-6586). Copernicus Meetings.

Forman, D.J., & Wales, D.W. (1981). *Geological evolution of the Canning Basin, Western Australia.* Geology and Geophysics Bulletin, Bureau of Mineral Resources, 210.

Forman, D.J., Wales, D.W., & Burne, R.V. (1981). *Geological evolution of the Canning Basin, Western Australia (Bulletin).* Department of National Development and Energy, Bureau of Mineral Resources, Geology and Geophysics.

Forsyth, D.W., & Uyeda, S. (1975). On the relative importance of the driving forces of plate motion. *Geophysical Journal of the Royal Astronomical Society* 43, 163–200.

Fossen, H., & Rotevatn, A. (2016). Fault linkage and relay structures in extensional settings—A review*. Earth-Science Reviews*, 154, 14-28.

Franke, D. (2013). Rifting, lithosphere breakup and volcanism: Comparison of magma-poor and volcanic rifted margins. *Marine and Petroleum Geology*, 43, 63-87.

Frizon de Lamotte, D., Fourdan, B., Leleu, S., Leparmentier, F., & de Clarens, P. (2015). Style of rifting and the stages of Pangea breakup. *Tectonics*, 34(5), 1009-1029.

Fyfe, W.S., & Leonardos, O.H. (1973). Ancient metamorphic-migmatite belts of the Brazilian African Coasts. *Nature* 224 (5417), 501–502.

Gaina, C., & Müller, R.D. (2007). Cenozoic tectonic and depth/age evolution of the Indonesian gateway and associated back-arc basins. *Earth Science Review*, 83 (3–4), 177–203.

Gartrell, A.P. (2000). Rheological controls on extensional styles and the structural evolution of the Northern Carnarvon Basin, North West Shelf, Australia. *Australian Journal of Earth Sciences*, 47(2), 231-244.

Gartrell, A., Keep, M., van der Riet, C., Paterniti, L., Ban, S., & Lang, S. (2022). Hyperextension and polyphase rifting: Impact on inversion tectonics and stratigraphic architecture of the North West Shelf, Australia. *Marine and Petroleum Geology*, 139, 105594

Gauchery, T., Rovere, M., Pellegrini, C., Cattaneo, A., Campiani, E., & Trincardi, F. (2021). Factors controlling margin instability during the plio-quaternary in the Gela basin (strait of Sicily, Mediterranean Sea). *Marine and Petroleum Geology*, 123, 104767.

Geoscience Australia. (2014a). Regional Geology of the Northern Carnarvon Basin, Offshore petroleum exploration acreage release, Australia. http://www.petroleum-acreage.gov.au/files/files/2014/documents/regional-geology/Regional_Geology-Northern_Carnarvon.pdf

Geoscience Australia. (2014b). Release areas W14-8, W14-9. W14-10, W14-11, W14-12, W14-13 and W14-22, Exmouth Plateau, Northern Carnarvon Basin Western Australia. http://www.petroleum-acreage.gov.au/files/files/2014/documents/geology/Geology-Exmouth_Plateau.pdf

Geoscience Australia. (2015). Regional Geology of the Northern Carnarvon Basin, Offshore Petroleum Exploration Acreage Release, Australia. http://www.petroleum-acreage.gov.au/2015/geology/northern-carnarvon-basin/geology

Geoscience Australia. (2019). Regional Geology of the Northern Carnarvon Basin, Offshore petroleum exploration acreage release, Australia. https://www.ga.gov.au/scientific-topics/energy/province-sedimentary-basin-geology/petroleum/acreagerelease/northerncarnarvon

Geoscience Australia. (2022). *Regional Geology of the Northern Carnarvon Basin.*

Gernigon, L., Blischke, A., Nasuti, A., & Sand, M. (2014). *Conjugate volcanic rifted margins, spreading and micro-continent: Lessons from the Norwegian-Greenland Sea*. In AGU Fall Meeting Abstracts (Vol. 2014, pp. T53B-4671).

Gernigon, L., Brönner, M., Roberts, D., Olesen, O., Nasuti, A., & Yamasaki, T. (2014). Crustal and basin evolution of the southwestern Barents Sea: From Caledonian orogeny to continental breakup. *Tectonics*, 33(4), 347-373.

Gibbons, A.D., Barckhausen, U., Van Den Bogaard, P., Hoernle, K., Werner, R., Whittaker, J.M., & Müller, R.D. (2012). Constraining the Jurassic extent of Greater India: Tectonic evolution of the West Australian margin. *Geochemistry, Geophysics, Geosystems*, 13(5).

Gibbons, A.D., Whittaker, J.M., & Müller, R.D. (2013). The breakup of East Gondwana: Assimilating constraints from Cretaceous ocean basins around India into a best-fit tectonic model. *Journal of Geophysical Research: Solid Earth,* 118, 808–822.

Gibbons, A.D., Zahirovic, S., Müller, R.D., Whittaker, J.M., & Yatheesh, V. (2015). A tectonic model reconciling evidence for the collisions between India, Eurasia and intra-oceanic arcs of the central-eastern Tethys. *Gondwana Research,* 28(2), 451-492.

Gilchrist, A.R., & Summerfield, M.A. (1994). *Tectonic models of passive margin evolution and their applications for theories of long term landscape development.* In: Kirkby (Ed.), Process Models and Theoretical Geomorphology. John Wiley and Sons, London.

Gillard, M., Autin, J., & Manatschal, G. (2016). Fault systems at hyper-extended rifted margins and embryonic oceanic crust: structural style, evolution and relation to magma. *Marine and Petroleum Geology*, 76, 51–67.

Gillard, M., Autin, J., Manatschal, G., Sauter, D., Munschy, M., & Schaming, M. (2015). Tectonomagmatic evolution of the final stages of rifting along the deep conjugate Australian-Antarctic magma-poor rifted margins: constraints from seismic observations. *Tectonics* 34 (4), 753–783.

Gillard, M., Tugend, J., Müntener, O., Manatschal, G., Karner, G.D., Autin, J., & Ulrich, M. (2019). The role of serpentinization and magmatism in the formation of decoupling interfaces at magma-poor rifted margins. *Earth Science Review,* 196, 102882.

Goldfarb, R.J., Taylor, R.D., Collins, G.S., Goryachev, N.A., & Orlandini, O.F. (2014). Phanerozoic continental growth and gold metallogeny of Asia. Gondwana Res. 25 (1), 48–102.

Gomez-Romeu, J., Kusznir, N., Roberts, A., & Manatschal, G. (2020). Measurements of the extension required for crustal breakup on the magma-poor Iberia-Newfoundland conjugate margins. *Marine and Petroleum Geology,* 118, 104403.

Goodwin, I.D., Mortlock, T.R., & Browning, S. (2016). Tropical and extratropical-origin storm wave types and their influence on the East Australian longshore sand transport system under a changing climate. *Journal of Geophysical Research: Oceans,* 121 (7), 4833–4853.

Gourlan, A.T., Meynadier, L., & Allègre, C.J. (2008). Tectonically driven changes in the Indian Ocean circulation over the last 25 Ma: neodymium isotope evidence. *Earth Planetary Science Letters,* 267 (1), 353–364.

Gradstein, F., & Ludden, L. (1992). *Radiometric age determinations for basement from Sites 765 and 766, Argo Abyssal Plain and northwestern Australian margin* [Paper presentation]. Proceedings of

the ODP, Science Results: Ocean Drilling Program, College Station, Texas.

Grain, S.L., Peace, W.M., Hooper, E.C.D., McCartain, E., Massara, P.J., Marshall, N.G., & Lang, S.C. (2013). *Beyond the deltas: late Triassic isolated carbonate build-ups on the Exmouth Plateau, Carnarvon Basin, Western Australia* [Paper presentation]. The Sedimentary Basins of Western Australia 4: Proceedings of the Petroleum Exploration Society of Australia Symposium, Perth, Western Australia.

Grantz, A., & May, S. D. (1982). *Rifting History and Structural Development of the Continental Margin North of Alaska: Rifted Margins: Field Investigations of Margin Structure and Stratigraphy.*

Grasemann, B., & Stuwe, K. (2011). Tectonics and Geodynamics. *Environmental and Engineering Geology*, II, 39.

Grotzinger, J., & Jordan, T.H. (2007). *Understanding Earth.* Freeman.

Gueydan, F., & J. Précigout. (2014), Modes of continental rifting as a function of ductile strain localization in the lithospheric mantle, *Tectonophysics,* 612, 18–25.

Gunn, P.J. (1988). *Bonaparte Basin: evolution and structural framework* [Paper presentation]. The North West Shelf, Australia. Proceedings of Petroleum Exploration Society Australia Symposium, Perth, Western Australia.

Haile, N.S. (1987). Time and age in geology: the use of Upper/Lower, late/early in stratigraphic nomenclature. *Marine and Petroleum Geology,* 4(3), 255-257.

Hall, R. (2012). Late Jurassic–Cenozoic reconstructions of the Indonesian region and the Indian Ocean. *Tectonophysics,* 570, 1-41.

Handy, M.R. (1989). Deformation regimes and the rheological evolution of fault zones in the lithosphere: the effects of pressure, temperature, grainsize and time. *Tectonophysics,* 163(1-2), 119-152.

Haq, B.U., Boyd, R.L., Exon, N.F., & Von Rad, U. (1992). *Evolution of the central Exmouth Plateau: a post-drilling perspective* [Paper presentation]. Proceedings of the ODP, Science Results: Ocean Drilling Program, College Station, Texas.

Harris, P.T. (1988). Large-scale bedforms as indicators of mutually evasive sand transport and the sequential infilling of wide-mouthed estuaries. *Sedimentary Geology*, 57 (3), 273–298.

Hearty, D.J., Ellis, G.K., & Webster, K.A. (2002). *Geological history of the western Barrow Sub-basin: implications for hydrocarbon entrapment at Woollybutt and surrounding oil and gas fields.*

Heezen, B.C. (1960). Geologic mapping of submerged continental margins. *AAPG Bulletin*, 44 (7), 1250-1250.

Heine, C., & Müller, R.D. (2005). Late Jurassic rifting along the Australian North West Shelf: margin geometry and spreading ridge configuration. *Australian Journal of Earth Sciences,* 52(1), 27-39.

Heine, C., Müller, R.D., & Gaina, C. (2004). Reconstructing the lost eastern Tethys Ocean basin: convergence history of the SE Asian margin and marine gateways. Continent-ocean interactions within East Asian Marginal Seas. *Geophysics Monograph Series,* 149, 37–54.

Heine, C., Zoethout, J., & Müller, R.D. (2013). Kinematics of the South Atlantic rift. *Journal of Geophysical Research, Solid Earth* 4, 215–253.

Helland-Hansen, W., & Martinsen, O.J. (1996). Shoreline trajectories and sequence description of variable depositional-dip scenarios. *Journal of Sedimentary Research,* 66 (4), 670–688.

Hengesh, J.V., & Whitney, B.B. (2014). *Quaternary reactivation of Australia's western passive margin: Inception of a new plate boundary* [Paper presentation]. International Union for Quaternary Research (INQUA) Focus Group on Paleo seismology and Active Tectonics, 5th International INQUA Meeting on Paleoseismology, Active Tectonics and Archeoseismology (PATA), Busan, South Korea.

Henza, A.A., Withjack, M.O., Schlische, R.W. (2010). Normal-fault development during two phases of non-coaxial extension: An experimental study. *Journal of Structural Geology,* 32, 1656–1667.

Herold, N., Buzan, J., Seton, M., Goldner, A., Green, J.A.M., Müller, R.D., Markwick, P., & Huber, M. (2014). A suite of early Eocene (~55 Ma) climate model boundary conditions. *Geoscientific Model Development,* 7 (5), 2077–2090.

Hocking, R. M. (1987). *Geology of the Carnarvon Basin, Western Australia.* Geological Survey of Western Australia Bulletin.

Hocking, R.M. (1988). *Regional geology of the northern Carnarvon Basin* [Paper presentation]. The North West Shelf, Australia: Proceedings of the Petroleum Exploration Society of Australia. Symposium, Perth, Western Australia.

Hocking, R.M (1990a). *Field Guide for the Carnarvon Basin (with notes and additions 1993).* Records of the Geological Survey of Western Australia (11).

Hocking, R.M., (1990b). *Carnarvon Basin.* In: Geology and Mineral Resources of Western Australia. Western Australia Geological Survey (Memoir 3).

Hocking, R.M (1992). *Jurassic deposition in the southern and central North West Shelf.* Western Australia Geological Survey Western Australia Record (199217, 101).

Hocking, R.M., Moors, H.T., & Van De Graaff, W.J.E. (1987). *Geology of the Carnarvon basin, Western Australia.* Geological Survey of Western Australia Bulletin (133).

Hoffman, P.F. (1991). Did the breakout of Laurentia turn Gondwanaland inside-out? *Science,* 252(5011), 1409-1412.

Horstman, E.L., & Purcell, P.G. (1988, August*). The offshore Canning Basin-a review* [Paper presentation]. The North West Shelf, Australia. Proceedings of Petroleum Exploration Society Australia Symposium, Perth, Western Australia.

Hu, S., O'Sullivan, P.B., Raza, A., & Kohn, B.P. (2001). Thermal history and tectonic subsidence of the Bohai Basin, northern China: a Cenozoic rifted and local pull-apart basin. *Physics of the Earth and Planetary Interiors,* 126(3-4), 221-235.

Hubbard, R.J. (1988). Age and significance of sequence boundaries on Jurassic and Early Cretaceous rifted continental margins. *AAPG Bulletin,* 72(1), 49-72.

Hughes, A.N., & Shaw, J.H. (2015). Insights into the mechanics of fault-propagation folding styles. Bulletin, 127(11-12), 1752-1765.

Huismans, R.S., Podladchikov, Y.Y., & Cloetingh, S. (2001). Transition from passive to active rifting: Relative importance of asthenospheric doming and passive extension of the lithosphere. *Journal of Geophysical Research, Solid Earth* 106 (B6), 11271–11291.

I'Anson, A. J. (2020). *Structural inheritance at extensional continental margins: Implications for the tectonic evolution of the Northern Carnarvon Basin, Western Australia* (Doctoral dissertation).

I'Anson, A., Elders, C., & McHarg, S. (2019). Marginal fault systems of the Northern Carnarvon Basin: Evidence for multiple Palaeozoic extension events, North-West Shelf, Australia. *Marine and Petroleum Geology,* 101.

Iasky, R.P., Mory, A.J., Ghori, K.A.R., & Shevchenko, S.I. (1998a). *Structure and petroleum potential of the southern Merlinleigh Sub-basin, Carnarvon Basin, Western Australia.* Geological Survey of Western Australia (61).

Iasky, R.P., Mory, A.J., & Shevchenko, S.I. (1998b). *A structural interpretation of the Gascoyne Platform, southern Carnarvon Basin, WA.* Geological Survey of Western Australia, (61).

Issautier, B., Saspiturry, N., & Serrano, O. (2020). Role of structural inheritance and salt tectonics in the formation of pseudosymmetric continental rifts on the European margin of the hyperextended Mauléon

Basin (Early Cretaceous Arzacq and Tartas Basins). *Marine and Petroleum Geology,* 118, 104395.

Jablonski, D. (1997). Recent advances in the sequence stratigraphy of the Triassic to Lower Cretaceous succession in the Northern Carnarvon Basin, Australia. *The APPEA Journal,* 37(1), 429-454.

Jablonski, D., & Saitta, A.J. (2004). Permian to Lower Cretaceous plate tectonics and its impact on the tectono-stratigraphic development of the Western Australian margin. *The APPEA Journal*, 44(1), 287-328.

Jackson, J., & McKenzie, D. (1983). The geometrical evolution of normal fault systems. *Journal of Structural Geology,* 5(5), 471-482.

Jitmahantakul, S., & McClay, K. (2013). *Late Triassic–Mid Jurassic to Neogene extensional fault systems in the Exmouth Sub-Basin, Northern Carnarvon Basin, North West Shelf, Western Australia.* In Proceedings Western Australian Basins Conference.

Johnson, B.D., Powell, C.M., Veevers, J.J. (1976). Spreading history of the eastern Indian Ocean and Greater India's northward flight from Antarctica and Australia. *Geological Society of America Bulletin*, 87, 1560–1566.

Johnson, B.D., Powell, C.M., Veevers, J.J. (1980). Early spreading history of the Indian Ocean between India and Australia. *Earth and Planetary Science Letters*, 47, 131–143.

Ju, Y., Wang, G., Li, S., Sun, Y., Suo, Y., Somerville, I., Li, W., He, B., & Yu, K. (2022). Geodynamic mechanism and classification of basins in the Earth system. *Gondwana Research*, 102 (2022): 200-228.

Ju, Y., Ying, S., Guochang, W., & Fengqi, T. (2015). Dynamic types of basin formation and evolution and its geodynamic mechanisms. *Chinese Journal of Geology,* 50(2), 503-523.

Karner, G.D., & Driscoll, N.W. (1999). Style, timing and distribution of tectonic deformation across the Exmouth Plateau, northwest Australia,

determined from stratal architecture and quantitative basin modelling. Geological Society, *London, Special Publications,* 164(1), 271-311.

Karner, G.D., Taylor, B., Driscoll, N.W., & Kohlstedt, D.L. (Eds.). (2004). *Rheology and deformation of the lithosphere at continental margins*. New York Chichester, West Sussex: Columbia University Press.

Kearey, P., Klepeis, K.A., & Vine, F.J. (2009*). Global tectonics.* John Wiley & Sons.

Keen, C. E. (1979). Thermal history and subsidence of rifted continental margins—evidence from wells on the Nova Scotian and Labrador shelves. *Canadian Journal of Earth Sciences,* 16(3), 505-522.

Keen, C.E., & Boutilier, R. (1990). Geodynamic modelling of rift basins: the syn-rift evolution of a simple half-graben. In: Pinet, B., Bois, C. (Eds.), *The Potential of Deep Seismic Profiling for Hydrocarbon Exploration*, Collection Colloques et Seminaires, 24. Editions Technip, Paris.

Keep, M., Clough, M., & Langhi, L. (2002). *Neogene tectonic and structural evolution of the Timor Sea region, NW Australia* [Paper presentation]. The Sedimentary Basins of Western Australia 3, Proceedings of Petroleum Exploration Society of Australia Symposium, Perth, Western Australia.

Keep, M., Harrowfield, M., & Crowe, W. (2007). The Neogene tectonic history of the North West Shelf, Australia. *Exploration Geophysics,* 38(3), 151-174.

Keep, M., Powell, C.M., & Baillie, P.W. (1998). *Neogene deformation of the North West Shelf, Australia* [Paper presentation]. The Sedimentary Basins of Western Australia 2: Proceedings of West Australian Basins Symposium Perth, Western Australia.

Khain, V. Y. (1992). The role of rifting in the evolution of the Earth's crust, *Tectonophysics,* 215, 1–7.

Kingston, D.R., Dishroon, C.P., & Williams, P.A. (1983). Global basin classification system. *AAPG Bulletin,* 67(12), 2175-2193.

Klootwijk, C.T., Gee, J.S., Peirce, J.W., Smith, G.M., & McFadden, P.L. (1992). An early India-Asia contact: paleomagnetic constraints from Ninetyeast ridge, ODP Leg 121. *Geology,* 20(5), 395-398.

Kooi, H., & Beaumont, C. (1994). Escarpment evolution on high-elevation rifted margin: insight from a surface processes model that combines diffusion, advection and reaction. *Journal of Geophysical Research,* 99 (B6), 12191–12209.

Korchinski, M.S. (2019). *Mechanical Analysis of Continental Rifting and Orogenic Collapse* (Doctoral dissertation, University of Minnesota).

Korchinski, M., Rey, P.F., Mondy, L., Teyssier, C., & Whitney, D.L. (2018). Numerical investigation of deep-crust behavior under lithospheric extension. *Tectonophysics,* 726, 137-146.

Korchinski, M., Teyssier, C., Rey, P.F., Whitney, D.L., & Mondy, L. (2021). Single-phase vs two-phase rifting: numerical perspectives on the accommodation of extension during continental break-up. *Marine and Petroleum Geology,* 123, 104715.

Krantz, R.W. (1988). Multiple fault sets and three-dimensional strain: theory and application. *Journal of Structural Geology,* 10 (3), 225–237.

Larsen, H.C., & Saunders, A.D. (1998). *41. Tectonism and volcanism at the Southeast Greenland rifted margin: a record of plume impact and later continental rupture.* In Proceedings of the Ocean Drilling Program, Scientific Results, 152, 503-533.

Larsen, H.C., Saunders, A.D., & Clift, P.D. Editors (1994). *Proceedings of the Ocean Drilling Program.* Ocean Drilling Program, Texas A and M University, College Station, TX.

Lavier, L.L., & Manatschal, G. (2006). A mechanism to thin the continental lithosphere at magma-poor margins. *Nature,* 440(7082), 324-328.

Lee, C.-T.A., Shen, B., Slotnick, B.S., Liao, K., Dickens, G.R., Yokoyama, Y., Lenardic, A., Dasgupta, R., Jellinek, M., & Lackey, J.S. (2013).

Continental arc–island arc fluctuations, growth of crustal carbonates, and long-term climate change. *Geosphere,* 9 (1), 21–36.

Lei, C., Alves, T.M., Ren, J., Pang, X., Yang, L., & Liu, J. (2019). Depositional architecture and structural evolution of a region immediately inboard of the locus of continental breakup (Liwan Sub-basin, South China Sea). *GSA Bulletin,* 131 (7–8), 1059–1074.

Li, Z. X., & Powell, C. M. (2001). An outline of the palaeogeographic evolution of the Australasian region since the beginning of the Neoproterozoic. *Earth-Science Reviews*, 53(3-4), 237-277.

Li, S.T., Xie, X.N.,Wang, H., Jiao, Y.Q., Ren, J.Y., & Zhuang, X.G. (2004). *Sedimentary basin analysis, principle and application.* Higher Education Press, Beijing (in Chinese).

Lister, G.S., Etheridge, M.A. & Symonds, P.A. (1986). Application of the detachment fault model to the formation of passive continental margins. *Geology,* 14, 246- 50.

Lister, G.S., Etheridge, M.A. & Symonds, P.A. (1991). Detachment models for the formation of passive continental margins. *Tectonics,* 10, 1038-64.

Longley, I.M., Buessenschuett, C., Clydsdale, L., Cubitt, C.J., Davis, R.C., Johnson, M.K., Marshall, N.M., Murray, A.P., Somerville, R., Spry, T.B. & Thompson, N.B. (2002). *The North West Shelf of Australia - a Woodside Perspective,* The Sedimentary Basins of Western Australia, ed. M. Keep and S. Moss, Proceedings Western Australian Basins Symposium 3, Perth, Western Australia,

Lorenzo, J.M., Mutter, J.C., & Larson, R.L. (1991). Development of the continent-ocean transform boundary of the southern Exmouth Plateau. *Geology,* 19(8), 843-846.

Lymer, G., Cresswell, D.J., Reston, T.J., Bull, J.M., Sawyer, D.S., Morgan, J.K., & Shillington, D.J. (2019). 3D development of detachment faulting during continental breakup. Earth Planet Sci. Lett. 515, 90–99.

MacNeill, M., Marshall, N., & McNamara, C. (2018). New Insights into a major Early-Middle Triassic rift episode in the NW Shelf of Australia. *ASEG Extended Abstracts,* 2018(1), 1-5.

Magoon, L.B., & Dow, W.G. (1994). *The petroleum system: chapter 1: Part 1, Introduction.* In E.A., Beaumont & N.H., Foster (Eds.), Treatise of Petroleum Geology, Handbook of Petroleum Geology, AAPG.

Manatschal, G., Chenin, P., Ghienne, J. F., Ribes, C., & Masini, E. (2022). The syn-rift tectono-stratigraphic record of rifted margins (Part I): Insights from the Alpine Tethys. *Basin Research,* 34(1), 457-488.

Manatschal, G., Chenin, P., Lescoutre, R., Miró, J., Cadenas, P., Saspiturry, N., Masini, E., Chervrot, S., Ford, M., Joilvet, L., Mouthereau, F., Thinon, I., Issautier, B., & Calassou, S. (2021). The role of inheritance in forming rifts and rifted margins and building collisional orogens: a Biscay-Pyrenean perspective. *BSGF-Earth Sciences Bulletin,* 192(1), 55.

Marshall, N.G., & Lang, S.C. (2013). A new sequence stratigraphic framework for the North West Shelf, Australia. In The Sedimentary Basins of Western Australia 4: Proceedings PESA Symposium. Perth, Western Australia.

Martins-Neto, M.A., & Catuneanu, O. (2010). Rift sequence stratigraphy. *Marine and Petroleum Geology,* 27(1), 247-253.

McClay, K.R., & White, M.J. (1995). Analogue modelling of orthogonal and oblique rifting. *Marine and Petroleum Geology,* 12(2), 137-151.

McCormack, K.D., & McClay, K.R. (2018). Orthorhombic faulting in the Beagle Sub-basin, North West Shelf, Australia. *Geological Society, London, Special Publications,* 476, SP476-3.

McDermott, K., & Reston, T. (2015). To see, or not to see? Rifted margin extension. *Geology,* 43 (11), 967–970.

McHarg, S. (2018). *Tectonostratigraphic evolution of the Dampier Sub-basin, Northern Carnarvon Basin, Western Australia* [Doctoral dissertation, Curtin University].

McHarg, S., l'Anson, A., & Elders, C. (2018). The Permian and Carboniferous extensional history of the Northern Carnarvon Basin and its influence on Mesozoic extension. *ASEG Extended Abstracts*, 2018(1), 1-8.

McKenzie, D. (1978). Some remarks on the development of sedimentary basins, *Earth and Planetary Science Letters,* 40, 25–32.

Meert, J.G., & Lieberman, B.S. (2008). The Neoproterozoic assembly of Gondwana and its relationship to the Ediacaran–Cambrian radiation. *Gondwana Research,* 14(1-2), 5-21.

Menzies, M.A., Klemperer, S.L., Ebinger, C.J., & Baker, J. (2002). *Characteristics of Volcanic Rifted Margins*. Special Papers-Geological Society of America.

Metcalfe, I. (1994). Gondwanaland origin, dispersion, and accretion of East and Southeast Asian continental terranes. *Journal of South American Earth Sciences,* 7 (3), 333–347.

Metcalfe, I. (1996). Gondwanaland dispersion, Asian accretion and evolution of eastern Tethys. *Australian Journal of Earth Sciences*, 43(6), 605-623.

Metcalfe, I. (1999). Gondwana dispersion and Asian accretion: an overview. *Gondwana Dispersion and Asian Accretion*, 9-28.

Metcalfe, I. (2006). Palaeozoic and Mesozoic tectonic evolution and palaeogeography of East Asian crustal fragments: the Korean Peninsula in context. *Gondwana Research,* 9 (1–2), 24–46.

Metcalfe, I. (2013). Gondwana dispersion and Asian accretion: Tectonic and palaeogeographic evolution of eastern Tethys. *Journal of Asian Earth Sciences,* 66, 1-33.

Merdith, A.S., Collins, A.S., Williams, S.E., Pisarevsky, S., Foden, J.D., Archibald, D.B., Morgan, L.B., Alessio, B.L., Armistead, S., Plavsa, D.,

Clark, C., & Müller, R.D. (2017). A full-plate global reconstruction of the Neoproterozoic. *Gondwana Research,* 50, 84-134.

Merdith, A.S., Williams, S.E., Collins, A.S., Tetley, M.G., Mulder, J.A., Blades, M.L., Young, A., Armistead, S.E., Cannon, J., Zahirovic, S. & Müller, R.D. (2020). Extending full-plate tectonic models into deep time: Linking the Neoproterozoic and the phanerozoic. *Earth-Science Reviews,* 10377.

Miall, A.D. (2013). *Principles of sedimentary basin analysis*. Springer Science & Business Media.

Milani, E.J., & Davison, I. (1988). Basement control and transfer tectonics in the Recôncavo-Tucano-Jatobá rift, Northeast Brazil. *Tectonophysics,* 154(1-2), 41-70.

Mohn, G., Manatschal, G., Beltrando, M., Masini, E., & Kusznir, N. (2012). Necking of continental crust in magma-poor rifted margins: Evidence from the fossil Alpine Tethys margins. *Tectonics,* 31(1).

Mohn, G., Manatschal, G., Müntener, O., Beltrando, M., Masini, E. (2010). Unravelling the interaction between tectonic and sedimentary processes during lithospheric thinning in the Alpine Tethys margins. *International Journal of Earth Sciences*, 99, 75e101.

Mohr, P. (1992). Nature of the crust beneath magmatically active continental rifts. Geodynamics of rifting, volume II. Case history studies on rifts: North and South America and Africa. *Tectonophysics,* 213, 269–284.

Mondy, L. (2019). *On the dynamics of continental rifting: a numerical modelling approach* (Doctoral dissertation).

Moore, M.E., Gleadow, A.J., & Lovering, J.F. (1986). Thermal evolution of rifted continental margins: new evidence from fission tracks in basement apatites from southeastern Australia. *Earth and Planetary Science Letters,* 78(2-3), 255-270.

Moresi, L., & Solomatov, V. (1998). Mantle convection with a brittle lithosphere: thoughts on the global tectonic styles of the Earth and Venus. *Geophysical Journal International,* 133 (3), 669-682.

Morag, N., Haviv, I., Eyal, M., Kohn, B.P., & Feinstein, S. (2019). Early flank uplift along the Suez Rift: Implications for the role of mantle plumes and the onset of the Dead Sea Transform. *Earth and Planetary Science Letters,* 516, 56-65.

Morgan, J.V., Gulick, S.P., Bralower, T., Chenot, E., Christeson, G., Claeys, P., Gebhardt, C., Goto, K., Jones, H., Kring, D.A., Le Ber, E., Lofi, J., Long, X., Lowery, C., Mellett, C., Ocampo-Torres, R., Osinski, G.R., Perez-Cruz, L., Pickersgill, A., Poelchau, M., Rae, A., Rasmussen, C., Rebolledo-Vieyra, M., Riller, U., Sato, H., Schmitt, D.R., Smit, J., Tikoo, S., Tomioka, N., Urrutia-Fucugauchi, J., Whalen, M., Wittmann, A., Yamaguchi, K.E., Zylberman, W. (2016). The formation of peak rings in large impact craters. *Science,* 354 (6314), 878–882.

Morley, C.K., Haranya, C., Phoosongsee, W., Pongwapee, S., Kornsawan, A., & Wonganan, N. (2004). Activation of rift oblique and rift parallel pre-existing fabrics during extension and their effect on deformation style: examples from the rifts of Thailand. *Journal of Structural Geology,* 26, 1803–1829.

Mosher, D.C., & Yanez-Carrizo, G. (2021). The elusive continental rise: Insights from residual bathymetry analysis of the Northwest Atlantic margin. *Earth-Science Reviews,* 217, 103608.

Müller, R.D., Gaina, C., & Clark, S. (2000). *Seafloor spreading around Australia*. Billion-year earth history of Australia and neighbours in Gondwanaland, 18-28.

Müller, R.D., Mihut, D., & Baldwin, S. (1998). *A new kinematic model for the formation and evolution of the west and northwest Australian margin*, in: Purcell, P.G., Purcell, R.R. (Eds.), The Sedimentary Basins of Western Australia. Petroleum Exploration Society of Australia, Perth, Western Australia.

Müller, R.D., Mihut, D., Heine, C., O'Neill, C., Russell, I., Keep, M., & Moss, S.J. (2002, October). *Tectonic and volcanic history of the Carnarvon Terrace: Constraints from seismic interpretation and geodynamic modelling* [Paper presentation]. The Sedimentary Basins of Western Australia 3, Proceedings of Petroleum Exploration Society of Australia Symposium, Perth, Western Australia.

Müller, R.D., Sdrolias, M., Gaina, C., Steinberger, B., & Heine, C. (2008). Long-term sea-level fluctuations driven by ocean basin dynamics. *Science,* 319 (5868), 1357.

Müller, R.D., Zahirovic, S., Williams, S.E., Cannon, J., Seton, M., Bower, D.J., Tetley, G., Heine, C., Le Breton, E., Liu, S., Russell, S.H., Yang, T., Leonard, J., & Gurnis, M. (2019). A global plate model including lithospheric deformation along major rifts and orogens since the Triassic. *Tectonics,* 38(6), 1884-1907.

Mutter, J.C., & Larson, R.L. (1989). Extension of the Exmouth Plateau, offshore northwestern Australia: Deep seismic reflection/refraction evidence for simple and pure shear mechanisms. *Geology,* 17(1), 15-18.

Mayall, M., & Kneller, B. (2021). Seismic interpretation workflows for deep-water systems: A practical guide for the subsurface. *AAPG Bulletin,* 105(11), 2127-2157.

Myers, J.S., Shaw, R.D., & Tyler, I.M. (1996). Tectonic evolution of proterozoic Australia. *Tectonics,* 15(6), 1431-1446.

Naliboff, J.B., Buiter, S.J., Péron-Pinvidic, G., Osmundsen, P.T., & Tetreault, J. (2017). Complex fault interaction controls continental rifting. *Nature communications,* 8(1), 1-9.

Neugebauer. H.J. (1978). Crustal doming and the mechanism of rifting. Part I: Rift formation. *Tectonophysics,* 45: 159- 186.

O'Brien, G.W. (1993). Some ideas on the rifting history of the Timor Sea from the integration of deep crustal seismic and other data. *The PESA Journal,* 21, 95-113.

O'Brien, G.W., Etheridge, M.A., Willcox, J.B., Morse, M., Symonds, P., Norman, C. & Needham, D.J. (1993). The structural architecture of the Timor Sea, north-western Australia: implications for basin development and hydrocarbon exploration. *The APEA Journal*, 33(1), 258-78.

O'Brien, G. W., Higgins, R., Symonds, P., Quaife, P., Colwell, J., & Blevin, J. (1996). Basement control on the development of extensional systems in Australia's Timor Sea: an example of hybrid hard linked/soft linked faulting?. *The APPEA Journal,* 36(1), 161-201.

O'Neill, C., Jellinek, A.M., Lenardic, A. (2007a). Conditions for the onset of plate tectonics on terrestrial planets and moons. *Earth and Planetary Science Letters*, 261 (1), 20-32.

O'Neill, C., & Lenardic, A. (2007). Geological consequences of super-sized Earths. *Geophysical Research Letters,* 34 (19).

O'Neill, C., Lenardic, A., Moresi, L., Torsvik, T.H., Lee, C.T. (2007b). Episodic precambrian subduction. *Earth and Planetary Science Letters*, 262 (3), 552-562.

O'Neill, C., & Zhang, S. (2019). *Modeling early Earth tectonics: the case for stagnant lid behaviour*. In Earth's oldest rocks. Elsevier.

Pattillo, J., & Nicholls, P.J. (1990). A tectonostratigraphic framework for the Vulcan Graben, Timor Sea region. *The APPEA Journal*, 30(1), 27-51.

Parmentier, E.M. (1987). Dynamic topography in rift zones: Implications for lithospheric heating. Philosophical Transactions of the Royal Society of London. *Series A, Mathematical and Physical Sciences,* 321(1557), 23-25.

Paumard, V., Bourget, J., Payenberg, T., Ainsworth, R.B., George, A.D., Lang, S., Posamentier, H.W., & Peyrot, D. (2018). Controls on shelf-margin architecture and sediment partitioning during a syn-rift to post-rift

transition: Insights from the Barrow Group (Northern Carnarvon Basin, North West Shelf, Australia). *Earth-Science Reviews,* 177, 643-677.

Pellegrini, C., Patruno, S., Helland-Hansen, W., Steel, R.J., & Trincardi, F. (2020). Clinoforms and clinothems: fundamental elements of basin infill. *Basin Research*, 32 (2), 187–205.

Péron-Pinvidic, G., & Manatschal, G. (2010). From microcontinents to extensional allochthons: witnesses of how continents rift and break apart?. *Petroleum Geoscience,* 16(3), 189-197.

Peron-Pinvidic, G., Manatschal, G., & Osmundsen, P.T. (2013). Structural comparison of archetypal Atlantic rifted margins: A review of observations and concepts. *Marine and Petroleum Geology,* 43, 21-47.

Pigram, C.J., & Panggabean, H. (1984). Rifting of the northern margin of the Australian continent and the origin of some microcontinents in eastern Indonesia. *Tectonophysics,* 107 (3), 331–353.

Pinto, V.H.G., Manatschal, G., Karpoff, A.M., & Viana, A. (2015). Tracing mantle-reacted fluids in magma-poor rifted margins: The example of Alpine Tethyan rifted margins. *Geochemistry, Geophysics, Geosystems,* 16(9), 3271-3308.

Pitman III, W.C., & Andrews, J.A. (1985). *Subsidence and thermal history of small pull apart basins.*

Plafker, G. (1987). *Regional geology and petroleum potential of the northern Gulf of Alaska continental margin.*

Playford, P.E., Cockbain, A.E., & Low, G.H. (1976). *Geology of the Perth Basin, Western Australia.* Western Australia Geological Survey.

Polomka, S.M., & Lemon, N.M. (1996). Tectono-Stratigraphic Evolution of the Barrow Sub-Basin, North West Shelf: A Discussion on Nomenclature Revision. *PESA Journal*, 24, 105–115.

Powell, C., & Johnson, B.D. (1980). Constraints on the Cenozoic position of Sunderland. *Tectonophpics,* 63, 91-109.

Powell, C.M., & Veevers, J.J. (1987). Namurian uplift in Australia and South America triggered the main Gondwanan glaciation. *Nature,* 326(6109), 177.

Powell, C.M., Roots, S.R., & Veevers, J.J. (1988). Pre-breakup continental extension in East Gondwanaland and the early opening of the eastern Indian Ocean. *Tectonophysics,* 155(1-4), 261-283.

Pryer, L.L., Romine, K.K., Loutit, T.S., & Barnes, R.G. (2002). Carnarvon basin architecture and structure defined by the integration of mineral and petroleum exploration tools and techniques. *The APPEA Journal,* 42(1), 287-309.

Pryer, L., Blevin, J., Nelson, G., Sanchez, G., Lee, J.D., Cathro, D., Graham, R., & Horn, B. (2014). Structural architecture and basin evaluation of the North West Shelf. *The APPEA Journal,* 54(2), 474-474.

Purcell, P.G., & Purcell, R.R. (1988). *The North West Shelf, Australia-An Introduction.* Proceedings of the North West Shelf Symposium. Petroleum Exploration Society of Australia.

Rad, U., Exon, N.F., & Haq, B.U. (1992). Rift–to drift history of the Wombat Plateau, northwest Australia etc. *Proceedings of Ocean Drilling Program., Science Results,* 122, 765-800.

Ranero, C.R., & Pérez-Gussinyé, M. (2010). Sequential faulting explains the asymmetry and extension discrepancy of conjugate margins. *Nature,* 468 (7321), 294–299.

Reches, Z.E. (1978). Analysis of faulting in three-dimensional strain field. *Tectonophysics,* 47 (1–2), 109–129.

Reston, T.J. (2005). Polyphase faulting during the development of the west Galicia rifted margin. *Earth and Planetary Science Letters,* 237 (3–4), 561–576.

Reston, T.J., & Pérez-Gussinyé, M. (2007). Lithospheric extension from rifting to continental breakup at magma-poor margins: rheology, serpentinisation and symmetry. *International Journal of Earth Science,* 96 (6), 1033–1046.

Ribeiro, A., Mateus, A., & Antonio Ribeiro, P. (2002*). Soft plate and impact tectonics.* Springer Science & Business Media.

Richter, F., & McKenzie, D. (1978). Simple plate models of mantle convection. *Journal of Geophysics,* 44, 441–471.

Ring, U. (1994). The influence of pre-existing structure on the evolution of the Cenozoic Malawi rift (East African rift system). *Tectonics,* 13 (2), 313–326.

Roberts, D.G., & Bally, A.W. (2012). *Some remarks on basins and basin classification and tectonostratigraphic megasequences*. In, Regional Geology and Tectonics: Principles of Geologic Analysis. Elsevier.

Roberts, D.G., & Schnitker, D. (1984*). Initial reports of the deep sea drilling project, 81.* US Govern. Printing Office, Initial Report, Deep Sea Drilling Project.

Rollet, N., Shi, Z., Morse, M., Djomani, Y.P., & Gunning, M. (2019*). Crustal structure and distribution of volcanics in the Northern Carnarvon and Roebuck basins, central Australian Northwest shelf: potential field modelling.* RECORD 2019/022.

Rohead-O'Brien, H., & Elders, C. (2018). Controls on Mesozoic rift-related uplift and syn-extensional sedimentation in the Exmouth Plateau. *ASEG Extended Abstracts,* 2018(1), 1-8.

Rohead-O'Brien, H., Elders, C., Cunneen, J. (2019). The variation of Mesozoic rift impact on the Exmouth Plateau and the depositional response. *West Australian Basin Symposium,* Perth, Australia. Withdrawn.

Rohrman, M. (2013). Intrusive large igneous provinces below sedimentary basins: An example from the Exmouth Plateau (NW Australia). *Journal of Geophysical Research: Solid Earth,* 118(8), 4477-4487.

Rohrman, M. (2015). Delineating the Exmouth mantle plume (NW Australia) from denudation and magmatic addition estimates. *Lithosphere*, 7(5), 589-600.

Romans, B.W., Castelltort, S., Covault, J.A., Fildani, A., & Walsh, J.P. (2016). Environmental signal propagation in sedimentary systems across timescales. *Earth Science Reviews,* 153, 7–29.

Romine, K., and Durrant, J. (1996). *Carnarvon Cretaceous-Tertiary Tie Report.* Australian Geological Survey Organisation, Record 1996/36.

Romine, K.K., Durrant, J.M., Cathro, D.L., & Bernardel, G. (1997). Petroleum play element prediction for the Cretaceous-Tertiary basin phase, Northern Carnarvon Basin. *The APPEA Journal,* 37(1), 315-339.

Rosendahl, B.R. (1987). Architecture of continental rifts with special reference to East Africa. *Annual Review of Earth and Planetary Sciences*, 15, 445.

Royden, L., & Keen, C.E. (1980). Rifting process and thermal evolution of the continental margin of eastern Canada determined from subsidence curves. *Earth and Planetary Science Letters,* 51(2), 343-361.

Rouby, D., Braun, J., Robin, C., Dauteuil, O., & Deschamps, F. (2013). Long-term stratigraphic evolution of Atlantic-type passive margins: A numerical approach of interactions between surface processes, flexural isostasy and 3D thermal subsidence. *Tectonophysics,* 604, 83-103.

Ruppel, C. (1995). Extensional processes in continental lithosphere. *Journal of Geophysical Research: Solid Earth,* 100(B12), 24187-24215.

Sakai, T., Saneyoshi, M., Sawada, Y., Nakatsukasa, M., Kunimtatsu, Y., & Mbua, E. (2013). *Early continental rift basin stratigraphy, depositional facies and tectonics in volcaniclastic system: examples from the Miocene successions along the Japan Sea and in the East African Rift Valley (Kenya).* In Mechanism of sedimentary basin formation-multidisciplinary approach on active plate margins.

Sandiford, M., Hand, M., & McLaren, S. (1998). High geothermal gradient metamorphism during thermal subsidence. *Earth and Planetary Science Letters,* 163(1-4), 149-165.

Sapin, F., Ringenbach, J.-C., & Clerc, C. (2021). Rifted margins classification and forcing parameters. *Scientific Reports,* 11, 8199.

Sawyer, D.S., Coffin, M.F., Reston, T.J., Stock, J.M., Hopper, J.R. (2007). COBBOOM: the continental breakup and birth of oceans mission. *Scientific Drilling,* 5, 13–25.

Scarselli, N. (2014*). Seismic Analysis of Gravity Driven Deformation at Passive Margins* [Doctoral dissertation, Royal Holloway University of London].

Schiffer, C., Doré, A.G., Foulger, G.R., Franke, D., Geoffroy, L., Gernigon, L., Holdsworth, B., Kusznir, N., Lundin, E., McCaffrey, K., & Welford, J.K. (2020). Structural inheritance in the North Atlantic. *Earth-Science Reviews,* 206, 102975.

Scotese, C.R. (2001). *Atlas of earth history,* 1. Paleogeography. PALEOMAP Project, Arlington, Tex.

Scotese, C., Boucot, A., & McKerrow, W. (1999). Gondwanan palaeogeography and paleoclimatology. *Journal of African Earth Science,* 28 (1), 99–114.

Seggie, R.J., Lang, S.C., Marshall, N.M., Cubitt, C.J., Alsop, D., Kirk, R., & Twartz, S. (2007). Integrated multi-disciplinary analysis of the Rankin Trend gas reservoirs North West Shelf, Australia. *The APPEA Journal,* 47(1), 55-69.

Seton, M., Müller, R.D., Zahirovic, S., Gaina, C., Torsvik, T., Shephard, G., Talsma, A., Gurnis, M., Turner, M., Maus, S., & Chandler, M. (2012). Global continental and ocean basin reconstructions since 200 Ma. *Earth-Science Reviews,* 113(3-4), 212-270.

Şengör, A.M.C., & Burke, K. (1978), Relative timing of rifting and volcanism on Earth and its tectonic implications. *Geophysical Research Letters,* 5(6), 419–421.

Shaw, R.P., Auton, C.A., Baptie, B., Brocklehurst, S., Dutton, M., Evans, D.J., Field, L.P., Gregory, S.P., Henderson, E., Hughes, A.J., Milodowski, A.E., Parkes, D., Rees, J.G., Small, J., Smith, N., Tye, A., & West, J. M. (2013). *Potential natural changes and implications for a UK GDF.*

Skogseid, J., Planke, S., Faleide, J.I., Pedersen, T., Eldholm, O., Neverdal, F. (2000). NE Atlantic continental rifting and volcanic margin formation. *Geological Society of London, Special Publication,* 167 (1), 295–326.

Sleep, N.H. (1971). Thermal effects of the formation of Atlantic continental margins by continental break up. *Geophysical Journal International,* 24(4), 325-350.

Smith, S.A., Tingate, P.R., Griffths, C.M., & Hull, J.N.F. (1999). The structural development and petroleum potential of the Roebuck Basin. *The APPEA Journal,* 39(1), 364-385.

Soares, D.M., Alves, T.M., & Terrinha, P. (2012). The breakup sequence and associated lithospheric breakup surface: their significance in the context of rifted continental margins (West Iberia and Newfoundland margins, North Atlantic). *Earth Planet Science Letters,* 355, 311–326.

Sømme, T.O., Helland-Hansen, W., Martinsen, O.J., & Thurmond, J.B. (2009). Relationships between morphological and sedimentological parameters in source-to-sink systems: a basis for predicting semi-quantitative characteristics in subsurface systems. *Basin Research,* 21 (4), 361–387.

Sømme, T.O., Jackson, C.A., & Vaksdal, M. (2013a). Source-to-sink analysis of ancient sedimentary systems using a subsurface case study from the Møre-Trøndelag area of southern Norway: Part 1 - depositional setting and fan evolution. *Basin Research,* 25 (5), 489–511.

Spasojevic, S. & Gurnis, M., (2012). Sea level and vertical motion of continents from dynamic earth models since the Late Cretaceous. *AAPG Bulletin,* 96 (11), 2037–2064.

Spencer, l., Needham, J., Bradshaw, J., Bradshaw, M., Foster, C., Noonan, J., Edgecombe, S. & Zuccaro, G. (1994). *Australian Petroleum Systems Barrow-Exmouth Sub-basins Module* (Record, 1994/19). Australian Geological Survey Organisation.

Spencer, l., Needham, J., Edgecombe, S., Bradshaw, J., Foster, C., Bradshaw, M., Vizy, J., & Zuccaro, G. (1993). *Australian Petroleum Systems Dampier Sub-basins Module* (Record, 1993/31). Australian Geological Survey Organisation.

Spencer, l., Sayers, J., Bradshaw, J., Bradshaw, M., Foster, C., Murray, A., Edwards, D., Zuccaro, G., Buchanan, C., & Apps, H. (1995*). Australian Petroleum Systems Exmouth Plateau & Outer Rankin Platform Module* (Record 1995/80). Australian Geological Survey Organisation.

Stagg, H.M.J., Alcock, M.B., Bernardel, G., Moore, A.M.G., Symonds, P.A. & Exon, N.F. (2004). *Geological framework of the outer Exmouth Plateau and adjacent ocean basins* (Record 2004/13). Geoscience Australia.

Stagg, H.M.J., & Colwell, J.B. (1994). *The structural foundations of the Northern Carnarvon Basin* [Paper presentation]. The Sedimentary Basins of Western Australia, Petroleum Exploration Society of Australia Symposium, Perth, Western Australia.

Stagg, H.M.J., Willcox, J.B., Symonds, P.A., O'Brien, G.W., Colwell, J.B., Hill, P.J., Lee, C-S., Moore, A.G.M., & Struckmeyer, H.I.M. (1999). Architecture and evolution of the Australian continental margin: AGSO *Journal of Australian Geology and Geophysics*, 17.

Steckler, M.S. (1985). Uplift and extension at the Gulf of Suez: indications of induced mantle convection. *Nature,* 317(6033), 135-139.

Steckler, M.S., & Watts, A.B. (1980). The Gulf of Lion: subsidence of a young continental margin. *Nature,* 287, 425–429.

Storti, F., & Poblet, J. (1997). Growth stratal architectures associated to decollement folds and fault-propagation folds. Inferences on fold kinematics. *Tectonophysics,* 282(1-4), 353-373.

Summons, R.E., Bradshaw, M., Crowley, J., Edwards D.S., George, S.C. & Zumberge, J.E. (1998). *Vagrant oils: geochemical signposts to unrecognised petroleum systems* [Paper presentation]. The Sedimentary Basins of Western Australia 2: Proceedings of West Australian Basins Symposium Perth, Western Australia.

Suppe, J., 1983. Geometry and kinematics of fault-bend folding. *American Journal of Science,* 283, 684–721.

Suppe, J., & Medwedeff, D.A. (1990). Geometry and kinematics of fault-propagation folding. *Eclogae Geologicae Helvetiae,* 83(3), 409-454.

Symonds, P.A., Collins, C.D.N. & Bradshaw, J. (1994). *Deep structure of the Browse Basin: Implications for basin development and petroleum exploration* [Paper presentation]. The Sedimentary Basins of Western Australia, Petroleum Exploration Society of Australia Symposium, Perth, Western Australia.

Swift, M.G., Stagg, H.M.J., & Falvey, D.A. (1988). *Heat flow regime and implications for oil maturation and migration in the offshore Northern Carnarvon Basin* [Paper presentation]. The Sedimentary Basins of Western Australia: Proceedings of West Australian Basins Symposium Perth, Western Australia.

Tackley, P.J. (2000). Self-consistent generation of tectonic plates in time-dependent, three-dimensional mantle convection simulations. *Geochemistry, Geophysics, Geosystems*, 1 (8).

Taylor, B., Goodliffe, A. M., & Martinez, F. (1999). How continents break up: insights from Papua New Guinea. *Journal of Geophysical Research: Solid Earth,* 104(B4), 7497-7512.

Tetreault, J.L., & Buiter, S.J.H. (2018). The influence of extension rate and crustal rheology on the evolution of passive margins from rifting to break-up. *Tectonophysics,* 746, 155–172.

Tibaldi, A. (1989). The Pleistocene fault pattern in northern Michoacan, Mexico: an example of three-dimensional strain. *Annales Tectonicae,* 3, 34–43.

Tibaldi, A., & Bonali, F.L. (2018). A model to explain joint patterns found in ignimbrite deposits. *Bulletin of Volcanology*, 80 (3), 26.

Tindale, K., Newell, N., Keall, J., Smith, N., Purcell, P.G., & Purcell, R.R. (1998). *Structural evolution and charge history of the Exmouth Sub-basin, northern Carnarvon Basin, Western Australia* [Paper presentation]. The Sedimentary Basins of Western Australia 2: Proceedings of West Australian Basins Symposium Perth, Western Australia.

Totterdell, J.M., Blevin, J.E., Struckmeyer, H.I.M., Bradshaw, B.E., Colwell, J. B., & Kennard, J.M. (2000). A new sequence framework for The Great Australian Bight: starting with a clean slate*. The APPEA Journal,* 40(1), 95-118.

Tortopoglu, B. (2015). *The Structural evolution of the Northern Carnarvon Basin, Northwest Australia* [Doctoral dissertation, Colorado School of Mines].

Trudgill, B., & Cartwright, J. (1994). Relay-ramp forms and normal-fault linkages, Canyonlands National Park, Utah. *Geological Society of America Bulletin,* 106(9), 1143-1157.

Tugend, J., Gillard, M., Manatschal, G., Nirrengarten, M., Harkin, C., Epin, M.-E., Sauter, D., Autin, J., Kusznir, N., & McDermott, K. (2020). *Reappraisal of the magma-rich versus magma-poor rifted margin archetypes.* Special Publication of the Geological Society of London, 476, 23–47.

Turcotte, D.L., & Emerman, S.H. (1983). Mechanisms of active and passive rifting. *Developments in Geotectonics,*19, 39-50.

Turcotte, D.L., & Oxburgh, E.R. (1973). Mid-plate tectonics. *Nature,* 244(5415), 337-339.

Van der Beek, P., Andriessen, P., & Cloetingh, S. (1995). Morphotectonic evolution of rifted continental margins: inferences from a coupled tectonic-surface processes model and fission track thermochronology. *Tectonics,* 14 (2), 406–421.

Van der Beek, P., Cloetingh, S.A.P.L., & Andriessen, P. (1994). Mechanisms of extensional basin formation and vertical motions at rift flanks: constraints from tectonic modelling and fission track thermochronology. *Earth and Planetary Science Letters,* 121, 417–433.

Veevers, J.J. (1974). *Western continental margin of Australia.* In The geology of continental margins. Berlin, Heidelberg: Springer Berlin Heidelberg.

Veevers, J.J. (1977). Rifted arch basins and post-breakup rim basins on passive continental margins. *Tectonophysics,* 41(4), T1-T5.

Veevers, J.J. (1986). *Phanerozoic earth history of Australia;* Oxford Monographs on Geology and Geophysics, 2. Clarendon Press Oxford.

Veevers, J.J. (1988). Morphotectonics of Australia's northwestern margin-a review. In: Purcell P.G. & R.R. (Eds), The North West Shelf Australia, Proceedings Of Petroleum Exploration Society Australia Symposium, Perth, 1988, 19-27.

Veevers, J.J. (2000). Change of tectono-stratigraphic regime in the Australian plate during the 99 Ma (mid-Cretaceous) and 43 Ma (mid-Eocene) swerves of the Pacific. *Geology,* 28, 47-50.

Veevers, J.J. (2006). Updated Gondwana (Permian–Cretaceous) earth history of Australia. *Gondwana Research,* 9(3), 231-260.

Veevers, J.J., & Cotterill, D. (1976). Western margin of Australia: a Mesozoic analog of the East African rift system. *Geology,* 4(12), 713-717.

Veevers, J.J., Powell, C.M., & Roots, S.R. (1991). Review of seafloor spreading around Australia. I. Synthesis of the patterns of spreading. *Australian Journal of Earth Sciences,* 38(4), 373-389.

von Rad, U., Exon, N.F. (1983). *Mesozoic-Cenozoic sedimentary and volcanic evolution of the starved passive continental margin off northwest*

Australia. In: Watkins, J., CDrake, C. (Eds.), Studies in Continental Margin Geology: AAPG Memoir.

von Rad, U., Exon, N.F., Haq, B.U. (1992). *46. Rift-to-drift history of the Wombat Plateau, Northwest Australia: Triassic to Tertiary Leg 122 Results.*

Wang, P. (2004). *Cenozoic deformation and the history of sea-land interactions in Asia.* Continent-Ocean Interactions Within East Asian Marginal Seas.

Watts, A.B. (1978). An analysis of isostasy in the world's oceans, 1. Hawaiian Emperor seamount chain. *Journal of Geophysical Research,* 83, 5989-6004.

Watts, A.B. (1989). Lithospheric flexure due to prograding sediments loads: implication for the origin of onlap/offlap patterns in sedimentary basins. *Basin Research*, 2, 133–144.

Watts, A.B. (2001). *Isostasy and Flexure of the Lithosphere.* Cambridge University Press.

Watts, A.B., & Fairhead, J.D. (1997). Gravity anomalies and magmatism along the western continentalmargin of the British Isles. *Journal of the Geological Society,* 154, 523–529.

Watts, A.B., Karner, G.D., & Steckler, M.S. (1982). Lithospheric flexure and the evolution of sedimentary basins: *Royal Society of London Philosophical Transactions Series A,* 305, 249-281.

Weaver, P.P.E., Wynn, R.B., Kenyon, N.H., & Evans, J. (2000). Continental margin sedimentation, with special reference to the north-east Atlantic margin. *Sedimentology,* 47 (1), 239–256.

Weissel, J.K., & Karner, G.D. (1989). Flexural uplift of rift flanks due to mechanical unloading of the lithosphere during extension. *Journal of Geophysical Research: Solid Earth*, 94(B10), 13919-13950.

Wessel, P., Müller, R.D. (2007). *Plate Tectonics*. Treatise on Geophysics, 6. Elsevier.

Wheeler, J., & Cheadle, M. (2014). *Geophysics, Reference Module in Earth Systems and Environmental Sciences*. Elsevier.

White, N., & McKenzie, D. (1988). Formation of the" steer's head" geometry of sedimentary basins by differential stretching of the crust and mantle. *Geology,* 16(3), 250-253.

Whittam, D.B., Norvick, M.S., & Mclntyre, C.L. (1996). Mesozoic and Cainozoic tectonostratigraphy of western ZOCA and adjacent areas. *The APPEA Journal,* 36(1), 209-232.

White, R., & McKenzie, D. (1989a). Magmatism at rift zones: the generation of volcanic continental margins and flood basalts. *Journal of Geophysical Research: Solid Earth,* 94(B6), 7685-7729.

White, R.S., & McKenzie, D.P. (1989b). Volcanism at rifts. *Scientific American,* 261(1), 62-71.

Williams, G.D. (1993). *Tectonics and seismic sequence stratigraphy: an introduction.* In: Williams, G.D., Dobb, A. (Eds.), Tectonics and Seismic Sequence Stratigraphy. Geological Society Special Publication.

Wilson, M. (1993). Magmatism and the geodynamics of basin formation. *Sedimentary Geology,* 86, 5–29.

Winata, M., Elders, C., Maselli, V., & Stephenson, R.A. (2021, Submitted). Regional seismic stratigraphic framework and depositional history of the post-Valanginian passive margin sequences in the Northern Carnarvon Basin, North West Shelf of Australia. *Marine Petroleum Geology.*

Woodside Offshore Petroleum (1988). *A review of the petroleum geology and hydrocarbon potential of the Barrow-Dampier Sub-basin and environs* [Paper presentation]. The Sedimentary Basins of Western Australia: Proceedings of West Australian Basins Symposium Perth, Western Australia.

Wopfner, H. (1994). The Malagasy Rift, a chasm in the Tethyan margin of Gondwana. *Journal of Southeast Asian Earth Sciences*, 9(4), 451-461.

Wulff, K., & Barber, P. (1995). Tectonic controls on the sequence stratigraphy of Late Jurassic fan systems in the Barrow-Dampier Basin, North West Shelf, Australia. *PESA Journal,* 23, 77-89.

Yeates, A.N., Bradshaw, M.T., Dickins, J.M., Brakel, A.T., Exon, N.F., Langford, R.P., Mulholland, S.M., Totterdell, J.M., & Yeung, M. (1987). *The Westralian superbasin: an Australian link with Tethys* [Paper presentation]. International Symposium on Shallow Tethys 2.

Yeh, M.W., & Shellnutt, J.G. (2016). The initial break-up of Pangæa elicited by Late Palæozoic deglaciation. *Scientific Reports,* 6(1), 1-9.

Zabanbark, A. (2010). The structural features and petroleum resource potential of basins in the western and northwestern Australian margins. *Oceanology,* 50, 268-280.

Zahirovic, S., Matthews, K.J., Flament, N., Müller, R.D., Hill, K.C., Seton, M., & Gurnis, M. (2016). Tectonic evolution and deep mantle structure of the eastern Tethys since the latest Jurassic. *Earth-Science Reviews,* 162, 293-337.

Zastrozhnov, D., Gernigon, L., Gogin, I., Planke, S., Abdelmalak, M.M., Polteau, S., Faleide, J.I., Manton, B., & Myklebust, R. (2020). Regional structure and polyphased Cretaceous-Paleocene rift and basin development of the mid-Norwegian volcanic passive margin. *Marine and Petroleum Geology*, 115, 104269.

Zaw, K., Meffre, S., Lai, C.-K., Burrett, C., Santosh, M., Graham, I., Manaka, T., Salam, A., Kamvong, T., & Cromie, P. (2014). Tectonics and metallogeny of mainland Southeast Asia—a review and contribution. *Gondwana Research,* 26 (1), 5–30.

Zhao, Q., Zhu, H., Zhou, X., Liu, Q., Cai, H., & Gao, W. (2021). Continental margin sediment dispersal under geomorphic control in Xihu Depression, East China Sea Shelf Basin*. Journal of Petroleum Science and Engineering,* 205, 108738.

Zhu, J., Wu, B., Wang, L., Peng, S., & Zhou, H. (2019). Neoproterozoic bimodal volcanic rocks and granites in the western Dabie area, northern margin of Yangtze block, China: implications for extension during the break-up of Rodinia. *International Geology Review*, 61(11), 1370-1390.

Ziegler, P.A. (1992), North Sea rift system, in Geodynamics of Rifting, Volume I. Case History Studies on Rifts: Europe and Asia, edited by P. A. Ziegler, *Tectonophysics,* 208, 55–75.

Ziegler, P.A. (1993). Plate-moving mechanisms: their relative importance. *Journal of the Geological Society,* 150, 927–940.

Ziegler, P.A. (1996). *Geodynamic processes governing development of rifted basins*. In: Roure, F., Ellouz, N., Shein, V.S., & Skvortsov, L. (Eds.), Geodynamic Evolution of Sedimentary Basins. Editions Technip, Paris.

Ziegler, P.A., & Cloetingh, S. (2004). Dynamic processes controlling evolution of rifted basins. *Earth-Science Reviews,* 64, 1–50.

Zuber, M.T., & Parmentier, E.M. (1986). Lithospheric necking: a dynamic model for rift morphology. *Earth and Planetary Science Letters,* 77(3-4), 373-383.

Zwaan, F., & Schreurs, G. (2017). How oblique extension and structural inheritance influence rift segment interaction: Insights from 4D analog models. *Interpretation,* 5, SD119–SD138.